Giacomo Cao · Roberto Orrù *Editors*

Current Environmental Issues and Challenges

Springer

Current Environmental Issues and Challenges

Giacomo Cao • Roberto Orrù
Editors

Current Environmental Issues and Challenges

Springer

Editors
Giacomo Cao
Roberto Orrù
Department of Mechanical,
Chemical and Materials Engineering
University of Cagliari
Cagliari, Italy

ISBN 978-94-017-8776-5 ISBN 978-94-017-8777-2 (eBook)
DOI 10.1007/978-94-017-8777-2
Springer Dordrecht Heidelberg New York London

Library of Congress Control Number: 2014938205

Printed on acid-free paper

Springer is part of Springer Science+Business Media (www.springer.com)

Preface

The purpose of this book is to put together in a single reference several topics related to current environmental issues and challenges. The latter ones have been presented and discussed during specific summer schools attended in the last years by PhD Students in Environmental Science and Engineering involved in the agreement signed by the Ecole Nationale de l'Industrie Minérale (Morocco), the Pushchino State Institute of Life Sciences (Russia), the University of Aveiro (Portugal) and the University of Cagliari (Italy). The agreement, which was approved and financially supported for the first time in 2001 by the Ministry of the University and the Scientific and Technological Research (MURST) of the Italian Government in the framework of the Three Years Plan 1998–2000 indicated as Internationalisation, was aimed to establish an international postgraduate education programme in environmental studies. It should be noted in passing that the objective of the agreement was to increase the academic, scientific and cultural relations among the involved institutions in the area of Environmental Science and Engineering and, particularly, to jointly award the corresponding PhD Degree.

This book covers quite diverse subjects which belong to significant environmental topics. In particular, the chapters dealing with air pollution from mobile sources, air pollution and health effects and air quality modelling fall in the air pollution category, while the ones related to microalgae for carbon dioxide sequestration/biofuels production, fuel cells and solar energy technology, respectively, can be ascribed to the energy topic. Then, several technologies to handle a wide spectrum of environmental pollutants are taken into account in the corresponding chapters: self-propagating high-temperature reactions, catabolic plasmids in biodegradation, dust removal, glyphosate biodegradation, bioleaching and probiotic bacteria for water sanitation. Moreover, the chapter on biodiversity is clearly related to the conservation issue, while the water pollution subject is tackled by the chapter on water quality monitoring. Finally, a general analysis on green business as well as on the grid/cloud computing technology to share resources management in environmental sciences is also provided.

Each chapter is a stand-alone to allow the user rapid access to the subject of interest. All chapters provide a reference section for further reading and research. Few books currently exist that cover such a wide spectrum of topics. For this reason it is intended as a text for graduate courses in environmental science and engineering as well as a reference book on the addressed topics.

Cagliari, Italy

Giacomo Cao
Roberto Orrù

Contents

Air Pollution and Health Effects

Ana Isabel Miranda, Joana Valente, Ana Margarida Costa, Myriam Lopes, and Carlos Borrego

Abstract

The quality of the air we breathe is still a major concern to human health. Notwithstanding the air pollution mitigation efforts that have been pursued since the last half of the twentieth century, the World Health Organization estimates that more than two million premature deaths each year can be attributed to the effects of urban outdoor air pollution and indoor air pollution. This chapter addresses the evolution of knowledge on the relationship between air pollution and human health, since the first records until nowadays. It also reviews the current approaches to do health impact assessment and the common air pollution – health indicators. A particular case study based on a chain of events, from emissions to the atmosphere until health, passing through exposure and inhaled dose, illustrates how this approach can be explored, providing useful and concrete information.

Keywords

Air pollution • Human health • Air emissions • Air quality modelling • Exposure • Inhaled dose

1 Introduction

Air is a natural resource from which the quality of human health depends nowadays and since the beginning of our history. It is a common belief that before the Industrial Revolution, our planet's atmosphere was still unattained by human-made pollutants. Recent studies (e.g. Fuller et al. 2011; Sapart et al. 2012), however, indicate that human activity, notably metallurgy and large-scale agriculture starting around 100 B.C., emitted enough methane gas to have had an impact on the methane signature of the entire atmosphere. According to Sapart et al. (2012), the ancient Romans kept domesticated livestock (cows, sheep and goats) which excrete methane gas, a by-product of digestion, and around the same time, in China, the Han dynasty expanded its rice fields, which harbour methane-producing bacteria. Also, blacksmiths in both empires produced methane gas when they burned wood to fashion metal weapons.

Although these signal that human activity could have had a contribution to air quality changes since hundreds of centuries ago, there is no registered information about their potential effects on human health. Brimblecombe (2011), however, in his history of air pollution since medieval times argues that smoke from fires within huts would have filled the whole space already, causing respiratory problems to cavemen, and that Seneca, Emperor Nero's tutor, suffered life-long ill health and was frequently advised by his physicians to leave Rome because of the oppressive fumes. There are records of complaints against smoke in the air in the thirteenth century when coal was used in London (Brimblecombe 2011), and Halliday (Halliday 1961) mentions the royal proclamation

A.I. Miranda (✉) • J. Valente • M. Lopes • C. Borrego
Centre for Environmental and Marine Studies (CESAM), Department of Environment and Planning, University of Aveiro, 3810-193 Aveiro, Portugal
e-mail: miranda@ua.pt

A.M. Costa
Institute of Environment and Development, Campus Universitário, 3810-193 Aveiro, Portugal

G. Cao and R. Orrù (eds.), *Current Environmental Issues and Challenges*,
DOI 10.1007/978-94-017-8777-2_1,

prohibiting the use of coal in London at the beginning of the fourteenth century.

Nevertheless, it was during the last century that clearer evidences of air pollution effects on human health came to the general public awareness with several well-known events of air pollution, such as the Meuse Valley smog in 1930, the Donora smog in 1948 or the Great London smog in 1952. Hedley (2009) reports that the dense fog that affected the Meuse Valley in Belgium, in December 1930, was associated with laryngeal symptoms, chest pain, coughing and breathlessness. Some patients showed signs of pulmonary oedema. Overall 60 deaths were attributed to the episode. According to this author (Hedley 2009), the health impacts of the Donora, Pennsylvania, poisonous cloud include 70 deaths and several hundreds with long-term respiratory and cardiovascular damage. The 1952 Great London smog is probably the best known and most catastrophic air pollution episode with about 4,000 deaths in 5 days, because of lung infections and heart disease, caused by high levels of particulates and sulphur dioxide (SO_2).

Since these air pollution events, particularly the Great London smog, several air pollution mitigation actions have been pursued, namely, the United Kingdom (1956), the United States of America (1963) and the New Zealand (1972) Clean Air Acts. The European Union has also been working to improve the quality of the air since the early 1970s by controlling emissions of harmful substances into the atmosphere, improving fuel quality and integrating environmental protection requirements into the transport and energy sectors, as well as by adopting an integrated strategy to tackle air pollution and to protect against its effects on human health and the environment – the Clean Air for Europe (CAFE) Programme. It is an indisputable fact that much has been done in the last decades to improve the quality of the air we breathe and live in. Policies, technology and increasing public awareness have taken us to an unprecedented level of protection, but in spite of the emission reduction achieved during the last decade, the World Health Organization (WHO) still estimates that more than two million premature deaths each year can be attributed to the effects of urban outdoor air pollution and indoor air pollution.

The main purpose of this chapter is to provide an overview of the current knowledge on air pollution and health effect assessment and to describe a particular case study that illustrates how the effects of air pollution on human health can be studied based on a chain of events, from emissions to the atmosphere until health, passing through exposure and dose.

2 Recent Developments on the Assessment of Health Effects of Air Pollution

In the late 1980s, research on the health effects of air pollution underwent a transformation with greater insights into the biological action of pollutants on animal and human cells, together with clinical and population studies of health outcomes and new methods for statistical analysis leading to a marked increase in the quality and quantity of reports about the influence of air pollutants on health, healthcare utilisation and premature deaths (Hedley 2009).

Nowadays knowledge on health effects of air pollution is mainly based on epidemiological study designs that include time-series, case-crossover, panel, cohort and birth outcome approaches. According to Ren and Tong (2008), who reviewed the major epidemiological studies of ambient air pollution on morbidity and mortality over the last two decades, many time-series, case-crossover and panel studies have shown that there are consistent short-term effects of air pollution on health outcomes (hospital visits or deaths). For instance, there is a general agreement (Ren and Tong 2008) about an increase of all-cause daily mortality and hospital admissions for asthma and chronic obstructive pulmonary disease (COPD) for each 10 $\mu g \cdot m^{-3}$ increase in particulate matter with an equivalent aerodynamic diameter lesser than 10 μm (PM10). Moreover, exposure to particulate matter with an equivalent aerodynamic diameter lesser than 2.5 μm (PM2.5) is associated with an increase in heart failure and in hospital admissions from heart failure on the same day. Ren and Tong (2008) also mention an association between ozone concentration and mortality with a 10-ppb increase in the previous week's ozone associated with increases in daily mortality and cardiovascular and respiratory mortality. Brunekreef and Holgate (2002) report that associations between nitrogen dioxide (NO_2) and mortality were found, but these were sensitive to adjustment for black smoke, suggesting that the nitrogen dioxide represented a mixture of traffic-related air pollution. Ren and Tong (2008) also realised that although time-series studies have shown that day-to-day variations in air pollutant concentrations are associated with daily deaths and hospital admissions, it is still unclear how many days, weeks or months of air pollution have brought such events forward.

Hedley (2009) describes the burden of ill health and the risk of future illness as a pyramid (Fig. 1) where many individuals experience the least serious, most common effects shown at the bottom of the pyramid, and fewer individuals experience the more severe effects such as hospitalisation or death.

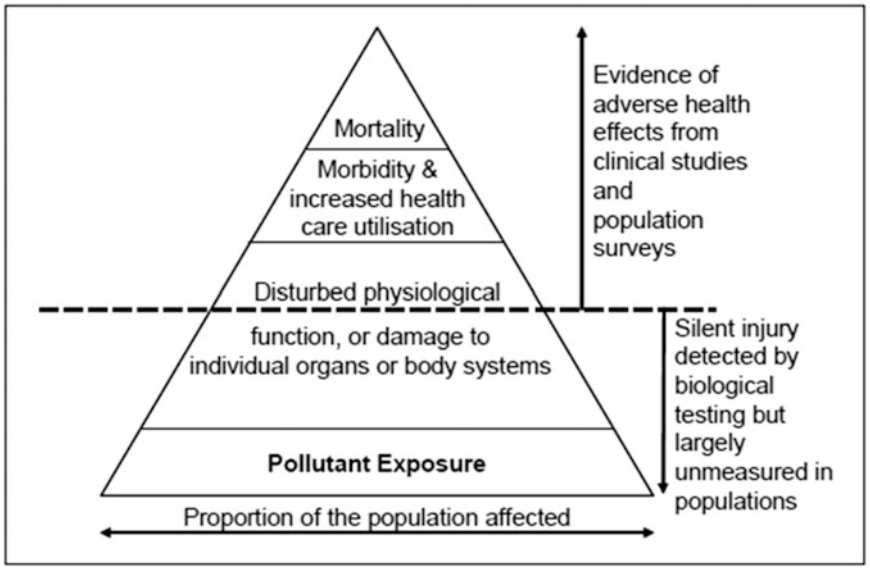

Fig. 1 The burden of ill health and the risk of future illness can be represented as a pyramid (Hedley 2009)

Table 1 Outdoor (WHO 2006) and indoor (WHO 2010) air quality guideline values established by the World Health Organization

		Air quality guideline ($\mu g \cdot m^{-3}$)	
Pollutant	Averaging time	Outdoor	Indoor
PM10	24 h	50	
	1 year	20	
PM2.5	24 h	25	
	1 year	10	
NO_2	1 h	200	200
	1 year	40	40
SO_2	10 min	500	
	24 h	20	
CO	15 min	100,000	100,000
	30 min	60,000	
	1 h	30,000	35,000
	8 h	10,000	10,000
	24 h		7,000
O_3	8 h, daily maximum	100	

Based on a systematic review of literature on adverse health effects of air pollution, the WHO published the first edition of the Air Quality Guidelines for Europe in 1987. Since then, updates were produced, and in 2005 the WHO published a new document, which is intended to be relevant and applicable worldwide and takes into consideration large regional inequalities in exposures to air pollution (Krzyzanowski and Cohen 2008). It recommends guideline levels for particulate matter, ozone (O_3), nitrogen dioxide and sulphur dioxide, as well as the set of interim targets for these pollutants' concentrations, encouraging gradual improvement of air quality and reduction of health impacts of the pollution (WHO 2006). Table 1 contains the updated WHO air quality guideline values, which are based on the now extensive body of scientific evidence relating to air pollution and its health consequences, including epidemiology, clinical studies and toxicological experiments.

An increasing range of adverse health effects has been linked to air pollution and at ever-lower air pollutant concentrations. This is especially true for airborne particulate matter. New studies use more refined methods and more subtle but sensitive indicators of effects, such as physiological measures (e.g. changes in lung function, inflammation markers). Therefore, the updated guidelines are based on these sensitive indicators as well as the most critical population health indicators such as mortality and unscheduled hospitalisations.

However, concern focuses not only on ambient air quality but also on indoor air quality in home and at workplace. In fact, the highest air pollution exposures occur in the indoor environment where people spend 80–90 % of their time, and the percentage is still overall higher for some specific groups such as children, elderly, disabled or sick people (EC 2006; WHO 2010). Some of the worst and most distressing respiratory problems triggered by air pollution are among children, since they can be particularly sensitive to environmental stresses (EEA 2005). Children, as sensitive human beings, can be regarded as 'biomarkers' for environmental threats, not only because they are more at risk but because they can also provide early warnings of hazards to others, as well as being effective points of intervention for the prevention of disease in their later lives (EEA 1999). In this sense, the WHO (2010) recently published guidelines for the protection of public health from risks due to a number of chemicals commonly present in indoor air (see Table 1). The substances considered, i.e. benzene, carbon monoxide (CO), formaldehyde, naphthalene, nitrogen dioxide, polycyclic aromatic hydrocarbons (especially benzo[a]pyrene),

Fig. 2 Chain of events related to the health effects of air pollution (Adapted from Hertel et al. 2001)

radon, trichloroethylene and tetrachloroethylene, have indoor sources and are known in respect of their hazardousness to health and are often found indoors in concentrations of health concern.

3 From Air Emissions to Health: A Chain of Events

Health effects of air pollution are a result of a chain of events, which include release of pollution, atmospheric transport, dispersion and transformation, and uptake of pollutants before the health effects take place (Fig. 2). The conditions for these events vary considerably and have to be accounted for, in order to ensure a proper assessment (Hertel et al. 2001).

Human exposure can be defined as an event that occurs when an individual is in contact with a pollutant. The European legislation recognises and recommends using human exposure as an assessment indicator of health impact. To have exposure, it is required that the concentration of a pollutant in a certain location should not be zero and, simultaneously, an individual be present in that location. Exposure does not necessarily imply a pollutant inhalation or ingestion; it is only related to the pollutant levels in the air. On the other hand, the dose concept is used when a pollutant crosses the physical barrier (body). When analysing the exposure to atmospheric pollutants, the inhaled dose is referred as the amount of pollutants inhaled by an individual in a determined time.

3.1 Emissions

Nowadays urban areas are considered major sources of air pollution. In the past, urban air pollution was considered a local problem mainly associated with domestic heating and industrial emissions, which are now controllable to a great extent. Despite significant improvements in fuel and engine technology, present-day urban environments are mostly dominated by traffic emissions (Fenger 1999; Colvile et al. 2001). The combination of traffic emissions and densely packed buildings flanking narrow streets (street canyons) that characterise most of the urban environments is responsible for complex air pollutant concentration patterns including high peak concentrations, commonly known as hot spots. This is often the case near busy traffic axis in city centres, where urban building arrangements and microclimate may contribute to the creation of poor air dispersion conditions at street level.

Streets are in fact one of the most important urban elements, where population and traffic density are relatively high and where human exposure to hazardous pollutants is expected to frequently occur (Xiaomin et al. 2006). Particulate matter (PM10 and PM2.5) and nitrogen oxides (NO_x) are considered as the most important traffic-related pollutants with known acute and chronic effects on human health (Curtis et al. 2006).

Moreover, due to traffic and industrial activities, ambient air pollution, in the absence of smoking, is a major source of pollutants in indoor air. Outdoor pollutants come into the building through the ventilation system or by infiltration (building envelop permeability) (Götschi et al. 2002; Liao et al. 2004; EC 2006). Local peak concentrations in residences can also be originated from specific sources, e.g. gas stoves, wood stoves, fireplaces, kerosene heaters and candles. In offices, electrostatic equipment (photocopying machines and laser prints) should be accounted as major sources of NO_2.

3.2 Air Concentrations

Air quality data from fixed monitoring sites are frequently used as an approach to characterise outdoor concentrations in urban areas. Nevertheless, these local measurements cannot reflect the complex temporal and spatial distribution of pollutant concentrations observed, and thus depending on the location and dimension of the region to be studied, monitoring data may not be sufficient to characterise pollutant levels or to perform population exposure estimations. Numerical models can complement measured concentration data because they are able to provide detailed information on atmospheric flow and pollutant transport using meteorological and emission data inputs. They simulate the changes of pollutant concentrations in the air using a set of mathematical equations characterising the chemical and physical processes in the atmosphere. In this sense, air quality models can be used as important tools for the assessment of exposure to atmospheric pollutants.

There are several types of air quality models. Dispersion models are usually simple; they estimate the concentration of a given pollutant at specified ground-level receptors,

considering only the dispersion and not the chemical transformation processes. They simulate the atmospheric transport and the turbulent atmospheric diffusion, and some are also able to simulate the ground deposition. The most simple dispersion models use the Gaussian approach.

Recently, and with the continuous increase of hardware capabilities and the optimisation of numerical methods, computational fluid dynamics (CFD) modelling has become an attractive tool to predict flow and concentration fields near buildings. CFD modelling is a general term used to describe the analysis of systems involving fluid flow, heat transfer and associated phenomena (e.g. chemical reactions) by means of computer-based numerical methods. CFDs are the only models that allow a detailed estimation of spatial and temporal distribution of air pollutants in complex urban areas, contributing to the identification of sensitive urban areas in terms of air quality and with potential harmful effects to human health.

Chemical transport models simulate the changes of pollutants in the atmosphere using a set of mathematical equations characterising the chemical and physical processes in the atmosphere. Most of the current chemical aerosol models have adopted the three-dimensional Eulerian grid modelling mainly because of its ability to better and more fully characterise physical processes in the atmosphere and predict the species concentrations throughout the entire model domain.

Once the outdoor concentration has been calculated by air quality models, the indoor pollutant concentration can be modelled based on an understanding of the ways in which indoor air becomes exchanged with outdoor air, together with the deposition or decay dynamics of the pollutants and with indoor emission source rate characterisation. Several methodologies exist to estimate indoor air pollution concentrations from outdoor modelled concentrations. These include a variety of empirical approaches based on statistical evaluation of test data and a least squares regression analysis, deterministic models based on a pollutant mass balance around a particular indoor air volume or a combination of both approaches. Most of the currently available studies (e.g. Monn 2001; Chau et al. 2002; Wu et al. 2005; Borrego et al. 2006) are based on experimental data, resulting from measurements of outdoor and indoor concentrations for different microenvironments in order to establish a relation between indoor and outdoor (I/O) concentrations. There are several parameters affecting the I/O ratio, such as the penetration coefficient, the deposition rate and the air exchange rate between the indoor and the outdoor air, and those are directly dependent on the types of ventilation used (natural ventilation, mechanical ventilation or both) (Liao et al. 2004). Ventilation is therefore a major driver of air quality in indoor environments since it, on one hand, promotes the dilution of concentrations from indoor sources and, on the other hand, works as a transport mechanism for outside pollutants be brought inside.

3.3 Exposure

Exposure studies can be carried out with the aim of obtaining estimates of the exposure of the individual (personal exposure) or for a larger population group (population exposure), through direct or indirect methods. Direct methods are measurements made by personal portable exposure monitors or biological markers. These are, however, invasive and expensive techniques. The personal exposure monitoring devices that people carry with them must be lightweight, silent and highly autonomous, and still 1 week is about the maximum time that any population representative sample of individuals will comply with personal exposure measurements. On the other side, biological markers are indicators of changes or events in human biological systems. For example, a metabolite of some exogenous substance found in a person's blood or urine might be considered a marker of the person's exposure to that substance in the environment.

In indirect methods, the exposure is determined by combining information about the time spent in specific locations, the microenvironments, with the pollutants concentrations at these same places. The microenvironment can be the interior of a car, inside a house, inside an office or school or outdoors. A constraint for using the indirect methods is that the residence time of the person (termed the time-activity pattern) needs to be known together with the pollution concentrations in each of the microenvironments at the time when the person is present.

In some cases, models have been developed specifically for exposure modelling based in a time-microenvironment-activity concept. This modelling approach calculates exposure as the product of the concentration in a microenvironment and the time spent in that microenvironment. Thus, total exposure is the sum of the exposures in all microenvironments during the time of interest, as expressed by Hertel et al. (2001):

$$E_i = \sum_j^J C_j t_{ij} \qquad \left[\mathrm{M} \cdot \mathrm{L}^{-3} \cdot \mathrm{T}\right] \tag{1}$$

where E_i is the total exposure for person i over the specified period of time, C_j is the pollutant concentration in microenvironment j, t_{ij} is the residence time of the person i in microenvironment j, and J is the total number of microenvironments.

Table 2 Ventilation rate for different activity levels and different individual characteristics

	Ventilation rate ($m^3 \cdot min^{-1}$)						
Level of physical activity	Child	Girl	Boy	Adult woman	Adult man	Woman (+65)	Man (+65)
Rest	0.0045	0.0053	0.0063	0.0050	0.0067	0.0050	0.0050
Sedentary	0.0048	0.0063	0.0075	0.0083	0.0100	0.0067	0.0083
Light	0.0110	0.0110	0.0130	0.0217	0.0283	0.0200	0.0230
Moderate	0.0220	0.0167	0.0250	0.0333	0.0417	0.0300	0.0350
High	0.0440	0.0530	0.0630	0.0533	0.0700	0.0500	0.0583

3.4 Dose

The concentration of a pollutant at which effects are first observed depends upon the level of sensitivity of the individual as well as the dose delivered to the respiratory tract. The inhaled dose, in turn, is a function of the air concentration, the minute ventilation and the duration of exposure. This can be expressed as

$$\text{Dose}_i = C_j \, t_{ij} \, V_{ij} \tag{2}$$

where V_{ij} is the person ventilation rate i in the microenvironment j.

Therefore, one important determinant of human exposure to pollutants via inhalation of contaminants in air is a person's ventilation rate, the volume of air inhaled in a specified time period (e.g. litres per minute, hour or day).

Individuals performing strenuous activity (higher minute ventilation) for several hours are likely to respond to lower concentrations than when exposed at rest (lower minute ventilation) for a shorter time. For instance, for the effects of exposure to ozone, the USEPA (2009) mentions:

- An average young adult playing an active sport such as soccer or full-court basketball outdoors for 2 h would be expected to experience small to moderate lung function and symptom effects as well as lung injury and inflammation following exposure to 120 ppb ozone.
- If the same average young adult is at rest outdoors for the 2 h, such effects would not be expected until exposures reach 300–400 ppb.
- An average outdoor labourer doing intermittent work might experience similar small to moderate lung function and symptom effects as well as lung injury and inflammation following an 8-h exposure to 60–70 ppb ozone.

More sensitive individuals will experience such effects at lower concentrations, while less sensitive individuals will experience these effects only at higher concentrations. Moreover, ventilation rates vary with several characteristics of the individuals, such as age, gender, body weight, health status and physical activity. Table 2 contains ventilation rates based on the USEPA (2009) report.

It is obvious from the data presented in Table 2 that individuals exposed to the same levels of air pollution can inhale different doses and hence present different health effects.

3.5 Health Effects and Indicators

Hedley (2009) describes several injuries resulting from the exposure to air pollution, such as cardiovascular disease (e.g. atherosclerosis, heart attacks and arrhythmia) and respiratory disease (e.g. initiation of exacerbation of asthma, lower respiratory tract inflammation and infection causing bronchitis and pneumonia). Exposure to air pollutants cause a specific decline in lung function, which can, for example, be measured as a test of the forced expiratory volume of air achieved in one second (FEV1).

Exposure to air pollution is thus associated with an increase of risks to diverse health effects, decreasing quality of life which may be translated in terms of health indicators. When different health effects are considered, it is important to distinguish between acute effects related with short-term exposures and chronic effects resulting from long-term exposure. There are several indicators to express the change in population health status due to exposure to air pollution. Bouland et al. (2013) identify premature mortality, with different variations, as the most used common indicator and morbidity, life expectancy and recently more and more popular disability-adjusted life year (DALY) as other common indicators.

According to Bouland et al. (2013), the mortality indicator measures the changes in the mortality rates due to exposure to environmental stressor(s), in particular, an air pollutant. It can be expressed as premature deaths, avoidable deaths, attributed cases of death, additional mortality or death postponed.

The morbidity indicator estimates the changes in new or existing diseases (e.g. pneumonia cases, cardiovascular diseases, respiratory diseases) in the target population. Morbidity cases are commonly divided into incidence and prevalence. Incidence means new cases of disease in a given period of time, for example, new pneumonia cases per year. Prevalence describes the proportion of population that has a particular disease.

The indicator years of life lost (YOLL) estimates the potential life years that were lost due to premature mortality. Other names for this indicator are, e.g. years of potential life lost (YPLL) or potential years of life lost (PYLL). Calculation of YOLL varies from simple comparison of the age of death, with the expected life expectancy of a person with that age, to multidimensional life table model that calculates

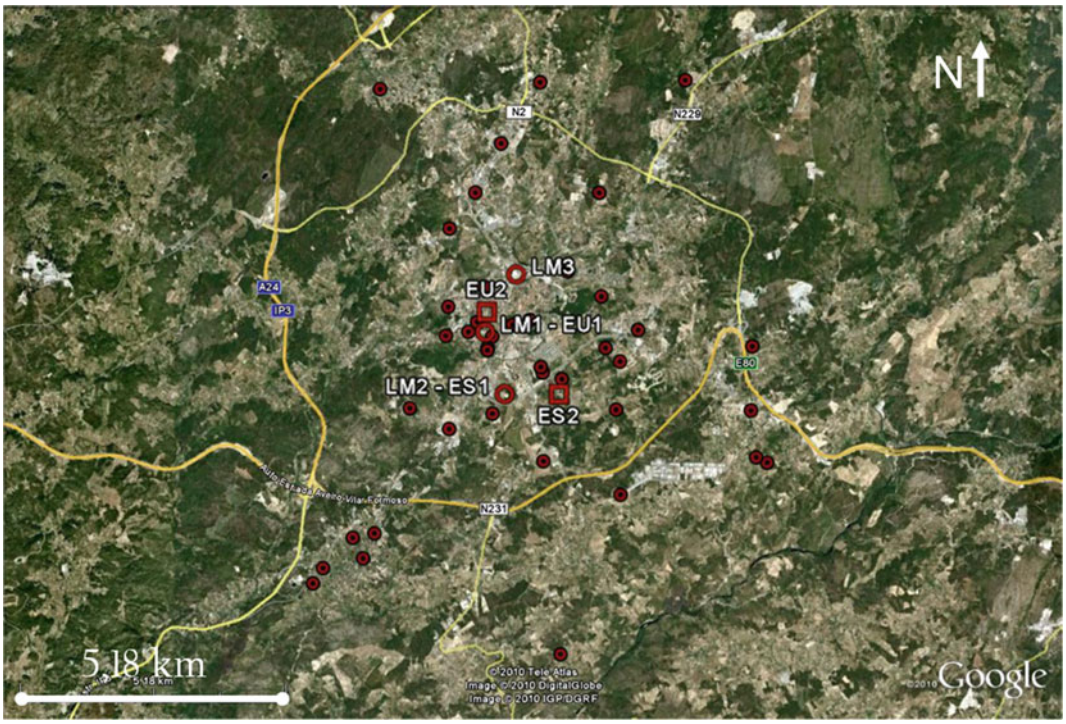

Fig. 3 Aerial photograph of the study area of Viseu, with the location of the four selected elementary schools (ES1, ES2, EU1 and EU2), the three mobile laboratories (LM1, LM2 and LM3) and the children houses (●)

YOLL and other indicators. YOLL is also one of two components of disability-adjusted life year (DALY), which is a measure of disease burden.

4 Case Study: The SAUDAR Project

SAUDAR is the Portuguese acronym of the project "the Health and the Air we breathe" that had as main goals to study the relation between air quality (indoor and outdoor) and human health in an urban area presently with no considerable air pollution problems – Viseu. Viseu is a town located in the interior of Portugal with approximately 93,000 inhabitants and an area of 507 km^2. Despite the lack of fixed monitoring sites, past field campaigns (1990, 1994, 1995, 2002) using a mobile air quality station located in the centre of the town show the fulfilment of air quality standards for the measured concentrations of NO_2, SO_2, O_3 and benzene (Borrego et al. 2007). Nevertheless, these past monitoring campaigns may not be considered representative of the air quality levels in all urban area of Viseu.

To study the relation between air quality and human health, a group of children was selected. Children represent one of the most vulnerable population groups, spending more time outdoors and having more immature lungs and higher ratios of ventilation rate to body weight than adults. Particularly, special attention was given to children with respiratory problems, as asthma, because there is a clear association between epidemics of asthma attacks in children and local peaks of air pollution (EEA 2005). In this sense, a large survey was made in four elementary schools located in the town of Viseu to identify children with respiratory problems, such as asthma (Martins et al. 2012).

A group of 51 children with asthma, attending 4 elementary schools in the town, were selected as a study case. Figure 3 presents an aerial photograph of the study area with the location of the four elementary schools, two in the town centre and the other two in the suburban area of Viseu. These 51 children live, study and have their activities within the town, providing the main criteria for their selection.

Experimental measuring campaigns for two winter and two summer periods were conducted, which comprised traffic counting for the main roads, indoor and outdoor air quality measurements in houses and schools attended by the group of the selected children with respiratory problems, air exchange rate measurements and children health examinations. Besides the measured data and their analysis, SAUDAR project also relied on a modelling approach. Despite the several pollutants addressed by the SAUDAR project, PM10 and NO_2 are specifically described here because of their strong contribution to health effects in urban environments.

4.1 Emissions

To study the main emission sources in the area of Viseu, the national inventory report was used (APA 2008). The inventory takes into account annual emissions from line sources (streets and highways), area sources (industrial and residential combustion, solvents and others) and large point sources. These annual emission data for each pollutant activity were spatially disaggregated in order to obtain the resolution required for the domain of study. The disaggregation was made in two steps. First, emissions were estimated at municipality level using adequate statistical indicators for each pollutant activity (e.g. types of fuel consumption) and then distributed according to the population density (Monteiro et al. 2007). Time disaggregation was obtained by application of monthly, weekly and hourly profiles from the University of Stuttgart (GENEMIS 1994).

4.2 Air Concentrations

The air quality assessment in the town of Viseu took place during the four mentioned periods. The outdoor and indoor concentrations of PM10 and NO_2 over Viseu were obtained based on measurements and modelling tools.

4.2.1 Air Quality Monitoring

The outdoor air concentrations of NO_2 and PM10 were measured continuously by three mobile laboratories: one in the town centre, one in a town centre school courtyard and another in a suburban school courtyard. NO_2 concentrations (5 days mean) were also measured using diffusive samplers in 20 points distributed over the town of Viseu, in an area of approximately 40 km^2. Moreover, NO_2 measurements (5 days mean) were carried out in the courtyard and classrooms of the four schools and in the sleeping room of the children's houses using diffusive samplers. All parents of the children included in the medical visits were asked to participate in the air quality studies. Additionally, at the schools, ambient and indoor PM10 values were measured by gravimetric methods (24-h mean).

Figure 3 shows the location of the four schools, the three mobile laboratories and the children houses.

4.2.2 Air Quality Modelling

The Eulerian air quality model CHIMERE (Vautard et al. 2001) was applied to estimate PM10 and NO_2 concentration levels over the town of Viseu during both winter and summer campaigns. Monteiro et al. (2005, 2007) present some examples of successful applications of this system to Portugal. The model was applied first to Portugal, then to the northern/central region of Portugal and finally to Viseu region using a one-way nesting technique that allowed increasing the spatial resolution of the simulation from 9 km × 9 km, to 3 km × 3 km and 1 km × 1 km, respectively. Figure 4 shows the nested domains used to better simulate the air quality in Viseu.

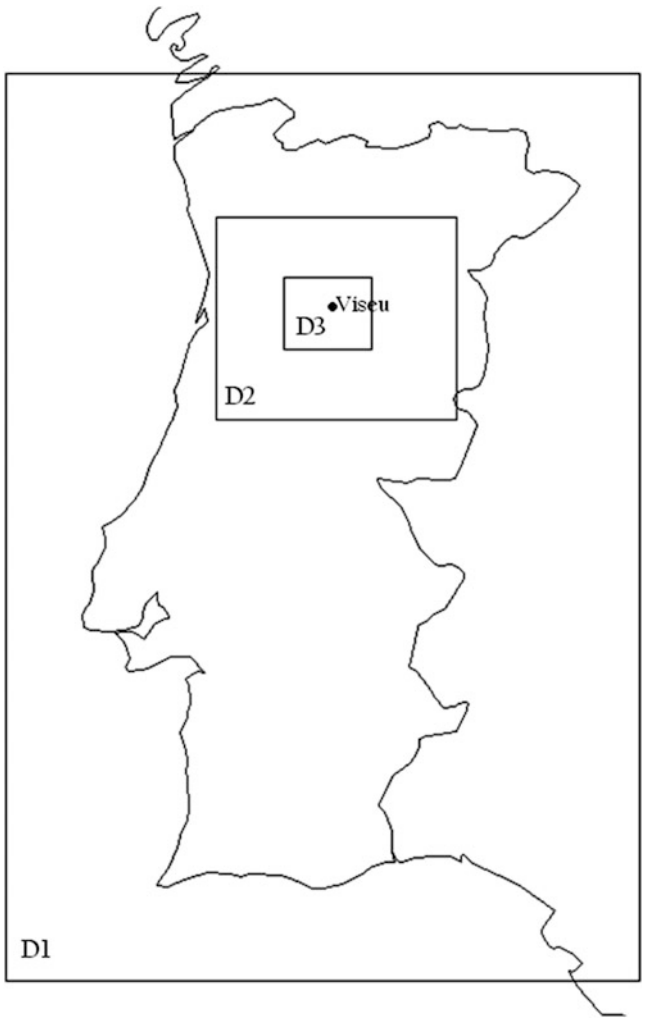

Fig. 4 Air quality modelling domains

This model needs specific input data to simulate PM10 and NO_2 levels in the town of Viseu, namely, meteorological data and air emissions. Meteorological data were provided by the mesoscale meteorological model MM5 (Dudhia 1993). Emission data were obtained from the Portuguese emission inventory, which was spatially downscaled to the sub-municipality level for each activity sector (traffic, solvents, industrial and residential combustion, and others), as previously described.

Hourly outdoor 3D fields of PM10 and NO_2, for 1 km model resolution, were simulated for both winter and summer

periods. Results were compared to measurement, and because of the weak performance of the model simulating PM10, a bias correction technique (Borrego et al. 2011) was applied, resulting in a considerable improvement of the simulation. PM10 is in fact a pollutant with emissions greatly uncertain. At winter time, there is the contribution of fireplaces that was not included in the emission inventory. Moreover, resuspension dust at summer time can also be a non-considered source of PM10. Table 3 presents the final statistical indicators of the model performance, namely, the correlation coefficient (r), the mean square error (MSE) and the bias.

Even with some drawbacks to improve, namely, concerning the correlation coefficients for PM10 and NO_2 for the 2007 campaigns, as shown by Table 3 values, the model performance is adequate and obtained data permit to trust the modelling results and to understand its capabilities.

Ten distinct microenvironments were taken into account in the modelling framework corresponding to the main locations where the selected children spend their time during the winter and summer campaigns: home indoor (homein) and home outdoor (homeout); school indoor (schoolin) and school outdoor (schoolout); sport indoor (sportin) and sport outdoor (sportout); after school activity centre (atl); vehicle (car); other outdoors (otherout); and other indoors (otherin). The air quality of each microenvironment was characterised using measured data and/or modelled results. In the absence of indoor data, adequate indoor/outdoor ratios from bibliography (Baek et al. 1997; USEPA 1997; Monn 2001; Gulliver and Briggs 2004; Wu et al. 2005) were used.

Table 3 Statistical indicators of the air quality performance simulating PM10 and NO_2 hourly values after the bias correction technique, for the four periods of campaign

	r (−)	MSE (μg·m^{-3})	BIAS (μg·m^{-3})
Jan06			
PM10	0.68	23.3	1.6
NO_2	0.73	8.,0	0.2
Jun06			
PM10	0.61	11.2	3.0
NO_2	0.62	9.2	2.4
Jan07			
PM10	0.52	31.9	0.4
NO_2	0.69	13.5	0.9
Jun07			
PM10	0.50	10.9	0.5
NO_2	0.49	7.2	0.3

4.3 Exposure

PM10 and NO_2 concentration matrixes were combined with information on the time-activity profiles of the children within the ten microenvironments (Fig. 5). These profiles characterise the movement of the children within the study domain during 1 day with hourly resolution in four distinct periods: winter/weekday, winter/weekend, summer/weekday and summer/weekend. In this sense, 3D matrixes of microenvironment/activity profiles were created for a typical weekday and weekend of both winter and summer campaigns.

At morning children were mainly at school and in the afternoon in an after school activity centre or at home. Durante winter outdoor activities are restricted to the school break time if it is not raining, while at summer time several children play outside between the end of study activities and dinner. Generally children go to school by private car.

The individual exposure of the SAUDAR children to PM10 and NO_2 was estimated for the winter and summer periods of the SAUDAR experimental campaigns. Figure 6 shows the average weekly exposure to NO_2 and PM10 during the four study periods.

Estimated exposure was generally higher at winter periods for both NO_2 and PM10. These exposure values

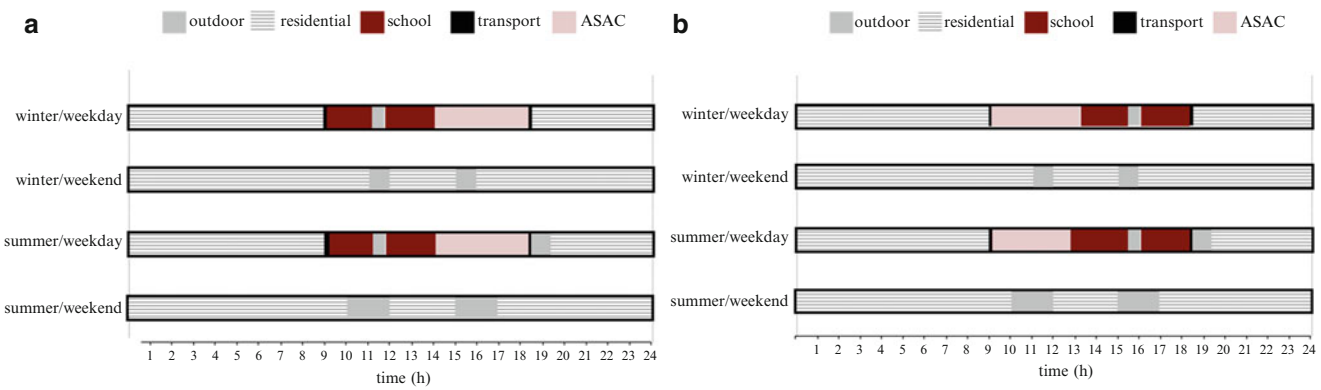

Fig. 5 Typical time-activity profiles of the selected children

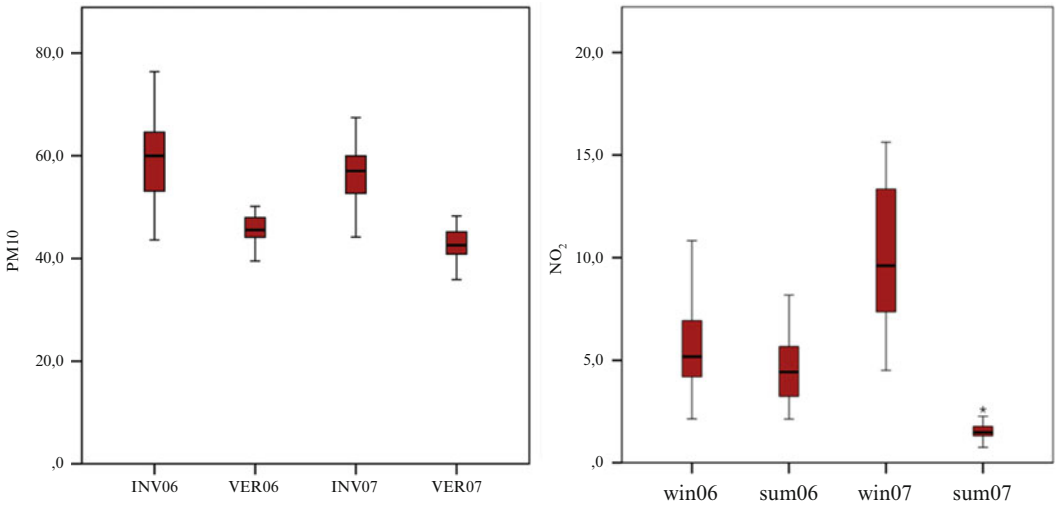

Fig. 6 Minimum, percentiles 25 and 75 and maximum exposure values (μg·m^{-3}·week), estimated for each studied period

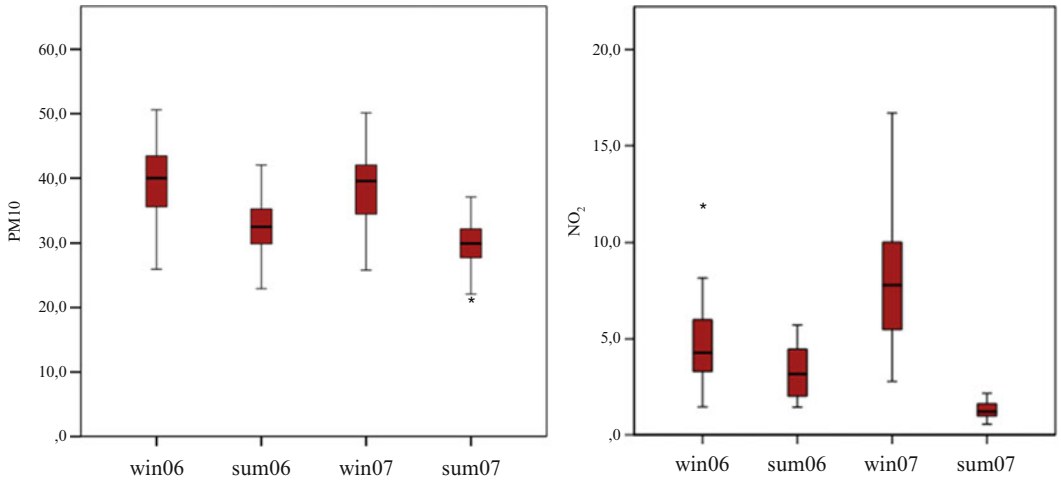

Fig. 7 Minimum, percentiles 25 and 75 and maximum dose values (μg·min^{-1}·week), estimated for each studied period

are going to be used to go further estimating the dose inhaled by the children and then the identified health effects.

4.4 Dose

The activity profiles of the SAUDAR children in which microenvironment were crossed with ventilation rates for five levels of physical activity (rest, sedentary, light, moderate and high) to deliver the inhaled dose. Figure 7 presents the weekly averaged dose of PM10 and NO_2 for the winter and summer periods.

These results are expressed in μg·min^{-1}·week, which means the average mass of pollutant inhaled per minute, by the children, during 1 week. Trying to better understand the relevance of the parameters exposure and dose independently from time, two factors were defined: exposure/time (ET) and inhaled dose/time (DT). These factors represent the ratio between the exposure and the inhaled dose, respectively, in each microenvironment, and the time in the same microenvironment:

$$\mathrm{ET} = \frac{e_i/e_T}{t_i/t_T} \quad \mathrm{DT} = \frac{d_i/d_T}{t_i/t_T} \tag{3}$$

where e_i is the exposure value in microenvironment i, e_T is the total exposure, d_i is the inhaled dose in microenvironment i, d_T is the total inhaled dose, t_i is the time spent in microenvironment i, and t_T is the total time.

A unit value of ET means that a specific microenvironment equally contributes for the exposure to a given pollutant and for the duration of this exposure. Figure 8 presents ET and DT values for PM10, based on averages for the four study periods.

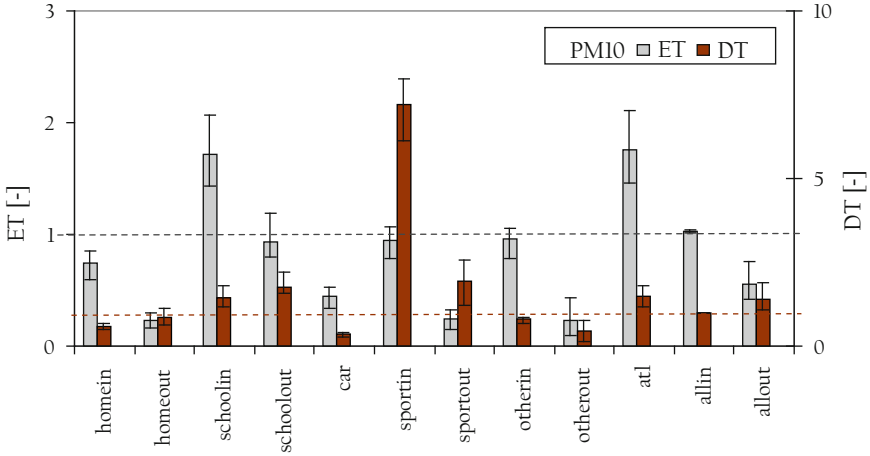

Fig. 8 ET and DT ratios for PM10 (*dotted lines* indicate ET = 1 and DT = 1)

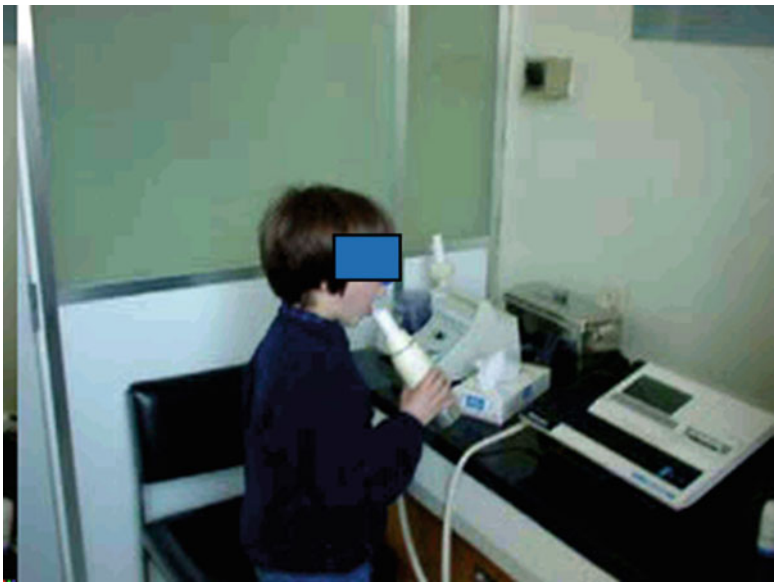

Fig. 9 Child doing the expiratory test

The most contributor microenvironments to PM10 exposure are indoor school and ASAC with ET values higher than 1.7, which represents one contribution to exposure 70 % larger than to the time spent. This result is in agreement with the high PM10 values estimated in schools. On the other hand, when analysing DT values, microenvironments with a high level of physical activity (sportin, sportout and schoolout) are highlighted because they combine high concentration levels with high ventilation rates. Thus, in spite of the higher contribution of indoor schools to exposure, the time spent in a sportin microenvironment could be more prejudicial to health.

4.5 Effect

Health effects can be studied based on dose-response relationships established by the simultaneous determination of individual exposure and associated health effects. Martins et al. (2012) performed medical tests to the SAUDAR children, who attended the local hospital where a medical team carried out several examinations to evaluate their respiratory function, namely, pH, NO, CO, % carboxyhaemoglobin (COHb) measurements on the breath condensate, broncodilation test with spirometry, urinary cotinine measurements, forced expiratory volume in one second (FEV1), forced vital capacity (FVC), ratio FEV1/FVC, peak expiratory flow (PEF), flow at 50 % of FVC (F50), forced expiratory flow between 25 and 75 % of FVC (F25) and mid-expiratory flow rate (MEF). These health indicators allowed identifying short-term cause-effect relations as a contribution to the assessment of air pollution impacts on human health. Figure 9 shows one child doing the expiratory test.

An exploratory analysis of potentially interesting variables was done aiming to find a relation between exposure, dose

and health effects. Chi-square test was used to compare proportions and Friedman's test to compare pollutants, weather conditions, and spirometric and inflammation outcomes along the four campaigns (Martins et al. 2012). Results revealed that the increasing mean personal exposure to PM10 in the studied week was associated with a trend of deterioration of airways, reaching significance with a decrease of the FEV1 and increase of ΔFEV1. Associations were found also for an increase of NO_2 exposure: a decrease of FEV1, FEV1/FVC, F25, pH on EBC and an increase of ΔFEV1. Exposure to PM10 as estimated using a function of both concentrations and daily activity patterns was related to lung function decline, even in a non-industrial town like Viseu (Martins et al. 2012).

5 Final Comments

The effects of air pollution on health are dependent on several factors. Apart from the concentrations and chemical properties of the pollutants, the person's age and general state of health, and the duration of exposure, factors such as the weather condition and the distance from the emission sources also affect the nature and extent of the health effects observed. Health impacts may be greater for individuals and groups that are more susceptible, more exposed or otherwise more vulnerable.

The case study here presented is based on a methodology that fills in the gap between air pollutant emissions and the inhaled dose and results from the cooperation between different fields of research toward a healthier life.

Regarding wheezing children, results suggest a relation between total exposure to the assessed air pollutants, namely, PM10 and NO_2, in various environments and airway changes. Attention should be dedicated to air quality in houses and schools in childhood as most part of the children's time is spent in these environments, but also to microenvironments where the ventilation rate is higher, such as sport spaces.

Future research areas to clarify the links between air pollution and respiratory effects should include a control group and a multipollution approach. New data have shown that multipollution is an important phenomenon to be taken into account in the assessment of health effect of air quality. Better understanding of population vulnerability can improve the scientific basis to assess risks and develop policies or other health protection initiatives to reduce the impacts of air pollution.

Acknowledgements The authors would like to acknowledge the financial support of the 3rd European Framework Programme and the Portuguese Ministry of Science, Technology and Higher Education, through the Foundation for Science and Technology (FCT), for the postdoc grant of J. Valente (SFRH/BPD/78933/2011). SAUDAR study was supported by the Fundação Calouste Gulbenkian. This work was supported by European Funds through COMPETE and by National Funds through the Portuguese Science Foundation (FCT) within project PEst-C/MAR/LA0017/2013.

References

Agência Portuguesa do Ambiente APA.: Alocação espacial de emissões em 2005: gases acidificantes, eutrofizantes e precursores de ozono; partículas; metais pesados; gases com efeito de estufa. Lisboa, APA (2008)

Baek, S., Kim, Y., Perry, R.: Indoor air quality in homes, offices and restaurants in Korean urban area – Indoor/outdoor relationships. Atmos. Environ. **31**(4), 529–544 (1997)

Borrego, C., Tchepel, O., Costa, A.M., Martins, H., Ferreira, J., Miranda, A.I.: Traffic-related particulate air pollution exposure in urban areas. Atmos. Environ. **40**, 7205–7214 (2006)

Borrego, C., et al.: "SaudAr – A Saúde e o Ar que respiramos" Relatório do 3º de actividades. Universidade de Aveiro. AMB-QA-3/2007, Aveiro (2007)

Borrego, C., Monteiro, A., Pay, M.T., Ribeiro, I., Miranda, A.I., Bassart, S., Baldasano, J.M.: How bias-correction can improve air quality forecasts over Portugal. Atmos. Environ. **45**(37), 6629–6641 (2011)

Bouland, C., et al.: Review and gaps identification in air quality and health assessment methodologies at regional and local scale. Deliverable D2.4 Health Impact Assessment. APPRAISAL Project. FP7 Grant 303895 (2013)

Brimblecombe, P.: The Big Smoke: A History of Air pollution in London Since Medieval Times. Routledge Revivals, New York, USA (2011)

Brunekreef, B., Holgate, S.T.: Air pollution and health. Lancet **360**, 1233–1242 (2002)

Chau, C.K., Tu, E.Y., Chan, D., Burnett, J.: Estimating the total exposure to air pollutants for different population age groups in Hong Kong. Environ. Int. **27**, 617–630 (2002)

Colvile, R.N., Hutchinson, E.J., Mindell, J.S., Warren, R.F.: The transport sector as a source of air pollution. Atmos. Environ. **35**, 1537–1565 (2001)

Curtis, L., Rea, W., Smith-Willis, P., Fenyves, E., Pan, Y.: Adverse health effects of outdoor air pollutants. Environ. Int. **32**, 815–830 (2006)

Dudhia, J.: A nonhydrostatic version of the Penn State–NCAR mesoscale model: Validation tests and simulation of an Atlantic cyclone and cold front. Mon. Weather Rev. **121**(5), 1493–1513 (1993)

European Commission EC: Strategies to determine and control the contributions of indoor air pollution to total inhalation exposure (STRATEX). Report No. 25 European Collaborative Action Urban Air, Indoor Environment and Human Exposure. Environment and Quality of Life. European Commission. Directorate Joint Research Centre – Institute for Health & Consumer. EUR 22503 EN, 79 pp (2006)

European Environmental Agency EEA: Environment in the European Union at the Turn of the Century. European Environment Agency, Copenhagen (1999)

European Environmental Agency EEA: The European Environment – State and Outlook 2005. European Environment Agency, Copenhagen (2005). ISBN 92-9167-776-0

Fenger, J.: Urban air quality. Atmos. Environ. **33**, 4877–4900 (1999)

Fuller, D.Q., et al.: The contribution of rice agriculture and livestock pastoralism to prehistoric methane levels: An archaeological assessment. Holocene **21**, 743–759 (2011)

GENEMIS (Generation of European Emission Data for Episodes) Project: "EUROTRAC Annual Report", Part 5. EUROTRAC International Scientific Secretariat, Garmisch-Partenkirchen (1994)

Götschi, T., et al.: Comparison of black smoke and PM2.5 levels in indoor and outdoor environments of four European cities. Environ. Sci. Technol. **36**(6), 1191–1197 (2002)

Gulliver, J., Briggs, D.J.: Personal exposure to particulate air pollution in transport microenvironments. Atmos. Environ. **38**, 1–8 (2004)

Halliday, E.C.: A historic review of atmospheric pollution. In: Air Pollution, WHO Monograph Series No. 46, WHO, Geneva (1961)

Hedley, A.J.: Air Pollution and Public Health. The Current Avoidable Burden of Health Problems, Community Costs and Harm to Future Generations. The University of Hong Kong. CB(1) 733/08-09(02) (2009)

Hertel, O., et al.: Human exposure to outdoor air pollution (IUPAC technical report). Pure Appl. Chem. **73**(6), 933–958 (2001)

Krzyzanowski, M., Cohen, A.: Update of WHO air quality guidelines. Air Qual. Atmos. Health **1**, 7–13 (2008)

Liao, C.-M., Huanga, S.-J., Yu, H.: Size-dependent particulate matter indoor/outdoor relationships for a wind-induced naturally ventilated airspace. Build. Environ. **39**(4), 411–420 (2004)

Martins, P., et al.: Airways changes related to air pollution exposure in wheezing children. Eur. Resp. J. **39**(2), 246–253 (2012)

Monn, C.: Exposure assessment of air pollutants: a review on spatial heterogeneity and indoor/outdoor/personal exposure to suspended particulate matter, nitrogen dioxide and ozone. Atmos. Environ. **35**, 1–32 (2001)

Monteiro, A., Vautard, R., Borrego, C., Miranda, A.I.: Long-term simulations of photo oxidant pollution over Portugal using the CHIMERE model. Atmos. Environ. **39**(17), 3089–3101 (2005)

Monteiro, A., Miranda, A.I., Borrego, C., Vautard, R., Ferreira, J., Perez, A.T.: Long-term assessment of particulate matter using CHIMERE model. Atmos. Environ. **41**, 7726–7738 (2007)

Ren, C., Tong, S.: Health effects of ambient air pollution – recent research development and contemporary methodological challenges. Environ. Health **7**(56) (2008)

Sapart, C.J., et al.: Natural and anthropogenic variations in methane sources during the past two millennia. Nature **490**, 85–88 (2012)

U.S. Environmental Protection Agency (EPA): Exposure Factor's Handbook. National Center for Environmental Assessment, Springfield (1997)

U.S. Environmental Protection Agency (EPA): Metabolically Derived Human Ventilation Rates: A Revised Approach Based upon Oxygen Consumption Rates. National Center for Environmental Assessment, Washington, DC; EPA/600/R-06/129F (2009)

Vautard, R., Beekmann, M., Roux, J., Gombert, D.: Validation of a hybrid forecasting system for the ozone concentrations over the Paris area. Atmos. Environ. **35**(14), 2449–2461 (2001)

World Health Organization: WHO Air Quality Guidelines for Particulate Matter, Ozone, Nitrogen, Dioxide and Sulfur dioxide – Summary of Risk Assessment. WHO Press, Geneva (2006)

World Health Organization: WHO Guidelines for Indoor Air Quality: Selected Pollutants. WHO Regional Office for Europe, Copenhagen (2010). ISBN 978 92 890 0213 4

Wu, J., Lurmann, F., Winer, A., Luc, R., Turco, R., Funk, T.: Development of an individual exposure model for application to the Southern California children's health study. Atmos. Environ. **39**, 259–273 (2005)

Xiaomin, X., Zhen, H., Jiasong, W.: The impact of urban street layout on local atmospheric environment. Build. Environ. **41**, 1352–1363 (2006)

Air Pollution from Mobile Sources: Formation and Effects and Abatement Strategies

Neal Hickey, Ilan Boscarato, and Jan Kaspar

Abstract

An overview of the issue of air pollution from mobile sources is presented in the present chapter. The chapter is divided into three sections. The first section contains a general introduction on specific aspects of air pollution from internal combustion engines. The topics covered include a description of the primary and secondary pollutants formed and their adverse effects on health and the environment; the mechanisms of pollutant formation and, consequently, the factors which affect their formation; and a historical perspective of the legislative measures progressively introduced over the years. Finally, a brief description of the abatement strategies which may be generally adopted will be given (primary methods vs. secondary methods). The second section describes the state-of-the-art pollution abatement technologies for gasoline, lean-burn and diesel engines. The third section describes aspects related to pollution abatement in the marine sector. Air pollution abatement from ships is of high current interest due to the recent and ongoing introduction of legislation in the area. The specific problems associated with the marine sector are described, along with the strategies/technologies adopted to affront these problems. Historically, thanks in part to the success achieved, there has been a shift in emphasis of the focus of the problem, which has evolved from gasoline-fuelled engines, to diesel and lean-burn gasoline engines, to, more recently, off-road vehicles and marine engines. The present contribution will centre on the development of emission abatement from road vehicles, which have been largely responsible for the technological advances made in the field, and marine engines, which have recently become the subject of attention and can be considered to represent the challenge for the future. The situation regarding off-road vehicles will not be specifically considered as related solutions are derived from the above quoted areas. The contribution is based on a seminar held at the summer school of the International PhD in Environmental Science and Engineering, Cagliari, September 2008.

Keywords

Air pollution • Mobile sources • Air quality strategies • Kyoto Protocol • Selective catalytic reduction (SCR)

1 Air Pollution: Formation and Effects

1.1 Introduction

Air pollution has been defined as "the presence in the earth's atmosphere of one or more contaminants in sufficient quantity to cause short- or long-term deleterious effects to human,

N. Hickey (✉) • I. Boscarato • J. Kaspar
Department of Chemical and Pharmaceutical Science, University of Trieste, Via L. Giorgieri 1, Trieste, Friuli Venezia Giulia, Italy
e-mail: nhickey@units.it

G. Cao and R. Orrù (eds.), *Current Environmental Issues and Challenges*,
DOI 10.1007/978-94-017-8777-2_2,

animal or plant life, or to the environment" (Painter 1974). These contaminants are divided into (1) primary pollutants, which are emitted directly into the atmosphere, and (2) secondary pollutants, which are formed in the atmosphere by subsequent reaction of primary pollutants or between primary pollutants and other gaseous species of the atmosphere.

The issue of air pollution and air quality is vast: A multitude of substances may be considered as pollutants and there are many sources which can result in the presence of polluting substances in the atmosphere. However, a limited number of anthropogenic activities are particularly problematic, and therefore, the substances related to these activities are of particular concern. For example, signatories to the United Nations Economic Commission for Europe (UNECE) Convention on Long-Range Transboundary Air Pollution (LRTAP) are required to provide inventories on a range of substances subdivided according to various categories (Adams et al. 2012):

Main pollutants: nitrogen oxides (NO_x), non-methane volatile organic compounds (NMVOC), sulphur oxides (SO_x), ammonia (NH_3), carbon monoxide (CO)

Particulate matter (PM): subdivided as primary PM (fine particulate matter (PM2.5) and coarse particulate matter (PM10)) and total suspended particulates (TSP)

Heavy metals (HMs): subdivided as priority heavy metals – lead (Pb), cadmium (Cd) and mercury (Hg) – and additional HMs: arsenic (As), chromium (Cr), copper (Cu), nickel (Ni), selenium (Se) and zinc (Zn)

Persistent organic pollutants (POPs): polychlorinated dibenzodioxins/dibenzofurans (PCDD/Fs), polycyclic aromatic hydrocarbons (PAHs), hexachlorobenzene (HCB), hexachlorocyclohexane (HCH) and polychlorinated biphenyls (PCBs)

In addition, reporting of a number of individual PAHs is required: benzo(a)pyrene, benzo(b)fluoranthene, benzo(k) fluoranthene and indeno(1,2,3-cd)pyrene. The US EPA controls 187 substances classified as toxic air pollutants (US EPA 2013b).

Activities or potential sources which lead to the formation of polluting substances in the atmosphere include biogenic sources, solvent use, agriculture, treatment and disposal of waste, extraction and distribution of fuels, combustion plants, electricity generation and transport. Combustion processes contribute enormously to the problem and the emergence of petroleum products added a new dimension to the problem of combustion-related pollution. More specifically, the massive increase in the use of internal combustion engines (ICE) in various forms of transport contributed to greatly increased problems of pollution, with the biggest concerns surrounding the problem of community pollution. Once the problem was identified, intense efforts have been devoted, since the second half of the twentieth century, to reduce the contribution associated with automotive sources. These efforts have met with significant success and, for example, have led to the introduction of catalytic control of exhaust gas emissions as a standard feature of modern automobiles. Indeed, thanks in part to the success achieved, there has been a shift in emphasis of the focus of the problem, which has evolved from gasoline-fuelled engines, to diesel and lean-burn gasoline engines, to, more recently, marine engines.

1.2 Pollutant Formation in the Internal Combustion Engine (ICE) (Hickey et al. 2006)

The ideal chemical reaction for a combustion process, and therefore also in an ICE, may be represented as in Eq. 1:

$$HC + O_2 \rightarrow CO_2 + H_2O + Q \qquad \text{unbalanced} \qquad (1)$$

where HC represents the fuel and Q the energy liberated in the form of heat from this highly exothermic process. However, a number of factors may interfere with this ideal process, with the result that substances (pollutants) other than carbon dioxide and water are present after the combustion process. Both physical (e.g., incomplete combustion) and chemical (e.g., fuel impurities and secondary reactions) factors are involved. In the following sections, the main pollutants found in engine exhaust and the variables or mechanisms which lead to their formation will be considered.

1.2.1 Carbon Monoxide (CO)

CO is produced when there is insufficient oxygen (O_2) for the complete oxidation of hydrocarbons, either on a global or on a local basis. Thus, on a global basis, CO emissions are high when the engine is operated under conditions in which there is an excess of fuel with respect to the oxygen necessary for its combustion. This can occur, for example, during acceleration. These are known as rich conditions. However, for local mixing reasons (local basis), CO formation does not reduce to zero under the so-called lean conditions, when there is an excess of O_2 (Fig. 1). Furthermore, the formation of CO is favoured by low combustion temperature, such as those encountered immediately after engine start-up, or by temperature inhomogeneity in the combustion chamber.

Although CO is considered as an ozone precursor (see sect. 1.2.3), the effects of CO alone on the environment are limited and the main concern surrounding this pollutant is its very high toxicity, which acts by limiting O_2 transport in the body. The affinity of CO for haemoglobin (carboxyhaemoglobin), which carries O_2 from the lungs to the tissues in the form of oxyhaemoglobin, is approximately 210 times greater than that of O_2 (Prockop and Chichkova 2007). Other known mechanisms of the detrimental effects of carbon monoxide on body processes include its ability to bind to myoglobin and mitochondrial cytochrome oxidase.

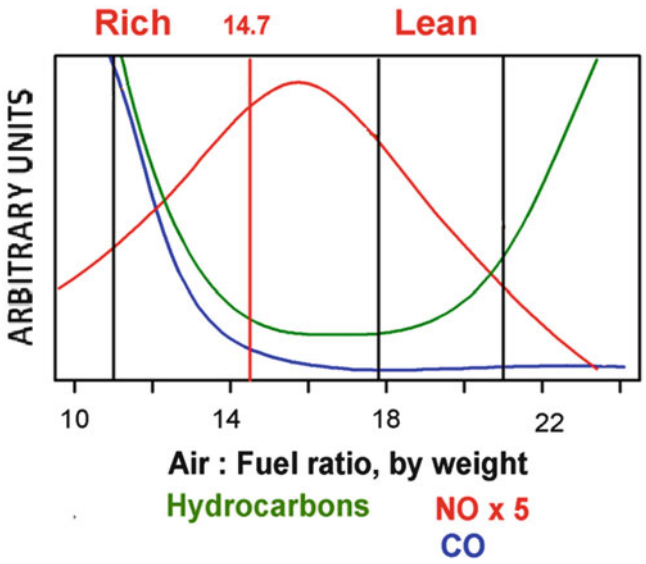

Fig. 1 Effect of air-to-fuel (A/F) ratio (w/w) on emissions of hydrocarbons, CO and NO_x. An A/F ratio of 14.7 corresponds to a stoichiometric mixture (Adapted from Kaspar et al. (2003))

1.2.2 Hydrocarbons (HCs)

Fuels for mobile sources contribute to the presence of hydrocarbons in the atmosphere at all stages of their use (from refining to refuelling) through evaporation losses. However, the emissions strictly associated with the combustion process itself are due to unburned or partially combusted fuel. In reality, the collective designation of HCs covers a multitude of specific compounds. The US EPA has listed more than 1,000 different compounds present in exhaust or evaporative emissions from on-road and non-road equipment, using conventional (gasoline, diesel) and various alternative fuels (e.g., ethanol, biodiesel, compressed natural gas) (US EPA 2013a). The nature of the HCs emitted depends on the characteristics of the fuel. For example, for light fuels, such as gasoline, the HCs emitted are not necessarily those present in the fuel. In fact, HCs with 1–3 carbon atoms (C1–C3) are common. For heavier fuels, such as diesel, they can also be the fuel itself.

The HCs emitted can also result from various reaction processes which take place during combustion, such as cracking, hydrogenation and dehydrogenation.

Various factors lead to the appearance of the unburned HCs, which is often linked with that of CO formation (Fig. 1): low temperature, lack of homogeneity during combustion (temperature or mixing) or physical factors which impedes combustion process. The temperature of the air/fuel mixture as it enters the combustion chamber can be a factor, as too low a temperature can result in poor mixing and consequently partial misfire. In general, engine misfire due to ignition, fuel delivery or air induction problems leads to the emission of HCs. For example, both inadequate spark (mixture too rich) and a non-combustible mixture (too lean) lead to HC emissions. Another potential reason for HC emissions is the phenomenon of wall quenching, in which the relatively cool temperature of the chamber walls causes the flame to extinguish prematurely and some of the fuel remains unburned. In addition, there are physical phenomena in the engine which contribute to HC emissions. During engine operation, porous coke chamber deposits are formed. Adsorption and trapping of the fuel in these deposits allow fuel to escape combustion, and this uncombusted fuel is subsequently expelled.

There are various health issues associated with the presence of HC in the atmosphere. From this point of view, unsaturated and aromatic HCs are considered to be the most problematic. HC emissions were initially thought to present a relatively low toxicity threat, and, as will be seen in the next section, the main concern was their determining role as precursors to the secondary pollutant ozone (O_3) and its build-up at a tropospheric level along with other hazardous secondary pollutants. In fact, both NO_x and HCs are often referred to as ozone precursors. However, the potential health hazards of specific HCs or categories of HC have, over time, become evident. Many are carcinogens or mutagens and the effects of long-term exposure to many of the individual substances have not been fully established. In the case of automotive emissions, benzene, buta-1,3-diene, formaldehyde, acetaldehyde and polynuclear aromatic hydrocarbons (PAHs) are of particular concern. Furthermore, when they react with the other components of the atmosphere or the exhausts, they can generate more dangerous secondary pollutants, such as polycyclic aromatic hydrocarbons (PAHs) and benzene derivatives. These secondary HC pollutants can reach the bloodstream when inhaled, so their abatement is therefore of the highest importance. From an environmental point of view, another potential problem is that of water pollution.

It should be noted that, given the large number of possible HC compounds, they are usually considered together and their concentrations are often reported as ppm of carbon equivalent (*ppm C*) (Kaspar et al. 2003).

1.2.3 Nitrogen Oxides (NO_x)

The designation "nitrogen oxides (NO_x)" is used to refer to any combination of NO and NO_2.

There are three recognised routes to NO_x formation during fuel combustion:

1. Thermal NO_x species are formed by the Zeldovich mechanism, in which atmospheric nitrogen and oxygen react together to form NO_x. This process is summarised as follows:

$$O + N_2 \rightarrow NO + N \quad (2)$$

$$N + O_2 \rightarrow NO + O \quad (3)$$

$$N + OH \rightarrow NO + H \quad (4)$$

The mechanism is favoured by high oxygen radical concentration and, above all, by high temperature.

2. Prompt NO_x species are formed in hydrocarbon-rich flames via the interactions of hydrocarbon radicals with nitrogen to produce various nitrogen-containing species (nitriles, amines, amides, cyanides, etc.,). These are then oxidised to produce NO_x. Prompt NO_x forms by the Fenimore mechanism (Fenimore 1975, 1976), which can be represented as follows:

$$CH + N_2 \rightarrow HCN + N \quad (5)$$

$$N + O_2 \rightarrow NO + O \quad (6)$$

$$N + OH \rightarrow NO + H \quad (7)$$

$$C_2 + N_2 \rightarrow 2CN \quad (8)$$

$$CN + O \rightarrow C + NO \quad (9)$$

$$CN + O_2 \rightarrow CO + NO \quad (10)$$

3. Fuel NO_x is formed by the oxidation of fuel-bound nitrogen, i.e., nitrogen-containing species in the fuel itself. Consequently, its contribution depends only on the quantity of nitrogen present in the fuel and is independent of the oxygen content and the temperature. During combustion, fuel compounds such as ammines amides, pyridines, etc., generate other volatile compounds of nitrogen, such as ammonia and cyanides, which are then oxidised to NO and CO_2

In relation to the formation of NO_x in gasoline-fuelled ICE, there are two important features, i.e., thermal NO_x is favoured under most engine conditions and therefore combustion temperature is the most important control factor, and NO is effectively the only NO_x species present. This is because at the temperature of fuel combustion, the equilibrium between NO and NO_2 (Eq. 11a) is shifted far to the left.

$$NO + ½O_2 \leftrightarrow NO_2 \quad (11a)$$

With regard to its environment effects, primary NO_x emissions contribute to the process of eutrophication of aquatic systems and, to a limited extent, to the formation of acid rain. From the point of view of health effects, NO presents a very low toxicological threat. NO_2 on the other hand is a highly toxic brown-red gas. Its presence in the atmosphere is therefore highly undesirable. As indicated earlier, a significant cause for concern surrounding the presence of NO in the atmosphere is its presence in combination with HCs and CO and their further reaction to form secondary pollutants during photochemical smog episodes. On cooling, atmospheric NO can be slowly converted into NO_2 via Eq. 11a, as the equilibrium lies to the right at low temperature. The NO_2 formed can undergo a photochemical dissociation to NO and atomic oxygen. The atomic oxygen produced reacts with O_2 to form ozone. A circular reaction process is completed when the NO reacts with O_3 to form NO_2 and O_2. The levels of O_3 (and NO_2) are regulated by this cycle. In the presence of hydrocarbons and CO, however, this cycle is broken, resulting in increased NO oxidation to NO_2, build-up of tropospheric ozone and the formation of hazardous secondary pollutants such as peroxyl acyl nitrates (PANs and formaldehyde). This type of air pollution episode is known as photochemical smog and was first unequivocally identified in Los Angeles in the mid-1940s. The European Environment Agency monitors levels of NO_x, CO, CH_4 and non-methane volatile organic compounds (NMVOCs) as ozone precursors (EEA 2013a).

1.2.4 Particulate Matter (PM)

Particulate matter is a collective term for an often highly complex mixture of solids and liquids (Matti Maricq 2007; Twigg and Phillips 2009). The issue of airborne PM and its relationship with transport is highly complex. A large number of interrelated factors are involved in the formation and development of airborne PM, for which the situation is probably more complex than for any other pollutant. In the following paragraphs, a number of relevant features with regard to PM will be discussed.

1.2.4.1 PM Composition

As indicated above, PM is a collective term for a mixture of substances. This mixture can include oxides, sulphates, sulphites, carbonates, chlorides, metal compounds, fuel and soot carbon. The composition of PM derived from combustion is related to the fuel type and purity. For road transport, diesel applications are the worst offenders, while PM emissions from gasoline engines are significantly smaller.

Diesel PM is divided into three main categories: soluble organic fraction (SOF), sulphates and soot. The SOF is composed of heavy HCs from the fuel and lubricating oil or is formed during combustion. This is often condensed on existing solid particles. Sulphates arise from the presence of sulphur in the fuel, which is converted into SO_2 during combustion and then into SO_3. These gases can also react with water in the exhaust gases to form hydrated sulphuric acid. More generally, sulphates form part of the so-called inorganic fraction of PM. Other potential contributors to this inorganic fraction are inorganic compounds added to lubrication oil (and sometimes to the fuel itself) for various reasons (as viscosity modifiers, as antioxidants, as anticorrosives, to keep solid matter, especially soot, in suspension).

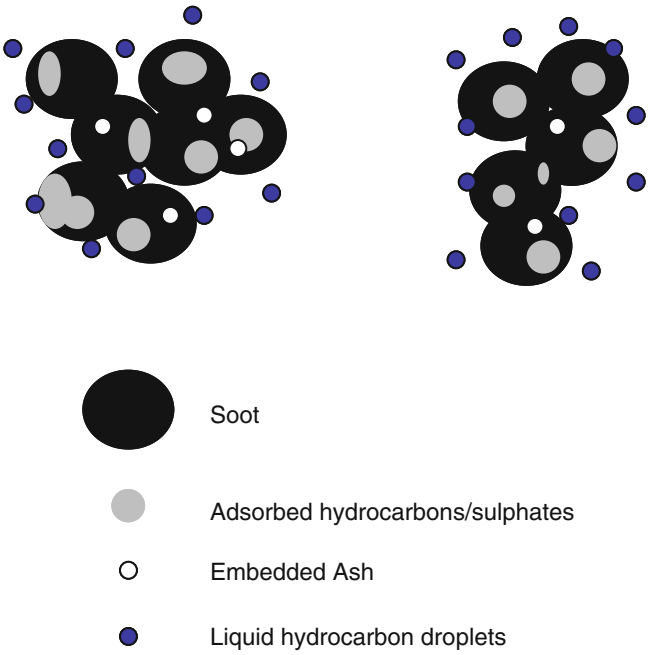

Fig. 2 Schematic representation of PM composition (Adapted from Matti Maricq 2007; Twigg and Phillips 2009)

Finally, soot is formed from incomplete combustion of the fuel. The complex nature of PM composition is illustrated schematically in Fig. 2.

As will be discussed later, the issue of marine fuel sulphur content is of fundamental importance in the formation/prevention of PM from marine engines.

1.2.4.2 PM Classification

PM is classified in a number of related ways. The most common classification of particulates is according to particle size, or fractions, which can range across four orders of magnitude. As particles are unlikely to be spherical, a generally accepted method of measurement and comparison must be adopted. The most widely used definition is the aerodynamic diameter: A particle with an aerodynamic diameter of 10 μm behaves in a gas like a sphere of unit density with a diameter of 10 μm. The notation PM10 is used to describe particles of 10 μm or less, whereas PM2.5 indicates particles with an aerodynamic diameter of less than 2.5 μm. Similarly, PM1 is another commonly used indication.

On this general basis, PM is often defined as coarse PM (2.5–10 μm), fine PM (particles from 0.1 to 2.5 μm) and ultra-fine PM (particles smaller than 0.1 μm). Another classification, related to their potential health effects, is based on their capacity to penetrate into the respiratory system.

1.2.4.3 PM Sources: Primary and Secondary PM

While there are usually multiple sources for any pollutant, in the case of PM there are a considerable number of natural sources. These include sea spray (sea salt), soil and sand moved by the wind, biogenic aerosols (e.g., pollen) and volcanic emissions. Furthermore, in the case of automotive transport, there are a number of sources of PM generally related to vehicle use, but not directly related to the combustion process. These include primary PM from attrition processes – wear of brakes and tyres, wear of the road surface and PM derived from suspension of deposited matter by passing vehicles. Finally, there is the PM derived from the combustion process itself. However, even this is further subdivided into primary PM from the combustion process (usually less than 1–2.5 μm) and secondary PM which form in the atmosphere through chemical and physical processes starting from the primary precursors. All of these possibilities, along with the above-discussed variable composition of PM, give rise to a very complex situation in which the various sources are not easily apportioned.

The issue of secondary PM formation is of fundamental importance because the PM present in the atmosphere does not necessarily correspond with that emitted from the engine during the combustion process. In fact, PM emissions are commonly studied with dilution tunnels in attempts to mimic the chemical and physical processes which lead to the growth and/or formation of secondary PM in the atmosphere. The process of transformation is illustrated in Fig. 3. Chemical reactions may also come into play. For example, the above-discussed hydrated sulphuric acid formed during combustion can in turn interact with other gases and particles in the air to form sulphates and other products.

The concerns surrounding PM have grown significantly in recent years, along with the observation that PM concentrations in urban areas are unacceptably high. As may be inferred from the above discussion, certain PM can reach the deepest recesses of the lungs, and many studies have linked PM with a series of respiratory related. In fact, the European Environmental Agency (EEA) report that "Two pollutants, fine particulate matter and ground-level ozone, are now generally recognised as the most significant in terms of health impacts" (EEA 2013b), while the US Environmental Protection Agency (US EPA) state that "Of the six (criteria) pollutants, particle pollution and ground-level ozone are the most widespread health threats" (US EPA 2013b).

1.2.5 Sulphur Oxides (SO_x)

The designation "sulphur oxides (SO_x)" is used to indicate any mixture of SO_2 and SO_3. In combustion processes, the SO_x formed originate from the sulphur present in the fuel. Both are toxic, colourless gases, with a pungent odour and a high solubility in water. This property is responsible for one of the main concerns surrounding SO_x emissions, i.e., their

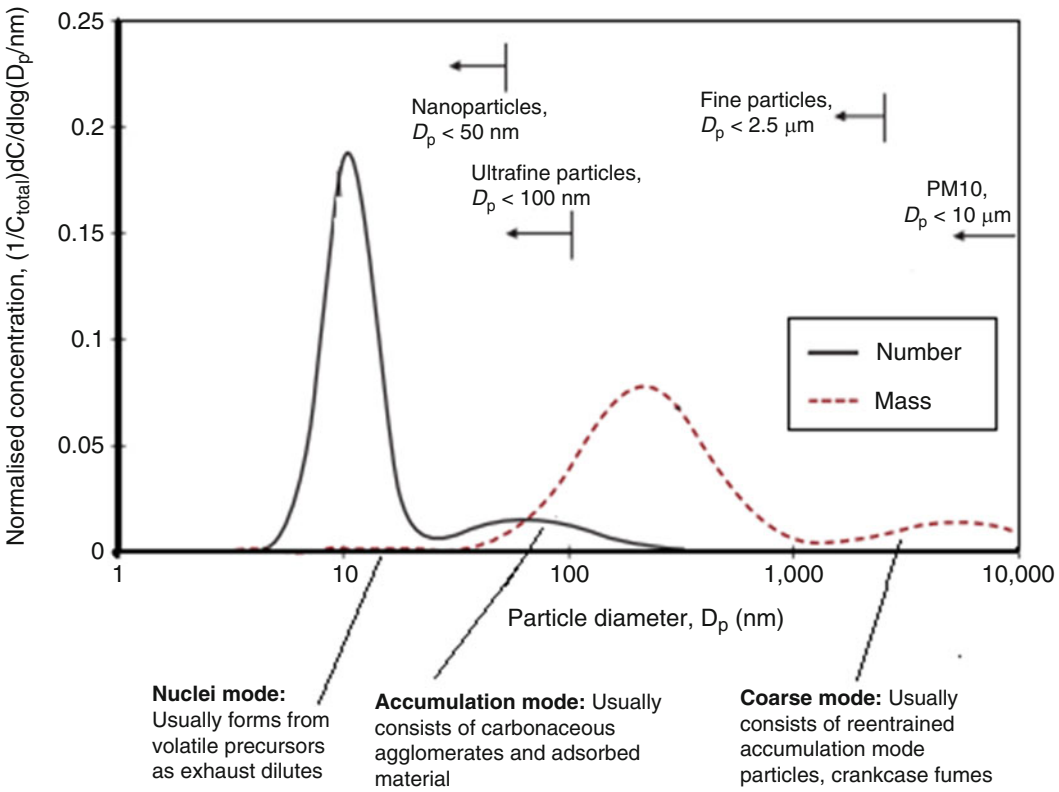

Fig. 3 Evolution of particulate matter (*PM*) (Adapted from Dieselnet 2013; Twigg 2011a)

acid nature. Dissolved in rainfall (acid rain), they can cause significant damage both to the environment and to buildings. In comparison, the acid-forming potential NO_x is much lower. As indicated above, the high solubility in water means that hydrated sulphuric acid can form during the combustion process itself. In the presence of high fuel sulphur concentrations, as in the case of marine fuels, the formation of the so-called acid mists gives rise to another potential problem relevant to the present discussion. These acid mists can cause severe corrosion damage to the post-treatment abatement systems. In addition, sulphur is a poison for many catalysts and its presence can determine catalyst choice in catalytic posttreatment systems.

As may be inferred from the discussion of PM, the issue of SO_x cannot be completely separated from that of PM. In the case of automotive fuels, as a pollution prevention measure, the level of the sulphur in the fuel has been progressively reduced to 10 ppm in Europe. This concentration leads to the formation of very low levels of SO_x and sulphate PM in the exhaust. For this reason, land-based transport makes a relatively small contribution to atmospheric SO_x levels. However, as will be outlined in Sect. 3, while similar measures are only now being adopted in the marine transport sector, the amount of sulphur in marine fuel is still high. This situation represents one of the biggest challenges for pollution abatement in the marine sector.

1.2.6 Carbon Dioxide (CO_2)

Combustion of fossil-based fuels necessarily leads to CO_2 formation. CO_2 is a direct greenhouse gas, and there is much debate centred on CO_2 because its atmospheric concentration is increasing, with transport in general making a significant contribution. The Kyoto Protocol, in which many countries committed to reduce CO_2 levels (UNFCCC 2013), is a direct consequence of the concerns surrounding the role of CO_2 in global warming. Furthermore, in 1998, the European Commission reached an agreement with the European Automobile Manufacturers' Association (ACEA), the Japanese Automobile Manufacturers Association (JAMA) and the Korean Automobile Manufacturers Association (KAMA) to comply with voluntary limits (140 g/km by 2008). After an initial period which saw significant CO_2 reductions, non-compliance resulted in the introduction of mandatory limits (vide infra).

1.3 Factors Which Affect Pollutant Formation

From the preceding paragraphs it emerges that the factors which affect pollution formation may be broadly divided into three main related categories. It is useful to summarise these below:

1.3.1 Engine Type (NO_x, CO, HCs)

For the purposes of pollution abatement, for simplicity, the discussion can be divided into two large categories, i.e., stoichiometric and lean engines. As will become evident, this distinction is useful for the discussion of the types of post-combustion depollution systems possible. The difference is related to air-to-fuel (A/F) ratio, usually denoted by λ (Fig. 1). A value of $\lambda = 1$ indicates the point where the amount of oxygen present is exactly that required for full stoichiometric combustion of all of the fuel present. This corresponds to an A/F ratio of 14.7 (w/w) for an oxygen-free gasoline. This discussion is also linked to the type of fuel used. Gasoline engines are typically run stoichiometric, while engines using heavier fuels (light-duty diesel, heavy-duty diesel, marine engines) are all operated under lean conditions, in which there is an excess of air ($\lambda > 1$). Here the discussion will be limited to the commonly engine types/fuels used. The situation for alternative fuels, e.g., methane, gpl and hydrogen, will not be specifically considered.

1.3.2 Engine Operating Conditions (NO_x, CO, HCs)

Within the framework of the engine and fuel type used, the engine operating conditions (or driving conditions) also come into play as this influences the A/F ratio and temperature. The exact composition at any given time thus strongly depends on these two factors.

1.3.3 Fuel Quality (SO_x, PM)

As discussed above, the fuel type and fuel quality are the determining factors in the formation of PM and SO_x species.

Figure 1 shows the variation in the production of NO_x, CO and HCs as the A/F ratio varies. In fuel-rich combustion mixtures ($\lambda < 1$, net reducing), the highest amounts of CO and HC are formed. Their levels of production decrease as the ratio approaches the stoichiometric point ($\lambda = 1$). Initially, in the fuel-lean situation ($\lambda > 1$, net oxidising), most of the fuel is consumed by the available O_2, which results in low production of CO and HCs. However, as λ increases, HCs output begins to increase because combustion becomes inefficient (or misfire occurs). This picture represents a general scheme since the region of misfire depends on the type of engine (lean or stoichiometric).

In the case of NO_x, its formation is low in fuel-rich conditions due to a scarcity of O_2. NO_x production increases to a maximum as the A/F ratio passes through stoichiometry ($\lambda = 1$) into fuel-rich stoichiometries ($\lambda > 1$). The amount formed then starts to decrease as the temperature of combustion falls, due to the presence of an increasing amount of air. This decrease in temperature results in a decrease in NO_x production. Another temperature-related feature is the situation immediately after start-up, when the engine temperature has not reached its normal operating level. In this period the lowest concentrations of NO are formed while CO and HCs levels are high.

All of this means that the amount and types of pollutants vary (Kaspar et al. 2003). It is important to note that, although related, reducing pollution from each engine type represents a different problem and, as will be seen later, for this reason the abatement solutions also vary. In fact, the dependency of the nature of the emission of the engine type has been recognised not only as composition but also in terms of their impact: In a recent meeting the International Agency for Research on Cancer (IARC; Lyon, France) classified diesel engine exhaust as "carcinogenic to humans" (Group 1), whereas gasoline engine exhaust was considered as "possibly carcinogenic to humans" (Benbrahim-Tallaa et al. 2012). Interestingly, this carcinogenic classification of diesel exhaust has been questioned (Pallapies et al. 2013) since it does not take into account the significant evolution of diesel engines, e.g., the introduction of common rail technology (Hesterberg et al. 2011; McClellan et al. 2012). Furthermore, it should be remembered that the nature of the fuel can affect the amount and nature of emissions, as indeed was observed when blends of regular and biodiesel were employed on the same engine (Magara-Gomez et al. 2012).

1.4 Pollution Legislation

Legislative measures progressively introduced over the years have been largely responsible for stimulating progress in the abatement technologies adopted in the automotive sector. The progressive introduction of increasingly stringent measures led first to the adoption of pollution prevention measures and then to the introduction and subsequent development of the so-called end-of-pipe technologies. In the following sections, an overview of legislative measure in the automotive sector will be considered.

Urban air pollution problems have existed for centuries and legislative measures to control the problem are underway for well over a century. Two particular types of urban air pollution came to the fore during the twentieth century: London-type smog and photochemical smog (Jacobson 2002). Initially, the focus was on London-type smog. This was caused by the burning of fossil fuels in the presence of fog (SMoke + fOG) and became a serious public health and safety issue with the Industrial Revolution. Episodes of this type of pollution were very frequent in London but the phenomenon was common in many industrial areas. The increasing frequency and seriousness of these episodes in the nineteenth and first half of the twentieth century lead to a greater attention to the problem. However, it was only after the Second World War that determined efforts were devoted to air pollution management, in particular after the so-called Great Smog of 1952 in London. In 1956, the UK passed its first Clean Air Act. The first federal "Pollution Control Act"

was passed in the USA in 1955, in which the Public Health Service was financed to study the sources and problems related to air pollution. For a variety of reasons, initial measures generally met with limited success. For example, compliance control measures were inadequate. Similarly, rather than on pollution prevention or control, the focus was on measures to reduce the presence of harmful gases in urban areas, for example, through the use of taller chimney stacks, thereby moving the pollution sources away from the cities. However, these laws represented the first steps towards a serious legislative effort to affront the problem of urban pollution.

With regard to photochemical smog, the problem is directly linked with the widespread diffusion of automobiles. By the late 1930s/early 1940s, the problem of reduced urban visibility became evident in Los Angeles, and by the mid-1940s, it was realised that the pollution was not only from smokestacks but from a wider variety of sources, including automobiles. In fact, the first legislative measures which identified automobiles as sources of pollution were introduced in California in 1947. However, no specific countermeasures were adopted. The first US Federal standards which specifically required control of automotive emissions were introduced by the Clean Air Act of 1970, while in 1970, Europe, with directive 70/220/CEE, fixed its first standards to control pollutants generated in internal combustion engines. Both have been frequently amended and updated in the intervening years. Californian legislation limits have been independently set since 1977 by the Californian Air Resources Board (CARB). Legislation in California represents the most severe emission standard in the world.

Initial US Federal legislation required a 90 % reduction of CO and HC emissions from 1970 model years by 1975 and a 90 % reduction of NO emissions from 1971 model years by 1976. Initial strategies to meet the targets were based on prevention: Engine modification allowed CO and HCs emissions to be reduced. However, the more demanding limits introduced for the 1975 model year meant that catalytic control had to be introduced. Significant reductions of CO and HC emissions were required, which led to the introduction of conventional oxidation catalysts (COCs – Pd, Pt/Al_2O_3), together with engine modifications and the use of unleaded gasoline. Engines were operated in lean conditions to provide the O_2 necessary for the oxidation catalyst to function. Some degree of NO_x control was achieved by non-catalytic methods, especially exhaust gas recirculation (EGR). As NO_x limits became stricter, COCs were superseded by a combination of COC and three-way catalysts (TWCs), to specifically tackle NO_x emissions, and, finally, by TWCs only. TWCs will be discussed in more detail in Sect. 2.

1.5 Automotive Emission Standards

The initial EU legislation closely reflected the legislation which had been recently introduced in the USA. However, in the successive development of its legislation, the EU began to introduce EU-specific standards. A very important consideration, for example, is the significantly higher incidence of diesel engines in the Europe. Consequently, from the early 1990s, there has been a gradual phasing-in of the modern European emission standards, known as Euro 1 to Euro 6 standards. Standards set before this are generally referred to as Euro 0. In the automotive sector, emission standards are set for various pollutants on the basis of vehicle/engine types and are divided into two main categories: (1) passenger cars and light-duty (LD) vehicles (<3.5 t) and (2) heavy-duty (HD) vehicles and buses. Other engine types, such as motorcycles and non-road diesel engines, are also legislated, but these will not be considered here. The situation in relation to marine engines will, however, be discussed in Sect. 3.

To exemplify the temporal development of legislation, Table 1 outlines European emission standards since 1993

Table 1 Selected EU emission standards for passenger cars

		CO	HC	NMHC	NO_x	HC + NO_x	*PM*
Standard	Year	(g/km)					
Diesel							
Euro 1[a]	1992	2.72 (3.16)	–	–	–	0.97 (1.13)	0.14 (0.18)
Euro 2	1996	1.0	–	–	–	0.7	0.08
Euro 3	2000	0.64	–	–	0.5	0.56	0.05
Euro 4	2005	0.50	–	–	0.25	0.30	0.025
Euro 5	2009	0.50	–	–	0.18	0.23	0.005
Euro 6	2014	0.50	–	–	0.08	0.17	0.005
Gasoline							
Euro 1[a]	1992	2.72 (3.16)	–	–	–	0.97 (1.13)	–
Euro 2	1996	2.2	–	–	–	0.5	–
Euro 3	2000	2.3	0.20	–	0.15	–	–
Euro 4	2005	1.0	0.10	–	0.08	–	–
Euro 5	2009	1.0	0.10	0.068	0.06	–	0.005
Euro 6	2014	1.0	0.10	0.068	0.06	–	0.005

[a]Vaules in parenthesis are conformity of production (COP) limits

Table 2 European Union sulphur limits in automotive fuel

Date	Maximum sulphur content
1993	0.2 % w/w
2000	350 ppm
2005	50 ppm
2010	10 ppm

for selected pollutants. Similarly, in the USA, Tier I standards were phased in between 1994 and 1997, while Tier II standards were phased in between 2004 and 2009. Even more stringent Tier III standards have been agreed, to be phased in between 2017 and 2025. It should be noted that a fundamental aspect in the application of emission legislation is the procedure used to test engine compliance. Compliance tests are performed on a chassis dynamometer and involve prescribed cycles, which, however, will not be further discussed here.

An important distinction exists between the emission measurement units for HD diesel vehicles and other categories. For HD diesel vehicles, the limits are expressed as a function of power output (g/kWh), while they are expressed as a function of the driving distance for the other categories (g/km). As will be discussed in Sect. 3, the recent introduction of emission limits in the marine sector treats such engines in the same way as land-based HD engines from this point of view.

The EU has recently adopted two regulations which address CO_2 emissions from passenger cars and light commercial vehicles. CO_2 emission targets for new passenger cars were adopted in April 2009. The regulation established a fleet-average CO_2 emission target of 130 g/km to be reached by 2015, with a target of 95 g CO_2/km to be reached from 2020 also defined. CO_2 emission targets for light commercial vehicles were proposed in October 2009. The regulation establishes a fleet-average CO_2 emission target of 175 g/km, fully phased-in from 2016, and a target of 135 g CO_2/km from 2020.

With regard to the emission of SO_x, EU legislation has implemented a progressive reduction of the sulphur content in automotive fuel since the beginning of the 1990s (Table 2). Currently, automotive fuel contains a maximum of 10 ppm of sulphur. In the USA, ultra low-sulphur diesel (ULSD) contains a maximum of 15 ppm S.

1.6 The Progress Made in Pollution Abatement

The efforts which have been made to reduce emissions of pollutants in recent years have been quite successful. This is illustrated in Fig. 4, which shows the decrease in emissions of airborne pollutants from road transport in the EU-27 countries between 1990 and 2010. Road transport represents one of the main pollution categories, and the regulation measures introduced have contributed significantly to specific and overall reductions. However, whereas this chapter is focussed essentially on automotive and marine emissions, it must be evidenced that off-road engines also significantly contribute to overall emissions and, accordingly, regulation limits have also been set for these engines. It is estimated that in 1996, before any standards had become effective, emissions from land-based off-road engines, locomotive engines and marine diesel engines accounted for about 40 % of the mobile source emissions of PM and 25 % of NO_x. Of this, land-based off-road diesel engines contributed about 47 % (Van Rensselar 2011).

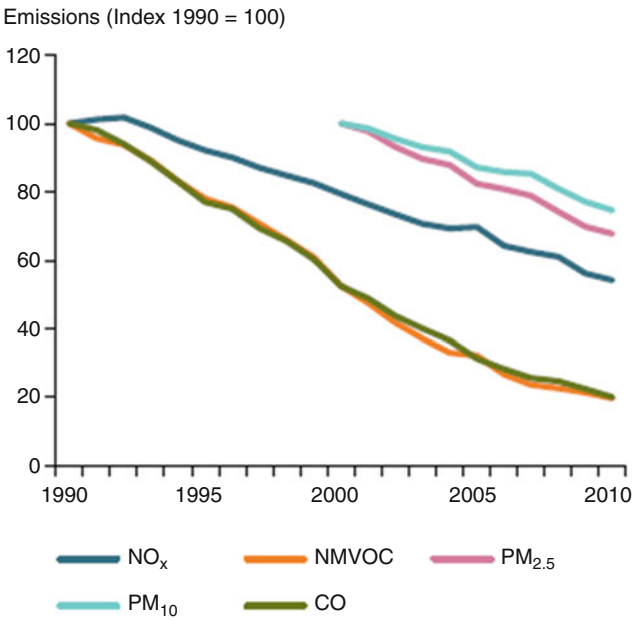

Fig. 4 EU-27 road transport emissions trends 1990–2010 for the main airborne pollutants (Adapted from Adams et al. 2012)

1.7 Pollution Abatement Strategies

Pollution abatement strategies may be divided into two categories: measures to prevent pollution (primary methods) and measures to reduce emission of the pollutants once formed (secondary methods). As may be inferred from the above discussion, both approaches have been extensively employed for pollution control from transport. Preventative measures include engine modification; the use of reformulated, Pb-free and low-sulphur fuels; and the use of alternative fuels such as liquefied petroleum gas (LPG) and natural gas (NG) which are intrinsically cleaner than diesel or gasoline. However, the very high limits imposed by legislation made it necessary to introduce post-combustion technologies, and preventative

measures must be used in combination with these, not as alternatives. In the following sections, the state of the art in automotive catalytic technologies will be discussed.

2 State of the Art in Automotive Pollution Technology

2.1 Three-Way Catalysts (TWCs)

Three-way catalysts (TWCs) are the current state-of-the-art technology for emission control for gasoline automobiles, and they are without doubt the most successful post-combustion catalytic technology introduced in the automotive sector. A schematic representation of a TWC is shown in Fig. 5. The name TWC derives from the ability to simultaneously convert the three primary pollutants CO, NO_x and HCs (Kaspar et al. 2003):

$$2CO + O_2 \rightarrow 2CO_2 \quad (12)$$

$$HC + O_2 \rightarrow H_2O + CO_2 \quad \text{(unbalanced)} \quad (13)$$

$$2NO + 2CO \rightarrow 2CO_2 + N_2 \quad (14)$$

$$NO + HC \rightarrow N_2 + CO_2 + H_2O \quad \text{(unbalanced)} \quad (15)$$

$$2NO + 2H_2 \rightarrow N_2 + 2H_2O \quad (16)$$

TWC formulations have evolved and improved remarkably in terms of performance since they were first introduced. However, the improvements observed are not the result of changes in formulation only. A large number of factors – materials advances, improved engine characteristics, improved engine control, improved fuel characteristics, etc., – have been responsible for their success.

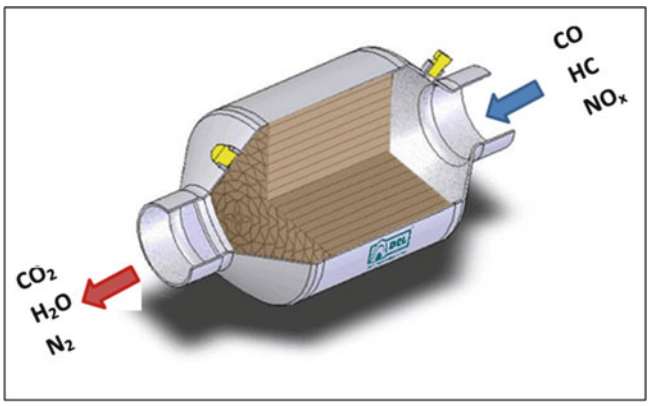

Fig. 5 Schematic arrangement of a three-way catalyst (*TWC*) (Adapted from Govconsys 2013)

The catalyst is formed by three main components:

- A *honeycomb* monolith substrate
- A *washcoat* support for the active phase
- An *active phase*

2.1.1 The Substrate

The substrate is a honeycomb monolith made of cordierite ($2MgO{\cdot}2Al_2O_3{\cdot}5SiO_2$) or metal. This is mounted in a steel container with a resilient matting material to ensure vibration resistance. This arrangement protects the catalyst and facilitates installation. Traditionally, cordierite monoliths have been extensively employed, primarily due to their lower production cost. Metallic substrates have a number of advantages however, such as a high thermal conductivity and low heat capacity, which allow very fast heating. In addition, they can be fabricated with very thin foil, which gives low back pressure and high geometric surface area, combined with good mechanical strength. These characteristics make metal monoliths suitable for specific applications such as close-coupled catalysts (CCCs), which are installed as close as possible to the engine in order to reduce the light-off time (vide infra).

A wide variety of substrate sizes with different cell densities and wall thicknesses are available. In fact, the cell density can range from 10 to more than 1,000 cells per square inch (cpsi), and various cross-channel sections are possible (triangular, hexagonal, trapezoidal and round). Very high cell densities (>1,000 cpsi) are common for TWCs, while densities in the range near 400 cpsi are more common for diesel applications (vide infra) (Dieselnet 2013).

2.1.2 The Catalyst: Washcoat + Active Phase

The active catalyst is supported (washcoated) onto the monolith by dipping it into a slurry which contains the catalyst precursors. After removal of the excess mixture, the honeycomb is calcined to obtain the finished catalyst.

The washcoat plays a number of key roles in the catalysis:

- It increases the surface area to maximise the contact between gas and active species. Consequently, it must have a high surface area which is stable at elevated temperatures.
- It ensures a high dispersion of the active phase. By interaction with the active phase, it should also maintain this high dispersion at elevated temperatures.
- In some cases, it acts as a co-catalyst.

Sintering of the either washcoat support or active phase results in dramatic loss of activity.

The exact composition of a TWC is a matter of confidentially. Different formulations exist for different manufacturers, and indeed formulations have varied significantly over the years, depending on a variety of factors, including economic considerations based on the price of the metals used in the active phase. However, modern

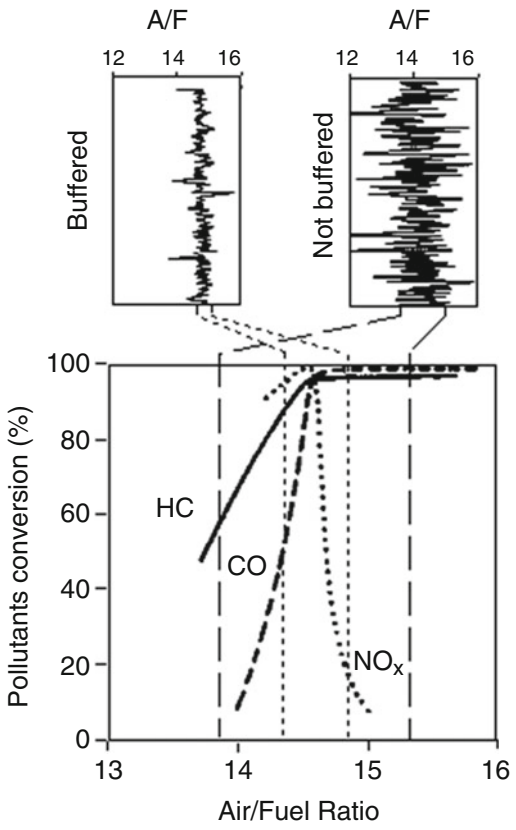

Fig. 6 Effect of air-to-fuel (*A/F*) ratio on the conversion efficiency of a three-way catalyst (*TWC*) (Adapted from Kaspar et al. 2003)

TWC all contain a number of main components in their formulations:

- Alumina, which is employed as a high surface area support (washcoat)
- CeO_2-ZrO_2 mixed oxides
- Precious Group Metals (PGMs) as active phases (Rh, Pt and Pd)
- Various oxides as stabilisers of alumina surface area, activity promoters and selectivity promoters

With regard to the last point, there are many possibilities: Iron, manganese, calcium, strontium, barium, lanthanum, neodymium, praseodymium and zirconium may all be used (Twigg 2011a). Formulations normally contain more than one of these additives.

2.1.3 TWC Operation

Before discussing the role of each component, a number of technological aspects regarding catalysis functionality will be outlined. These aspects may be useful to fully understand the role of each component.

In order to function correctly, TWCs require that stoichiometric conditions are maintained over the catalyst. The dependence on conversion efficiency A/F ratio is indicated in Fig. 6. Very high conversion is observed only if the A/F is maintained within a narrow operating window. Achieving this narrow window is achieved by the integrated engine on-board diagnostics (EOBD) system. The system is composed of two oxygen sensors, known as λ sensors, located at the inlet and outlet of the converter. The signal from the first sensor is used as a feedback for the fuel and air injection control loop. Ceria-based oxides are included in the catalyst formulations to further buffer the A/F fluctuations over the catalyst, through the redox properties of this element (vide infra). By comparing the oxygen concentration before and after the catalyst, A/F fluctuations are detected. Excessive fluctuations of A/F at the outlet signal system failure.

A further important feature which should be considered is the position of the catalyst. TWCs are capable of converting close to 100 % of the three pollutants once they reach their operating temperature and efficient A/F control is maintained. Heating of the catalyst is achieved by the exhaust gases themselves. However, in the time take to reach this temperature, conversion is low and a significant proportion of the overall emissions occur in this warm-up period after engine start-up (cold start). This may result in non-compliance during test procedures, especially for the more demanding legislation. The solution to this problem is to use a close-coupled catalyst (CCC). Basically, the catalyst is positioned closer to the engine, which significantly reduces the time it takes to reach operating temperature and dramatically affects vehicle emissions immediately after the start-up of the engine. As temperatures up to 1,100 °C are routinely met as a consequence of this location of the catalyst, an extremely efficient and robust catalyst is required.

2.1.4 The Role of PGMs

The PGMs represent the key component of the TWC, as the catalytic activity occurs at the metal centre. Rh, Pd and Pt have long been employed in TWCs. There is general agreement on the specificity of Rh to promote NO removal, while Pt and Pd are used mainly to perform the oxidation reactions, even though the oxidation activity of Rh is also good. In the early COCs, Pt was used, along with smaller amounts of either Pd or Rh to provide durability under lean conditions. However, once catalytic NO_x reduction became necessary, Rh/Pt was used. With improvements in catalyst performance, lower cost Pd/Rh TWCs were developed. The choice of Pt/Rh or Pd/Rh strongly depended on the balance of HC/CO/NO_x from a particular engine and application (Twigg 2011a). Pd was extensively added to TWC formulations starting from the mid-1990s being, at that time, cheaper than other PGMs. Formulations with Pd as the only PGM were in fact developed and commercialised for a period. Better A/F control and modification of the support provided adequate NO_x conversion even in the absence of Rh. Economic factors did to some extent come into play in this choice. However, the increased use of Pd in the TWC

technology also resulted in strong increases in Pd market price. In the past, a strongly disadvantage of the use of Pd was sensitive to poisoning by sulphur or lead. However, lead levels are now close to zero and fuel sulphur levels have been markedly reduced so these considerations are less important than previously. Consequently, most modern TWCs are based on Pd/Rh formulations.

2.1.5 The Role of Al_2O_3

The main role of Al_2O_3 is as a high surface area support to promote PGM dispersion and stability. In most cases γ-Al_2O_3 is employed due to its high surface area and good thermal stability under the hydrothermal conditions of the exhausts. However, other aluminas such as δ- and θ-Al_2O_3, which exhibit even higher thermal stability, can also be employed for specific applications such as in the CCCs (Kaspar et al. 2003), for which the issue of thermal stability is particularly important. Alumina stabilisation is necessary to prevent its transformation to the low surface area α-Al_2O_3 (surface areas typically below 10 m^2 g^{-1}). A number of stabilising agents have been reported in the literature: Lanthanum, barium, strontium, cerium and zirconium oxides or salts have been widely investigated. Efforts to produce highly stabilised alumina-based oxides, along with efforts to understand the stabilisation mechanisms, remain an ongoing area of research (Hernandez-Garrido et al. 2013).

2.1.6 The Role of CeO_2

A number of beneficial effects have been attributed to CeO_2 (Kaspar et al. 2003; Trovarelli 1996):

- It promotes the PGM metal dispersion.
- It increases the thermal stability of the Al_2O_3.
- It promotes the water-gas shift (WGS) reaction
- It favours catalytic activity at the interfacial metal-support sites.
- It promotes CO removal trough oxidation by lattice oxygen.
- It stores and releases oxygen under respectively lean and rich conditions

Of particular importance is the ability of ceria to store and release oxygen under lean and rich conditions, respectively. In reducing conditions, the excess reductant reacts with the ceria, which is reoxidised in oxidising conditions:

$$CeO_2 + xCO \rightarrow CeO_{2-x} + xCO_2 \quad (17)$$

$$CeO_{2-x} + \tfrac{1}{2}xO_2 \rightarrow CeO_2 \quad (18)$$

This redox ability is known as the oxygen storage capacity (OSC) and the net effect is that the OSC buffers oscillations in the A/F ratio. It is an important control factor in maintaining the stoichiometric conditions necessary for efficient conversion. Maintaining the OSC is highly important for both catalytic and technological reasons. From the catalytic point of view, the TWC activity is directly related to the OSC performance, while from a technological point of view, as above-discussed, the OBD technology is based on monitoring OSC efficiency.

Clearly, the OSC also contributes to removal of CO (and HC) in lean conditions. Another important means of CO removal is the WGS reaction, which is catalysed by ceria:

$$CO + H_2O \rightarrow H_2 + CO_2 \quad (19)$$

From the mid-1990s, CeO_2-ZrO_2 mixed oxides have gradually replaced pure CeO_2 as the OSC materials in TWCs. The replacement of CeO_2 with CeO_2-ZrO_2 mixed oxides in TWC formulations has significantly increased their performance due to the high thermal stability of these materials (Hernandez-Garrido et al. 2013).

2.2 Diesel and Lean-Burn Gasoline Engines

As outlined in Sect. 1, diesel and lean-burn gasoline engines operate at A/F ratios higher than stoichiometric (>14.7). These engines, due to the high A/F used in the combustion process, can achieve significant fuel savings. This reduction in fuel consumption translates to reduced emissions of CO_2. However, as these engines present a different composition with respect to gasoline engines, the problem of pollution abatement must be resolved by different methods. The TWC in fact does not work efficiently for NO_x reduction as the excess of O_2 competes for the reducing agent, in particular CO. The issue of diesel engines is particularly relevant in Europe, where there is a very high incidence of automotive diesel engines.

It is worth recalling that such engines operate at lower temperatures with respect to gasoline engines, which results in the production of lower amounts of NO_x. However, it is in fact the problem of NO_x reduction under oxidising condition which represents the biggest difficulty. The second "peculiarity" is the formation of significant amounts of PM in the case of diesel engines, although some PM is also formed in lean-gasoline engines which use direct fuel injection (DI). Importantly, nowadays many modern gasoline engines use DI technology and accordingly mostly run under lean conditions (Wang-Hansen et al. 2013).

In order to comply with the stringent legislation introduced for these engines, a number of specific post-combustion technologies have been successfully introduced and developed for the individual pollutants from these engines. The following discussion will be organised according to the solutions proposed for individual pollutants. For the sake of completeness, some discussion will also be

devoted to potential solutions which have been tested at the development/research stage, but which, for various reasons, have not been commercialised.

2.2.1 NO_x Technologies

There are two major strategies to control NO_x emissions under oxidising conditions:

- $deNO_x$ (lean-$deNO_x$) catalysts
- NO_x adsorbers (NO_x traps)

It should be noted that a significant amount of research was in the past devoted to a third option, that of direct catalytic decomposition of NO_x (Imanaka and Masui 2012; Roy and Baiker 2009).

$$NO \rightarrow \tfrac{1}{2}N_2 + \tfrac{1}{2}O_2 \qquad (20)$$

This reaction is in fact thermodynamically very favourable. However, despite the significant amount of early research, a catalyst which shows suitable activity and, above all, stability under the severe conditions of automobile exhaust has not been found and the focus has shifted to the other options.

2.2.1.1 NO_x Storage-Reduction (NSR) Catalysts

The NO_x storage-reduction (NSR) catalyst (concept), sometimes called lean NO_x trap (LNT) or NO_x adsorber catalyst (NAC), was developed and commercialised by Toyota (Matsumoto 1997; Miyoshi et al. 1995; Takahashia et al. 1996) for lean-burn engines. The operating principle is illustrated in Fig. 7. Under oxidising conditions, NO is oxidised to NO_2, which is stored at the surface of an alkaline storage component. The storage component is usually barium, but strontium may also be used. Periodic switching to a fuel-rich exhaust, achieved by fuel injection, results in release of the stored NO_x species, which are reduced to N_2 over a TWC-type catalyst.

The mechanism of NO_x adsorption and desorption/reduction has been extensively investigated. Although the storage/reduction is rather complex process, there is general consensus that the majority of NO_x is stored as nitrate species. The process of nitrate release has been represented as the reverse of adsorption, due to instability of the stored species in conditions of low O_2 partial pressure (Twigg 2011a).

$$2M(NO_3)_2 \rightarrow 2MO + 4NO + 3O_2 \qquad (21)$$

A major drawback of the NSR catalyst is its sensitivity to SO_x, as surface sulphates are invariably more thermally stable than nitrates. Poisoning of the NO_x storage function is directly related to the amount of SO_2 passed over the catalyst. Although the sulphur content of automotive fuels has now reached very low levels, even trace amounts

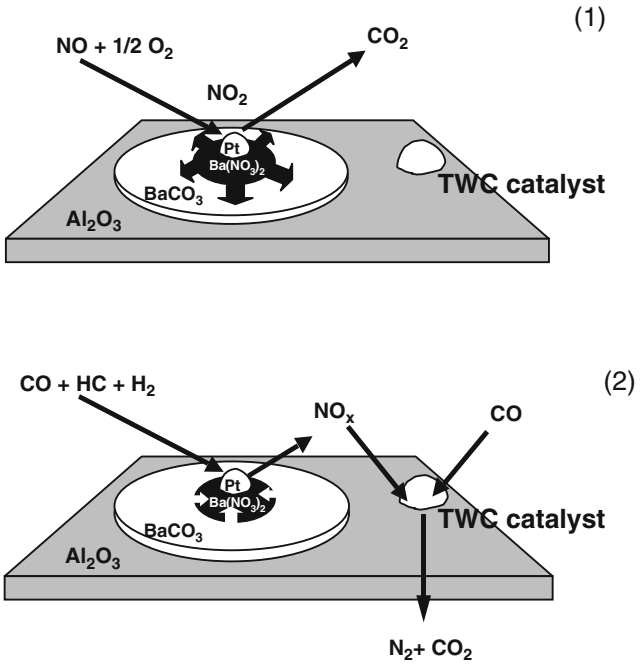

Fig. 7 Principle of operation of a NSR catalyst: NO_x are stored under oxidising conditions (*1*) and then reduced on a TWC when the A/F is temporarily switched to rich conditions (*2*) (Adapted from Twigg 2011b)

cumulatively reduce capacity. It is therefore necessary to periodically apply high temperature regeneration treatments to restore the full storage capacity to the catalyst. For this reason, thermal deactivation due to sintering of the barium species and formation of barium aluminates is an issue in terms of durability of the catalyst. Accordingly, thermally stable Ba-containing materials are desirable as NO_x absorbers. Alternative strategies to protect the storage capacity include:

1. Adoption of a SO_x adsorber to the NO_x trap. This is then periodically regenerated.
2. Modification of the catalyst composition to promote of the removal efficiency of the adsorbed SO_x.

2.2.1.2 Selective Catalytic Reduction (SCR)

SCR refers to the selective reduction of NO_x in the presence of excess O_2. Reduction of NO_x under lean conditions using a NO_x reduction catalyst may be achieved by either utilising the unburnt HCs present in the exhaust or injecting a reducing agent after the combustion to achieve this goal. Of these, the most advanced technology, which is in fact used in diesel applications, is SCR using NH_3 as the reducing agent. In fact, SCR originally referred to this process. However, SCR is normally used to indicate the process for any reducing agent, although SCR-HC and SCR-NH_3 are often used to distinguish the two.

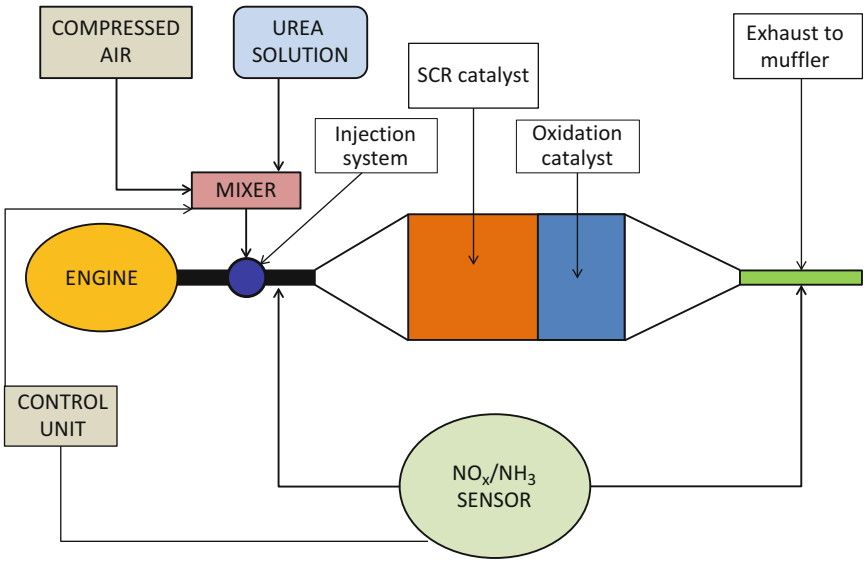

Fig. 8 A typical arrangement for abatement of NO_x from a heavy-duty diesel engine using urea as reducing agent (Adapted from Kaspar et al. 2003)

SCR-HC has been the subject of intensive investigations for over 20 years and represents an important area in ongoing automotive catalytic research. Studies on NO_x removal under oxidising conditions were triggered by the discovery in 1991 that hydrocarbons could act as selective reducing agents in an excess of O_2 (Iwamoto and Hamada 1991). This topic has been regularly reviewed in the intervening years. A large number of catalysts have been investigated, which can be generally divided into three categories (Brandenberger et al. 2008; Burch et al. 2002; He et al. 2008; Liu and Woo 2006):

- Metal-loaded zeolites
- Pt/Al_2O_3 and derived systems
- Ag-cased catalysts (e.g., Ag/Al_2O_3 and Ag/ZrO_2)

Despite the large research effort which has been devoted to this process (Burch 2004), no catalyst has been found which shows an overall adequate conversion, although the last-mentioned systems, which are the most recent to receive attention, do show some very interesting results, e.g., the promotion of low temperature deNO_x activity of H_2 promoted Ag/Al_2O_3 (Breen and Burch 2006) or by using ZrO_2-based supports (Hickey et al. 2010).

SCR-NH_3 is a well-established technology for NO_x abatement from stationary sources (Forzatti 2001). Typically, vanadia supported on TiO_2, with different promoters (WO_3 and MoO_3), are employed in monolith-type catalysts (Forzatti 2001; Sagar et al. 2011), but use of metal-loaded zeolites has also received great attention (Brandenberger et al. 2008). The use of WO_3 and MoO_3 is dictated by the need to increase both the sulphur tolerance and acid properties of the surface. SCR-NH_3 has significant disadvantages when applied to passenger cars or trucks, particularly space and weight requirements. The fact that an engine normally operates in nonstationary conditions is a further difficulty. Nevertheless, SCR using NH_3 has been successfully transferred to the automotive sector, especially for heavy-duty applications.

As ammonia is highly toxic, with consequent storage and transport problems, ammonia or ammonium solutions are not used. Urea solutions are instead used as an alternative in-situ ammonia source for NO_x reduction from heavy-duty diesel vehicles.

A urea-based SCR system is schematically illustrated in Fig. 8. The urea solution is vaporised and injected into a preheated zone where hydrolysis occurs in two steps according to Eqs. 22 and 23:

$$H_2N - CO - NH_2 + \Delta \rightarrow NH_3 + HNCO \quad (22)$$

$$HNCO + H_2O \rightarrow NH_3 + CO_2 \quad (23)$$

The second step is crucial (Koebel and Strutz 2003), in that, if inappropriate conditions are used, the isocyanic acid (HNCO) may polymerise. The products formed are thermally more stable than urea and they may be deposited on the catalyst. This results not only in ammonia loss but may also cause catalyst deactivation. This can be avoided by correct engineering of the injection system. In fact, if the injection nozzle is too close to curves in the exhaust conduit, the formation of solid deposits is possible.

Ammonia then reacts with NO and NO_2 over the catalyst:

$$4NO + 4NH_3 + O_2 \rightarrow 4N_2 + 6H_2O \quad (24)$$

$$6NO_2 + 8NH_3 \rightarrow 7N_2 + 12H_2O \quad (25)$$

The reaction of NO_2 with NH_3 is much slower. However, when equal amounts of NO and NO_2 are present, another reaction mechanism can be involved, the so-called fast SCR.

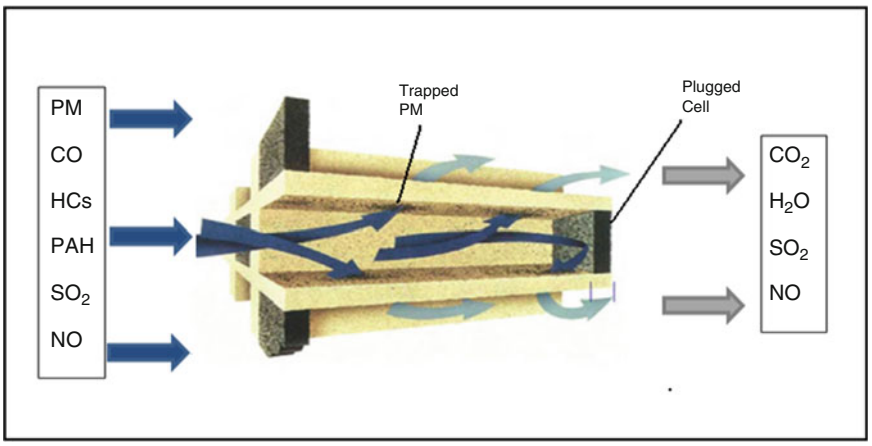

Fig. 9 Schematic representation of a diesel particle filter (*DPF*) (Adapted from Twigg 2011a; Twigg and Phillips 2009)

$$2NH_3 + NO + NO_2 \rightarrow 2N_2 + 3H_2O \qquad (26)$$

As it is fast, this reaction is desirable and it is promoted by placing an oxidation catalyst placed before the SCR catalyst, to oxidise the required amount of NO in the exhaust.

This approach has proved to be quite successful and has been commercially applied in HD diesel engines. High NO_x (up to 80 %) can be achieved on HD engines under driving conditions (Koebel et al. 2004). A major challenge of such system is that an extreme care must be used to develop a suitable urea injection strategy that avoids overloading of the system, leading to ammonia slip. To avoid odour and pollution problems, ammonia slip should not exceed 10 ppm. Nevertheless, this solution is the most reliable for the high NO_x abatement required by incoming EU and US regulations.

2.2.2 CO and HC Emissions

2.2.2.1 Diesel Oxidation Catalyst (DOC)

Abatement of CO and HC is generally achieved by monolithic Pt-based oxidation catalysts. These were first introduced by Volkswagen in 1989, before legislation made their use necessary. However, the introduction of the severe legislation in 1993 made them necessary in all new European diesel cars. Although the excess of oxygen in the exhaust might suggest that oxidation of HC and CO under such conditions is a facile process, the situation is complicated by the fact that the temperatures reached by diesel exhaust and therefore by the diesel oxidation catalysts are low (150–250 °C), especially in urban driving conditions, in addition to other factors, e.g., PM interference/deactivation, which makes the technology quite complex (Russell and Epling 2011).

On engine start-up, the catalyst is unheated and is therefore not active, which results in significant cold-start emissions. In addition, the HCs present can adsorb and block the catalytic sites. At higher temperatures, conversion occurs. Incorporation of thermally stable zeolite adsorbers, which trap the HCs at low temperature and subsequently release them for oxidation at high temperature, significantly improves this situation and reduces cold-start emissions. More serious problems may be encountered in the presence of SO_2 as the temperature is insufficiently high for its subsequent removal. However, the low-sulphur levels now present in automotive fuel means that this is now less problematic. In fact, it has allowed incorporation of Pd into catalyst formulations, which, although less costly, is very susceptible to sulphur poisoning. In such systems, Pd/Pt alloys form, which show higher stability against sintering and higher activity after ageing (Twigg 2011a).

2.2.3 PM Emissions

Diesel particle filters (DPFs) are used to reduce PM emissions from diesel engines. The name is in fact somewhat misleading as such systems are in fact much more complicated than simple filter systems and normally incorporate catalytic functions, using Pt- or Pt/Pd-based catalysts. The most commonly used are porous ceramic wall-flow filters. This is illustrated in Fig. 9. Alternate channels are blocked, which forces the flow through the filter walls, where PM is retained. Accumulation of PM results in gradual build-up of backpressure across the filter which interferes with engine performance and will, if left unchecked, cause the engine to stop. Periodic removal of accumulated PM is therefore necessary. Modern technologies use NO_2 to promote low temperature soot oxidation for diesel particulate filter regeneration, in view of the high oxidation ability of the NO_2 with respect to O_2. However, the efficiency of the process is strongly linked to the exhaust temperature and therefore to driving conditions. It should also be recalled that engine-out NO_2 is usually negligible, so it must be generated in situ with a catalyst.

The reactions involved take place in two separate sections of the device. In the first section, a platinum-based catalyst oxidises the NO to NO_2 according to Eq. 11b.

$$NO + \tfrac{1}{2}O_2 \rightarrow NO_2 \qquad (11b)$$

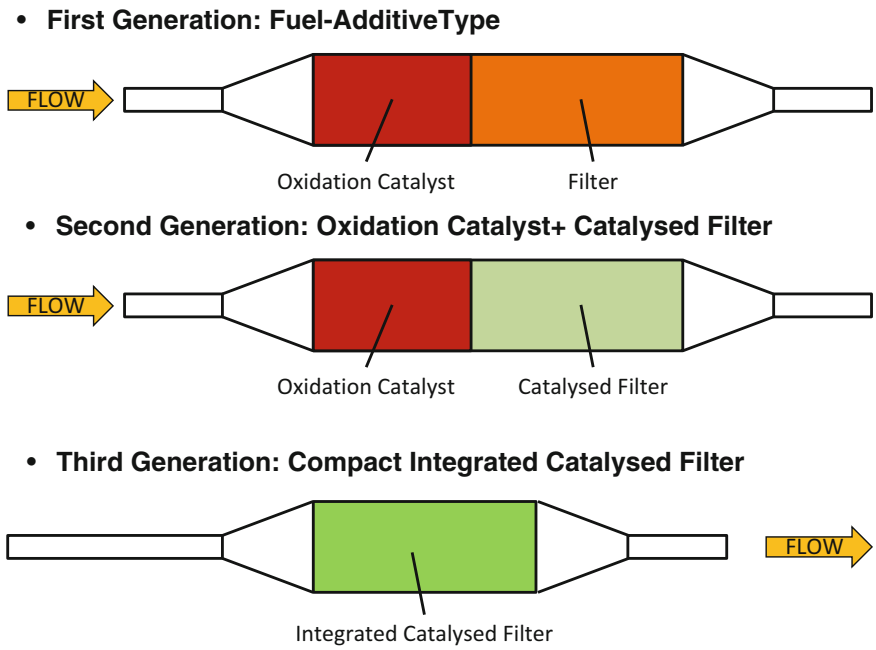

Fig. 10 Diesel particle filter system arrangements (Adapted from Twigg 2011a)

The NO_2 thus produced is then used to oxidise the particulate and uncombusted hydrocarbons, which may be represented by as follows:

$$NO_2 + \text{“CH”} \rightarrow NO + CO_2 + H_2O \quad \text{(unbalanced)} \qquad (27)$$

In urban driving conditions, the temperature usually is too low for this form of regeneration to take place. However, in extra-urban or motorway driving conditions, the exhaust temperature can reach sufficiently high temperatures to promote NO oxidation to NO_2 over the upstream oxidation catalyst and subsequent oxidation of PM by NO_2 on the downstream filter. This is known as passive generation and the concept, developed by Johnson Matthey, is called the Continuously Regenerating Trap (CRT®). It should be noted that NO is produced in the soot oxidation process. In this case, therefore, NO_x abatement is not achieved. When the temperature is too low, as it is under most driving conditions, a form of active regeneration must be used. Additional fuel may be injected and oxidised over the oxidation catalyst. The heat liberated is utilised to initiate PM combustion. Alternatively, the catalyst may be heated electrically.

As outlined by Twigg, three oxidation catalyst/filter arrangements have been developed and commercialised to reduce HC, CO and PM from diesel engines (Fig. 10). The first system employs an oxidation catalyst (or more than one) upstream of a filter. The oxidation catalyst(s) convert(s) NO to NO_2 for passive PM combustion when conditions permit this to take place. CO and HCs are also removed. The catalyst(s) also oxidise(s) extra fuel during active PM combustion. A fuel additive, often ceria based, is used with this system. This is converted to an oxide during the combustion, which, on retention by the filter, catalyses PM combustion. The main disadvantages of these systems are the high cost and partial blocking of the filter by the retained oxide, leading to increased backpressure. Lager filters may be employed to overcome this problem.

The second type is similar to the first in that it contains two separate functions placed in series: oxidation catalyst(s) upstream of a filter. However, in this case the filter is also catalysed. PGMs (Pt or Pt/Pd) are dispersed in the filter channels to promote PM combustion. This is a commonly used configuration. Fuel additives are not use in this system and thus they do not have their associated disadvantages.

The third system, introduced by Johnson Matthey in 2005, combines the oxidation and filter functions in a single design. This system, in addition to HC and CO oxidation, allows both active and passive filter regeneration. This compact design results in a higher thermal efficiency with respect to the other systems.

To summarise, the present and future developments in the field of automotive pollution abatement are strongly linked to market situation. As far as LD vehicles are concerned, Fig. 11 reports the market share of the diesel-powered new LD vehicles sold in Italy. Introduction of the common-rail diesel engine on the market clearly boosted sales of diesel-powered cars peaking at 60 % of market share in year 2006. In the short term, this clearly influenced global emissions and the global warming effect (Tanaka et al. 2012).

Generally speaking, as low CO_2 emissions are pursued in Europe, the recent trend has been towards downsizing of engines (Johnson 2011, 2013), particularly in the A (minicars) and B (small cars) car segments. This favours adoption of the new lean-gasoline engine technology which allows significant fuel saving. Due to the lower emission rates, catalysts containing lean NO_x trap components can

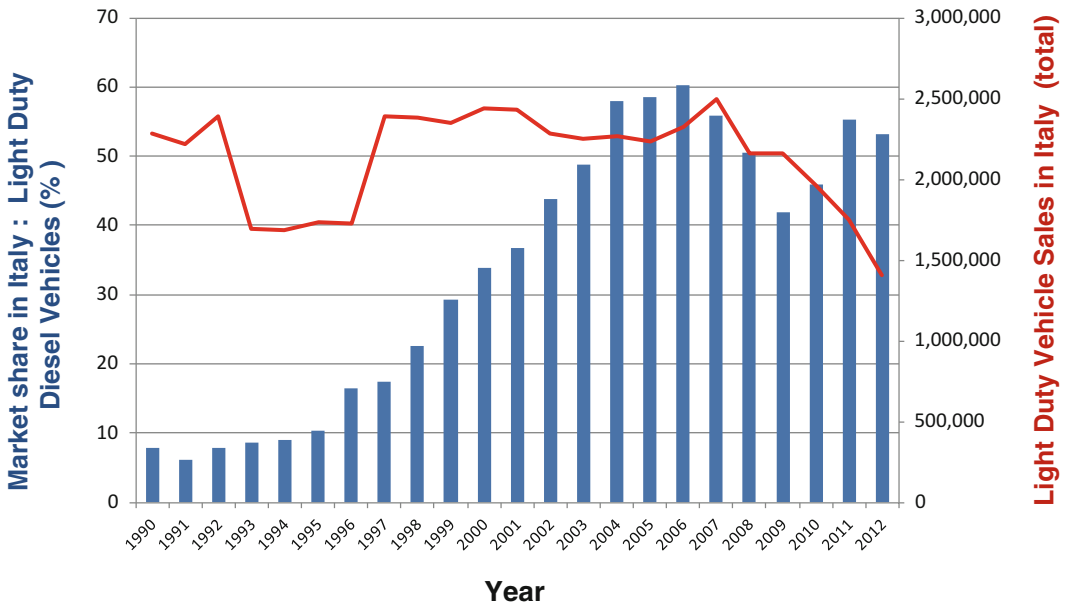

Fig. 11 Market share of diesel-powered new LD vehicles sold in Italy

Fig. 12 Implementation of urea-SCR for LD vehicles would require the installation of a urea distribution network

cope with the issue of NO_x abatement for this type of vehicle. On the other hand, lean-gasoline engines also emit particulates, which requires inclusion of filtering capability to the three-way/lean NO_x catalyst (Twigg 2013).

C– (medium cars) and higher segment light-duty vehicles are mostly equipped with diesel engines. Due to the high emission rates, efficient NO_x control can be achieved only using urea-SCR technology as already used on HD vehicles (Jayat et al. 2011). This will require an extended network of refilling stations (Fig. 12), as the consumption of the urea solution (Ad-blue) accounts for 3–5 % of the diesel fuel consumption. Refilling of urea may also be problematic

since high purity of Ad-blue must be ensured at the refuelling station: Even slight oil contamination can lead to urea-SCR system failure, accordingly research is aimed at finding alternative ammonia sources (Fulks et al. 2009). DOC and catalysed particulate filters represent the state-of-art technology for PM and HC abatement. Combination of DOC, PM filter and SCR and/or NO oxidation functionality catalyst into a single catalyst/filter body represents today's challenge aimed at simplifying the pollution control system.

3 Pollution Abatement for Marine Diesel Engines

3.1 Introduction

Sea transportation, which represents the most economic method of transportation of goods, has increased steadily over the last 30 years or so. In 2007, it was reported that ocean-going vessels transport ca. 90 % of all trade by volume to and from the 25 EU member states and 80 % by weight of all trade in and out of the USA (Friedrich et al. 2007). An obvious consequence of this increase in the world's ocean-going fleet is that it has given rise to a significant increase in airborne emissions from shipping sources. Thus, there is growing awareness that sea traffic has become a major contributor to airborne pollutants (Eyring et al. 2010; Lack et al. 2009; Winebrake et al. 2009). For example, ship numbers and cargo movements indicate that international shipping in 2001 was responsible for ca. 30 % of global NO_x emissions, 9 % of SO_x emissions and 3 % of CO_2 emissions (Eyring et al. 2005; Friedrich et al. 2007).

The problem is especially acute in relation to often more environmentally sensitive coastal areas. Estimates indicate that at any given time, 80 % of the world fleet is either harboured (55 % of the time) or near a coast (25 % of the time), with the result that 70–80 % of all ship emissions occur within 400 km of land (Friedrich et al. 2007; Corbett et al. 1999), although such estimates do vary significantly (Ritchie et al. 2005a). In any case, port areas are often highly populated, and, clearly, the potential health concerns are appreciable. Pollution abatement from seagoing vessels has therefore become a topic of high current interest (Corbett et al. 1999, 2007).

Historically, the absence of specific legislation governing emissions in the marine sector has meant that the development of specific pollution abatement solutions has somewhat lagged behind the automotive and stationary sectors. Thus, while there has been in a sharp decrease in emissions from road transport (Sect. 1.6) and land-based sources in general, those from international shipping sources continue to grow. It was estimated that, in the absence of countermeasures, total NO_x and SO_x emissions from international shipping sources will surpass those from land-based sources in the 25 EU member states by 2020, as illustrated in Fig. 13. However, the recent introduction of legislation and the proposed legislation in the coming years has prompted an upsurge in research interest in methods or technologies to control pollution from ships. Consequently, it is possible to envisage an analogous development to that observed in the automotive and stationary sectors. Indeed, there appears to be considerable overlap between the areas and the same or similar solutions may be transferred from the automotive and stationary sectors to the marine sector. However, as seen from the experience gained in the automotive sector, the specific problems to be resolved and the potential

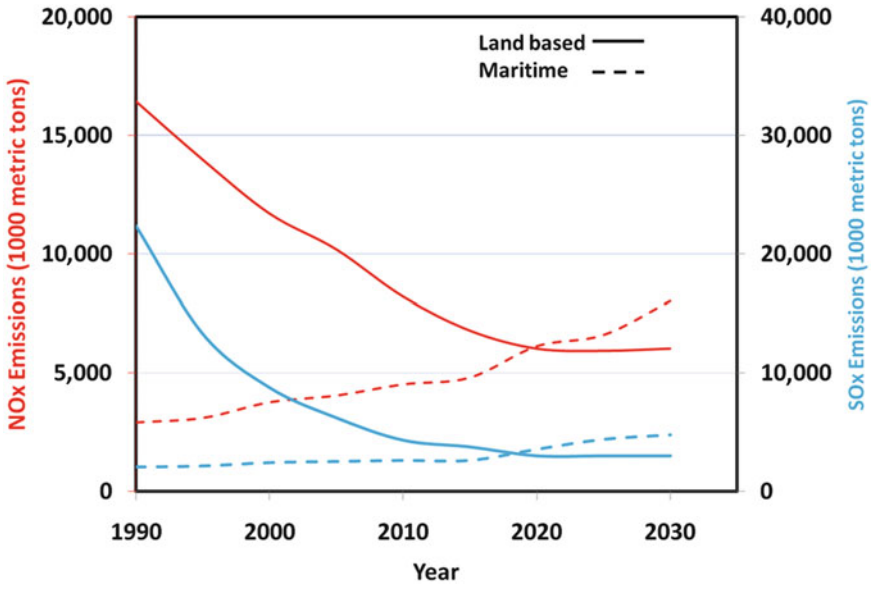

Fig. 13 Inventories and projections of NO_x and SO_x emissions in Europe from land-based and international shipping sources (Adapted from Friedrich et al. 2007)

methods which can be adopted strongly depend on the exact nature of the exhaust gas composition, in addition to a range of other considerations, such as space requirements.

3.2 Emission Legislation in the Marine Sector

The increase in interest in pollution abatement in the marine sector has seen the introduction of a number of general strategic responses. These include legislative measures; voluntary programmes, such the US Environmental Protection Agency's (EPA) voluntary Blue Sky emission standards; and market-based incentive programmes, such as Sweden's Environmentally Differentiated Fairway Dues Program. The last-mentioned programme has been responsible for an increase in the use of low-sulphur fuel in Sweden's ports through the lowering of the fairway dues to be paid in that case. However, the most significant development regards the legislative measures which are coming into force, essentially through the MARPOL 73/78 convention of the International Maritime Organization (IMO) (IMO 2013). Given the international nature of marine transport, it is important to stress the unique position occupied by the IMO, which represents more than 98 % of the global fleet, to introduce a coordinated global response to the problem. MARPOL (Marine Pollution) 73/78 is in fact a voluntary programme, but it is the basis of most proposed legislation for airborne emissions from ocean-going vessels. Born in the aftermath of the Torrey Canyon oil spill, MARPOL 73/78 is an international convention to prevent marine pollution by ships which was adopted in 1973 by the IMO and revised and expanded in 1978. Since then it has been expanded by Annexes specifically addressing various aspects of marine pollution. The issue of environmental problems associated with the marine sector is the responsibility of the IMO's Marine Environment Protection Committee (MEPC), which can propose modification to MARPOL 73/78.

The MARPOL protocol is composed of six annexes, each of which deals with specific aspects related to marine pollution (adoption date indicated in parenthesis):

- Annex I: Regulations for the Prevention of Pollution by Oil (2 October 1983)
- Annex II: Regulations for the Control of Pollution by Noxious Liquid Substances in Bulk (2 October 1983)
- Annex III: Prevention of Pollution by Harmful Substances Carried by Sea in Packaged Form (1 July 1992)
- Annex IV: Prevention of Pollution by Sewage from Ships (27 September 2003)
- Annex V: Prevention of Pollution by Garbage from Ships (31 December 1988)
- Annex VI: Prevention of Air Pollution from Ships (19 May 2005)

Initially, problems related to airborne emissions were not a priority. The first specific air pollution measures, adopted in 1985, were concerned only with SO_x, while in 1988, NO_x limits were incorporated, along with limits for chlorofluorocarbons (CFCs) used as refrigerants. However, the lenient limits for engine emissions did not result in significant advancements towards air pollution reduction and they were replaced by Annex VI. This protocol was ratified by 15 signatory states to MARPOL on the 18th of May 2004 and entered into force on the 19th of May 2005. Since its ratification, the number of signatories to the protocol has grown from 15 (representing 50 % of world tonnage) to the actual value of 170 states, representing more than 97 % of world tonnage (IMO 2013).

The limits fixed by the MPEC in Annex VI for NO_x and SO_x are specified in regulation 13 and regulation 14, respectively. It is important to underline that the two sets of emission and fuel quality requirements are defined by Annex VI: (1) global requirements and (2) more stringent requirements applicable to ships in special Emission Control Areas (ECAs).

3.2.1 MARPOL 73/78 Annex VI, Regulation 14: Sulphur Oxides (SO_x)

In regulation 14, the recommended strategy for decreasing SO_x emissions is based on a significant reduction of the sulphur content in the fuel. This is due to the high sulphur content of currently used marine fuel. It should be recalled that the sulphur content of the fuel is the sole source of SO_x emissions from any internal combustion engine (ICE). The proposed reductions in maximum fuel sulphur content are indicated in Fig. 14. A number of different fuels are available for marine engines. For example, marine heavy fuel oil (HFO) has an average sulphur content of 2.7 % or 27,000 ppm, in comparison to a maximum European sulphur content of 0.001 % or 10 ppm in the automotive sector. The adoption of low-sulphur content fuels is the one of the main reasons for the sharp decrease of SO_x emissions from land-based sources illustrated in Fig. 13. It should be noted that the 4.5 % maximum on the sulphur content of marine fuels is significantly higher than the present average of HFO.

Reduction in the sulphur will also result in a decrease in PM emissions. A US EPA study has estimated that a decrease in fuel sulphur content from 2.7 to 1.5 % would result in PM reductions of 18 %, while a decrease to 0.5 % sulphur would decrease PM emissions by about 63 % (Ritchie et al. 2005b; US EPA 2003). The effect of the quality of the fuel used on PM composition is illustrated in Table 3, which compares the composition and quantity of the PM produced from low- and high-sulphur diesel fuels. With HFO, more PM is produced and it is composed of approximately 65 % sulphates and metal oxides, compared with 15 % with truck diesel. It is clear that the two systems

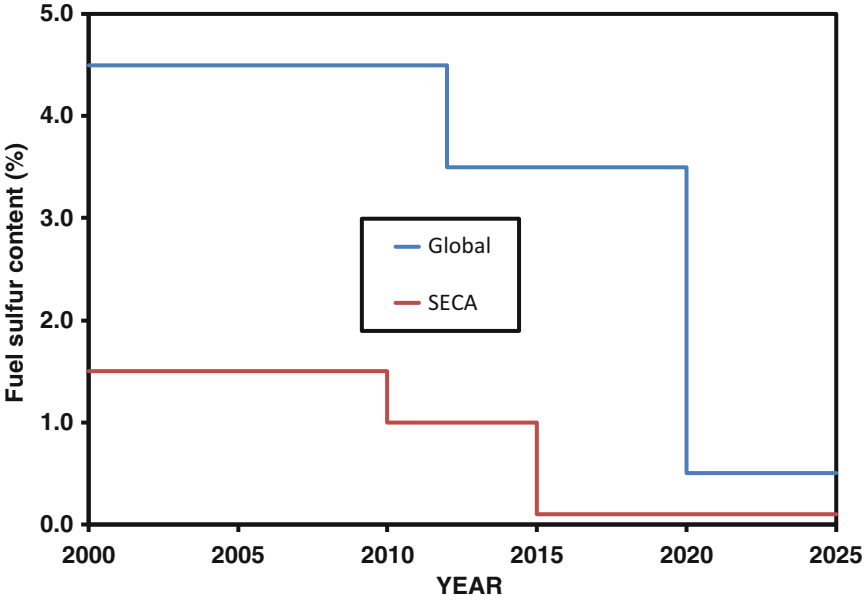

Fig. 14 Development of maximum allowed marine fuel sulphur content proposed by the International Maritime Organization (*IMO*). SECA = Sulphur Emission Control Area

Table 3 Comparison of particulate emission composition

Parameter	Truck diesel engine operating on diesel oil[a]	Medium-speed diesel engine operating on heavy fuel oil[a]
Carbon soot	35 %	25 %
Hydrocarbons (fuel oil, lubrication oil)	50 %	10 %
Ash metal (oxides, sulphates)	15 %	65 %
Typical value	0.15 g/kWh	0. 4 g/kWh
Measurement method	ISO 8178	ISO 9096

Data reproduced from US EPA (2003)
[a]Values are approximate

present rather different challenges in attempts to reduce emissions. This is especially true from the point of view of any catalytic solution. This interrelationship between SO_x and PM emissions illustrates a very important point in the complex process of pollution abatement: Any measure designed to reduce the emissions of one pollutant can also have a strong effect on the emission of others.

3.2.2 MARPOL 73/78 Annex VI, Regulation 13: Nitrogen Oxides (NO_x)

Regulation 13 defines three emission Tiers. Tiers I and II are global requirements, while Tier III is to be applied in any proposed NO_x ECA (NECA). The standards are applied to any marine diesel engine with a power output of more than 130 kW installed after 2000, and any marine diesel engine with a power output of more than 130 kW which has undergone a major conversion after the 1st of January 2000. The emission limits for the three Tiers are reported in Table 4. The emissions are defined in terms of the engine's operating speed, or rpm values, at any given time. Figure 15 illustrates the NO_x limit variations as a function of the engine speed. Comparison of Fig. 15 with the EURO limits for trucks is instructive. For example, the Euro 5 and 6 limits, imposes maximum NO_x emission values of 2 and 0.4 g/kWh. It is evident that only the Tier III NECA NO_x limits have comparable values, but they are still up to five times higher than the automotive HD limits (Lovblad and Fridell 2006).

Table 4 NO_x emission limits for the marine sector

NO_x limit (g/kWh)				
Tier	Date	$n < 130$	$130 < n < 2{,}000$	$n > 2{,}000$
Tier I	2000	17.0	45. $n^{-0.2}$	9.08
Tier II	2011	14.4	44. $n^{-0.23}$	7.07
Tier III	2016[a]	3.4	9. $n^{-0.2}$	1.96

[a]In NO_x emission control areas (tier II standards apply outside ECAs)
n = rotations per minute (rpm)

In an analogously manner to the automotive sector, regulation 13 establishes that the marine engine must have a compliance certificate. To evaluate this compliance, the MPEC has adopted various engine test cycles. Moreover, the compliance of the engine must be certified on a yearly basis.

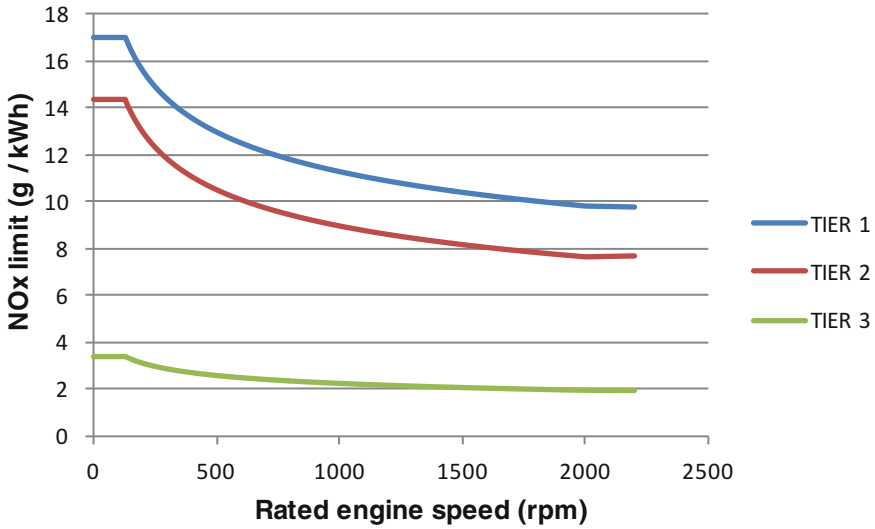

Fig. 15 Evolution of the International Maritime Organization (*IMO*) NO_x limits on the basis of the engine speed

Finally, it is worth noting that Annex VI leaves to the individual states the responsibility to impose limits for the other pollutants, such as CO, HC and PM.

3.2.3 Emission Control Areas

An important provision of Annex VI is that of the possibility to designate ECAs. Two Sulphur Emission Control Areas (SECAs) were established immediately. The Baltic Sea, which came into force on 19 May 2006, was the first SECA, while the second SECA is composed of the North Sea and the English Channel and came into force on 22 July 2007. More recently, in 2012, North American Emission Control Areas (SECA and NECA) were established. This includes all of the North American coastline and the Caribbean Sea. France was a co-proposer of this ECA on behalf of its island territories of Saint Pierre and Miquelon. On a worldwide level, further ECAs are planned, including the Mediterranean Sea.

In 2002, the European Commission adopted a strategy to reduce atmospheric emissions from seagoing ships. The current EU position, which is a modification and extension of Annex VI of MARPOL, is outlined in EU Directive 2005/33 on the sulphur content of marine fuel.

The provisions adopted include:

- Implementation of the SO_x Emission Control Areas defined in the IMO's MARPOL Annex VI convention.
- The use of <1.5 % sulphur after 2007 by all passenger vessels on regular services to or from any port within the EU.
- The use of <0.2 % sulphur fuel (0.1 % by 2008) by all ships at berth in all EU ports. Ships which use shoreside electricity are exempt from this requirement.
- The use of 0.1 % sulphur fuel from 2010 by ships travelling on inland waterways.

In addition, ratification of MARPOL Annex VI, including the NO_x emission standard, was encouraged.

In 2003 the USA adopted the Annex VI NO_x standards for international marine diesel engines built after 2004. In addition, the voluntary US EPA Blue Sky standards set much more stringent limits than the rather lenient MARPOL initial standards.

It should be apparent from the above discussion that there is a clear movement towards the introduction of worldwide mandatory limits on emissions from ocean-going vessels. In regulation 14, the strategy of switching to low-sulphur fuels is emphasised. However, alternative approaches are possible. Regulation 4 of Annex VI, *Equivalents*, establishes that any alternative method of reducing emissions is permitted if the method can be shown to be "at least as effective in terms of emissions reductions as that required by this Annex". Alternative methods comprise "any fitting, material, appliance or apparatus to be fitted in a ship or other procedures, alternative fuel oils or compliance methods". Broadly speaking, this means that any pollution abatement measure which meets the emission standards for SO_x or NO_x may be employed. This, of course, opens the possibility of the introduction of post-combustion pollution abatement technologies.

In the case of SO_x emissions, the high costs associated with a switching from high-sulphur content residual oils (ROs) to low-sulphur content marine distillates (MDs) make such measures unattractive mainly from an economic point of view. Thus, "low"-sulphur-containing fuels employed in international shipping are often made of blends, leading to a low environmental advantage (Mestl et al. 2013). Consequently, post-combustion treatment of the flue gas is an approach which has attracted strong interest. Moreover, the possibility to use abatement systems eliminates the problem of switching between different fuels while entering or leaving an ECA (see sect. 3.3.2), which is necessary under the MARPOL

convention. In the case of NO_x emissions, the introduction of post-combustion emission control technologies will almost certainly be necessary. In fact, according to the US EPA, Tier I standards were already respected by the engines and engine modifications were needed to respect Tier II standards, while Tier III standards can only be met by pollution abatement systems.

3.3 Strategies to Reduce Pollutant Emissions in the Marine Sector

As in the automotive sector, both *primary methods* and *secondary methods* are strategies which are actively pursued to reduce emissions from ships, as both offer the possibility to achieve significant reductions. In the following sections, the possible solutions adopted in both cases will be outlined and analysed. It should be noted that the abatement performance data cited in the present section have been taken from references de Jong et al. (2005) and Wahlström et al. (2006) and references therein.

One of the proposed strategies to reduced emissions from ships is the use of shoreside electricity by ships at berth. This is a measure which would considerable reduce *local* emission given the amount of time that ships spend at berth. However, with this measure the problem of pollution abatement is merely shifted to the source of the electricity used and, clearly, the emissions inventory depends on the method of electricity generation. This option will not be further discussed here. Similarly, emissions trading and other market-based solutions will not be considered.

The nature of the problem of abatement of airborne emissions from marine sources is on one level similar to that of diesel engines for road vehicles, especially in relation to NO_x and particulates PM, for which the same problems have been addressed. It is therefore unsurprising that inspiration has been sought from the wealth of experience gained in this area. However, as already indicated, marine diesel and other heavy fuel oils have the added complication of very high sulphur content relative to that found in fuels for road vehicles. In the following, the technical options in relation to NO_x abatement will first be discussed, before addressing the problem of SO_x emissions. As will become clear, the two subjects are not completely independent.

3.3.1 NO_x Reduction Methods

A considerable number of technological options are available for reduction of NO_x from marine vessels (de Jong et al. 2005). These include:

- Internal engine modifications (IEM)
- Technologies which introduce water in the combustion process
- Exhaust gas recirculation (EGR)
- Selective catalytic reduction

The first three options are preventative measures whose aim is to reduce NO_x formation during the combustion process by optimising the combustion conditions or controlling the combustion temperature. Such changes include addition of water to the combustion chamber to decrease the combustion temperature, improved air charge characteristics or altered fuel injection systems (Lovblad and Fridell 2006).

3.3.1.1 NO_x Reduction Through Internal Engine Modification

A large number of parameters influence the combustion process in the reaction chamber: the compression ratio, injection and valve timing, the size and dimension of the fuel spray, etc. Engine modifications which influence these parameters have therefore been adopted to reduce emissions.

Internal engine modifications (IEM) are divided into two categories: basic IEM and more advanced IEM. Basic IEM essentially involves installation of slide valves, which offer the possibility of better fuel spray characteristics. This type of injector optimises the combustion temperature with a better atomisation of the fuel, thus avoiding the characteristic temperature spike on fuel injection. In this way, a 20 % decrease in NO_x emission is possible. Moreover, fuel combustion is improved, minimising the emissions of HC and PM. The main drawback of this solution is that it is applicable only to the slow two-stroke engines. However, the costs are limited and the modifications can be realised during a routine maintenance work.

Advanced IEM include:

- Retarded injection/Miller cycle valve timing
- Higher compression ratio/adjustable compression
- Increased turbo efficiency/two-stage turbocharger
- Common-rail injection/flexible injection system/two-stage injection
- Higher cylinder pressure
- Low intake air temperature

Retarded fuel injection optimises combustion efficiency. The premixing burning phase is reduced, thereby reducing the temperature and pressure in the cylinder, which leads to NO_x reductions of up to 30 %. This solution can be adopted using both mechanical and electronic control devices. The former system implies that the efficiency is achieved only in a limited range of engine regimes, while the second allows high efficiency to be obtained across a wide range of regimes but is applicable only to engines using light fuels.

The main drawbacks of this measure are increased PM emission and a reduction in specific power output, together with higher consumption of fuel. Moreover, significant engine modifications are necessary to efficiently apply this technology.

In the multiple injection solution, the fuel is injected in a calibrated sequence instead of a single injection. A first injection is made to create a homogeneous flame front and this is followed by another injection containing the rest of the fuel. This limits the pressure and temperature peaks typical of the single injection systems, which in turn leads to a maximum decrease in NO_x of ca. 20 %, while avoiding an increase in PM emission. The main disadvantages of the system are related to the costs of installation and maintenance.

In the common-rail fuel injection system, the injection temperature and pressure are controlled electronically, and the fuel injection pressure, which reaches values 2 or 3 times higher than that reached by systems utilising the traditional fuel pump, is maximised. The resulting accurate control in the flame characteristics leads to a decrease in both NO_x formation and fuel consumption. As with retarded fuel injection, this system is not easy to apply to heavy fuel oil (HFO) and is more suitable to engines running on marine distillates (MD).

Cooling of the inlet air decreases the maximum temperature reached in the combustion chamber, which reduces NO_x emissions by about 10–14 %. As the air used is already cold before entering the combustion chamber jet for the medium-speed and low-speed engine, the solution is applicable only to the fast diesel engine. Moreover the solution implies an investment cost to install the air treatment system.

Sometimes a combination of these primary techniques is adopted. In general, the main combinations involve an increase in the injection pressure and optimisation of fuel atomisation, to achieve a more homogeneous combustion.

3.3.1.2 NO_x Reduction by Decreasing the Combustion Temperature

Another general strategy to reduce NO_x emissions is to lower the combustion temperature. A number of conceptually similar techniques operate by introducing water into the combustion process. These are often used in conjunction with exhaust gas recirculation (EGR). General drawbacks of these systems are that they require additional treatment and mixing apparatus and many require freshwater storage. Many are still at a development stage.

3.3.1.2.1 Direct Water Injection (DWI)

In this system, developed by Wärtsilä, a calibrated amount of water is introduced into the combustion chamber. To avoid effects on engine operation, if the water is stopped, the water injection apparatus is independent from that of the fuel. The water to fuel ratio is typically 0.4–0.7 and NO_x reduction of 50–60 % is achieved. The main drawbacks are a significant increase in both fuel consumption and particulate emissions. The system is not suitable for high-sulphur fuels and residual oils, and it is expensive, due to the need to have freshwater storage and treatment systems as well as the need to frequently substitute the injector.

3.3.1.2.2 Combustion Air Saturation System (CASS)

This is a similar system developed by Wärtsilä, in which water is injected into the combustion air and enters the combustion chambers as steam. This can result in a 30–50 % decrease in NO_x emissions.

3.3.1.2.3 Water in Fuel Emulsion, Water-Fuel Emulsion (WiFE, WFE)

The WiFE method is a well-established technology which has been the subject of attention for marine engines over the last 20 or so years. The water and fuel are mixed before the injection to form a micro-emulsion in which small water droplets are surrounded by the fuel. The injection produces a fine spray in which the droplets explode due to rapid water evaporation, thereby increasing the air/fuel mixing. This reduces NO_x formation, with a simultaneous reduction in CO, PM and HC formation. The NO_x and PM emission reductions observed are proportional to the water content in the fuel. The general consensus seems to be that the reductions achievable depend on the water percentage of the emulsion, with a 1:1 ratio in the case of NO_x and a 1:2 to 1:3 ratio in the case of PM (i.e., 30 % of water reduces NO_x by 30 % and PM by 60–90 %). The technique is limited by an upper limit of water which can be effectively employed, which is approximately 30 %. The process also results in an increase in fuel consumption.

3.3.1.2.4 Humid Air Motor Technology (HAM)

Developed by MAN, combustion temperature reduction and elimination of temperature spikes are both achieved by the addition of steam to the inlet air. To reach significant reductions, the amount of steam introduced must be at least three times higher than the amount of fuel. Importantly, seawater can be used in this system. The main disadvantages are the costs and complexity of the steam plant. This solution is cheaper than the costly ammonia SCR approach to NO_x abatement (vide infra). However, HAM technology can reach 70 % NO_x reduction, while SCR reaches 90 % (see Table 5).

3.3.1.2.5 Exhaust Gas Recirculation (EGR)

EGR is a well-established method of pollution abatement in the automotive sector which can be applied to any engine. The exhaust is filtered and reintroduced into the combustion chamber after cooling. Due to the higher thermal capacity of

Table 5 Estimated emission reduction efficiencies of various deNO$_x$ techniques

	% Emissions reduction (−)/increase (+) per vessel			
Measure	NO$_x$ (%)	SO$_2$ (%)	PM (%)	VOC (%)
Basic IEM (2 stroke slow speed only)	−20	0	0	0
Advanced IEM	−30	0	0	0
Direct water injection	−50	0	0	0
Humid air motors	−70	0	0	0
Exhaust gas recirculation[a]	−35	−93	≥63[b]	±[c]
Selective catalytic reduction (2.7 % residual oil (*RO*))	−90	0	0	0
Selective catalytic reduction (1.5 % RO)	−90	−44	−18	±
Selective catalytic reduction (0.1 % marine distillate (*MD*))	−90	−96	≥63[d]	±

Data reproduced from de Jong et al. (2005)
[a]Assumed switch from 2.7 % sulphur residual oil (*RO*) to marine diesel (*MD*) for technical reasons
[b]US EPA 2003 outline that a switch from 2.7 % sulphur RO to 0.3 % MD reduces PM by 63 %. The PM reduction to 0.1 % MD will therefore be slightly higher than 63 %
[c]± no or not conclusive information available
[d]PM reductions estimated in the same way as for EGR

the exhausts, the combustion temperature, and consequently the emitted NO$_x$, is reduced. The main problem is related to PM removal because its introduction in the chamber can lead to the formation of solid deposits, to lubricating oil contamination, to valve fouling, etc. Due to the difficulty to remove or reduce PM emission for HFO, the system should be applicable only with low-sulphur fuel (LSF) and distillate fuel.

3.3.1.3 NO$_x$ Reduction Through the Use of Alternative Fuels

The possible use of alternative fuels has also received attention in recent years and the main fuels studied are methanol and liquefied petroleum gas (LPG). The potential use of methanol is still at a research stage because of the great differences in density, viscosity, heat capacity and ignition temperature between methanol and oil fuels. LPG is a more developed alternative because its characteristics are more similar to marine fuel oil. The use of LPG can result in significant decreases in NO$_x$ emission, but security problems related to fuel storage are an issue.

The abatement efficiencies of the various prevention measures discussed above are summarised in Table 5. The efficiency of ammonia SCR (vide infra) is included in the comparison to offer an overall comparison of the efficiencies of the various deNO$_x$ methods discussed.

3.3.1.4 Selective Catalytic Reduction

SCR with urea has been successfully transferred from stationary and automotive sources to the marine sector and is, thus far, the only commercial post-combustion deNO$_x$ solution applied on board ships. The on-board SCR was pioneered by Haldor-Topsøe A/S and MAN B&W Diesel A/S which lead, in 1989, to the installation of the first marine SCR deNO$_x$ unit on a 37,000 tdw deep-sea bulk carrier the Pacific Princess. The system was installed for the first time on a ferry, the M/S Stena Jutlandica, in 1997, on all main as well as auxiliary engines. Other commercially available SCR system are the Siemens SINO$_x$ system and the Munters Diesel Emission Control Selective Catalytic Reduction (DEC SCR) Converter System, which was first delivered in 1991. An on-board SCR system is analogous to that described for heavy-duty diesel applications, the differences being mainly related to the scale. The catalyst housing usually replaces the silencer in the exhaust uptake as SCR systems also effectively reduce noise. The SCR catalyst can be fitted with the optional of an oxidation catalyst, which can effectively reduce emissions of VOCs from the exhaust. Cooper and Gustafsson report that 45 % of ships on international routes which are fitted with an SCR system also have an oxidation catalyst (Cooper and Gustaffson 2004). Catalyst formulations are similar to those used in stationary sources (sect. 2.2.1.2).

3.3.1.4.1 Advantages and Disadvantages of Ammonia SCR

The SCR technique has a number of advantages which render it particularly suitable for installation in seagoing vessels (see below). The disadvantages associated with this technology are mostly the same as those which encountered for on-road diesel engines, with some differentiation due to scale, disadvantages which have not been overcome but which must be accepted. There are, however, a number of specific problems related to the marine sector that must be considered. The most important aspect is the high content of sulphur in the marine fuel which detrimentally affects the activity of the SCR catalyst, particularly those based on V_2O_5 (Huang et al. 2002, 2003). As a matter of fact, SO_2 is easily oxidised to SO_3 and this species tends to strongly bind to the surface. Both ammonia sulphates and bisulphates may form at low reaction temperature which, being solid, leads to pore plugging and catalyst deactivation. Furthermore, the ammonia that reacts is not used for the reduction process, leading to a decrease of the efficiency of ammonia

utilisation. Despite these disadvantages, urea-SCR offers one of the very few established post-combustion techniques to achieve significant NO_x reductions in the marine sector.

Flexibility

It has no effect on engine operation or design and can be easily fitted on a new engine or retrofitted on an existing engine, with no apparent limitation on ship or engine type.

Catalyst Lifetime

SCR catalysts are not resistant to sulphur poisoning. While catalyst formulations can be varied to strike a balance between high SCR activity and tolerable SO_2 resistance, catalyst performance invariable does degrade upon sulphur exposure and catalyst lifetime can be prolonged by using low-sulphur content fuels. Thus, the optimum situation, from the point of view of catalytic performance, is an SCR system running with such a fuel. However, these fuels are considerably more expensive. On the other hand, the use of more expensive fuels with low sulphur and other impurities may reduce overall costs by less frequent catalyst substitution, so the situation must be carefully evaluated. The experience gained indicates that with <1.5 % sulphur, the reactor may have to be replaced every 4–5 years, while with 2.7 % sulphur replacement may be necessary every 3 years (de Jong et al. 2005; Lovblad and Fridell 2006). With this information, the costs of catalyst replacement and fuel switching can therefore be compared and optimised.

A further significant problem in the case of marine diesel engines is pore blockage through deposition of calcium sulphate ($CaSO_4$) which forms after the combustion chamber. This drastically reduces the number of active sites available to the gas and will eventually result in a complete loss of activity. Other potential poisons include oxides of potassium, sodium, calcium, arsenic and phosphorous. The problem of deactivation of the catalyst through deposition of solid matter, in particular at the front of the catalyst, can be rather effectively attenuated by the incorporation of dust blowing systems into the catalytic system. Another technological option to prevent this problem is incorporation of filters before the catalyst.

Operating Materials

Aqueous solutions of urea are used as the source of ammonia. Urea solutions are commonly available, so supply is not a problem and cost is relatively low. In addition, they are non-poisonous and odourless and are considered relatively safe to transport and store at ambient temperature and pressure. However, at low ambient temperatures, the solution may freeze, which necessitates suitable storage conditions.

Space and Weight

SCR installations have considerable space and weight requirements: In addition to the space required for the SCR system (and the oxidation catalyst, if installed), large urea storage tanks are necessary.

Installation and Operation Costs

From a commercial point of view, the cost of installing the SCR plant is one of the biggest disadvantages. In addition to the basic investment for the system, other costs include the raw materials needed to operate the system, the higher fuel consumption due to the added weight of the catalytic reactor and urea storage tank and the need to dedicate specialised personnel to operate and maintain the system, which usually include sophisticated control systems. Routine maintenance, such as cleaning of the urea spray nozzles, is particularly important as their blockage can result in ammonia slip. As always, the issue of cost/benefit is often intangible and difficult to assess. However, the fact that SCR systems are now rather well established removes much of the guesswork.

Variables in Operating Costs

The concentration of the solution is an important consideration, and, from the point of view of minimising on-board storage space requirements, which in turn affects operational costs, very concentrated solution would clearly be preferred. However, there are limitations. A 40 % solution can be stored and used where the temperature remains above 0 °C. A 35 % solution, on the other hand, can be stored at temperatures down to −15 °C. Thus, in colder seas, such as the Baltic Sea SECA, 35 % solutions must be used. If it is necessary to use very large amounts of ammonia, such as in the case of longer voyages, another option is to store urea in the form of pellets and prepare the urea solution on-board. The cost of these possibilities must be evaluated on a case-by-case basis.

Catalyst Warm-Up

As discussed in Sect. 2, this is a problem common to many depollution catalysts. SCR catalysts have a minimum useful operational temperature (in the case of SCR catalysts, about 270 °C). However, as the heating process is normally achieved by the exhaust gases themselves, there is a time delay between start-up and adequate functioning of the catalyst. This result in a warm-up time (around 20–30 min), during which the NO_x reduction is non-existent or low. This may be a problem in a harbour, where the lowest emissions possible are necessary.

Urea Economy and Ammonia Slip

Urea reaction economy indicates the actual amount of used urea, with respect to reaction stoichiometry. In particular, it has been reported that the formation of various types of ammonium sulphates and bisulphates, as well as the polymers

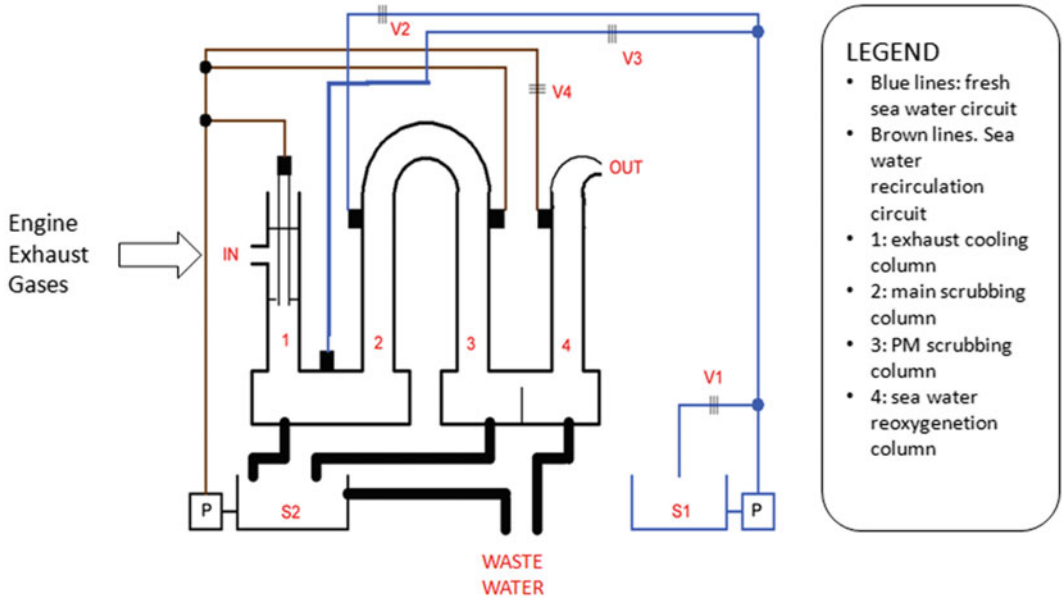

Fig. 16 Schematic representation of an on-board seawater scrubbing system

mentioned above (sect. 2.2.1.2), decreases the NO_x conversion to N_2. To maximise the conversion, an excess of urea is generally used. This varies in function of the sulphur content in the fuel. Ratios of 1.2:1 or higher are usually used.

Under normal operating conditions, the problem of ammonia slip is most likely to occur with load variations. The consequent odour problems are especially unwelcome in the case of passenger ships. The phenomenon can also result in downstream corrosion problems. Although SCR systems incorporate a feedback control loop to address the issue of correct dosage of the urea solution, brief episodes of ammonia slip can still occur due to control response factors. The possibility of ammonia slip is enhanced at higher space velocities, even when the system is operating correctly. Another possible source of ammonia slip is incorrect or inadequate maintenance of the urea injection system. Ensuring that the urea injection nozzles do not become blocked is a vital part of the maintenance procedures.

3.3.2 SO_x Reduction Methods

Two main options are considered as potential SO_x reduction methods in marine applications:

1. Fuel switching
2. Seawater scrubbing (SWS)

The fuel switching option includes both the reduction of fuel sulphur content and the practice of on-board fuel switching when necessary, for example, when entering a port or a SECA. Reducing sulphur content represents a concrete preventative abatement measure which is immediately applicable. However, there are a number of disadvantages associated with this approach. The high costs associated with a switching from high-sulphur content residual oils (ROs) to the low-sulphur content marine distillates (MDs) make such measures unattractive from an economic point of view for the shipowners, even though such option can be attractive on a global scale (Wang et al. 2007). In addition, for application of on-board fuel switching, significant changes to the ship would be required: extra fuel tanks and modifications to fuel pumps, fuel circuits and even to the engine. This overall increase of complexity of the system, along with the concomitant necessity of more expensive maintenance, is another economic drawback. Finally, fuel switching has only a moderate effect in the case of NO_x emissions, which means that separate solutions need to be found for this pollutant.

Several pollution control techniques have been evaluated for shipping (Farrell et al. 2002), but seawater scrubbing is the only technological option considered suitable. In general, SO_x scrubbing is a consolidated technology which has been used for many years in flue gas desulphurisation (FGD) applications (Rajendran et al. 1999; Srivastava et al. 2001). A number of options are available: the limestone/gypsum system, the spray dry system, the Wellman-Lord process and seawater scrubbing. The first large-sized FGD process was installed at the Battersea in London in 1930. The first seawater scrubber was introduced in 1988 at the Statoil refinery in Mongstad, Norway. Seawater scrubbing installations are now quite common all around the world.

The transfer of the SWS process from land-based applications to marine applications is a process in an advanced state of development. Commercial on-board SWS systems are now available, such as the Krystallon Seawater Scrubber (BP Marine and Kittiwake Developments Ltd). A schematic representation of a SWS system is illustrated in Fig. 16. It is clear that the overall systems are complicated and

Fig. 17 Scheme of the strategy adopted in the ECOMOS project, aimed at developing an integrated method for abatement of the main pollutants emitted from a marine engine

involve elaborate systems for water treatment and process control. The common factor in all seawater scrubbing systems is intimate contact between the exhaust gas and seawater, during which the SO_2 present is transferred to the seawater.

3.3.2.1 Advantages and Disadvantages of Seawater Scrubbing

Very high SO_x and PM abatement efficiencies can be achieved using the SWS technique. An important characteristic of seawater is its pH: Seawater is naturally basic with a pH which ranges from 8.0 to 8.2. It is therefore a more effective scrubbing medium than freshwater. The capacity of the scrubbing water can be increased by addition of alkaline (usually lime), but this has added cost and space requirements.

Formation of sulphuric acid mists is a potential problem associated with sulphur scrubbing processes. Their formation depends on the concentrations of SO_3 and water vapour in the gas stream as well as the temperature. The process is a well-known phenomenon in SO_2 scrubbing processes *after* the scrubbing step, where the temperature of the flue gas is below the sulphuric acid dew point. A number of consolidated countermeasures, above all droplet separators, are available to combat the problem.

The main environmental concern surrounding seawater scrubbing is the quality of the water discharged from the scrubbing unit. Factors which must be considered include the pH of the discharged liquid, the presence of sulphites and the presence of other potentially harmful species. Due to the high quantity of sulphates already present in seawater, it is commonly considered that sulphates which remain in the used scrubbing water can be safely discharged into the sea without significant environmental impact. The IMO OILPOL fixes a maximum concentration of petroleum hydrocarbons which can be discharged overboard at 15 ppm (IMO 2013). The IMO has not specified limits for other components and characteristics of discharge water, such as pH, suspended solids and heavy metals. Ideally, the discharge water should not significantly affect the pH of seawater (a very sensitive parameter for sea life), but it should be oxygenated to ensure that the chemical oxygen demand (COD) is not high (thus, sulphite discharge should be avoided) and PM discharge is undesirable. With regard to pH, seawater contains a natural carbonate buffer system and the indications from the test results are that dilution of the used water does not result in significant pH variations. Water treatment procedures are incorporated in the commercial systems to ensure both oxygenation of the scrubbing liquid and PM abatement (see Fig. 16).

3.3.2.2 Integrated NO_x/SO_x Abatement Systems

Integrated systems are not commercially available. An early demonstration of a seawater scrubber in conjunction with a selective catalytic reduction unit and particle eductor has been reported. This was installed in 1993 and showed an SO_2 removal efficiency of 90 %, with the conclusion that there was potential for even more efficient abatement (Ritchie et al. 2005b). It is not clear why this approach has not been pursued, but it is not difficult to imagine high costs, both for installation and operation, especially with the two technologies in their infancy from the point of view of shipboard application. However, such systems are the subject of current research. We have, in fact, within the ECOMOS[1] project analysed feasibility of an integrated process using an abatement strategy illustrated in Fig. 17. The process was scaled up from laboratory to a pilot plant and showed promising results: removal efficiencies for PM, CO, HC and SO_x of over 90 % and for NO_x of over 35 % could be achieved, highlighting the possibility of integrating the catalytic technology into seawater scrubber pollution control devices, which could make the use of SCR technology onboard ships unnecessary.

[1] The ECOMOS project (Ecological compatibility of ships cruising the motorways of the sea) was cofunded by the Italian Ministry of Education (MIUR) and accomplished by a Consortium lead by Fincantieri C.N.I. and RAM (Mediterranean Network of Motorways of the Sea). Project partners are CETENA (Italian Ship Research Centre), INCA (Inter-university Consortium "Chemistry for the Environment"), University of Genoa, RINA Services, I.M.–C.N.R. ("Engines Institute"-National Research Council), ISSIA – CNR (Institute of intelligent systems for automation), ISMAR – CNR (Institute of Marine Sciences) and CONSAR (Shipowners Research Consortium).

References

Adams, M., van Aatdenne, J., Kampbel, E., Tista, M., Zuber, A.: European Union emission inventory report 1990–2010 under the UNECE Convention on Long-range Transboundary Air Pollution (LRTAP), EEA technical report no. 8/2012, ISSN 1725-2237, (2012) http://www.eea.europa.eu/publications/eu-emission-inventory-report-1990–2010

Benbrahim-Tallaa, L., Baan, R.A., Grosse, Y., Lauby-Secretan, B., El Ghissassi, F., Bouvard, V., Guha, N., Loomis, D., Straif, K., International Agency for Research on Cancer Monograph Working, G.: Carcinogenicity of diesel-engine and gasoline-engine exhausts and some nitroarenes. Lancet Oncol. **13**, 663–664 (2012)

Brandenberger, S., Kröcher, O., Tissler, A., Althoff, R.: The state of the art in selective catalytic reduction of NOx by ammonia using metal-exchanged zeolite catalysts. Catal. Rev. Sci. Eng. **50**, 492–531 (2008)

Breen, J.P., Burch, R.: A review of the effect of the addition of hydrogen in the selective catalytic reduction of NOx with hydrocarbons on silver catalysts. Top. Catal. **39**, 53–58 (2006)

Burch, R.: Knowledge and know-how in emission control for mobile applications. Catal. Rev. Sci. Eng. **46**(3–4), 271–333 (2004)

Burch, R., Breen, J.P., Meunier, F.C.: A review of the selective reduction of NOx with hydrocarbons under lean-burn conditions with non-zeolitic oxide and platinum group metal catalysts. Appl. Catal. B Environ. **39**, 283–303 (2002)

Cooper, D. A., Gustaffson, T.: Methodology for Calculating Emissions from Ships – 1. Update of Emission Factors. IVL report U 878. IVL Swedish Environmental Research Institute, Gothenburg, Sweden. Report series SMED and SMED&SLU Nr 4 2004. http://www.smed.se/wp-content/uploads/2011/05/SMED_Report_2004_4.pdf (2004)

Corbett, J.J., Fischbeck, P.S., Pandis, S.N.: Global nitrogen and sulfur inventories for oceangoing ships. J. Geophys. Res. D Atmos. **104**, 3457–3470 (1999)

Corbett, J.J., Winebrake, J.J., Green, E.H., Kasibhatla, P., Eyring, V., Lauer, A.: Mortality from ship emissions: a global assessment. Environ. Sci. Technol. **41**, 8512–8518 (2007)

de Jong, E., Hugi, C., Cooper, D.: Entec UK Ltd (2005), Report: "Service Contract on Ship Emissions: Assignment, Abatement and Market-based Instruments, Task 2b NOx Abatement" (2005)

Dieselnet: www.dieselnet.com (2013). Accessed in June 2013

EEA: http://themes.eea.eu.int/ (2013a). Accessed in June 2013

EEA: www.eea.europa.eu/themes/air/intro (2013b). Accessed in June 2013

Eyring, V., Kohler, H.W., van Aardenne, J., Lauer, A.: Emissions from international shipping: 1. The last 50 years. J Geophys Res D: Atmos **110**(17), 171–182 (2005). Article number D17305

Eyring, V., Isaksen, I.S.A., Berntsen, T., Collins, W.J., Corbett, J.J., Endresen, O., Grainger, R.G., Moldanova, J., Schlager, H., Stevenson, D.S.: Transport impacts on atmosphere and climate: shipping. Atmos. Environ. **44**, 4735–4771 (2010)

Farrell, A.E., Corbett, J.J., Winebrake, J.J.: Controlling air pollution from passenger ferries: cost-effectiveness of seven technological options. J. Air Waste Manage. Assoc. **52**, 1399–1410 (2002)

Fenimore, C.P.: The ratio NO_2 NO in fuel-lean flames. Combust. Flame **25C**, 85–90 (1975)

Fenimore, C.P.: Reactions of fuel-nitrogen in rich flame gases. Combust. Flame **26C**, 249–256 (1976)

Forzatti, P.: Present status and perspectives in de-NOx SCR catalysis. Appl. Catal. A Gen. **222**, 221–236 (2001)

Friedrich, A., Heinen, F., Kamakaté, F., Kodjak, D.: Air Pollution and Greenhouse Gas Emissions from Ocean-Going Ships: Impacts, Mitigation Options and Opportunities for Managing Growth. The International Council on Clean Transport (ICCT) (2007)

Fulks, G., Fisher, G. B., Rahmoeller, K., Wu, M. C., D'Herde, E., Tan, J.: A review of solid materials as alternative ammonia sources for lean NOx reduction with SCR. SAE Technical Papers, vol. 2009-01-0907 (2009)

Govconsys.: www.govconsys.com/dd_emissions_3-way_catalyst.html. Accessed in June 2013

He, H., Zhang, X., Wu, Q., Zhang, C., Yu, Y.: Review of Ag/Al_2O_3-reductant system in the selective catalytic reduction of NOx. Catal. Surv. Jpn. **12**(1), 38–55 (2008)

Hernandez-Garrido, J.C., Desinan, S., Di Monte, R., Fonda, E., Midgley, P.A., Calvino, J.J., Kaspar, J.: Self-assembly of one-pot synthesized CexZr1-xO 2-BaO-ÀnAl$_2O_3$ nanocomposites promoted by site-selective doping of alumina with barium. J. Mat. Chem. A **1**(11), 3645–3651 (2013)

Hesterberg, T.W., Long, C.M., Sax, S.N., Lapin, C.A., McClellan, R. O., Bunn, W.B., Valberg, P.A.: Particulate matter in new technology diesel exhaust (NTDE) is quantitatively and qualitatively very different from that found in traditional diesel exhaust (TDE). J. Air Waste Manag. Assoc. **61**(9), 894–913 (2011)

Hickey, N., Fornasiero, P., Graziani, M.: Hydrogen-based technologies for mobile applications In: Graziani, M., Fornasiero, P. (eds.) Renewable Resources and Renewable Energy: A Global Challenge, pp. 225–272. CRC Press, Taylor & Francis Group, Boca Raton, Florida, New York (2006)

Hickey, N., Boscarato, I., Kaspar, J., Bertinetti, L., Botavina, M., Martra, G.: Effect of the support on activity of silver catalysts for the selective reduction of NO by propene. Appl. Catal. B – Environ. **100**(1–2), 102–115 (2010)

Huang, Z., Zhu, Z., Liu, Z.: Combined effect of H_2O and SO_2 on V_2O_5/AC catalysts for NO reduction with ammonia at lower temperatures. Appl. Catal. B – Environ. **39**, 361–368 (2002)

Huang, Z., Zhu, Z., Liu, Z., Liu, Q.: "Formation and reaction of ammonium sulfate salts on V_2O 5/AC catalyst during selective catalytic reduction of nitric oxide by ammonia at low temperatures. J. Catal. **214**, 213–219 (2003)

Imanaka, N., Masui, T.: Advances in direct NO x decomposition catalysts. Appl. Catal. Gen. **431–432**, 1–8 (2012)

IMO: http://www.imo.org/. Accessed in June 2013 (2013)

Iwamoto, M., Hamada, H.: Removal of nitrogen monoxide from exhaust gases through novel catalytic processes. Catal. Today **10** (1), 57–71 (1991)

Jacobson, M.Z.: Atmospheric Pollution. History, Science and Regulation. Cambridge University Press, Cambridge (2002)

Jayat, F., Reck, A., Babu, K.V.R.: SCR and SCRI as After-Treatment Systems for Low CO_2 and Low NOx Vehicles. SAE Technical Papers, vol. 2011-26-0038 (2011)

Johnson, T.V.: Diesel Emissions in Review. SAE Technical Papers vol. 4, pp. 143–157 (2011)

Johnson, T.V.: SAE 2012 world congress. Platin. Met. Rev. **57**, 117–122 (2013)

Kaspar, J., Fornasiero, P., Hickey, N.: Automotive catalytic converters: current status and some perspectives. Catal. Today **77**(4), 419–449 (2003)

Koebel, M., Strutz, E.O.: Thermal and hydrolytic decomposition of urea for automotive selective catalytic reduction systems: thermochemical and practical aspects. Ind. Eng. Chem. Res. **42**, 2093–2100 (2003)

Koebel, M., Elsener, M., Kroecher, O., Schaer, C., Roethlisberger, R., Jaussi, F., Mangold, M.: NOx reduction in the exhaust of mobile heavy-duty diesel engines by urea-SCR. Topics Catal. **30/31**, 43–48 (2004)

Lack, D. A., Corbett, J. J., Onasch, T., Lerner, B., Massoli, P., Quinn, P. K., Bates, T. S., Covert, D. S., Coffman, D., Sierau, B., Herndon, S., Allan, J., Baynard, T., Lovejoy, E., Ravishankara, A. R., Williams, E.: Particulate emissions from commercial shipping: chemical, physical, and optical properties. Geophys Res D: Atmos. **114**, D00F04-1–D00F04/16 (2009)

Liu, Z.M., Woo, S.I.: Recent advances in catalytic DeNO(X) science and technology. Catal. Rev.-Sci. Eng. **48**, 43–89 (2006)
Lovblad, G., Fridell, E.: Experiences from Use of Some Techniques to Reduce Emissions from Ships. Swedish Maritime Administration, Goteborg (2006)
Magara-Gomez, K.T., Olson, M.R., Okuda, T., Walz, K.A., Schauer, J. J.: Sensitivity of diesel particulate material emissions and composition to blends of petroleum diesel and biodiesel fuel. Aerosol Sci. Tech. **46**, 1109–1118 (2012)
Matsumoto, S.: Recent advances in automobile exhaust catalyst. Catal. Surv. Jpn. **1**(1), 111–117 (1997)
Matti Maricq, M.: Chemical characterization of particulate emissions from diesel engines: a review. J. Aerosol Sci. **38**(11), 1079–1118 (2007)
McClellan, R.O., Hesterberg, T.W., Wall, J.C.: Evaluation of carcinogenic hazard of diesel engine exhaust needs to consider revolutionary changes in diesel technology. Regul. Toxicol. Pharmacol. **63**(2), 225–258 (2012)
Mestl, T., Løvoll, G., Stensrud, E., Le Breton, A.: The doubtful environmental benefit of reduced maximum sulfur limit in international shipping fuel. Environ. Sci. Technol. **47**, 6098–6101 (2013)
Miyoshi, N., Matsumoto, S., Katoh, K., Tanaka, T., Harada, J., Takahashi, N., Yokota, K., Sugiura, M., Kasahara, K.: Development of New Concept Three-Way Catalyst for Automotive Lean-Burn Engines. SAE Technical Papers (1995)
Painter, D.E.: Air Pollution Technology. Reston Publishing Company Inc., Reston (1974)
Pallapies, D., Taeger, D., Bochmann, F., Morfeld, P.: Comment: carcinogenicity of diesel-engine exhaust (DE). Arch. Toxicol. **87**, 547–549 (2013)
Prockop, L.D., Chichkova, R.I.: Carbon monoxide intoxication: an updated review. J. Neurol. Sci. **262**(1–2), 122–130 (2007)
Rajendran, N., Latha, G., Ravichandran, K., Rajeswari, S.: Flue gas desulphurisation systems – a review. Corrosion Rev. **17**, 443–465 (1999)
Ritchie, A., de Jong, E., Hugi, C., Coooper, D: Entec UK Ltd (2005), Report: Service Contract on Ship Emissions: Assignment, Abatement and Market-based Instruments, Task 2, General Report (2005a)
Ritchie, A., de Jong, E., Hugi, C., Coooper, D.: Entec UK Ltd (2005), Report: Service Contract on Ship Emissions: Assignment, Abatement and Market-based Instruments, Task 2c, $SO_{2\ Abatement}$ (2005b)
Roy, S., Baiker, A.: NOx Storage-reduction catalysis: from mechanism and materials properties to storage-reduction performance. Chem. Rev. **109**(9), 4054–4091 (2009)
Russell, A., Epling, W.S.: Diesel oxidation catalysts. Catal. Rev. Sci. Eng. **53**, 337–423 (2011)
Sagar, A., Trovarelli, A., Casanova, M., Schermanz, K.: A new class of environmental friendly vanadate based NH3 SCR catalysts exhibiting good low temperature activity and high temperature stability. SAE Int. J. Engines **4**, 1839–1849 (2011)
Srivastava, R.K., Jozewicz, W., Singer, C.: SO_2 scrubbing technologies: a review. Environ. Prog. **20**, 219–227 (2001)
Takahashia, N., Shinjoh, H., Iijima, T., Suzuki, T., Yamazaki, K., Yokota, K., Suzuki, H., Miyoshi, N., Matsumoto, S.I., Tanizawa, T., Tanaka, T., Tateishi, S.S., Kasahara, K.: The new concept 3-way catalyst for automotive lean-burn engine: NOx storage and reduction catalyst. Catal. Today **27**(1–2), 63–69 (1996)
Tanaka, K., Berntsen, T., Fuglestvedt, J.S., Rypdal, K.: Climate effects of emission standards: the case for gasoline and diesel cars. Environ. Sci. Technol. **46**, 5205–5213 (2012)
Trovarelli, A.: Catalytic properties of ceria and CeO_2-containing materials. Catal. Rev.-Sci. Eng. **38**, 439–520 (1996)
Twigg, M.V.: Catalytic control of emissions from cars. Catal. Today **163**(1), 33–41 (2011a)
Twigg, M.V.: Haren Gandhi 1941–2010: contributions to the development and implementation of catalytic emissions control systems. Platin. Met. Rev. **55**(1), 43–53 (2011b)
Twigg, M.V.: CAPoC 9: 9th international congress on Catalysis and Automotive Pollution Control. Platin. Met. Rev. **57**, 192–201 (2013)
Twigg, M.V., Phillips, P.R.: Cleaning the air we breathe – controlling diesel particulate emissions from passenger cars. Platin. Met. Rev. **53**(1), 27–34 (2009)
UNFCCC.: http://unfccc.int/resource/docs/convkp/kpeng.html (2013). Accessed in June 2013
US EPA: Final Regulatory Support Document: Control of Emissions from New Marine Compression-Ignition Engines at or Above 30 Liters per Cylinder. U.S. Environmental Protection Agency, Ann Arbor (2003)
US EPA.: http://www.epa.gov/otaq/toxics.htm (2013a). Accessed in June 2013
US EPA.: www.epa.gov/air/toxicair/newtoxics.html (2013b). Accessed in June 2013
Van Rensselar, J.: Tier 4 engines: setting a new standard. Tribol. Lubr. Technol. **67**(2), 32–41 (2011)
Wahlström, J., Karvosenoja, N., Porvari, P.: Ship Emissions and Technical Emission Reduction Potential in the Northern Baltic Sea. Report of the Finnish Environment Institute, Helsinki (2006)
Wang, C., Corbett, J.J., Winebrake, J.J.: Cost-effectiveness of reducing sulfur emissions from ships. Environ. Sci. Technol. **41**, 8233–8239 (2007)
Wang-Hansen, C., Ericsson, P., Lundberg, B., Skoglundh, M., Carlsson, P.A., Andersson, B.: Characterization of particulate matter from direct injected gasoline engines. Top. Catal. **56**, 446–451 (2013)
Winebrake, J.J., Corbett, J.J., Green, E.H., Lauer, A., Eyring, V.: Mitigating the health impacts of pollution from oceangoing shipping: an assessment of low-sulfur fuel mandates. Environ. Sci. Technol. **43**, 4776–4782 (2009)

Air Quality Modelling and Its Applications

Isabel Ribeiro, Joana Valente, Jorge Humberto Amorim, Ana Isabel Miranda, Myriam Lopes, Carlos Borrego, and Alexandra Monteiro

Abstract

Air quality numerical modelling systems are powerful tools for research and policy-making purposes. They describe mathematically the innumerable physical and chemical processes that characterise the atmosphere, with the aim of estimating the air quality levels over a region, ranging from the entire globe to a street, through a long- or short-term analysis. In this chapter an overview on selected air quality models is provided, with examples of numerical applications in the scope of the assessment of the air quality impacts caused by hypothetical changes on emissions, climate and other conditions.

Keywords

Atmosphere • Air quality modelling systems • Emission scenarios • Air quality assessment • Air quality forecasting

1 Introduction

The atmosphere is a complex dynamic and natural gaseous system, essential to support life on planet. Particulate matter and gaseous material emissions from both natural events (like volcanic eruptions, ground dust and salt spray from oceans, among others) and anthropogenic actions (industrial activities, transport services, etc.) may however affect the balance of the atmospheric system and cause air pollution, which could affect human health and damage plants and materials (Jacobson 1999).

The innumerable physical and chemical processes that characterise the atmosphere occur simultaneously and in inter-dependent ways. The dilution and dispersion of pollutants by turbulent transport, their photochemical transformation, the removing of these pollutants by clouds and precipitation and also their agglomeration and deposition via physical-chemical action on soil surface are the most important processes in the atmosphere when assessing air quality. These processes have been studied over the last decades by physicists and chemists, but a full explanation of their atmosphere behaviour is still a challenge in atmospheric sciences (Atkinson 1989; Seinfeld and Pandis 1998; Jacob and Winner 2009).

Nowadays it is possible to predict air quality through numerical air quality models, with uncertainty estimation. These air quality models describe mathematically the behaviour of the pollutants in the atmosphere taking into account the atmospheric processes.

2 Modelling Approaches

Modelling tools to assess the air quality are diverse and based on different approaches. Probably the most important challenge is to select the right model to the intended application, taking into account its main characteristics and the quality of the data available to run the simulation. In this section, an overview about the characteristics of air quality numerical models is performed.

I. Ribeiro • J. Valente • J.H. Amorim • A.I. Miranda • M. Lopes • C. Borrego • A. Monteiro (✉)
Centre for Environmental and Marine Studies (CESAM), Department of Environment and Planning, University of Aveiro, 3910-193 Aveiro, Portugal
e-mail: alexandra.monteiro@ua.pt

G. Cao and R. Orrù (eds.), *Current Environmental Issues and Challenges*,
DOI 10.1007/978-94-017-8777-2_3,

2.1 Types of Models

Several numerical models for the simulation of the dispersion of gaseous pollutants and particulate matter at different scales are currently available. These may go from simple to extremely complex, including box models, Lagrangian or Eulerian models, Gaussian models and computational fluid dynamics (CFD) models (Kumar et al. 2011).

Dispersion aerosol air quality models are usually simple. These models estimate the concentration of air pollutants at specified receptors, considering the dispersion (atmospheric transport, the turbulent atmospheric diffusion and surface wet/dry deposition) but not the chemical transformation processes. The most simple dispersion models use the Gaussian approach (Lutman et al. 2004).

Chemical transport models simulate the changes of pollutants in the atmosphere using a set of mathematical equations characterising the chemical and physical processes in the atmosphere. They became widely recognised and routinely utilised tools for regulatory analysis and attainment demonstrations by assessing the effectiveness of control strategies.

Based on the mathematical approach, models can be classified as Lagrangian or Eulerian models. Lagrangian models consider air parcels that follow a trajectory defined by the atmospheric circulation. The trajectories are normally calculated as linear segments, with the segment length and direction determined by the average wind speed and direction over the appropriate time step (Draxier and Hess 1998). Figure 1 represents the Draxler and Rolph (2011) work under the Fukushima Daiichi nuclear disaster, as an example of a Lagrangian model application (HYSPLIT4 Trajectory Model). Lagrangian models are computationally relatively simple, and they allow an easy determination of transboundary fluxes, and thus Lagrangian models are especially suitable for small number of sources or receptors. On the other hand, Eulerian models consider a mathematical approach anchored to the atmosphere surface (until few kilometres high). Eulerian models are often referred to as grid models, since the framework is a three-dimensional grid, with pollutants being emitted into the grid at the appropriate points (Fig. 2). Unlike Lagrangian models, Eulerian models can include nonlinear phenomena, especially those associated with physical and chemical processes (emissions, dispersion, transport, chemistry and deposition). Therefore, Eulerian models are computationally more demanding than Lagrangian. To simulate and integrate such processes, these models require input data provided by other models (e.g. meteorological or emission data). It is therefore more correct to refer to a system of models, rather than a model (Reid et al. 2007).

Air quality models can also be classified with respect to the scale of the phenomena they are developed to simulate. In fact, scale separation has proven to be a quite successful approach for atmospheric modelling, because different approximations and parameterisations can be applied for the different phenomena occurring at the different scales.

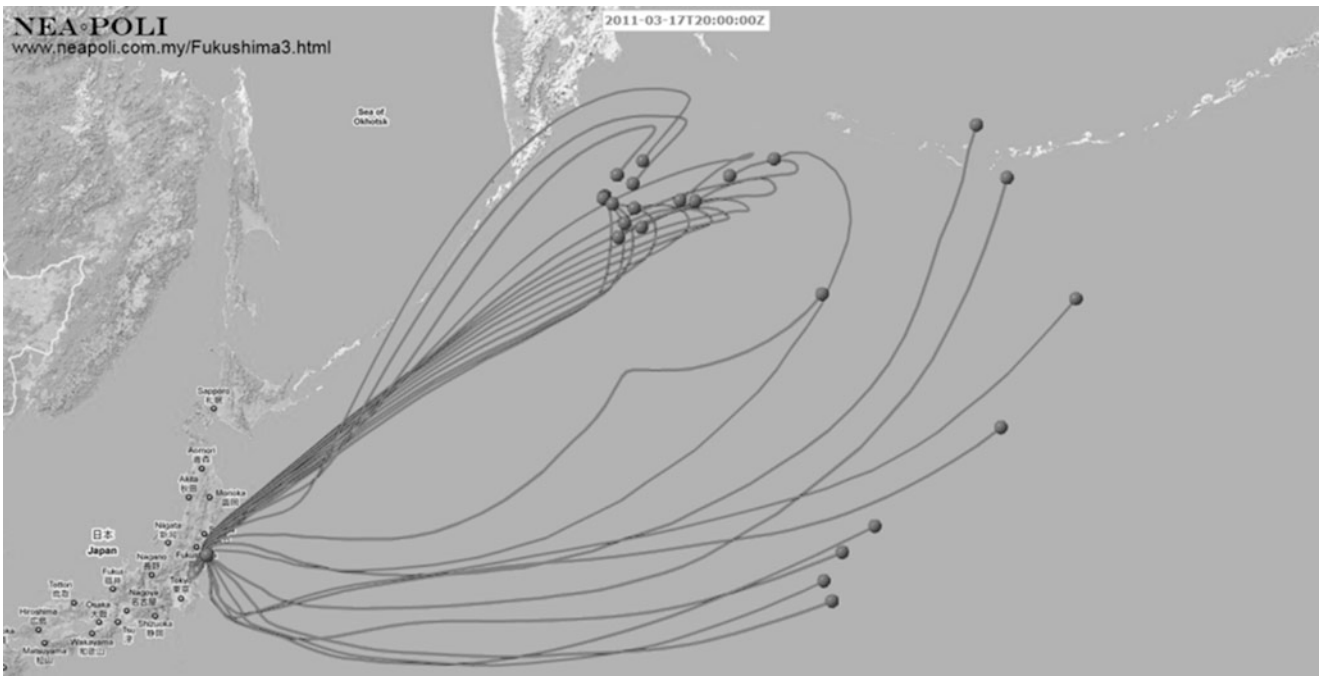

Fig. 1 Dispersion of possibly leaking radioactive substances using HYSPLIT4 Trajectory Model and 5-day forecast meteorological fields from the Global Forecast System Model (*GFM*) (From Draxler and Rolph 2011)

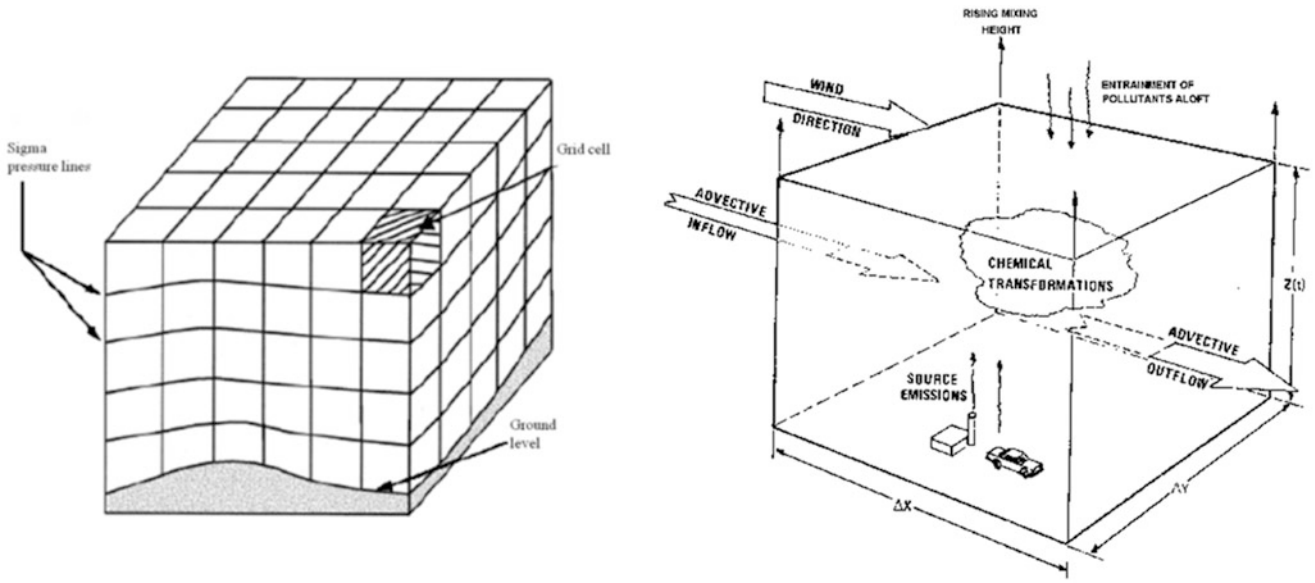

Fig. 2 Eulerian modelling framework (From Reid et al. 2007)

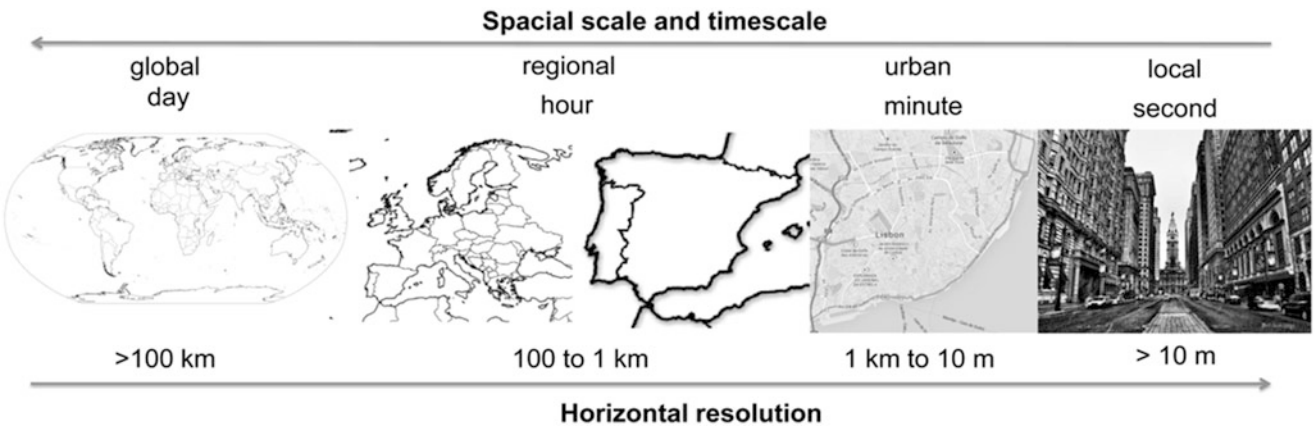

Fig. 3 Time and spatial scales regarding air quality model application

Hence, models can be classified into global, mesoscale (including regional and urban) and local (Fig. 3).

Global models consider the transport of pollutant throughout the atmosphere over the entire surface of the planet. Most global modelling has been confined to climate change issues (with carbon dioxide, CO_2, as the base) with a simplified chemical transport approach. However, expansion to other pollutants has taken place, such as gases (Horowitz et al. 2003) and aerosols (Ginoux et al. 2001), which allow a tighter description and prediction of the chemical composition and evolution of the atmosphere in a future climate. The large spatial extent of these models dictates that the spatial resolution must be relatively coarse to keep the computational demands within reasonable bounds. Mesoscale models consider spatial scales ranging from a few hundred to a few thousand kilometres. This is the spatial scale over which many of the most pressing air pollution concerns are important and is also the scale that often crosses jurisdictional boundaries. In the last years, an increasing body of scientific evidence has demonstrated that air pollution and their mitigation strategies can have significant effects, both positive and negative, on medium-term climate change at the local, regional, and global scales. Increasing evidence also shows that global warming aggravates existing air pollution problems, but most climate change mitigation efforts could have significant co-benefits for air pollution reduction, a win-win opportunity (Borrego 2013).

Local scale modelling is typically used to assess the impact of single sources, or small groups of sources, over distances ranging up to tens of kilometres. CFD modelling is a general term used to describe the analysis of systems involving fluid flow, heat transfer and associated phenomena (e.g. chemical reactions) by means of computer-based numerical methods. These models are based on a better knowledge of the

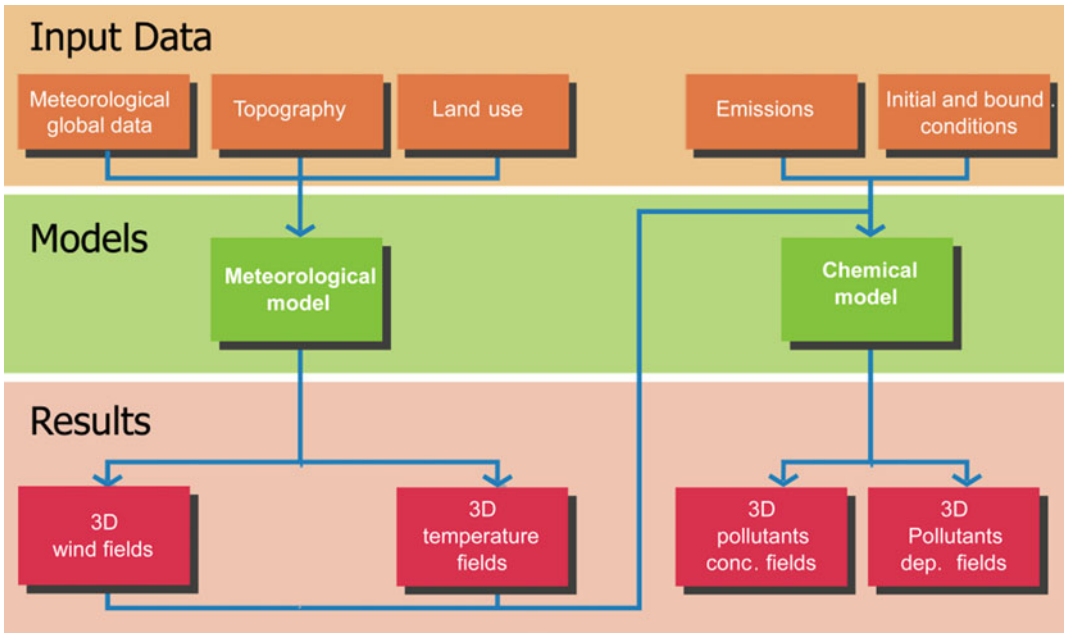

Fig. 4 Scheme of an air quality modelling system

atmosphere structure, using parameterisations of the boundary layer and solving of the Navier-Stokes equations through finite difference and finite volume methods.

The current computational advances allow air quality models to fully couple the meteorology within a unified modelling system (online models) with two-way interactions. However, the most common approach is still the offline system, which only allows one-way coupling from the meteorology – sampled at fixed time intervals – to the chemistry (Grell et al. 2004). This two-way interaction is important because not only can meteorology affect the chemistry through transport, precipitation and radiation processes at each time of the model simulation, but the chemical fields can also impact the meteorological variables. Therefore, online modelling systems are a very promising way for future atmospheric simulations leading to a new generation of models for environmental and chemical weather predictions (Baklanov et al. 2007).

2.1.1 Input/Output Data

Air quality models require a considerable volume of data. The specific needs reflect the methodological approach incorporated in the model, but it typically includes the following variables (Fig. 4):

- Emissions – for all sources treated by the model, the emission is required for each of the chemical species simulated by the model (including each of the species or categories used in the model chemistry), both anthropogenic and biogenic. These emissions should relate to a specific time period being studied.
- Geophysical data – information is required for a range of surface parameters, such as topography, land use and vegetation, and additional data for small-scale modelling, such as building geometry and trees.
- Meteorology – meteorological information is used to force the transport in the air quality model. This information is needed at one or several vertical levels in the atmosphere.
- Initial and boundary conditions – it is usual to specify the initial concentrations for the pollutant species in the model. These will be taken from typical or average values measured, or previously modelled, for the region of interest. It is also necessary to specify concentrations at the boundaries of the model, except for global models. It is relatively simple to estimate initial and boundary conditions at the surface based on measurements, these values are also required at higher levels in the atmosphere, where measurements are sparser. Current practice, which addresses the specification of initial and boundary conditions, is to nest the model.

Output data are usually the temporal and spatial distribution of the air pollutants concentration values.

2.1.2 Model Uncertainty Estimation

Modelling systems can represent suitable tools for air quality studies with an adequate spatial detail and the verification of the limit targets fulfilment and threshold values imposed by the legislative frameworks. Modelling approaches can provide complete spatial coverage information, but models always have uncertainties associated. According to Borrego et al. (2008), total modelling system uncertainty is defined as the sum of model uncertainty, variability and uncertainty on input data. Uncertainties

associated with model formulation may be due to erroneous or incomplete representation of the dynamic and chemistry of the atmosphere, incommensurability, numerical solution techniques and choice of modelling domain and grid structure. Variability refers to stochastic atmospheric and anthropogenic processes. It contributes to uncertainties associated with emission estimation and representations of chemistry and meteorology.

The most common way to determine the total air quality modelling system uncertainty is the comparison between observations and predictions data through the application of data quality indicators that reflect the ability of a model (or modelling system) to simulate real phenomena (Borrego et al 2008). According to Chang and Hanna (2004), there are three main components for the evaluation of air quality modelling systems:

- The scientific evaluation, requiring an in-depth knowledge of the model code, examines in detail the model algorithms, physics, assumptions and codes for their accuracy, efficiency and sensitivity.
- The statistical evaluation compares model predictions to observations in order to estimate how well predictions match the observations. However, this direct comparison method may cause misleading results because uncertainties in observations and model predictions arise from different sources (Chang and Hanna 2004).
- The operational evaluation component mainly considers issues related to the user-friendliness of the model (user's guide, user interface, etc.).

However, over the last years, several workshops and papers have addressed that model evaluation criteria are dependent on the context in which models are to be applied (Steyn and Galmarini 2008). For regulatory applications, a model must be able to provide adequate description of the relationships among atmospheric processes and variables in addition to adequate quantitative estimates of species concentrations. On the other hand, under a forecasting activity, a model is judged by its ability to simulate the temporal evolution of chosen forecast variables. Therefore, Dennis et al. (2010) proposed a new framework for model evaluation to determine the suitability of a modelling system for a specific application, composed by four evaluation types:

- The operational evaluation is based on statistics to compare the magnitudes between model estimations and observations, to some selected criteria, through standard metrics (mean bias, root mean square error and correlation factor) and graphical techniques, such as Taylor diagram, time series, scatter plots and performance goal plots ("soccer plots" and "bugle" plots). This type of evaluation makes use of routine observations of ambient pollutant concentrations, emissions, meteorology and other relevant variables.
- The diagnostic evaluation examines the ability of the model to simulate each of the interacting atmospheric processes with implications on air quality. Since a change in a model input does not always lead to a linear response in the model output, diagnostic evaluations are usually complexes. Usually to ascertain whether inputs have influence on model performance issues, sensitivity tests are applied (Saltelli et al. 2004).
- The dynamic evaluation focuses on the ability of the model to predict changes on ambient air pollutant concentrations in response to changes in either source emissions or meteorological conditions. An example of dynamic evaluation would be modelling assessments of the weekday/weekend concentration differences where mobile source emissions are known to significantly change (Chow 2003).
- The probabilistic evaluation acknowledges the uncertainty in model inputs and formulation of processes by focusing on the modelled distributions of selected variables rather than individual model estimates at specific time and location. According to Foley et al. (2008), this approach provides an estimated probability distribution of pollutant concentrations at any given location and time, which can be used to estimate a range of likely concentration values or the probability of exceeding a given threshold value for a particular pollutant.

The framework for model evaluation proposed by Dennis et al. (2010) is used on the Air Quality Modelling Evaluation International Initiative (AQMEII, http://aqmeii.jrc.ec.europa.eu/). Moreover, the Forum for Air Quality Modelling (FAIRMODE activity – http://fairmode.ew.eea.europa.eu/) that aims to promote synergy between the users and exchange of relevant information is also taking into account the same framework. In this sense, a procedure for the benchmarking of air quality models has been developing in order to evaluate model performance and indicate a way to improve their use. The benchmarking model, DELTA Tool (Thunis et al. 2011), takes into account the Air Quality Directive (2008/50/EC) as well as several scientific works related to model evaluation (Hanna et al. 1993; Nappo and Essa 2001; Olesen et al. 2001; Ichikawa and Sada 2002; Pielke 2002; Delle Monache et al. 2006).

3 Applications of Air Quality Modelling

Air quality modelling approaches can successfully support research and policy-making activities, allowing to (1) assess the impacts of changes on urban planning (including green infrastructures) (e.g. Amorim et al. 2013; Borrego et al. 2006, 2011b; Martins 2012), emissions (e.g. Miranda et al. 1993; Borrego et al. 2004) and climate scenarios (e.g. Carvalho et al. 2010); (2) assess the long-term air quality (for 1 year periods, at least) (e.g. Monteiro et al. 2007; Ribeiro et al. 2013); and

(3) forecast the air quality for a short period, commonly from tomorrow to next 2 or 3 days (e.g. Borrego et al. 2011a; Kukkonen et al. 2012). Selected examples of these applications are described in this Section.

3.1 Scenario Analysis

As mentioned before, air quality modelling systems need input variables, such as emissions, meteorological parameters, land use and topography. Different input scenarios can be created to evaluate the potential impact of these changes on the air quality. This kind of application is especially useful for territory planning and policy strategies, as well as for air quality impact assessment studies. Despite the uncertainty of the scenarios, they provide alternative images of how the future might unfold.

3.1.1 Emission and Climate Scenarios

Emission scenarios describe different options for release of pollutants into the atmosphere. They may be based on assumptions about driving forces such as patterns of economic and population growth, technology development and other factors, with pollutant emissions associated. Moreover, emission scenarios drive forces to the design of climate scenarios, because climate is sensitive to greenhouse gases and other atmospheric pollutants. In fact, with a growing concern on climate change consequences in several areas of interest, including the air quality, climate scenarios became widely used.

The impact of climate change on the air quality over Europe was illustrated by Carvalho et al. (2010), using a reference year (1990) and the IPCC SRES A2 year (2100) (Fig. 5). The modelling results suggest that the O_3 and PM10 levels in the atmosphere levels will be deeply impacted, depending on the region and the month. The Western and Central Europe will be the most affected areas: the predictions from this study point out that the variations of O_3 monthly mean surface concentration may reach an increase of 50 $\mu g \cdot m^{-3}$ in July 2010. Regarding PM10 monthly mean surface concentration, the biggest variation predicted is on October (almost 30 $\mu g \cdot m^{-3}$). Also in accordance with Carvalho et al. (2010), the changes in the boundary layer height, relative humidity, temperature, solar radiation, wind speed and precipitation may be responsible for significant differences in pollutant concentration patterns. In this sense, it is important to understand how future air quality will be under future climate scenarios and therefore contribute to the definition of adaptation and mitigation measures (Jacob and Winner 2009; Dawson and Winner 2012).

3.1.2 Plans and Programmes

In order to reduce and control the effects of air pollution on human health and in the environment, the European Air Quality Directive (Directive 2008/50/EC) established the obligations of the member states to elaborate and implement plans and programmes (PP) to improve air quality when the air quality standards are not met. The implementation of PP to air quality improvement should be based on the design of measures to reduce the pollutant atmospheric concentrations and meet the legal limits. In other words, PP are a set of scenarios developed to reduce atmospheric emissions and, consequently, improve air quality over a specific region.

These emission reduction scenarios can imply, for instance, the replacement of technologies in industrial sources or in residential combustion fireplaces (Borrego et al. 2012a) or decrease of heavy-duty vehicles circulating in city centres and the implementation of washing and sweeping city street actions (Borrego et al. 2012b). The efficiencies of the PP are assessed through the application of an air quality modelling system in order to identify the most adequate measures to be adopted. Figure 6 illustrates two examples of the implementation of PP to reduce PM10 concentrations through the emission reduction from traffic, industry and residential combustion sectors (Fig. 6a) and to reduce NO_2 concentrations reducing emissions from traffic (Fig. 6b) over the northern region of Portugal (Borrego et al. 2012a, b).

3.1.3 Urban Planning

Despite the progress made in controlling local air pollution, urban areas still show increasing signs of environmental stress, and air quality is one of the major concerns. The findings of several studies (e.g. Minnery 1992) provide evidence that the shape of a city and the land use distribution determine the location of emission sources and the pattern of urban traffic, ultimately affecting urban air quality. Urban sprawl is altering the landscape, with current trends pointing to further changes in land use that will, in turn, lead to changes in population, energy consumption, atmospheric emissions and air quality. Urban planners have debated on the most sustainable urban structure, with arguments in favour and against urban compaction and dispersion (Martins 2012). In this sense, air quality models can be a helpful tool for urban planners aiming to develop successful urban growth strategies to a city while tackling the multivariate dimensions of sustainability (Borrego et al. 2006). In this sense, these advanced tools can provide information to better select the most adequate location for new communication routes and industry, residential or recreational areas.

As an example of the role of green infrastructures on air quality, Amorim et al. (2013) evaluated the impact of trees over the dispersion of carbon monoxide (CO) emitted by

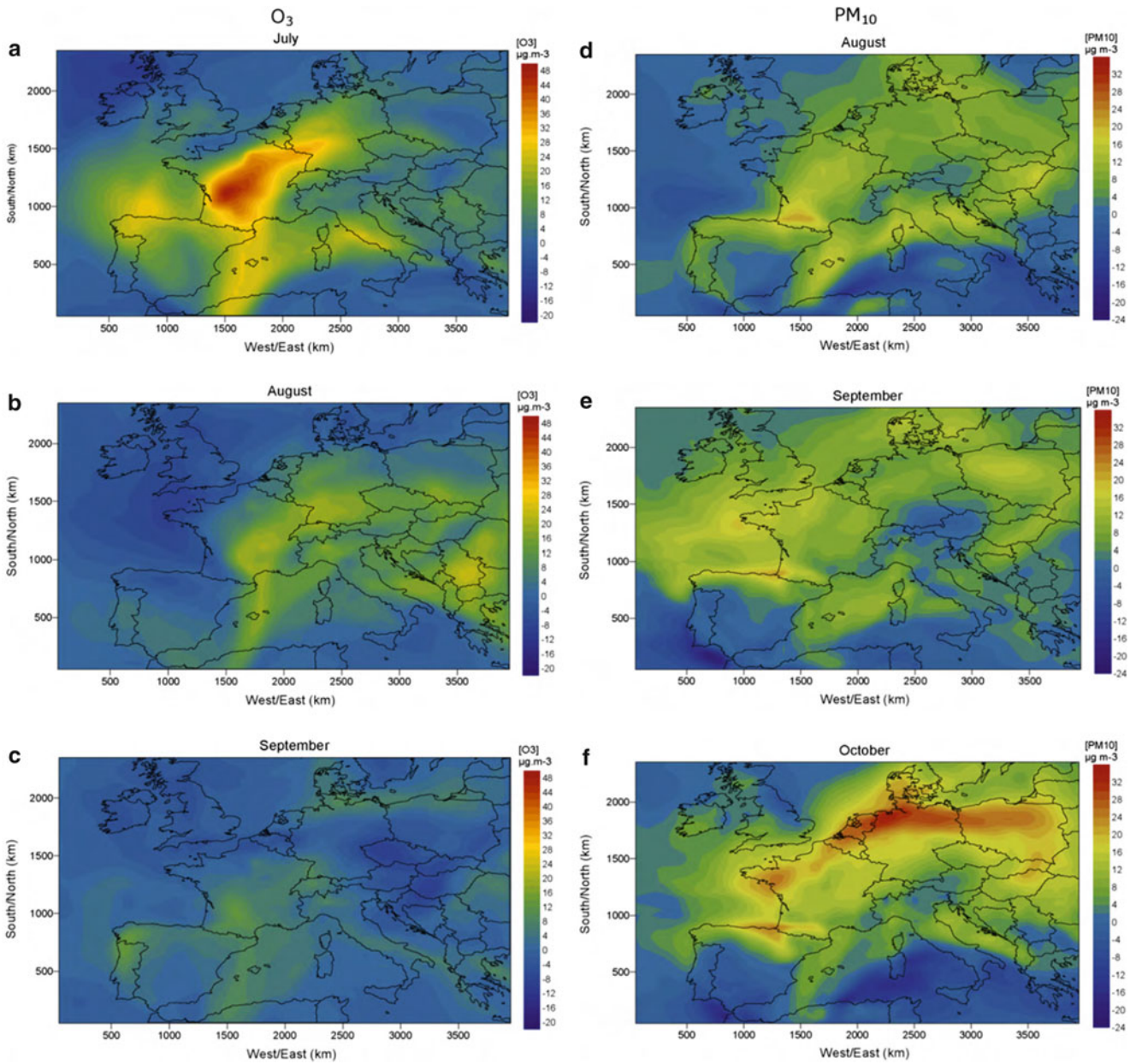

Fig. 5 Monthly mean surface O_3 (**a**–**c**) and PM10 (**d**–**f**) concentration changes ($\mu g \cdot m^{-3}$) simulated across Europe, only considering climate change from July to October (1990–2010) (From Carvalho et al. 2010)

road traffic in the city centre of two Portuguese cities (Fig. 7). The results indicated that the effect of the urban canopy on the dispersion of road traffic emitted air pollutants is highly complex and very spatially dependent. These conclusions support the importance of integrating the knowledge provided by the application of CFD models when defining strategies to optimise the role of green areas on human comfort and health.

As another example of the role of city planning on urban sustainability, Borrego et al. (2011b) applied an advanced Gaussian dispersion model (URBAIR) to previously selected intervention areas in three European cities with distinct characteristics: Helsinki, Athens (Fig. 8) and Gliwice (González et al. 2013). The model simulated the impact of different traffic management options on air quality, reinforcing that distinct urban planning options strongly influence local air pollutant levels. This work showed that the model used is capable of providing guidelines to urban planners and policy decision makers, on different traffic management strategies and their resultant air quality levels, supporting the decision processes on urban planning.

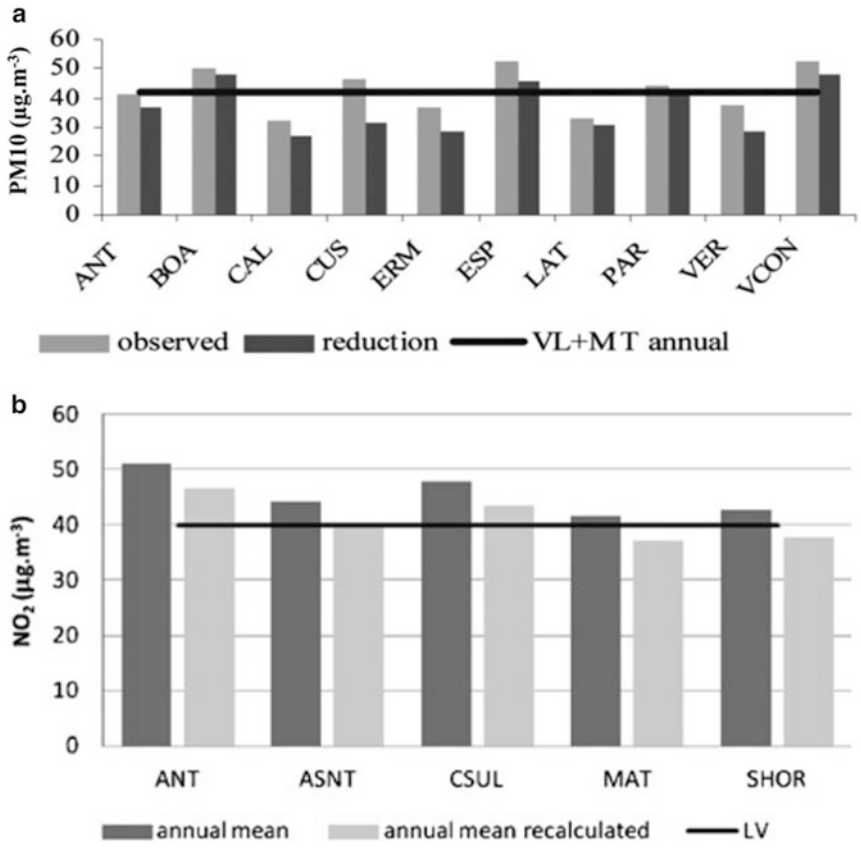

Fig. 6 Annual mean concentrations before and after the implementation of plans and programmes and limit value plus margin of tolerance (LV + MT) over the northern region of Portugal: (**a**) to reduce PM10 emissions from traffic, industry and residential combustion sectors (From Borrego et al. 2012a) and (**b**) to reduce NO_2 emissions from traffic (From Borrego et al. 2012b)

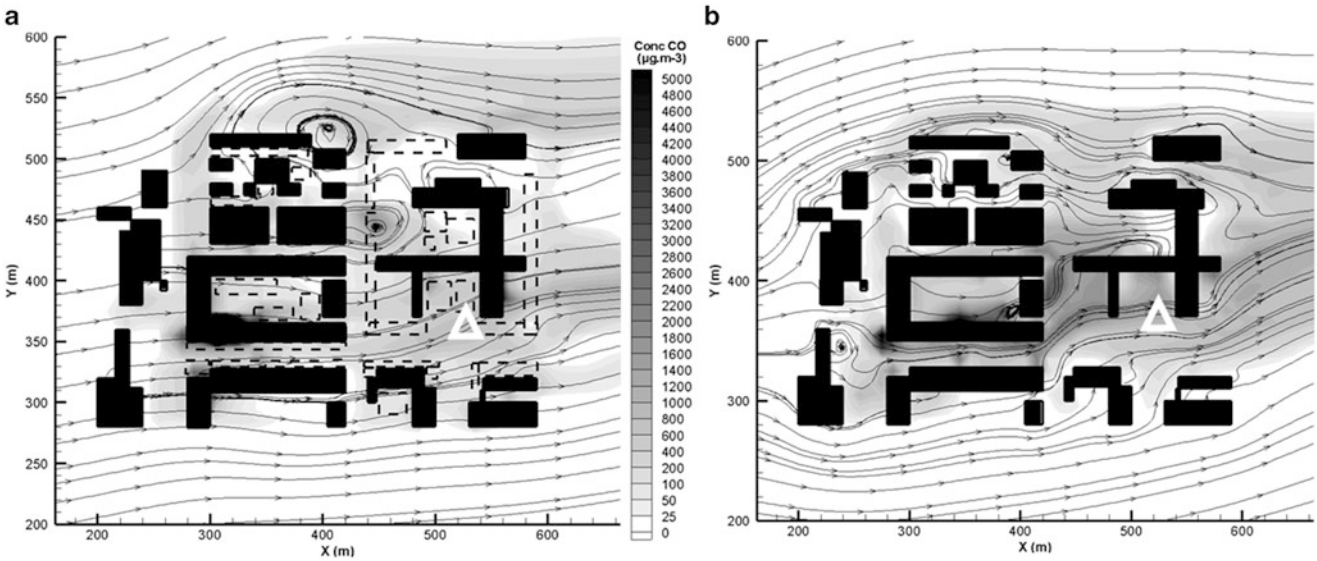

Fig. 7 Horizontal streamlines (3 m high) and CO concentration field with (**a**) and without (**b**) the effect of trees at the Aveiro city centre (in Portugal) between 10 and 11 a.m. *Unfilled rectangles* indicate tree blocks and the *white triangle* is the AQS location (From Amorim et al. 2013)

3.2 Long-Term Assessment

Especially in Europe and North America, air quality assessment is regularly based on the long-term application of modelling systems (van Loon et al. 2007; Thunis et al. 2011; Zhang et al. 2011; Emery et al. 2012; Solazzo et al. 2012). One of the main objectives of long-term air quality assessment is the verification of both limit targets and threshold values fulfilment imposed by legislation with respect to relevant pollutants in order to minimise the impacts on human health and natural ecosystems.

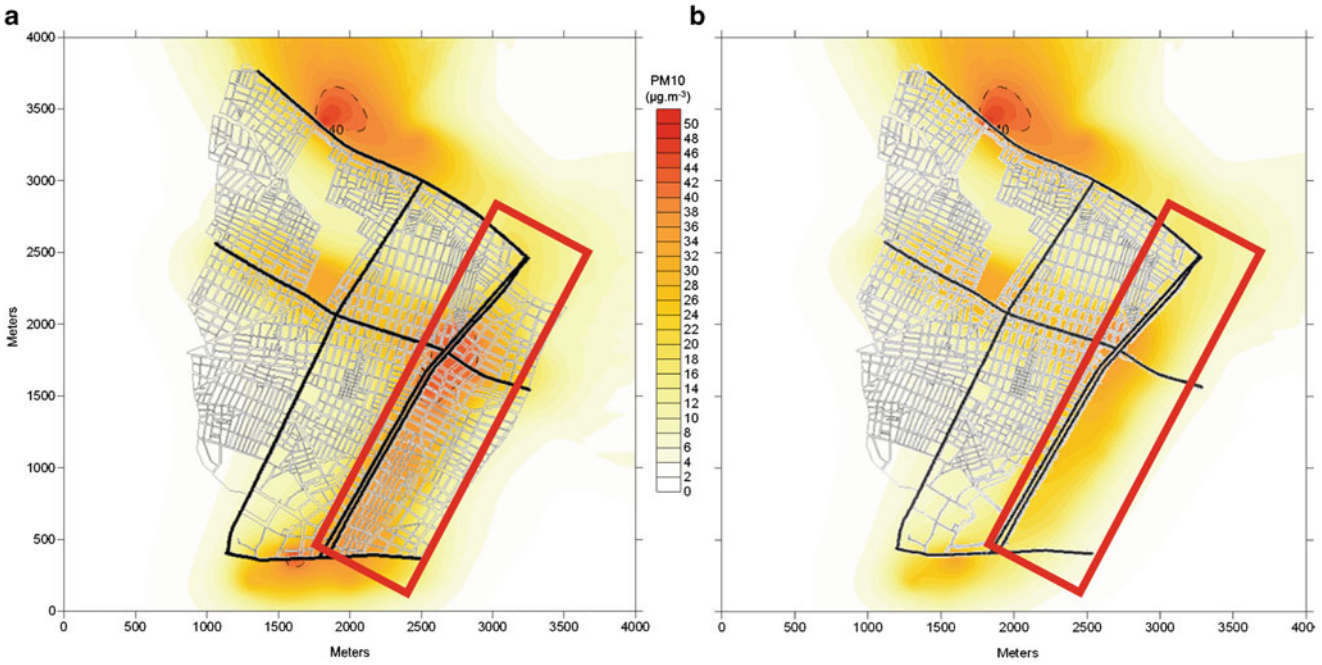

Fig. 8 Comparison of 1.5 m-high horizontal annual average PM10 concentration fields in Athens domain for two different intervention strategies in Western Athens. The planning alternative shown in image (**a**) consists on the construction of new residential buildings, while (**b**) corresponds to the conversion into a green area. The *red rectangle* indicates the intervention area, located at an industrial degraded area in the municipality of Egaleo (From Borrego et al. 2011b)

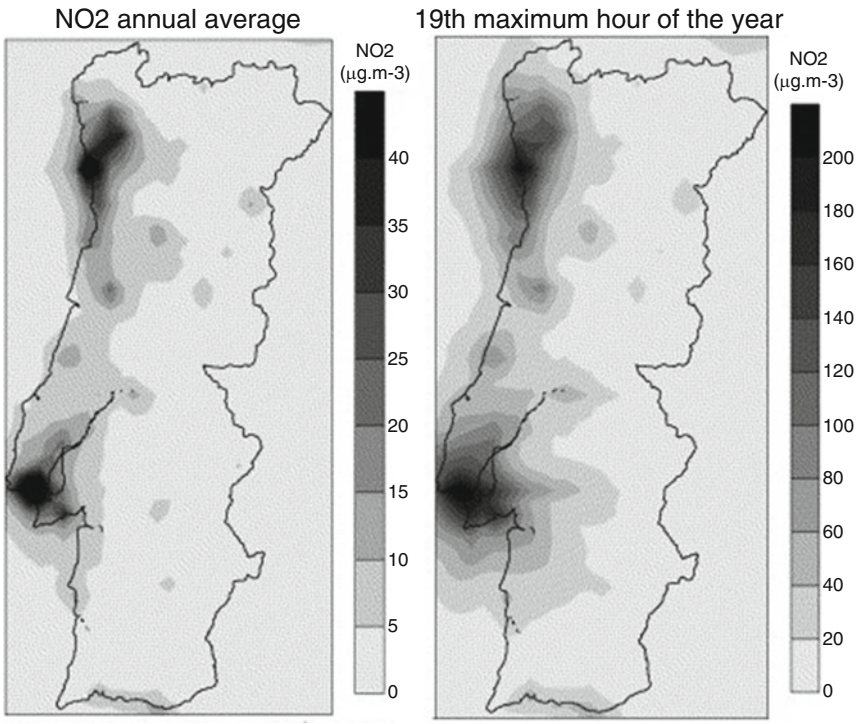

Fig. 9 Modelling results for NO_2 considering human health protection limit values (Directive 1999/30/EC) for the year 2001 (From Monteiro et al. 2007)

The European Union Member States must report annually the air quality assessment. Traditionally, this report has been based on monitored data, but due to sparse or non-existent fixed monitoring stations, this assessment has some limitations. Modelling approaches can contribute to this assessment by providing air quality concentration fields and thus the spatial distribution of pollutants (Fig. 9) (Monteiro et al. 2007), allowing the crossing of this information with other type of information such as the population density (Ribeiro et al. 2013).

The long-term air quality assessment based on modelling application could also be useful to study the representativeness and spatial coverage of the monitoring network, improving air quality assessment activities (Monteiro et al. 2005).

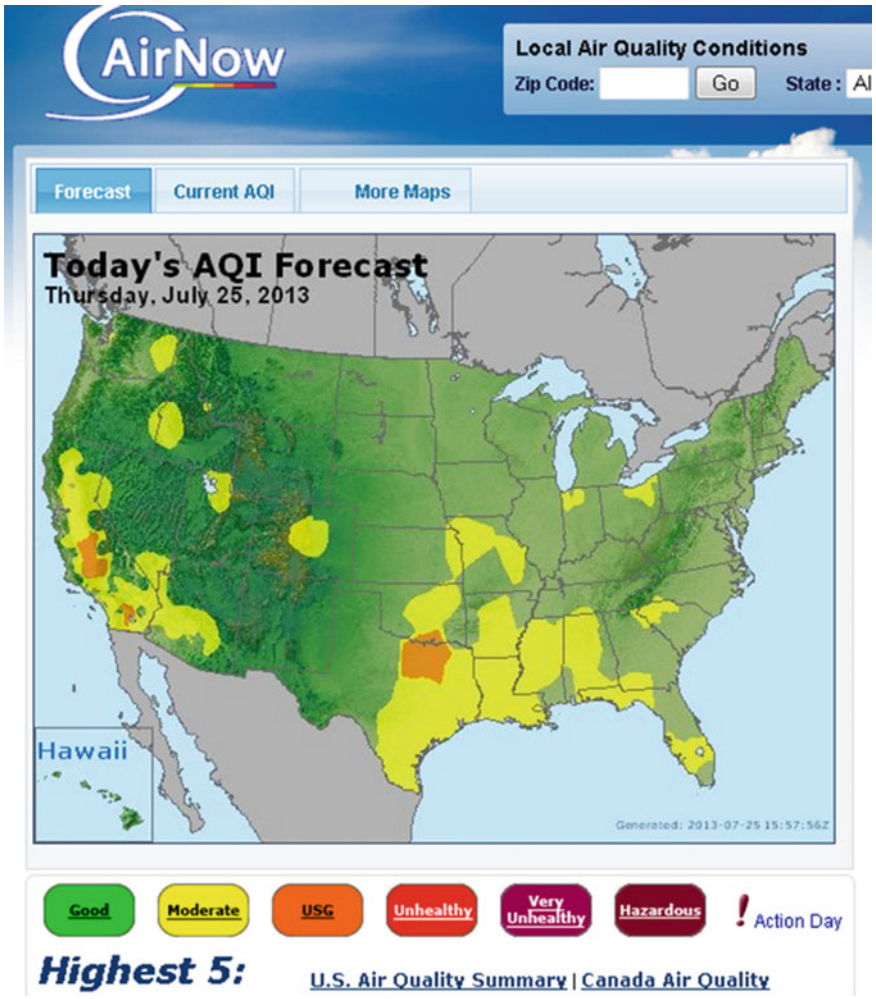

Fig. 10 Air quality index forecast for July 25, 2013, over the USA (From http://www.airnow.gov/)

3.3 Air Quality Forecast

Air quality forecasting is both a challenge and a scientific problem which has recently emerged as a major priority in many urbanised and industrialised countries due to increasing consciousness of the effect of airborne pollutant emissions on health and the environment. The goals of reliable air quality forecasts are evident: exposure of the population can be more efficiently reduced and better protection can be ensured by means of information and short-term action plans. For this purpose, European legislation has set ambient air quality standards for acceptable levels of air pollutants (like O_3, NO_2, SO_2, PM2.5 and PM10) and has also recommended the use of modelling tools to assess and forecast air quality in order to develop emission abatement plans and to alert the population when health-related issues occur (Borrego et al. 2011a).

There are currently several air quality modelling forecasting systems on a local, regional and continental scale in Europe and worldwide (see http://www.chemicalweather.eu for Europe and http://www.airnow.gov/ for the USA). Their forecast maps usually show the predicted Air Quality Index (AQI) (Fig. 10), which is an indicator/classification used to communicate to the public how polluted the air is currently or how polluted it is forecast to become. This will allow the authorities to take actions to prevent or reduce the adverse effects of the exposure of the population through early warnings and to implement alert systems for the population when exceedances of air quality targets are predicted.

4 Final Remarks

The atmosphere is a complex and natural gaseous system, which balance may be affected by the introduction of gaseous or particulate compounds emitted by natural and/or anthropogenic sources and affecting human health and causing damage to plants and materials. Focused on these concerns, atmospheric sciences have been moving forwards. Nowadays, the air quality prediction, for an area ranging from the entire globe to a street, is possible through numerical models, describing mathematically the behaviour of

the pollutants in the atmosphere taking into account the atmospheric processes. For that, the models require diverse input information, such as meteorological fields, terrain characterisation (topography, land use or roughness), atmospheric pollutant emissions and boundary conditions.

There are several numerical modelling tools to predict the air quality based on different approaches. To select the right model to the intended application and taking into account its main characteristics is the first and, probably, the most important step on air quality prediction activity.

Air quality models are considered as powerful tools in research and policy-making activities, allowing the assessment of the impacts from emission, climate or other type of variable scenarios. This kind of application provides appropriate information to analyse how driving forces may influence air quality outcomes. Thus, it is especially useful for environmental impact assessment studies, urban planning and to structure policy strategies. The scenario analysis provides alternative images of how the future might unfold, in spite of the high uncertainty associated with the scenario development.

Especially in North America and Europe, public administrations and environmental authorities are mandated to control and manage air quality in order to minimise air pollution effects on human health and natural ecosystems. In this sense, long-term air quality assessment should be performed annually verifying the fulfilment of the limit targets and threshold values imposed by legislation with respect to the relevant pollutants. This kind of assessment application based on an air quality modelling system also contributes to the identification of air quality problems and causes and therefore to the development and implementation of measures to reduce air pollution levels (plans and programmes). Moreover, there are tens of air quality forecasting systems providing predictions of air pollution concentration fields for the next 2 or 3 days, allowing the authorities to take actions to prevent or reduce the adverse effects of the exposure of the population through early warnings and to implement alert systems for the population when exceedances of air quality targets are predicted.

In spite of the uncertainty associated with the air quality models and the required input data, air quality modelling can provide, with enough accuracy, useful information to decision-making support techniques that may assist in moving towards more sustainable practices, ensuring a better quality of life for the citizens from global to local scale.

Acknowledgements The authors acknowledge the Portuguese Science Foundation for the financing of BIOGAIR project (PTDC/AAC-AMB/103866/2008; FCOMP-01-0124-FEDER-008587), for the Ph.D. grant of Isabel Ribeiro (SFRH/BD/60370/2009) and the post doc grants of Alexandra Monteiro (SFRH/BPD/63796/2009), Joana Valente (SFRH/BPD/78933/2011) and Jorge Humberto Amorim (SFRH/BPD/48121/2008). Thanks are extended to the Portuguese Agency for the Environment for supporting the air quality assessment and forecasting over Portugal and the "Comissão de Coordenação e Desenvolvimento Regional do Norte" for the coordination and responsibility of the plans and programmes.

References

Amorim, J.H., Rodrigues, V., Tavares, R., Valente, J., Borrego, C.: CFD modelling of the aerodynamic effect of trees on urban air pollution dispersion. Sci. Total Environ. **461–462**, 541–551 (2013)

Atkinson, B.W.: Meso-scale atmospheric circulations, 495 p. Academic, London (1989)

Baklanov, A., Fay, B., Kaminski, J., (eds.): Overview of existing integrated (offline and online) mesoscale systems in Europe; COST 728 D2.1 report, p 108, April (2007)

Borrego, C.: Air pollution and climate change: two slides of the same coin. In: EuNetAir Newsletter COST action TD1105. **Iss. 2**, June. http://www.eunetair.it/cost/newsletter/Newsletter_EuNetAir-Issue2_June2013.pdf (2013)

Borrego, C., Martins, H., Carvalho, A., Carvalho, A.C., Lopes, M., Valente, J., Miranda, A.I.: Portuguese power plants impact on air quality. In: Air Pollution 2004, 30 June – 2 July, Rhodes, Greece (2004)

Borrego, C., Martins, H., Tchepel, O., Salmim, L., Monteiro, A., Miranda, A.I.: How urban structure can affect city sustainability from an air quality perspective. Urb. Air Qual. Model. **21**(4), 461–467 (2006)

Borrego, C., Monteiro, A., Ferreira, J., Costa, A.M., Carvalho, A.C., Lopes, M.: Procedures for estimation of modelling uncertainty in air quality assessment. Environ. Int. **34**, 613–620 (2008)

Borrego, C., Monteiro, A., Pay, M.T., Ribeiro, I., Miranda, A.I., Basart, S., Baldasano, J.M.: How bias-correction can improve air quality forecast over Portugal. Atmos. Environ. **45**, 6629–6641 (2011a)

Borrego, C., Cascão, P., Lopes, M., Amorim, J.H., Tavares, R., Rodrigues, V., Martins, J., Miranda, A.I., Chrysoulakis, N.: Impact of urban planning alternatives on air quality: URBAIR model application. In: Brebbia, C.A., Longhurst, J.W.S. (eds.) XIX International Conference on Modelling, Monitoring and Management of Air Pollution. WIT Transactions on Ecology and the Environment, vol. 147, p. 12. WIT, Southampton (2011b)

Borrego, C., Sá, E., Carvalho, A., Sousa, S., Miranda, A.I.: Plans and programmes to improve air quality over Portugal: A numerical modelling approach. Int. J. Environ. Pollut. **48**(1–4), 60–68 (2012a)

Borrego, C., Monteiro, A., Sa, E., Carvalho, A., Coelho, D., Dias, D., Miranda, A.I.: Reducing NO_2 pollution over urban areas: Air quality modelling as a fundamental management tool. Water Air Soil Pollut. **223**(8), 5307–5320 (2012b)

Carvalho, A., Monteiro, A., Solman, S., Miranda, A.I., Borrego, C.: Climate-driven changes in air quality over Europe by the end of the 21st century, with special reference to Portugal. Environ. Sci. Policy **13**, 445–458 (2010)

Chang, J.C., Hanna, S.R.: Air quality model performance evaluation. Meteorol. Atmos. Phys. **87**, 167–196 (2004)

Chow, J.C.: Introduction to special topic: Weekend and weekday differences in ozone levels. J. Air Waste Manage. Assoc. **53**, 771 (2003)

Dawson, J.P., Winner, D.A.: New directions: Adapting air quality management to climate change: A must for planning. Atmos. Environ. **50**, 387–389 (2012)

Delle Monache, L., Deng, X., Zhou, Y., Stull, R.: Ozone ensemble forecasts: 1. A new ensemble design. J. Geophys. Res. **111**(D05307) (2006)

Dennis, R., Fox, T., Fuentes, M., Gilliland, A., Hanna, S., Hogrefe, C., Irwin, J., Rao, S.T., Scheffe, R., Schere, K., Steyn, D., Venkatram, A.: A framework for evaluating of regional-scale numerical

photochemical modeling systems. Environ. Fluid Mech. **10**(4), 471–489 (2010)
Draxier, R., Hess, G.D.: An overview of the HYSPLIT_4 modelling system for trajectories, dispersion and deposition. Aust Meteorol. Mag. **47**(4), 295–308 (1998)
Draxler, R.R., Rolph, G.D.: HYSPLIT (HYbrid Single-Particle Lagrangian Integrated Trajectory) Model access via NOAA ARL READY website (http://ready.arl.noaa.gov/HYSPLIT.php). NOAA Air Resources Laboratory, Silver Spring, MD (2011)
Emery, C., Jung, J., Downey, N., Johnson, J., Jimenez, M., Yarwood, G., Morris, R.: Regional and global modeling estimates of policy relevant background ozone over the United States. Atmos. Environ. **47**, 206–217 (2012)
Foley, K., Pinder, R., Napelonak, S.: New directions in air quality model evaluation: probabilistic model evaluation. Poster presented at the CMAS conference; Chapel Hill, NC. http://www.cmascenter.org/conference/2008/agenda.cfm (2008)
Ginoux, P., Chin, M., Tegen, I., Prospero, J.M., Holben, B., Dubovik, O., Lin, S.J.: Sources and distributions of dust aerosols simulated with the GOCART model. J. Geophys. Res. **106**, 20255–20273 (2001)
González, A., Donnelly, A., Jones, M., Chrysoulakis, N., Lopes, M.: A decision-support system for sustainable urban metabolism in Europe. Environ. Impact Asses. Rev. **38**, 109–119 (2013)
Grell, G., Knoche, R., Peckham, S.E., McKeen, S.A.: Online versus offline air quality modeling on cloud-resolving scales. Geophys. Res. Lett. **31**, L16117 (2004)
Hanna, S.R., Chang, J.C., Strimaitis, D.G.: Hazardous gas model evaluation with field observations. Atmos. Environ. **27A**, 2265–2285 (1993)
Horowitz, L., Walters, S., Mauzeralles, D., Emmonds, L., Rash, P., Granier, C., Tie, X., Lamarque, J., Schultz, M., Tyndall, G., Orlando, J., Brasseur, G.: A global simulation of tropospheric ozone and related tracers: Description and evaluation of MOZART, version 2. J. Geophys. Res. **108**(D24), 4784 (2003)
Ichikawa, Y., Sada, K.: An atmospheric dispersion model for the environment impact assessment of thermal power plants in Japan – a method for evaluating topographical effects. J. Air Waste Manage. Assoc. **52**, 313 (2002)
Jacob, D.J., Winner, D.A.: Effect of climate change on air quality. Atmos. Environ. **43**, 51–63 (2009)
Jacobson, M.Z.: Fundamentals of atmospheric modelling. Cambridge University Press, Cambridge, UK (1999)
Kukkonen, J., Balk, T., Scultz, M., Baklanov, A., Klein, T., Miranda, A. I., Monteiro, A., Hirtl, M., Tarvainen, V., Boy, M., Peuch, V.-H., Poupkou, A., Kioutsioukis, I., Finardi, S., Sofiev, M., Sokhi, R., Lehtinen, K., Karatzas, K., San José, R., Astitha, M., Kallos, G., Schaap, M., Reimer, E., Jakobs, H., Eben, K.: A review of operational, regional-scale, chemical weather forecasting models in Europe. Atmos. Chem. Phy. **12**, 1–87 (2012)
Kumar, P., Ketzel, M., Vardoulakis, S., Pirjola, L., Britter, R.: Dynamics and dispersion modelling of nanoparticles from road traffic in the urban atmospheric environment – a review. J. Aerosol. Sci. **42**(9), 580–603 (2011)
Lutman, E.R., Jones, S.R., Hill, R.A., McDonald, P., Lambers, B.: Comparison between the predictions of a Gaussian plume model and a Lagrangian particle dispersion model for annual average calculations of long-range dispersion of radionuclides. J. Environ. Radioact. **75**, 339–355 (2004)
Martins, H.: Urban compaction or dispersion? An air quality modelling study. Atmos. Environ. **54**, 60–72 (2012)
Minnery, J.: Urban Form and Development Strategies: Equity, Environmental and Economic Implications. The National Housing Strategy Background, Paper 7. AGPS, Canberra (1992)
Miranda, A.I., Conceição, M.S., Borrego, C.: A contribution to the air quality impact assessment of a roadway in Lisbon. The air quality model APOLO. Sci. Total Environ. **134**(1–3), 1–7 (1993)
Monteiro, A., Vautard, R., Borrego, C., Miranda, A.I.: Long-term simulations of photo oxidant pollution over Portugal using the CHIMERE model. Atmos. Environ. **39**, 3089–3101 (2005)
Monteiro, A., Miranda, A.I., Borrego, C., Vautard, R., Ferreira, J., Perez, A.T.: Long-term assessment of particulate matter using CHIMERE model. Atmos. Environ. **41**, 7726–7738 (2007)
Nappo, C.J., Essa, K.S.M.: Modeling dispersion from near-surface tracer releases at Cape Canaveral. Atmos. Environ. **35**, 3999–4010 (2001)
Olesen, H.R.: Ten years of harmonisation activities: past, present and future. In: 7th International Conference on Harmonisation Within Atmospheric Dispersion Modelling for Regulatory Purposes. European Commission, Joint Research Centre (2001)
Pielke, R.A.: Mesoscale meteorological modeling. Academic, San Diego (2002)
Reid, N., Misra, P.K., Amman, M., Hales, J.: Air quality modeling for policy development. J. Toxicol. Environ. Health **70A**(3–4), 295–310 (2007)
Ribeiro I., Monteiro A., Fernandes A.P., Monteiro A.C., Lopes M., Borrego C., Miranda A.I.: Air quality modelling as a supplementary assessment method in the framework of the European air quality Directive. In: 15th International Conference on Harmonisation within Atmospheric Dispersion Modelling for Regulatory Purposes, 6–9 May 2013, Madrid, Spain (2013)
Saltelli, A., Tarantola, S., Campolongo, F., Ratto, M.: Sensitivity Analysis in Practice. A Guide to Assessing Scientific Models. Wiley, Chichester (2004)
Seinfeld, J.H., Pandis, S.N.: Atmospheric Chemistry and Physics: From Air Pollution to Climate Change. Wiley, New York (1998). ISBN 9780471178163
Solazzo, E., Bianconi, R., Vautard, R., Appel, K.W., Moran, M.D., Hogrefe, C., Bessagnet, B., Brandt, J., Christensen, J.H., Chemel, C., Coll, I., van der Gon, H.D., Ferreira, J., Forkel, R., Francis, X.V., Grell, G., Grossi, P., Hansen, A.B., Jeričević, A., Kraljević, L., Miranda, A.I., Nopmongcol, U., Pirovano, G., Prank, M., Riccio, A., Sartelet, K.N., Schaap, M., Silver, J.D., Sokhi, R.S., Vira, J., Werhahn, J., Wolke, R., Yarwood, G., Zhang, J., Rao, S.T., Galmarini, S.: Model evaluation and ensemble modelling of surface-level ozone in Europe and North America in the context of AQMEII. Atmos. Environ. **53**, 60–74 (2012)
Steyn, D.G., Galmarini, S.: Evaluating the predictive and explanatory value of atmospheric numerical models: Between relativism and objectivism. Open Atmos. Sci. J. **2**, 38–45 (2008)
Thunis, P., Georgieva, E., Pederzoli, A., Pernigotti, D.: "The DELTA Tool and Benchmarking Report Template", Concepts and User's Guide, p. 31. Join Research Centre, Ispra (2011)
van Loon, M., Vautard, R., Schaap, M., Bergström, R., Bessagnet, B., Brandt, J., Builtjes, P.J.H., Christensen, J.H., Cuvelier, C., Graff, A., Jonson, J.E., Krol, M., Langner, J., Roberts, P., Rouil, L., Stern, R., Tarrasón, L., Thunis, P., Vignati, E., White, L., Wind, P.: Evaluation of long-term ozone simulations from seven regional air quality models and their ensemble. Atmos. Environ. **41**(10), 2083–2097 (2007)
Zhang, L., Jacob, D.J., Downey, N.V., Wood, D.A., Blewitt, D., van Carouge, C.C., Donkelaar, A., Jones, D.B.A., Murray, L.T., Wang, Y.: Improved estimate of the policy-relevant background ozone in the United States using the GEOS-Chem global model with $1/2^\circ \times 2/3^\circ$ horizontal resolution over North America. Atmos. Environ. **45**(37), 6769–6776 (2011)

Fuel Cell Technology and Materials

Lorenzo Pisani, Bruno D'Aguanno, Vito Di Noto, and John Andrews

Abstract

In this chapter, the key role of fuel cells and regenerative fuel cell technologies, in the future energetic scenarios based on renewable energy sources, is described. The fuel cell technology is reviewed; its working principles are summarized and mathematically described by means of a simple analytical model. It is found that the limits of fuel cell competitiveness can be overcome only through a specific design of its key component materials: the electrolyte and the electrocatalyst. Examples of material design research achievements are reported for both fuel cells and regenerative fuel cells.

Keywords

Fuel cells • Fuel cell modeling • Fuel cell materials • PEMFC • URFC

1 Introduction

The first commercial application of fuel cells (FC) goes back to the years 1965–1966 and to the Project Gemini. Since that time, although the energy production–storage–consumption issue became a worldwide critical issue, both economically and ecologically, and despite the many progresses in the field, fuel cells are still "searching to find a killer application that allows their penetration into the market" (Winter and Brodd 2004).

Fuel cells belong to the class of electrochemical devices in which the atomic bond energy is directly converted to electrical energy. To the same class belong batteries and electrochemical capacitors. All these systems have two electrodes in contact with an electrolytic solution, and all energy production processes are happening at the interface electrode–electrolyte solution. Fuel cells are open systems in which reactants have to be provided from outside (storage outside), while batteries are closed systems containing the reactant in their interior (storage inside). Electrochemical capacitors, which store energy in electrical double layer at the electrode–electrolyte interface, may deliver energy also in the absence of redox reactions.

Fuel cells have been considered as a replacement to the internal combustion engines and combustion power plants, due to a possible lower ecological impact and comparable, or higher, energy conversion efficiency.

The best way to compare between each other all these devices, and to understand their domains of applicability, is via the so-called Ragone plot, in which the specific energy (Wh/kg) is reported in the abscissa and the specific power (W/kg) is reported in the ordinate. The Ragone plot of Fig. 1 shows that fuel cells are high energy systems of quite low power, while supercapacitors and capacitors can deliver the low energy content at a high rate (high power). Batteries have an intermediate behavior, but the combustion energy is at the upper right part of the plot, showing that, at the

L. Pisani (✉) • B. D'Aguanno
Department of Renewable Energy, Center for Advanced Studies, Research and Development in Sardinia (CRS4), Building 1, Technological Park Polaris, 09010 Pula, Italy
e-mail: pisani@crs4.it

V. Di Noto
Department of Chemical Sciences, University of Padua, Via Marzolo 1, 35131 Padova (PD), Italy

J. Andrews
School of Aerospace, Mechanical and Manufacturing Engineering, RMIT University, Melbourne, VIC 3001, Australia

G. Cao and R. Orrù (eds.), *Current Environmental Issues and Challenges*,
DOI 10.1007/978-94-017-8777-2_4,

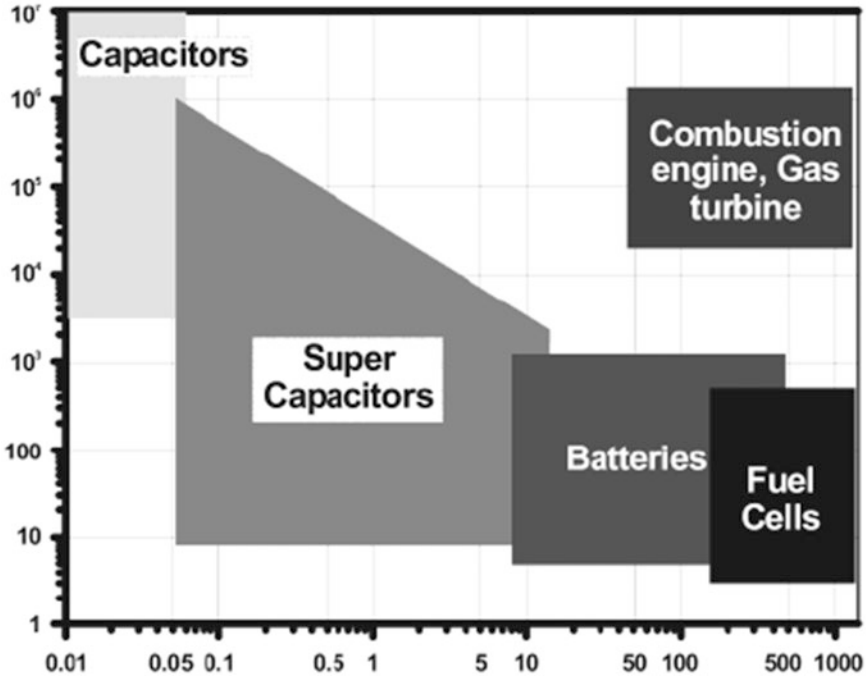

Fig. 1 Ragone plot with the energy/power storage domains of electrochemical devices as compared to that of combustion engines. *Abscissa*: specific energy, Wh/kg; *ordinate*: specific power, W/kg (Adapted from Winter and Brodd 2004)

moment, "no single electrochemical power source can match the characteristics of the internal combustion engine" (Winter and Brodd 2004).

Then, fuel cells alone are best suited for specific stationary energy applications and to replace batteries and super capacitors in electronic devices. In addition, and from life cycle assessment, FC are expected to have a very low ecological impact.

To enhance at the same time the specific power and the specific energy, and also to try to bridge the gap with the internal combustion engines, R&D activities are running in the direction of hybridization, in which, for example, carbon nanotube or graphene-enhanced ultracapacitors are coupled with fuel cells. Transition metal and light metal-decorated graphenes are expected to have a very high specific power (see Figure 1 in Ref. (Tozzini and Pellegrini 2013)), and their hybridization with fuel cells, in devices which can be classified either as electrochemical asymmetric ultracapacitor or as modified FC (Signorelli 2009), can deliver high energy at high power.

Aside from these specific applications, fuel cells have a key role in all energetic scenarios based on renewable energy sources. In such scenarios, CO_2 is strongly reduced and the energy is produced/distributed on small scale. The reduction of CO_2 is achieved by the production of electricity, heat, and "solar fuels," mainly hydrogen, from renewable sources, while the small scale is achieved by scalable power and storage systems managed by smart grids. In the production schemes of hydrogen, fuel cells are coupled with a sun-powered thermo-catalytic reactor able to split the water molecule or with a system producing electricity from renewables plus an electrolyzer. In both schemes, the renewable energy is transferred to the hydrogen obtained from the water splitting, and water is re-obtained from a hydrogen fuel cell able to deliver back part of the renewable energy as electricity.

The coupling of a fuel cell with an electrolyzer is realized via the regenerative fuel cells (RFC) or, better, via the unitized RFC (URFC) in which a single device is able to work as an electrolyzer and as a fuel cell (Andrews and Doddathimmaiah 2008; Mitlitsky et al. 1998).

The aim of this paper is to present the basic definitions, the basic role and properties, and the basic mechanisms of transport in all the components making a fuel cell. The same presentation is given for the URFCs. It is only from this starting point that deeper analysis aimed to optimize and to enhance fuel cell, and hybrid fuel cell performances can be understood and developed.

The paper is organized as follows. The next Section, Sect. 2, introduces the FC working principle, the role of each FC component, and the classification scheme of the known FCs. Sect. 3 introduces the quantities which enter in the description of the FC performance curve and the FC potential as a function of the FC current density, and it explains, through a simple analytical model, the overall shape of the curve, from low to high current density. Section 4 is devoted to the main materials used as electrolyte in the membrane region and as catalyst in the reactive

regions. The section points out the phenomena happening in the involved materials. The final section, Sect. 5, deals with regenerative and unitized regenerative FCs. Also in this case, the working principle, the basic roles and properties of involved materials, and the transport mechanisms are presented and explained.

2 The Fuel Cell Technology: Working Principle

Redox reactions involve the transfer of electrons between species. By separating oxidation and reduction half-reactions and by leading the electron transfer through an external circuit, chemical energy is transformed directly into electrical energy.

In an electrochemical cell, oxidation and reduction reactions are separated in space and connected by an external electric circuit. The two separated regions, where the two half-reactions take place, are called the electrodes: the anode for the oxidation and the cathode for the reduction reaction. The separator, capable to transport the ionic species to provide a complete electric circuit, is called the electrolyte.

Fuel cells are electrochemical cells, which use a fuel as reductant and oxygen as oxidant (see Fig. 2). Hydrogen is the most common fuel, but hydrocarbons and alcohols are sometimes used.

In principle, fuel cell operation can be reversed, and the FC can work as an electrolyzer producing oxygen and hydrogen molecules from water and electricity. In the reversible fuel cell concept, the same physical cell is used for both operation modes.

In the next subsection, we schematically list all the main components of a fuel cell, their functions and phenomena, and the constituting materials. Afterwards, we will give some more details on the key FC components, the electrolyte, and the reactive regions of the electrodes.

2.1 The FC Components

2.1.1 Flow Channels and Current Collectors

Main function: (1) The flow channels must drive the fuel to the anode and the oxidant to the cathode and allow the removal of the reaction products (H_2O, CO_2). (2) The current collector must collect the electrons produced by the

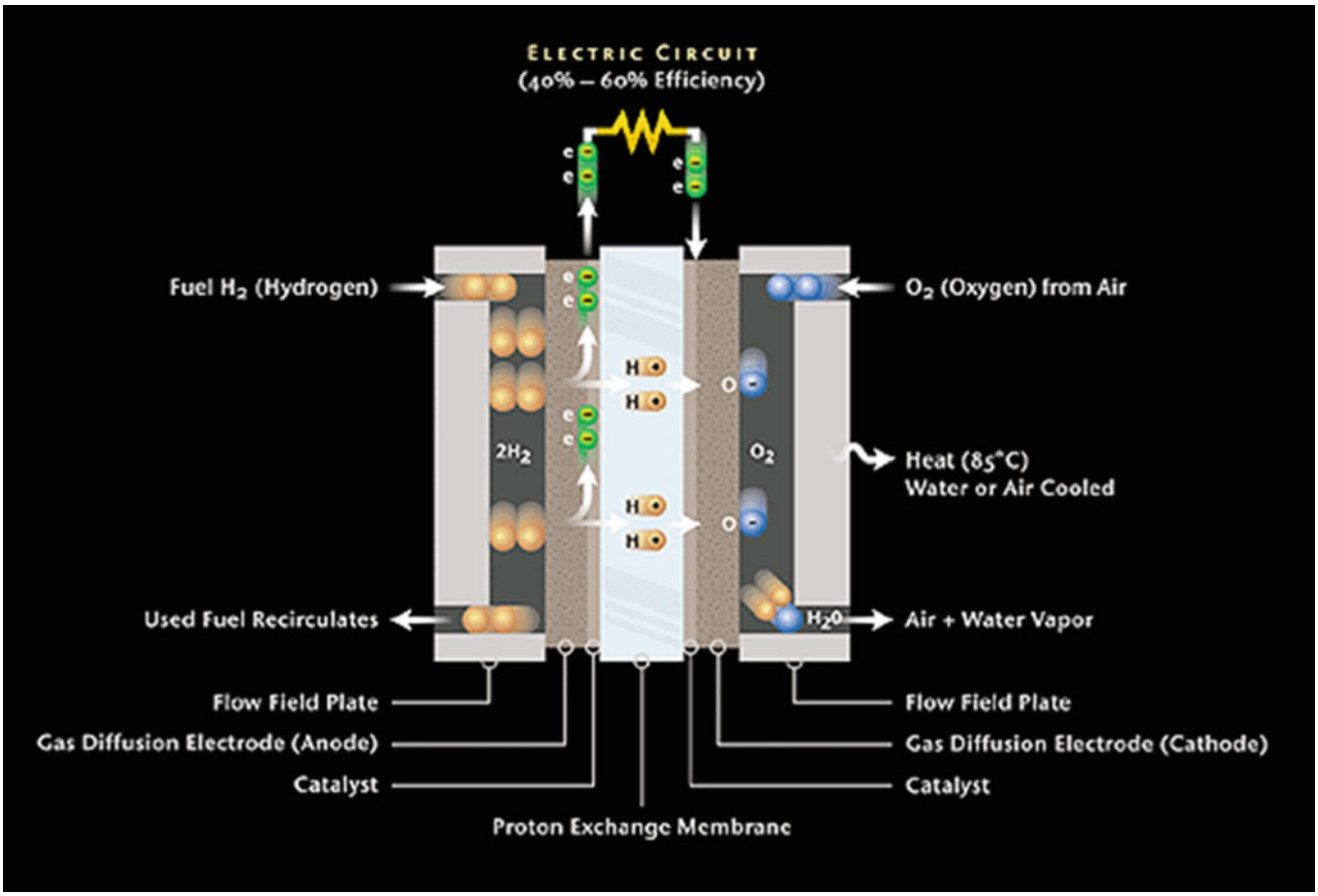

Fig. 2 FC working principle

electrochemical reaction at the anode and, through the external circuit, bring them at the cathode.

Auxiliary functions: In polymer electrolyte membrane fuel cells (PEMFC), the current collectors have also a mechanical support function and a thermal control function.

Material properties: Good electronic and thermal conductor

Phenomena: Reactant flow conduction, thermal and electronic conduction

2.1.2 Electrode Diffusion Layers

Main functions: The function of the electrode diffusion layers is to drive the reactants from the flow channels to the electrochemically reactive regions and the electrons from the electrochemically reactive regions to the current collectors.

Auxiliary functions: In solid oxide fuel cells (SOFC), electrodes can have also a mechanical support function and can catalyze the methane reforming reaction.

Material properties: Porous material, good electronic conductor

Phenomena: Reactant diffusion, electronic conduction, nonelectrochemical reactions (shift reaction, reforming reaction)

2.1.3 Electrodes Reactive Layer

Main functions: The function of the electrode reactive layers is to catalyze the electrochemical reactions.

Material properties: Porous material, electronic and ionic conductor, high catalytic activity

Phenomena: Electrochemical reaction, catalysis, electronic and ionic conduction, reactant diffusion

2.1.4 The Electrolyte

Main functions: The function of the electrolyte is to conduct an ionic current between the two electrodes while constraining the electrons to pass through the external circuit.

Auxiliary function: In most of the cells, the electrolyte should keep the fuel separated from the oxidant in order to avoid direct (nonelectrochemical) reactions.

Phenomena: Ionic conduction, reactant crossover

Material properties: Good ionic conductor, electronic insulator, minimum permeability to reactant

2.2 The FC Types

As schematically described in the previous section, the main physical phenomena occurring inside the fuel cells are transport of ions, electrons and neutral species, and electrochemical reactions. While chemical diffusion and electronic conduction phenomena are common to a very wide number of applications, electrocatalysis and ionic conduction are much more specific and complex. Therefore, the key FC components are the electrolyte and the reactive regions of the electrodes.

Different strategies have been studied to make these components efficient, robust, and economically affordable, but none of them has shown a clear and general advantage. Thus, different types of FC have been developed, or are still under development, and are classified following the operating temperature range and the electrolyte material.

2.2.1 Temperature Classification

The reaction kinetics should be as fast as possible in order to minimize activation losses. Three main factors influence the reaction kinetics: the catalyzers quality, the temperature, and the availability of reaction sites.

In practice, a good structural design of the reactive layer should guarantee the simultaneous presence of ions, electrons, and reactant fluxes on the catalyst surface (triple phase boundaries). Beside this, either very efficient catalyzer or very high temperature is needed to minimize the activation losses. As a consequence, a first main FC classification is based on the operating temperature range.

At low temperatures ($\leq$100 °C), precious metals and, in particular, platinum are the catalyzers of choice. On the other hand, at such "low" temperatures, the fuel cell is easy to manage, with quick start-up times and no thermal breaking risk. Moreover, liquid water can be used to transport ions through the electrolyte. Low-temperature fuel cells (LTFC) include PEMFC and alkaline fuel cells (AFC).

At very high temperatures (>600 °C), platinum is not necessary anymore and less costly catalyzers (e.g., nickel) can be used. Moreover, catalyzer sensibility to poisoning substances is strongly reduced and a larger variety of fuels can be used. However, such high temperature brings strong material issues and long start-up times. High-temperature fuel cells (HTFC) include SOFC and molten carbonate fuel cells (MCFC).

Intermediate temperature FC exists as well, which share the main disadvantages of the other two classes, including the need of precious metal catalysts and long start-up times. Among this class, we mention the phosphoric acid fuel cells (PAFC).

2.2.2 Electrolyte Classification

The function of the electrolyte is to conduct an ionic current between the two electrodes while constraining the electrons to pass through the external circuit. The main issue is to find a manageable ionic conductor material, with a good ionic conductivity in order to minimize ohmic losses.

Different ionic conduction mechanisms can be used, including:

- Water electrolytic solutions (acid or basic) (PEMFC, AFC) (low temperatures—not much larger than the water boiling temperature)
- Anhydrate liquids as phosphoric acid (PAFC) or molten salts (MCFC) (intermediate to high temperatures)
- Conduction in solids (SOFC) (high temperatures)

A number of different ionic species can be used as charge carriers. For example, in hydrogen fuel cells which separate the hydrogen oxidation reaction $2H_2 + O_2 \rightarrow 2H_2O$, the following ions are commonly used:

Protons H^+ (PEMFC, PAFC, and proton SOFC):

$$2H_2 \rightarrow 4H^+ + 4e^- \quad O_2 + 4H^+ + 4e^- \rightarrow 2H_2O. \tag{1}$$

Hydroxide OH^- (AFC, anion electrolyte membrane FC, AEMFC):

$$2H_2 + 4OH^- \rightarrow 4H_2O + 4e^- \quad O_2 + 2H_2O + 4e^- \rightarrow 4OH^-. \tag{2}$$

Oxygen ions O^- (SOFC):

$$2H_2 + 2O^-{}_2 \rightarrow 2H_2O + 4e^- \quad O_2 + 4e^- \rightarrow 2O^-{}_2. \tag{3}$$

Carbonate ions $CO^{2-}{}_3$ (MCFC):

$$2H_2 + 2CO_3^{2-} \rightarrow H_2O + 2CO_2 + 4e^- \quad O_2 + 2CO_2 + 4e^- \rightarrow 2CO_3^{2-}. \tag{4}$$

3 FC Performances: Analysis and Optimization

The fuel cell operation is characterized by the cell potential versus current density I: the $V(I)$ performance curve. This curve provides direct information on:

- Electric power density, which can be obtained as $V(I) \times I$. The maximum of this function has an important role in dimensioning the FC system for applications requiring high power peaks (e.g., automotive applications).
- Energy conversion efficiency, which can be obtained as $V(I)/V_0$, where V_0 is the theoretical potential. Efficiency is a fundamental parameter for all applications.
- Maximum current density, I_{lim}.
- Dissipated power, which can be obtained as $(V_0 - V(I)) \times I$. This quantity is the heat generated by the fuel cell.

In the next subsections, we will derive a simple but quite accurate analytical expression for $V(I)$, from which all the above information can be easily derived and analyzed.

3.1 The Fuel Cell Potentials

The theoretical potential, V_0, is a thermodynamic quantity that depends on the specific electrochemical reaction, temperature, and chemical concentrations. It corresponds to the maximum potential achievable with a 100 % conversion efficiency. Potential losses inside a fuel cell originate either at the interfaces between ionic and electronic conducting phases, where all the electrochemistry takes place, or internally to each single phase. The single phase losses, η, are essentially of Ohmic origin, linear with the cell current density, and, therefore, they have a trivial effect on the performance curves:

$$\eta_{\text{ohm}}(I) \approx RI, \tag{5}$$

where R is the fuel cell resistance.

More complex is the I-behavior of the interface overpotentials, η_{int}, which, as illustrated in Fig. 3, originate in the small electrode reactive region, where the two phases coexist.

In the Figure, we have arbitrarily represented the theoretical potential V_0 as the sum of an anodic, E_A, and a cathodic, E_C, contributions.

Therefore, we write the cell potential as made up of zero-current term, E; a potential drop term of Ohmic origin, η_{ohm}; and potential drop terms originated by the interface electrochemistry in the anode and cathode reactive regions, η_{int}:

$$V(I) \approx E_A + E_C - \eta_{\text{ohm}}(I) - \eta_{\text{int}}^{C}(I) - \eta_{\text{int}}^{A}(I). \tag{6}$$

3.2 The Interface Phenomena

At open circuit, ions and electrons produced by the electrochemical reactions are accumulated around the electrode–electrolyte interface. The reaction goes on until the electrostatic potential of this "double electric layer" equals the reaction potential, E_A or E_C (see Fig. 3).

When the circuit is closed, electronic and ionic current tends to cancel polarizations, while reactions tend to restore them. When reactions are not fast enough, depolarizations, or overpotentials, are created which contribute to accelerate reactions. Equilibrium is reached that, in general, is well described by the Butler–Volmer formula, which links the current density production to the depolarization η_{int}:

$$\nabla \cdot I = a i_{0,\text{ref}} \left(\frac{c_{\text{RL}}}{c_{\text{ref}}} \right)^{\gamma} \left(e^{\alpha\beta\eta_{\text{int}}} - e^{-\alpha\beta\eta_{\text{int}}} \right), \tag{7}$$

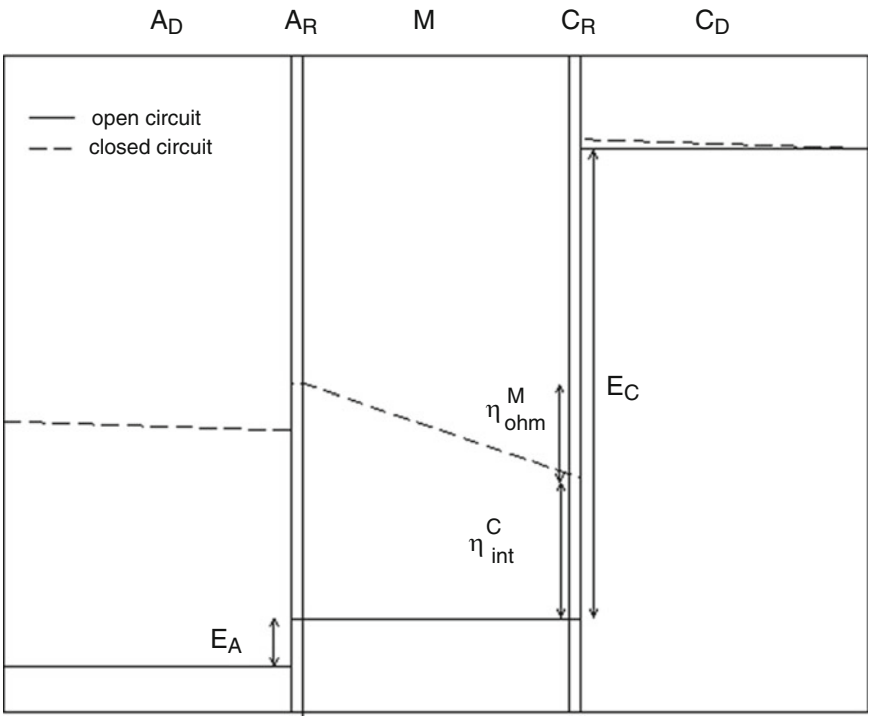

Fig. 3 I-behavior of the potentials in the FC regions

in which a is the catalyst area per unit volume, $i_{0,\mathrm{ref}}$ the reference current density, c_{RL} the reactant concentration in the reactive layer, c_{ref} the reference concentration, α and γ the kinetic parameters, and $\beta = 1/k_{\mathrm{B}}T$.

The cell current density can be obtained by integrating the Butler–Volmer equation within the reactive layer thickness, L_{RL}:

$$I = I_0 + ai_{0,\mathrm{ref}} \int_{L_{\mathrm{RL}}} \left(\frac{c_{\mathrm{RL}}}{c_{\mathrm{ref}}}\right)^{\gamma} \left(e^{\alpha\beta\eta_{\mathrm{int}}} - e^{-\alpha\beta\eta_{\mathrm{int}}}\right) \mathrm{d}V, \qquad (8)$$

from which we can get $\eta_{\mathrm{int}}(I)$.

3.3 The Interface Overpotential

By using the assumptions:

1. The electrochemical reaction follows the phenomenological Butler–Volmer equation.
2. The potentials and the reactant concentration are approximately constant inside the reactive layer.
3. The electrolyte does not conduct electronic current.

It follows that the crossover current is zero and η_{int} and c_{RL} are constant. The integral in Eq. 8 becomes trivial:

$$I = ai_{0,\mathrm{ref}} L_{\mathrm{RL}} \left(\frac{c_{\mathrm{RL}}}{c_{\mathrm{ref}}}\right)^{\gamma} \left(e^{\alpha\beta\eta_{\mathrm{int}}} - e^{-\alpha\beta\eta_{\mathrm{int}}}\right). \qquad (9)$$

Equation 9 can be easily inverted to get η_{int} as a function of I:

$$\eta_{\mathrm{int}} = \frac{1}{\alpha\beta} \ln\left\{ \frac{I}{2ai_{0,\mathrm{ref}} L_{\mathrm{RL}}} \left(\frac{c_{\mathrm{ref}}}{c_{\mathrm{RL}}}\right)^{\gamma} + \sqrt{1 + \left(\frac{I}{2ai_{0,\mathrm{ref}} L_{\mathrm{RL}}}\right)^{2} \left(\frac{c_{\mathrm{ref}}}{c_{\mathrm{RL}}}\right)^{2\gamma}} \right\}. \qquad (10)$$

In the Tafel limit $\alpha\beta\eta_{\mathrm{int}} >> 1$, the second exponential term in Eq. 9 can be neglected and the expression becomes much simpler:

$$\eta_{\mathrm{int}} = \frac{1}{\alpha\beta} \ln\left\{ \frac{I}{ai_{0,\mathrm{ref}} L_{\mathrm{RL}}} \left(\frac{c_{\mathrm{ref}}}{c_{\mathrm{RL}}}\right)^{\gamma} \right\}. \qquad (11)$$

The equations above express η_{int} as a function of the current density I and of the reactant concentration inside the reactive layer c_{RL}, which, on its hand, depends on the current density. In the next section, in order to derive the performance curve, we make such dependency explicit.

3.4 Reactant Concentration

Reactant concentrations can be obtained by using the following assumptions:

1. The gradient of the reactant concentration is proportional to the molar flux, N.
2. The molar flux is proportional to the current density.
3. The fluxes are 1D in the direction perpendicular to the FC plane.

The first assumption implies that the reactant diffuses through the electrode with a constant diffusion coefficient D. This can be written as

$$\nabla c = -\frac{N}{D}, \tag{12}$$

which is a phenomenological diffusion equation. The second assumption implies that all the reactant flux is consumed by the electrochemical reaction and no flux crosses through the electrolyte. In this condition, the molar flux, N, can be expressed through the Faraday relation:

$$N = \frac{I}{nF}, \tag{13}$$

where F is the Faraday constant and n is the number of electrons exchanged in the electrochemical reaction for each reactant molecule.

Substituting this expression of N in Eq. 12 and integrating through the electrode diffusion layer, we easily get

$$c_{\mathrm{RL}} = c_{\mathrm{in}}\left(1 - \frac{I}{I_{\mathrm{lim}}}\right), \quad I_{\mathrm{lim}} = \frac{nFDc_{\mathrm{in}}}{L_{\mathrm{D}}}, \tag{14}$$

where I_{lim} represents the value of current density at which the reactant concentration in the reactive layer becomes 0, c_{in} is the value of reactant concentration in the gas channel, and L_{D} is the thickness of the diffusion layer.

By inserting this expression of c_{RL} in Eq. 10 or 11, we get explicit expressions for the interface overpotential; in the Tafel limit:

$$\eta_{\mathrm{int}} = \frac{1}{\alpha\beta}\ln(I) - \frac{\gamma}{\alpha\beta}\ln\left(1 - \frac{I}{I_{\mathrm{lim}}}\right) + \frac{1}{\alpha\beta}\ln\left\{\frac{1}{ai_{0,\mathrm{ref}}L_{RL}}\left(\frac{c_{\mathrm{ref}}}{c_{\mathrm{in}}}\right)^{\gamma}\right\}. \tag{15}$$

3.5 Analytical Expression for the Performance Curve

By using Eqs. 5, 6, and 15, we finally get

$$V = V_0 - RI - \frac{1}{\alpha\beta}\ln(I) + \frac{\gamma}{\alpha\beta}\ln\left(1 - \frac{I}{I_{\mathrm{lim}}}\right) - \frac{1}{\alpha\beta}\ln\left\{\frac{1}{ai_{0,\mathrm{ref}}L_{\mathrm{RL}}}\left(\frac{c_{\mathrm{ref}}}{c_{\mathrm{in}}}\right)^{\gamma}\right\}. \tag{16}$$

In Fig. 4, the different terms of the above expression are associated to the various characteristic behaviors of the performance curve.

The term aL_{RL} reflects the effective catalyzer volume and $i_{0,\mathrm{ref}}$ its quality. It is seen that changing the catalyzer, the entire performance curve is shifted vertically by a constant amount.

The quantity R reflects the electrolyte conductivity and is responsible for the slope of the performance curve in its quasi-linear portion.

The value I_{lim} reflects the quality of oxygen or fuel transport. Its effect on the performance curve is a sharp voltage fall at high current densities.

Equation 16 is, in fact, the result of the simplest model representation describing all the main characteristics of the performance curve. Note that this model is general, while most, if not all, of the literature models are specific to particular FC types. A large number of more accurate and complex models exist in the literature, but their use and description lay beyond the scope of this chapter (e.g., Bernardi and Verbrugge 1992; Pisani et al. 2002a, b).

The present model can be easily and effectively used to perform parametric studies, optimizations, and cost analysis. It can also be used as a "semiempirical" function, by fitting the parameters to experimental performance curves and by using their physical meaning to analyze the FC working behavior and identify possible failures.

In the next section, Eq. 16 is analyzed to provide some general information on the fuel cell performances.

3.6 A Simple Analysis of the Performance Curve

The potential in Eq. 16 is a monotone decreasing function of the current density. The fuel cell conversion efficiency, which is proportional to V, is, as well, a decreasing function of I. Therefore, maximal efficiency is obtained for I close to 0. On the other hand, the electric power $P = V(I) \times I$ is 0 for both $I = 0$ and $V(I) = 0$, while it is positive in between, where, obviously, it reaches a maximum value $P = P_{\mathrm{max}}$. Optimal operating conditions, in general, depend on the particular application and range between $I = 0$ and $I = I(P_{\mathrm{max}})$, depending on the relative importance of efficiency versus produced power. For current density larger than $I(P_{\mathrm{max}})$, both power and efficiency decrease and operating in that range should be avoided.

The limiting current density depends mainly on the reactant transport and the concentration overpotential is relevant only near I_{lim}. A good design of the cell should guarantee $I_{\mathrm{lim}} >> I(P_{\mathrm{max}})$. In such conditions, indeed, concentration overpotential plays a marginal role and can be neglected.

The maximal efficiency, near $I = 0$, depends only on the reaction kinetics, while the maximal power density depends both on kinetics and on the cell resistance R.

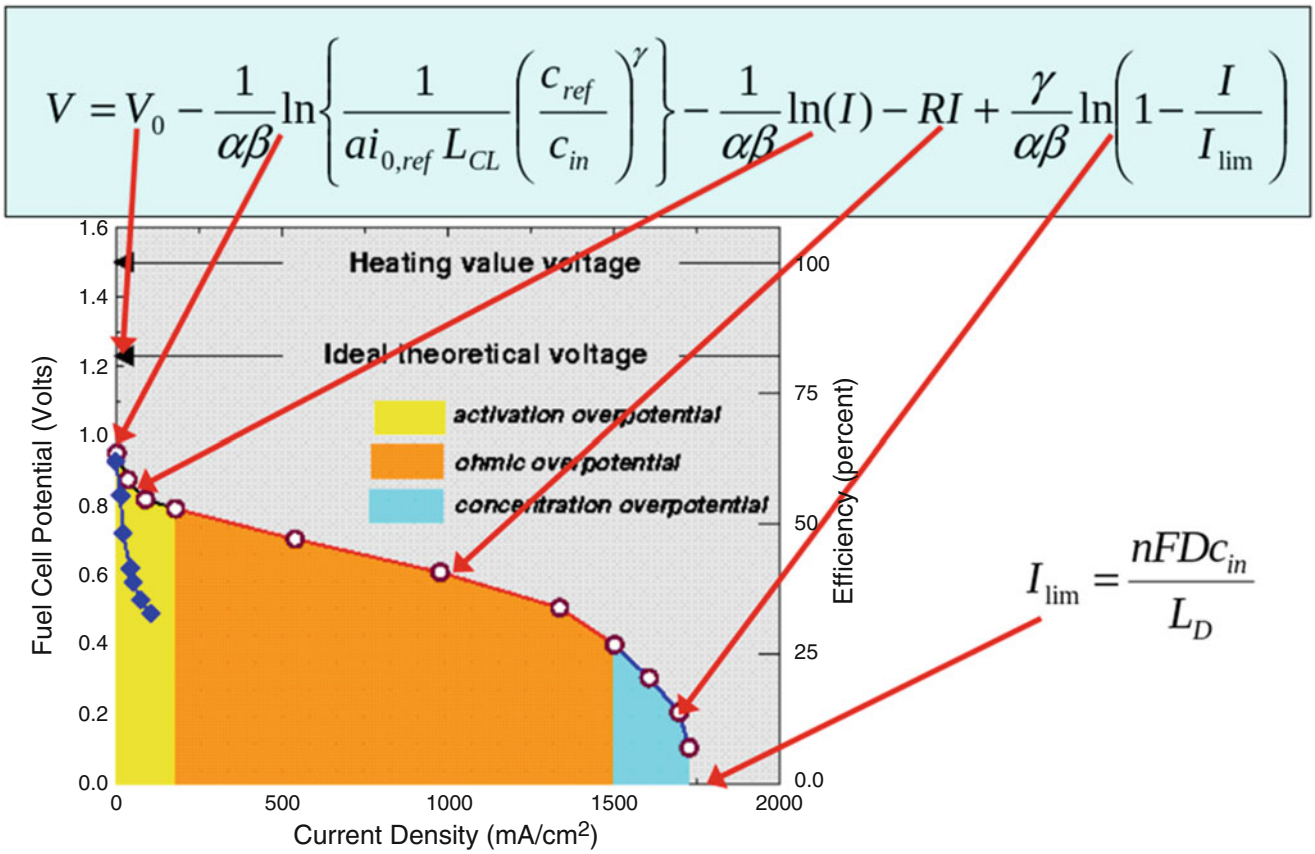

Fig. 4 The performance curve of a FC

In summary, it can be stated that efficiency and power losses depend mainly on electrolyte and electrocatalyst materials. The research on the optimization and design of materials for these crucial components is very much alive as exemplified in the next Section.

4 FC Materials

The function of the electrolyte is to conduct an ionic current between the two electrodes while constraining the electrons to pass through the external circuit. The main issue is to find a manageable ionic conductor material, with a good ionic conductivity in order to minimize ohmic losses.

Different ionic conduction mechanisms can be used, including:

- Conduction in water electrolytic solutions (acid or basic)
- Conduction in unhydrated ionic liquids as phosphoric acid or molten salts
- Conduction in solids

The materials allowing the above ion transport mechanisms are very different and range from polymeric membranes to ceramic materials. None of the known materials possessed the characteristics of conductivity, durability, and cheapness required to make the fuel cell technology competitive in large-scale applications, and, thus, a large amount of scientific work has been devoted in the development of "new" electrolytic materials optimized for the fuel cell technology.

In this section, as an example of such "material design," we focus, in general, on the LTFC technology and, in particular, on the polymer electrolyte membranes. Similar efforts and improvements have been obtained in the field of ceramic materials for the SOFC technology.

The modern state of the art of functional materials for application in LTFCs consists in:

(a) Proton-conducting membranes based on pristine perfluorinated ionomers operating at a high hydration degree at ca. 80 °C
(b) Supported platinum electrocatalysts

These FCs must be fueled with very pure reactants to achieve the optimal performance. As of today, there are significant obstacles for the implementation of FC technology in practical applications. In particular (Di Noto et al. 2012d):

- Operation at 80 °C in humidified conditions adds significantly to the complexity and cost of the FC power plant, which must include bulky and expensive heat and water management modules.

- Functional materials are very expensive; large amounts of scarce elements (i.e., platinum-group metals, PGMs, such as Pt) are needed, or a very complex synthetic procedure (e.g., in the case of perfluorinated ionomers) must be followed.
- Durability should be improved, to match the requirements of applications (up to ca. 5,000 h for the automotive sector and 40,000 h for stationary systems).
- Very pure reactants are expensive, but are a necessity since state-of-the-art electrocatalysts are characterized by a low tolerance to common contaminants (e.g., CO found in H_2 fuel obtained by steam-reforming processes).

To address these issues, one of the main approaches is to increase the operating temperature of the FC up to 120 °C and higher, without humidifying the reactant streams. In these conditions, the management of heat and water in the FC power plant becomes much easier, yielding much cheaper and compact systems. Furthermore, at T > 120 °C, the tolerance of the electrocatalysts to the contaminants increases dramatically, and the FC can run directly on cheap hydrogen obtained from steam-reforming processes. Another possibility is to devise FC systems based on anion-exchange membranes, AEMs, capable to carry OH^- anions; indeed, in an alkaline environment, it is possible to prepare highly efficient electrocatalysts that do not require PGMs. However, significant efforts are still to be spent in this area as AEM performance is compromised by the exposure to the traces of CO_2 found in air; in addition, AEMs are not as durable as state-of-the-art perfluorinated ionomers.

As of today, significant efforts are also spent in the development of oxygen reduction reaction (ORR), electrocatalysts for application in an acid environment (i.e., in PEMFCs, and high-temperature PEMFCs, HT-PEMFCs) which are not based on PGMs. Very promising results have been achieved, even if the durability and current density yielded by the electrodes mounting these PGM-free electrocatalysts are still to be increased to be of interest for practical applications.

4.1 Electrolyte Membranes for FCs

The electrolyte membranes for application in FCs must ensure a facile and selective transport of the ions involved in the operation of the device.

To maximize the FC performance, as a function of the operative temperature and of the ion type involved in the transport (e.g., in PEMFC or AEMFC), several types of widely different materials are used in the fabrication of the electrolyte membranes. However, the vast majority of these materials share some common fundamental features, the most important of which is a clear phase separation between highly polar domains (where the ions actually migrate) and a supporting matrix, providing the electrolyte membrane with its mechanical properties.

Perfluorinated ionomers are the reference materials to manufacture proton-conducting membranes for application in PEMFCs. These materials include a perfluorocarbon backbone and perfluoroethereal side chains tipped with $-SO_3H$ groups, giving rise to the polar domains (see Fig. 5).

The various ionomers are differentiated by the exact chemical structure and linear density of side chains along the backbone. As of today, most research has been devoted to Nafion™; recently, other ionomers have attracted attention such as the 3 M ionomers (Giffin et al. 2012a). The latter systems are characterized by shorter side chains in comparison with Nafion, including only one ether linkage (see Fig. 5); this has significant repercussions on the domain separation and proton conduction mechanism of the material (Giffin et al. 2012a). In particular, it is observed that the short side chains of 3 M ionomers yield an improved proton conductivity to the final electrolyte membrane in comparison with Nafion.

Water plays a crucial role in the phase separation and proton conduction mechanism of regular perfluorinated ionomers. However, if water is not present (e.g., in a PEMFC operating at T > 90 °C, or if the reactant feeds are not humidified properly), the drop in proton conductivity is dramatic, compromising the operation of the PEMFC. One way to address this issue is to dope a perfluorinated ionomer with a proton-conducting ionic liquid, PCIL (Di Noto et al. 2010). In the resulting systems, the PCIL substitutes water as the ion-conducting medium in the polar domains (see Fig. 6), ensuring remarkable proton conductivity even at high temperatures and in dry conditions.

While perfluorinated ionomers show an excellent proton conductivity in hydrated conditions and a very good chemical and electrochemical stability, they are also very expensive owing to a complex synthetic process involving very hazardous intermediates. One way to address these issues is to develop other ionomers based on much cheaper polyaromatic backbones such as polyethersulfone (PSU), polyphenylenesulfone (PPSU), and polyetheretherketone (PEEK). The proton conductivity is bestowed by functionalizing these polymeric backbones with suitable amounts of $–SO_3H$ groups (see Fig. 5). The phase separation properties and proton-conducting mechanisms of these materials are significantly different in comparison with standard perfluorinated ionomers (Di Noto et al. 2012b).

Another possibility is to devise hybrid materials, where a polymeric matrix characterized by a high chemical and electrochemical stability (e.g., PTFE blended with silicone rubber) is used to disperse an inorganic component bearing sulfonated groups, which allow the hybrid to conduct protons (see Fig. 7) (Di Noto et al. 2012c).

The electrolyte membranes for application in HT-PEMFCs show a completely different chemical composition and structure in comparison with those adopted in PEMFCs. In general, the HT-PEMFC membranes consist of (a) a polymer matrix able to tolerate high temperatures and

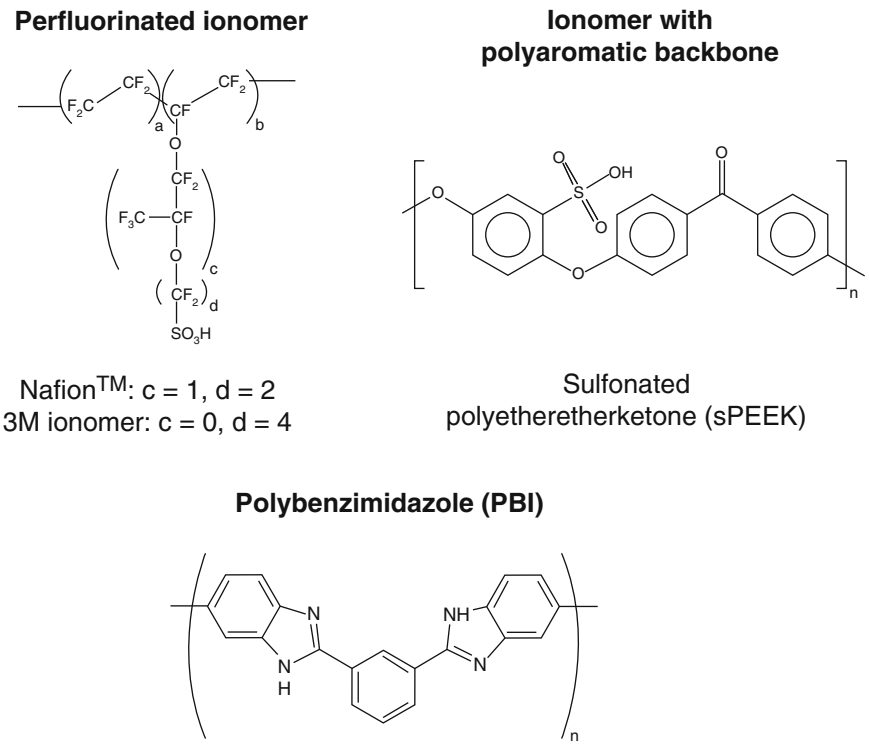

Fig. 5 Some common matrices used in the fabrication of electrolyte membranes for PEMFCs and HT-PEMFCs (Adapted from Di Noto et al. 2012d)

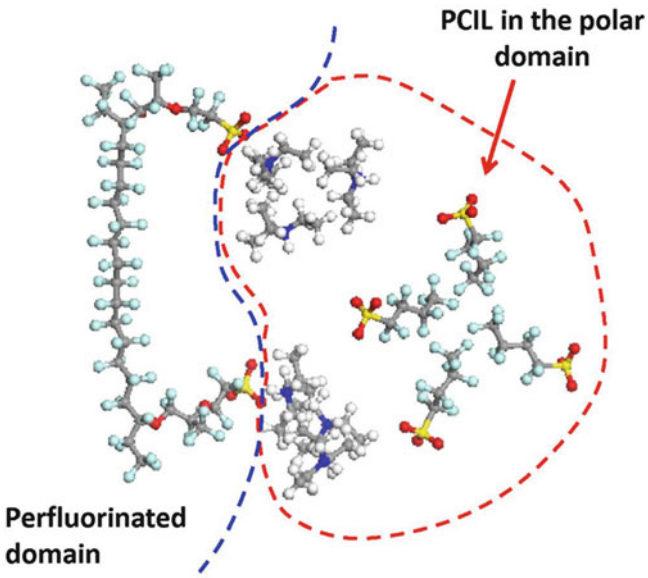

Fig. 6 Typical morphology of a perfluorinated ionomer doped with a PCIL

bearing a large concentration of functionalities bestowing to the system a high Lewis basicity (e.g., polybenzimidazole or its derivatives; see Fig. 6) and (b) phosphoric acid, which is used to soak the polymer matrix and acts as the proton-conducting medium.

Acid–base proton exchange reactions are known to take place between the phosphoric acid and the imidazole moieties in the polymer chains. This gives rise to a perturbation in the extended conjugated systems of the resulting protonated diimidazolium cations, allowing rotation of the benzimidazole monomer units along the polymer chain.

Finally, the ionomers used to fabricate the anion-exchange membranes (AEMs) for application in AEMFCs are characterized by backbone chains, which may be comprised of block copolymers, which are functionalized with the anion-exchange groups allowing the system to carry ions. Very little information is available on the details of the ion conduction mechanism of these systems. However, it was demonstrated that in the case of the commercial Selemion AMV™ anion-exchange membrane, the dynamics of the membrane are not significantly involved in the mechanism of long-range conduction, unlike most of the ionomers used in PEMFCs (Giffin et al. 2012b).

One of the most fruitful avenues of research in the field of electrolyte membranes for application in FCs is the development of hybrid materials, obtained by doping a pristine ionomer with one or more additional components (e.g., ceramic oxide nanoparticles, ionic liquids). This approach gives rise to the formation of additional interfaces in the hybrid material, where a variety of new interactions between the host ionomer and the guest component(s) take place. Consequently, it becomes possible to modulate the properties of the host ionomer, so that the final hybrid electrolyte membrane is optimized for the intended application. In general, the introduction of a filler based on oxide nanoparticles improves the mechanical properties of the host ionomer, owing to

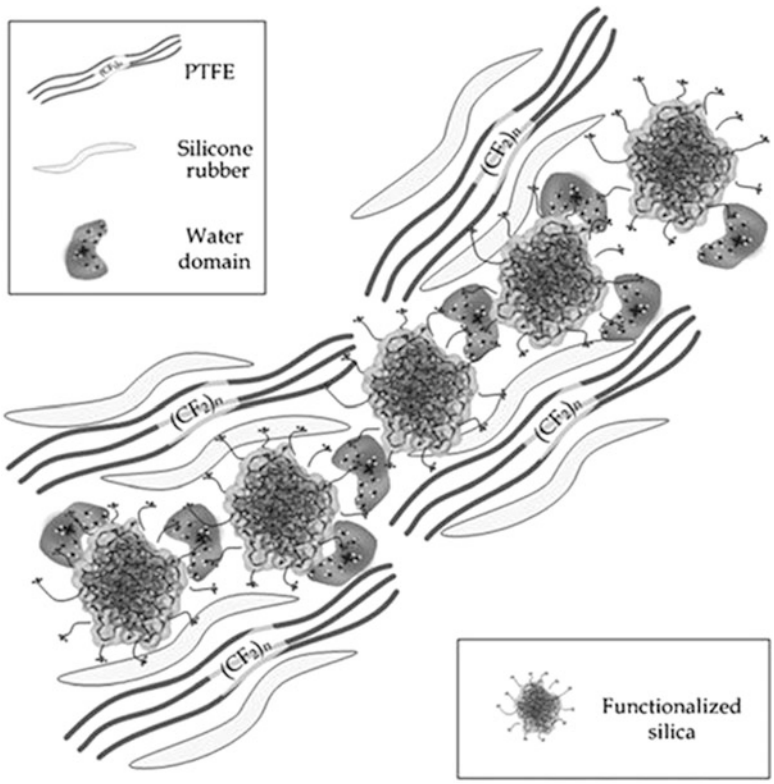

Fig. 7 Structure of a proton-conducting hybrid membrane consisting of PTFE, silicone rubber, and functionalized silica (Adapted from Di Noto et al. 2012c)

the formation of dynamic cross-links between the two components (see Fig. 8) (Di Noto et al. 2009).

The large body of research carried out in this area yielded, until today, an improved understanding of (a) the complex interplay between the composition, morphology, thermo-mechanical properties and electric response and (b) the long-range charge transport mechanism of ion-conducting membranes. This information is of fundamental importance to devise new electrolyte membranes for application in energy conversion and storage devices other than FCs, e.g., dye-sensitized solar cells, DSSCs, and redox flow batteries, RFBs.

4.2 ORR Electrocatalysts for Application in FC

The kinetics of the electrochemical processes involved in the operation of PEMFCs must be promoted by suitable electrocatalysts to achieve a performance level compatible with the applications. Today's state-of-the-art electrocatalysts for PEMFCs are characterized by platinum nanocrystals supported on active carbons featuring a large surface area such as Vulcan XC-72R (see Fig. 9).

The hydrogen oxidation reaction, HOR, is a relatively facile process; on the other hand, the oxygen reduction reaction (ORR) is much more sluggish, giving rise to significantly higher overpotentials. Thus, most of the Pt loading in a PEMFC fueled with H_2 is located at the cathode electrode. For these reasons, most of today's research efforts are focused to devise new ORR electrocatalysts characterized by a higher activity, a lower loading of Pt or other scarce elements, and a better durability in comparison with the state of the art.

In the last few years, a large number of innovative preparation methods are described in the literature (see, e.g., Ref. (Di Noto and Negro 2010)), allowing to introduce in the final electrocatalysts the desired concentration of metal atoms. The latter become embedded in metal alloy nanoparticles, which bear on their surface the active sites of the electrocatalyst. The best performance in the ORR is achieved with bi-/plurimetal active sites, comprising a platinum-group metal (PGM), e.g., Pt or Pd, together with one or more first-row transition metals such as Fe, Co, or Ni (Di Noto and Negro 2010). The PGM must be in its (0) oxidation state, allowing an easy adsorption of the incoming oxygen molecules. The other metals must be in their most stable oxidized state (e.g., III in the case of Fe) and act as cocatalysts; the nitrogen atoms of the coordination nests bind them to the surface of the active sites, preventing their facile removal during FC operation. The cocatalysts are strong Lewis acids; thus, they facilitate the protonation of ORR intermediates on the active sites, prompting the removal of ORR products. Consequently, the active sites are regenerated more quickly, boosting the kinetics of the ORR process according to a bifunctional mechanism. On the other hand, the introduction of a first-row transition

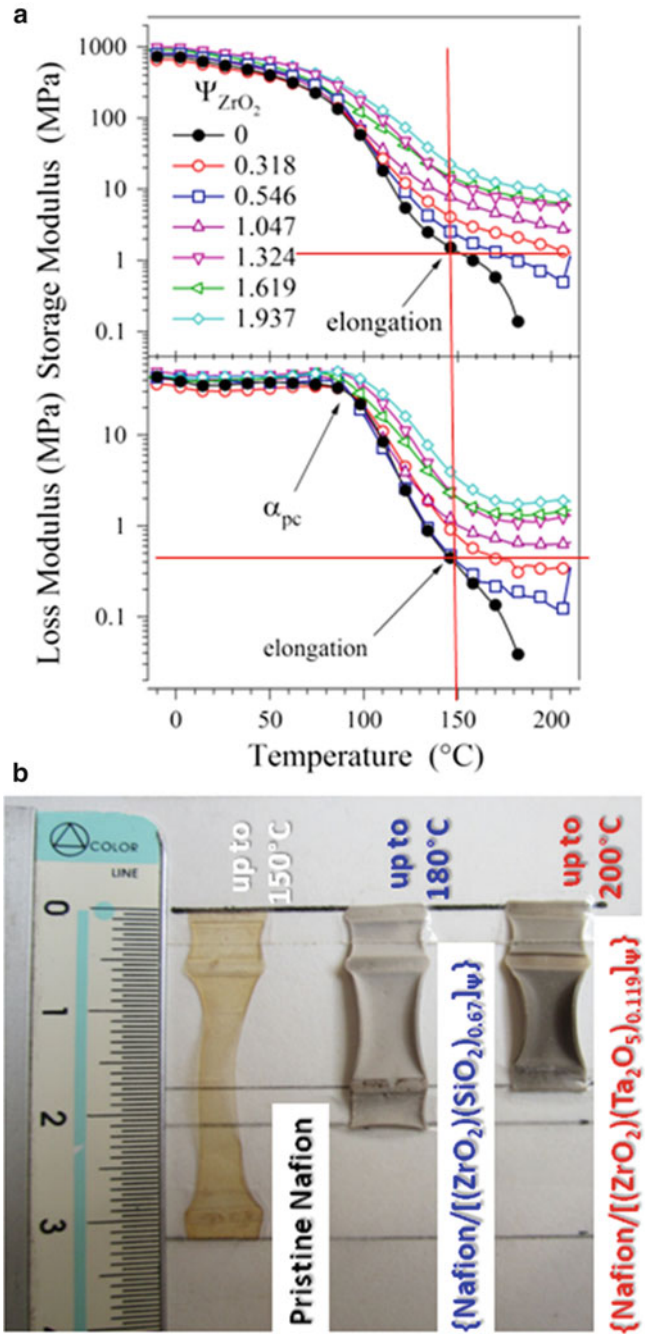

Fig. 8 Effect of the doping with a "core–shell" inorganic nanofiller on the mechanical properties of hybrid inorganic–organic Nafion-based nanocomposite membranes. (**a**) Trends of storage and loss moduli versus T in {Nafion/[$(ZrO_2)(Ta_2O_5)_{0.119}$]Ψ} membranes. (**b**) Samples after DMA measurements

metal in the PGM lattice of the metal alloy nanoparticles of the electrocatalysts also gives rise to a contraction of the unit cell; correspondingly, the center of the d-band is lowered, pushing to higher potentials the blocking of ORR active sites by oxygen-based adsorbates. As a result, the minimum ORR overpotential is lowered, improving the kinetics of the process by means of an electronic mechanism.

A major breakthrough in the development of this family of electrocatalysts was achieved with the ideation of "core–shell" materials (see Fig. 9) (Di Noto and Negro 2010).

The morphology of a "core–shell" electrocatalyst allows a better dispersion of the active sites in comparison with a similar pristine material, facilitating the transport of reactants and products in the electrode layer (Di Noto et al. 2012a). Moreover, very small metal alloy nanoparticles can be formed, maximizing the area of the active sites. Consequently, a much-improved FC performance is achieved.

5 Regenerative FC

A regenerative fuel cell (RFC) is a single device or system capable of functioning as either an electrolyzer or a fuel cell (Andrews and Doddathimmaiah 2008). Usually the reversible reaction employed is the decomposition of water into hydrogen and oxygen and their recombination to form water. Among other reversible reactions studied for RFCs have been hydrogen–halogen reactions (in particular bromine) and the zinc–oxygen reaction (Mitlitsky et al. 1998).

In a discrete regenerative fuel cell (DRFC), the device used to perform the electrolysis is separate to that used as a fuel cell, but these two devices are both integrated into a single system. However, it is only in what is called a unitized regenerative fuel cell (URFC) that the RFC concept is fully manifest, by using the same physical cell in both electrolyzer and fuel cell modes (see Fig. 10). When a DC electricity is applied to the cell in electrolyzer (E) mode, water is dissociated into hydrogen and oxygen gas, which are stored. In fuel cell mode, these gases fed back into the cell to regenerate electricity and reform water. More commonly, just the hydrogen is stored and the RFC draws on oxygen from the air when operating as a fuel cell.

A URFC offers potential cost, space, and mass savings over the conventional hydrogen-based electrical energy storage system and a DRFC, in that only one electrochemical cell is required rather than two. The concomitant technical challenge is getting a round-trip energy efficiency in a URFC close to or equal to that of a separate electrolyzer and fuel cell. Andrews and Doddathimmaiah's (Andrews and Doddathimmaiah 2008) review found the highest reported round-trip energy efficiency for a URFC was 38.3 % (E mode, 85.3 %; FC mode, 44.9 %). It was suggested that raising this to 45 % should be achievable, some 5 % points lower than that achievable with the best performing discrete electrolyzer and fuel cell in combination.

The design of URFC stacks involves some special challenges. In particular, similar operating conditions must be maintained in both modes in all cells within the stack in terms of gas flows, water flows, pressure, and temperature,

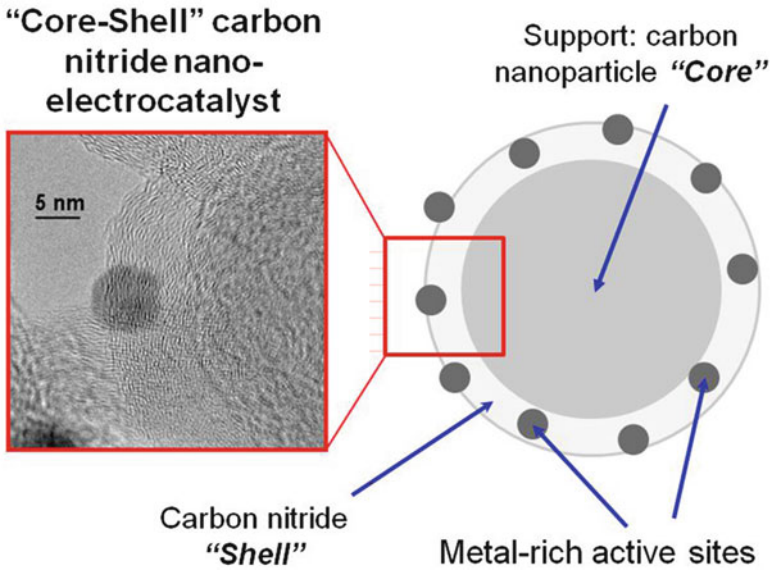

Fig. 9 Morphology of a "core–shell" carbon nitride nano-electrocatalyst (Adapted from Di Noto et al. 2012a)

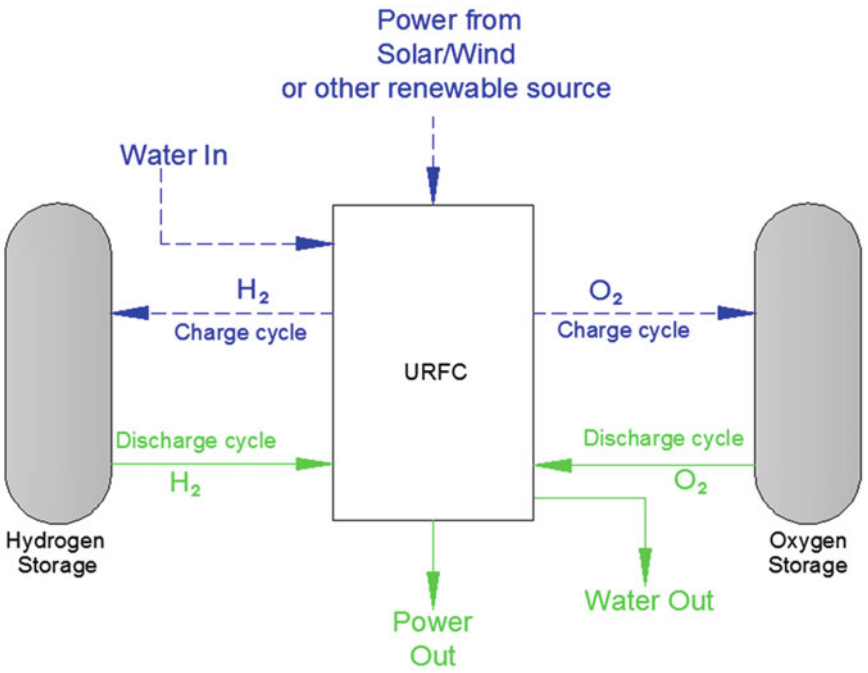

Fig. 10 A schematic of a unitized regenerative fuel cell system (URFC) supplied by renewable energy sources of electricity

so that each cell output is around the same value. The water management system must in E mode ensure sufficient water is available on the O-side electrodes of each cell in the stack, and remove water that gathers on the H-side electrodes due to osmotic drag of water molecules by H^+ ion across the membrane. On switching to FC mode, this system must remove any excess water in O-side GDBs and flow channels, remove water vapor produced by the overall electrochemical reaction, and ensure the membrane remains hydrated.

Functioning URFC stacks with up to seven cells in series have recently been reported in the literature (e.g., Ref. (Su et al. 2009; Grigoriev et al. 2011)).

5.1 Materials

Most URFCs to date have employed a proton exchange membrane (PEM) as a solid electrolyte, since they work at relatively low temperatures up to 80 ºC. However, high-temperature (600–1,000 °C) solid oxide cells have also been used.

In the most common type of URFC, the electrode from which hydrogen is evolved in E mode and consumed in FC mode stays the same (see Fig. 11). In E mode, the catalyst layer in the oxygen electrode must facilitate the water-molecule splitting reaction, and in FC mode the reverse

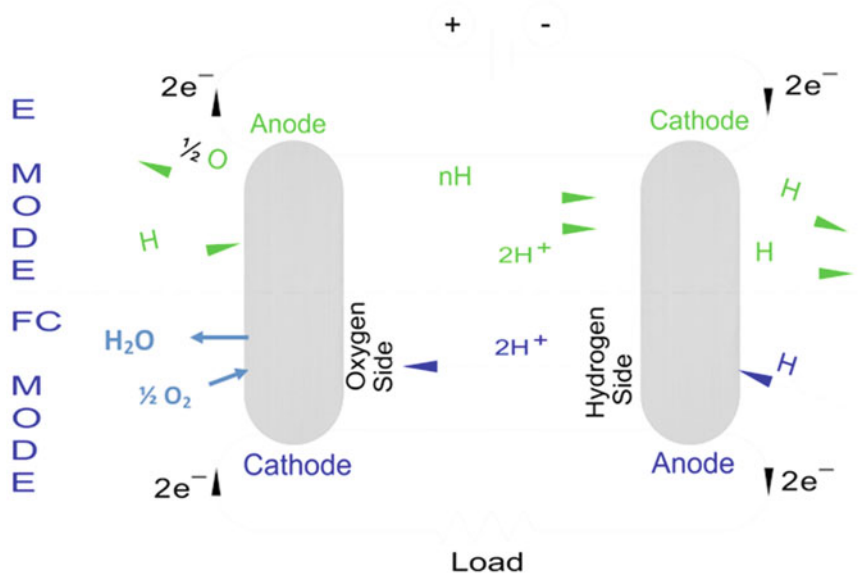

Fig. 11 The electrolyzer (*E*) mode (*top*) and fuel cell (*FC*) mode (*bottom*) reactions in a URFC in which the oxygen and hydrogen electrodes remain the same in the two modes

water-formation reaction. So this layer must be bifunctional and usually contains a mix of catalysts: Pt for use in FC mode with the addition of other elements and/or their oxides to enhance the water splitting reaction. The catalyst layer on the hydrogen side typically contains just Pt, which functions equally well in the hydrogen molecule formation and dissociation reactions.

The main catalysts reported as being used on URFCs on the oxygen side over the past few years are still Pt plus Ir, IrO_2, RuO_2, IrO2/RuO_2, Pt/TiO_2, and Ir/TiO_2 (see, e.g., Ref. (Jung et al. 2009; Cruz et al. 2012)). A lot of the emphasis in research on these has been on fabricating porous structures of these mixed catalysts to maximize the effective reaction areas.

The support medium for the catalysts on the oxygen side is also ideally porous and must be resistant to the water and oxidizing environment. Materials employed include the usual Nafion and carbon cloth and paper, graphitized carbon (see Ref. (Pai and Tseng 2012)), titania (Huang et al. 2012), Sb-doped SnO_2 (ATO), plasma-assisted deposition of nanoparticles of catalyst (Pt and Pd) on carbon powder, nanotubes and nanofibers (Fedotov et al. 2013), titanium carbide, TiC, and TiCN (Garcia et al. 2013; Sui et al. 2011).

Materials being investigated for the GDL on the oxygen side to prevent degradation and corrosion include a conventional carbon substrate with a protective microporous layer of iridium–titanium nitride, titanium felt (Ito et al. 2012), and metallic ceramics such as titanium carbide (TiC) (Chen et al. 2010).

5.2 Challenges

A key challenge in future URFC design is to obtain a round-trip energy efficiency very close that of a system with a separate electrolyzer and fuel cell, with an oxygen-side catalyst layer that performs equally well in both E and FC modes remaining a focus in research. The development of long-lived cells resistant to corrosion or other degradation, and retention of structural integrity and strength after repeated cycling and mode switching, is another important goal. There is still a lack of practical designs and operating experience for URFC stacks with more than six or seven cells. URFC stacks must be able to operate in E mode at pressures up to 10 or 20 bar, so that hydrogen can be stored as compressed gas or metal hydrides in vessels of practical size in stand-alone power supplies, without the need for an external compressor.

If these technical challenges can be overcome, the potential cost, space, and mass savings that a URFC offers compared to conventional hydrogen-based electrical energy storage system open up numerous applications in space vehicles and satellites, submarines, aircraft, remote or distributed terrestrial energy supply systems, electricity storage in central grids or at a local level when there is variable energy input from solar or wind power, electricity storage at a local level, and possibly in hydrogen electric cars capable of generating some of their own hydrogen fuel when parked.

Acknowledgements The financial support of the Sardinia Region Authority is gratefully acknowledged.

References

Andrews, J., Doddathimmaiah, A.: Regenerative fuel cells. In: Fuel Cell Materials, pp. 344–385. Woodhead Publishing, Cambridge, UK (2008)

Bernardi, D.M., Verbrugge, M.: A mathematical model of the solid-polymer-electrolyte fuel cell. J. Electrochem. Soc. **139**, 2477 (1992)

Chen, G., Zhang, H., Zhong, H., Na, H.: Gas diffusion layer with titanium carbide for a unitized regenerative fuel cell. Electrochem. Acta **55**, 8801 (2010)

Cruz, J., Baglio, V., Siracusano, S., Ornelas, R., Arriaga, L., Antonucci, V., Arico, A.: Nanosized Pt/IrO_2 electrocatalyst prepared by modified polyol method for application as dual function oxygen electrode in unitized regenerative fuel cells. Int. J. Hydrog. Energy **37**, 5508 (2012)

Di Noto, V., Negro, E.: Development of nano-electrocatalysts based on carbon nitride supports for the ORR processes in PEM fuel cells. Electrochem. Acta **55**, 7564 (2010)

Di Noto, V., Lavina, S., Negro, E., Vittadello, M., Conti, F., Piga, M.: Hybrid inorganic-organic proton conducting membranes based on nafion and 5 wt% of MxOy(M = Ti, Zr, Hf, Ta and W). Part ii: relaxation phenomena and conductivity mechanism. J. Power Sources **187**, 57 (2009)

Di Noto, V., Negro, E., Sanchez, J.Y., Iojoiu, C.: Structure-relaxation interplay of a new nanostructured membrane based on tetraethylammonium trifluoromethanesulfonate ionic liquid and neutralized nafion 117 for high-temperature fuel cells. J. Am. Chem. Soc. **132**, 2183 (2010)

Di Noto, V., Negro, E., Polizzi, S., Agresti, F., Giffin, G.A.: Synthesis-structure-morphology interplay of bimetallic "core-shell" carbon nitride nano-electrocatalysts. Chem. Sus. Chem. **5**, 2451 (2012a)

Di Noto, V., Piga, M., Giffin, G.A., Pace, G.: Broadband electric spectroscopy of proton conducting SPEEK membranes. J. Membr. Sci. **58**, 390–391 (2012b)

Di Noto, V., Piga, M., Giffin, G., Negro, E., Furlan, C., Vezzù, K.: New nanocomposite hybrid inorganic–organic proton-conducting membranes based on functionalized silica and PTFE. Chem. Sus. Chem. **5**, 1758–1766 (2012c)

Di Noto, V., Zawodzinski, T.A., Herring, A.M., Giffin, G.A., Negro, E., Lavina, S.: Polymer electrolytes for a hydrogen economy. Int. J. Hydrog. Energy **37**, 6120 (2012d)

Fedotov, A., Grigoriev, S., Millet, P., Fateev, V.N.: Plasma-assisted Pt and Pt–Pd nano-particles deposition on carbon carriers for application in PEM electrochemical cells. Int. J. Hydrog. Energy **38**, 8568 (2013)

Garcia, G., Roca-Ayats, M., Lillo, A., Galante, J.L., Pena, M.A., Martinez-Huerta, M.V.: Catalyst support effects at the oxygen electrode of unitized regenerative fuel cells. Catal. Today **210**, 67 (2013)

Giffin, G.A., Haugen, G.M., Hamrock, S.J., Di Noto, V.: Interplay between structure and relaxations in perfluorosulfonic acid proton conducting membranes. J. Am. Chem. Soc. **135**, 822 (2012a)

Giffin, G.A., Lavina, S., Pace, G., Di Noto, V.: Interplay between the structure and relaxations in selemion amv hydroxide conducting membranes for AEMFC applications. J. Phys. Chem. C **116**, 23965 (2012b)

Grigoriev, S., Millet, P., Porembsky, V., Fateev, V.N.: Development and preliminary testing of a unitized regenerative fuel cell based on PEM technology. Int. J. Hydrog. Energy **36**, 4164 (2011)

Huang, S.-Y., Ganesan, P., Jung, H.-Y., Popov, B.N.: Development of supported bifunctional oxygen electrocatalysts and corrosion-resistant gas diffusion layer for unitized regenerative fuel cell applications. J. Power Sources **198**, 23 (2012)

Ito, H., Maeda, T., Nakano, A., Hwang, C.M., Ishida, M., Kato, A., Yoshida, T.: Int. J. Hydrog. Energy **37**, 7418 (2012)

Jung, H.-Y., Park, S., Popov, B.N.: Electrochemical studies of an unsupported PtIr electrocatalyst as a bifunctional oxygen electrode in a unitized regenerative fuel cell. J. Power Sources **191**, 357 (2009)

Mitlitsky, F., Myers, B., and Weisberg, A.H.: Regenerative fuel systems R & D. Proceedings of the U.S. DOE Hydrogen Program Review, Arlington (1998)

Pai, Y.-H., Tseng, C.-W.: Preparation and characterization of bifunctional graphitized carbon-supported Pt composite electrode for unitized regenerative fuel cell. J. Power Sources **202**, 28 (2012)

Pisani, L., Murgia, G., Valentini, M., D'Aguanno, B.: A new semi-empirical approach to performance curves of polymer electrolyte fuel cells. J. Power Sources **108**, 192 (2002a)

Pisani, L., Murgia, G., Valentini, M., D'Aguanno, B.: A working model of polymer electrolyte fuel cells: comparison between theory and experiments. J. Electrochem. Soc. **149**, A898 (2002b)

Signorelli, R. High energy and power density nanotube-enhanced ultracapacitor design, modeling, testing, and predicted performance. PhD thesis, MIT (2009)

Su, H.N., Liao, S.J., Xu, L.M.: Design, fabrication and preliminary study of a mini power source with a planar six-cell PEM unitised regenerative fuel cell stack. Fuel Cells **9**, 522 (2009)

Sui, S., Ma, L., Zhai, Y.: Tic supported Pt-Ir electrocatalyst prepared by a plasma process for the oxygen electrode in unitized regenerative fuel cells. J. Power Sources **196**, 5416 (2011)

Tozzini, V., Pellegrini, V.: Prospects for hydrogen storage in graphene. Phys. Chem. Chem. Phys. **15**, 80–89 (2013)

Winter, M., Brodd, R.: What are batteries, fuel cells, and supercapacitors? Chem. Rev. **104**, 4245–4269 (2004)

Engineering Aspects Related to the Use of Microalgae for Biofuel Production and CO_2 Capture from Flue Gases

Alessandro Concas, Massimo Pisu, and Giacomo Cao

Abstract

The recent achievements in the field of CO_2 capture and biofuel production through microalgae are presented in this chapter. Specifically, after a brief analysis of the main biological, chemical, and physical phenomena involved in the photosynthetic conversion of CO_2 to biofuels, the current technologies for CO_2 capture, microalgae growth, biomass harvesting, and lipid extraction are critically assessed with a particular focus on the potential exploitation of recent research results at the industrial scale. Finally, future scientific and technological directions for the direct CO_2 capture from flue gases through microalgae are also proposed.

Keywords

Microalgae • Biofuels • CO_2 capture • Photobioreactors • Microalgae harvesting • Lipid extraction • Photosynthesis

1 Introduction

World economy is strictly linked to the availability of fossil fuels, which nowadays meet the world's growing energy demand. However, the intensive exploitation of fossil fuels as main source of energy is currently recognized to be not sustainable due to the continuous depletion of available resources as well as to their contribution to environmental pollution and greenhouse gases emissions (Ahmad et al. 2011). Moreover, the inhomogeneous distribution of oil reservoirs around the world can lead to economic dependence issues which can give rise to geopolitical instabilities in several countries (Gupta 2008). For this reason, the production of renewable sources of energy such as biofuels is recognized to be critical to fulfill a sustainable economy and face global climate changes (Cheng and Timilsina 2011). Therefore, biofuels deriving from feedstocks such as plants, organic wastes, or algae could help to reduce the world's oil dependence (Naik et al. 2010). In fact, biomass feedstocks are intrinsically renewable since they are produced through a natural process, i.e. photosynthesis, that is continuously replenished by sunlight. Moreover, biofuels would mitigate global warming problems since all the CO_2 emitted during their burning can be fixed by plants used as biomass feedstock, through photosynthetic mechanisms. On the other hand, first- and second-generation biofuels are characterized by several drawbacks which can limit their exploitation as alternative source of energy.

1.1 First-Generation Biofuels

First-generation biofuels are mainly biodiesel (or bio-esters in general) ethanol and biogas which can be produced starting from biomass feedstocks such as rapeseed, sugarcane, maize, soybeans, palm oil, and sunflower. The

A. Concas • M. Pisu
Center for Advanced Studies, Research and Development in Sardinia (CRS4), Loc. Piscina Manna, Building 1, 09010 Pula (CA), Sardinia, Italy

G. Cao (✉)
Department of Mechanical, Chemical and Materials Engineering, University of Cagliari, Piazza d'Armi, 09123 Cagliari, Italy
e-mail: giacomo.cao@dimcm.unica.it

G. Cao and R. Orrù (eds.), *Current Environmental Issues and Challenges*,
DOI 10.1007/978-94-017-8777-2_5,

industrial processes which transform the biomass feedstock into biofuel clearly depend upon the starting feedstock as well as the desired biofuel (Naik et al. 2010). Nowadays, the most widespread processes for converting biomass into first-generation biofuels are the following: fermentation for producing ethanol, anaerobic digestion to obtain biogas, and oil extraction followed by transesterification for the production of biodiesel (Fig. 2). Moreover, physical methods are also extensively used for transforming raw biomass into briquettes or pellets to be used for feeding domestic boilers. In addition, even if less widespread, thermochemical processes such as pyrolysis are exploited for converting biomass into useful bio-oil (Naik et al. 2010). First-generation biofuels have now attained economic levels of production, and their use is continuously increasing all over the world. On the other hand, the large-scale production of crops to obtain biofuels is currently recognized to be unsustainable from the ethical and environmental point of view because of the significant stress that their production may determine on world food market (Brennan and Owende 2010). In fact, the large-scale diverting of farmlands or crops for biofuels can provoke the detriment of the food supply as well as a dramatic increase of food price which mainly impacts on the most vulnerable regions of the world. In the US, for example, during the last 10 years the percentage of the corn crop that has been used for biofuel production increased from about 10 % to about a third, causing a significant increase in the global corn price (Brennan and Owende 2010). Another important concern is related to the low areal productivity of energetic crops which results in the need of huge land areas for meeting the global demand of biofuels (Chisti 2007). This aspect places important concerns related to the conversion of forests into energetic crops which can, in turn, contribute to enhance problems such as soil erosion, loss of habitat, and reduction of valuable biodiversity. Finally, life cycle assessments of first-generation biofuels clearly demonstrated that their production and transportation can result in the emission of CO_2 amounts that approach those ones typical of traditional fossil fuels.

1.2 Second-Generation Biofuels

The food versus fuel competition triggered by first-generation biofuels has stimulated a greater interest for the development of biofuels produced from nonfood biomass, commonly referred to as second-generation biofuels (Timilsina et al. 2010). Biomasses to produce the latter ones are basically organic wastes and by-products that may result from different manufacturing processes. Among the others, feedstocks include, for example, agricultural residues, domestic wastes, wood/forestry residues, exhausted cooking oils, and food wastes, even if also nonedible oil crops are counted among the suitable feedstock (Ahmad et al. 2011; Brennan and Owende 2010). The most promising second-generation biofuels are those produced starting from residual of non-edible lignocellulosic biomasses derived from plants. Lignocellulosic biomass is actually one of the most abundant and less exploited biological resources on the planet, and thus today there is a great interest in developing suitable technologies for transforming it into liquid biofuels (Naik et al. 2010). The major components of lignocellulosic biomass are cellulose and hemicellulose (over 67 % of dry mass), which can be converted to different biofuels depending upon the specific thermochemical and/or biological processes adopted (Carriquiry et al. 2011). Currently, there are a lot of technologies for converting cellulose into viable biofuels being developed, but, from a conceptual point view, they can be divided into two fundamental categories. The first ones display a biochemical character since cellulose and hemicellulose are subjected to enzymatic hydrolysis to obtain sugars that are subsequently fermented for producing bioethanol. The second ones are the thermochemical, also known as biomass-to-liquids (BTL) technologies, where lignocellulosic materials are converted through pyrolysis/gasification processes to syngas mainly consisting of CO and H_2. The latter ones can be then burnt for producing electricity or, alternatively, converted into a wide range of long carbon chain biofuels, such as synthetic diesel, aviation fuel, or ethanol by means of the Fischer–Tropsch conversion technology (Sims et al. 2010). In addition, plant biomass can be also simply chopped and then conformed into briquettes or pellets, to be burnt for the production of electric energy or heat (Naik et al. 2010). When compared to first-generation ones, second-generation biofuels do not involve "*food* versus fuel" antagonism, are more efficient and more environmentally friendly, require less farmland, and can be grown in lands that are not suitable for food crops. However, since their production is strictly related to by-products availability, second-generation biofuels may not be abundant enough to meet the fuel demand on a large scale (Ahmad et al. 2011). Moreover, at present, the technology for producing second-generation biofuels from lignocellulosic biomass is still under development and has not still attained economic levels of production (Naik et al. 2010). More specifically the feedstock pretreatment technologies (cellulose hydrolysis and gasification) are still inefficient and costly and need to be drastically optimized in order to become economically viable (Sims et al. 2010).

1.3 Third-Generation Biofuels: Microalgae

Microalgae are microorganisms living in sea or freshwater that convert sunlight, water, carbon dioxide, and inorganic

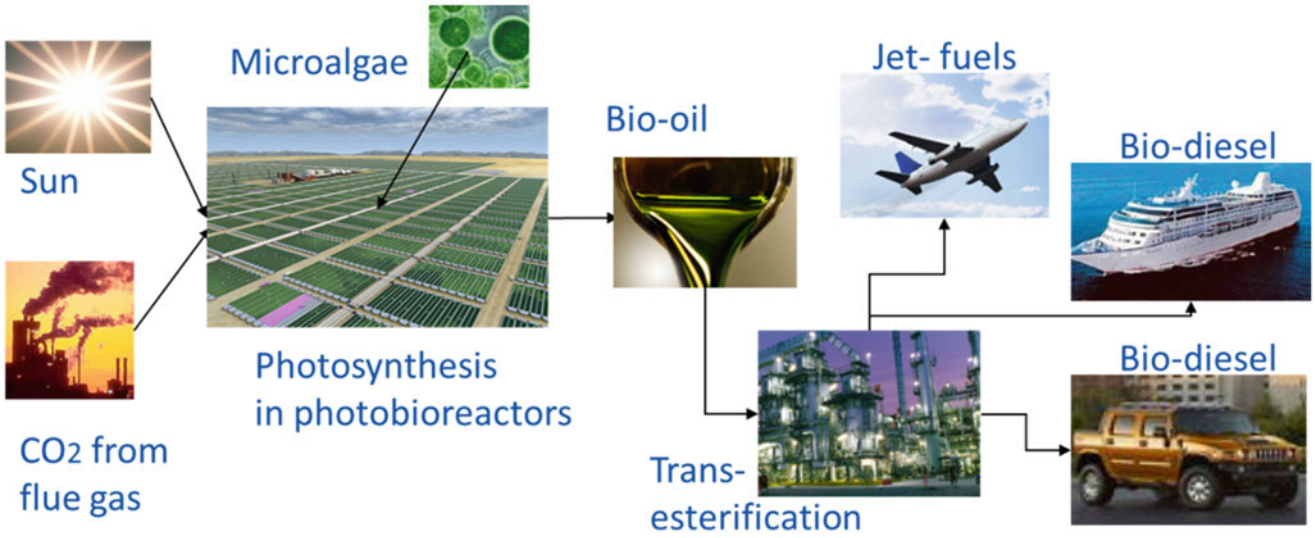

Fig. 1 Conceptual scheme for the production of biofuels and CO_2 capture through microalgae

salts to algal biomass through photosynthesis. Several microalgae are exceedingly rich in oil, which can be extracted and subsequently converted to biodiesel using existing technologies (Chisti 2008). When compared to crops used for first-generation biofuels, microalgae display superior biomass growth rates. Moreover, the corresponding oil content is higher than the one of terrestrial crops since it can exceed 80 % of the dry weight of biomass. For these reasons, the oil productivity of microalgae exceeds that one of terrestrial crops even 10–100 times (Chisti 2008). Microalgae, differently from crops, are cultured in aquatic environments. For these reasons, cultivation of microalgae can be carried out in less extended and lower-quality lands, thus avoiding the exploitation of arable ones. In addition, cultivation of microalgae might be coupled with the direct bio-capture of CO_2 emitted by industrial activities. Therefore, the potential use of microalgae as renewable feedstock for the massive production of liquid biofuels is receiving a rising interest mostly driven by the global concerns related to the depletion of fossil fuel supplies and the increase of CO_2 levels in the atmosphere. From a conceptual point of view, the process shown in Fig. 1 can be carried out for producing biofuels and capturing CO_2 through microalgae.

Despite the apparent simplicity of the process, its implementation to the industrial scale is still not widespread since it is characterized by technical and economic constraints that might hinder its full scale-up. Moreover, the complexity of the biological phenomena involved during the algal growth further complicates the optimization of the process through the classical process engineering techniques. In what follows, the biochemical phenomena involved during microalgae growth and lipid accumulation are briefly discussed.

1.3.1 Photosynthesis and Lipid Production in Microalgae

The process exploited by microalgae for converting sunlight energy and inorganic compounds into the energy-rich molecules constituting the microalgal biomass is called photosynthesis. A simplified scheme of the photosynthetic phenomena occurring in vegetal cells is shown in Fig. 2.

Basically, the photosynthetic process can be divided into two sets of reactions: the light-dependent (light) reactions and the light-independent (dark) reactions. The first ones, which convert the energy of light into chemical energy, take place within the thylakoid membranes of the chloroplasts, whereas the dark reactions, which use the produced chemical energy to fix CO_2 into organic molecules, occur in the stroma of the chloroplast. During the light reactions, the energy transported by incident photons is captured by specific pigments and then used to "split water" into molecular oxygen, into two H^+ ions, and into one pair of electrons, respectively. The energy of light is thus transferred to these electrons and is, finally, used to generate adenosine triphosphate (ATP) and the electron carrier nicotinamide adenine dinucleotide phosphate (NADPH). These two compounds carry the energy and the electrons generated during the light reactions to the stroma, where they are used by the enzymatic dark reactions of the Calvin cycle to synthesize sugars from CO_2. The main sugar synthesized during the Calvin cycle is glyceraldehyde 3-phosphate (G3P). Therefore, the net result of the photosynthesis is the conversion of light, water, and CO_2 into G3P and molecular oxygen.

The synthesized G3P finally passes into the cytosol where it will be involved as intermediate in the central metabolic

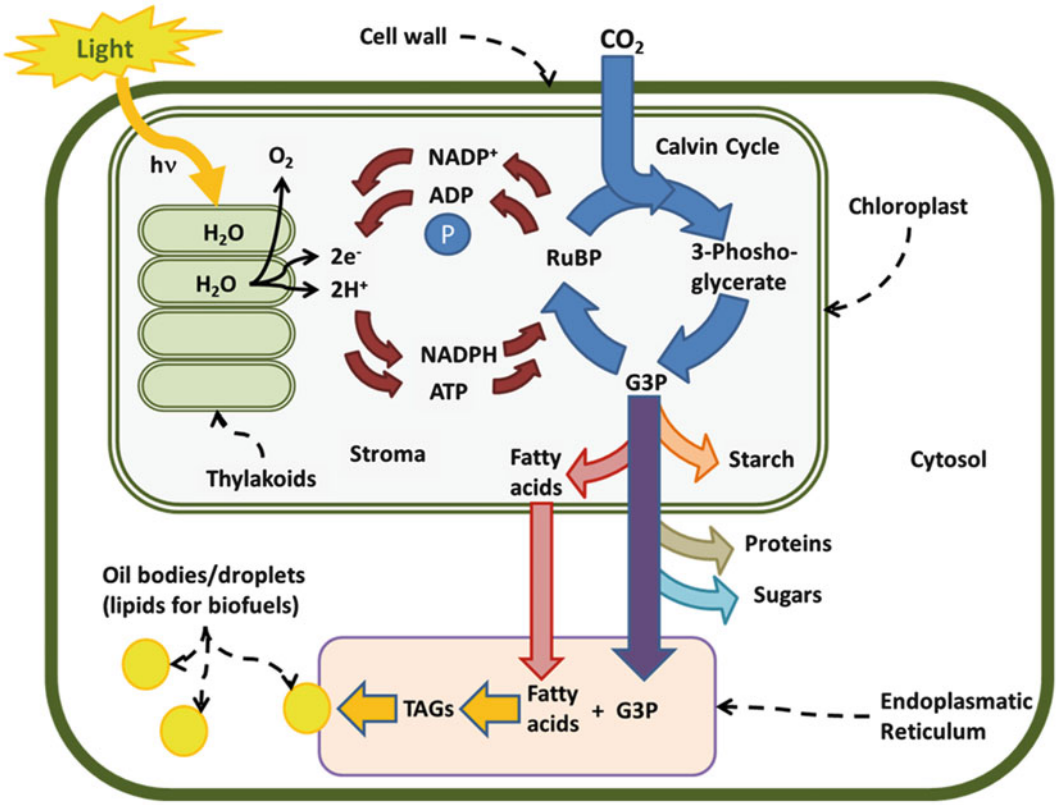

Fig. 2 Simplified scheme of photosynthesis in microalgae and lipid production metabolic pathways (Adapted from Yonghua 2012)

pathways of the cell that lead to the production of several macromolecules such as starch, proteins, and sugars. In the chloroplast also free fatty acids are synthesized starting from G3P. Fatty acids, along with G3P, are then transferred to the endoplasmic reticulum where they are further converted into nonpolar storage lipids, such as triacylglycerides (TAGs), through a number of enzymatic reactions. Finally, TAGs are packaged into oil bodies that bud off into the cytosol (Sakthivel 2011). These oil bodies have a fatty acid composition comparable to vegetable oils and thus can be extracted from the microalgae cell and subsequently converted to useful biofuels (Klok et al. 2013). Specifically, oils from algae can yield biodiesel through transesterification and gasoline (petrol) or jet fuels through distillation and cracking, respectively (Georgianna and Mayfield 2012). When compared with first-generation biomass feedstocks, microalgae have been found to contain higher concentrations of lipids. The average lipid content varies between 1 and 70 %, while under specific operating conditions certain species can reach 90 % of oil weight by weight of dry biomass (Mata et al. 2010). Depending on the specific strain considered, microalgae can be characterized by high biomass growth rates which, coupled with the intrinsic high lipid content, can lead to very high oil productivity. Table 1 shows lipid content as well as lipid and biomass productivities of different microalgae species. From Table 1, it can be observed that volumetric lipid productivity of microalgae is extremely variable depending upon the specific strain considered and goes from 0.01 to 3.67 g_{oil} L^{-1} day^{-1}. However, it is worth noting that lipid productivity can be strongly affected by the specific culturing conditions adopted, i.e., growth medium composition, light regime, photobioreactor configuration, operation mode, etc. Consequently, it can be argued that, by suitably choosing the best performing strains, very high volumetric productivities of lipids can be achieved by using algae. In particular, from Fig. 3 it can be observed that oil yields per area (areal productivity) of microalgae could greatly exceed the one of the best oilseed crops. This aspect clearly determines up to 20 times smaller land areas to produce the same amount of biofuels (e.g., biodiesel) through microalgae.

Furthermore, since the cultivation of microalgae is carried out in open ponds and photobioreactors which can be located in marginal lands that are unsuitable for conventional agriculture, the competition with arable ones is drastically reduced. In addition, microalgae are not directly involved in the human food supply chain, thus eliminating the food versus fuel dispute that represents the main drawback related to

Table 1 Biomass productivities, lipid content, and lipid productivities of different microalgae species

Strain	Biomass productivity (g/L/day)	Lipid content (% biomass)	Lipid productivity (mg/L/day)	Reference
Botryococcus braunii	0.35	17.9	61.8	Orpez et al. (2009)
Botryococcus braunii	0.29	17.9	51.4	Orpez et al. (2009)
Botryococcus braunii	0.03	36.1	12.3	Sydney et al. (2011)
Botryococcus braunii[a]	0.02	50.0	10.0	Mata et al. (2010)
Botryococcus braunii	0.04	22.0	9.5	Dayananda et al. (2007)
Chaetoceros calcitrans	0.04	39.8	17.6	Rodolfi et al. (2009)
Chaetoceros muelleri	0.07	33.6	21.8	Rodolfi et al. (2009)
Chaetoceros muelleri[a]	0.07	33.6	21.8	Mata et al. (2010)
Chlamydomonas reinhardtii	2.00	25.3	505.0	Kong et al. (2010)
Chlorella[a]	0.00	37.5	18.7	Mata et al. (2010)
Chlorella emersonii[a]	0.04	44.0	30.2	Mata et al. (2010)
Chlorella protothecoides	7.30	50.3	3,671.9	Xiong et al. (2008)
Chlorella protothecoides	4.10	43.0	1,763.0	Cheng et al. (2009)
Chlorella protothecoides	4.85	36.2	1,214.0	Mata et al. (2010)
Chlorella protothecoides	2.02	55.2	1,115.0	Xu et al. (2006)
Chlorella pyrenoidosa[a]	3.27	2.0	65.4	Mata et al. (2010)
Chlorella sorokiniana IAM-212	0.23	19.3	44.7	Rodolfi et al. (2009)
Chlorella sp.	0.00	32.6	110.0	Hsieh and Wu (2009)
Chlorella sp.	0.08	66.1	51.0	Hsieh and Wu (2009)
Chlorella sp.[a]	1.26	29.0	42.1	Mata et al. (2010)
Chlorella vulgaris	0.35	42.0	147.0	Feng et al. (2011)
Chlorella vulgaris	0.35	42.0	147.0	Feng et al. (2011)
Chlorella vulgaris	0.20	18.4	36.9	Rodolfi et al. (2009)
Chlorella vulgaris	0.15	23.0	35.0	Liang et al. (2009)
Chlorella vulgaris	0.17	19.2	32.6	Rodolfi et al. (2009)
Chlorella vulgaris	0.09	34.0	31.0	Liang et al. (2009)
Chlorella vulgaris[a]	0.11	31.5	25.6	Mata et al. (2010)
Chlorella vulgaris	0.10	22.0	22.0	Liang et al. (2009)
Chlorococcum sp.	0.28	19.3	53.7	Rodolfi et al. (2009)
Chlorococcum sp.[a]	0.28	19.3	53.7	Mata et al. (2010)
Crypthecodinium cohnii[a]	10.00	35.6	3,555.0	Mata et al. (2010)
Dunaliella primolecta[a]	0.09	23.1	20.8	Mata et al. (2010)
Dunaliella salina[a]	0.28	15.5	116.0	Mata et al. (2010)
Dunaliella sp.[a]	0.00	42.3	33.5	Mata et al. (2010)
Dunaliella tertiolecta[a]	0.12	43.9	52.6	Mata et al. (2010)
Ellipsoidion sp.	0.17	27.4	47.3	Rodolfi et al. (2009)
Euglena gracilis[a]	7.70	17.0	1,309.0	Mata et al. (2010)
Haematococcus pluvialis[a]	0.06	25.0	13.8	Mata et al. (2010)
Isochrysis galbana[a]	0.96	23.5	225.6	Mata et al. (2010)
Isochrysis galbana	0.17	22.3	38.0	Su et al. (2007)
Isochrysis galbana	0.12	14.3	17.2	Su et al. (2007)
Isochrysis sp.	0.14	27.4	37.8	Rodolfi et al. (2009)
Isochrysis sp.[a]	0.13	20.1	37.8	Mata et al. (2010)
Isochrysis sp.	0.17	22.4	37.7	Rodolfi et al. (2009)
Monallanthus salina[a]	0.08	21.0	16.8	Mata et al. (2010)
Monodus subterraneus	0.19	16.1	30.4	Liang et al. (2009)
Monodus subterraneus[a]	0.19	16.0	30.4	Mata et al. (2010)
Nannochloris sp.[a]	0.34	38.0	68.7	Mata et al. (2010)
Nannochloropsis	0.17	29.2	49.7	Rodolfi et al. (2009)
Nannochloropsis sp.	0.21	29.6	61.0	Rodolfi et al. (2009)
Nannochloropsis sp.	0.20	24.4	48.2	Rodolfi et al. (2009)
Nannochloropsis sp.	0.17	21.6	37.6	Rodolfi et al. (2009)

(continued)

Table 1 (continued)

Strain	Biomass productivity (g/L/day)	Lipid content (% biomass)	Lipid productivity (mg/L/day)	Reference
Neochloris oleoabundans	0.31	40.0	125.0	Li et al. (2008b)
Neochloris oleoabundans	0.63	15.0	98.0	Li et al. (2008b)
Neochloris oleoabundans	0.15	28.0	37.8	Gouveia et al. (2009)
Neochloris oleoabundans	0.03	52.0	14.4	Gouveia et al. (2009)
Neochloris oleoabundans[a]	0.00	47.0	112.0	Mata et al. (2010)
Pavlova lutheri	0.14	35.5	50.2	Rodolfi et al. (2009)
Pavlova salina	0.16	30.9	49.4	Rodolfi et al. (2009)
Phaeodactylum tricornutum	0.24	18.7	44.8	Rodolfi et al. (2009)
Porphyridium cruentum	0.37	9.5	34.8	Rodolfi et al. (2009)
Scenedesmus obliquus[a]	0.37	33.0	122.8	Mata et al. (2010)
Scenedesmus quadricauda	0.19	18.4	35.1	Rodolfi et al. (2009)
Scenedesmus sp.	0.26	21.1	53.9	Rodolfi et al. (2009)
Scenedesmus sp.[a]	0.15	20.4	47.4	Mata et al. (2010)
Scenedesmus sp.	0.21	19.6	40.8	Rodolfi et al. (2009)
Skeletonema costatum	0.08	21.1	17.4	Rodolfi et al. (2009)
Skeletonema sp.	0.09	31.8	27.3	Rodolfi et al. (2009)
Skeletonema sp.[a]	0.09	22.6	27.3	Mata et al. (2010)
Spirulina maxima[a]	0.23	6.5	15.0	Mata et al. (2010)
Spirulina platensis[a]	2.18	10.3	224.5	Mata et al. (2010)
Tetraselmis sp.[a]	0.30	13.7	43.4	Mata et al. (2010)
Tetraselmis suecica	0.28	12.9	36.4	Rodolfi et al. (2009)
Tetraselmis suecica[a]	0.22	15.8	31.7	Mata et al. (2010)
Tetraselmis suecica	0.32	8.5	27.0	Rodolfi et al. (2009)
Thalassiosira pseudonana	0.08	20.6	17.4	Rodolfi et al. (2009)

[a]Average values are reported

first-generation biofuels (Ahmad et al. 2011). Further advantages of microalgae over higher plants as feedstock for biofuel production are summarized as follows:

- Microalgae are able to double their biomass in very short times (4–24 h), thus allowing harvesting cycles of 1–10 days which are much shorter as compared with those ones of crop plants, i.e., only once or twice for each year (Schenk et al. 2008; Ahmad et al. 2011).
- Microalgae grow in aquatic media but less water is needed with respect to terrestrial crops (Rodolfi et al. 2009).
- Microalgae display larger light capture and conversion efficiency than crop plants which leads to reduce fertilizer and nutrient inputs, thus resulting in less waste and pollution (Schenk et al. 2008). Moreover, fertilizers suitable for microalgae cultivation (especially nitrogen and phosphorus) can be obtained from wastewaters (Cao and Concas 2011; Rodolfi et al. 2009).
- Cultivation of microalgae might be coupled with the direct bio-capture of CO_2 emitted by industrial activities that use fossil fuels for energy generation (Concas et al. 2012).
- Microalgae can be used for producing valuable copro ducts or by-products such as biopolymers, proteins, carbohydrates, vitamins, antioxidants, PUFAs, etc. (Ahmad et al. 2011).
- Cultivation of microalgae does not require the use of herbicides or pesticides (Rodolfi et al. 2009).
- Oil content of microalgae can be further increased by adopting specific operating conditions during their growth (i.e., nitrogen starvation).

Ultimately, when compared to first- and second-generation biofuels, microalgae are characterized by a more sound environmental sustainability and economic viability (Quinn et al. 2011). For these reasons, the potential exploitation of microalgae as renewable resource for the production of liquid biofuels is receiving a rising interest (Olguin 2003; Mulbry et al. 2008).

2 Parameters Affecting Microalgae Growth

It is well known that algae growth in batch cultures proceeds according to the five main phases depicted in Fig. 4 and described in what follows (Jalalizadeh et al. 2012):

- A lag phase, where a growth delay takes place when cultivation starts due to physiological adjustments of the inoculum to changes in nutrient concentration, light intensity, and other culture conditions

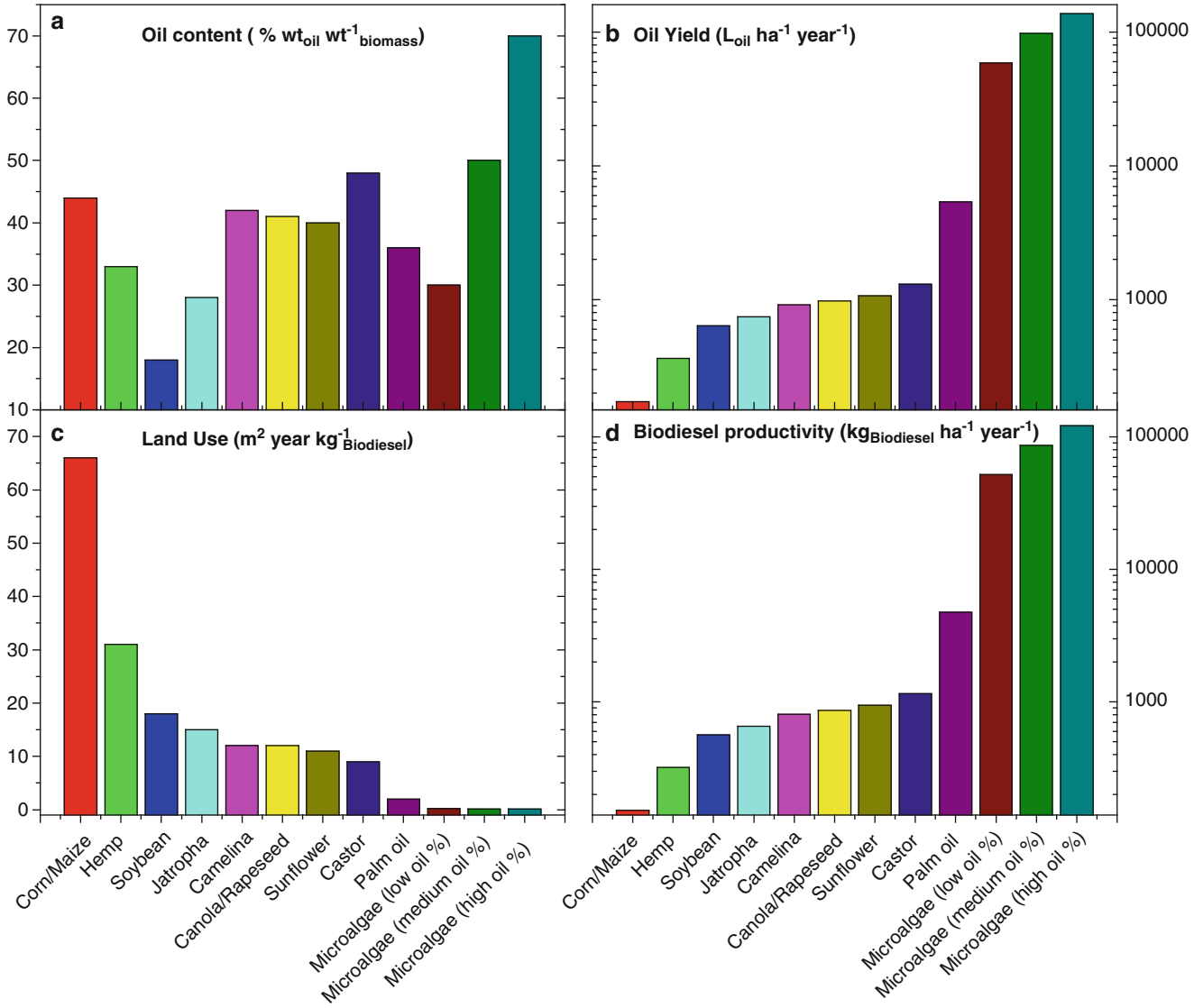

Fig. 3 Comparison of microalgae with oil crops in terms of biodiesel productivity and land area needs (Adapted from Mata et al. 2010)

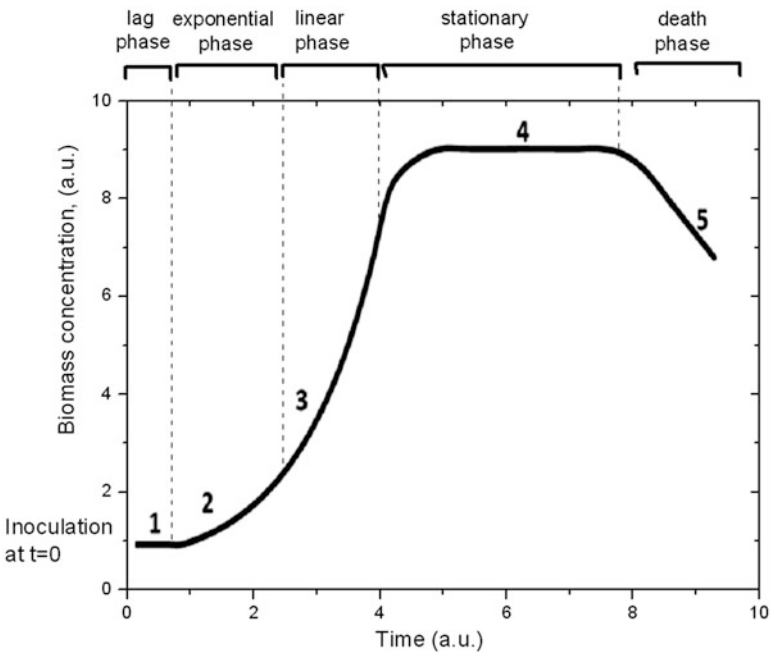

Fig. 4 Schematic representation of biomass growth in a batch culture (Adapted from Jalalizadeh et al. 2012)

- An exponential phase, where cells grow and replicate exponentially with time, as long as all the conditions affecting algae growth are optimized, i.e., nutrients and light availability, optimal temperature, pH, etc.
- A linear growth phase, where biomass concentration grows linearly as a function of time
- A stationary growth phase, where the biomass concentration remains constant as a result of the reduced availability of nutrients and light that lead the death rate to equal the growth one
- A decline or death phase, where the decrease in the concentration of nutrients and/or the accumulation of toxic waste products lead the death rate to overcome the growth one

Such a growth behavior can be well described by the mass balance for microalgae biomass reported in what follows:

$$\frac{dX}{dt} = (\mu - k_d)X$$

where X is the microalgal biomass concentration (mass/volume), μ is the specific growth rate (1/time), and k_d is the specific mass loss rate (1/time) which accounts for all the phenomena that are responsible of biomass depletion, i.e., cell catabolism, apoptosis, lysis, etc. The term $(\mu - k_d)$ is the net growth rate.

While k_d is usually considered to be constant, the growth rate μ depends upon several factors which can affect microalgae growth. Among them, light, nutrient concentration, pH, and temperature (T) are quite important. From a mathematical point of view, the influence of each parameter on the growth rate μ can be expressed as follows:

$$\mu = \mu_{max} \cdot g(I_{av}) \cdot h(S) \cdot f(pH) \cdot \psi(T)$$

where μ_{max} is the maximum growth rate which can be achieved under optimal growth conditions for the specific strain considered, I_{av} is the light intensity available during cultivation, and S the generic substrate concentration. The functions expressing the influence of each parameter on the specific growth rate will equal to 1 when the parameter value is optimal for microalgae growth. In what follows, the effects of each operating parameter are analyzed and discussed.

2.1 Effect of Light

Light is essential for the phototropic growth of microalgae. Spectrum, intensity, and photoperiod of light influence microalgae growth. Photosynthetically active radiation (PAR) designates the spectral range (wave band) of solar radiation from 400 to 700 nm that microalgae are able to use during the process of photosynthesis. It should be noted that photons at shorter wavelengths (<400 nm) carry a very high energy content that can damage microalgal cells, while at longer wavelengths (>700 nm) the energy carried does not allow photosynthesis to take place. Therefore, if we denote by I_λ ($\mu mol_{photons}\ m^{-3}\ s^{-1}$ or $\mu E\ m^{-3}\ s^{-1}$) the intensity of light at the generic wavelength λ (m), the total intensity I exploitable by algae for phototrophic growth can be calculated as follows:

$$I(t) = \int_{400\ (nm)}^{700\ (nm)} I_\lambda\ (t, \lambda) d\lambda$$

When light penetrates in an optically dense medium such as a microalgal culture, it experiences attenuation phenomena due to absorption by the medium as well by the pigments of microalgal cells. Such effect is usually represented by the Lambert–Beer's law:

$$I(r, t) = I(0, t) \cdot \exp(-k_a \cdot r \cdot X)$$

where r is the path length traveled by the light ray within the culture, k_a is the extinction coefficient, and X is the biomass concentration. Thus, the light intensity reaching a microalgal cell depends upon its position with respect to the light direction. While it can be difficult to identify the light intensity reaching each single cell in a culture, it is simpler to evaluate the average light irradiance in the culture vessel. For this reason, the light-dependent kinetics of microalgae growth are usually expressed with reference to the averaged light intensity which can be calculated as follows (Sevilla and Grima 1997):

$$I_{av}(t) = \frac{\int_V I(r, t) \cdot dV(r)}{V}$$

where V is the culture volume. The effect of average light intensity on microalgae growth and photosynthesis has been extensively studied in the literature. Typically, the concentration of microalgae in solution increases with the intensity of light up to a certain level (saturation intensity), beyond which a further increase of light intensity does not provoke the increase of algal growth rate that remains almost constant (Fig. 5a). Such a behavior is quantitatively well described by the classical saturation kinetics:

$$\mu = \mu_{max} \cdot g(I_{av}) = \mu_{max} \cdot \frac{I_{av}}{I_K + I_{av}}$$

where I_K represents the half saturation constant for light intensity. On the other hand, when light intensities overcome a certain threshold, a damage of the microalgae photosystem can take place, which ultimately results in a decrease of the growth rate as shown in Fig. 5b (Grima et al. 1999). In Table 2, a list of suitable equations for the specific growth

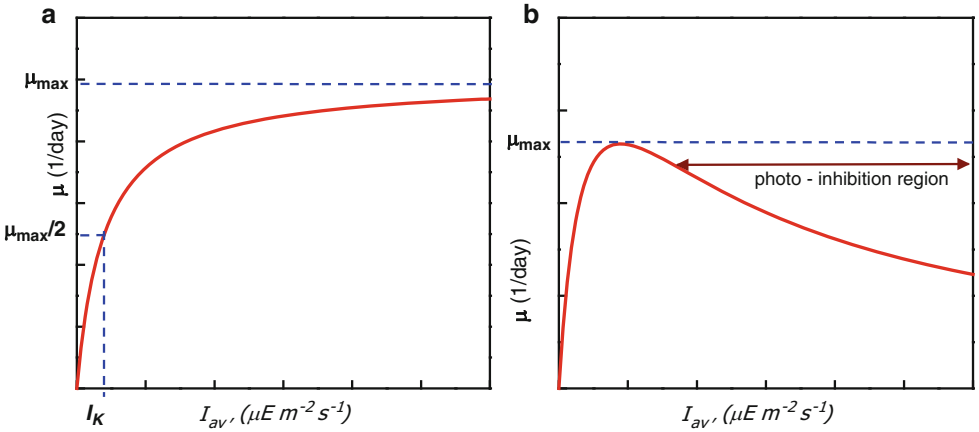

Fig. 5 Effect of light intensity on growth rate without (**a**) and with (**b**) photoinhibition (Adapted from Chisti 2007)

Table 2 Specific growth rate expressions available in the literature as a function of light intensity (Sevilla and Grima 1997)

Kinetic model
$\mu = \mu_{\max} \cdot g(I_{av}) = \mu_{\max} \cdot \frac{I_{av}^n}{I_K^n + I_{av}^n}$
$\mu = \mu_{\max} \cdot g(I_{av}) = \mu_{\max} \cdot \exp\left(1 - \frac{I_{av}}{I_{\max}}\right)$
$\mu = \mu_{\max} \cdot g(I_{av}) = \mu_{\max} \cdot \frac{I_{av}}{I_{\max}} \cdot \exp\left(1 - \frac{I_{av}}{I_{\max}}\right)$
$\mu = \mu_{\max} \cdot g(I_{av}) = \mu_{\max} \cdot \frac{I_{av}}{I_K + I_{av} + I_{av}^2/K_I}$

rate as a function of light intensity which are also able to quantitatively describe photoinhibition phenomenon is reported. Such expressions have been successfully used to simulate experimental data obtained either in batch or turbidostat mode with optically thin cultures (Sevilla and Grima 1997).

2.2 Effect of Nutrients

The medium where microalgae grow basically consists of water enriched by macro- (C, N, P, S) and micronutrients (Mg, Zn, Fe, K, Na, etc.) as well as by the CO_2 transferred from the gas phase (i.e., flue gas or air). Besides CO_2, whose role in photosynthesis has been already discussed in Sect. 1.3.1, nitrogen and phosphorous are key elements for algae metabolism. Their suitable balancing in the growth medium is thus critical for an effective process design (Mandalam and Palsson 1998). Ammonia, urea, and nitrate are often selected as a nitrogen source for the mass cultivation of microalgae. Although ammonia and urea are often used in mass cultivation owing to their relatively low cost, selecting proper nitrogen source for each algal species is important in improving biomass and oil productivity (Li et al. 2008b). Urea and nitrate were found to be better nutrients than ammonia for the growth and lipid accumulation when considering *Chlorella* sp., *Chlorella vulgaris*, *Neochloris oleoabundans*, and *Scenedesmus rubescens* (Li et al. 2008b; Hsieh and Wu 2009). On the contrary, for different strains, the use of ammonia has been demonstrated to provoke higher biomass and lipid content than urea and nitrate (Xu et al. 2001). It should be noted that the optimal concentration of nitrogen to be assured in the growth medium depends upon two counteracting effects. Specifically, while a high availability of nitrogen typically leads to a high biomass productivity, a decrease of nitrogen concentration in the cultivation broth typically results in higher lipid contents counteracted by lower growth rates. Such behavior depends upon the fact that, under starvation conditions, nitrogen concentration is not enough for activating the metabolic pathways leading to protein synthesis required by growth so that the excess of carbon coming from photosynthesis is channeled into storage molecules such as triacylglycerides or starch (Scott et al. 2010). This inverse relationship between biomass productivity and lipid content makes the choice of the suitable nitrogen concentration not straightforward since a trade-off value should be assured in order to maximize lipid productivity (Concas et al. 2013, 2014). When considering phosphorus, microalgae are capable of metabolizing it mainly in polyphosphate form. Orthophosphate is generally considered the main limiting nutrient for freshwater strains, but also in this case, its optimal concentration depends upon contrasting effects. In fact, phosphorus starvation can result in higher lipid productivity, as reported for *Monodus subterraneus*, while may provoke changes in fatty acids composition for *Phaeodactylum tricornutum* and *Dunaliella tertiolecta* (Liu et al. 2007).

For all these reasons, the preparation of the culture broth is a critical step for the entire process of biofuel production through microalgae. Moreover, the need of a continuous replenishment of macronutrients during algal cultivation is one of the most impacting cost items of the entire process. In fact, as rule of thumb, about 1.8 kg of CO_2, 0.33 kg of nitrogen, and 0.71 kg of phosphate are consumed to produce 1 kg of microalgal biomass. Since large-scale cultivation of microalgae implies the consumption of huge amounts of

such macronutrients, the economic feasibility of the entire process could be seriously affected by the erroneous evaluation of their depletion kinetics. Therefore, in view of industrial scaling-up, the effect of nutrients concentration in the medium on biomass composition and productivity should be quantitatively evaluated (Concas et al. 2013). Since nutrients concentration and supplies are among the most controllable factors in microalgae cultivation, at least the main macronutrients uptake rates need to be quantitatively evaluated for the microalgae strains candidate to industrial exploitation. In this way, macronutrients concentrations might be properly controlled during cultivation. Hence, biomass production can be optimized with respect to the required process end products by means of suitable growth kinetics and broth composition. The Monod equation is the most common kinetic model used for describing the relationship between the microalgae growth rate and the concentration of the limiting nutrient:

$$\mu = \mu_{\max} \cdot h(S) = \mu_{\max} \cdot \frac{[S]}{K_S + [S]}$$

where K_s (g/L) is the half saturation constant and $[S]$ (g/L) the substrate concentration. When multiple nutrient limitations take place, the Monod model can be written as follows:

$$\mu = \mu_{\max} \prod_{j=1}^{\text{Nutrients}} \frac{[S_j]}{K_{S,j} + [S_j]}$$

On the other hand, the use of the Monod model is limited to the case where no luxury uptake of nutrients and nutrient storage phenomena takes place. However, the last ones are common phenomena in microalgae and lead to a temporal uncoupling between growth rate and dissolved nutrient concentrations (Jalalizadeh et al. 2012). Therefore, when intracellular storage of nutrients takes place, the cell quota of the limiting nutrient, expressed as the total amount of nutrient contained within the cell per cell weight, better describes the nutritional status than does the concentration in solution. Ultimately, the growth rate of algae is more dependent on the internal cellular concentrations than on the external ones (Richmond 2008). Under such conditions the Droop model (Droop 1983), which is capable to relate growth rate to the internal cell quota, may properly simulate microalgae growth kinetics. The Droop model can be written as

$$\mu = \mu_{\max} \cdot \left(1 - \frac{q_{\min}}{q}\right)$$

where q is the internal cell quota of the limiting nutrient ($g_{nutrient}/g_{cell}$) while q_{min} is the minimal internal cell quota below which algae growth does not take place.

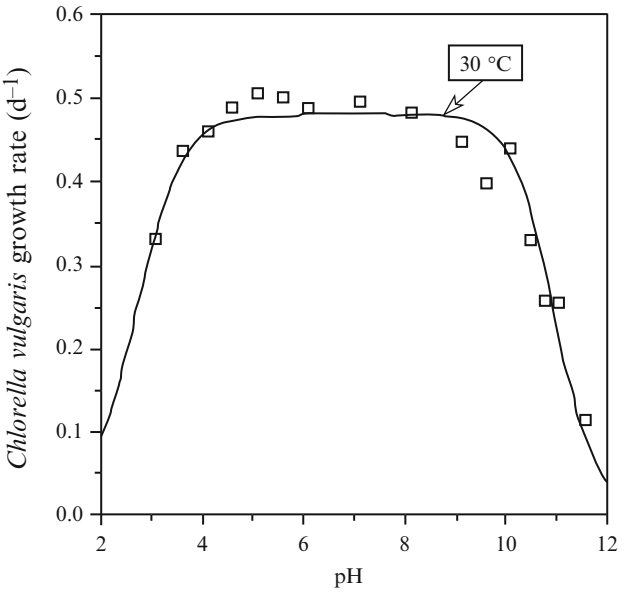

Fig. 6 Effect of pH on the growth of Chlorella vulgaris at 30 °C (Adapted from Mayo 1997)

2.3 Effects of pH

The time evolution of a medium's pH during algal growth is a significant indicator of how well are evolving photosynthetic processes. In fact, as algae grow, dissolved CO_2 is consumed by photosynthesis and, consequently, pH increases. However, pH variation not only represents a fundamental indicator of the evolution of photosynthetic activity but can also, in turn, strongly affect the growth kinetics of microalgae influencing the distribution of carbon dioxide species and carbon availability thus causing direct physiological effects (Cornet et al. 1995; Chen and Durbin 1994). Moreover, in microalgal cultures, the hydrogen ion is recognized to be a noncompetitive inhibitor near neutral conditions, while it can limit photosynthetic growth and substrate utilization rates at very low or very high pH levels (Mayo 1997). Furthermore, pH can affect the enzymatic activity of intra- and extracellular carbonic anhydrase, thus influencing the carbon capture mechanism of some microalgal strains (Concas et al. 2012). In order to evaluate the dependence of growth rate upon pH, the following expression has been proposed by Mayo (1997):

$$\mu = \mu_{\max} \cdot f(\text{pH}) = \frac{\mu_{\max} \cdot [H^+]}{[H^+] + K_{OH} + [H^+]^2 / K_H}$$

which states that $[H^+]$ can be considered as a noncompetitive substrate when the medium pH is high while displays an inhibition effect when the pH of the medium is low (Mayo 1997). The resulting dependence of growth rate from pH is depicted in Fig. 6.

As it can be observed from Fig. 6, the kinetic model proposed by Mayo (1997) well describes the fact that each strain of microalgae has a relatively narrow optimal range of pH and most microalgal species are favored by neutral pH.

2.4 Effect of Temperature

Temperature is one of the main factors which regulate cellular, morphological, and physiological responses of microalgae (Mayo 1997; Durmaz et al. 2007). High temperatures generally accelerate the metabolic rates of microalgae, whereas low ones lead to inhibition of microalgal growth (Munoz and Guieysse 2006). Under optimal temperature condition, the enzymes of microalgal cells show the highest activity. The optimal temperature range for microalgal growth depends on the specific strain considered, but in general, it typically goes from a minimum of 5 °C to a maximum of 35 °C (Abu-Rezq et al. 1999).

As far as the kinetic dependence of growth rate from temperature is concerned, different relationships have been proposed in the literature. One of the most used equations, according to an Arrhenius-type dependence, is reported as follows (Mayo 1997):

$$\mu = \mu_{\max} \cdot \psi(T) = \mu_{\max} \cdot \frac{A \cdot \exp\left(-E_1/R \cdot T\right)}{\left[1 + K \cdot \exp\left(-E_2/R \cdot T\right)\right]}$$

where A and K are preexponential factors (−), E_1 and E_2 are the activation energies (J/mole), R is the universal gas constant, and T is the absolute temperature (K). This equation well interprets experimental data.

The control of temperature is a key factor for cultivating microalgae outdoors. Actually, temperature can vary depending upon the geographic region of cultivation. Seasonal and even daily fluctuations in temperature can interfere with algae production. The internal temperature in photobioreactors can reach values that are 30 °C higher than ambient one if suitable temperature control equipment is not used. To overcome this problem, evaporation, cooling, or shading techniques are successfully employed.

3 Production of Biodiesel from Microalgae

Microalgae cultivation systems are very different from those ones typically used for producing biomass feedstock for first- and second-generation biofuels. This is mainly due to the fact that, while biomass used for first- and second-generation biofuels consists mainly of terrestrial crops, the life of the microalgae and their proliferation occurs in liquid environments. Therefore, when compared to terrestrial crops, the production of microalgae requires specific cultivation, harvesting, and processing techniques which should be correctly implemented to the aim of viably producing biodiesel (Mata et al. 2010).

Basically, the current processes for biodiesel production from microalgae involve distinct operating steps where cells are grown, separated from the growing media, dried (or disrupted), and finally undergone to lipid extraction processes. Once extracted, microalgal lipids are processed through technologies similar to the existing ones for the production of biodiesel or other biofuels starting from first-generation biomass feedstocks. While different biofuels can be produced from microalgae in this work, we will focus on the production of biodiesel. Figure 7 shows a schematic representation of the process for the CO_2 capture and biodiesel production through microalgae. As it can be seen, the process starts with the CO_2 capture and its conveying in the cultivation system where microalgae grow exploiting the sunlight and the nutrients suitably provided. Then, it follows the biomass harvesting, downstream processing, and oil extraction to supply the biodiesel production unit.

As reported in Fig. 7, cultivation of microalgae can be performed in open systems (ponds, raceways, lakes) or in closed ones, i.e., photobioreactors. Whatever the system being used, a suitable source of CO_2 must be supplied to microalgae. To this aim, atmospheric air (0.03 %v/v of CO_2), flue gas (9–15 % of CO_2), or pure concentrated CO_2 (100 %v/v) can be used. Atmospheric air as CO_2 source significantly simplifies the layout and the operation of the plant, while, because of the lower CO_2 concentration in air, high volumes of air are required in order to sustain microalgae growth at an acceptable rate. This can result in very large cultivation systems that require a high land availability. On the contrary, when flue gases are used as carbon source, lower flow rates of gases should be pumped into the cultivation system for supplying the necessary amounts of carbon to sustain microalgae growth. Moreover, the use of costless feedstocks such as flue gases as source of CO_2 might greatly improve the economic feasibility of the microalgae-based technology while, simultaneously, producing a positive impact on significant environmental concerns such as air pollution and climate changes. For this reason, the potential exploitation of CO_2 from flue gases is one of the main targets of scientists and technicians operating in this field (Cao and Concas 2011; Francisco et al. 2010). However, the use of flue gas as carbon source might raise specific concerns related to the toxicity of some of its constituents with respect to algae. For this reason, the flue gas should be pretreated before feeding it in the cultivation system. A further challenge in the carbon capture through microalgae is the use of pure concentrated CO_2 (100 %v/v) obtained from flue gas. In this case in fact, besides the lesser volumes of photobioreactors that are needed, the potential poisoning effects provoked by other compounds in flue gas

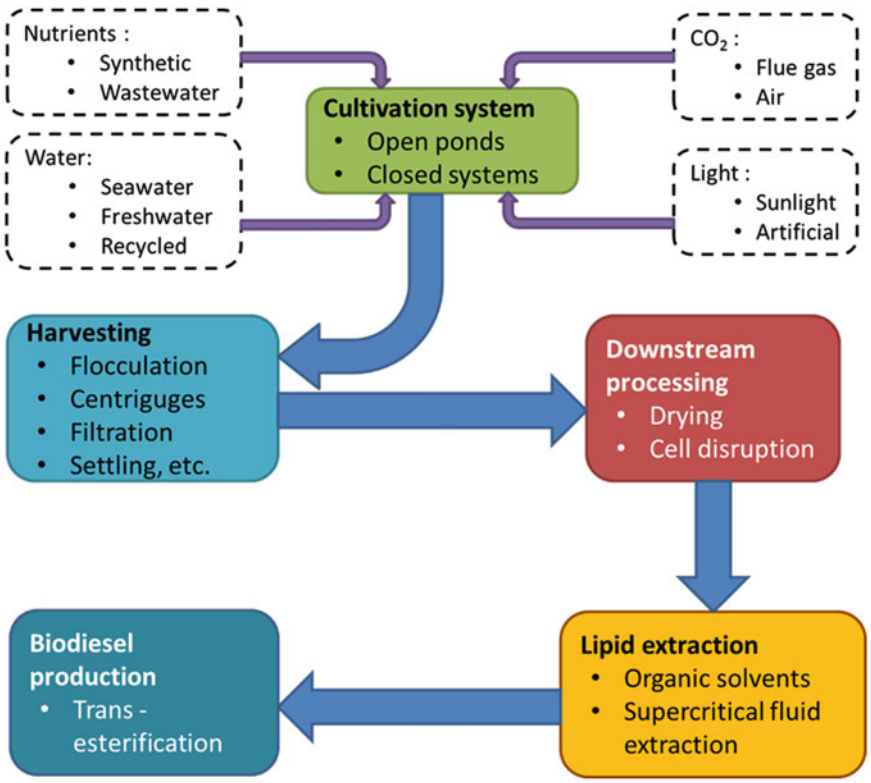

Fig. 7 Schematic representation of the "algae to biodiesel" process

(NOx, SOx, etc.) could be reduced, thus increasing the net growth rate of microalgae.

Besides CO_2, several micro- and macronutrients must be supplied to the culture in order to sustain microalgal growth. While the importance of the nutrients has been already discussed in Sect. 2.2, it is noteworthy to underline that the exploitation of costless feedstocks such as wastewaters as sources of macronutrients might greatly improve the economic feasibility of the microalgae-based technology while simultaneously producing a positive impact on important environmental concerns such as water pollution. In fact, wastewaters, even if pretreated, may contain residual concentration of nitrogen and phosphorus which are capable to sustain microalgal growth (Cao and Concas 2011). In particular, industrial and agricultural wastewater and secondary sewage-treated effluent can be used as source of nitrogen and phosphorus (Devi et al. 2012). For this reason, the operation step of medium preparation can involve a premixing with wastewater.

Finally, in order to suitably cultivate microalgae, large amounts of water must be available. Depending upon the specific microalgal strain to be cultivated, freshwater or seawater can be used for preparing the growth medium. The use of marine strains would be convenient since seawater can contain suitable concentrations of micronutrients whose purchase could be so avoided. Moreover, seawater would be available in large amounts without affecting water resources to be exploited for other uses. Since water consumption might be significant, the recycling of the exhaust growth medium at the outlet of the cultivation systems should be always considered in an optimized flow sheet.

Finally, water and nutrients are dosed and mixed within a suitable premixing unit. The obtained mixture is then filtered, sterilized, and finally pumped into the cultivation systems.

3.1 Cultivation of Algae in Open Ponds

Different designs have been proposed for open ponds, natural or artificial ones, operating at large scale. Typical examples are the unstirred ponds (lakes and natural ponds), the inclined ones, central pivot, and the raceway ponds. Among the others, the most widespread typology of open pond is the so-called raceway pond. It basically consists of open channels where a paddle wheel is used to drive the flow, while algae are kept suspended in water around a racetrack. Baffles in the channels guide the flow in order to minimize space. Raceways are typically made by concrete but can be simply dug into the soil and waterproofed with a plastic liner to prevent the liquid filtration through the ground. These systems are usually operated in a continuous mode, where the fresh medium (containing macro- and micronutrients) is fed in front of the paddle wheel and algal broth is harvested behind it after being circulated through the loop (Singh and Sharma 2012). The raceways

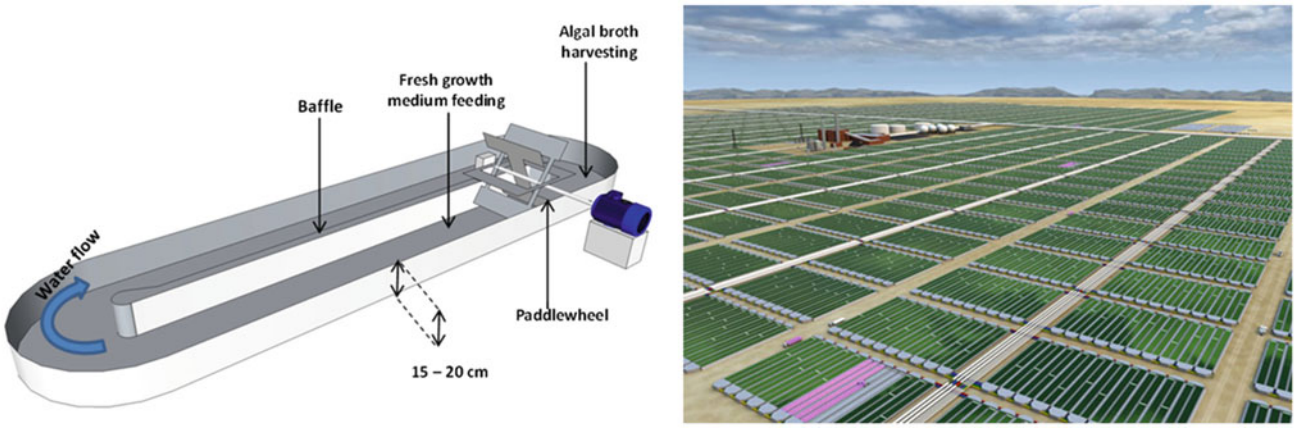

Fig. 8 Scheme of a single raceway pond and photography of raceway pond farm (Adapted from Rapier 2012)

(Fig. 8) are characterized by low water depths of about 15–20 cm in order to assure a suitable light penetration along the hydraulic section, thus avoiding dark zones where microalgae cannot grow. At such depths biomass concentrations of 1 g L^{-1} can be achieved and productivities ranging from 15 to 25 g m^{-2} day^{-1} are possible (Schenk et al. 2008).

In general, these cultivation systems are less expensive to build and simpler to operate than closed ones. For this reason, they are currently considered as the most cost-effective way for the massive production of microalgae at a large scale. However, open ponds display several limitatons. In particular, when compared to close systems, open raceways are characterized by a lower productivity that is the result of a number of factors. Evaporative losses can lead to changes in the ionic composition of the growth medium, thus potentially provoking negative effects on culture growth such as hypersalinity, nutrient's precipitation, etc. Changes in temperature and photoperiod deriving from seasonal variation cannot be suitably controlled in open ponds (Rawat et al. 2013). These systems are more susceptible to contaminations by competing organisms such as mushrooms, bacteria, and protozoa. Furthermore, since atmospheric carbon dioxide is used as carbon source, its transfer rate is very low and consequently carbon starvation phenomena could take place. Finally, sunlight is available only at the surface of the pond, and hence, in the deeper strata of the liquid bulk, light limitation phenomena can arise. Improved mixing and bubbling the air at the bottom of the ponds by means of suitable spargers can minimize impacts of both CO_2 and light limitation, but in general the productivity of these systems is very low whereby large areas of land may be required to meet the desired output of cultivation (Rawat et al. 2013).

To overcome limitations related to open system and in the meantime keeping their low operating cost, the potential use of closed raceway ponds is currently under study. These systems consist essentially of an open pond covered by a transparent or translucent barrier which turns it into a greenhouse (Singh and Sharma 2012). This configuration prevents the microalgae to be contaminated by competing bacteria and allows a better control of crucial operating parameters such as temperature, evaporation, etc. Moreover, by using closed raceways the amount of CO_2 provided can be increased since the gas bubbled at the bottom cannot escape to the atmosphere.

3.2 Closed Systems (Photobioreactors)

Photobioreactors (PBR) are closed systems having no direct exchange of gases and contaminants with the environment where culture broth and microalgae are exposed to a photonic energy flux which triggers photosynthetic phenomena hence allowing biomass growth. Since they are closed reactors, the crucial operating parameters such as temperature, pH, nutrient concentration, light intensity distribution, mixing, and gas mass transfer rate can be suitably controlled and optimized. As a result photobioreactors typically have higher biomass productivities than open ponds. On the contrary, photobioreactors are more expensive and complicated to operate than open ponds. A qualitative comparison between photobioreactors and open ponds is summarized in Table 3.

Ideally, a photobioreactor for production of biomass should catch all sunlight available and dilute and distribute it uniformly in the growth medium where algae are suspended in such a way that all the caught light energy can be suitably exploited by algae for biomass formation. For this reason, a critical design parameter of photobioreactors is the illumination surface area per unit volume. Typically, a high illuminated surface area-to-volume ratio (SVR) results in a higher light availability in the liquid bulk and consequently in higher volumetric productivities of the systems. The surface-to-footprint ratio (SFR) is another critical design

Table 3 Comparison between open ponds and photobioreactors

Parameter	Open systems	Photobioreactors
Contamination risk	High	Low
Sterility	None	Achievable
Species control	Difficult	Easy
Area/volume ratio	Low	High
Water losses	High	Low
CO_2 losses	High	Depends on pH, alkalinity
O_2 inhibition	Low	Problematic
Mixing	Very poor	Uniform
Light utilization efficiency	Poor	High
Temperature control	Difficult	Less difficult
Evaporation of growth medium	High	Low
Hydrodynamic stress on algae	Very low	Low–High
Process control	Complicated	Less complicated
Maintenance	Easy	Difficult
Yield	Low	High
Population (algal cell) density	Low	High
Biomass concentration	1 g L^{-1}	3–5 g L^{-1}
Constructions costs	Low	High
Weather dependence	High	Low
Overheating problems	Low	High
Dissolved oxygen concentration	Low	High
Scale-up	Difficult	Difficult
Surface-to-volume ratio, SVR (m^2/m^3)	<4	<100
Surface-to-footprint ratio, SFR (m^2/m^2)	1	<10

Adapted from Lutzu (2012)

parameter. Higher values of SFR correspond to a larger areal productivity of the photobioreactor, and consequently, the lesser is the land area needed for producing the required output of microalgal biomass. Different types of photobioreactors are currently under study and development with the aim of reaching the more suitable configuration where SVR and SFR are maximized.

3.2.1 Vertical Tubular Photobioreactors

The classical configuration of vertical tubular photobioreactor is the bubble column. It is basically a cylinder with radius of up to 0.2 m and height of up to 4 m. The height to diameter ratio is typically kept greater than 2 in order to maximize the SVR ratio. The CO_2 is provided to the algae by bubbling the gas from the bottom upwards through suitable spargers. While allowing a better CO_2 mass transfer, the bubble flow provides also the suitable mixing degree without provoking significant shear stresses on microalgae. Moreover, the gas flow enables the effective removal of photosynthetic O_2 produced by algae which, if accumulated in the liquid, can inhibit the growth. The height constrain of these columns (<4 m) depends upon the gas transfer limitations and the strength of the transparent materials used to construct the columns. Since CO_2 supply and O_2 removal is optimized, in such type of reactors algal growth is often limited by other parameters such as light (Wang et al. 2012). A schematic representation of different types of vertical tubular photobioreactors is shown in Fig. 9.

A specific configuration of vertical tubular photobioreactors is the so-called airlift reactor. It consists of a vessel with two interconnecting zones (i.e., the riser and the downcomer). The gas flow is introduced at the bottom of the riser and carries the liquid upward. At the top of the column liquid/gas separation takes place in the freeboard regime thus allowing the removal of accumulated photosynthetic oxygen (Krichnavaruk et al. 2005). Subsequently, the degassed liquid falls downward in the downcomer. Mixing is therefore guaranteed by aeration and liquid circulation. This system allows a better exposure of microalgal cells to light radiation than classical bubble columns as well as an effective mixing and degassing of the liquid. Airlift PBR configurations may include an internal loop airlift, split column airlift, and external loop airlift.

3.2.2 Flat Panel Photobioreactors

Flat panels (Fig. 10) are parallelepiped-shaped photobioreactors having a minimal light path and a large illumination surface area (SVR) which can reach values of up to 40 m^{-1} (Singh and Sharma 2012). The thickness of the plate is the crucial parameter in the design of flat panels

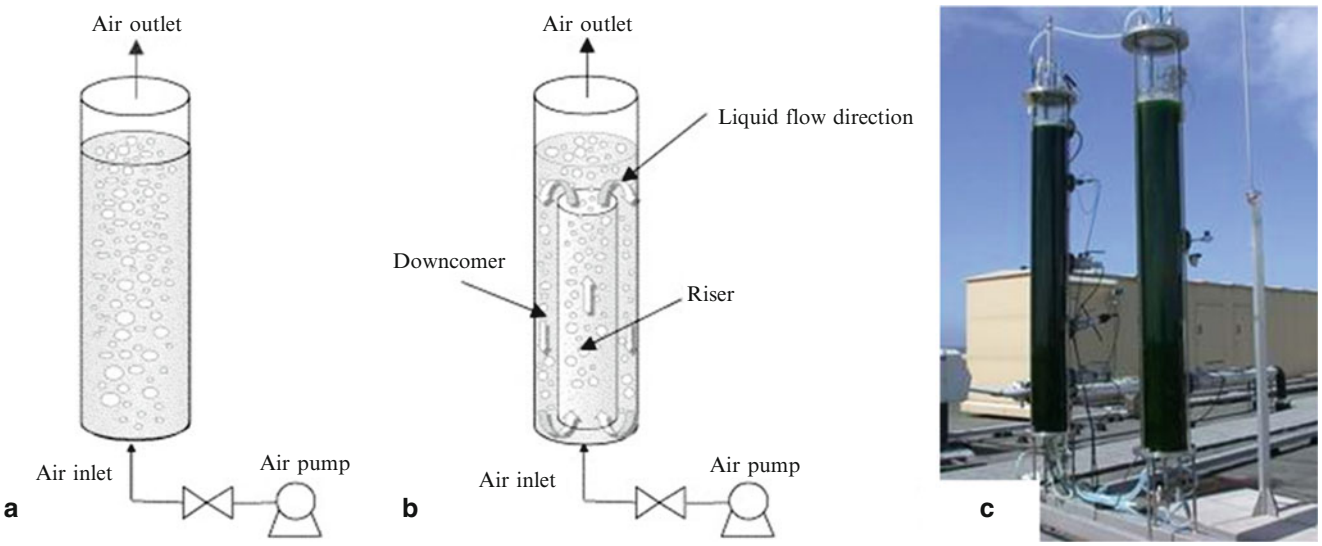

Fig. 9 Schematic representation of bubble column (**a**) and airlift (**b**) photobioreactors and picture (**c**) of an industrial bubble column photobioreactor (Adapted from Krichnavaruk et al. 2005)

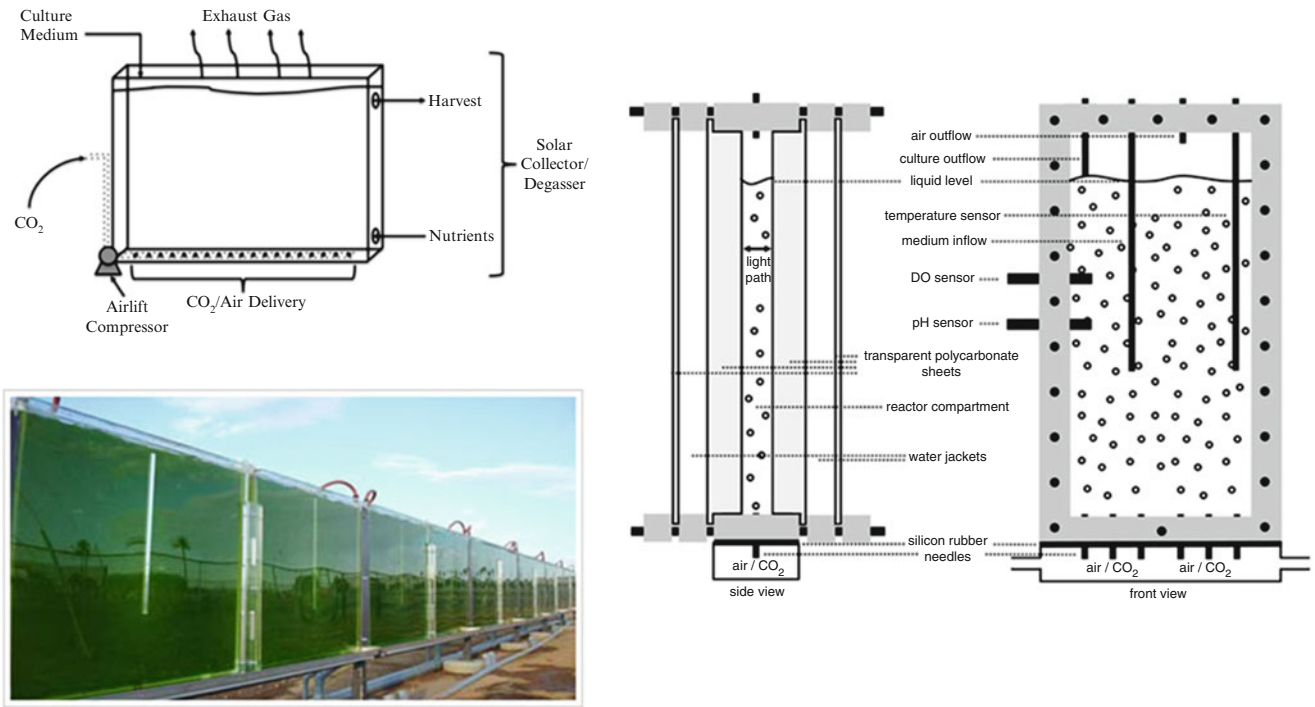

Fig. 10 Schematic representations and picture of flat panel photobioreactors (Adapted from Carter (2012) and Zijffers et al. (2010))

because it determines the surface area/volume ratio and the length of light path (Wang et al. 2012). They can be made from transparent materials like glass, plexiglass, polycarbonate, etc. The CO_2 is provided by bubbling the gas from one side of the panel through suitable perforated tubes. Mixing of the liquid is assured by the gas flow or by rotating the photobioreactor through a motor (Singh and Sharma 2012).

Major limitations of conventional flat panels are the difficulties of controlling the liquid flow and the relatively high construction costs. To overcome these problems, vertical alveolar panels, made in plexiglass, were proposed (Tredici and Materassi 1992). These systems allow to obtain a high surface-to-volume ratio of about 80 m^{-1}. A good biomass productivity can be achieved by using these alveolar panels as well as a good mixing degree and suitable mass

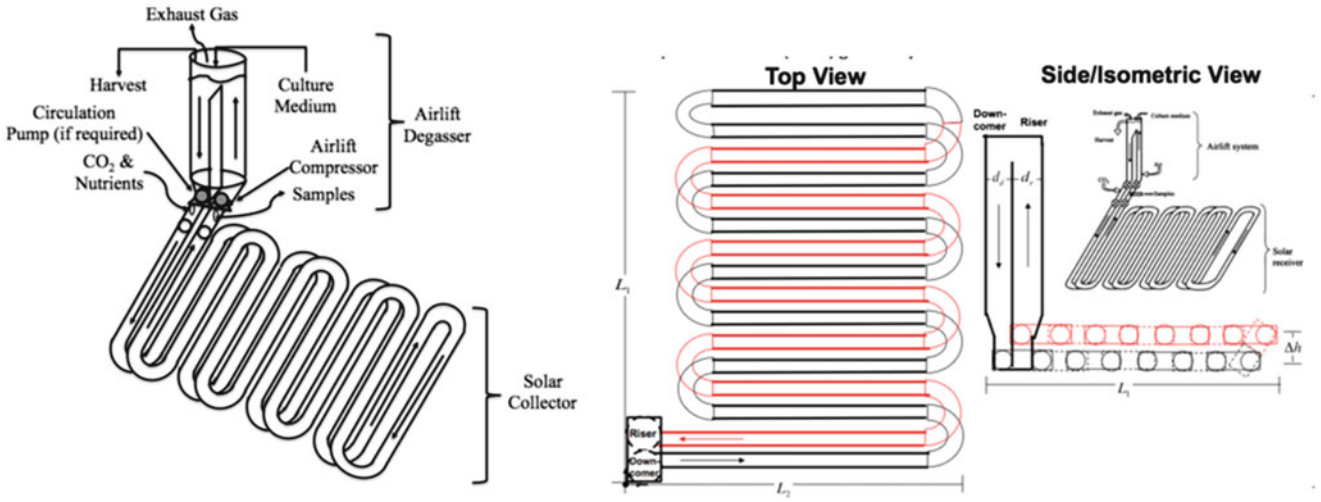

Fig. 11 Schematic representations of horizontal (serpentine type) photobioreactors (Adapted from Carter 2012)

transfer rates. Moreover, the manufacturing costs of these reactors are quite low. However, critical operating parameters such as temperature and light penetration should still be optimized in such a PBR (Wang et al. 2012).

3.2.3 Horizontal Tubular Photobioreactors

Horizontal tubular reactors typically consist of arrays of transparent thin tubes built in different patterns (i.e., straights, loop, serpentine shaped, etc.). The arrays of tubes can be arranged in parallel or in series and then placed horizontally on the ground. Horizontal placement of these tubes results in a better angle for incident light compared to vertical tubular reactors, allowing for more efficient light harvesting (Wang et al. 2012). Moreover, the tubes are preferably oriented towards the sunlight in order to maximize the light capture, and the ground under the tubes can be covered with white plastic sheets in order to increase the albedo. In fact, a high albedo results to an increase of the total light received by the tubes. Typically, these tubes are less than 0.1 m in diameter since otherwise the light does not suitably penetrate in the less exposed zones of dense cultures (Chisti 2007). However, larger diameters may be used when suitable regimes of turbulence of the fluid are employed in order to assure the movement of algae from the illuminated part of the tube to the dark one and vice versa. Prolonged exposure to light in the illuminated part of the tube can trigger photoinhibition phenomena while a long time exposure to darkness can inhibit photosynthesis. Furthermore, the tubes should not be longer than 80 m in order to avoid the accumulation of photosynthetic oxygen in the culture and a too high increase of pH as algae grow (Cao and Concas 2011). Besides the tubes, which act as solar collectors, the horizontal photobioreactors include the following components: the harvesting unit to separate algae from the suspension, a degassing column for gas exchange and cooling (or heating), and a circulation pump (Wang et al. 2012). In Fig. 11, a specific configuration of horizontal photobioreactors is shown.

In the degassing device, air or CO_2-enriched air is injected in order to strip dissolved oxygen and at the same time provide the CO_2 to algae culture. In the degasser, also the feeding of fresh medium can be carried out. Typically, horizontal photobioreactors are capable to capture light better than other photobioreactors, thus potentially assuring higher productivities. On the other hand, just this characteristic can cause the onset of photoinhibition phenomena as well as the accumulation of high amounts of heat. Thus, expensive temperature control systems such as heat exchangers are often required during large-scale cultivation of algae. Furthermore, long tubular PBRs are characterized by gradients of oxygen, CO_2, and pH along the tubes. The increase in pH of the cultures would also lead to frequent recarbonation of the cultures, which would consequently increase the cost of algal production. Finally, it should be noted that adherence of the cells to the walls of the tubes is common. This results in a progressive fouling of the tubes and a consequent worsening of light penetration in the culture.

3.2.4 Advantages and Drawbacks of Different Types of Photobioreactors

Each photobioreactor configuration described above is characterized by specific advantages and drawbacks that should be considered when designing the cultivation system. A summary of the main features of these three configurations is shown in Table 4.

Table 4 Prospects and limitations of different photobioreactors

Culture systems	Advantages	Disadvantages
Horizontal tubular PBRs	Large illumination surface area, suitable for outdoor cultures, fairly good biomass productivities, relatively cheap	Gradients of pH, dissolved oxygen and CO_2 along the tubes, fouling, some degree of wall growth, require large land space
Vertical-column PBRs	High mass transfer, good mixing with low shear stress, low energy consumption, high potentials for scalability, easy to sterilize, readily tempered, good for immobilization of algae, reduced photoinhibition and photooxidation	Small illumination surface area, their construction require sophisticated materials, shear stress to algal cultures, decrease of illumination surface area upon scale-up
Flat-plate PBRs	Large illumination surface area, suitable for outdoor cultures, good for immobilization of algae, good light path, good biomass productivities, relatively cheap, easy to clean up, readily tempered, low oxygen buildup	Scale-up requires many compartments and support materials, difficulty in controlling culture temperature, some degree of wall growth, possibility of hydrodynamic stress to some algal strains

Adapted from Lutzu (2012)

3.3 Harvesting of Microalgae

At the outlet of the photobioreactor, the bulk culture medium is characterized by a water content ranging from 99.5 to 99.9 %, and thus, the harvesting of microalgal biomass is basically carried out through a dewatering/concentrating phase. Such operating phase is usually accomplished through a two-step process (Pragya et al. 2013). The first step, where biomass is concentrated to 2–7 % dry weight, is called bulk harvesting. In the second one, called thickening, the algal slurry is further concentrated to about 15–25 % in order to obtain better manageable slurry in the subsequent operations of lipid extraction (Pragya et al. 2013). Thickening is more energy intensive than bulk harvesting (Chen et al. 2011). Either bulk harvesting or thickening can be performed by means of different techniques which will be briefly summarized in what follows.

3.3.1 Gravity Sedimentation and Flocculation

This technique is typically used for the bulk harvesting of microalgae and refers to a process by which microalgal cells settle to the bottom of a liquid under the action of gravity and subsequently form a sediment which can be easily harvested. Sedimentation is performed through thickeners and clarifiers that are similar to those ones used in standard wastewater treatment plants. It is an energy-efficient method while the separation yield depends upon several factors such as microalgae cell size as well their tendency to aggregate. Because of the relatively small diameter of cells (5–50 μm) and the colloidal character of microalgal suspensions, gravity settling is typically a very slow process (settling rates of 0.1–2.6 cm h^{-1}) which requires large tanks in order to give an effective solid/liquid separation. Fortunately, sedimentation rate can be enhanced by the addition of flocculants to the system. The latter ones are chemicals which improve the rate of sedimentation of the microalgae by aggregating the dispersed microalgal cells into larger colonies which can settle down faster. Common inorganic flocculants are aluminum- and iron-based metal salts. However, metallic salts are quite expensive and require an acidic pH as well as a high dosage to provide an adequate result. On the other hand, cell apoptosis can be induced by the addition of aluminum salts. Residual metal salts after harvesting may negatively affect both the medium recycling and the quality of the desired products. For this reason, organic flocculants or polyelectrolytes which are cationic polymers that physically link cells together are generally preferred. Such flocculants are better tolerated by algae, require a lower dosage, and do not affect medium recycling. Among the different types of organic flocculants available on the market, the most used are chitosan and grafted starch (Kim et al. 2013). After flocculation the microalgae settle down faster and can be harvested from the bottom of the settler. Another technique for increasing the settling rate of algae is the auto-flocculation. In this case, chemicals such as carbonates and hydroxides (NaOH) are added to induce physiochemical reaction between algae and promote auto-flocculation due to carbonates precipitation when pH rises as a result of the photosynthetic phenomena (Kim et al. 2013).

A further technique is the bio-flocculation which consists in culturing microalgae with another microorganism that promotes sedimentation. Example is the use of microbial flocculants for harvesting mass culture of *Chlorella vulgaris* from *Paenibacillus* sp. AM49 (Richmond 2008; Chen et al. 2011).

3.3.2 Centrifugation

Centrifugation is a process that involves the use of the centrifugal force for the stratification of algal culture into regions with different solid concentration that are subsequently separated by draining the less concentrated phase (supernatant). Centrifugation can also be followed by sedimentation to separate the supernatant. This technique allows an effective separation of microalgae in a relatively short time. According to Pragya et al. (2013), about 80–90 % microalgae can be recovered within 2–5 min. For these

reasons, centrifugation is one of the most preferred methods for harvesting of algal biomass. On the other hand, this method is high energy consuming thus potentially being able to negatively affect the CO_2 balance of the process. Energy requirement consumption for various types of centrifuge is estimated to range from 0.3 to 8 kWh m^{-3} (Alabi et al. 2009). Some authors claimed that centrifugation process needs about 48.8 % of the total energy consumption during algal biofuel production. For all these limitations alternative methods for algae harvesting are currently under study and development.

3.3.3 Filtration

Filtration can be used to concentrate microalgal cells. The technique is based on the use of specific filters such as screens, micro-strainers, or membranes through which the algal suspension is passed. Microalgae or microalgae colonies are retained by the filter depending on the difference between the cell size and mesh dimension of the filter. The conventional filtration processes are suitable for the harvesting of microalgae having a relatively large (>70 μm) cell size such as *Spirulina*. It cannot be used for microalgae species having diameters lower than 30 μm such as *Scenedesmus*, *Dunaliella*, and *Chlorella*. Different filtration techniques can be used. Micro-strainers are rotating filters with fine mesh screens. They are simple to operate, require low investment, and have high filtration ratios. Other methods of filtration include dead-end filtration, vacuum or pressure filtration, and cross-flow filtration (Ahmad et al. 2011). In dead-end filtration the fluid flows perpendicularly to the filter, and the trapped particles start to build up a "filter cake" on the surface of the membrane which reduces the efficiency of the filtration process until the filter cake is washed away in back flushing. Dead-end filtration of large amounts of algal broth can only be accomplished using packed bed filters (made from sand), and its application is limited to the removal of algae culture having low solid concentration due to the rheological properties of microalgae which produce compressible cakes and hence clog the filters (Alabi et al. 2009). To overcome such limitation, dead hand filtration vacuum filters can be used. They are able to recover large amounts of microalgae, although they are less effective when applied to organisms approaching bacterial dimensions. A recovery of 80–90 % of freshwater algae is achievable with vacuum tangential flow filtration. Tangential flow filtration is widely used to decrease filter or membrane fouling and performs more efficiently than does dead-end filtration. In cross-flow filtration, backwashing and ventilation of the algae medium can help control the fouling and recover flux (Pragya et al. 2013). Ultrafiltration is another technique that is capable to concentrate an algal suspension up to 150-fold (from 1 to 154.85 g/L) under conditions of pulsated air scouring combined with backwashing (Kim et al. 2013). Filtrations are basically simple but potentially very expensive depending on specific operating parameters such as filter pore size, algae aggregation rate, microalgae species, filter materials, etc. (Greenwell et al. 2010). Energy consumptions range from 0.2–0.88 kWh m^{-3} to 0.1–5.9 kWh m^{-3} for vacuum or pressure filtration, respectively (Alabi et al. 2009).

3.3.4 Flotation

Laboratory experiments have shown that also flotation is suitable for harvesting small, unicellular algae. The separation of suspended microalgae from the liquid bulk phase is achieved through the use of air or gas bubbles which flow upwards within a flotation tank or basin. The small bubbles adhere to the suspended microalgae and then carry them to the liquid surface where they may be removed by a skimming device (Pragya et al. 2013). Microalgal cells with a diameter from 10–30 μm to 500 μm are preferred for effective flotation. Typically, the flotation efficiency depends on the size of the bubbles: nanobubbles (< μm), microbubbles (1–999 μm), and fine bubbles (1–2 mm). As a rule of thumb, the smaller is the bubble size, the longer is their longevity and the larger is their carrying capacity due to the increased surface area-to-volume ratio. Moreover, small bubbles rise slowly and thus can more easily adhere to microalgal cells and more stably transport them to the water surface than large bubbles (Kim et al. 2013). Depending on the bubble size, flotation can be carried out through dissolved air, dispersed air, or electrophoresis. In dissolved air flotation the water stream is pre-saturated with pressurized air. The pressurized air is then released at atmospheric pressure in a flotation tank or basin. The released air forms tiny bubbles of 10–100 μm in size. On the contrary, dispersed air floatation is achieved by injecting air bubbles into the water through an air injection system and a high speed mechanical agitator. In this way, bubbles having diameter ranging from 700 to 1,500 μm can be produced. In both dissolved and dispersed air flotation, flocculants can be added to increase the microalgae separation yield. Electrophoresis techniques exploit the hydrogen bubbles generated by electrolysis of water for transporting microalgal flocs to the water surface. Moreover, since microalgal cells have a negatively charged surface, the application of an electric field can cause algae to migrate towards the positively charged anode where they can be harvested (Pragya et al. 2013). The major benefit of approaches based on electrophoresis is that no chemical addition is required; however, the high power requirements and electrode costs do not make for an appealing harvesting method, especially for large-scale applications (Christenson and Sims 2011).

3.3.5 Final Considerations About Harvesting of Microalgae

It is worth noting that, according to some authors, harvesting alone is one of the most expensive steps of the overall process of microalgae production since it accounts for

Table 5 Comparison of mechanical harvesting methods for algae

Method	Solid concentration after harvesting (%)	Recovery yields (%)	Major benefits	Major limitations
Centrifugation	12–22	>90	Reliable, high solids conc.	Energy intensive, high cost
Tangential filtration	5–27	70–90	Reliable, high solids conc.	Membrane fouling, high cost
Gravity sedimentation	0.5–3	10–90	Low cost	Slow, unreliable
Dissolved air flotation	3–6	50–90	Proven at large scale	Flocculants usually required

Adapted from Christenson and Sims (2011)

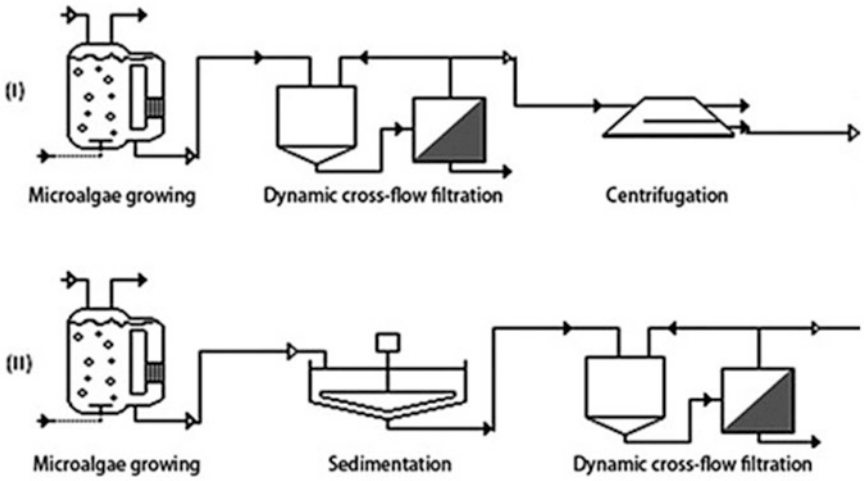

Fig. 12 Diagrams of two possible concentration paths: from photobioreactor to (*I*) final concentrated biomass passing through dynamic microfiltration followed by centrifugation and (*II*) final concentrated biomass passing through pH-induce flocculation sedimentation and dynamic microfiltration (Adapted from Rios et al. 2013)

20–30 % of the total production cost (Rawat et al. 2011). Therefore, in order to assure the economic sustainability of the process, efficient and inexpensive harvesting methods should be developed and subsequently adopted at the industrial scale. Moreover, the correct choice of the technique for dewatering the microalgal culture is critical in order to reduce water consumption. In fact, the exhaust liquid growth media separated during this operating phase should be recycled for preparing the fresh growth medium. In Table 5, a comparison made by Christenson and Sims (2011) between the advantages and limitations of the main techniques for microalgae harvesting is reported.

Finally, it is worth noting that also suitable combinations of the methods described above can be exploited in order to increase harvesting efficiency. In Fig. 12, two possible combinations of different harvesting techniques proposed by Rios et al. (2013) are shown.

3.4 Downstream Processing

The harvested biomass slurry is characterized by a solid content ranging from 5 to 15 % dry weight. Lipid extraction can be performed both from wet and dry biomass. Depending upon the specific lipid extraction route adopted, specific pretreatments should be carried out. In particular, if lipid extraction will be carried out from dry biomass, a drying/dehydration pretreatment will be necessary, while, if the wet route is chosen, microalgae must be undergone to a specific pretreatment aimed to break their cell wall (Fig. 13).

Since, after harvesting microalgal biomass is perishable, it must be processed rapidly. In what follows, the main techniques for performing drying and cell disruption will be summarized.

3.4.1 Drying Methods

The target of the drying process is to extend the viability of the desired product and prevent the degradation of the harvested biomass slurry. It can be performed basically by sun drying, spray drying, solar drying, drum drying, fluidized bed drying, freeze drying, and refractive window technology (Brennan and Owende 2010). Other techniques include flash drying and rotary dryers. The selection of the drying process depends on the scale of operation and the use for which the product is intended. Sun drying is a method based on natural evaporation of water. It is a slow drying technique which depends on weather conditions and requires large evaporation basins. On the other hand, it is the cheapest way for drying microalgae since it consumes low energy. Spray drying is a technique of producing a dry biomass from slurry by rapidly drying it with a hot gas (Alabi et al. 2009). All spray dryers use some type of atomizer or spray nozzle to

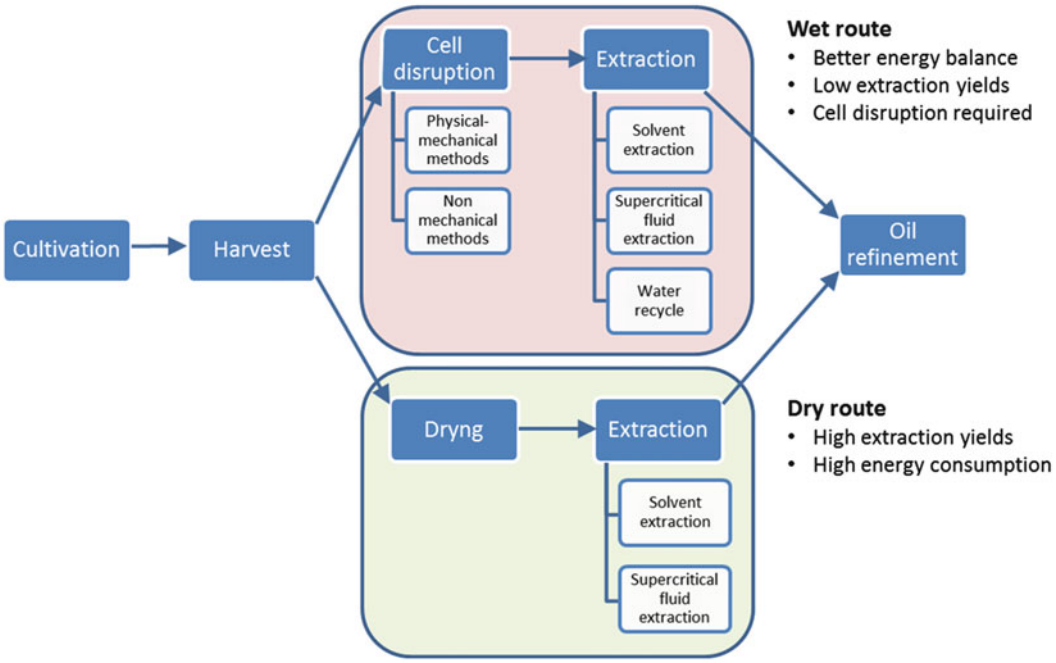

Fig. 13 Comparison of dry and wet route of lipid extraction (Adapted from Kim et al. 2013)

disperse the liquid or slurry into a controlled drop size spray. This method is quite expensive but can be used for the extraction of higher value products from microalgae (Brennan and Owende 2010). Freeze drying, also known as lyophilization, is a dehydration process which works by freezing the algal biomass at −20 °C and then reducing the surrounding pressure to allow the frozen water in the material to sublimate directly from the solid to the gas phase. While allowing good oil extraction yields, freeze drying is relatively expensive and thus is rarely used for large-scale operations (Brennan and Owende 2010). In drum drying, the wet biomass is applied as a thin film to the surface of a heated drum, and the dried biomass solids are then scraped off with a knife. Drum drying is fast and efficient but is both cost and energy intensive (Alabi et al. 2009).

Since it involves high energy consumptions, drying is one of the main costs of the whole process of oil production from algae. It can represent 70–75 % of the processing cost. Thus, while allowing subsequent good extraction yields, drying as a pretreatment process is not an economical process. For this reason, drying is often skipped and the wet route is generally preferred. An improvement of the economic sustainability of the drying step can be achieved by suitably exploiting the energy of flue gas at the outlet of the emission source for heating the wet biomass (Cao and Concas 2011).

3.4.2 Cell Disruption Methods

Cell disruption is an essential pretreatment when lipid extraction is carried out directly from wet biomass. In fact, lipid extraction from wet biomass is characterized by low yields due to the immiscibility of water with organic solvents typically used for dissolving lipids from algae. Therefore, when solvent extraction is applied to a wet biomass, the microalgal cells tend to remain in the water phase due to their surface charges, and thus, they cannot contact the organic solvent phase which is able to extract lipids (Kim et al. 2013). On the other hand, this phenomenon can be prevented by suitably breaking the cell wall of microalgae and thus facilitating the release of intracellular lipids from the microalgal cellular matrix. Once released from the algal cell, lipids pass to the organic phase from which they can be extracted by evaporating the solvent. The cell disruption is therefore a method for breaking the cell wall of algae. Since microalgae have a cell wall, which is a thick and rigid layer composed of complex carbohydrates and glycoproteins with high mechanical strength and chemical resistance, this operating step can require high-energy inputs. Cell disruption techniques can be conceptually divided into physical or mechanical methods and nonphysical methods.

3.4.2.1 Physical Mechanical Methods

The physical or mechanical methods include high-pressure homogenization, ball milling, microwaving, ultrasonication, and cavitation. The process of high-pressure homogenization is a mechanical method which consists in pumping the cell suspension to a high pressure through a narrow opening of a valve before the cell suspension is released into a chamber of a lower pressure (Halim et al. 2012). High-pressure homogenizers can greatly enhance the availability and the extraction of pigments from the cells. On the other hand, it can cause high energy consumptions which can be up to 750 kWh/dry ton for 4–7 wt% solids

(Alabi et al. 2009). Ball milling is a very simple cell disruption technique that breaks cells by means of spheres made of quartz or metal that are shaken within a closed container filled with the target cells. The cells are disrupted by collision or friction with the spheres. This method is very simple and rapid but is hard to scale up and requires extensive cooling systems for preventing thermal degradation of lipids (Kim et al. 2013). Microwaves break cells using the shocks generated by high-frequency electromagnetic waves (about 2,500 MHz). This method has been successfully applied for disrupting vegetal cell walls and subsequently extracting lipids. The main limitation deriving from using microwaves at large scale is the high energy consumption (about 70 kW). Ultrasonication exploits the cavitation phenomena induced by ultrasounds (18–50 kHz) in a liquid. Cavitation leads to the formation and the immediate implosion of cavities (microbubbles) in the liquid. Such implosions result in the production of shockwaves which can disrupt the cell wall of microalgae thus allowing the release of intracellular lipids. The main advantage of this method is the high yields of cell disruption. On the other hand, the main limitations are the high energy consumptions which range from 60 to 120 MJ/$kg_{wet\ biomass}$ and the low scalability deriving from the fact that cavitation occurs only in small regions near the ultrasonic probes (Kim et al. 2013). Finally, a relatively new technique for cell disruption is the electroporation. The latter one consists in the increase of the electrical permeability of cells by applying a pulsed electromagnetic field. It is usually applied in molecular biology for introducing specific substance into a cell, such as drugs or piece of DNA as well as for extracting intracellular compounds. No permanent effects are detected in the cells. However, if a very strong intensity of the electric field is applied, the cell wall can be destroyed, thus allowing the subsequent extraction of lipids. Electroporation is very simple and low energy consuming since in the few studies carried out on microalgae, an energetic input of about 36 kWh/m^3 was sufficient for disrupting algal cells (Lee et al. 2012).

3.4.2.2 Nonmechanical Methods

The main nonmechanical methods for microalgal cell disruption are osmotic shocks, enzymatic hydrolysis, and physicochemical methods. Osmotic shock is caused by a sudden change in the solute concentration which provokes a rapid change in the movement of water across the cell wall. This results in the creation of a pressure gradient between the inner and the outside of the cells which can disrupt the cell envelopment. Both hyper-osmotic shocks and hypo-osmotic shocks can be used for breaking the cell wall. When the salt concentration is higher in the exterior, the cells suffer hyper-osmotic stress. As a result, the cells shrink since the inner cell fluids diffuse outwards, and a damage is caused to the cell walls. On the contrary, hypo-osmotic stress takes place when the salt concentration within the cell is lower than the exterior one. In this case, water permeates into the cells which consequently swell or burst if the stress is too high. Osmotic shock is a relatively cheap and simple method for disrupting algal cell walls. On the other hand, it produces high amounts of saline wastewater which must be treated (Kim et al. 2013). Enzymatic hydrolysis exploits specific enzymes to lyse algal cell walls. Specific enzymes such as papain, pectinase, snailase, neutrase, lipase, and alcalase can react with the cellulose and phospholipids of the cell wall converting them into glucose, fatty acids, and glycerol, respectively (Young et al. 2011). This way enzymatic reactions can break the cell wall, thus facilitating the subsequent phase of lipid extraction. Even though the enzymatic hydrolysis can lead to high yields of cell disruption, the cell lysing enzymes are still cost prohibitive and thus unsuitable for massive production.

Physicochemical methods include alkaline and acid hydrolysis through NaOH, HCl, and H_2SO_4. They are typically carried out within autoclaves at a temperature of about 90 °C (Sathish and Sims 2012). Among the others, chemicals such as lysine acetone, methanol, dimethyl sulfoxide (DMSO), and organic acids can be used for lysing the cell wall of algae. Despite the fact that chemical methods have high cell disruption performances, they show some significant limitations. The chemicals must be continuously supplied and this aspect greatly affects the economic sustainability of the method when large-scale production is considered. Furthermore, acids and alkalis can corrode the surface of reactors and attack target products (i.e., lipids) of the microalgal cell. Therefore, physicochemical methods must be coupled with a mechanical pretreatment aimed to reduce the chemical usage (Kim et al. 2013).

3.4.2.3 Comparison Between Main Techniques for Cell Disruption

A comparison between the different techniques can be performed in terms of disruption efficiency. The following parameter defined by Halim et al. (2012) as average disruption yield L can be used for comparing different techniques:

$$L = \left(1 - \frac{C}{C_0}\right) \cdot 100\ \%$$

where C/C_0 is the average ratio between the number of intact (not disrupted cells) cells before and after disruption procedure. By comparing the main techniques summarized above in terms of such parameter, the result shown in Fig. 14 was obtained.

3.5 Lipid Extraction

The feasibility of biofuel production from algae cultivation depends basically on their content of lipids (Jones et al. 2012). Amounts and typology of lipids in microalgae vary from strain to strain. However, the lipid categories are basically divided into neutral lipids (e.g., triglycerides, cholesterol, polyunsaturated fatty acids) and polar lipids (e.g., phospholipids, galactolipids). Triacylglycerides (TAGs) as neutral lipids are the most useful precursors for the production of biodiesel (Kirrolia et al. 2013). However, as shown in Fig. 15, TAG are contained within the microalgae cells, surrounded by a rigid cell wall, and thus extraction is needed for being suitably exploited. To this aim, dewatered biomass is processed in a pretreatment step aimed to dry the biomass or alternatively to break the cell wall of microalgae to facilitate the subsequent step of lipid extraction. Therefore, depending on the specific pretreatment adopted, microalgal biomass to undergo lipid extraction can assume one of the following physical states: disrupted concentrate or dried powder. Several methods for lipid extraction from microalgae are currently under investigation at the laboratory scale, but only solvent extraction appears to be the viable way for an effective lipid extraction at the industrial scale. Typically, solvent extraction is carried out by contacting microalgal biomass with an eluting solvent which extracts TAG and fatty acids out of the cells (Halim et al. 2011). The most suitable solvents for extracting lipids from microalgae are the organic ones and supercritical carbon dioxide. In what follows, we will focus on these two techniques.

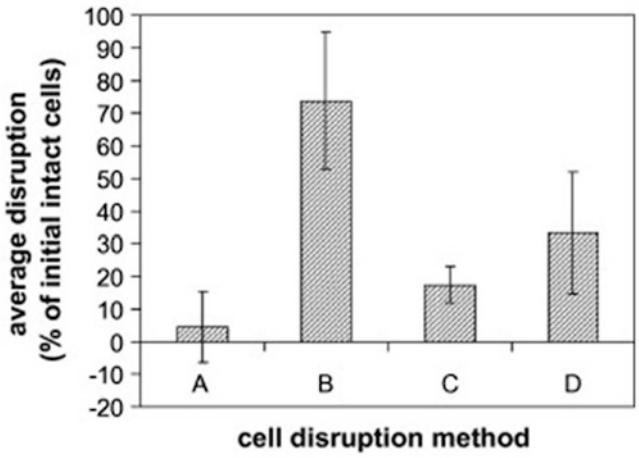

Fig. 14 Comparison of the different cell disruption methods. Average disruption (± standard deviation) of each method is reported. Average disruption is expressed as % of initial intact cells. *A*: ultrasonication. *B*: high-pressure homogenization. *C*: bead beating. *D*: sulfuric acid treatment (Adapted from Halim et al. 2012)

3.5.1 Organic Solvent Extraction

This technique is based upon the fact that when a microalgal cell is contacted with a nonpolar organic solvent, such as hexane or chloroform, a static film of solvent surrounding the algal cell is formed as a result of the interactions between solvent molecules and the cell wall constituents (Fig. 15). The film thickness depends also upon hydrodynamics parameters such as stirring speed, solvent flow rate, and cell diameter (Halim et al. 2012). Subsequently, the organic solvent diffuses through the cell membrane into the cytoplasm and interacts, through van der Waals-type bindings, with the neutral lipids

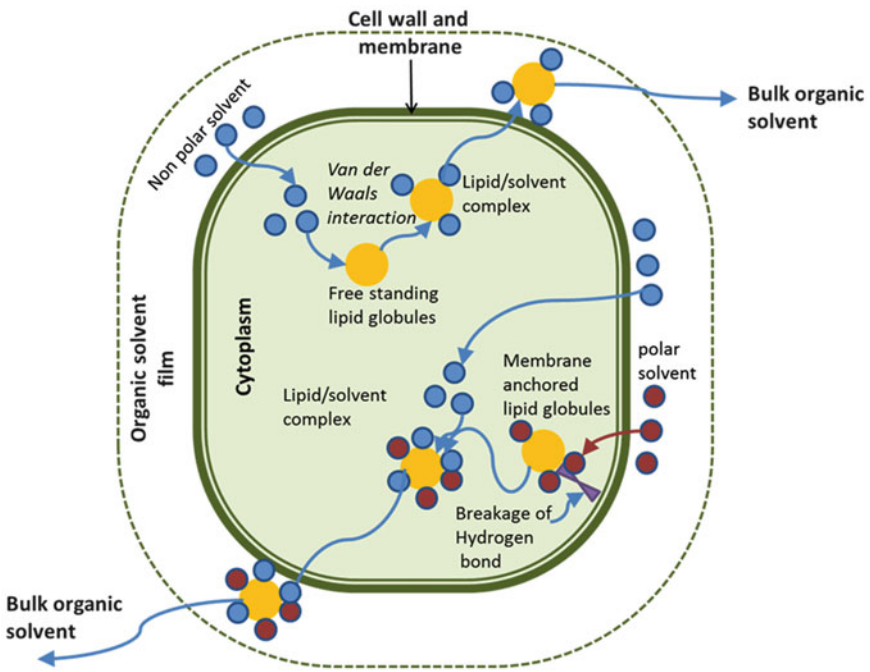

Fig. 15 Simplified scheme of the main phenomena involved in lipid extraction through organic solvents (Adapted from Halim et al. 2012)

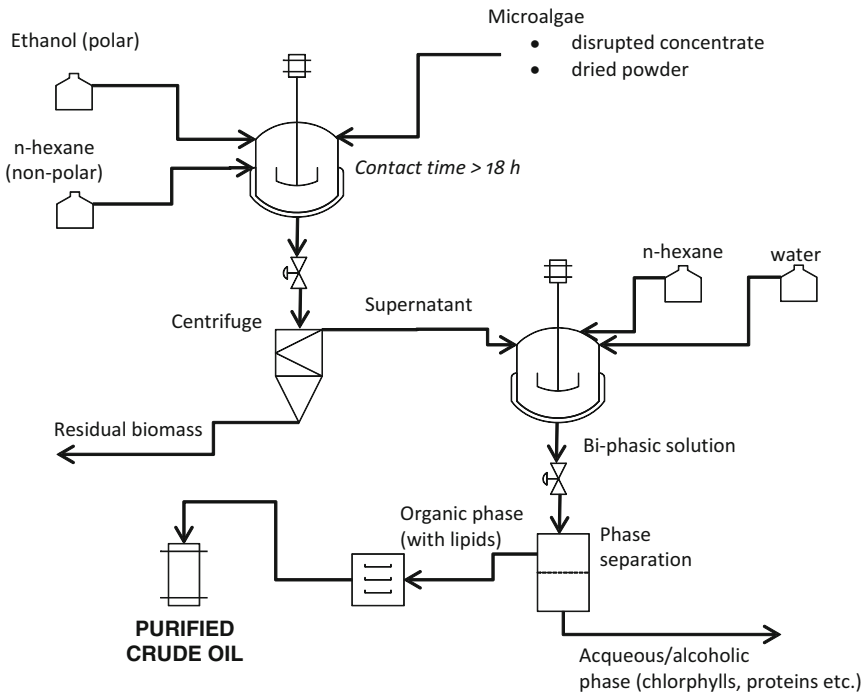

Fig. 16 Scheme of a classical solvent extraction process

by forming organic solvent–lipid complexes. The latter ones, driven by a concentration gradient, counter-diffuses across the cell wall towards the static organic solvent film surrounding the cell and then towards the bulk organic solvent. As a result, the neutral lipids are extracted out of the cells and remain dissolved in the nonpolar organic solvent. This method permits the extraction of free-standing lipid globules that float in the cytoplasm. However, some lipid bodies are linked via hydrogen bonds to the proteins of the cell membrane. The van der Waals interactions promoted by nonpolar organic solvents are not strong enough to break the above bonds which anchor lipid bodies to the cell membrane (Halim et al. 2012). On the contrary, polar solvents such as methanol ethanol or isopropanol are capable of breaking such bonds. For this reason, organic polar solvents are often used in synergy with nonpolar ones for extracting lipids from microalgae. Once the lipid bodies are undocked from the membrane, they form complexes with the organic solvents and counter-diffuse towards the solvent bulk outside the cell driven by concentration gradients (Halim et al. 2012).

Therefore, for an effective extraction of lipids, mixtures of polar and nonpolar solvent are often used. Useful combinations of nonpolar/polar solvents are hexane/isopropanol, chloroform/methanol, hexane/ethanol, etc. As shown in Fig. 16, the two kinds of solvents are typically added simultaneously with a volumetric ratio which is established by means of specific experimental trials. If extraction is performed on wet biomass, the cell debris should be removed by means of a suitable liquid solid separation such as centrifugation. Once cell debris is removed, biphasic separation is induced by further adding suitable amounts of polar solvent and water.

After biphasic separation, neutral and polar lipids are concentrated in the organic phase which is a mixture of nonpolar (e.g., hexane) and polar (e.g., ethanol) solvents and the aqueous/alcoholic phase which is a mixture of water and polar organic solvent (e.g., ethanol) where other cellular molecules such as chlorophylls, proteins, and carbohydrates have been transferred. Therefore, biphasic separation allows not only the removal of residual water but also non-lipid contaminants from the mixture of organic solvents and lipids. The organic phase is then decanted and evaporated to yield purified crude lipids, which can be then fractionated and transesterified to produce biodiesel. Since the evaporation phase could be energy consuming, volatile solvents are typically preferred in order to reduce time and cost of the evaporation step. Moreover, specific solvents such as chloroform are effective but highly toxic, and their use should be avoided. For this reason, the most suitable combination of nonpolar/polar solvents appears to be a mixture of hexane and ethanol (Fajardo et al. 2007).

The main operating parameter affecting the extraction yield is the contact time t (h). In particular, according to Halim et al. (2011), the lipid extraction process is observed to follow a first-order kinetics which results in the following relationship between the cumulative amount of lipid extracted in the organic solvent m_e ($g_{lipid}/g_{dried\ microalgae}$) and time t:

$$m_e = m_{s,0}\left(1 - e^{-kt}\right)$$

where $m_{s,0}$ is the amount of lipid originally present in the cells ($g_{lipid}/g_{dried\ microalgae}$) and k is the lipid mass transfer coefficient from the cells into the organic solvent

(min^{-1}). Such kind of relation indicates that the cumulative mass of extracted lipids increases with time until a plateau is reached. Typically, extraction time depends on the specific algal strain. Extracting 90 % of lipids may need up to 12 h depending upon the value of the mass transfer coefficient k. The latter one is found to be a function of other operating parameters such as temperature T (°C), solvent/biomass ratio s/b ($mL_{solvent}/g_{biomass}$), and stirring speed ω (rpm). The higher is the value of these parameters the higher is the value of k. However, usual values of T range from 25 to 60 °C, stirring speed ω can vary from 500 to 800 rpm while the solvent/biomass ratio can vary from 5 to 250 ($mL_{solvent}/g_{biomass}$) (Fajardo et al. 2007; Lee et al. 1998).

The main limitations of the solvent extraction techniques are the need of a continuous supply of expensive solvents since not all of the organic ones can be recycled. Moreover, the high toxicity of solvents arises environmental and safety concerns.

3.5.2 Supercritical CO_2 Extraction

Supercritical fluid extraction (SFE) is the process of separating one component (e.g., lipids) from another (e.g., microalgae) using supercritical fluids as extracting solvent. A supercritical fluid is any substance at a temperature and pressure above its critical point (Tc, Pc), where distinct liquid and gas phases do not exist. Under such thermobaric conditions, supercritical fluids behave like solvents, thus becoming a suitable substitute of organic solvents in a range of industrial and laboratory processes. The capability of behaving like a solvent depends on the fact that supercritical fluids have density similar to the one of liquids while their viscosity and diffusivity are closer to the ones of gases. For this reason, the solubility approaches that of the liquid phase while penetration and diffusion into a solid matrix is facilitated by the gas-like transport properties. As a consequence, the rates of extraction and phase separation can be significantly faster than that one for conventional extraction processes.

Among the various fluids, supercritical carbon dioxide ($SCCO_2$) is becoming an important solvent due to its low toxicity, its low flammability, and its lack of reactivity which result in a low environmental impact. Moreover, its relatively low critical pressure (7.39 MPa) results in low compression cost, while its modest critical temperature (31.1 °C) permits a successful extraction of thermally sensitive lipid fractions without degradation. The principle through which lipids can be extracted from microalgae through $SCCO_2$ is similar to the one schematically shown in Fig. 16 for the extraction with organic solvent. First, $SCCO_2$ rapidly diffuses into the algal cell and then lipid bodies dissolve in the supercritical fluid by forming lipid-CO_2 complexes through van der Waals interactions. Subsequently, the so formed complexes counter-diffuse from the inner of the cell towards the static film and then towards the bulk driven by concentration gradients. While the phenomena on the base of lipid extraction are very similar to the ones involved in the organic solvent extraction, by using supercritical fluids the extraction rate can be up to ten times faster. Nevertheless, the properties of $SCCO_2$ can be altered by suitably tuning pressure and temperature for performing a selective extraction. Since $SCCO_2$ is unable to interact with either polar lipids or neutral lipids, a polar modifier, often referred to as cosolvent, is added to CO_2. The target is to improve the affinity of the resulting fluid for polar lipids and lipid complexes. Common polar modifiers are methanol ethanol, toluene, and methanol–water mixture. A simplified scheme of the $SCCO_2$ extraction process is shown in Fig. 17. It involves the use of a source of pure CO_2 which, in the case where algae are cultivated near a coal-fired power station, can be conveniently obtained from the scrubbed flue gas of the station. The microalgal biomass, in the form of disrupted concentrate or dried powder, is placed in a packed bed previously filled with suitable packing elements. The CO_2 along with the cosolvent is heated through heat exchangers and compressed through compressors until the desired supercritical conditions of temperature and pressure are achieved.

The $SCCO_2$ is then pumped into the column from the bottom and flows upwards through the packed bed thus contacting microalgae and desorbing lipids according to the mechanisms depicted above. Therefore, lipids enter in the bulk $SCCO_2$ flow which subsequently leaves the packed column to enter in the so-called blow down vessel. Here, the pressure is reduced until CO_2 returns to the gaseous state. The lipids then precipitate down in a collection vessel while the gaseous CO_2 flows upwards. The CO_2 is then collected for being recirculated. As such, SFE-derived crude lipids are free from any extraction solvent and do not need to undergo an extraction solvent removal step (Halim et al. 2012).

Also for the case of supercritical lipid extraction, the process is observed to follow a first-order kinetics. The time evolution of the cumulative amount of extracted lipids during the process can be described by a mathematical relationship similar to the one reported for organic solvent extraction. However, in this case the mass transfer coefficient is a function of different operating parameters (Halim et al. 2012) such as the extraction pressure, the temperature, the concentration of cosolvent, and the $SCCO_2$ flow rate. Typical range of operating pressure for extracting lipids from algae is from 200 to 450 bar. The extraction temperatures can vary from 40 to 60 °C, and the $SCCO_2$ flow rate range is 0.4–500 l/min (Andrich et al. 2005; Cheung 1999; Mendes et al. 2003; Sajilata et al. 2008). The $SCCO_2$ extraction technique is a very promising method for extracting lipids from microalgae since it can assure high extraction yields in relatively short

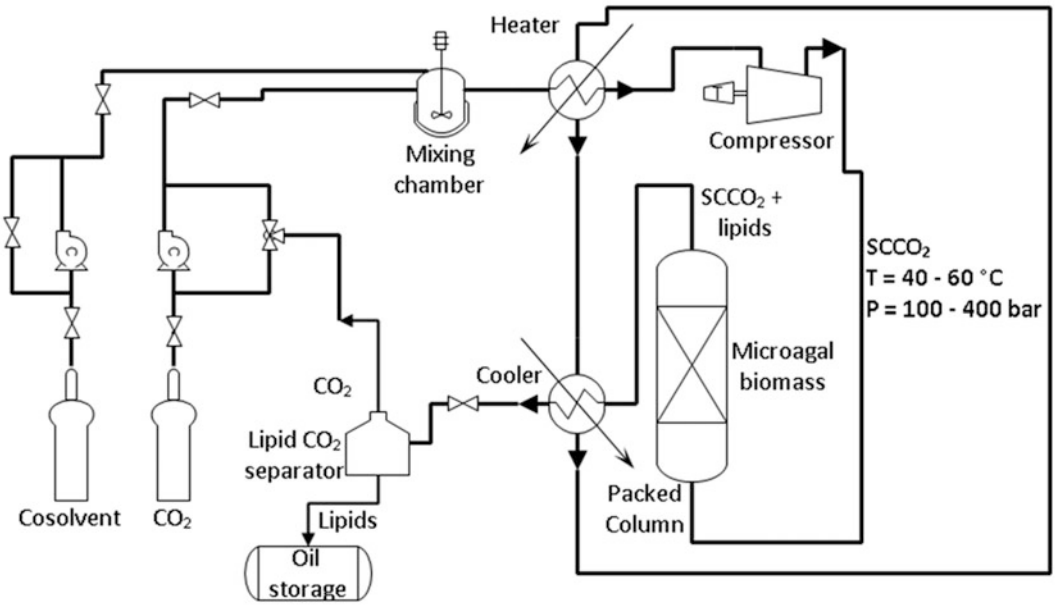

Fig. 17 Scheme of the $SCCO_2$ extraction of microalgal lipids

times. Moreover, no concerns related to solvent toxicity can arise. Unfortunately, the main limitations of this method are the high energy consumption related to the operating phases of fluid heating and compression as well as the potentially high costs of investment.

3.6 Conversion of Microalgal Lipids for the Production of Biodiesel

Once extracted the algal crude oil must be further processed to be used as fuel. Depending on the specific postprocessing technology, different kinds of biofuels can be produced. However, in this work we will focus only on the production of biodiesel which can be obtained through the well-known process of transesterification. The need of further processing the oil depends on the fact that its viscosity is too high for its exploitation in internal combustion engines. Hence, to produce a useful biodiesel, the viscosity of microalgal oil must be reduced. The most common method to produce biodiesel from vegetal oil is just the transesterification alcoholysis. It consists in the reaction between triglycerides of the oil with methanol. Such reaction leads to the formation of methyl esters of fatty acids (FAMEs) that are biodiesel and glycerol (Fig. 18).

The reaction can be catalyzed by acids, alkalis, and lipase enzymes, but usually, alkalis such as sodium and potassium hydroxide are used since they are able to speed up the reaction about 4,000 times than acids. Alkali-catalyzed transesterification is carried out at approximately 60 °C under atmospheric pressure. Under these conditions, reaction takes about 90 min to complete (Chisti 2007). When transesterification reaction is completed, the two phases (glycerine and esters) are separated by gravimetric methods such as decanting and centrifuging. It has been reported that the achievable conversion of algal triglycerides to biodiesel is about 98 % (Amin 2009) and the produced biodiesel can be compatible with conventional petroleum-derived diesel (Table 6). The biodiesel produced can thus be used in the internal combustion engines.

4 Carbon Capture by Microalgae

As discussed above, cultivation of microalgae might be coupled with the direct bio-capture of CO_2 emitted by industrial activities that use fossil fuels for energy generation (Usui and Ikenouchi 1997; Francisco et al. 2010). For this reason, microalgae can be seen as a new technology for carbon mitigation. Driven by the increasing concerns related to the effects of CO_2 levels on global warming, several technologies for carbon mitigation are currently being developed around the world. Among those, carbon capture coupled with geological storage (CCS) is considered the most realistically feasible and economically viable method for reducing CO_2 concentration in the atmosphere (Zhang and Sahinidis 2012). However, CCS techniques are characterized by several limitations that might hinder their application at the real scale, whereby biological carbon capture through microalgae is today becoming a realistic alternative to CCS technologies.

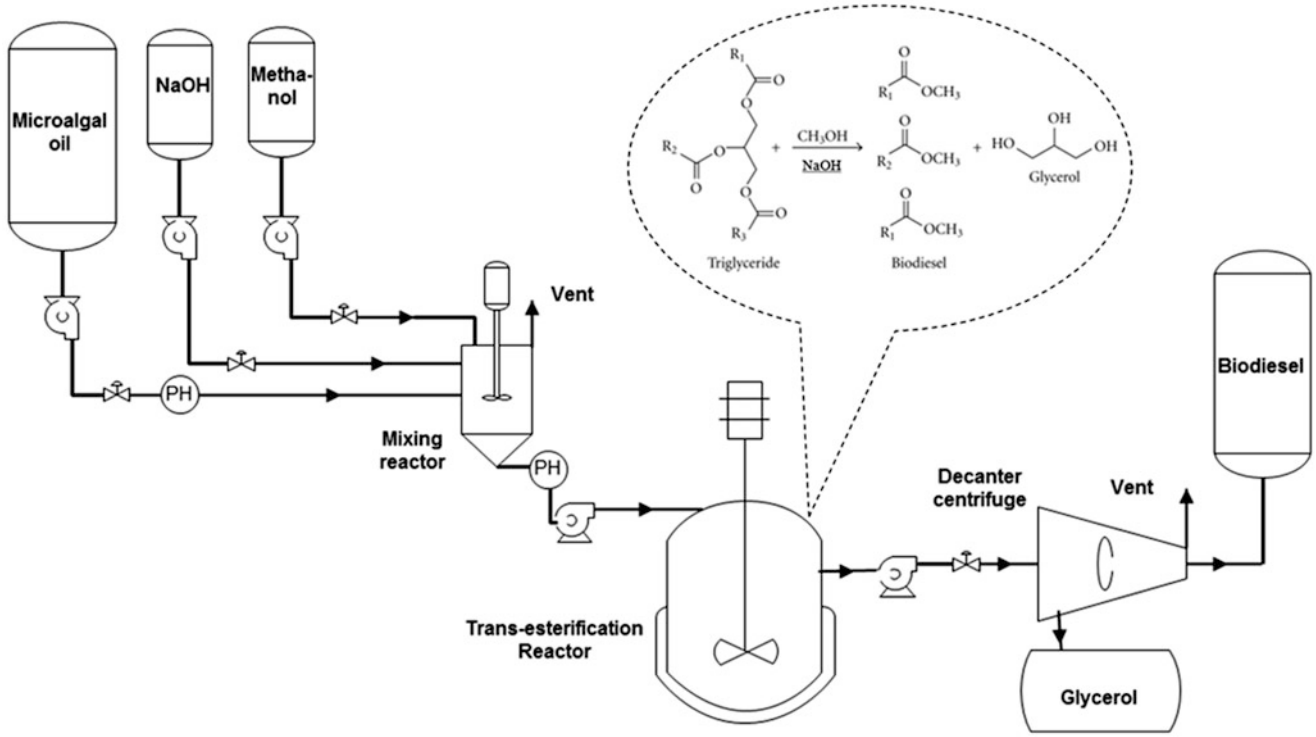

Fig. 18 Scheme of the transesterification process

Table 6 Comparison of properties of biodiesel, diesel fuel, and ASTM standard

Properties	Biodiesel from microalgae	Diesel fuel	ASTM standard
Density (kg L^{-1})	0.864	0.838	0.86–0.90
Kinematic viscosity at 40 °C (mm^2 s^{-1})	5.2	1.9–4.1	3.5–5.0
Flash point (°C)	115	75	Min 100
Solidifying point (°C)	−12	−50–10	–
Cold filter plugging point (°C)	−11	−3.0 (max. −6.70)	Summer max 0; winter max −15; max 0.5
Acid value (mg KOH g^{-1})	0.374	Max 0.5	–
Heating value (MJ kg^{-1})	1.81	1.81	–

Adapted from Amin (2009)

4.1 Limitations of the Current Carbon Capture and Sequestration (CCS) Technology

Basically, CCS techniques are characterized by a first step, called capture, where the CO_2 is separated from the other constituents of the flue gas emitted by a point source such as a power station or a generic CO_2-emitting facility. The separated CO_2 is then compressed and transported (usually through pipelines) to the storage site. Finally, in the sequestration step, compressed CO_2 is injected into deep geological formations, such as saline aquifers, depleted oil/gas reservoirs, or deep un-mineable coal seams (Zhang and Sahinidis 2012). In an alternative version, storage can be carried out by injecting CO_2 in the bottom of oceans. However, both the steps of capture and of sequestration are characterized by specific concerns which can limit the application at the industrial scale of the CCS technologies. A simplified scheme of the CCS technology is shown in Fig. 19.

The chemical–physical capture technologies fundamentally include the chemical absorption, adsorption onto solid materials, membrane-based technology, and cryo-fractionation (Fig. 20). In absorption processes, the flue gas is continuously passed through the liquid solvent, which absorbs the CO_2. However, this technique, which typically involves the use of a MEA (monoethanolamine) solution for absorbing CO_2, can be affected by several operating problems such as corrosion, liquid channeling, flooding, foaming, etc. (Lv et al. 2013). The adsorption techniques are based on the ability of some porous solids (adsorbents) to selectively bind the molecules of CO_2 in the flue gas by exploiting van der Walls forces (physical adsorption) or

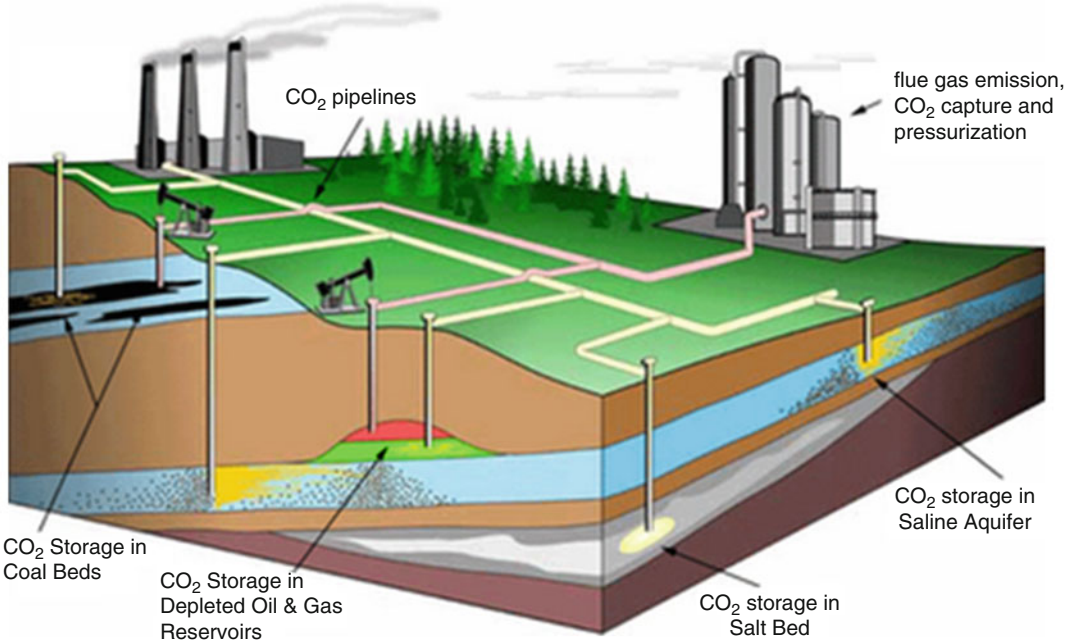

Fig. 19 Conceptual scheme of carbon capture and storage (Adapted from O'Neill 2009)

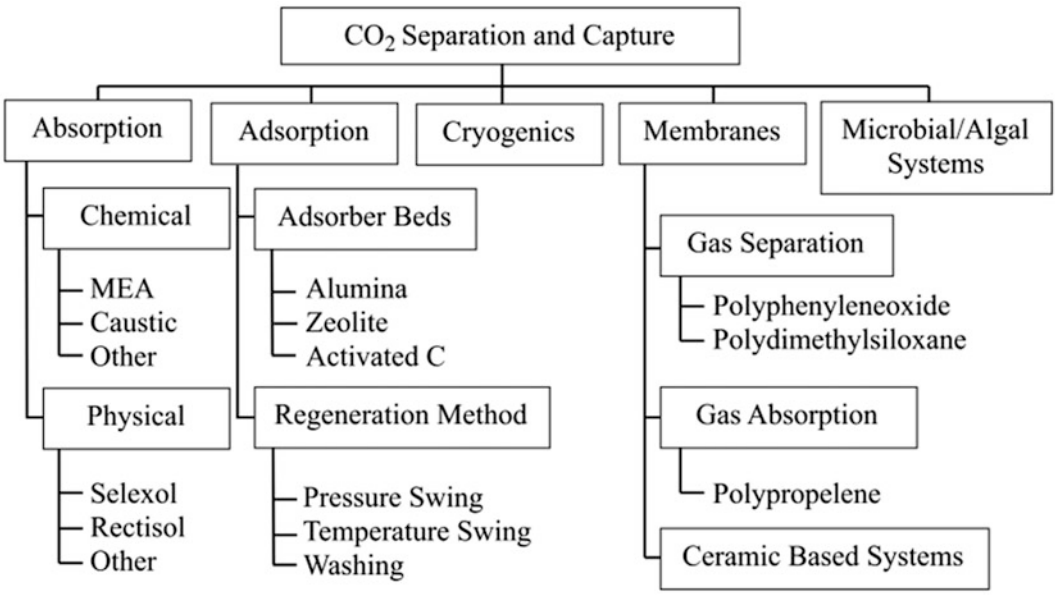

Fig. 20 Chemical–physical methods for carbon capture (Adapted from Lam et al. 2012)

real chemical bonds (chemical adsorption). The most important adsorbents are activated carbon, zeolite, silica gel, aluminum oxide, etc. The main drawbacks related to the use of solid adsorbents for CO_2 capturing are the need to remove moisture and contaminants from flue gas before conveying it to the adsorber (Lam et al. 2012). In fact, NO_x and SO_x, which can be present in untreated flue gas, can poison the adsorbents while moisture, which accounts for up to 15 %v/v in a typical flue gas, can reduce the CO_2 recovery from 75 to 60 % (Li et al. 2008a). The membrane technologies are based on the specific permeability and selectivity of polymeric membranes which, working like a filter, allows the separation of CO_2 from the other constituents of the flue gas. The main limitations of membrane technologies are related to high manufacturing cost, the fouling effect, as well as the high membrane surface area that is needed for the treatment (Lam et al. 2012). Finally, the cryogenic fractionation technology exploits the

difference in boiling points of the various gas species to separate CO_2. However, the cryogenic method is high energy consuming and is strongly affected by moisture of flue gas (Tuinier et al. 2010).

Once captured and concentrated, carbon dioxide must be permanently stored. To this aim, geological carbon sequestration is currently seen as the only realistic method for CO_2 mitigation. As mentioned above, it consists basically in the injection of CO_2 into deep rocks, aquifers, or oceans. However, also carbon sequestration in geological formations may raise significant safety concerns (Mazzoldi et al. 2012). In particular, the major issue related to the geological carbon sequestration into rocks or aquifers is the potential triggering of seismicity phenomena owing to the large-scale pressurization resulting from CO_2 injection (Cappa and Rutqvist 2011). Furthermore, over a long time scale, the presence of unknown faults in the rocks hosting the CO_2 may provide preferential paths for CO_2 leakage out of reservoirs (Mazzoldi et al. 2012). This phenomenon potentially thwarts the efforts made for storing the CO_2 which can pass to the atmosphere through these faults. Moreover, when stored into aquifers, CO_2 can cause the acidification of the water body thus rising important risks for the potential users of the acidified groundwater (Wilkin and DiGiulio 2010). Finally, ocean sequestration is based on the fact that at great depths, because of the increased pressure, CO_2 is denser than sea water, and hence, it may be theoretically stored on the bottom as liquid or deposits of icy hydrates, thus preventing its contact with the atmosphere. However, also in this case, several concerns may rise. In fact, at whatever depth, dissolved CO_2 induces water acidification thus negatively affecting all the ecosystems and the biogeochemical cycles hosted by deep sea (Yamada et al. 2010).

When considering the economic aspects, it is noteworthy that the cost of the capture might be significant depending on CO_2 concentration in the flue gas and the used chemical process. Moreover, the cost of transportation and storage is estimated to be about US 5–15 $ for each ton of CO_2 captured. For CCS methodology, there is not any valuable product to balance other costs. Therefore, considering the carbon cost established by Kyoto protocol (270 $ t^{-1}), the CCS methodologies are not economically feasible. Only a carbon cost of 330 $ t^{-1} is assumed to make CCS competitive (Pires et al. 2012). Furthermore, CCS methodologies will face the opposition of the populations near the storage locations, due to the possible CO_2 leakage and the consequent environmental hazards.

4.2 Direct Carbon Bio-Fixation by Microalgae

Since the CCS technologies may give rise to significant concerns which may affect their application to the large scale, the potential exploitation of microalgae as a method for the CO_2 capture and bio-fixation is receiving a rising interest (Olguin 2003; Mulbry et al. 2008). In fact, when compared to CCS technologies, biological carbon mitigation through microalgae shows a number of potential advantages. Among the last ones, there is the possibility of performing CO_2 capture and fixation in well-controlled photobioreactors. Moreover, biological CO_2 fixation techniques do not use hazardous chemicals, do not affect the environment, can exploit directly flue gases evading the costs of CO_2 separation/capture, and finally lead to the production of valuable products such as biofuels, food, and fine chemicals (Farrelly et al. 2013).

Microalgal photosynthesis is capable to exploit CO_2 in both atmosphere and flue gases. The CO_2 uptake capacity of microalgae is ten times higher than terrestrial plant. Furthermore, they can accumulate inorganic carbon in their cytoplasm to concentrations several orders of magnitude higher than that on the outside, a phenomenon called CO_2 concentrating (Pires et al. 2012). The use of flue gases as source of CO_2 can theoretically result in positive effects on microalgae growth. In fact, being equal the gas flow rates, the carbon provided by flue gases to microalgae is much higher than the one supplied by air. This could lead to higher biomass and oil productivities that are critical to ensure a sustainable production of biofuels through microalgae.

On the contrary, the industrial production of microalgae has been so far carried out by using atmospheric CO_2 as carbon source. Under such operating conditions, the diffusion of CO_2 from the atmosphere into a microalgal culture is not effective enough to achieve high biomass productivity due to the low CO_2 content of air (380 ppmv CO_2) and the high surface tension of water (Van Den Hende et al. 2011). Moreover, since the mass transfer of CO_2 in water is very low, atmospheric air must be continuously pumped at a very high flow rate into the microalgal broth for supplying the amounts of carbon needed by microalgae to grow. This leads to high energy consumptions and consequently to high operating costs during algae cultivation (Lam et al. 2012). In addition, the higher is the gas flow rate the higher is the gas holdup and therefore the larger is the volume of photobioreactors. To the aim of overcoming such limitations, suitable amounts of commercially available CO_2 are usually supplied to the microalgal cultures in the industrial practice. However, this can result in a relatively large cost since the current price for commercially delivered CO_2 ranges from 30 to 40 € per ton of CO_2. While these costs can be sustainable when the final product extracted from microalgae is a fine chemical characterized by a high commercial value, in the case where massive production of biofuels is the final target of the cultivation, such operating costs might become prohibitive.

In the light of what is above, several advantages might derive from the exploitation of costless flue gases as carbon source for growing microalgae and producing biofuels. More

specifically, reduction of green house gas (GHG) emission, the increase of biomass and lipid productivity, as well as the reduction of operating costs are the main advantages which potentially derive from the use of flue gas as carbon source. Moreover, high concentration of CO_2 in the flue gas increases its mass transfer from the gas phase to the medium, being the last one a limiting step of CO_2 fixation by microalgae. For these reasons, the potential exploitation of microalgae for the CO_2 capture from flue gases and the subsequent production of liquid biofuels is currently the subject of a continuously growing number of studies reported in literature. Most of these works shows that using simulated flue gases (15 %v/v of CO_2) has a positive effect towards carbon fixation rate and biomass productivity (Sydney et al. 2010; Ho et al. 2010; Tang et al. 2011; Lam et al. 2012). In particular, growth rate of microalgae has been improved due to the feeding of gases having a concentration of CO_2 (1–15 %) higher than the typical one of atmospheric air (0.04 % CO_2) thus leading to a higher biomass productivity as well as shorter cultivation time (Lam et al. 2012). Moreover, it is noteworthy that, under specific cultivating conditions, the feeding of CO_2 concentrations of 10–15 %v/v led also to the increase of the lipid content of microalgal cells even if such increment was limited to 1–6 % wt/wt (Tang et al. 2011). Finally, it is found that the increase of CO_2 concentration in the gas fed to microalgae can provoke the accumulation of polyunsaturated fatty acids which are a viable form of lipids since they can reduce the pour point of the resulting biodiesel (Tang et al. 2011). Table 7 shows the CO_2 tolerances and removal rates as well as the corresponding biomass productivities observed for several microalgal strains cultivated under different operating conditions. These values can be used to estimate the volume needed for the photobioreactor implementation for CO_2 fixation.

The comparison of the performance of microalgal strains shown in Table 7 is difficult because of the different operating conditions adopted in each experiment. In fact, besides the intrinsic properties of the specific strain, the CO_2 removal rate is affected by several operating parameters such as photobioreactors typology, gas flow rate, illumination, cell density, growth rate, etc. However, from the data shown in Table 7 it can be observed that, under specific operating conditions and by using specific strains, high CO_2 removal rates can be achieved with microalgae. Moreover, it has been shown that CO_2 concentration in the feed gas up to 50 %v/v can be tolerated by specific microalgal strains.

On the other hand, it is worth noting that all the data shown in Table 7 refer to experiments carried out at the laboratory scale, while, to the best of our knowledge, no data are available about the performance of microalgae in removing CO_2 at the industrial scale. Furthermore, all the experiments of Table 7 have been carried out by using CO_2-enriched gases obtained by mixing in suitable amounts pure CO_2 and air or nitrogen, while only rarely real flue gases have been used. For this reason, the information reported in the literature about the possibility of exploiting flue gases for growing microalgae and producing biofuels are not completely established. In fact, flue gases, besides CO_2, N_2, and O_2, can contain high concentrations of several compounds which may be highly toxic for microalgae.

4.2.1 Potential Limitations to the Use of Microalgae for Capturing CO_2 from Real Flue Gases

As argued above, flue gases are the only viable way of supplying the CO_2 that is needed for the production of large amounts microalgal biomass. On the other hand, the direct use of raw flue gases can be limited by different factors. In fact, even if treated before discharge, flue gases typically contain several compounds which can be toxic to microalgae even at low concentrations. Specifically, as shown in Table 8, besides CO_2, H_2O, O_2, and N_2, flue gas can contain a number of compounds such as nitrogen oxides (NO_x), sulfur oxides (SO_x), unburned carbohydrates (C_xH_y), CO, heavy metals, halogen acids, and particulate matter (PM) (Van Den Hende et al. 2011).

As mentioned above, while some of such compounds can be highly toxic to microalgae, other compounds can affect microalgae cultivation in different ways. Specifically, due to its high volumetric concentrations, N_2 lowers the concentration of CO_2 in flue gas, thus leading to a decreased CO_2 mass transfer towards the liquid medium. Oxygen is necessary for photorespiration of microalgae but when is present at high concentrations and under high illumination intensities may form toxic radicals which can damage cell membranes (Pulz 2001). Moreover, high concentrations of oxygen may inhibit CO_2 uptake by competing for Rubisco in the Calvin cycle (Richmond 2008). NOx and SOx can be toxic for specific strains of microalgae (Radmann and Costa 2008; Baker et al. 1983). Moreover, SOx can lower culture pH thus affecting microalgae growth (Yang et al. 2004). High concentrations of heavy metals have been found to be toxic for microalgae. Furthermore, relatively high concentrations of chlorine compounds have been found to induce cellular damage in Chlorella salina (Ebenezer et al. 2012). As far as the other compounds are concerned, less is known about their interactions with microalgae, but it might be guessed, for example, that particulate matter, in large quantities, might lower light penetration as a result of the increased turbidity of growth medium. Ultimately, depending on the chemical composition of the specific flue gas considered, several negative phenomena might be provoked on microalgae growth by its use as carbon source. In this regard, it is worth noting that industrial flue gases can show a very wide range of chemical compositions depending on the specific industrial process by which they are produced.

Table 7 Biomass productivity, CO_2 tolerance, and removal rate of different microalgal strains

Species	CO_2 conc. tolerance (%v)	CO_2 removal rate ($g_{CO2}\ L^{-1}\ day^{-1}$)	Biomass productivity ($mg\ L^{-1}\ day^{-1}$)	Reference
Anabaena sp.	10	1.010	–	Chiang et al. (2011)
Anabaena sp.	0.03	1.450	–	Gonzalez Lopez et al. (2009)
Aphanothece microscopic N.	15	40.333	0.754	Francisco et al. (2010)
Aphanothece microscopic N.	15	1.430	0.77	Jacob-Lopes et al. (2010)
Aphanothece microscopic N.	15	0.550	0.301	Jacob-Lopes et al. (2010)
Aphanothece microscopic N.	15	0.513	–	Jacob-Lopes et al. (2010)
Aphanothece microscopic N.	15	16.793	–	Jacob-Lopes et al. (2010)
Botryococcus braunii	10	0.500	–	Sydney et al. (2010)
Botryococcus braunii	10	–	–	Yoo et al. (2010)
Chlorella	15	0.460	–	Jin et al. (2006)
Chlorella	10	–	–	Yue and Chen (2005)
Chlorella pyrenoidosa	0.03	0.136	0.065	Tang et al. (2011)
Chlorella pyrenoidosa	5	0.246	0.133	Tang et al. (2011)
Chlorella pyrenoidosa	10	0.260	0.144	Tang et al. (2011)
Chlorella pyrenoidosa	30	0.150	0.075	Tang et al. (2011)
Chlorella pyrenoidosa	50	0.106	0.054	Tang et al. (2011)
Chlorella pyrenoidosa	20	0.224	0.121	Tang et al. (2011)
Chlorella sp.	5	35 %	–	Chiu et al. (2009)
Chlorella sp.	5	24 %	–	Chiu et al. (2009)
Chlorella sp.	15	–	–	Lee et al. (2002)
Chlorella sp.	5	0.700	–	Ryu et al. (2009)
Chlorella sp.	5	0.704	0.336	Ryu et al. (2009)
Chlorella sp.	2	0.517	0.295	Ryu et al. (2009)
Chlorella sp.	5	0.583	0.335	Ryu et al. (2009)
Chlorella sp.	–	1.380	–	Zhao et al. (2011)
Chlorella sp. (marine)	10	13.970	0.458	Chiu et al. (2008)
Chlorella sp. (marine)	2	7.847	0.528	Chiu et al. (2008)
Chlorella sp. (marine)	15	17.197	0.369	Chiu et al. (2008)
Chlorella sp. (marine)	5	9.497	0.491	Chiu et al. (2008)
Chlorella sp. KR-1	15	–	0.78	Lee et al. (2002)
Chlorella sp. KR-1	15	–	1.24	Lee et al. (2002)
Chlorella sp. KR-1	15	–	0.71	Lee et al. (2002)
Chlorella sp. KR-1	15	–	–	Lee et al. (2002)
Chlorella sp. P12	6–8	6.56	3.8	Doucha et al. (2005)
Chlorella sp. T-1	13	–	–	Maeda et al. (1995)
Chlorella sp. T-1	15	–	–	Maeda et al. (1995)
Chlorella sp. T-1	15	–	–	Maeda et al. (1995)
Chlorella sp. T-1	15	–	–	Maeda et al. (1995)
Chlorella vulgaris	1	6.23	–	Cheng et al. (2006)
Chlorella vulgaris	1	0.28	–	Fan et al. (2007)
Chlorella vulgaris	1	0.14	–	Fan et al. (2007)
Chlorella vulgaris	1	0.14	–	Fan et al. (2007)
Chlorella vulgaris	1	0.04	–	Fan et al. (2007)
Chlorella vulgaris	0.093	3.55	–	Fan et al. (2008)
Chlorella vulgaris	15	25.67	0.482	Francisco et al. (2010)
Chlorella vulgaris	15	0.48	1.85	Jin et al. (2006)
Chlorella vulgaris	12		–	Radmann and (Costa 2008)
Chlorella vulgaris	2	0.430		Yeh and Chang (2011)
Chlorella vulgaris	5	0.249	0.81	Sydney et al. (2010)
Chlorococcum littorale	20	0.902	0.53	Kurano et al. (1995)

(continued)

Table 7 (continued)

Species	CO_2 conc. tolerance (%v)	CO_2 removal rate ($g_{CO2}\ L^{-1}\ day^{-1}$)	Biomass productivity ($mg\ L^{-1}\ day^{-1}$)	Reference
Cyanidioschyzon merolae	2–6.5	–	–	Kurano et al. (1995)
Cyanidium caldarium	2–6.5	–	–	Kurano et al. (1995)
Dunaliella tertiolecta	15	21.340	0.367	Francisco et al. (2010)
Dunaliella tertiolecta	15	–	–	Nagase et al. (1997)
Dunaliella tertiolecta	15	–	–	Nagase et al. (1997)
Dunaliella tertiolecta	15	–	–	Nagase et al. (1997)
Dunaliella tertiolecta	15	–	–	Nagase et al. (1997)
Dunaliella tertiolecta	15	–	–	Nagase et al. (1997)
Dunaliella tertiolecta	5	0.271	0.65	Sydney et al. (2010)
Euglena gracilis	11	–	0.114	Chae et al. (2006)
Galdieria partita	2–6.5	–	–	Kurano et al. (1995)
Haematococcus pluvialis	0.03	0.143	76	Huntley and Redalje (2007)
Microalgal bacterial flocs	12	0.363	0.181	Van Den Hende et al. (2011)
Microcystis aeruginosa	15	0.491	1.9	Jin et al. (2006)
Monoraphidium minutum	13.6	90.00 %	1	Brown (1996)
Microcystis ichthyoblabe	15	0.521	2.14	Jin et al. (2006)
Nannochloropsis oculata	2	–	–	Su et al. (2011)
Nannochloropsis sp.	15	–	–	Jiang et al. (2011)
Phaeodactylum tricornutum	15	2.163	0.007	Francisco et al. (2010)
Phormidium sp.	15	27.097	0.415	Francisco et al. (2010)
Scenedesmus	15	0.610	–	Jin et al. (2006)
Scenedesmus obliquus	15	16.867	0.655	Francisco et al. (2010)
Scenedesmus obliquus	20	0.390	–	Ho et al. (2010)
Scenedesmus obliquus	10	0.550	–	Ho et al. (2010)
Scenedesmus obliquus	20	61.80 %	–	Li et al. (2011)
Scenedesmus obliquus	20	–	–	Li et al. (2011)
Scenedesmus obliquus	12	–	–	Radmann and Costa (2008)
Scenedesmus obliquus	0.03	0.150	0.083	Tang et al. (2011)
Scenedesmus obliquus	5	0.286	0.158	Tang et al. (2011)
Scenedesmus obliquus	10	0.290	0.155	Tang et al. (2011)
Scenedesmus obliquus	20	0.246	0.134	Tang et al. (2011)
Scenedesmus obliquus	30	0.150	0.081	Tang et al. (2011)
Scenedesmus obliquus	50	0.106	0.056	Tang et al. (2011)
Scenedesmus obliquus	20	–	–	Li et al. (2011)
Scenedesmus obliquus	18	–	–	Li et al. (2011)
Scenedesmus obliquus	12	–	–	Li et al. (2011)
Scenedesmus obliquus	18	–	–	Li et al. (2011)
Scenedesmus sp.	15	0.612	2.01	Jin et al. (2006)
Scenedesmus sp.	15	–	0.35	Santiago et al. (2010)
Scenedesmus sp.	20	–	–	Westerhoff et al. (2010)
Scenedesmus sp.	10	–	–	Yoo et al. (2010)
Spirulina platensis	15	0.920	–	Kumar et al. (2010)
Spirulina platensis	10	0.320	–	Sydney et al. (2010)
Spirulina platensis	5	0.319	0.44	Sydney et al. (2010)
Spirulina sp.	12	–	–	Radmann and Costa (2008)
Synechococcus nidulans	12	–	–	Radmann and Costa (2008)
Synechococcus sp.	0.55	4.440	–	Takano et al. (1992)
Synechocystis sp.	–	2.070	–	Martinez et al. (2011)

Table 8 Range of concentrations of compounds found in different treated flue gases

Compound	Unit	Concentration in flue gas	
		Min	Max
N_2	%	72	77
CO_2	%	3	16
H_2O	%	9	14
O_2	%	1	15
NO	mg Nm^{-3}	50	1,500
NO_2	mg Nm^{-3}	2	75
SO_2	mg Nm^{-3}	0	1,400
SO_3	mg Nm^{-3}	0	32
CO	mg Nm^{-3}	2.5	11,250
C_xH_y	%	0.008	0.4
Heavy metals	mg Nm^{-3}	0	2.2
Chlorine and its compounds	mg Nm^{-3}	0	1,400
Fluorine and its compounds	mg Nm^{-3}	0.5	5
Particulate matter	mg Nm^{-3}	120	15,000

Adapted from Van Den Hende et al. (2011)

For this reason, the possibility of using microalgae for the CO_2 capture from flue gases should be preceded by a detailed analysis of their chemical composition.

Further limitations to the direct use of flue gas as carbon source for microalgae are those related to the high gas flow rates to be sent to the photobioreactors. In fact, once the residence time is fixed by algal growth metabolism, high flow rates result in large volume of the photobioreactors. This aspect, in turn, might result in high footprints of the plant for capturing CO_2 and producing biofuels. Moreover, according to Fernandez et al. (2012), if flue gas is directly injected into the photobioreactors, most of the CO_2 is released into the atmosphere. Furthermore, the flue gas should be injected in the liquid medium by means of suitable diffusers which are able to supply the gas in form of thin bubbles in order to maximize the mass transfer of CO_2. However, the presence of high concentrations of particulate matter in the flue gas can provoke clogging of the diffusers and consequent difficulties in providing CO_2 to the culture. For all the above reasons, new processes allowing for CO_2 capture and concentration from flue gases before transferring it to microalgal culture should be developed.

5 Microalgae Growth with Pure CO_2 (100 %v/v) Obtained from Flue Gases

5.1 Rationale Behind the Use of Pure CO_2 from Flue Gases

Since flue gases contain several compounds which may be toxic for microalgae growth, a suitable processing step should be implemented with the aim of removing such compounds from flue gas before injecting it into the microalgal culture. Moreover, in order to reduce the gas flow rates to be fed to the photobioreactors, the above preliminary step should be also able to separate the main components of flue gas such as N_2, O_2, and H_2O from CO_2 which could be concentrated up to values close to 100 %v/v in the resulting gas. In fact, by assuming that CO_2 concentration is about 12 %v/v in the raw flue gas, its separation from the other compounds can result in a net reduction of 88 % of the volumes of gas to be fed in the reactors. This way the photobioreactor volumes could be dramatically reduced. Moreover, the higher is the CO_2 concentration in the gas phase, the faster and the more effective is its mass transfer towards the liquid medium. Since CO_2 mass transfer is one of the main limiting steps of CO_2 fixation by microalgae, the use of pure CO_2 could greatly improve the whole process yield. For similar reasons, the use of high concentrated CO_2 gases enhances O_2 stripping from the liquid phase where it is accumulated as a result of algal photosynthesis. Thus, since photosynthetic oxygen can inhibit microalgae growth, its effective removal might lead to higher growth rates and biomass productivities. Moreover, it should be noted that CO_2 mass transfer rate could be further enhanced by supplying it in the form of microbubbles with sizes 10–50 μm through suitable membrane spargers which could not be used with raw flue gas because of its high content of particulate matter which can lead to membrane's clogging (Lam et al. 2012). Ultimately, the separation of CO_2 from other compounds of the flue gas could potentially lead to a great increase of the whole process efficiency.

As stated above, the CO_2 capture and concentration from a flue gas may be accomplished by different methods such as absorption, adsorption, cryogenics, and membrane-based techniques. Among these techniques, the most consolidated one at the industrial scale as well as the most energy efficient and cheaper one is the chemical absorption (Farrelly et al. 2013). A typical scheme for CO_2 capture through chemical absorption–desorption is shown in Fig. 21.

The most preferred solvent for chemical absorption of CO_2 from flue gas is amines such as monoethanolamine (MEA). As it can be seen from, after the solvent has reached its maximum absorption capacity, it is sent to the desorption section where it is heated to 100–150 °C to release almost pure CO_2. Since the flue gas at the outlet from the chimney has a temperature of about 100 °C, its enthalpy can be suitably exploited for desorbing CO_2 from the solvent.

Ultimately, a stream of pure CO_2 can be easily produced for flue gas through this simple process. The CO_2 produced can be thus sent to photobioreactors. A suitable amount of CO_2 separated might be also used for extracting lipids from microalgae through supercritical fluid extraction methods (Fig. 17). This way the high costs and hazards related to the use of organic solvents for extracting lipids form microalgae could be avoided.

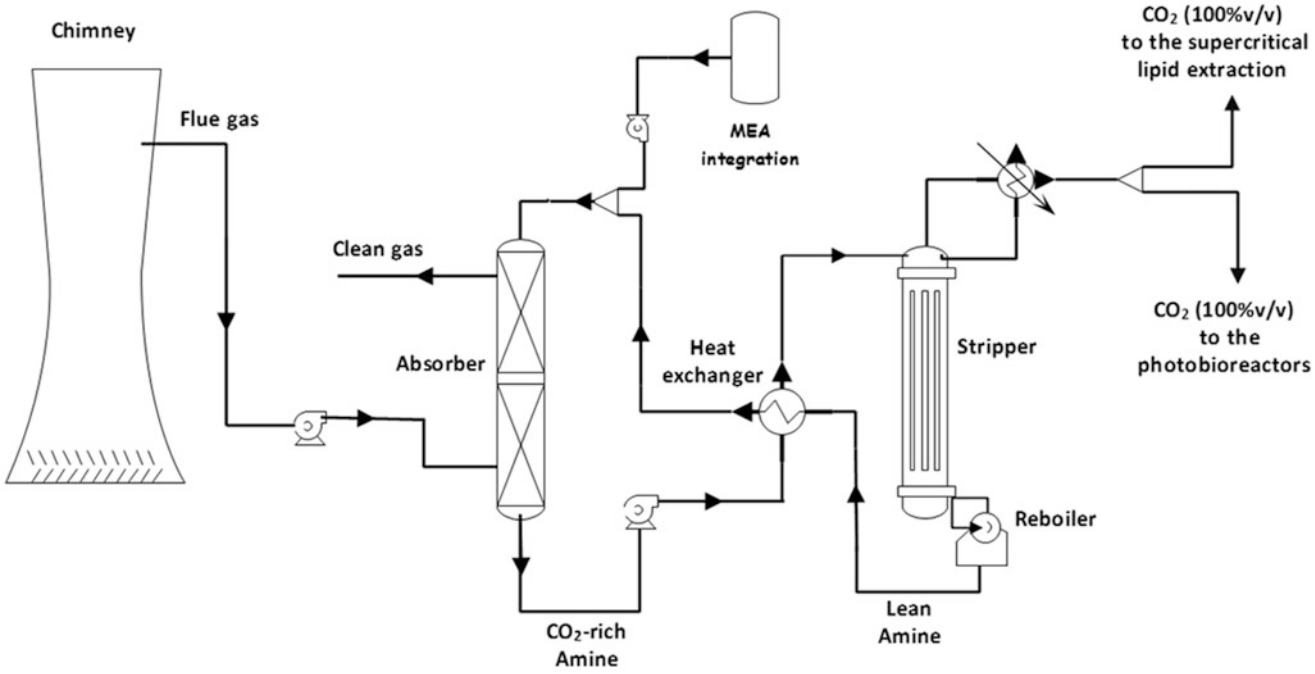

Fig. 21 Typical scheme for the CO_2 capture and concentration through absorption with MEA

5.2 Recent Experimental and Modeling Results When Using Pure CO_2

Despite the significant improvements of the microalgal technology potentially deriving from the use of pure CO_2 separated from flue gases, very few experimental studies have been carried out along these lines. This is mainly due to the fact that high loadings of CO_2 are well known to drastically lower the pH of the growth medium thus provoking inhibitory effects on microalgae growth. Moreover, when microalgae strains acclimated to low CO_2 concentrations are suddenly exposed to high concentrations of CO_2, the efficiency of photosystem might be reduced (Van Den Hende et al. 2011). In fact, the few experiments carried out using pure CO_2 as carbon source showed that under such conditions, microalgae growth is strongly inhibited (Goldman and Graham 1981).

However, a recent work has demonstrated that specific strains of microalgae are capable to adapt to high levels of CO_2 if previously exposed to high dissolved CO_2 for prolonged times (Baba and Shiraiwa 2012). This behavior is probably due to the fact that the prolonged exposition to high CO_2 concentrations may prompt the expression of specific genes that may generate changes in the carbon capture mechanism (CCM) of several strains of microalgae as well as of their structural anatomy and in the redistribution of certain cellular organelles (Baba and Shiraiwa 2012). Thus, high CO_2 tolerant strains of microalgae can be created by acclimating them to high CO_2 concentrations for very long times. Moreover, the low pH of the medium can be suitably buffered by properly designing the growth medium as well as by optimizing specific operating parameters such as gas flow rate, CO_2 bubble size, and illumination. The optimization of design and operating parameters may be accomplished by exploiting suitable process engineering techniques. To this aim, mathematical models that are capable to quantitatively describe the influence of the crucial operating parameters (i.e., photobioreactor geometry, heat and mass transfer conditions, growth medium composition, pH, etc.) on microalgae growth and lipid accumulation are needed. However, in spite of the large number of mathematical models available in the literature (Cornet et al. 1995; Sevilla and Grima 1997; Acien Fernandez et al. 1999; Rubio et al. 1999; Grima Molina et al. 2001; Berenguel et al. 2004; Pruvost et al. 2008; Concas et al. 2010), to the best of our knowledge, very few of them were able to quantitatively describe the evolution of pH during photosynthetic growth of microalgae (Rubio et al. 1999). Moreover, such models were typically characterized by the questionable assumption of steady state conditions and inorganic carbon species as the sole ones able to affect the solution pH (Rubio et al. 1999), while the effect of other ionic species in solution was neglected. Nevertheless, the quantitative description of pH evolution during microalgal growth is crucial since it can influence photosynthetic phenomena as already discussed in Sect. 2.3. Therefore, the quantitative description of pH evolution in microalgal cultures seems to be a key goal in order to properly control and optimize microalgae

photobioreactors. In particular, this aspect is of crucial importance when high CO_2 concentrated gases are used as carbon source. In fact, in this case the medium pH can reach very low values that might inhibit microalgae growth. On the other hand, the potential exploitation of costless feedstocks such as flue gases as source of CO_2 is one of the main targets of scientists and technicians operating in this field for the reasons previously discussed. Thus, the correct evaluation of the effect of pH is critical also for assuring the possibility of exploiting/capturing CO_2 from flue gases through microalgae. For the abovementioned reasons, microalgae strains capable to survive under elevated CO_2 concentration might represent a suitable candidate for the industrial cultivation of microalgae for biofuel production and CO_2 capture. Among such strains the unicellular eukaryotic green alga *Chlorella vulgaris* is characterized by high growth rates (Radakovits et al. 2012), coupled with a significant lipid content. Moreover, according to Baba and Shiraiwa (2012), *C. vulgaris* is one among those strains which is capable of developing suitable molecular mechanisms that allows its adaptation to extremely high CO_2 concentrations. For all these reasons *C. vulgaris* is potentially one of the more useful strains for biofuel production and CO_2 capturing from flue gases. Along these lines, a recent work by Concas et al. (2012) proposed a novel mathematical model of the growth of *Chlorella vulgaris* in semi-batch photobioreactors fed with pure CO_2 (100 %v/v). In particular, the proposed model was capable of simulating temporal evolution of cells, light intensity, and nutrient concentration within the growth medium as well as carbon dioxide and oxygen concentration in the liquid and gas phase. Moreover, by taking advantage of comprehensive kinetics and considering the ion speciation phenomena taking place, the model was able to quantitatively describe the dynamics of pH evolution and its effect on microalgae growth. The adjustable parameters of the proposed model were fitted against experimental data obtained when starting from a specific set of initial concentration of nutrients in the growth medium. Then, the reliability of the mathematical model was successfully tested through the prediction of the temporal evolution of microalgae concentration and pH when using different initial concentrations of nutrients. Moreover, experimental results obtained by Concas et al. (2012) have confirmed that *C. vulgaris* strain is capable to adapt to high levels of CO_2, probably by changing the carbon uptake mechanisms. From the kinetics point of view, such aspect may cause the variation of the relevant values of the half saturation constant and the biomass yield related to carbon species with respect to the typical ones obtained for *C. vulgaris* cultured under atmospheric CO_2. Ultimately, both experimental and modeling investigation carried out by Concas et al. (2012) confirmed the possibility of cultivating microalgae with pure CO_2, which, as mentioned above, represents a possible strategy for improving the CO_2 capture from flue gas. Finally, the model proposed by Concas et al. (2012) might represent a useful tool to develop suitable control and optimization strategies to improve microalgal cultures fed by pure CO_2 obtained from flue gas.

6 Concluding Remarks

The production of biofuels from renewable feedstocks is recognized to be critical to fulfill a sustainable economy and face global climate changes. When compared to first- and second-generation biofuel feedstocks, microalgae are characterized by higher growth rates and lipid content which result in larger bio-oil productivities. Moreover, cultivation of microalgae can be carried out in less- and lower-quality lands, thus avoiding the exploitation of arable ones. In addition, cultivation of microalgae might be coupled with the direct bio-capture of CO_2 emitted by industrial activities that use fossil fuels for energy generation. Ultimately, when compared to first- and second-generation biofuels, microalgae are characterized by a greater environmental sustainability and economic viability. For these reasons, the potential exploitation of microalgae as renewable resource for the production of liquid biofuels is receiving a rising interest mostly driven by the global concerns related to the depletion of fossil fuel supplies and the increase of CO_2 levels in the atmosphere. The high potential of algae-based biofuels is confirmed by the number of recent papers available in the literature on the subject. In spite of such interest, the existing microalgae-based technology for CO_2 sequestration and biofuel production is still not widespread since it is affected by economic and technical constraints that might limit the development of industrial scale production systems. In particular, the main obstacles are related to the extensive land areas needed as well as the estimated high costs of the operating phases of microalgae cultivation, harvesting, and lipid extraction. Therefore, in view of industrial scaling-up, the current technology should be optimized in terms of selected algal strains as well as design/operating parameters. The latter target may be accomplished by exploiting suitable process engineering techniques. Along these lines significant efforts are currently in progress around the world. In the light of what is above, this chapter has been aimed to present the recent achievements related to the engineering aspects connected with the use of microalgae for biofuel production and CO_2 capture from flue gases. It has been shown that cultivation of microalgae can be performed in closed ones, i.e., photobioreactors, or in open systems. The first ones can be bubble columns,

airlift, flat panel, and horizontal tubular photobioreactors. While photobioreactors are characterized by high biomass productivity, a better process control and lower contamination risks, if used for producing low value products, such as biofuels, they have still not attained economic levels of production. Significant efforts are currently being performed to decrease the operating and capital costs linked to the construction and the operation of photobioreactors for producing biofuels. The major achievements in this direction are those related to the use of very low-cost materials for the construction of photobioreactors, the use of flue gases and wastewaters as source of macronutrients, and finally the use of engineered algae that are characterized by extremely high oil productivity, thus allowing the compensation of high operating costs with potentially large incomes. Also, the valorization of microalgal compounds separated by lipids, such as chlorophylls, pigments, and proteins, might improve the economical sustainability of photobioreactors-based processes. On the other hand, open raceways, which are less expensive, show several drawbacks such as low oil productivity, high risks of contamination, high losses of water due to evaporation, scarce process control, and high susceptibility to different weather conditions. To overcome limitations related to open system and in the meantime keeping their low operating cost, the potential use of closed raceway ponds is currently under study. These systems essentially consist of an open pond covered by a transparent or translucent barrier which turns it into a greenhouse. This configuration prevents the microalgae to be contaminated by competing bacteria and allows a better control of crucial operating parameters such as temperature, evaporation, etc.

Another bottleneck of the process is related to the harvesting step of microalgae. Essentially, harvesting can be performed by centrifugation, filtration, flotation, and flocculation. It is worth noting that harvesting alone can be the most expensive step of the overall process of microalgae production. Therefore, in order to assure the economic sustainability of the process, efficient and inexpensive harvesting methods should be developed and subsequently adopted at the industrial scale. In this regard, the most promising processes for microalgae harvesting are those ones which combine different technologies such as microfiltration followed by centrifugation or pH-induced flocculation sedimentation and dynamic microfiltration. Also, auto-flocculation and bio-flocculation are promising techniques. However, they are still in the embryonic phase, and their potential use at the industrial scale for harvesting large amounts of microalgae still needs to be investigated.

Since biomass drying after harvesting and before the lipid extraction is very expensive, the direct extraction from wet biomass seems to be the only economically feasible way to recover lipids from microalgae. Therefore, the downstream process of cell disruption represents an essential pretreatment when lipid extraction is carried out directly from wet biomass. Among the techniques which can be realistically applied at the industrial scale, the most efficient ones for cell disruption are high-pressure homogenization, bead beating, and sulfuric acid treatment.

Lipid extraction is typically carried out by contacting microalgal biomass with an eluting solvent which extracts triacylglycerides and fatty acids out of the cells. The most suitable solvents for extracting lipids from microalgae are the organic ones and supercritical carbon dioxide ($SCCO_2$). The main limitation related to the use of organic solvents is their high cost and the need of their continuous supply since not all of them can be suitably recycled. Moreover, the toxicity of organic solvents arises environmental and safety concerns. On the other hand, the extraction technique based on the use of $SCCO_2$ is a very promising method for extracting lipids from microalgae since it can assure high extraction yields in relatively short times. Moreover, no concerns related to solvent toxicity can arise. Unfortunately, the main limitations of this method are the high energy consumption related to the operating phases of CO_2 heating and compression as well as the potentially high costs of investment.

Finally, in this chapter a possible novel method for the CO_2 capture from flue gases through microalgae is proposed. The method consists in the concentration of CO_2 up to 100 % v/v before feeding it to the photobioreactors. This way, specific compounds of flue gas which could be toxic for microalgae can be removed and the photobioreactor volumes could be dramatically reduced. Moreover, the higher is the CO_2 concentration in the gas phase, the faster and the more effective is its mass transfer towards the liquid medium. Based on these considerations, a recent work by Concas et al. (2012) confirmed the possibility of cultivating microalgae with pure CO_2 streams, which, as mentioned above, represents a possible strategy for improving the CO_2 capture from flue gas. The strategy is based on triggering of physiological changes in microalgae by exposing them to high CO_2 concentrations for prolonged times. Such changes allow microalgae to grow under the acidic conditions provoked by CO_2 concentration level adopted. Finally, the model proposed by Concas et al. (2012) might represent a useful tool to develop suitable control and optimization strategies to improve microalgal cultures fed with pure CO_2 obtained from flue gas by taking advantage of standard technologies.

References

Abu-Rezq, T.S., Al-Musallam, L., Al-Shimmari, J., Dias, P.: Optimum production conditions for different high-quality marine algae. Hydrobiologia **403**, 97–107 (1999)

Acien Fernandez, F., Garcia Camacho, F., Chisti, Y.: Photobioreactors: light regime, mass transfer, and scaleup. Prog. Ind. Microbiol. **35**, 231–247 (1999)

Ahmad, A., Yasin, N., Derek, C., Lim, J.: Microalgae as a sustainable energy source for biodiesel production: a review. Renew. Sustain. Energy Rev. **15**(1), 584–593 (2011)

Alabi, A.O., Bibeau, E., Tampier, M., Council, B.C.I.: Microalgae Technologies and Processes for Biofuels-Bioenergy Production in British Columbia: Current Technology, Suitability and Barriers to Implementation: Final Report. British Columbia Innovation Council, Vancouver (2009)

Amin, S.: Review on biofuel oil and gas production processes from microalgae. Energ. Convers. Manage. **50**(7), 1834–1840 (2009)

Andrich, G., Nesti, U., Venturi, F., Zinnai, A., Fiorentini, R.: Supercritical fluid extraction of bioactive lipids from the microalga Nannochloropsis sp. Eur. J. Lipid Sci. Tech. **107**(6), 381–386 (2005)

Baba, M., Shiraiwa, Y.: High-CO_2 response mechanisms in microalgae. In: Advances in Photosynthesis-Fundamental Aspects, pp. 12–435. In Tech, New York (2012)

Baker, M., Mayfield, C., Inniss, W., Wong, P.: Toxicity of pH, heavy metals and bisulfite to a freshwater green alga. Chemosphere **12**(1), 35–44 (1983)

Berenguel, M., Rodriguez, F., Acien, F., Garcia, J.: Model predictive control of pH in tubular photobioreactors. J. Process Contr. **14**(4), 377–387 (2004)

Brennan, L., Owende, P.: Biofuels from microalgae: a review of technologies for production, processing, and extractions of biofuels and co-products. Renew. Sustain. Energy Rev. **14**(2), 557–577 (2010)

Brown, L.M.: Uptake of carbon dioxide from flue gas by microalgae. Energ. Convers. Manage. **37**(6), 1363–1367 (1996)

Cao, G., Concas, A.: Process for bio-oil production involving the use of CO2. Patent 2371940 (2011)

Cappa, F., Rutqvist, J.: Impact of CO_2 geological sequestration on the nucleation of earthquakes. Geophys. Res. Lett. **38**(17) (2011). http://dx.doi.org/DOI:10.1029/2011GL048487

Carriquiry, M.A., Du, X., Timilsina, G.R.: Second generation biofuels: economics and policies. Energy Policy **39**(7), 4222–4234 (2011)

Carter, N.A.: Environmental and economic assessment of microalgae-derived jet fuel. Ph.D. dissertation, Massachusetts Institute of Technology (2012)

Chae, S., Hwang, E., Shin, H.: Single cell protein production of *Euglena gracilis* and carbon dioxide fixation in an innovative photo-bioreactor. Bioresour. Technol. **97**(2), 322–329 (2006)

Chen, C., Durbin, E.G.: Effects of pH on the growth and carbon uptake of marine phytoplankton. Mar. Ecol. Prog. Ser. **109**, 83–94 (1994)

Chen, C.-Y., Yeh, K.-L., Aisyah, R., Lee, D.-J., Chang, J.-S.: Cultivation, photobioreactor design and harvesting of microalgae for biodiesel production: a critical review. Bioresour. Technol. **102** (1), 71–81 (2011). Special Issue: Biofuels - II: Algal Biofuels and Microbial Fuel Cells

Cheng, J.J., Timilsina, G.R.: Status and barriers of advanced biofuel technologies: a review. Renew. Energy **36**(12), 3541–3549 (2011)

Cheng, L., Zhang, L., Chen, H., Gao, C.: Carbon dioxide removal from air by microalgae cultured in a membrane-photobioreactor. Sep. Purif. Technol. **50**(3), 324–329 (2006)

Cheng, Y., Zhou, W., Gao, C., Lan, K., Gao, Y., Wu, Q.: Biodiesel production from Jerusalem artichoke (Helianthus Tuberosus L.) tuber by heterotrophic microalgae Chlorella protothecoides. J. Chem. Technol. Biotechnol. **84**(5), 777–781 (2009)

Cheung, P.C.: Temperature and pressure effects on supercritical carbon dioxide extraction of n-3 fatty acids from red seaweed. Food Chem. **65**(3), 399–403 (1999)

Chiang, C.-L., Lee, C.-M., Chen, P.-C.: Utilization of the cyanobacteria *Anabaena sp*. CH1 in biological carbon dioxide mitigation processes. Bioresour. Technol. **102**(9), 5400–5405 (2011)

Chisti, Y.: Biodiesel from microalgae. Biotechnol. Adv. **25**(3), 294–306 (2007)

Chisti, Y.: Biodiesel from microalgae beats bioethanol. Trends Biotechnol. **26**(3), 126–131 (2008)

Chiu, S.-Y., Kao, C.-Y., Chen, C.-H., Kuan, T.-C., Ong, S.-C., Lin, C.-S.: Reduction of CO_2 by a high-density culture of Chlorella sp in a semicontinuous photobioreactor. Bioresour. Technol. **99**(9), 3389–3396 (2008)

Chiu, S.-Y., Tsai, M.-T., Kao, C.-Y., Ong, S.-C., Lin, C.-S.: The air-lift photobioreactors with flow patterning for high-density cultures of microalgae and carbon dioxide removal. Eng. Life Sci. **9**(3), 254–260 (2009)

Christenson, L., Sims, R.: Production and harvesting of microalgae for wastewater treatment, biofuels, and bioproducts. Biotechnol. Adv. **29**(6), 686–702 (2011)

Concas, A., Pisu, M., Cao, G.: Novel simulation model of the solar collector of BIOCOIL photobioreactors for CO_2 sequestration with microalgae. Chem. Eng. J. **157**(2), 297–303 (2010)

Concas, A., Lutzu, G.A., Pisu, M., Cao, G.: Experimental analysis and novel modeling of semi-batch photobioreactors operated with Chlorella vulgaris and fed with 100%(v/v) CO_2. Chem. Eng. J. **213**, 203–213 (2012)

Concas, A., Lutzu, G.A., Locci, A.M., Cao, G.: Nannochloris eucaryotum growth in batch photobioreactors: kinetic analysis and use of 100% (v/v) CO_2. Adv. Environ. Res. **2**(1), 19–33 (2013)

Concas, A., Steriti, A., Locci, A.M., Cao, G.: Comprehensive modeling and investigation of the effect of iron on the growth rate and lipid accumulation of Chlorella vulgaris cultured in batch photobioreactors. Bioresour. Tehcnol. **153**, 340–350 (2014)

Cornet, J.-F., Dussap, C.G., Gros, J.-B., Binois, C., Lasseur, C.: A simplified monodimensional approach for modeling coupling between radiant light transfer and growth kinetics in photobioreactors. Chem. Eng. Sci. **50**(9), 1489–1500 (1995)

Dayananda, C., Sarada, R., Kumar, V., Ravishankar, G.A.: Isolation and characterization of hydrocarbon producing green alga Botryococcus braunii from Indian freshwater bodies. Electron. J. Biotechnol. **10**(1), 78–91 (2007)

Devi, M.P., Subhash, G.V., Mohan, S.V.: Heterotrophic cultivation of mixed microalgae for lipid accumulation and wastewater treatment during sequential growth and starvation phases: effect of nutrient supplementation. Renew. Energy **43**, 276–283 (2012)

Doucha, J., Straka, F., Livansky, K.: Utilization of flue gas for cultivation of microalgae Chlorella sp.) in an outdoor open thin-layer photobioreactor. J. Appl. Phycol. **17**(5), 403–412 (2005)

Droop, M.: 25 Years of algal growth kinetics. A personal view. Bot. Mar. **26**(3), 99–112 (1983)

Durmaz, Y., Monteiro, M., Bandarra, N., Gökpinar, S., Işik, O.: The effect of low temperature on fatty acid composition and tocopherols of the red microalga, Porphyridium cruentum. J. Appl. Phycol. **19**(3), 223–227 (2007)

Ebenezer, V., Nancharaiah, Y.V., Venugopalan, V.: Chlorination-induced cellular damage and recovery in marine microalga, Chlorella salina. Chemosphere **89**(9), 1042–1047 (2012)

Fajardo, A.R., Cerdan, L.E., Medina, A.R., Fernandez, F.G.A., Moreno, P.A.G., Grima, E.M.: Lipid extraction from the microalga Phaeodactylum tricornutum. Eur. J. Lipid Sci. Tech. **109**(2), 120–126 (2007)

Fan, L.-H., Zhang, Y.-T., Cheng, L.-H., Zhang, L., Tang, D.-S., Chen, H.-L.: Optimization of carbon dioxide fixation by Chlorella vulgaris

cultivated in a membrane-photobioreactor. Chem. Eng. Technol. **30**(8), 109–1099 (2007)
Fan, L.-H., Zhang, Y.-T., Zhang, L., Chen, H.-L.: Evaluation of a membrane-sparged helical tubular photobioreactor for carbon dioxide biofixation by *Chlorella vulgaris*. J. Membr. Sci. **325**(1), 336–345 (2008)
Farrelly, D.J., Everard, C.D., Fagan, C.C., McDonnell, K.P.: Carbon sequestration and the role of biological carbon mitigation: a review. Renew. Sustain. Energy Rev. **21**, 712–727 (2013)
Feng, Y., Li, C., Zhang, D.: Lipid production of *Chlorella vulgaris* cultured in artificial wastewater medium. Bioresour. Technol. **102**(1), 101–105 (2011)
Fernandez, F.G.A., Gonzalez-Lopez, C., Sevilla, J.F., Grima, E.M.: Conversion of CO_2 into biomass by microalgae: how realistic a contribution may it be to significant CO_2 removal? Appl. Microbiol. Biotechnol. **96**(3), 577–586 (2012)
Francisco, E.C., Neves, D.B., Jacob-Lopes, E., Franco, T.T.: Microalgae as feedstock for biodiesel production: carbon dioxide sequestration, lipid production and biofuel quality. J. Chem. Technol. Biotechnol. **85**(3), 395–403 (2010)
Georgianna, D.R., Mayfield, S.P.: Exploiting diversity and synthetic biology for the production of algal biofuels. Nature **488**(7411), 329–335 (2012)
Goldman, J.C., Graham, S.J.: Inorganic carbon limitation and chemical composition of two freshwater green microalgae. Appl. Environ. Microbiol. **41**(1), 60–70 (1981)
Gonzalez Lopez, C., Acien Fernandez, F., Fernandez Sevilla, J., Sanchez Fernandez, J., Ceron Garcia, M., Molina Grima, E.: Utilization of the cyanobacteria *Anabaena sp*. ATCC 33047 in CO_2 removal processes. Bioresour. Technol. **100**(23), 5904–5910 (2009)
Gouveia, L., Marques, A.E., da Silva, T.L., Reis, A.: Neochloris oleoabundans UTEX 1185: a suitable renewable lipid source for biofuel production. J. Ind. Microbiol. Biot. **36**(6), 821–826 (2009)
Greenwell, H.C., Laurens, L.M.L., Shields, R.J., Lovitt, R.W., Flynn, K.J.: Placing microalgae on the biofuels priority list: a review of the technological challenges. J. R. Soc. Interface, **7**(46), 703–726 (2010)
Grima Molina, E., Fernandez, J., Acien, F., Chisti, Y.: Tubular photobioreactor design for algal cultures. J. Biotechnol. **92**(2), 113–131 (2001)
Grima, E.M., Fernandez, F.G.A., Camacho, F.G., Chisti, Y.: Photobioreactors: light regime, mass transfer, and scaleup. J. Biotechnol. **70**(1–3), 231–247 (1999). Biotechnological Aspects of Marine Sponges
Gupta, E.: Oil vulnerability index of oil-importing countries. Energy Policy **36**(3), 1195–1211 (2008)
Halim, R., Gladman, B., Danquah, M.K., Webley, P.A.: Oil extraction from microalgae for biodiesel production. Bioresour. Technol. **102**(1), 178–185 (2011)
Halim, R., Danquah, M.K., Webley, P.A.: Extraction of oil from microalgae for biodiesel production: a review. Biotechnol. Adv. **30**(3), 709–732 (2012)
Ho, S.H., Chen, W.-M., Chang, J.-S.: Scenedesmus obliquus CNW-N as a potential candidate for CO_2 mitigation and biodiesel production. Bioresour. Technol. **101**(22), 8725–8730 (2010)
Hsieh, C.-H., Wu, W.-T.: Cultivation of microalgae for oil production with a cultivation strategy of urea limitation. Bioresour. Technol. **100**(17), 3921–3926 (2009)
Huntley, M.E., Redalje, D.G.: CO_2 mitigation and renewable oil from photosynthetic microbes: a new appraisal. Mitig. Adapt. Strat. Glob. Chang. **12**(4), 573–608 (2007)
Jacob-Lopes, E., Gimenes, C.H., Queiroz, M.I., Franco, T.T.: Biotransformations of carbon dioxide in photobioreactors. Energ. Convers. Manage. **51**(5), 894–900 (2010)
Jalalizadeh, M.: Development of an integrated process model for algae growth in a photobioreactor. Ph.D. dissertation, University of South Florida (2012)
Jiang, L., Luo, S., Fan, X., Yang, Z., Guo, R.: Biomass and lipid production of marine microalgae using municipal wastewater and high concentration of CO 2. Appl. Energ. **88**(10), 3336–3341 (2011)
Jin, H.-F., Lim, B.-R., Lee, K.: Influence of nitrate feeding on carbon dioxide fixation by microalgae. J. Environ. Sci. Heal. A **41**(12), 2813–2824 (2006)
Jones, J., Manning, S., Montoya, M., Keller, K., Poenie, M.: Extraction of algal lipids and their analysis by HPLC and mass spectrometry. J. Am. Oil Chem. Soc. **89**(8), 1371–1381 (2012)
Kim, J., Yoo, G., Lee, H., Lim, J., Kim, K., Kim, C.W., Park, M.S., Yang, J.-W.: Methods of downstream processing for the production of biodiesel from microalgae. Biotechnol. Adv. (2013) http://dx.doi.org/10.1016/j.biotechadv.2013.04.006
Kirrolia, A., Bishnoi, N.R., Singh, R.: Microalgae as a boon for sustainable energy production and its future research \& development aspects. Renew. Sustain. Energy Rev. **20**, 642–656 (2013)
Klok, A.J., Martens, D.E., Wijffels, R.H., Lamers, P.P.: Simultaneous growth and neutral lipid accumulation in microalgae. Bioresour. Technol. **134**, 233–243 (2013)
Kong, Q.-X., Li, L., Martinez, B., Chen, P., Ruan, R.: Culture of microalgae Chlamydomonas reinhardtii in wastewater for biomass feedstock production. Appl. Biochem. Biotechnol. **160**(1), 9–18 (2010)
Krichnavaruk, S., Loataweesup, W., Powtongsook, S., Pavasant, P.: Optimal growth conditions and the cultivation of Chaetoceros calcitrans in airlift photobioreactor. Chem. Eng. J. **105**(3), 91–98 (2005)
Kumar, A., Yuan, X., Sahu, A.K., Dewulf, J., Ergas, S.J., Van Langenhove, H.: A hollow fiber membrane photo-bioreactor for CO2 sequestration from combustion gas coupled with wastewater treatment: a process engineering approach. J. Chem. Technol. Biotechnol. **85**(3), 387–394 (2010)
Kurano, N., Ikemoto, H., Miyashita, H., Hasegawa, T., Hata, H., Miyachi, S.: Fixation and utilization of carbon dioxide by microalgal photosynthesis. Energ. Convers. Manage. **36**(6), 689–692 (1995)
Lam, M.K., Lee, K.T., Mohamed, A.R.: Current status and challenges on microalgae-based carbon capture. Int. J. Greenhouse Gas Contr. **10**, 456–469 (2012)
Lee, S.J., Yoon, B.-D., Oh, H.-M.: Rapid method for the determination of lipid from the green alga Botryococcus braunii. Biotechnol. Techs. **12**(7), 553–556 (1998)
Lee, J.-S., Kim, D.-K., Lee, J.-P., Park, S.-C., Koh, J.-H., Cho, H.-S., Kim, S.-W.: Effects of SO_2 and NO on growth of *Chlorella sp*. KR-1. Bioresour. Technol. **82**(1), 1–4 (2002)
Lee, A.K., Lewis, D.M., Ashman, P.J.: Disruption of microalgal cells for the extraction of lipids for biofuels: processes and specific energy requirements. Biomass Bioenerg. **46**, 89–101 (2012)
Li, G., Xiao, P., Webley, P., Zhang, J., Singh, R., Marshall, M.: Capture of CO_2 from high humidity flue gas by vacuum swing adsorption with zeolite 13X. Adsorption. **14**(2–3), 415–422 (2008a)
Li, Y., Horsman, M., Wang, B., Wu, N., Lan, C.Q.: Effects of nitrogen sources on cell growth and lipid accumulation of green alga Neochloris oleoabundans. Appl. Microbiol. Biotechnol. **81**(4), 629–636 (2008b)
Li, F.-F., Yang, Z.-H., Zeng, R., Yang, G., Chang, X., Yan, J.-B., Hou, Y.-L.: Microalgae capture of CO_2 from actual flue gas discharged from a combustion chamber. Ind. Eng. Chem. Res. **50**(10), 6496–6502 (2011)
Liang, Y., Sarkany, N., Cui, Y.: Biomass and lipid productivities of Chlorella vulgaris under autotrophic, heterotrophic and mixotrophic growth conditions. Biotechnol. Lett. **31**(7), 1043–1049 (2009)
Liu, J., Huang, J., Chen, F.: Microalgae as feedstocks for biodiesel production. In: Stoytcheva M., Montero, G. (eds.) Feedstocks and Processing Technologies, pp. 133–160, 458p. InTech. ISBN 978-953-307-713-0, doi:10.5772/1094 (2007)

Lutzu, G.A.: Analysis of the growth of microalgae in batch and semi-batch photobioreactors. Ph.D. dissertation, Universita'degli Studi di Cagliari (2012)

Lv, Y.X., Yan, G.H., Xu, C.Q., Xu, M., Sun, L.: Review on membrane technologies for carbon dioxide capture from power plant flue gas. Adv. Mater. Res. **602**, 1140–1144 (2013)

Maeda, K., Owada, M., Kimura, N., Omata, K., Karube, I.: CO_2 fixation from the flue gas on coal-fired thermal power plant by microalgae. Energ. Convers. Manage. **36**(6), 717–720 (1995)

Mandalam, R.K., Palsson, B.: Elemental balancing of biomass and medium composition enhances growth capacity in high-density Chlorella vulgaris cultures. Biotechnol. Bioeng. **59**(5), 605–611 (1998)

Martinez, L., Redondas, V., Garcia, A.-I., Moran, A.: Optimization of growth operational conditions for CO2 biofixation by native Synechocystis sp. J. Chem. Technol. Biotechnol. **86**(5), 681–690 (2011)

Mata, T.M., Martins, A.A., Caetano, N.: Microalgae for biodiesel production and other applications: a review. Renew. Sustain. Energy Rev. **14**(1), 217–232 (2010)

Mayo, A.W.: Effects of temperature and pH on the kinetic growth of unialga Chlorella vulgaris cultures containing bacteria. Water Environ. Res. **69**(1), 64–72 (1997)

Mazzoldi, A., Rinaldi, A.P., Borgia, A., Rutqvist, J.: Induced seismicity within geological carbon sequestration projects: maximum earthquake magnitude and leakage potential from undetected faults. Int. J. Greenhouse Gas Contr. **10**, 434–442 (2012)

Mendes, R.L., Nobre, B.P., Cardoso, M.T., Pereira, A.P., Palavra, A.F.: Supercritical carbon dioxide extraction of compounds with pharmaceutical importance from microalgae. Inorg. Chim. Acta **356**, 328–334 (2003)

Mulbry, W., Kondrad, S., Pizarro, C., Kebede-Westhead, E.: Treatment of dairy manure effluent using freshwater algae: algal productivity and recovery of manure nutrients using pilot-scale algal turf scrubbers. Bioresour. Technol. **99**(17), 8137–8142 (2008)

Munoz, R., Guieysse, B.: Algal–bacterial processes for the treatment of hazardous contaminants: a review. Water Res. **40**(15), 2799–2815 (2006)

Nagase, H., Yoshihara, K.-I., Eguchi, K., Yokota, Y., Matsui, R., Hirata, K., Miyamoto, K.: Characteristics of biological removal from flue gas in a Dunaliella tertiolecta culture system. J. Ferment. Bioeng. **83**(5), 461–465 (1997)

Naik, S., Goud, V.V., Rout, P.K., Dalai, A.K.: Production of first and second generation biofuels: a comprehensive review. Renew. Sustain. Energy Rev. **14**(2), 578–597 (2010)

O'Neill, J.: The carbon debate. http://forums.canadiancontent.net/news/83028-carbon-capture-storage.html (2009)

Olguin, E.J.: Phycoremediation: key issues for cost-effective nutrient removal processes. Biotechnol. Adv. **22**(1–2), 81–91 (2003). VI International Symposium on Environmental Biotechnology

Orpez, R., MartInez, M.E., Hodaifa, G., El Yousfi, F., Jbari, N., Sanchez, S.: Growth of the microalga *Botryococcus braunii* in secondarily treated sewage. Desalination **246**(1), 625–630 (2009)

Pires, J., Alvim-Ferraz, M., Martins, F., Simoes, M.: Carbon dioxide capture from flue gases using microalgae: engineering aspects and biorefinery concept. Renew. Sustain. Energy Rev. **16**(5), 3043–3053 (2012)

Pragya, N., Pandey, K.K., Sahoo, P.: A review on harvesting, oil extraction and biofuels production technologies from microalgae. Renew. Sustain. Energy Rev. **24**, 159–171 (2013)

Pruvost, J., Cornet, J.-F., Legrand, J.: Hydrodynamics influence on light conversion in photobioreactors: an energetically consistent analysis. Chem. Eng. Sci. **63**(14), 3679–3694 (2008)

Pulz, O.: Photobioreactors: production systems for phototrophic microorganisms. Appl. Microbiol. Biotechnol. **57**(3), 287–293 (2001)

Quinn, J., de Winter, L., Bradley, T.: Microalgae bulk growth model with application to industrial scale systems. Bioresour. Technol. **102**(8), 5083–5092 (2011)

Radakovits, R., Jinkerson, R.E., Fuerstenberg, S.I., Tae, H., Settlage, R. E., Boore, J.L., Posewitz, M.C.: Draft genome sequence and genetic transformation of the oleaginous alga Nannochloropsis gaditana. Nat. Commun. **3**, 686 (2012)

Radmann, E.M., Costa, J.A.V.: Conteúdo lipídico e composição de ácidos graxos de microalgas expostas aos gases CO_2, SO_2 e NO. Quim. Nova. **31**(7), 1609–1612 (2008)

Rapier, R.: Current and projected costs for biofuels from algae and pyrolysis. http://www.energytrendsinsider.com/2012/05/07/current-and-projected-costs-for-biofuels-from-algae-and-pyrolysis/ (2012). Accessed 10 June 2013

Rawat, I., Ranjith Kumar, R., Mutanda, T., Bux, F.: Dual role of microalgae: phycoremediation of domestic wastewater and biomass production for sustainable biofuels production. Appl. Energ. **88**(10), 3411–3424 (2011)

Rawat, I., Ranjith Kumar, R., Mutanda, T., Bux, F.: Biodiesel from microalgae: a critical evaluation from laboratory to large scale production. Appl. Energ. **103**, 444–467 (2013)

Richmond, A.: Handbook of Microalgal Culture: Biotechnology and Applied Phycology. Wiley-Blackwell, Oxford/Ames (2008)

Rios, S.D., Castaneda, J., Torras, C., Farriol, X., Salvado, J.: Lipid extraction methods from microalgal biomass harvested by two different paths: screening studies toward biodiesel production. Bioresour. Technol. **133**, 378–388 (2013)

Rodolfi, L., Chini Zittelli, G., Bassi, N., Padovani, G., Biondi, N., Bonini, G., Tredici, M.R.: Microalgae for oil: strain selection, induction of lipid synthesis and outdoor mass cultivation in a low-cost photobioreactor. Biotechnol. Bioeng. **102**(1), 100–112 (2009)

Rubio, F.C., Fernandez, F.G.A., Perez, J.A.S., Camacho, F.G., Grima, E.M.: Prediction of dissolved oxygen and carb Stephanopoulos on dioxide concentration profiles in tubular photobioreactors for microalgal culture. Biotechnol. Bioeng. **62**(1), 71–86 (1999)

Ryu, H.J., Oh, K.K., Kim, Y.S.: Optimization of the influential factors for the improvement of CO_2 utilization efficiency and CO_2 mass transfer rate. J. Ind. Eng. Chem. **15**(4), 471–475 (2009)

Sajilata, M., Singhal, R.S., Kamat, M.Y.: Supercritical CO_2 extraction of γ-linolenic acid (GLA) from *Spirulina platensis* ARM 740 using response surface methodology. J. Food Eng. **84**(2), 321–326 (2008)

Sakthivel, R.: Microalgae lipid research, past, present: a critical review for biodiesel production, in the future. J. Exp. Sci. **2**(10), 29–49 (2011)

Santiago, D.E., Jin, H.-F., Lee, K.: The influence of ferrous-complexed EDTA as a solubilization agent and its auto-regeneration on the removal of nitric oxide gas through the culture of green alga *Scenedesmus* sp. Process Biochem. **45**(12), 1949–1953 (2010)

Sathish, A., Sims, R.C.: Biodiesel from mixed culture algae via a wet lipid extraction procedure. Bioresour. Technol. **118**, 643–647 (2012)

Schenk, P.M., Thomas-Hall, S.R., Stephens, E., Marx, U.C., Mussgnug, J.H., Posten, C., Kruse, O., Hankamer, B.: Second generation biofuels: high-efficiency microalgae for biodiesel production. Bioenerg. Res. **1**(1), 20–43 (2008)

Scott, S.A., Davey, M.P., Dennis, J.S., Horst, I., Howe, C.J., Lea-Smith, D.J., Smith, A.G.: Biodiesel from algae: challenges and prospects. Curr. Opin. Biotechnol. **21**(3), 277–286 (2010)

Sevilla, J.F., Grima, E.M.: A model for light distribution and average solar irradiance inside outdoor tubular photobioreactors for the microalgal mass culture. Biotechnol. Bioeng. **55**(5), 701 (1997)

Sims, R.E., Mabee, W., Saddler, J.N., Taylor, M.: An overview of second generation biofuel technologies. Bioresour. Technol. **101**(6), 1570 (2010)

Singh, R., Sharma, S.: Development of suitable photobioreactor for algae production – a review. Renew. Sustain. Energy Rev. **16**(4), 2347–2353 (2012)

Su, C.-H., Giridhar, R., Chen, C.-W., Wu, W.-T.: A novel approach for medium formulation for growth of a microalga using motile intensity. Bioresour. Technol. **98**(16), 3012–3016 (2007)

Su, C.-H., Chien, L.-J., Gomes, J., Lin, Y.-S., Yu, Y.-K., Liou, J.-S., Syu, R.-J.: Factors affecting lipid accumulation by Nannochloropsis oculata in a two-stage cultivation process. J. Appl. Phycol. **23**(5), 903–908 (2011)

Sydney, E.B., Sturm, W., de Carvalho, J.C., Thomaz-Soccol, V., Larroche, C., Pandey, A., Soccol, C.R.: Potential carbon dioxide fixation by industrially important microalgae. Bioresour. Technol. **101**(15), 5892–5896 (2010)

Sydney, E., Da Silva, T., Tokarski, A., Novak, A., De Carvalho, J., Woiciecohwski, A., Larroche, C., Soccol, C.: Screening of microalgae with potential for biodiesel production and nutrient removal from treated domestic sewage. Appl. Energ. **88**(10), 3291–3294 (2011)

Takano, H., Takeyama, H., Nakamura, N., Sode, K., Burgess, J.G., Manabe, E., Hirano, M., Matsunaga, T.: CO_2 removal by high-density culture of a marine cyanobacterium Synechococcus sp. using an improved photobioreactor employing light-diffusing optical fibers. Appl. Biochem. Biotechnol. **34**(1), 449–458 (1992)

Tang, D., Han, W., Li, P., Miao, X., Zhong, J.: CO_2 biofixation and fatty acid composition of *Scenedesmus obliquus* and *Chlorella pyrenoidosa* in response to different CO_2 levels. Bioresour. Technol. **102**(3), 3071–3076 (2011)

Timilsina, G.R., Du, X., Carriquiry, M.A.: Second-Generation Biofuels. Policy Research Working Paper 5406 (2010). doi:10.1596/1813-9450-5406

Tredici, M.R., Materassi, R.: From open ponds to vertical alveolar panels: the Italian experience in the development of reactors for the mass cultivation of phototrophic microorganisms. J. Appl. Phycol. **4**(3), 221–231 (1992)

Tuinier, M., van Sint Annaland, M., Kramer, G., Kuipers, J.: Cryogenic CO_2 capture using dynamically operated packed beds. Chem. Eng. Sci. **65**(1), 114–119 (2010)

Usui, N., Ikenouchi, M.: The biological CO_2 fixation and utilization project by RITE (1) "Highly-effective photobioreactor system". Energ. Convers. Manage. **38**, S487–S492 (1997)

Van Den Hende, S., Vervaeren, H., Desmet, S., Boon, N.: Bioflocculation of microalgae and bacteria combined with flue gas to improve sewage treatment. N. Biotechnol. **29**(1), 23–31 (2011)

Wang, B., Lan, C.Q., Horsman, M.: Closed photobioreactors for production of microalgal biomasses. Biotechnol. Adv. **30**(4), 904–912 (2012)

Westerhoff, P., Hu, Q., Esparza-Soto, M., Vermaas, W.: Growth parameters of microalgae tolerant to high levels of carbon dioxide in batch and continuous-flow photobioreactors. Environ. Technol. **31**(5), 523–532 (2010)

Wilkin, R.T., DiGiulio, D.C.: Geochemical impacts to groundwater from geologic carbon sequestration: controls on pH and inorganic carbon concentrations from reaction path and kinetic modeling. Environ. Sci. Tech. **44**(12), 4821–4827 (2010)

Xiong, W., Li, X., Xiang, J., Wu, Q.: High-density fermentation of microalga Chlorella protothecoides in bioreactor for microbio-diesel production. Appl. Microbiol. Biotechnol. **78**(1), 29–36 (2008)

Xu, N., Zhang, X., Fan, X., Han, L., Zeng, C.: Effects of nitrogen source and concentration on growth rate and fatty acid composition of Ellipsoidion sp. (Eustigmatophyta). J. Appl. Phycol. **13**(6), 463–469 (2001)

Xu, H., Miao, X., Wu, Q.: High quality biodiesel production from a microalga *Chlorella protothecoides* by heterotrophic growth in fermenters. J. Biotechnol. **126**(4), 499–507 (2006)

Yamada, N., Tsurushima, N., Suzumura, M.: Effects of seawater acidification by ocean CO_2 sequestration on bathypelagic prokaryote activities. J. Oceanogr. **66**(4), 571–580 (2010)

Yang, S., Wang, J., Cong, W., Cai, Z., Ouyang, F.: Effects of bisulfite and sulfite on the microalga *Botryococcus braunii*. Enzyme Microb. Technol. **35**(1), 46–50 (2004)

Yeh, K.-L., Chang, J.-S.: Nitrogen starvation strategies and photobioreactor design for enhancing lipid content and lipid production of a newly isolated microalga Chlorella vulgaris ESP-31: Implications for biofuels. Biotechnol. J. **6**(11), 1358–1366 (2011)

Yonghua, L.-B.: Triacylglycerol biosynthesis in eukaryotic microalgae. http://lipidlibrary.aocs.org/plantbio/tag_algae/index.htm (2012)

Yoo, C., Jun, S.-Y., Lee, J.-Y., Ahn, C.-Y., Oh, H.-M.: Selection of microalgae for lipid production under high levels carbon dioxide. Bioresour. Technol. **101**(1), S71–S74 (2010)

Young, G., Nippen, F., Titterbrandt, S., Cooney, M.J.: Direct transesterification of biomass using an ionic liquid co-solvent system. Biofuels. **2**(3), 261–266 (2011)

Yue, L., Chen, W.: Isolation and determination of cultural characteristics of a new highly CO_2 tolerant fresh water microalgae. Energ. Convers. Manage. **46**(11), 1868–1876 (2005)

Zhang, Y., Sahinidis, N.V.: Uncertainty quantification in CO_2 sequestration using surrogate models from polynomial chaos expansion. Ind. Eng. Chem. Res. **52**(9), 3121–3132 (2012)

Zhao, B., Zhang, Y., Xiong, K., Zhang, Z., Hao, X., Liu, T.: Effect of cultivation mode on microalgal growth and CO_2 fixation. Chem. Eng. Res. Des. **89**(9), 1758–1762 (2011)

Zijffers, J.-W., Schippers, K., Zheng, K., Janssen, M., Tramper, J., Wijffels, R.: Maximum photosynthetic yield of green microalgae in photobioreactors. Marine Biotechnol. **12**(6), 708–718 (2010)

Concentrating Solar Energy Technologies

Erminia Leonardi and Bruno D'Aguanno

Abstract

Concentrating solar power is one of the fastest growing industries in the market of the renewable energy technologies. The main reason for this increasing interest lies in the fact that most of the power generated nowadays is produced using fossil fuels, which are very pollutant and damaging for the environment. People are, therefore, looking for new sources of substitute clean energy to assure a sustainable development of our civilization. There are several kinds of concentrating solar power techniques that are currently available, and in this chapter they will be described and compared. Also research trends will be discussed, taking account of the most recent market analysis.

Keywords

CSP • TES • Parabolic trough • Linear Fresnel • Solar tower • Parabolic dish • Multi-tower • Shading • Blocking and cosine effect

1 Introduction

Concentrating solar power (CSP) technologies, together with nonconcentrating solar technology, define the class of renewable energy technologies capable of exploiting the immense solar radiation resource available on the earth surface. Such an exploitation can ensure a transition from the economy based on fossil, and finite, sources of energy to a new economy based on renewable energies.

By concentrating the otherwise diluted solar radiation ($\approx$1 kW/m^2), CSP technologies open the access to the high power production/dispatching of energy. The fluids on which the solar radiation is concentrated can reach temperatures well above 1,000 °C, and the heat in such an extended range of temperature can be used in a variety of applications, of which the electricity production is the main one. By coupling CSP technologies with thermal energy storage (TES) systems, the produced solar heat can be delivered in a continuous way, bypassing all possible intermittencies in the solar source. The coupling of CSP technologies with TES systems allows the production of heat at the same conditions at which it is produced in any power plant based on fossil fuels. The exploitation of the solar radiation becomes "only" a question of competitiveness and of R&D efforts to reach such a competitiveness.

Aside from the seminal projects of Maadi, Egypt (a parabolic solar thermal energy system to pump water for irrigation realized in 1913 (Cleveland 2008)), and the plant of Sant'Ilario, Italy (a 1 MW central solar tower plant built in 1968 (Butti and Perlin 1980)), the beginning of the market exploitation of CSP technologies can be traced back to the parabolic trough plant known as Solar Energy Generating Systems (SEGS) of Mojave Desert, California, whose realization started in 1984. Along the years, this plant has been updated and extended reaching the present power of 354 MW SEGS (Wikipedia 2013), and, at the moment, it is still the largest CSP plant in the world. By analyzing the market situation at the year 2013, it results that 47 plants are

E. Leonardi (✉) • B. D'Aguanno
Reneable Energy, Center for Advanced Studies,
Research and Development in Sardinia (CRS4), Edificio 1,
Parco Tecnologico Polaris, cap 09010 Pula, Sardinia, Italy
e-mail: ermy@crs4.it

G. Cao and R. Orrù (eds.), *Current Environmental Issues and Challenges*,
DOI 10.1007/978-94-017-8777-2_6,

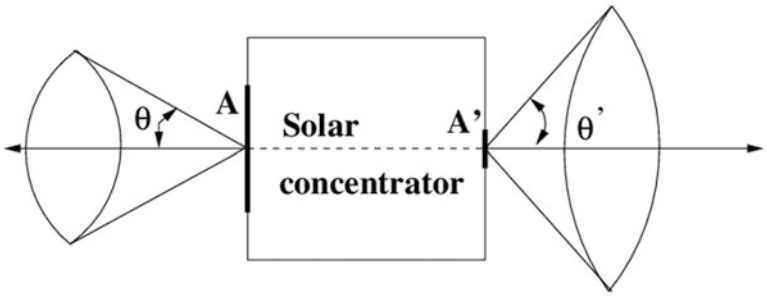

Fig. 1 Scheme of a generic solar concentrator

operative for a total of 2,691 MWp, while 40 new plants are announced for a total of 8,949 MWp.

Aim of this chapter is to review the state of the art of the CSP technologies used to produce electricity and of the key research topics which are needed to bring CSP plants at an open market level.

To this purpose, this chapter is organized as follows: The next section, Sect. 2, introduces the basic facts and relations about solar energy concentration and derives the attainable concentration limits. Section 3 illustrates the thermodynamics needed to describe the efficiency of the solar energy conversion from the concentrator to the receiver. Section 4 describes the concentration techniques and their use to make real CSP plants and the main characteristics of the major realized CSP plants. Section 5 illustrates the use of the thermal energy storage (TES) to achieve a continuous heat production out from a CSP plant. Finally, Sect. 6 shows the market trends for the realization of CSP plants and the critical research topics to be developed in order to guarantee a true competitiveness and deployment of the CSP technologies.

This chapter is closed by Sect. 7. There all the pro making CSP technologies as the key technologies for power generation from solar radiation are shortly revised and summarized.

2 The Solar Energy Concentration

The solar radiation has a relatively low energy density with respect to conventional sources of energy; therefore, optical concentration is required to increase the density allowing its exploitation for technical applications.

In a CSP system, the concentrated solar rays are reflected onto a receiver, which generates heat that can be used for many industrial applications (production of electricity, desalination, chemical reactions, etc.).

The design of solar concentrators is based on the principle of the nonimaging optics, which is the branch of optics concerned with the optimal transfer of light radiation between a source and a target, without any attempt to form an image of the source. On the basis of nonimaging optics, a solar concentrator is defined as an optical device that collects the solar radiation incident on some aperture area A and delivers it to an absorber (receiver) area A'. The light enters the system (the solar concentrator) within a cone defined by $\pm\theta$ and exits from it within a cone defined by $\pm\theta'$ as measured from the optical axis, as shown in Fig. 1.

In general, concentrators can be divided into two groups: 2D concentrators and 3D concentrators. 3D concentrators change all three direction vectors, direction cosines, of the incoming rays, and will typically concentrate the incoming irradiation into a spot. 2D concentrators are symmetric around one axis, and only two of the direction cosines are affected by the concentrator. In the following discussion, only 3D concentrators will be considered.

We start the derivation of the concentration limits of solar radiation with the description of the properties of the solar source.

The Sun can be considered as a Lambertian emitter since it obeys to the Lambert's cosine law, where the radiant intensity observed from an ideal diffuse radiator is proportional to the cosine of the angle θ between the observer's line of sight and the surface normal. Therefore, the Sun has the same radiance when viewed from any angle. This happens because, although the emitted power from a given area element is reduced by the cosine of the emission angle, the apparent size (solid angle) of the observed area, as seen by a viewer, is decreased by a corresponding amount. Therefore, its radiance (power per unit solid angle per unit projected source area) is the same.

The solar power flux, Φ, incident on the enter aperture of a solar concentrator, A, can be expressed as the integral of the radiance, L, times the area and the projected solid angle (Smestad et al. 1990; Welford and Winston 1989):

$$\Phi = \int LA\cos\theta \ \mathrm{d}\Omega$$

$$= \int_0^{2\pi} \mathrm{d}\phi \int_0^{\theta} LA\cos\theta \ \ \sin\theta \ \ \mathrm{d}\theta$$

$$= 2\pi LA \int_0^{\theta} \cos\theta \ \ \sin\theta \ \ \mathrm{d}\theta = \pi LA \sin^2\theta \qquad (1)$$

where θ is commonly called the acceptance angle of the solar concentrator. An expression similar to Eq. 1 can be obtained for the power flux, Φ', exiting the concentrator from the aperture A'.

Then, a geometric concentration ratio can be defined as

$$C \equiv \frac{\Phi/A}{\Phi'/A'}. \qquad (2)$$

If there are no losses within the concentrator, $\Phi = \Phi'$, and therefore

$$C = \frac{A'}{A}. \qquad (3)$$

By using thermodynamic relations, it is possible to demonstrate that for an ideal concentrator the product of the aperture area times the sinus squared of the acceptance angle of the radiation cone is conserved (Welford and Winston 1978):

$$A \sin^2\theta = A' \sin^2\theta' \qquad (4)$$

This means that if $A' \leq A$, then $\theta' \geq \theta$. Therefore,

$$C \leq \frac{\sin^2\theta'}{\sin^2\theta}. \qquad (5)$$

From Eq. 5, we can see that maximum theoretical concentration is achieved when $\theta' = 90°$. The acceptance angle, θ, cannot be greater than the Sun's half angle, $\theta_S = 4.653$ mrad, for which $C_{max} = 46{,}200$.

Instead, for a 2D concentrator, the concentration ratio is the square root of the 3D value:

$$C_{\downarrow}\max^{\uparrow}2D = \sqrt{\left(C_{\downarrow}\max^{\uparrow}3D\right)}. \qquad (6)$$

3 Thermodynamics of Solar Energy

The means by which sunlight can be used to produce heat is provided by the fundamental laws of the thermodynamics. In particular, from thermodynamics we know that the higher the temperature at which solar energy is provided to a given system, the more vast the field of technical applications is. If we concentrate and collect the diluted sunlight over a small receiver area, we could be able to obtain heat at high temperatures for producing electricity or storable fuels via thermochemistry, and the theoretical maximum efficiency of such energy conversion process is limited by the Carnot efficiency of an equivalent heat engine. In order to derive an expression for the temperature at which a solar collector can operate, as a function of the sunlight concentration, some gross assumptions are needed. We assume that the Sun and the absorber are black bodies, at temperatures T_S and T_{abs}, respectively. The rest of the universe (other than the Sun and the absorber), collectively called ambient, has a temperature $T_{amb} = 0$.

The Sun emits an amount of radiation according to the Stefan-Boltzmann equation:

$$Q_S = 4\pi R^2 \sigma T_S^4 \qquad (7)$$

where R is the radius of the Sun and $\sigma = 5.67 \times 10^{-8}$ $\mathrm{Wm^{-2}\ K^{-4}}$ is the Stefan-Boltzmann constant. Only the fraction $A = (4\pi\ D^2)$ (D is the distance between the Sun and the solar collector) of the emitted amount of radiation enters the solar concentrator. If we assume an ideal behavior of the solar concentrator (so that no radiative losses occur between the concentrator and the absorber), the incoming solar radiation absorbed by the receiver can be expressed as

$$Q_{abs} = \tau\alpha \frac{AR^2}{D^2} \sigma T_S^4 \qquad (8)$$

where τ is a reduction factor accounting for all possible radiation losses and α is the absorptance of the receiver.

On the other hand, the receiver loses energy corresponding to its temperature, T_{abs}:

$$Q_{lost} = \in A' \sigma T_{abs}^4, \qquad (9)$$

where $\in$ is the emissivity of the receiver.

If a fraction η_{abs} of Q_{abs} is extracted from the receiver, an expression relating T_{abs} to η_{abs} and C can be easily obtained by using the balance relation $(1 - \eta_{abs})\ Q_{abs} = Q_{lost}$ and Eqs. 8 and 9:

$$T_{abs} = T_S \left[(1 - \eta_{abs}) \frac{\tau\alpha C}{\in C_{max}} \right]^{1/4}. \qquad (10)$$

For $\eta_{abs} = 0$, all the absorbed heat is reradiated from the receiver, and T_{abs} is called the stagnation temperature of the solar collector. A graphic representation of the stagnation temperature versus C is shown in Fig. 2, for the simplified case of a receiver with $\tau = 1$, $\alpha = 1$ and $\in = 1$.

More importantly, by using Eq. 10 to write η_{abs} as a function of T_{abs}, we can clearly see that η_{abs} is a decreasing function of T_{abs}.

If we indicate with η_{carnot}, the well-known efficiency of the Carnot cycle is

$$\eta_{carnot} = 1 - \frac{T_{cold}}{T_{abs}}, \tag{11}$$

where T_{cold} and T_{abs} are the cold and hot temperatures of the Carnot machine, respectively. Then, the overall conversion efficiency, $\eta_{overall}$, of solar energy into work is

$$\eta_{overall} = \eta_{abs} \times \eta_{carnot}. \tag{12}$$

For each value of the concentration ratio, there is an optimal value of T_{abs}, which maximizes $\eta_{overall}$, as shown in Fig. 3.

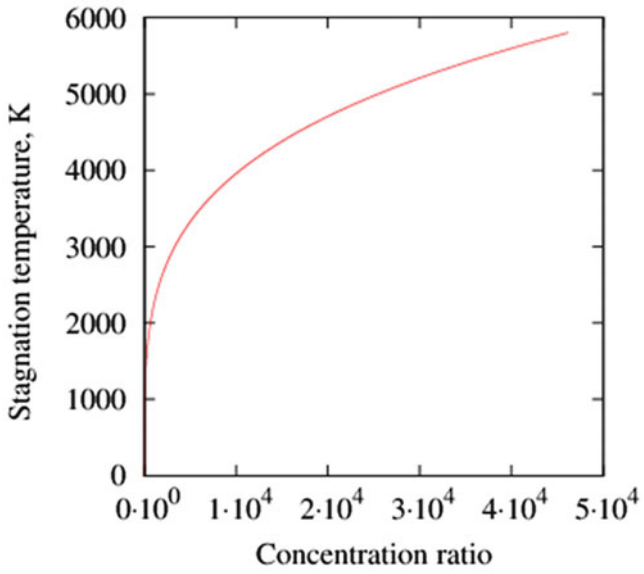

Fig. 2 Stagnation temperature as function of the concentration ratio

4 Collecting Solar Radiation Systems and Plants

The CSP systems can be considered to all intents and purposes thermoelectric plants, with the unique difference that the heat used in the thermodynamic cycle comes from the concentrated sunlight rather than from the combustion of fossil fuels.

Presently, there are four categories of concentrating collectors:

- Parabolic trough (PT) collectors
- Linear Fresnel (LF) collectors
- Solar towers (ST)
- Parabolic dish (PD) collectors

Regarding the way in which sunlight is concentrated, in general, a distinction can be made between one-axis (2D collectors) and two-axis (3D collectors) tracking systems. PT and LF belong to the first category, while ST and PD belong to the second one.

4.1 Parabolic Trough Systems

PT collectors use curved mirrors and single-axis tracking to intercept the Sun rays and concentrate them onto a receiver tube, located along the focus line of the mirrors. A heat transfer fluid (HTF), typically synthetic oil, molten salt, or steam, circulates in the tubes absorbing the Sun's heat before passing through multiple heat exchanger to produce steam. A sketch of the system is shown in Fig. 4.

The efficiency and cost of the PT systems is influenced by structural stiffness, choice of material, mirror cleanliness, and wear. Currently, PT technology is the most proven solar thermal electric technology, mainly due to the installation of many large commercial-scale plants. PT systems can effectively produce HTF heated to approximately 390 °C (actual concentration ratios are in the range of 70–80 suns).

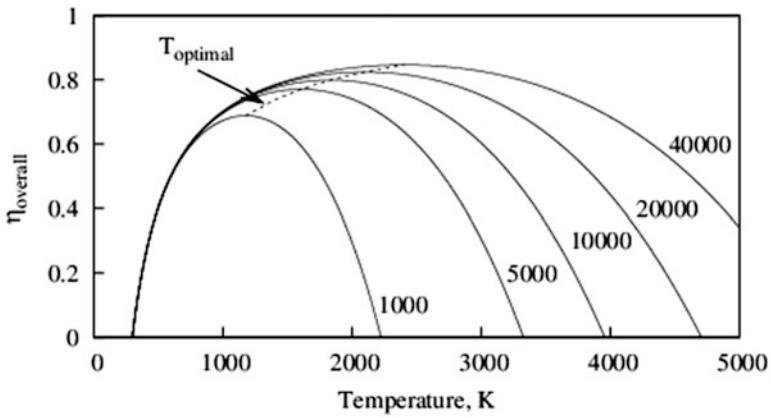

Fig. 3 Dependence on temperature of the overall conversion efficiency, for different values of the concentration ratio. Optimal temperature is also indicated. $T_{cold} = 298$ K

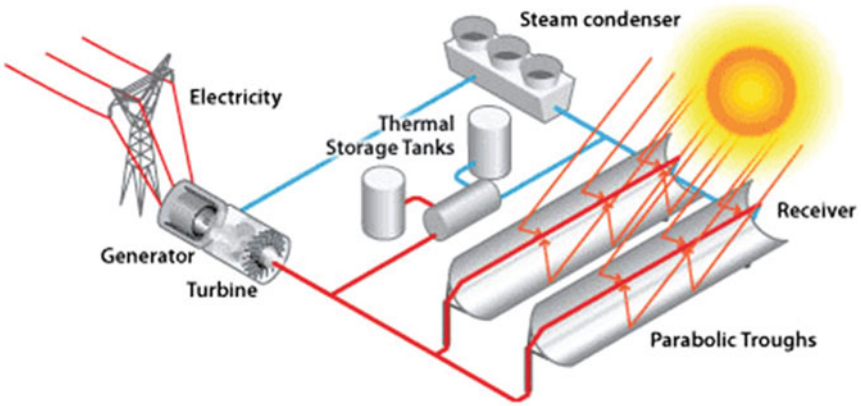

Fig. 4 Scheme of a parabolic trough system (*Source*: eere.energy.gov)

Table 1 Parabolic trough projects in the world

Project	Country	Capacity (MW_e)	Status	Start year
AndasoI-3	Spain	50	Operational	2011
Archimede	Italy	5	Operational	2010
Helios II	Spain	50	Operational	2012
Bokpoort	South Africa	50	Under development	2015
Diwakar	India	100	Under construction	2013
Genesis Solar Energy	United States	250	Under construction	2014
Godawari Solar Project	India	50	Operational	2013
KaXu Solar One	South Africa	100	Under construction	2015
TSEl	Thailand	5	Operational	2012
Shams 1	United Arab Emirates	100	Operational	2013
Pedro de Valdivia	Chile	360	Under construction	2015
Solana	United Stales	280	Under construction	2013
Ouarzazate	Morocco	160	Under construction	2015

The design-point solar-to-electric conversion efficiency ranges from 24 to 26 %, and the overall annual average conversion efficiency is about 13–15 %. The typical size of the plants ranges between 10 and 300 MWe, with a production of about 60–80 MWe/km^2. Table 1 indicates some of the most recent and representative PT plants.

4.2 Linear Fresnel Reflectors

Among other CSP technologies, the LF reflector is considered a very promising solution, thanks to its design and installation simplicity, raw material use, cost attractiveness, and relatively small land requirement, since more mirrors can be squeezed onto a small parcel of land.

The system is constituted of a field of linear heliostats that reflects and concentrates the sunlight onto an absorber tube (the receiver) horizontally arranged above the collectors. The heliostats can rotate along a longitudinal axis to track the Sun rays and constantly maintain the sunlight reflected on the receiver (see Fig. 5). The absorber tube is generally realized in steel and covered with glass.

The main advantage of this type of system is that it uses flat or elastically curved reflectors which are cheaper compared to parabolic glass reflectors. Additionally, these are mounted close to the ground, thus minimizing structural requirements. Moreover, the mirrors do not need to support the receiver, so they are structurally simple. In recent designs, mirrors can aim, at different times of the day, at different receivers thus allowing a denser packing of mirrors on the available land area (compact linear Fresnel reflectors).

However LF reflectors are less efficient than troughs in converting solar energy to electricity, and it is more difficult to incorporate storage capacity into their design.

The LF plants so far realized produce steam at about 270 °C and 40 bar, although demonstration plants with higher operating temperatures are under study (NovatecSolar 2013). Recently, superheated steam at about 380 °C has been demonstrated in an LF plant, and there are proposals for producing steam at 450 °C. The typical size of the LF plants ranges between 5 and 10 kWe, with a production of order 100–125 MWe/km^2. Table 2 indicates the most recent LF projects realized in the world.

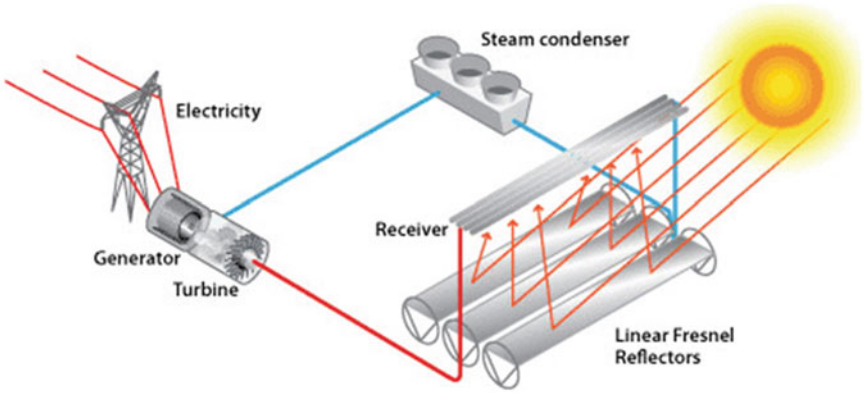

Fig. 5 Scheme of a linear Fresnel collector plant (*Source*: eere.energy.gov)

Table 2 Linear Fresnel reflectors projects in the world

Project	Country	Capacity (MW_e)	Status	Start year
Alba Nova 1	France	12	Under construction	2014
Augustin Fresnel 1	France	250	Operational	2012
Dhursar	India	100	Under construction	2013
Kimberlina	United States	5	Operational	2008
Kogan Creek	Australia	44	Under construction	2013
Liddell Power Station	Australia	9	Operational	2012
PE2	Spain	30	Operational	2012

4.3 Solar Tower Systems

The ST system is constituted of a field of heliostats that reflects and concentrates the solar radiation onto a receiver located atop a tower. A large ST plant can require from several thousands to more than one hundred thousand heliostats, each under computer control. Because they typically constitute about 50 % of the plant cost, the optimization of the solar field design is a crucial issue. A lot of R&D is focused on the optimal shape, size, and weight of the heliostats as well as on the relative arrangement in the solar field. A schematic of the system is shown in Fig. 6.

The heat transfer fluid, circulating within the receiver, can reach, in principle, very high temperatures because of the high concentration ratios achievable (up to 1,000 suns). Depending on the receiver design and the working fluid, the upper working temperatures can range from 250 °C to perhaps as high as 1,000 °C for future plants.

If the fluid is water, high-pressure steam can be directly produced at the receiver, with successive expansion in turbine. Current steam conditions for direct-steam generation range from saturated steam at 250 °C to superheated steam at over 550 °C. If an intermediate fluid circulates in the receiver, like air or molten salts, the steam is directly produced in the power block. If molten salt (typically a mixture of 60 % $NaNO_3$ and 40 % KNO_3) is used as HTF, the salt at about 290 °C is pumped from a cold storage tank to the receiver, where concentrated sunlight from the heliostat field heats it to about 565 °C. The hot salt is held in a storage tank, from which is pumped to a steam generator system for electricity production.

The size of the ST systems is limited by the accuracy of the tracking system. Presently, the maximum radius of a solar field is estimated of the order of 1,000 m, for a tower of about 200–250 m high. The nominal power estimated for the ST plants is evaluated in the order of 10–200 MWe. The design-point solar-to-electric conversion efficiency ranges from 20 to 24 %, and the overall annual average conversion efficiency is about 14–18 %. The land usage is in the range of 80–120 MWe/km^2.

Table 3 reports the ST plants in operation and in construction in the world, while Table 4 reports the characteristics of the heliostats and the tower height of some of them.

4.4 Parabolic Dish Collectors

The PD collector consists of a two-axis tracking parabolic dish reflector that concentrates the incoming sunlight onto a receiver located at the focal point of the dish (see Fig. 7).

The solar energy absorbed by the receiver can be converted into heat in a circulating fluid and transported through pipes to a central power-conversion system, or it can be directly converted into electricity by means of an engine-generator coupled to the receiver. The first method should be preferred

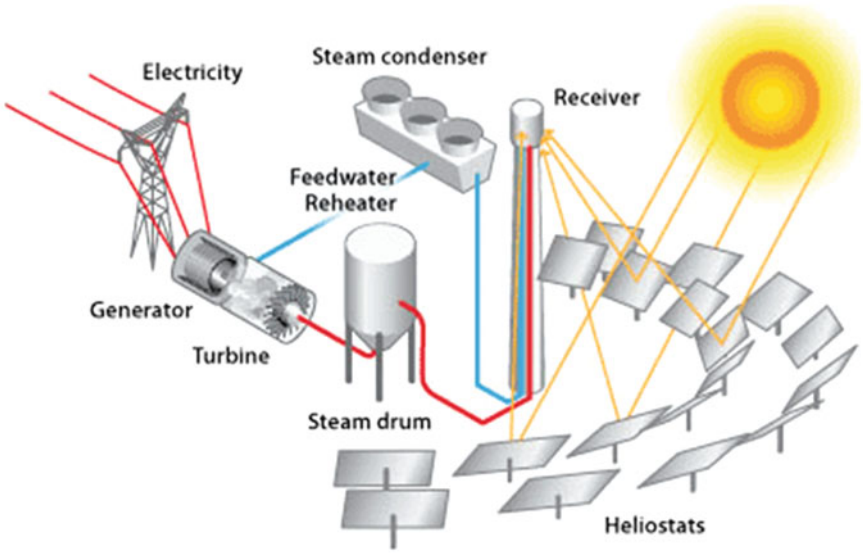

Fig. 6 Scheme of a solar tower system (*Source*: eere.energy.gov)

Table 3 Solar tower projects in the world

Project	Country	Capacity (MW_e)	Status	Start year
ACMR solar tower	India	2.5	Operational	2011
Beijing Badaling Solar	China	1.5	Operational	2012
Coyote Spring 1	United States	200	Under development	2014
Tonopah	United States	110	Under construction	2013
Gemasolar	Spain	19.9	Operational	2011
ISEGS	United States	392	Under construction	2013
PS20	Spain	20	Operational	2009
Sierra	United States	5	Operational	2009
RSEP	United States	150	Under construction	2016
Supcon Solar Project	China	50	Under construction	–
Lake Cargeligo	Australia	3	Operational	2011
Khi Solar One	South Africa	50	Under construction	2014
Panel Solar Electric generating System	United States	500	Under development	2016

Table 4 Characteristics of some ST plants operational or under construction

Project	N. of heliostats	Heliostat aperture area (m^2)	Tower height (m)
Tonopah	17,170	624	165
Gemasolar	2,650	120	140
PS20	1,255	120	165
ACME Solar Tower	14,380	1.136	40
Khi Solar One	4,120	140	200

when many dishes are arranged in a so-called distributed system for large-scale production, although, at present, there are no large-scale solar dish power plants.

Typically, the PD is coupled with a Stirling engine in a dish-Stirling engine system (Kongtragool and Wongwises 2003). The peculiarity of a Stirling engine is that the associated thermodynamic cycle produces electricity without producing steam as an intermediate step.

Due to its tracking system (always pointing to the Sun), the PD collector typically reaches concentration ratio in the range of 1,000–3,000 suns, which in turn can result, in principle, in temperatures of 1,500 °C and more (Sorenson and Breez 2009), thus allowing the most efficient energy conversions (above 30 %) (West 1986; Walker 1980) compared with the other CSP technologies.

Despite their high energy conversion efficiency, the PD collectors present some technological constrains. The electricity output of a single dish-Stirling unit is limited to small ratings due to geometric and physical reasons. Projection of capital costs, operation and maintenance costs, system

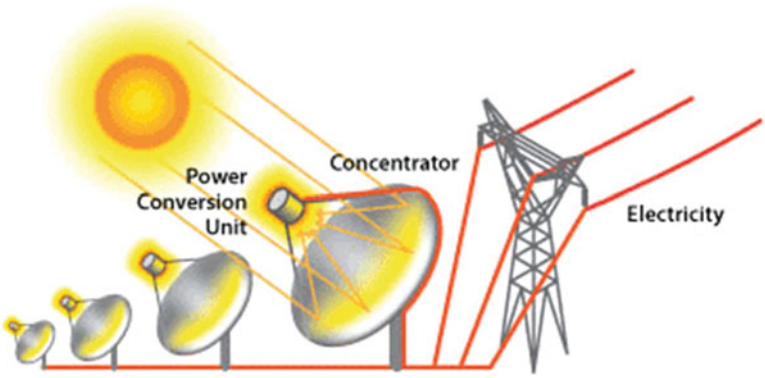

Fig. 7 Scheme of a parabolic dish collector (*Source*: eere.energy.gov)

Table 5 Dish/engine projects in the world

Project	Country	Capacity (MW_e)	Status	Start year
Maricopa	United States	1.5	Operational (demonstration)	2010
Tooele Army Depot	United States	1.5	Under construction (commercial)	2013

performance, and annual plant availability over the long term are not available or verified. Adequate energy storage is not yet available. The energy conversion system involves moving parts and this implies maintenance. The Stirling engine is a heavy part of the system, which therefore needs a strong tracking device to maintain the adequate tracking precision. At present, there are no utility-scale PD projects in development. The capacity of the PD systems ranges between 5 and 50 kWe with a typical land usage between 80 and 120 MWe/km^2. The design-point solar-to-electric efficiency is about 30 %, while the annual average conversion efficiency is in the low 20 % range.

Table 5 indicates the most recent PD projects realized in the world.

5 CSP and Thermal Storage

Solar energy is, by nature, unpredictable, intermittent and periodic, and subject to environmental conditions and climate changes. Therefore, the generation of electricity from a CSP system is also intermittent and unpredictable, unless a thermal energy storage (TES) is included in the plant. Storage also enables the production of electricity to be shifted to periods of highest demand, allowing a flexible use of the CSP plant, which is a very important parameter for optimal grid operation.

The concept of TES is simple: throughout the day, excess heat is diverted to a storage material (e.g., molten salts). When production is required (typically after sunset), the stored heat is released into the thermodynamic cycle of an appropriate engine-generator allowing the plant to continue the production of electricity.

Adding a TES to a CSP plant can increase its capacity factor significantly at all of the locations. For the sake of clarity, we recall that the capacity factor of a power plant is defined as the ratio of its actual output over a period of time to its potential output if it were possible for it to operate at full installed capacity in the same period of time.

At present, four kinds of TES configurations can be distinguished:

- *Intermediate load*: designed to produce electricity when the sunshine available covers peak and shoulder loads (from 08:00 to 19:00 h). Typically, it requires only small amount of storage. It has the smallest investment costs and the least-expensive electricity output.
- *Delayed intermediate load*: designed to collect solar energy all day but to produce electricity from noon on and after sunset, corresponding to peak and shoulder loads (from 12:00 to 23:00 h). It has the same size turbine as the intermediate load plant but requires a larger amount of energy.
- *Base load*: designed to run 24 h per day; it needs a larger amount of storage and a smaller turbine. If the costs of storage capacity are lower than those of larger turbines, electricity from the base load is slightly cheaper than that of delayed intermediate load plants. This will likely be the case with higher working temperatures, which will allow for less-expensive storage but require more sophisticated and costly turbines.
- *Peak load*: designed to provide electricity only for a few hours to meet the extreme peak loads (from 11:00 to 15:00 h). It requires a large turbine and a large amount of storage. Of all four designs, it produces the most expansive but also the most valuable electricity.

The four CSP technologies described above differ significantly from one another, not only with regard to technical

Table 6 Comparison of different CSP technologies

	Parabolic trough	Solar tower	Linear Fresnel	Dish-Stirling
Typical size MW	10–300	10–200	10–200	0.00 L–0.025
Maturity of technology	Commercially proven	Pilot commercial projects	Pilot projects	Demonstration projects
Technology development risk	Low	Medium	Medium	Medium
Operating temperature (°C)	350–550	250–565	300	550–750
Plant peak efficiency (%)	14–20	23–35	18	30
Annual solar-to-electricity efficiency (%)	11–16	7–20	13	12–25
Annual capacity factor (%)	25–28 (no TES) 29–43 (7 h TES)	55 (10 h TES)	22–24	25–28
Collector concentration	70–80	>1,000	>60	>1,300
TES system	Indirect two-tank molten salt at 380 °C ($\Delta T = 100$ K) or Direct two-tank molten salt at 550 ° C ($\Delta T = 300$ K)	Direct two-tank molten salt at 550 °C ($\Delta T = 300$ K)	Short term pressurized steam storage (<10 min)	No storage, chemical under development
Storage with molten salt	Commercially available	Commercially available	Possible, but not proven	Possible, but not proven
Hybridization	Yes and direct	Yes	Yes, direct (steam boiler)	Not planned
Grid stability	Medium to high (TES or hybridization)	High (large TES)	Medium (back-up firing possible)	Low
Cycle	Superheated Rankine steam cycle	Superheated Rankine steam cycle	Saturated Rankine steam cycle	Stirling
Steam conditions (°/bar)	380 to 540/100	540/100 to 160	260/50	n.a.
Maximum slope of solar field (%)	<1–2	<2–4	<4	10 % or more
Application type	On-grid	On-grid	On-grid	On-grid/Off-grid

and economic aspects, but also in relation to their reliability, maturity, and operational experience in utility-scale conditions. An attempt of comparison of their major features is given in Table 6, where data are produced by an analysis of IRENA (International Renewable Energy Agency) (IRENA 2013). From such analysis results that although parabolic trough plants are the most widely commercialized, currently, most of them are not provided of a TES system and only generate electricity during daylight hours. Solar tower and linear Fresnel systems are only beginning to be deployed with a potential significant reduction of the capital costs and improvement of the performances.

6 Research Trends

Since the SEGS plant realized in 1984, the number of CSP plants increased a lot, and today (2013), 47 plants are operating for a total of 2,691 MWp (see Fig. 8). As shown in Fig. 9, the 96 % of realized plants use linear parabolic concentrators, the 2 % linear Fresnel concentrators, and the other % solar tower point-like concentration. However, the 2013 announced plants, which amount to a total of 8,949 MWp (more than three times the all power built since 1984), have a completely different distribution. Such distribution is shown in Fig. 10, from which we note that the percentage of the solar towers is growing rapidly and it is reaching that of parabolic troughs, while the linear Fresnel continue to have almost the same 2013 percentage.

The quantitative plant growth, the technology polarization between solar tower and parabolic trough, and the growth of the solar tower plants are a result of several factors. Between them, we cite the following: (i) the free access to a very high direct normal irradiation in the Sunbelt regions, (ii) national rules to subsidize the generation of the market and of technical and institutional experience, and, last but not least, (iii) the national and international efforts to develop extended research activities in the field.

Lists of research topics, on which such efforts are focused, are reported in the studies promoted by the SunShot Initiative of the DOE (USA) (SunShot 2013) and in those promoted by the European Union Commission and by

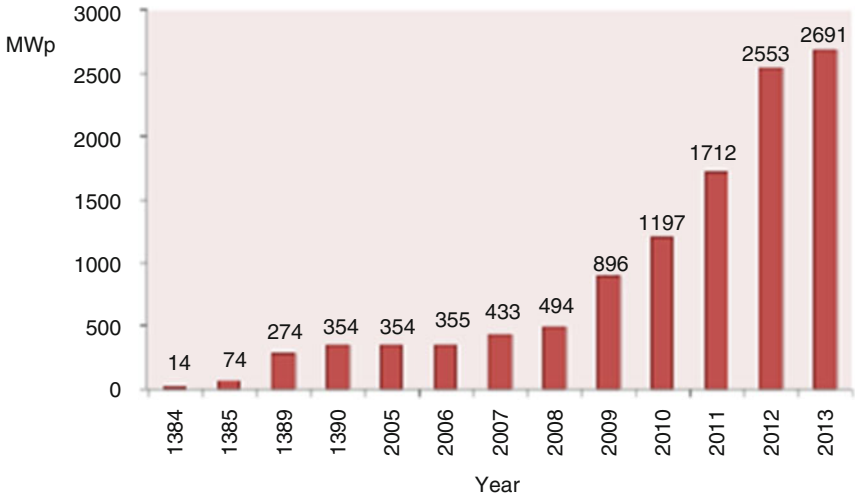

Fig. 8 Growth of CSP plants expressed in cumulative MWp

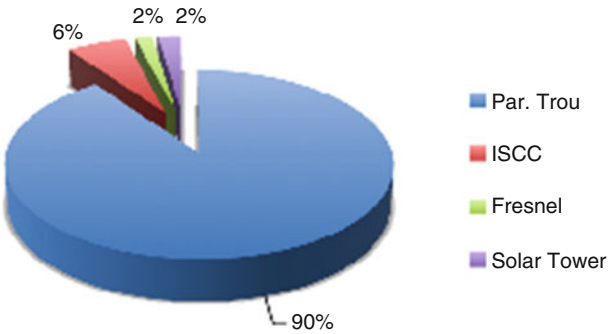

Fig. 9 Distribution of the 2013 installed power according to concentration technology (the ISCC plants use parabolic trough, too)

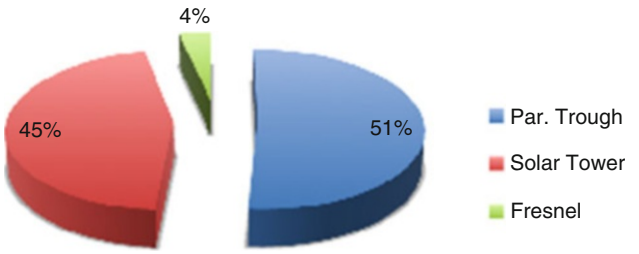

Fig. 10 Distribution of the 2013 announced power according to concentration technology

International Organizations (ESTELA 2013; EASAC 2013; IEA 2013; Pitz-Paal et al. 2013). The main research topics of the mentioned programs are summarized in Table 7.

The relevance of the research advancement on the levelized cost of energy (LCOE) is well illustrated in Fig. 11, from which it is clear that the research advancement will decrease the costs of all the subcomponents of a CSP plant and that the highest reduction is expected for the solar tower. This last observation also explains the growth of the ST plants illustrated in Fig. 10.

As examples of research activities are able to reduce the LCOE, we shortly illustrate the case of the thermal storage based on the thermocline phenomenon and that of solar multi-tower systems.

The thermocline is a region of a system in which a temperature gradient is present. The thermocline separates a region at uniform high temperature from another one at uniform low temperature. Thermoclines are quite stable, and the stability can be used to have, just in one container, a thermal storage at high temperature and a thermal storage at low temperature.

A thermocline can be generated in a storage tank filled by pebbles, or sand-like materials, and in which a stream of a fluid at high/low temperature is allowed to flow. The transient thermal behavior of such fixed bed systems can be modeled through a system of coupled partial differential equations in terms of solid- and fluid-phase temperatures. The most used models are the continuous phase model of Ismail and Stuginsky (1999) and the Schumann's model (Schumann 1929). These models introduce in their equations an extended set of material properties (thermal conductivities, heat transfer coefficients, pebble diameter, pebble heat capacity, etc.) as well as of operative conditions (working pressure, fluid velocity, storage tank geometrical dimension, etc.). Then, the overall heat storage system can be optimized by varying all the involved parameters in order to achieve a maximum storage capacity (very steep thermocline) and a stable thermocline, both at rest and during the charge/discharge cycles. An example of the effect of the pebble diameter on the amount of heat stored is given in Fig. 12. It is obvious that the more heat is stored in the tank, the more "cheap" is the heat storage system. More R&D work is needed along the optimization line.

Table 7 Research priorities

	Topics	Parameters
Increase efficiency and reduce generation, operation and maintenance costs	*Solar field*	
	New concept to reduce the cost of solar field by up to 50 % with significant material reduction	Collected energy for unitary surface of mirrors and site area
	Front-surface mirrors and polymeric reflectors with high reflectivity	Mirror reflectivity
	Independent and self-assembled heliostats, fast to install and with minimal site preparation	Mirror durability
	Anti-soiling coatings and low-to-no water cleaning techniques	Water consumption for mirror washing
		Tracker precision
	Solar receiver and HTF fluids	
	New solar selective and oxidation resistant coatings	Coating emittance and absorbance
	New oxidation resistant coatings	Melting temperature and thermal stability limits of salt mixtures
	HTF with nano-particles	
	New salt mixtures for extended temperature ranges	Thermal and mechanical stability of pressurized receivers
	Pressurized gases	Fluid viscosity and pumping work
	Site preparation	
	Solar field design wit minimal site disruption	Minimal work for site preparation
	Solar field design for non-flat area	Mirror density coverage of the site
	Power plant	
	Advanced power cycles	Conversion efficiency of thermal cycles
	Thermal flux management code	Real-time answer of management tools
Improve dispatchability	*Hybridization and integration*	
	Hybridization with steam plants	Specific design of demo plants
	Integration with gas turbine and combined cycles	Combined efficiency
	Integration with biomass plants	
	New storage concepts	
	Storage design (for oil molten salt, steam)	Specific costs
	Storage optimization (multi storage and optimized charging/discharging)	
	New storage concept (thermo-chemical storage)	
	Forecasting tools	
	Improved DNI ground measurements	Solar resource data
	New tools for meteorological satellite images	Forecast reliability
	DNI forecasting codes and tools	DNI variability
	Balance between DNI and wind resources	Deviation from planned to production
		Correlation between wind and DNI
Improve environmental profile	HTF and environment impact	Level of risk for water
	Reduction of water consumption	Cost of materials and systems
	Integration of CSP plants with desalination plants	Power block water consumption
		Combined power and water production

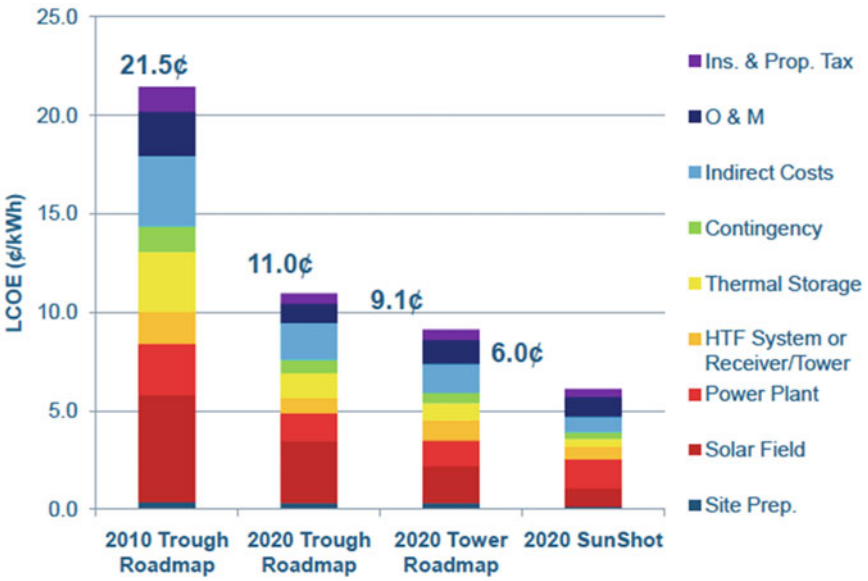

Fig. 11 Levelized cost of energy from USA and SunShot roadmaps (Picture from Steckli 2011)

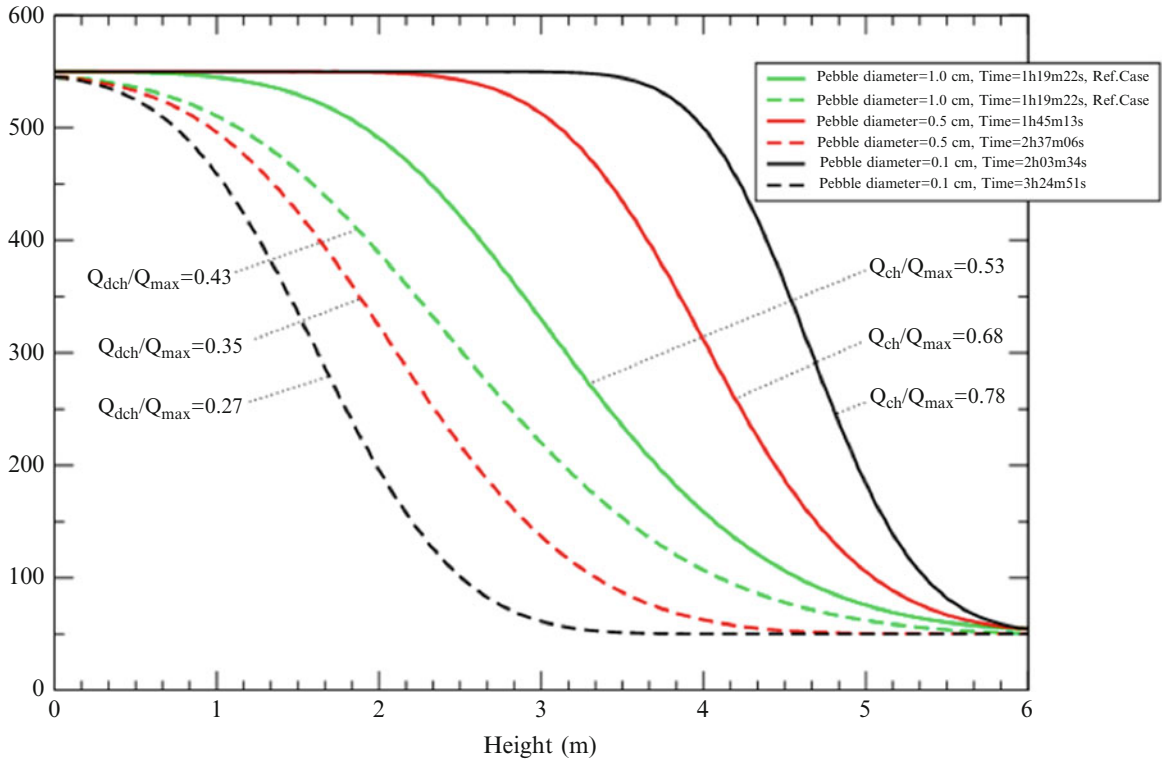

Fig. 12 Effect of pebble diameter on the amount of heat stored in a charge/discharge cycle. Smaller pebbles generate a steeper thermocline and an increase in the stored heat. Temperatures are in ordinate and tank length in abscissa. Q_{max}, maximum storable heat; Q_{ch}, stored heat; Q_{dch}, left heat (Picture from Pili et al. 2006)

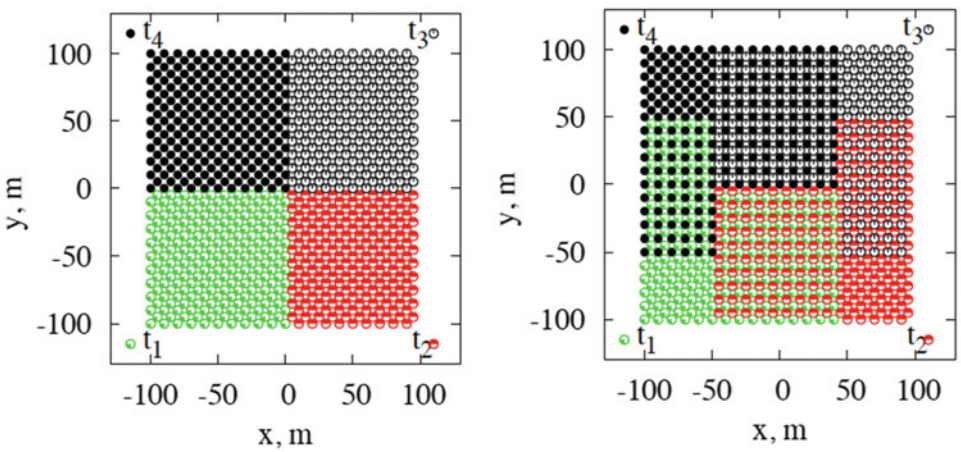

Fig. 13 Four towers system. Solar field in the "modular scheme" (*left*) and in the "alternate scheme" (*right*). The positions of the four two towers are indicated with the same symbols of the heliostats which reflect the sunlight toward them

In solar tower plants, the solar field can be made "cheaper" by coupling the solar field in a multi-tower system. In the paper of E. Leonardi (Leonardi 2013), three different ways of managing the heliostat in the field of multi-tower systems have been considered: (i) the modular scheme, where the solar field is partitioned into non-overlapping subfield around each tower (see Fig. 13 left); (ii) the alternate scheme, where the solar field presents overlapping regions of heliostats pointing to different towers (see Fig. 13 right); and (iii) the cosine scheme, where the heliostats are pointed toward the towers which allows the lower cosine effect. By evaluating the solar energy collected at the receivers placed at the top of the towers for the all year round, E. Leonardi (2013) found that the "alternate scheme" of a sixteen-tower system collects 15 % more energy than a single central tower system with a tower twice higher and that also reaches significantly higher peak power. In addition, the "cosine scheme" slightly increases the performances of the multi-tower system with respect to the "modular scheme" by using, however, higher towers and lower land coverage. The performance comparison of this system with a single central tower system with a very high

tower favors the multi-tower configuration, with an increase of the collected solar energy of about 11 % with respect to the single tower system. More R&D work is needed to fully exploit the optimization of the behavior of the heliostats for the all year along.

7 Conclusions

Concentrating solar energy technologies are recognized as belonging to those key technologies urgently needed to enforce the change from the economy based on fossil fuel to a new economy based on renewable energy. This belonging is worldwide recognized.

The main reasons of this recognition are the following:

- In nature, Sun energy is the most available renewable energy.
- Sun radiation arriving on a given land at a given time is one of the most predictable renewable energies.
- The concentration techniques allow the production of large amount of heat in an extended range of temperature, the upper limit being above 1,000 ºC.
- The easy access to heat in an extended range of temperature allows the coupling of CSP technologies with a huge number of specific applications, ranging from electricity production, seawater desalination, and solar fuel thermochemical production to heating and cooling of greenhouses and buildings, to name a few.
- The easy access to heat allows the coupling of CSP technologies with thermal energy storage (TES) systems overcoming, in this way, all problems connected with the intermittency of the solar radiation.
- Thanks to the coupling of CSP with TES, heat can be supplied to the final specific application in a continuous way, solving the problems connected with the dispatchability of renewable energies.
- The life-cycle assessment analysis shows that CSP technologies, as compared to other renewable energy technologies, have the lowest environmental impacts associated with all the stages of their production-disruption phases (from cradle to grave), specially for what concerns the use and consumption of rare elements.

The awareness of all these positive aspects has been the driving factor to push research activities in the field.

At the moment, R&D activities are focused on the following three groups of problems:

- Increasing efficiency and costs reduction
- Improving dispatchability
- Improving environmental profile

It is expected that the advancements induced by R&D activities, together with the know-how coming from the already realized CSP systems, will make CSP technologies competitive, as compared with any sort of corresponding system based on fossil fuels, within the next decade (≈2025).

Acknowledgments The financial support of the Sardinia Region Authority is gratefully acknowledged.

References

Butti, K., Perlin, J.: A Golden Thread: 2500 Years of Solar Architecture and Technology. Cheshire Books, Palo Alto (1980)

Cleveland, C.J.: Shuman, frank. www.eoearth.org/view/article/156005/ (2008). Accessed: 04/09/2013

EASAC: Concentrating solar power: its potential contribution to a sustainable energy future. EASAC policy report 16, Nov 2011. www.easac.eu/fileadmin/Reports/Easac_CSP_Web-Final.pdf (2013). Accessed: 02/08/2013

ESTELA: Strategic research agenda 2020–2025. ESTELA, Dec 2012. www.estelasolar.eu/fileadmin/ESTELAdocs/documents/Publications/ESTELA-Strategic_Reseach_Agenda_2020-2025_Summary.pdf (2013). Accessed: 02/08/2013

IEA: Technology roadmap – IEA 2010. www.iea.org/publications/freepublications/publication/csp_roadmap (2013). Accessed: 02/08/2013

IRENA: Renewable energy technologies: cost analysis series. concentrating solar power. www.irena.org/DocumentDownloads/Publications/RE_Technologies_Cost_Analysis-CSP.pdf (2013). Accessed: 02/08/2013

Ismail, K., Stuginsky Jr., R.: A parametric study on possible fixed bed models for pcm and sensible heat storage. Appl. Therm. Eng. **19**, 757 (1999)

Kongtragool, B., Wongwises, S.: A review of solar-powered stirling engines and low temperature differential stirling engines. Renew. Sust. Energ. Rev. **7**, 131–154 (2003)

Leonardi, E.: A systematic analysis of multi-tower systems. Technical report, CRS4 (2013). http://publications.crs4.it/pubdocs/2014/Leo14/

NovatecSolar: Novatec solar. www.novatecsolar.com/49-1-PE-1.html (2013). Accessed: 02/08/2013

Pili, P., Murgia, G., Varone, A., D'Aguanno, B.: Study of the efficiency of heat storage tanks for a single thermal charge-discharge cycle. Technical report, CRS4 (2006). http://publications.crs4.it/pubdocs/2014/Leo14/

Pitz-Paal, R., Dersch, J., Milow, B.: ECOSTAR-European Concentrated Solar Thermal Roadmapping. ECOSTAR 2005. www.promes.cnrs.fr/uploads/pdfs/ecostar/ECOSTAR.Roadmap.pdf (2013). Accessed: 02/08/2013

Schumann, T.: Heat transfer: a liquid flowing through a porous prism. J. Franklin Inst. **208**, 16 (1929)

Smestad, G., Ries, H., Winston, R., Yablonovitch, E.: The thermodynamic limit of light concentrators. Sol. Energy **21**, 99–111 (1990)

Sorenson, B., Breez, P.: "Renewable Energy". Focus Handbook. Academic Press, Oxford/San Diego (2009)

Steckli, J.: "DOE-CSP industry meeting": technical track recap doe-csp industry meeting, 9 Mar 2011. www1.eere.energy.gov/solar/pdfs/csp_sunshot_2011march_stekli.pdf (2011). Accessed: 02/08/2013

SunShot: SunShot Vision study – February 2012. www1.eere.energy.gov/solar/pdfs/47927.pdf (2013). Accessed: 02/08/2013
Walker, G.: Stirling Engines. Clarendon, Oxford (1980)
Welford, W.T., Winston, R.: The Optics of Nonimaging Concentrators. Light and Solar Energy. Academic, San Diego (1978)
Welford, W.T., Winston, R.: High Collection Non-Imaging Optics. Academic, New York (1989)
West, C.D.: Principles and Applications of Stirling Engines. Van Nostrand Reinhold, New York (1986)
Wikipedia: Solar energy generating systems. http://en.wikipedia.org/wiki/Main_Page (2013). Accessed 02/08/2013

Probiotics for Environmental Sanitation: Goals and Examples

Mikhail Vainshtein

Abstract

Bacterial probiotics are well-known paramedical tools to improve health and nutrition. These traditional applications are based on abilities of the probiotics to degrade complicated organic compounds and to suppress hazardous microorganisms in the intestinal tract. During the last decades, probiotic bacteria have been used also for sanitation of water for aquacultures. The chapter surveys possible application of probiotics in the environmental remediation. More specifically, utilization and sanitation of terrestrial wastes, especially manure and farm litter, with probiotic bacilli are discussed.

Keywords

Probiotic • Bacteria • Bacilli • Manuring • Remediation • Sanitation

1 Introduction

It is well known that the improvement of modern technologies results in an increase of production of wastes from all the industrial fields, including agriculture and farming.

In particular, cattle breeding, swine breeding, poultry, and any animal husbandry are related with increasing output of pollutants which include manure, guano, and bedding and litter mixed with the animal excrements. All these wastes contain organic matter enriched with biogenic elements (P, N, etc.), and as well, usually these pollutants are infected with some harmful enteric bacteria from the digestive tract of the animals. Historically, traditions of the European agriculture suggested utilization of the wastes for manuring, i.e., fertilization of soils with rich organic matter of dung and litter. Old traditional methods of natural digestion or composting proved to be insufficient, since it does not keep pace with the modern industrial scale of accumulation of the wastes. Increasing bulk of accumulating manure and litter threatens environment in total, and what is more, they serve as a possible source of spreading enteric bacteria (Dolgov 1984; Kisil 2007; Lysenko 2007).

Some modern biotechnologies suggested solution of the mentioned problems that involve new bacterial strains and/or microbial associations which are able to accelerate the organic matter recycling (Kovalev and Glazkov 1989; Zenikov 2006). One of these approaches consists of a microbial methane-containing gas mixture, known as biogas that is used in the same households as a source of energy (Ilyin 2005; Mironov et al. 2006). Another approach is related to the selection of microbial agents to speed up the decomposition process (Podgornov et al. 2009).

An additional problem in the utilization of these wastes is their sanitation. Manure and litter can contain not only enteric bacteria but, as well, some other hazardous groups of microorganisms. Natural digestion of the wastes does not provide a guaranty of disinfection. Introduction of antibiotics in the environment to suppress harmful microorganisms is not rational, and in some countries it is prohibited by laws and regulations to avoid appearance of

M. Vainshtein (✉)
Pushchino State Institute of Natural Sciences, Russian Academy of Sciences, Prospect Nauki 3 and 5, Pushchino, Moscow Region 142290, Russia

Institute of Biochemistry and Physiology of Microorganisms, Russian Academy of Sciences, Prospect Nauki 3 and 5, Pushchino, Moscow Region 142290, Russia
e-mail: vain@ibpm.pushchino.ru

G. Cao and R. Orrù (eds.), *Current Environmental Issues and Challenges*,
DOI 10.1007/978-94-017-8777-2_7,

antibiotic-resistant bacterial forms in the environment (Kümmerer 2008; De Knecht 2010). On the other hand, chemical treatment of waste is expensive, it does not provide complete disinfection, and, what is more, it prevents an active natural degradation of wastes (Gehan et al. 2009). Thus, the most promising utilization of organic pollutants combined with sanitation could be provided by those microbial strains which inhibit pathogenic bacteria. In this regard, significant potential interest is the search of helpful strains among probiotic cultures because of their ability both to degrade complex organic compounds and to suppress hazardous intestinal organisms (Li and Ni 2000).

Thus, study on utilization of litter and sanitation of polluted environment by bacterial probiotic strains is a modern upcoming trend of environmental microbiology and biotechnology.

2 Bacterial Probiotics for Nutrition and Sanitation

2.1 Definition of the Term

By the end of the nineteenth century, physicians and biologists proved that the intestinal microorganisms and their balance determine not only the presence/absence of infectious intestinal diseases but also the total human health. In recognition of the importance of the intestinal microbiota, there was even a popular term to describe it as an additional "invisible organ of the body" (Bogadelnikov and Vyaltseva 2011). In fact, different kinds of intestinal microorganisms may produce both positive and negative effects on metabolic processes in the host organism, and thus composition and stability of the microbiota shall determine health and growth of the host organism as a whole. The importance of the intestinal microbiota has led to artificial direct introduction of additional helpful microorganisms into the alimentary system. The cure with microbial cultures is especially important in case when a host organism is in short or limited with usual components of its intestinal microbiota (e.g., the host is a gnotobiont (Tlaskalová-Hogenová et al. 2011)). The intestinal microorganisms can be refunded with the help of additional bacterial mixtures ("bacterial cocktails"), the composition of which is selected by medical microbiologists for each patient individually. Health and weight of people and animals are highly dependent on the gut bacteria. A human being himself/herself cannot break down even cellulose of cucumber or chitin of mushrooms – all these processes are accomplished by intestinal bacteria. It was shown that intestinal bacteria affect also the nerve system and mood (Bravoa et al. 2011).

Microorganisms of intestinal biota are responsible for several different activities, namely:

1. Splitting of complex chemical compounds, foremost – ones which are not digestible or destroyed by the host – to easily digestible compounds.
2. Synthesis of vitamins, essential amino acids, and other valuable compounds.
3. Providing a constant presence of defensive bacteria which suppress any incoming dangerous pathogenic microorganisms.
4. Suppression of pathogenic forms can be carried out both directly by the intestinal microbiota and by strengthening the host immune system. The last thesis includes data showing that intestinal bacteria can enter the bloodstream and transferred inside the host organism. In this case, they can increase the total immune defense with no manifestation of a disease (Berdichevsky 2001).

Live microbial cultures, which are supplemented to enhance the intestinal microbiota in respect of the mentioned four activities, are called "probiotic(s)." Perhaps, the term "probiotic" in the literal sense of this word ("for life") is not the best choice, but it is accepted for decades (Parker 1974). The current variations in the definitions of probiotics depend on the position of the expert and the specific intended use: nutrition and feeding or medical purposes.

Accordingly, these are the following generalized definitions of the term "probiotic":

- Food supplement containing live bacteria or yeast that completes normal gastrointestinal microflora, given especially after its depletion caused by preliminary infection or effect of an antibiotic drug (American Heritage Dictionaries 2007)
- Useful bacteria used to colonize the intestinal tract (Jonas 2005)

Thus, probiotics are generally considered as a therapeutic tool to enhance the normal gastrointestinal microbiota. In livestock, they are used for the same purpose, but keep in mind primarily the increase in production (Core 2004). Application of probiotics to improve quality of the environment, for environmental remediation and sanitation, is clearly in progress in the last decades only. In this chapter these different applications of bacterial probiotics are compared.

2.2 Bacterial Probiotics for Medical Purposes

In the medical and paramedical literature, probiotics are suggested as a tool for treatment or prevention of any disease. The most known and most common probiotic bacteria belong to (1) bifidobacteria (genus *Bifidobacterium*), (2) lactic acid bacteria or lactobacilli (genus *Lactobacillus* and some species

Table 1 Microbial composition of probiotic preparations (information from official descriptions of preparations)

Name of preparation	Microorganisms/additions
Bifidumbacterin	*Bifidobacterium bifidum*
Lactobacterin	*Lactobacillus plantarum*
Colibacterin	*Escherichia coli* M-17
Bactisporin	*Bacillus subtilis* (*Paenibacillus subtilis*) 301
Bactisubtil	*B. cereus* Ir583t
Sporobacterin	*B. subtilis* 534
Bifilong	*B. bifidum*, *B. longum*
Bificol	*B. bifidum* 1 and *E. coli* M-17
Acilact	*L. acidophilus* 100 AIII, NKI, K3III24
Acipol	*L. acidophilus*/polysaccharide of kefir
Linex	*L. acidophilus*, *B. infantis*, *Enterococcus faecalis*
Biosporin	*B. subtilis*, *B. licheniformis*
Bifidumbacterin forte	*B. bifidum*/activated charcoal
Bifiliz	*B. bifidum*/lysozyme
BifiDoc	*B. bifidum*/complex of organic acids
Hylac forte	Complex of *E. coli* metabolites
Enterol	*Saccharomyces boulardii*

which were initially included into this genus), and (3) bacilli (genera *Bacillus* and *Paenibacillus*) capable of producing lactic acid (Table 1). Since the first two mentioned groups are endogenous to the human intestinal microbiota, they were used as probiotics initially and most commonly in the form of some soured or fermented milk beverages (kefir, yogurt, etc.) and later as preparations in the form of bacterial lyophilized biomass. One of the beneficial properties of probiotics is a good fixation to the epithelium of the intestinal mucosa that ensures a stable colonization and competitive inhibition of adhesion of pathogenic microorganisms.

An example of a well-studied probiotic for humans is represented by bifidobacteria (Pikasova 2009). Indeed, they are active producers of lactic and acetic acids and suppress the spoilage and enteric bacteria (*Salmonella*, etc.) both via competition for substrates and with acidification. In addition, bifidobacteria produce metabolites which have a direct inhibitory effect on some pathogens (Ivanova 2010).

The most recent publications showed that the medical role of probiotics is much wider than the opposition of intestinal infectious diseases; they provide the state of the organism as a whole (Million et al. 2013; Murphy et al. 2013). A similar suggestion was published by the founder of immunology E. Metchnikoff in 1903 (Metchnikoff 2010). He believed that aging is an accumulated result of putrescent products of the intestinal microbiota and suggested that any "old age" and senile decrepitude are just consequence and effect of the harmful agent assemblage in the host body, and a scale of this accumulation is proportional to the time of the life. E. Metchnikoff made some investigations and statistics for centenarians and concluded that all humans could live at least up to 150 years. He was enough logical to assume that this harmful agent is presented by putrefactive bacteria in the intestines, and as well, he proposed to include lactobacilli with the sour milk products into the diet as a method to suppress intestinal spoilage and, accordingly, to increase longevity.

Publications of different scientists throughout the years highlighted some possibility of bacteria to shift from the intestine into the body. These works were analyzed by B. Berdichevsky (2001) who examined the "autoinfection" not only as a seeming pathogenic process but also as a common symbiotic defense against other incoming microorganisms. He showed that bacteria, which had been labeled with tritium (^{3}H), penetrated from the rat intestinal tract into the kidneys and translocated into the newborn skin on the healing up wound.

Thus, the intestinal microbiota not only provides digestion of complicated compounds and inhibits pathogens, but it also changes the state of the host organism. Possible bacterial spreading from the intestinal tract into the host body is a basis for new sight on role of probiotics.

2.3 Probiotics in Aquaculture Sanitation

Similar to the application for human health and nutrition, probiotics are widely used to increase the livestock by improving balance of the digestive animals. For cattle, the lactic acid bacteria were used historically in silage. Particular attention was paid to the application of probiotics in aquacultures where they generally provide a more rapid increase of production than, for example, in cattle (10 % versus 3 %). In 1980 K. Yasuda and N. Taga proposed to use probiotic bacteria both as a food additive for fish and as an agent against fish diseases (Yasuda and Taga 1980). Typical well-known probiotics for aquaculture are represented by bacteria of the genera *Lactobacillus*, *Vibrio*, *Bacillus*, and *Pseudomonas*, and they provide major advantages due to the suppression of pathogenic bacteria. The application of bacterial probiotics replaced the use of antibiotics. For example, application of probiotic *Carnobacterium divergens* for Atlantic salmon and rainbow trout decreased the number of pathogenic *V. anguillarum* and *Aeromonas salmonicida* from 10^5 to 10^2 CFU (colony-forming units)/g of feces in 3 days (Balcázar et al. 2006; Verschuere et al. 2000).

In 1992, bacterial strain *Vibrio alginolyticus* was used as a probiotic in shrimp farming in Ecuador, and its application increased profit in the shrimp larvae production up to four times (Grifftih 1995). In contrast, chemical disinfectants and antimicrobial compounds gave little result in the disease control and resulted in the emergence of some new pathogens resistant to these agents. Thus, the problem was solved with introduction of new component into the

ecosystem, where new probiotic habitants affected as bacterial antagonists. Food and Agriculture Organization (FAO) has already recognized that application of probiotics is one of the main methods for improving production and development of aquaculture while maintaining environmental safety.

There is a fundamental difference in the use of probiotics for aquaculture compared with any animal breeding: the introduced bacteria act not only on the digestive tract but also on the whole water environment. Pathogenic microorganisms in aquatic environments can be located not only in the digestive system of the host organism (shrimp, fish) but inhabit and remained in high concentrations outside. These bacteria can easily penetrate into the host organism with coming water. That is why the use of probiotics is particularly important for filter-feeding invertebrates (shrimp) and for the fish in the larval stage.

Industrial aquaculturing is affiliated with risks of diseases of fishes, shrimps, etc., and with deoxygenation of water resulted in loss of yield. Massive development of putrefactive bacteria in shrimp ponds leads both to decrease of the shrimp crop and to their death. Usually, this mortal suffocation is accompanied with change of color of the bottom sediments (pond soils) from yellow/brown to black that is an indicator of anaerobic conditions produced via sulfide iron production. In these cases, the added probiotic bacteria inhibited the hazardous anaerobic bacteria (Farzanfar 2006) and provided sanitation of the ponds (Mayer et al. 2012). Application of probiotics and biodegrading microorganisms to the pond is a sustainable approach to minimize the environmental impact of aquaculture. These experiments showed that the strain *Paracoccus pantotrophus* 768 is able to reduce undesirable waste compounds and had a positive impact on pond soil quality. A field study using a commercial probiotic product (2×10^9 CFU/g) containing the abovementioned strain 768 was conducted during intensive farming of white shrimp *Litopenaeus vannamei* to effect environment quality in a commercial pond. The trial was carried out for 57 days with a dosage of 600 g/ha applied every 5 days. It was confirmed that the ponds with the bacterial supplement reached better environmental conditions and enhanced shrimp parameters. Average daily growth of shrimps with the probiotic treatment was improved up to 36 %.

During the performed experiments (Sklyarov et al. 2004), we proved effect of probiotic on the fish eggs and the larvae of the endogenous nutrition (Tables 2 and 3). Obviously, positive effects in these stages could not be affiliated with the alimentary tract but with the surface of the body and the water quality only. The obtained results mean that use of probiotics in aquaculture is important not only for nutrition as the target in the host organisms but also for the rehabilitation of water in whole (Verschuere et al. 2000).

Table 2 Effect of the probiotic *B. subtilis* on the carp fertilized spawn (Sklyarov et al. 2004)

	Larvae yield, % (number of surviving)		
Spawn, g	Probiotic	Blank	*d*, %
500	86	71	+15
500	74	58	+16
450	97	73	+24
450	90	74	+16
350	18	12	+6

Thus, there are no doubts that probiotic bacteria can carry out their functions to suppress pathogens and improve the treated environment both within and, as well, outside of the host organism in the aquatic ecosystems. Obviously, this trend may represent a significant biotechnological approach for treatment of the terrestrial environments too.

2.4 Bacterial Sanitation and Utilization of Poultry Litter and Manure (Our Proprietary Experimental Data)

We studied the possibility to use probiotic bacilli for sanitation and utilization of the poultry farm litter and manure in special experiments. In the first stage, we checked the distribution of enteric bacteria in the different layers of the bedding. Next, we tested the possibility of suppression of enteric bacteria in the model bedding samples which have been artificially infected with *E. coli* and *Salmonella enteritidis*. Finally, we compared utilizing activities of different commercial biopreparations and probiotic strain.

The total number of microorganisms in the exhausted bedding was presented with billions of colony-forming units (CFU) per 1 g (Table 4), which generally is normal for the bedding contaminated and enriched with litter. Coliform bacteria (*E. coli*) were counted by the CFU number on the Chromocult Coliform Agar, and the *Salmonella* CFU were counted on the chromogenic nutrient Rambach Agar by their indicative color, while the spore-forming acid-producing bacteria ("*B. subtilis*-like bacilli") CFU were counted on the Dextrose Casein-Peptone Agar in accordance with changing of the pH indicator color. To be sure that the last enumeration includes the spore-forming bacteria only, the inoculum was injected directly into the melted hot medium. Table 4 presents the distribution of the enumerated groups in three different layers of the exhausted bedding. Only two studied samples (Table 4, Nos. 3 and 9) contained *E. coli*-type colonies; all other enteric bacteria were presented with the *Salmonella* type. In the most cases, the enteric bacteria were discovered in the lowest layer only. In contrast, acidifying spore-forming bacteria were absent or were scared in the lower layers: as a rule,

Table 3 Effect of the probiotic *B. subtilis* on the crucian fertilized spawn and larvae (Sklyarov et al. 2004)

		Result: number of surviving fishes, %			
		Probiotic suspension, ml per 1,000 fishes			
Fish form	Stage to treat with the probiotic suspension	0 ml (blank)	5 ml	10 ml	15 ml
Spawn	1.5 h after beginning of incubation	27	65	75	77
Larvae	Change to exogenous feed	27	59	74	75
Larvae	10 days after change to exogenous feed	27	36	40	45

Table 4 Numbers and distribution of bacteria in the samples of the poultry bedding

Nos.	Chicken group	Bedding layer	Total number, 10^9 CFU/g	Number of coliform bacteria, 10^6 CFU/g	Number of acidifying spore-forming bacilli, 10^6 CFU/g
1	1	Upper	**10.6**	<0.1	**10.0**
2		Middle	2.5	0.2	0.7
3		Lowest	3.2	**40.0**	<0.1
4	2	Upper	3.0	<0.1	<0.1
5		Middle	5.5	<0.1	3.2
6		Lowest	4.3	**16.0**	0.5
7	3	Upper	**11.0**	<0.1	0.5
8		Middle	0.9	<0.1	0.7
9		Lowest	10.8	**34.0**	<0.1
10	4	Upper	1.4	<0.1	2.6
11		Middle	0.6	<0.1	<0.1
12		Lowest	1.8	**43.0**	2.7
13	5	Upper	**11.5**	<0.1	**10.0**
14		Middle	1.1	<0.1	0.4
15		Lowest	4.7	**20.0**	0.1
16	6	Upper	**8.0**	<0.1	2.0
17		Middle	4.8	<0.1	**10.0**
18		Lowest	2.2	**50.0**	5.0

The maximum numbers are in bold

Table 5 Ratios of bacterial number in the upper layer to bacterial number in the lower layer of the poultry bedding

		Ratio of the CFU number in the upper layer to the CFU number in the lower layer	
Group	Cage	Coliform bacteria	Acid-forming bacilli
2	1	0	350
2	2	2.5	0.25
2	3	0	175
3	1	0	2,000
3	2	0	10
3	3	0	200

The data presented are for enteric bacteria and acidifying bacilli

they were located in the top layer. Such distribution may be due to a large access of air to the upper layer of litter and drawback in the bottom. Accordingly, the greater the number of acidifying bacilli, the lesser the number of enteric bacteria (Table 5).

To avoid unevenness in the bacteria distribution and irregularity in the bedding composition, we studied the forthcoming suppressing effect of the probiotic acidifying bacilli on the model samples of unused bedding, which had been infected with *E. coli* O115 or *S. enteritidis*. The probiotic bacilli were presented with the strains *B. subtilis* and *B. licheniformis* from Provimi Corp., Moscow, and *B. polymyxa* B-514 from All-Russian Collection of Microorganisms (VKM). Results of the number relation of the enteric bacteria and the mentioned bacilli in 4 days under the modeled conditions – with nutrients and under air – are presented in the diagrams (Fig. 1). There are no doubts that probiotic bacteria can provide sanitation of litter (in our case – exhausted poultry bedding) by suppressing hazardous enteric bacteria. The specific bacterial agent has to be chosen for the treatment according to the composition of the litter and to the autochthonous pathogens.

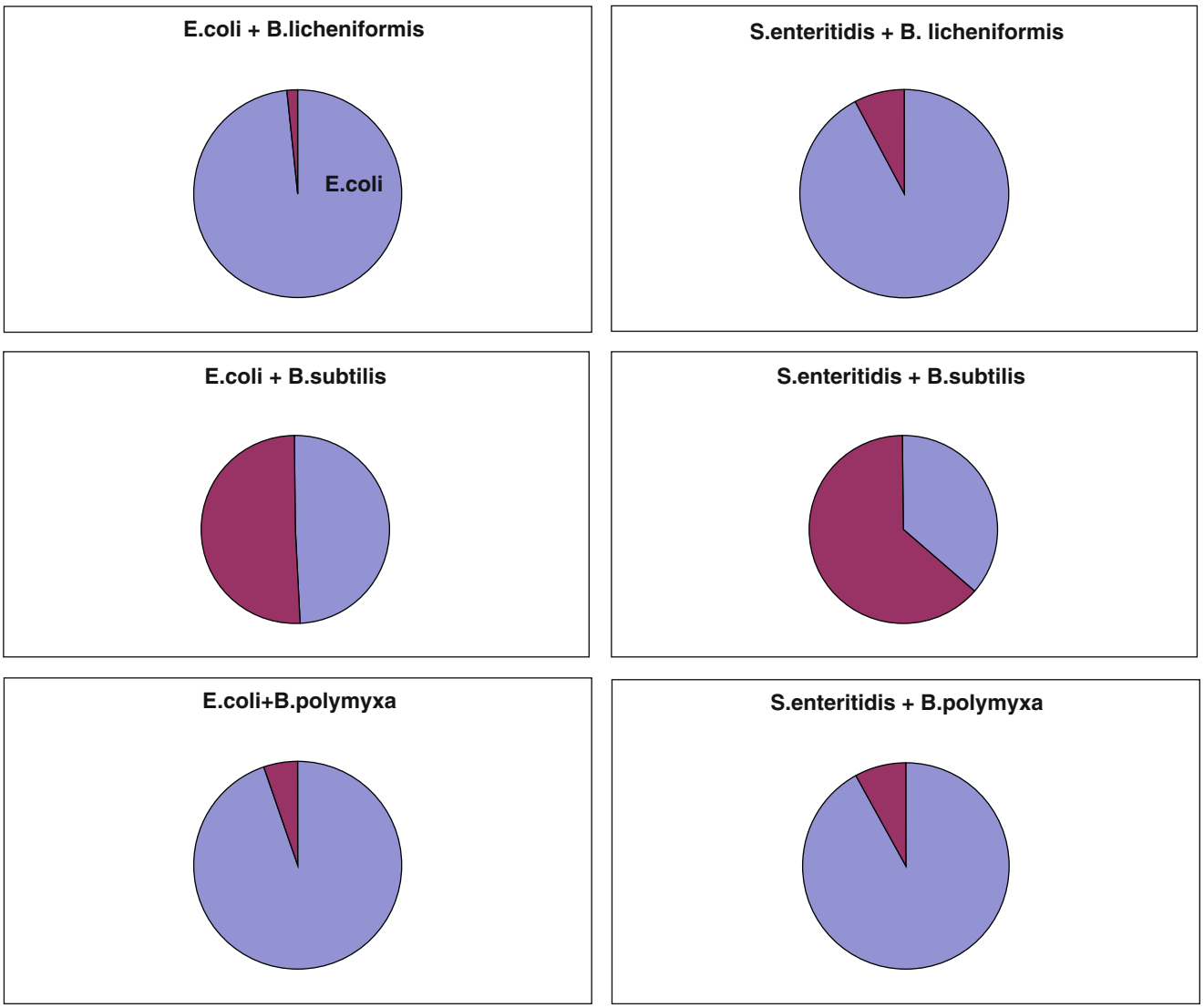

Fig. 1 Ratios of bacilli (*red*) and enteric bacteria (*blue*) in the infected samples in 4 days of their combined growth in model experiments. The data compared the numbers of the viable cells

Sanitation is one side of the whole remediation process, and the other one is utilization of the wastes. The ideal degradation of organic pollutants is a complete oxidation of the matter to carbon dioxide. In this case, we can evaluate the degradation level by the weight loss. Accordingly, we studied a possible role of the probiotic strains in utilization of the model (unused) bedding. The results showed that active utilization of the bedding by probiotic bacteria needed more than 3 weeks at room temperature and exceeded 10 % in 1 month (Table 6).

Exhausted bedding is just a kind of great output of poultry and cattle wastes where the most problematic pollutants are affiliated with animal excrements. There are numerous commercial biopreparations oriented to improve soils and to restore the contaminated and polluted sites. Some of these preparations (e.g., commercial one "Baikal EM1" or "EM – Effective Microorganisms," see Table 6) suggested to present all kinds of probiotic properties (Higa and Parr 1994; Yamada and Xu 2001; Szymanski and Patterson 2003). We proved the effectiveness of different commercial biopreparations in comparison with the probiotic strain *Bacillus sp.* (by the courtesy of A. Repina). It was shown that in a week some commercial preparations and the probiotic strain *Bacillus sp.* increased the rate of degradation of the poultry manure about twice comparatively to natural process (Table 7). However, the non-fresh samples of cattle dung were too complicated for most of the preparations, and just the probiotic strain and "Biokompostin" exceeded the level in a week (Table 8). There are no doubts that different strains (preparations) will produce different effects depending on the composition of the manure and its autochthonous microbiota. Meanwhile, the presented data are an evidence

Table 6 Decrease of the bedding weight affected by its inoculation with bacterial cultures

	Change of the bedding weight, % from the initial weight			
Exposure interval, days	*Bacillus sp.* (*mucilaginosus*)	*Bacillus subtilis*	*Bacillus licheniformis*	Preparation "Baikal EM1"
0	0	0	0	0
10	−3.5	+1.5	−2.0	+0.5
21	+1.0	0	−1.0	−3.0
27	−3.0	−9.5	−4.5	−8.0
33	−13.5	−16.0	−11.0	−14.0

Table 7 Degradation of the poultry manure by *Bacillus sp.* and by commercial preparations

		Decrease in weight in 6 days			
Degrading agent (commercial titles of preparations are in capital letters)	Poultry manure: initial weight, g	g	%	g/day	%/day
– (blank)	15.0	2.3	15.33	0.38	2.56
Bacillus sp.	15.0	4.0	26.67	0.67	**4.44**
BIOFORCE SEPTIC	15.0	2.2	14.67	0.37	2.44
ROEBIC	15.0	4.2	28.00	0.70	**4.67**
SANEX	15.0	2.7	18.00	0.45	3.00
SCHASTLIVYI DACHNIK, SEPTIC SYSTEM MAINTAINER DWT-360	15.0	4.6	30.67	0.77	**5.11**
SCHASTLIVYI DACHNIK, BIOKOMPOSIN BK	15.0	4.8	32.00	0.80	**5.33**

The maximum numbers are in bold

Table 8 Degradation of the cattle manure by *Bacillus sp.* and by commercial preparations

Degrading agent (commercial titles of preparations are in capital letters)	Cattle manure: initial weight, g	Exposition, days	Decrease in weight, g	Decrease in weight, g/day	Decrease in weight, %/day
– (blank)	18.0	13	2.4	0.185	**1.0**
Bacillus sp.	15.0	13	3.5	0.269	**1.8**
BIODESANT	28.0	8	0.0	0.0	0.0
ROEBIC	21.0	8	1.0	0.125	0.6
SANEX	18.0	8	1.0	0.125	0.7
SCHASTLIVYI DACHNIK, SEPTIC SYSTEM MAINTAINER DWT-360	21.0	8	0.0	0.0	0.0
SCHASTLIVYI DACHNIK, BIOKOMPOSIN BK	19.0	8	2.0	0.250	**1.3**

The maximum numbers are in bold

that probiotic bacteria can be used not only for purposes of improvement of health in the digestive tract of different living creatures, but they could provide a health of the treated environment in whole.

3 Discussion and Suggestions

It was mentioned above that selection and choice of probiotic species and strains shall be an individual work for each treated object accordingly to its nature. Introduction into the bowels suggests that these bacteria are affected with acid of gastric juice. By this reason, a special attention was dedicated to spore-forming bacteria which can be introduced into the host organism as spores, i.e., without loss because the spores are not injured with the gastric acid.

Some of these spore-forming strains have additional advantages: they inhibit hazardous bacteria because they produce specific antagonistic compounds. There are East countries that in their cuisine traditionally preserved their food using sour-producing fermentation. The milk-soured food includes not only the fermented milk beverages but sour-fermented vegetables too. For example, soybeans fermented with the spore-forming bacilli are a popular food in China as "Dajiang," in Japan as "Natto," and in Korea as "Doenjang." In scientific literature, this fermenting industrial group of bacteria was published usually under the name *Bacillus subtilis natto*. Recently the medical benefits of the Natto have become widely recognized in Japan, resulting in its increased popularity. Some of the Natto's beneficial effects are preventions of heart attacks, strokes, cancer, osteoporosis, obesity, and intestinal diseases caused by pathogens. The bacterium *B. subtilis natto* produces various enzymes, vitamins, amino acids, and other nutrients during the fermentation; nattokinase and pyrazine prevent or resolve blood clots (Fujita et al. 1993). The *B. subtilis* probiotics produce digestive enzymes (proteolytic, amylolytic, lipolytic, pectinolytic) and biologically active compounds (lysine, histidine, valine,

threonine, glutamate, tyrosine, ornithine, alanine). As well, the probiotics based on these bacilli inhibited wide spectra of hazardous bacteria and fungi (including *Salmonella*, *Escherichia*, and other enteric bacteria).

Bacilli in the commercial probiotics can be presented mostly by spores. Survival of the spores at high temperature and under unfavorable conditions and long-term storage provide their commercial preference. The abovementioned examples of the bacillary probiotics in medical and animal breeding practice showed that the listed properties are helpful. Our proprietary experimental data witnessed that this group of probiotics can be applied, as well, for sanitation of environment.

References

American Heritage Dictionaries: The American Heritage Medical Dictionary. Houghton Mifflin Company, Boston (2007)

Balcázar, J.L., de Blas, I., Ruiz-Zarzuela, I., Cunningham, D., Vendrell, D., Múzquiz, J.L.: The role of probiotics in aquaculture. Vet. Microbiol. **114**(3–4), 173–186 (2006)

Berdichevsky, B.: Autobakteria. Stress and a Person (An Anthology of One Observation) (in Russian), p. 410. Meditsinskaya Kniga, Moscow (2001)

Bogadelnikov, I.V., Vyaltseva, Y.V.: Microbiota – an invisible organ of the human organism (in Russian). Zdorovie Rebenka **8**(36), 113–122 (2011)

Bravoa, J.A., Forsythe, P., Chew, M.V., Escaravage, E., Savignac, H.M., Dinan, T.G., Bienenstock, J., Cryan, J.F.: Ingestion of Lactobacillus strain regulates emotional behavior and central GABA receptor expression in a mouse via the vagus nerve. Proc. Natl. Acad. Sci. U.S.A. **108**(38), 16050–16055 (2011)

Core, J.: Probiotics protect poultry from pathogens. Agricultural Research Magazine **52** (1) (2004). http://www.ars.usda.gov/is/ar/archive/jan04/biotic0104.pdf

De Knecht, J. (Chairman): Pharmaceuticals in the environment. Results of an European Environment Agency Workshop. EEA Technical Report No. 1. EEA, Copenhagen, 29p. (2010)

Dolgov, V.S.: Hygiene of Cleaning and Utilization of Manure (in Russian), p. 175. Rosselkhozizdat, Moscow (1984)

Farzanfar, A.: The use of probiotics in shrimp aquaculture. FEMS Immunol. Med. Microbiol. **48**(2), 149–158 (2006)

Fujita, M., Nomura, K., Hong, K., Ito, Y., Asada, A., Nishimuro, S.: Purification and characterization of a strong fibrinolytic enzyme (nattokinase) in the vegetable cheese natto, a popular soybean fermented food in Japan. Biochem. Biophys. Res. Commun. **197**(3), 1340–1347 (1993)

Gehan, Z.M., Anwer, W., Amer, H.M., El-Sabagh, I.M., Rezk, A., Badawy, E.M.: In vitro efficacy comparisons of disinfectants used in the commercial poultry farms. Int. J. Poultry Sci. **8**(3), 237–241 (2009)

Grifftih, D.R.W.: Microbiology and the role of probiotics in Ecuadorian shrimp hatcheries. In: Lavens, P., Jaspers, E., Roelants, I. (eds.) Abstracts of Larvi'95, Fish and Shellfish Larviculture Symposium, p. 478. European Aquaculture Society (Special Publication No. 24), Ghent (1995)

Higa, T., Parr, J.: Beneficial and Effective Microorganisms for a Sustainable Agriculture and Environment, p. 7. International Nature Farming Research Center, Atami (1994)

Ilyin, S.N.: Resource-saving technology of swine manure recycling with biogas manufacture (in Russian). Thesis. Cand. Tech. Sci. (PhD), Ulan-Ude (2005)

Ivanova, E.V.: Biological features of bifidum bacteria and their interaction with microsymbionts of human intestinal microflora (in Russian). Thesis Cand. Med. Sci. (PhD), Orenburg (2010)

Jonas, W.B.: Mosby's Dictionary of Complementary and Alternative Medicine. Elsevier, San Francisco (2005)

Kisil, N.: Ways of manure recycling (in Russian). Poultry Farming **8**, 48–50 (2007)

Kovalev, N.G., Glazkov, I.K.: Engineering of Manure Utilization Systems in Complexes (in Russian), p. 160. Agropromizdat, Moscow (1989)

Kümmerer, K.: Antibiotics in the environment. In: Pharmaceuticals in the Environment. Sources, Fate, Effects and Risks, pp. 75–93, 334p. Springer, Berlin/Heidelberg (2008)

Li, W., Ni, Y.: Use of probiotics to suppress mal-odors of poultry manure. J. Crop. Prod. **3**(1(15)), 215–221 (2000)

Lysenko, V.: Waste recycling in poultry farming – a way to the complex decision of bird influenza problem (in Russian). Ptitsefabrika **6**, 32–35 (2007)

Mayer, E., Gössl, E.M., Santos, G.A., Mohnl, M.: Bioremediation with probiotics in shrimp farming. Environm. Engineer. Manag. J. **11**(3 Suppl), S18 (2012)

Metchnikoff, E.: Etudes Sur La Nature Humaine: Essai de Philosophie Optimiste, 418p. Kessinger Publishing, United States (in French) (2010)

Million, M., Lagier, J.C., Yahav, D., Paul, M.: Gut bacterial microbiota and obesity. Clin. Microbiol. Infect. **19**(4), 305–313 (2013)

Mironov, V.F., Minzanova, S.T., Mindubaev, A.Z., Skvortsov, E.V., Mironova, L.G., Konovalov, A.I., Ryzhikov, D.V.: Method to increase biogas production. Patent RU 2351552 (in Russian) (2006)

Murphy, E.F., Cotter, P.D., Hogan, A., O'Sullivan, O., Joyce, A., Fouhy, F., Clarke, S.F., Marques, T.M., O'Toole, P.W., Stanton, C., Quigley, E.M., Daly, C., Ross, P.R., O'Doherty, R.M., Shanahan, F.: Divergent metabolic outcomes arising from targeted manipulation of the gut microbiota in diet-induced obesity. Gut **62** (2), 220–226 (2013)

Parker, R.B.: Probiotics, the other half of the antibiotic story. Anim. Nutr. Health **29**, 4–8 (1974)

Pikasova, O.V.: A new approach to the molecular diagnostics of bifidum bacteria (in Russian). Thesis. Cand. Biol. Sci. (PhD), Moscow, MSU (2009)

Podgornov, P.A., Ufimtseva, N.F., Anaprienko, T.R.: Method to convert poultry manure and swine dung to organic fertilizer. Patent RU 2409537 (in Russian) (2009)

Sklyarov, V.Y., Mikryakov, V.R., Kulakov, G.V., Kudryashova, E.B., Vainshtein, M.B.: Prospects of preparation application of "Subtilis" probiotics in piscatology for cultivation of fish spawn, embryos, and larvae on the examples of crucian Carassius carassius and carp Cyprinus carpio (order Cypriniformes, family Cyprinidae) (in Russian). Voprosy Rybolovstva **5**(3 (19)), 514–521 (2004)

Szymanski, N., Patterson, R.A.: Effective Microorganisms (EM) and wastewater systems in future directions for on-site systems: best management practice. In: Patterson, R.A., Jones, M.J. (eds.) Proceedings of On-site '03 Conference, pp. 347–354. Lanfax Laboratories, Armidale (2003)

Tlaskalová-Hogenová, H., Štěpánková, R., Kozáková, H., Hudcovic, T., Vannucci, L., Tučková, L., Rossmann, P., Hrnčíř, T., Kverka, M., Zákostelská, Z., Klimešová, K., Přibylová, J., Bártová, J., Sanchez, D., Fundová, P., Borovská, D., Šrůtková, D., Zídek, Z., Schwarzer, M., Drastich, P., Funda, D.P.: Gut microbiota (commensal bacteria) and mucosal barrier in pathogenesis of inflammatory, autoimmune diseases and cancer: contribution of germ-free and gnotobiotic models of human diseases. Cell. Mol. Immunol. **8**, 110–120 (2011)

Verschuere, L., Rombaut, G., Sorgeloos, P., Verstraete, W.: Probiotic bacteria as biological control agents in aquaculture. Microbiol. Mol. Biol. Rev. **64**(4), 655–671 (2000)

Yamada, K., Xu, H.: Properties and applications of an organic fertilizer inoculated with effective microorganisms. J. Crop Prod. **3**(1), 255–268 (2001)

Yasuda, K., Taga, N.: A mass culture method for Artemia salina using bacteria as food. Mer (Bull. Soc. Franco-Jap. Oceanogr.) **18**, 53–62 (1980)

Zenikov, V.I.: Method to prepare compost. Patent RU 2462439 (in Russian) (2006)

Dust Removal and Collection Techniques

Mostafa Maalmi

Abstract

In this chapter, dust elimination, which is an operation for the separation of solid particles from a gas carrier, will be addressed. In particular, the devices which are used in such an operation, i.e., scrubbers or dust separators, will be analyzed and discussed from several points of view.

Keywords

Mechanical separators • Wet scrubbers • Gas-solid filtration • Bag filters • Electrostatic filters

1 Preface

Nowadays, requirements and limitations of dust concentrations in the air are more and more stringent mainly for health and environmental reasons. At the industrial level, dust removal can be for compliance with environmental laws and for the preservation of citizen's health, but may have also an economic objective. Indeed, in many industry sectors (mining, cement, chemical industry, etc.), it is often necessary to recover much of the fine dust of the solid being treated or produced, otherwise this solid will be lost and the performance of transformations or processes will be low. The principles of the techniques used for recovery or disposal of dust and fine solid particles have not changed very much over the years. There are mainly two families of dust removal systems: Those that enable the recovery of the solid, such as sedimentation or decanting for coarse particles, and filtration by dry electrostatic precipitator or baghouses for fine particles. The second family of techniques does not allow the recovery or recycling of the solid, wet scrubbers (venturi and cyclones), as the solid is recovered as sludge of solid-liquid mixture. In this second case, the recovery of the solid can only be done after separation of the solid-liquid phase, but this is not usually done on the industrial level for fine solid particles, for technical and economical reasons.

Dust elimination or collection is an operation for the separation of solid particles from a gas carrier. The devices used in such an operation are called scrubbers or dust separators. There are different types of scrubbers depending on the separation mechanism involved. Dust collectors can be grouped into four distinct classes:

- Mechanical separators
- Wet scrubbers
- Electrostatic precipitators
- Bag filters

The study and rational choice of dust elimination system depend, in addition to the technical and economic aspects, on the gas-solid suspension nature, namely:

- Dust characteristics: particle size, composition, density, shape and surface area, chemical composition, the falling speed, and concentration
- Characteristics of the gas carrier: velocity, temperature, pressure, and chemical composition

The first section of this chapter will deal with mechanical separators and wet scrubbers. Electrostatic precipitators and bag filters will be discussed in the second section.

M. Maalmi (✉)
Department of Industrial Processes Engineering, Ecole Nationale de l'Industrie Minérale, Rue Hajj Cherkaoui, B.P 753, Agdal Rabat, Morocco
e-mail: maalmi@enim.ac.ma; mostafa.maalmi@yahoo.com

G. Cao and R. Orrù (eds.), *Current Environmental Issues and Challenges*,
DOI 10.1007/978-94-017-8777-2_8,

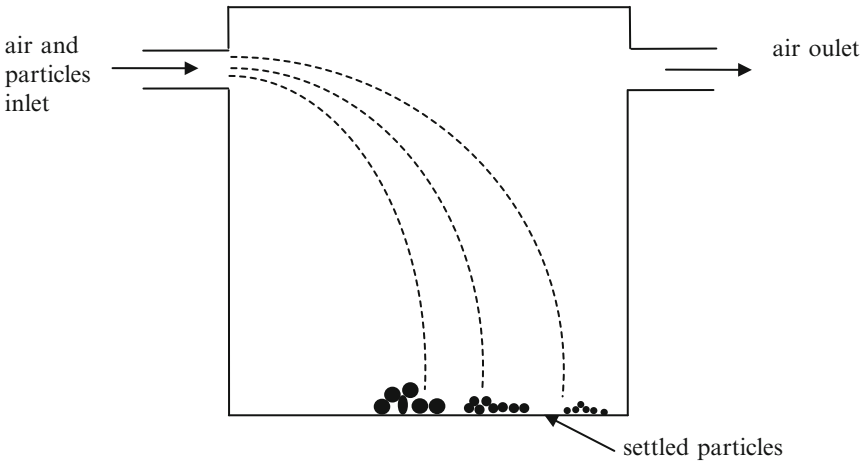

Fig. 1 Schematic representation of a settling chamber

2 Mechanical Separators and Wet Scrubbers

2.1 Mechanical Separators

Mechanical separators are used, primarily, to precipitate particles larger than 5 μm present in the gas to be treated by the following mechanical forces:

- Gravity
- Inertia
- Centrifugal force

Depending on the importance of one of these forces, three types of mechanical separators are considered:

- Settling chambers
- Inertial devices
- Cyclones

2.1.1 Settling Chambers

They are characterized by the existence of chambers where the flow rate of gas is minimized, so the particles are deposited by the action of gravity, minimizing re-entrainment (Fig. 1).

Settling chambers are generally horizontal and rectangular with a single input and a single output. The key parameter used to determine the size of a sedimentation chamber and the cut diameters (the smallest particle that can be captured) is the falling velocity.

2.1.1.1 Acting Forces

The forces involved in settling systems are mainly the force of gravity G and the resistance to movement of the particle in the fluid F, given by the following relationships:

$$F = C_D\left(\frac{\rho u^2}{2}\right)A_p \tag{1}$$

$$G = g\left(\frac{\pi d^3}{6}\right)(\rho_P - \rho_g) \tag{2}$$

The meanings of the symbols used in previous equations are reported below:

ρ_P: density of solid particles
ρ_g: density of gas
A_p: the particulate surface projected onto a plane perpendicular to the direction of motion, for a sphere, $A_p = (\pi d^2/4)$
d: solid particle mean diameter
g: gravity acceleration
u: flow velocity
C_D: drag coefficient

A schematic representation of a typical settling chamber is reported in Fig. 1.

Drag coefficient is a function of Reynolds (relative to the particle). On the basis of the flow regimes, the correlations useful for the calculation of this parameter are reported in the literature. In particular, for their practical aspects, the following correlations are worth citing:

Lamb (1945):

$$C_D = (24/Re)(1 + 3Re/16), \quad Re \leq 1 \tag{3}$$

- Allen (1900):

$$C_D = \left(10/Re^{1/2}\right), \quad (30 \leq Re \leq 300) \tag{4}$$

- Schiller and Naumann (1933):

$$C_D = (24/Re)\left(1 + 0.15Re^{0.687}\right), \quad 0.5 \leq Re \leq 800 \tag{5}$$

- McCabe et al. (1993):

$$C_D = a/Re^b \tag{6}$$

with $2 \leq Re \leq 500$, $a = 18.5$ and $b = 0.6$

$$500 \leq Re \leq 2.10^5, \quad a = 0.44 \text{ and } b = 0$$

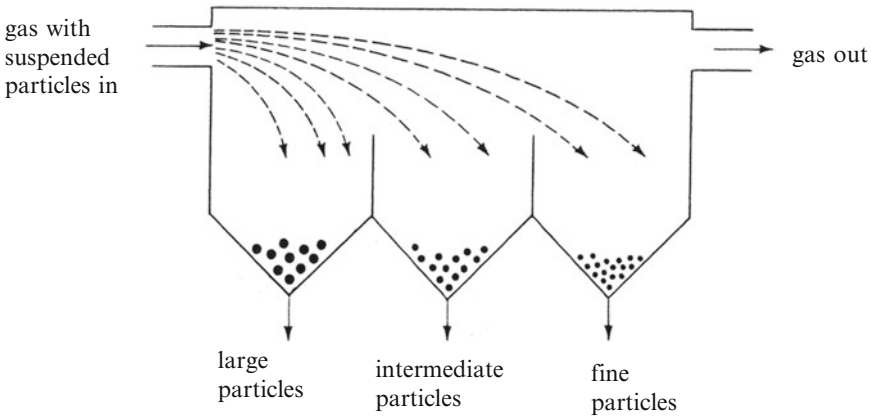

Fig. 2 Schematic representation of a sedimentation chamber with vertical baffles

2.1.1.2 Falling Velocity

For particles larger than 1 mm or Reynolds "particle" number greater than 1,000, the falling velocity is calculated by the Newton's law, equating forces F and G, as follows (with $C_D \sim 0.5$):

$$v = \sqrt{\frac{8gd(\rho_p - \rho_g)}{3\rho_g}} \tag{7}$$

On the other hand, for particles smaller than ~80 μm, the falling velocity is calculated using the Stokes' law (with $C_D = 24/Re$) through the following relationship:

$$v = \frac{d^2(\rho_p - \rho_g)g}{18\eta_g} \tag{8}$$

where d is the particle diameter and η_g the gas viscosity.

Equation 8 is typically applied as long as Reynolds number of the particles does not exceed the value of 1. For Reynolds numbers between 1 and 1,000, the sedimentation rate is given by the following relationship:

$$v = \left[2.32d^{1.6}(\rho_p - \rho_g)\rho_g{}^{-0.4}\eta_g{}^{-0.6}\right]^{0.714} \tag{9}$$

and the corresponding drag coefficient is calculated through $C_D = 18.5/(Re)^{0.6}$ (McCabe et al. 1993).

Finally, for particles smaller than 1 μm, it is necessary to apply the Cunningham velocity correction: $v_C = v(1 + 1.72 \cdot \lambda/d)$, where λ is the mean free path of the molecules. Anyway this aspect has little practical interest, because it is not possible to separate submicron particles by gravity anyway.

Nowadays the settling chambers are less and less used because of their size and their limited performance. In fact, it is difficult to separate particles with dimension smaller that 50 μm. The cutoff diameter can be estimated by assuming that the terminal settling velocity of a particle, which is deposited at a distance equal to the depth of the settling tank (Z), is defined by

$$v = \frac{Z}{\text{retention time}} = \frac{Z}{Z \cdot A/Q} = Q/A \tag{10}$$

And therefore,

$$d_c = \sqrt{\frac{18\eta_g Q}{glL\rho_p}} \tag{11}$$

where Q is the flow rate (m^3/s), g the gravity acceleration, l the chamber width (m), L the chamber length (m), and A the chamber surface (i.e., L times l).

For practical applications, the sedimentation chambers will be used for preliminary treatments or to remove larger particles. We can consider that the cutoff diameter does not drop off below 20 μm, although theoretically smaller particles can be allowed to settle down.

This process has the following advantages:

- Simple construction
- Low investment and operating and maintenance costs
- No limitation for operating temperature and pressure

However, settling chambers have two major drawbacks:

- Big dimensions
- Low efficiency

2.2 Inertial Devices

These separators are formed by baffles. The larger particles, due to their inertia, will strike the baffle and deposit as shown in Fig. 2. The diameter for which these separators are effective is 20–30 mμ, for simple shapes with vertical baffles. The cost of these facilities is low, but the efficiency is too limited given the large volume occupied by these units. Improvements have been proposed to force the gas to undergo several changes in

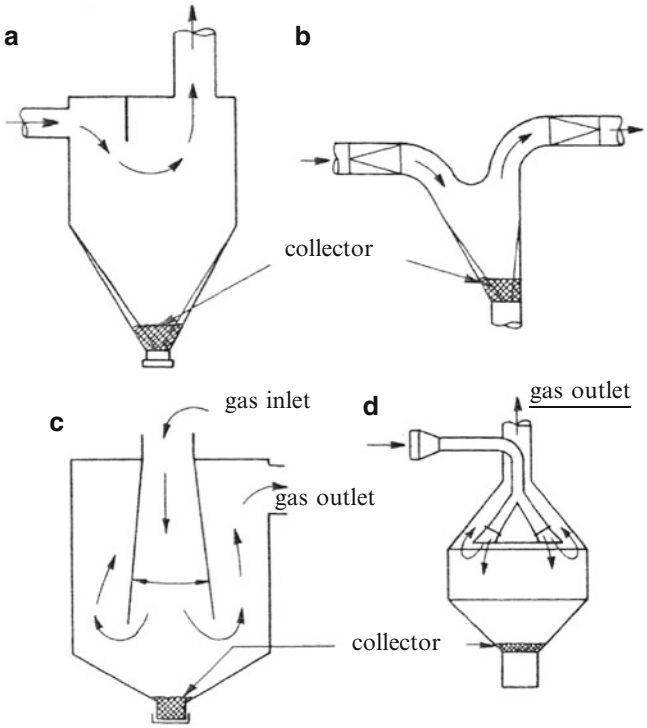

Fig. 3 Inertial separation devices with changes in the flow direction

direction as shown in Fig. 3. The efficiencies are thus increased, and pressure losses can reach 1,000 Pa for cutoff diameters of about 4 µm. The main limitation to the use of these devices is the re-entrainment of particles that have already hit a wall. These separators are rarely used for dust removal, because their ratio performance/necessary energy is low compared to cyclones. However, they are very used as mist eliminators (Perry and Green 1998).

2.2.1 Cyclones

Cyclones have been used in the process industry for over a century since 1880 for gas separation. However, the first publication on the prediction of their performance has been published only after 1930 (Cooper and Alley 1994).

2.2.1.1 Classification of Cyclones

They can be either of axial or tangential type:

- *Axial type*
  - At one end: axial and helical gas inlet
  - At the other: gas outlet in the center and dust outlet at the periphery
- *Tangential type*
  - Tangential inlet by volute or helical from above
  - A gas outlet from the top central duct
  - Dust outlet to the base of the conical portion of the cyclone

Cyclones can be used either individually or by group: these are multicellular cyclones that have a certain number of small diameter centrifugal elements grouped in an envelope containing both the input and output gas trunk and a common hopper to all cells for dust collection.

2.2.1.2 Cyclones Design

There is no optimal design for all applications. The appropriate design of a cyclone for a given task involves trade-offs between the number of cyclones to implement the flow rate per unit, the pressure drop, and the efficiency. Figure 5 shows important dimensions characterizing a cyclone of tangential type, and Table 1 gives the standard features proposed by different authors.

The diameter D of the cylindrical body has been chosen as reference, and the other parameters are parameterized on the value of D, as reported in what follows:

De: diameter of the central tube

H-h: height of the conical portion and h is the height of the cylindrical portion

$A = a \times b$: the gas inlet canal section

B: diameter of the discharge orifice

S: the length of the output

2.2.1.3 Optimal Design of a Cyclone

The collection efficiency of a cyclone η for particles having a given size and density can be determined from the following empirical relationship proposed by Koch and Licht (1977):

$$\eta = 1 - \exp\left(-2\left[\frac{G\tau}{D^3}\frac{Q(1+\gamma)}{}\right]^{\frac{0.5}{1+\gamma}}\right) \qquad (12)$$

where G is a configuration factor (shown in Table 1), D is the diameter, τ is the relaxation time ($d^2\rho_p/18\mu$), and γ is a parameter which depends on temperature T (K) and diameter D according to the following relationship:

$$\gamma = 1 - \left[1 - \frac{(39.4D)^{0.14}}{2.5}\right]\left(\frac{T}{283}\right)^{0.3} \qquad (13)$$

The design method proposed by Koch and Licht and briefly described below gives, for a given capacity, the diameter D of a cyclone with fixed dimensions for an optimum efficiency (i.e Eq. (12)).

By considering v_d as the speed necessary to avoid dropping or settling of particles and v_i as the velocity of the gas entering the cyclone, the ratio v_i/v_d is an important factor for the optimization of the cyclone design. This ratio should be equal to 1.25 $(v_i/v_d)_0$. Taking into account the

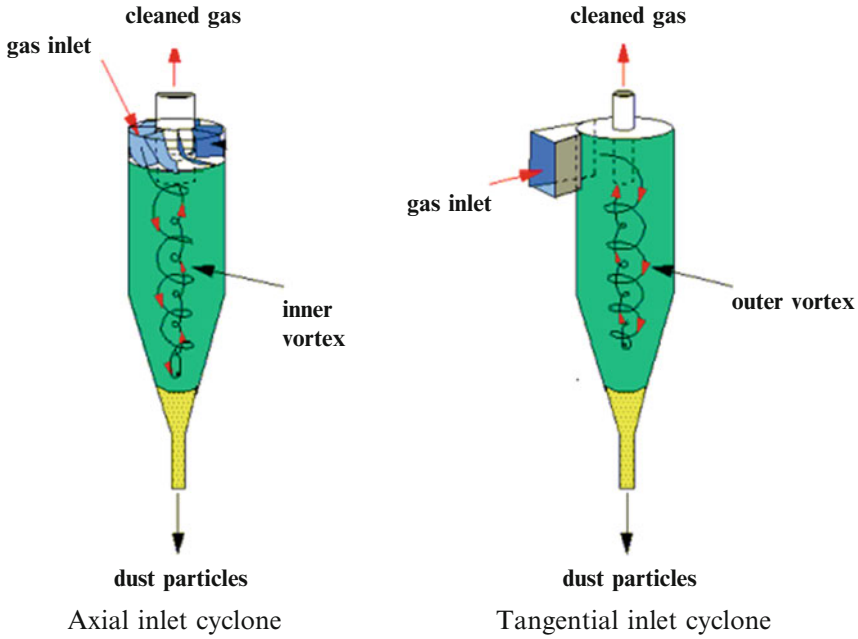

Fig. 4 Types of cyclones

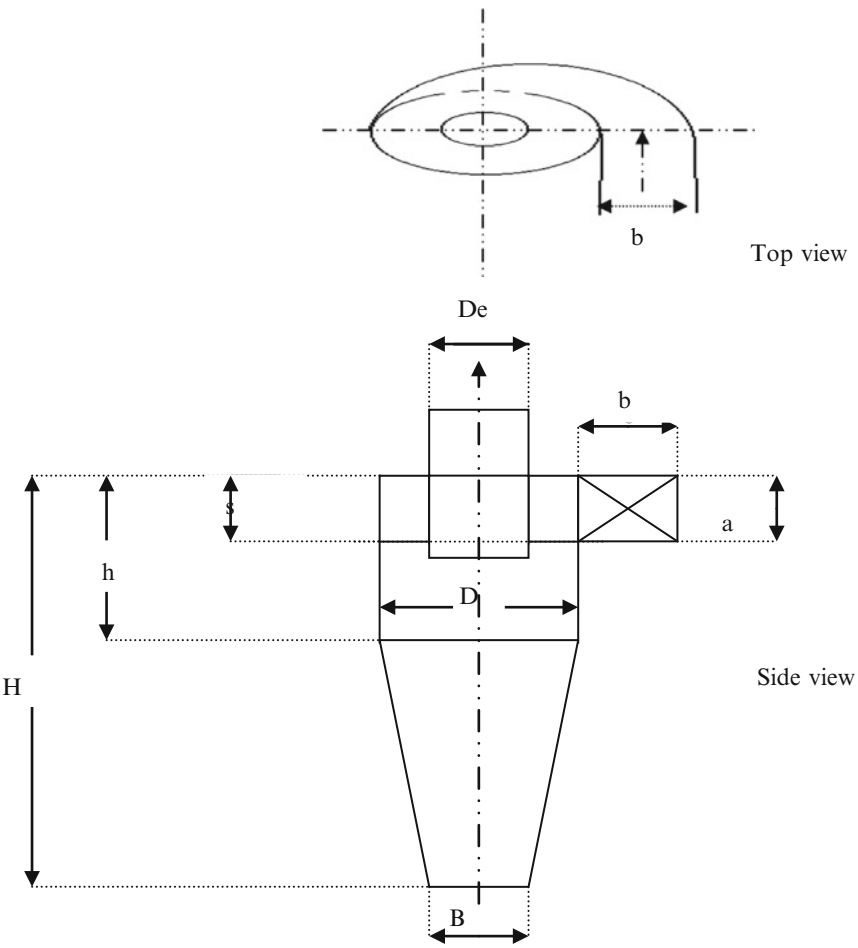

Fig. 5 Main dimensions of a cyclone

Table 1 Standard design of a cyclone: all parameters are relative to D (Dullien 1989)

	High efficiency cyclone		Conventional cyclone	
Symbol	Stairmand (1951)	Swift (1969)	Lapple (1967)	Swift (1969)
D	1	1	1	1
a	0.5	0.44	0.5	0.5
b	0.2	0.21	0.25	0.25
S	0.5	0.5	0.625	0.6
De	0.5	0.4	0.5	0.5
h	1.5	1.4	2	1.75
H-h	2.5	2.5	2	2
H	4	3.9	4	3.75
B	0.375	0.4	0.25	0.4
G	551.3	699.2	402.9	381.8

correction of temperature and density of the particles, this ratio is then given by

$$\frac{v_i}{v_d} = \frac{1.25}{f_T \cdot f_\rho} = \frac{(v_i/v_d)_0}{f_T \cdot f_\rho} \tag{14}$$

where f_T and f_ρ are correction factors given by

$$f_T = \frac{6.88}{10.52 - \mathrm{Ln}(T)} \tag{15}$$

$$f_\rho = \frac{2.25}{3.11 - \mathrm{Ln}(\rho_p)} \tag{16}$$

In previous relationships, temperature is expressed in °C and density in g/cm^3.

Koch and Licht (1977) have shown that the velocity of equilibrium can be written in terms of the system parameters as follows:

$$v_d = 0.228\, v_a \left[\frac{(b/D)^{0.4}}{(1-(b/D))^{1/3}}\right] D^{0.067} v_i^{2/3} \tag{17}$$

where $v_a = 1.1\left[g\mu\frac{(\rho_p-\rho)}{\rho^2}\right]^{1/3}$ is expressed in cm/s.

The complete procedure of design and the different steps of calculation are described elsewhere (Dullien 1989).

2.2.1.4 Pressure Drop Estimation

Generally, the pressure drop (and power consumption) in a cyclone increases with its efficiency. So it is important to estimate the pressure drop as a measure of the effectiveness of a given cyclone. Among the correlations and empirical techniques described in the literature, the method of Stairmand (1949) gives satisfactory results:

$$\Delta P = \frac{\rho}{2}\left[v_i^2\left\{1 + 2\phi^2\left[\frac{2(D-b)}{D_e} - 1\right]\right\} + 2v_e^2\right] \tag{18}$$

The meanings of the symbols used in the previous formulas are reported in what follows:
v_e: velocity at the gas outlet duct ($v_e = 4Q/\pi D_e{}^2$) (m/s)
ρ: density (kg/m^3)
v_i: inlet velocity (m/s)
v_d: saltation velocity (m/s)
ϕ: friction constant given by

$$\phi = \frac{\sqrt{(D_e/2)(D-b)} + \sqrt{(D_e/2)(D-b) + (4\Gamma A/ab)}}{(2\Gamma A/ab)} \tag{19}$$

where
Γ: a constant, for gases = 0.0005
A: cyclone surface exposed to the gas

2.2.1.5 Advantages and Disadvantages

The many advantages of cyclones are the installation and low maintenance cost. In addition, pressure drops are relatively small as compared to their efficiency and compactness. The only constraints related to their application are temperature and pressure values which must not exceed certain limits.

The major drawback of cyclones is that they are relatively ineffective for the retention of fine particles. This aspect may limit their use, especially since fine particulate matter is dangerous because it is easier to inhale and new regulations on air pollution do not permit the production of dust with diameter less than 10 μm.

2.2.2 Wet Scrubbers

Wet scrubbers are specific devices used for the removal of contaminants (either solid or liquid) from a gas stream using a washing liquid. The separation is accomplished by dissolving, by trapping, or by chemical reaction with the element to be separated.

The operation of gas scrubbing consists of three steps:

1. Movement of particles from the gas phase to the liquid surface that occurs as a result of the following different mechanisms:
   - Impact force
   - Interception
   - Diffusion
2. Transport of the particles in the liquid by adhesion and penetration
3. Separation of the drops from the treated gas

2.2.2.1 Advantages and Disadvantages (Raguin 1994)

The main advantages of wet scrubbers are briefly reported in what follows:

- They can handle high concentration of particles.
- They can stand high temperatures of the incoming gas.
- Fluctuations in load do not affect the efficiency significantly.
- Wet scrubbers can handle explosive gases with little risk.
- The absorption of gas and dust are handled in a single unit.

On the other hand, the main disadvantages are as follows:

- High potential for corrosion problems.
- The scrubbing liquid poses a pollution problem, which requires secondary treatment for sludge or wastewater that is generated at the output.

2.2.2.2 Different Types of Wet Scrubbers

Wet scrubbers used in industrial applications for dust removal operations are classified on a basis of:

- The amount of energy employed to make contact between the particles and the liquid, which results in pressure losses.
- The quantity of liquid brought into contact with the gas to be treated. It should be noted that the consumption of water corresponds to the supply of fresh water to compensate for evaporation losses and the flow of sludge (if water can be separated from the sludge and recycled).
- The contacting mode of the slurry with the scrubbing liquid.

According to these criteria the main types of wet scrubbers are as follows: spray towers, packed towers, and venturi scrubbers.

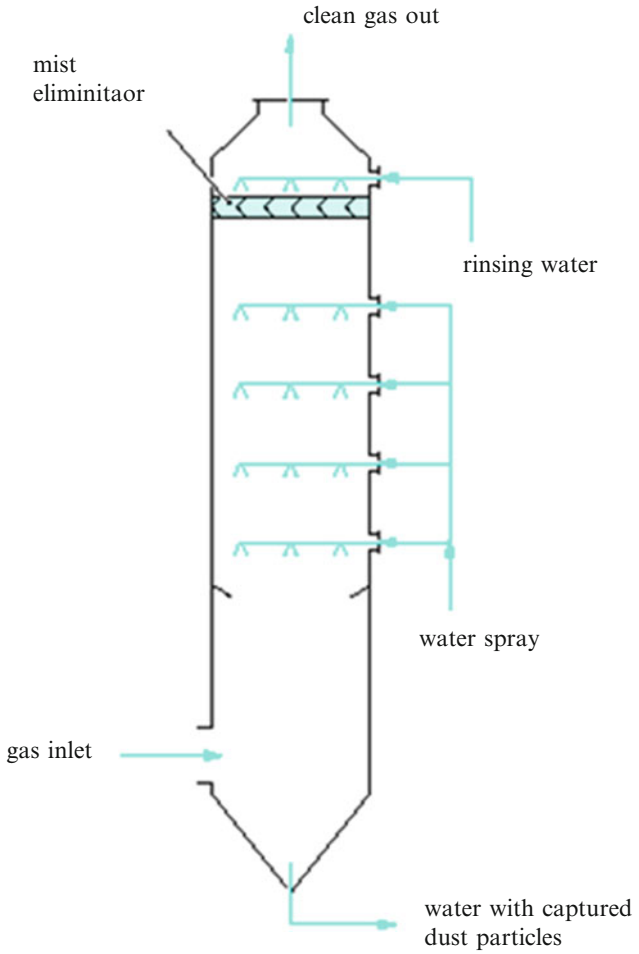

Fig. 6 Schematic of a spray scrubber column

2.2.2.3 Scrubbing Spray Towers

This dust removal system involves spraying a liquid phase under pressure through a spray nozzle. Then, the liquid droplets fall countercurrently with respect to the gas stream (Fig. 6). To avoid their re-entrainment by the gas stream, the droplets must have a sufficiently high speed relative to the gas flow.

The droplets used in this process have a diameter ranging from 0.1 to 1 mm, since particles that are collected by these droplets are relatively large. The most dominant mechanisms of collection are:

- *Inertial impact*. It is considered that the capture by inertial impact of a particle depends only on the mass of the particle and not on its size. Each particle is then considered to be a material point where all the mass is concentrated. In a gas stream, in which body collectors (droplets) are present, the solid particles follow the streamlines of the gas until these diverge around the collectors. Particles with sufficient inertia will continue their paths toward the droplet and thus leave the gas streamlines as indicated in Fig. 7. Among the streamlines of the gas current, there is one particular line situated at y_{lim} (initial ordinate of the critical path of the particles) from which the particle path, after leaving the streamlines, would be tangent to the collector.
- *Interception*. The mechanism for collecting solid particles by interception takes into account only the particle size and ignores their inertia (Strauss 1975). Under this mechanism, the particles follow exactly the streamlines of the gas flow. The collected particles (having diameter d_p) are those for which the centers are situated on the streamlines and their distance to the collector is equal to $d_p/2$, as illustrated in Fig. 8. This figure shows, for example, particles with diameters d_{p1} and d_{p3} will be captured, while d_{p2} and d_{p4} particles will not, because of their size. Concerning the collection efficiency, studies have shown that it depends on several parameters such as droplet size and the amount of water flowrate.

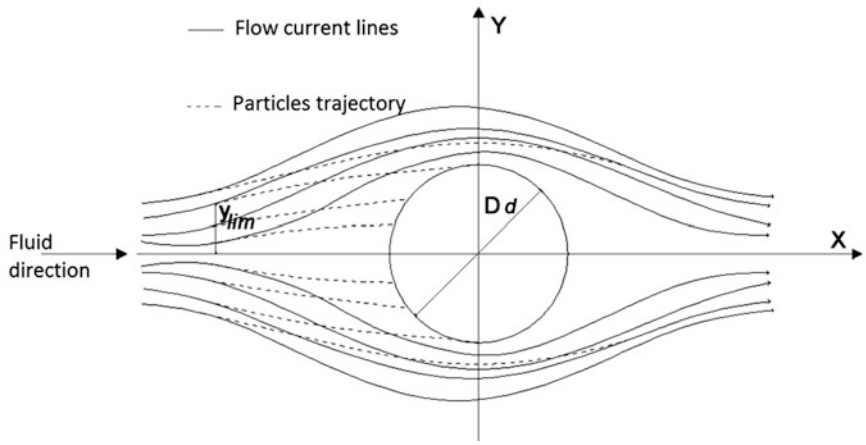

Fig. 7 Capturing of dust particles by inertial impact by a water droplet (Bouziani et al. 2006)

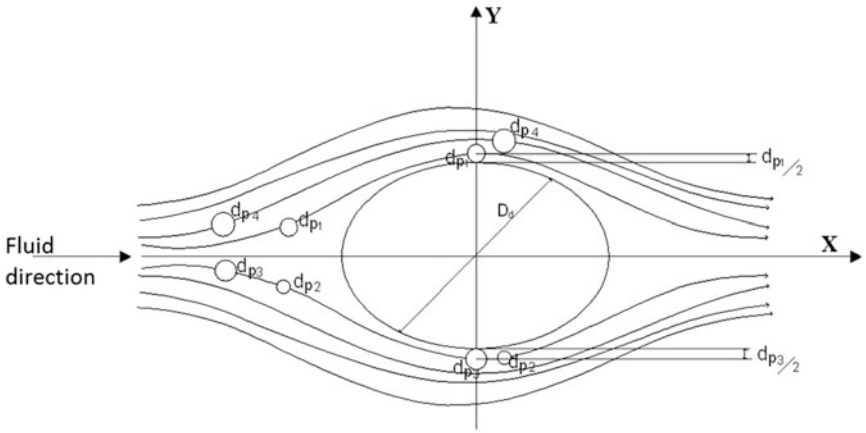

Fig. 8 Capture of a particle by interception (Bouziani et al. 2006)

The performance analysis of the collection is based on the uniformity of the distribution of droplet sizes, while the expression of the tower efficiency is given by (Calvert et al. 1974):

$$\eta = 1 - \exp\left(\frac{-3}{2}\frac{\eta_{IC}}{D}\frac{Q_L}{Q_G}\frac{v_d}{(v_d - v_G)}H\right) \qquad (20)$$

where η_{IC} is the abatement efficiency (for interception and inertia mechanisms combined) determined for a single spherical water droplet, D the droplet diameter, H the tower height, Q_L the water flow rate, Q_G the gas flow rate, v_d the velocity of the liquid droplet, and v_G the gas velocity. η_{IC} is obtained by considering the inertial impaction and interception mechanisms to be statistically independent (more details are given by Bouziani et al. 2006).

The spray tower has many advantages, as briefly described in what follows. It is especially suitable and effective for the capture of particles with a diameter greater than 10 µm. It requires low energy consumption and causes low pressure drops (between 2 and 4 in. water column), which results in low investment and operating and maintenance cost.

However, the major disadvantages of this process are:

- Difficulty to capture particles smaller than 5 µm
- Necessity of an important irrigation water flow rate
- Generation of polluted water

2.2.2.4 Packed Tower

This type of scrubber is rarely used for the collection of particles because of its high resistance to gas flow (high pressure drop). However, it is sometimes used to capture dispersed liquids droplets. Packed towers use a system of distribution of liquid at the top of the tower (as shown schematically in Fig. 9), and the liquid flows through random or structured packing. The random packing may consist of crushed stones or saddles etc. However, structured forms of packing can maximize the liquid surface and minimize pressure drop.

The demister aims to remove entrained liquid by the gas stream before exiting the tower from the top. The introduction of the gas to be treated can be done at any point of the system depending on the following configurations:

- *Cross flow configuration*
  This design is not very effective and is only applicable in cases where the gas to be treated is soluble. However, it does not require much energy (low pressure drop).
- *Countercurrent flow configuration*
  This design is the most widely used given its very high performance as the exiting gas is in contact with the fresh liquid (with low pollutant loaded), which maximizes the potential for absorption. This design requires a very large flow-rate ratio liquid/gas and is suitable in the case of relatively highly charged gas particles.

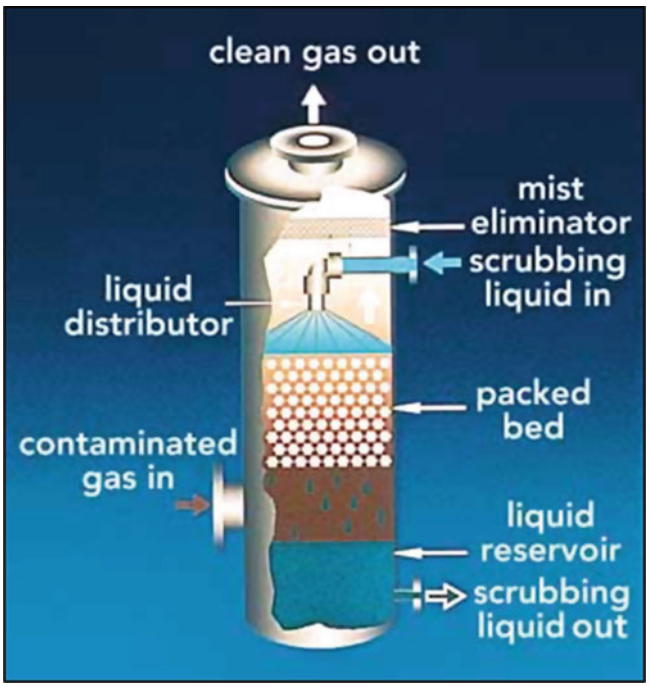

Fig. 9 Wet scrubbing packed tower: type countercurrent

- *Cocurrent flow conception*
  It is more effective for the collection of fine particles. However, the capture is limited when the gas–liquid system approaches equilibrium at the bottom of the tower.

Packed towers can accomplish a very high collection efficiency with relatively low liquid–gas ratio. However, they are characterized by high energy consumption (pressure loss varies between 3 and 8 in. water column). In addition, they require also high investment at the initial installation and relatively high operating and maintenance costs. Packed towers are also characterized by generating large amounts of polluted water as compared to that ones of the spray tower.

2.2.2.5 Venturi Scrubber

The venturi scrubber is an efficient device for air pollution control. It is used worldwide in various applications and configurations. The two best-known types are cocurrent and cross flow, as shown in Fig. 10.

The scrubbing liquid is injected via a spray nozzle. Because of the large pressure drop through the nozzle, the liquid flows at high speed by capturing solid particles from the gas stream under the effect of impact by inertia and then the liquid–gas mixture passes through a separator (cyclone) which will separate the clean gas from the rest (polluted liquid and the condensed gases) as shown in Figs. 11, 12, and 13.

The two criteria of performance of venturi scrubbers are the collection efficiency and pressure drop. These two criteria are influenced by several parameters such as:

- The size of the particles
- The liquid–gas fraction
- The droplet size distribution
- The geometric configuration of the process

According to Calvert et al. (1972), the collection efficiency can be calculated according to the following empirical correlation:

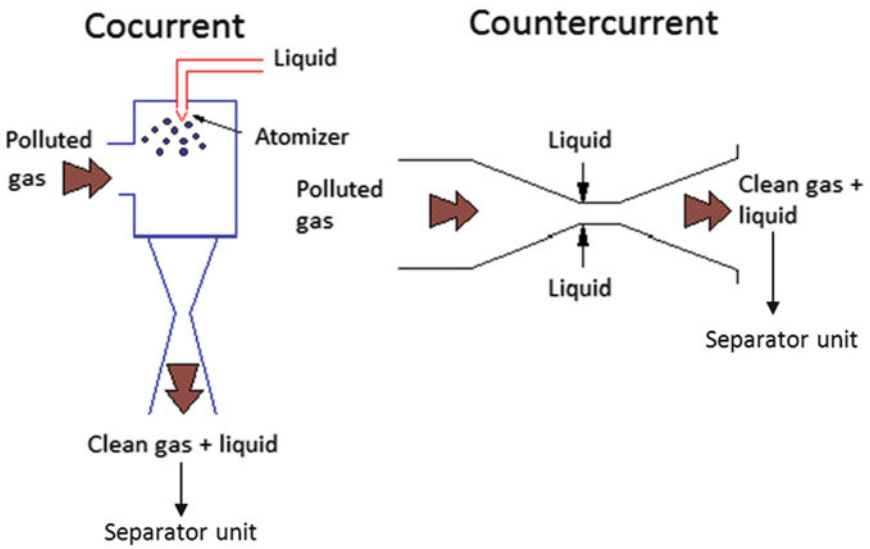

Fig. 10 Types of venturi scrubbers: cocurrent and countercurrent configurations

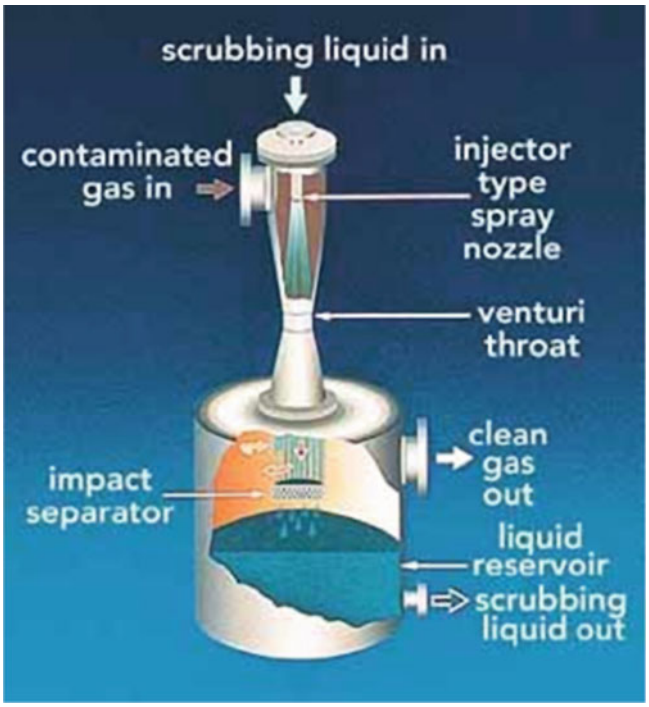

Fig. 11 Schematic of a cocurrent venturi scrubbing system

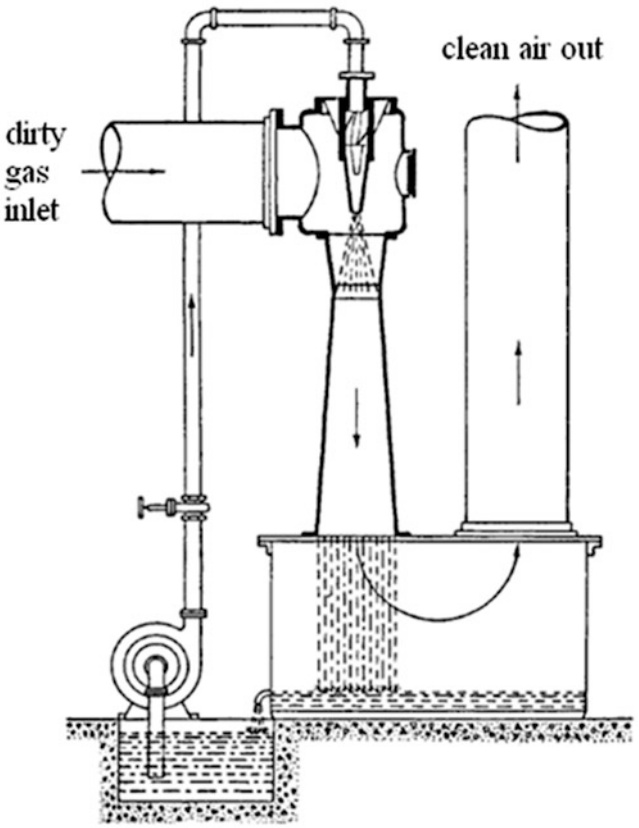

Fig. 12 Schematic of a venturi scrubber with gas–liquid separation equipment and water recycling (Pell and Dunson 1998)

Fig. 13 Example of a "Venturi Scrubbing System" with industrial dimensions

$$\eta_0 = 1 - \exp\left[\frac{2}{55}\frac{Q_L}{Q_G}\frac{v_G \cdot \rho_L}{\mu_G} D_G \cdot F(\psi,f)\right] \tag{21}$$

in which

$$F(\psi,f) = \frac{1}{2\psi}\left[-0.7 - 2\psi \cdot f + 1.4\ln\left(\frac{2\psi \cdot f + 0.7}{0.7}\right) + \left(\frac{0.49}{0.7 + 2\psi \cdot f}\right)\right] \tag{22}$$

$$\psi = \frac{N_S}{2} \tag{23}$$

where Q_L is liquid flow rate, Q_G the gas flow-rate, v_G the gas velocity, ρ_L the liquid density, μ_G the gas viscosity, f an empirical coefficient which varies between 0.1 and 0.5, D_G the diameter of the liquid droplet, and N_S the Stokes number given by

$$\frac{C\rho_p D_p^2 v_0}{18\mu_G(D_G/2)} \tag{24}$$

N_S represents the ratio of the force required to stop the particles at a distance $D_G/2$ to the force of resistance of the fluid on the particle (having density ρ_p) and when the velocity of the particle relative to the fluid is v_0.

The diameter D_G of a droplet can be calculated using the following correlation (Nukiyama and Tanasawa 1938, 1939):

$$D_G = \frac{58{,}600}{v_G}\left(\frac{\sigma}{\rho_L}\right)^{1/2} + 597\left(\frac{\mu_L}{\sqrt{\rho_L \sigma}}\right)^{0.45}\left(1{,}000\frac{Q_L}{Q_G}\right)^{1.5} \quad (25)$$

This correlation gives D_G in μm if all the other parameters are expressed in the cgs unit system. The parameter σ is the surface tension of water and C the Cunningham correction factor given by

$$C = (1 + 1.72 \cdot \lambda/d) \quad (26)$$

where λ is the mean free path of the particles.

The pressure drop can be estimated according to the following correlation (Hesketh 1974):

$$\Delta P = 190 {v_G}^2 \rho_G {A_t}^{0.133}\left(\frac{Q_L}{Q_G}\right)^{0.78} \quad (27)$$

where A_t represents the section of the venturi throat.

The importance of venturi scrubbers is represented by the fact they are characterized by a good efficiency with little energy requirements (i.e., they do not require fans to move the gas stream). However, the following drawbacks of venture scrubbers are reported in what follows:

- Pressure drop can be very important.
- Require a very large flow rate of water.
- The operating and maintenance costs are relatively important.

3 Gas-Solid Filtration: Bag Filters and Electrostatic Filters

3.1 Introduction

The different types of equipment described in Part 1 are mainly used for collecting dust processes from industrial activity generating relatively large amount of solid, while the gas-solid filters (described here) are intended and designed for the collection of solid particles at low concentrations; it is usually atmospheric dust.

The theoretical treatment of gas-solid "dust-air" filtration begins with the depositing process of solid particle on the collector (filtration medium). Several mechanisms that come into play in the gas-solid filtration are inertial deposition, interception, and diffusion deposition. Electrostatic precipitation can become a major mechanism if the collector, the dust particle, or both are electrically charged. The gravitational sedimentation has a minor influence for particle sizes typically encountered in this field.

In this chapter, the most important techniques used for dust elimination are presented.

3.2 Bag Filters

This type of dust collector is reserved to equipment where dust-laden fumes or gases go through a filter layer in which the particles are deposited. Contrary to what happens in the cyclonic separators or scrubbers in which the particles are continuously removed, here dust is accumulated and periodically must be separated from the gas phase by a cleaning process. The filtering layer may consist of:

- Woven media
- Bulk fiber or felt
- Porous membranes
- Filter paper

The filters are characterized by different level of efficiency: high values (e.g., used in nuclear and clean rooms) or normal ones. In the first case, the accumulated dust is often removed with the filter media itself (disposable filter), while in the second one, the filter media can last several years.

Moreover, in the case of a high efficiency filter, it is almost always required to protect the filter with a prefilter unit to limit the frequency of media replacement. In the last few years, this class of separators has undergone a rapid development since there initial investment and the cost of maintenance are relatively low.

3.2.1 Definition and Principle of Operation

In the baghouse, the dust-laden fumes or gases are passed through a filter medium which will retain the dust. The filter medium is arranged, generally in bags formed by large socklike fabric or felt, with a length between 3 and 6 m and a diameter of about 150 mm. These bags are usually suspended from the top. There are different types of bags and other technical solutions, while the operating principle remains the same. The gases are usually fed at the bottom and inside the bag, travel through the bags, and are discharged through the upper portion. In this arrangement, dust is collected inside the bags. It is also possible to have filters in which the dust is collected on the outside or in which the gas flows from top to bottom. For large units, it is common to divide the filter in compartments (as explained later) and may well have inactive compartments at a given time.

Filtration rate is calculated by dividing the actual flow through the active surface (for bags which are not in cleaning mode). This speed is generally quite low and usually ranges between 0.01 and 0.1 m/s.

A cleaning device is always used to remove the deposited dust on the filtering media. The cleaning is achieved either

Table 2 Coefficient of specific resistance K_2' of certain dusts (Williams et al. 1940)

	K_2' for particle size <						
Dust	20 mesh	140 mesh	375 mesh	90 μm	45 μm	20 μm	2 μm
Granite	1.58	2.20				19.8	
Cast iron	0.62	1.58	3.78				
Gypsum			6.30			18.9	
Feldspath			6.30			27.3	
Stone	0.96			6.30			
Zinc Oxide							15.7
Wood				6.30			
Resin (cold)		0.62				25.2	
Oats	1.58			9.60	11.0		
Corn	0.62		1.58	3.78	8.8		

These data have been obtained for the ambient air; for other gases, the coefficient K_2' must be multiplied by the ratio of viscosities (gas/air)

by countercurrent (reverse flow) air blowing, by mechanical shaking, or by pulse jet, as explained in more details next. Collected solids fall into a hopper and are discharged by screws, locks, or rotary air lock. Filtration efficiency can be estimated from Eqs. (28) and (29). Important factors affecting the efficiency or design filters are reviewed below.

3.2.2 Efficiency

The collection efficiency of a bag filter can be calculated from the efficiency of the fiber used and other physical characteristics of the filter (Chen 1955):

$$\eta_{\text{filter}} = \frac{4\eta_t \ L(1-\varepsilon)}{\pi D_b \varepsilon} \tag{28}$$

η_t *is the* efficiency of a single fiber in a filter:

$$\eta_t = \eta_0[1 + K_\alpha(1-\varepsilon)] \tag{29}$$

where η_0 is the efficiency of a single isolated fiber, D_b is the diameter of the fiber and L is the thickness of the filter medium, and K_α is a constant (approximately equal to 4.5 for values of porosity ε between 0.9 and 0.99).

Equation (29) indicates that the effectiveness of a fiber increases with the proximity of other fibers. Equation (29) implies also that:

1. η_t is the same throughout the filter (uniformity), and the solid particles are the same size.
2. All the fibers have the same diameter D_b, are cylindrical, and are placed perpendicularly to the direction of gas flow.
3. The fraction of particles deposited in any layer of the fiber is relatively small.
4. The gas passing through the filter keeps the same characteristics from a layer of the fiber to another.

3.2.3 Pressure Drop

The pressure drop depends on the nature of the filter media and the dust that is collected. It varies with time as the dust is accumulated between two successive cleaning operations. Since dust is more or less compressible, the pressure loss does not vary linearly with time. The following equation (similar to the Kozeny-Carman or Darcy equation for solid–liquid filtration) reflects the fact that the pressure loss is made up of two factors, one related to the media and the other to the filter cake (dust) (Billings and Wilder 1970):

$$\Delta p = K_1' v_f + K_2' w v_f \tag{30}$$

where Δp is expressed in kPa, w is the dust load on the filter (g/m^2), v_f is the superficial filtration velocity (m/min), and K_1' and K_2' are two constants related to the conditioned media "fabric" and to the dust layer respectively. The conditioned medium is one that maintains relatively the same amount of dust deposited in depth after several cycles of filtration and cleaning. The value of K_1' in kPa/(m/min) can be 10 times greater than the resistance value of new (clean) medium.

The coefficients K_1' and K_2' are determined from experimentation. Corrections should be made to these coefficients if the operating temperature is different from that of the experiment (using a viscosity ratio). Values of K_2' for certain types of dust are given the Table 2.

In practical applications, dust will accumulate until a pressure loss predetermined threshold is reached. After cake removal or cleaning, the pressure loss drops to a low value and the cycle resumes. The pressure drop is usually between 300 Pa and 2,500 kPa. It should be noted that we are not particularly interested in operating at too low pressure drop, as some permanent dust layer present continuously a protection to the media against deep fouling. In addition, too violent cleaning will wear prematurely the bags.

3.2.4 Filtration Velocity

Filtration rate is an essential element and is closely linked to the filter media used and the application. The lack of sufficiently advanced theory implies that the selection of the filtration velocity is based on experience or on what is already applied and used in one specific area. It is worth noting that an increase in temperature should lead to lower velocity because the gas viscosity increases. Similarly, finer particles than those ones of reference should lead to lower rates. Table 3 gives few figures of merit for velocity to be used for a fabric filter with dust collection from the outside of the bags. The other main factor affecting the rate of filtration is the method of cleaning (jet impulse or shaking).

3.2.5 Nature of Media

Several types of fibers are available and used in industrial applications. The selection criteria are mainly related to technical and economical considerations. Natural fibers such as wool, linen, and cotton are less and less used. From the chemical point of view, we note that it must take into account the resistance to oxidizing agents (oxygen and nitrogen oxides) as well as resistance to acids and bases. The resistance against high temperature is also crucial. It should be noted that a distinction between the temperature during normal operation and the temperature which can be reached as peaks needs to be taken into account. Table 4 gives some properties of commonly used media.

The method of preparation of a medium can be of three types: woven fabrics, felts, and needles. Figure 14 shows an example of two types of media: woven and felts (Siret 1994).

Table 3 Filtration rate recommended for fabric filters depending on the application

Application	Velocity (m/s)
Carbon	0.03
Cement	0.04
Incineration	0.02
Sand	0.05
Alumina	0.03

3.2.6 Cleaning of Bag Filters

Three main types of bag cleaning are generally used:

- Cleaning by shaking
- Cleaning by reverse flow of gas
- Cleaning by pulse jet

Cleaning may, in addition, be made for each category online or off-line as explained a little further.

3.2.6.1 Cleaning by Shaking

The shaking is historically the oldest method of bag filters cleaning. It should be seen, in this mode of cleaning, an analogy with household "beating" of a carpet to remove dust. The upper part of the sleeve (bag) is attached to a mechanical device that will give a vertical (or horizontal) movement, or a combination of both. The mechanical system is usually constituted by a system of shafts and cams. The vibration amplitude is limited so that two sleeves cannot touch each other during the cleaning operation and is of the order of 20–50 mm.

The vibration frequency is low enough and is usually between 4 and 8 Hz. The impact of an increase in frequency is rather beneficial. The duration time of the shaking is around 15–30 s. Cleaning by shaking has the advantages of a relatively low sleeves wear but has the drawbacks associated with all mechanical shaking, especially in terms of maintenance. This mode of cleaning is generally applied off-line and to woven media. Its performance, in terms of dust removal, is very good, as long as care is taken not to work at excessive filtration rate.

3.2.6.2 Cleaning by Reverse Air Flow

Reverse flow bag filters must, necessarily, be compartmentalized. Indeed, during cleaning, the gas flow is cut off in a compartment and a clean gas which can be air or just the filtered gas is forced, through the sleeves, in the direction opposite to that of filtration (as shown in Fig. 15). The diagram in Fig. 16 shows the operation for three compartments, two can be in filtration mode (F) and the third in cleaning or shaking mode (S).

When the dust collection is carried out inside the sleeve, which is frequent, support rings avoiding the complete collapse or folding of the sleeve on itself must be installed (as

Table 4 Properties of fibers used in fabric filters (Siret 1994)

Fiber	Maximum working temperature (°C)	Maximum peak temperature (°C)	Resistance to oxidization	Resistance to acids	Resistance to bases
Cotton	90	120	Good	Poor	Good
Wool	100	130	Good	Good	Average
Polyamides	100	110	Average	Average-good	Good
Polyester	150	180	Good	Good	Average
Glass	250	310	Good	Good except HF	Average
Fluorocarbons	260	280	Good	Good	Good
Polypropylene	100	120	Good	Good	Good
Polysulfides	170	190	Poor	Good	Good

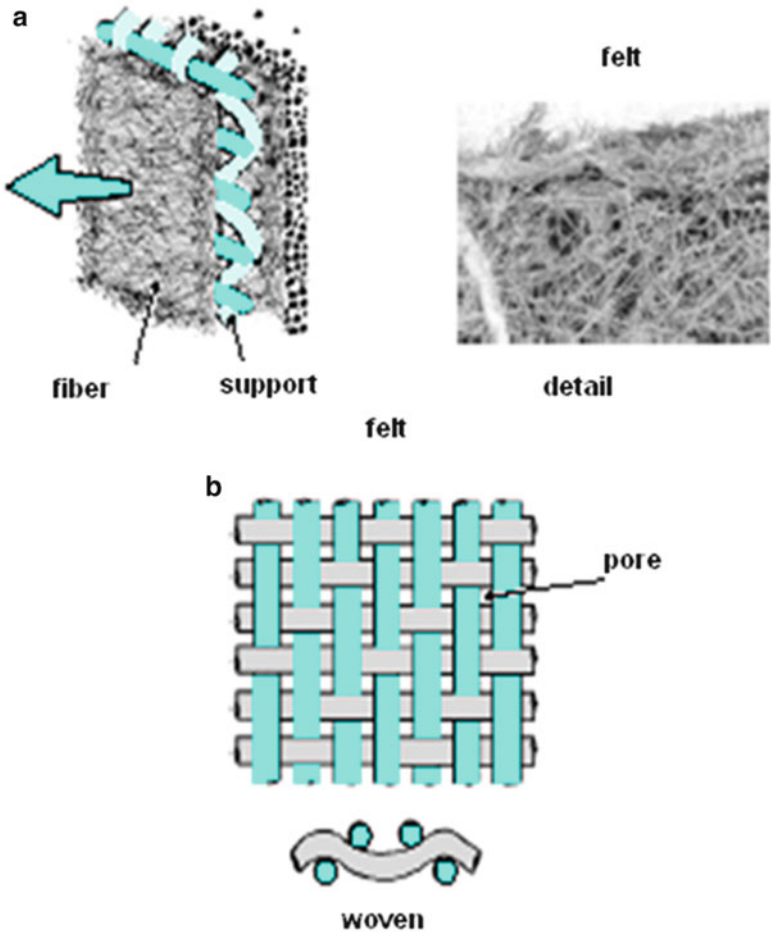

Fig. 14 Different filter media (felt and woven)

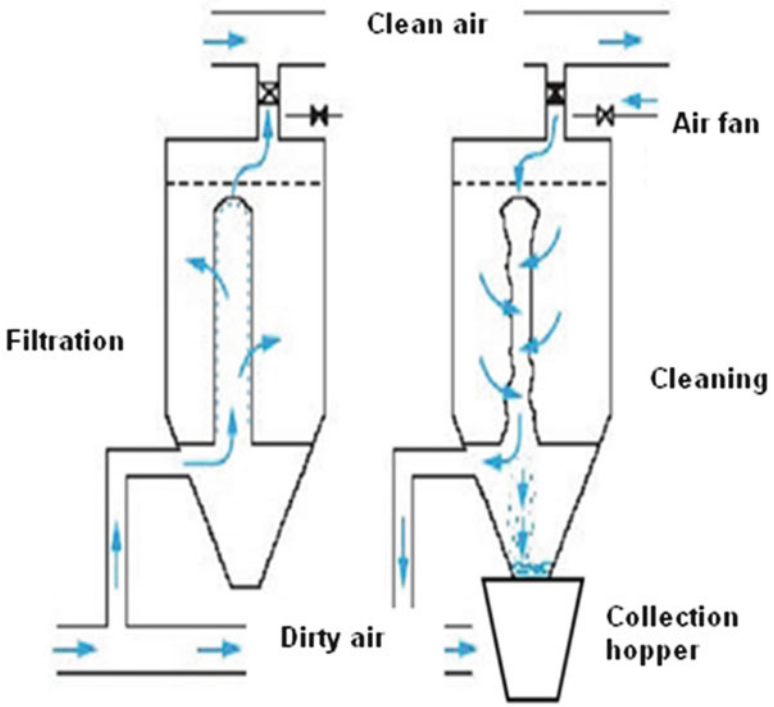

Fig. 15 Schematic representation of the reverse flow cleaning process

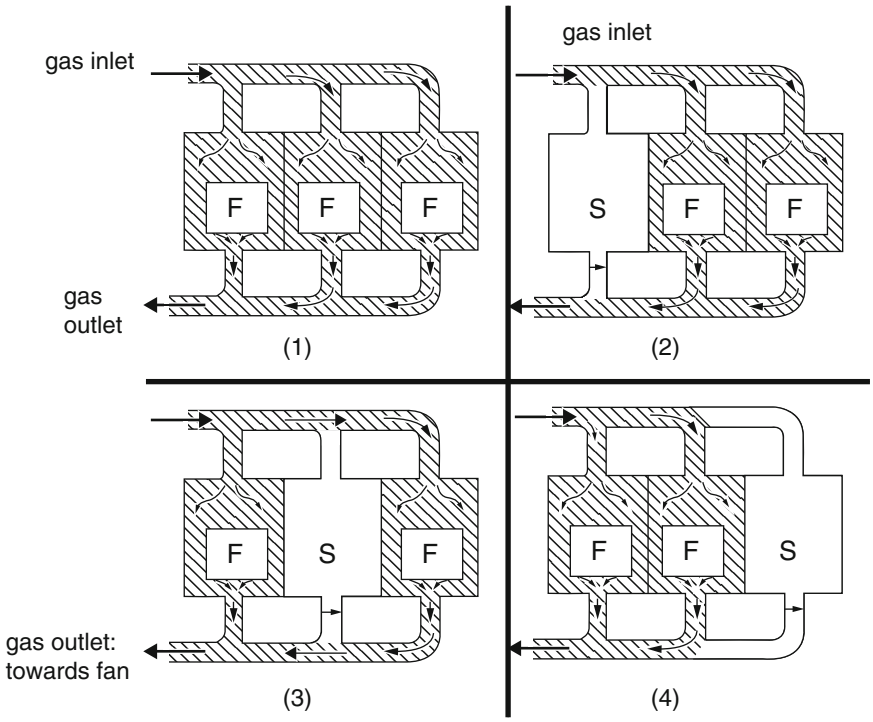

Fig. 16 Three-compartment bag filter at various stages (*1–4*) in the cleaning cycle (Perry and Green 1998). *F* mode filtration, *S* cleaning mode

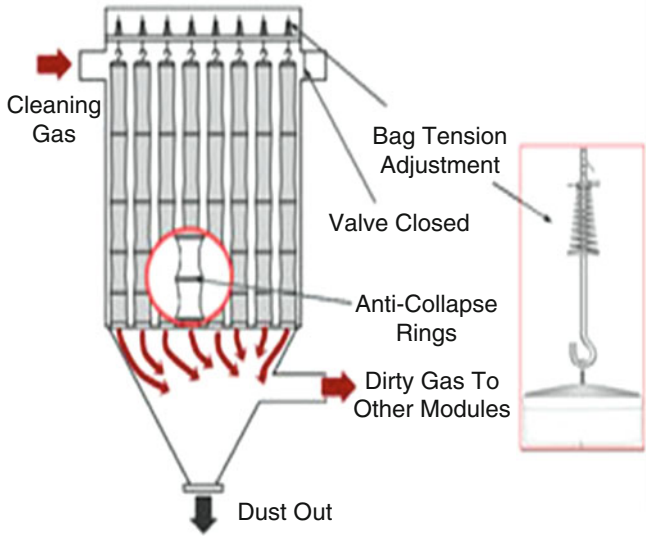

Fig. 17 Example of reverse flow bag filter with anti-collapse rings

shown in Fig. 17). Support cages are almost never used with this cleaning mode. The time of air blowing for reverse flow cleaning ranges from half a minute to several minutes.

The device used for reversing the flow direction of the gas is a pulling device (with the aid of a small fan) either of the already filtered gas or from the dry outdoor air. It is advisable to heat the air to avoid problems related to moisture condensation. Generally, reverse flow filters are more expensive than those based on shaking alone. An example of this type of filter is shown in Fig. 17.

3.2.6.3 Cleaning by Pulse Jet

The cleaning by pulse jet is a more recent application and has known large use with the emergence and development of needle felts; woven media is indeed not suited to this type of cleaning. In a forced air device, air pulse is supplied at medium pressure to the inside of the bag through a port located near its open end. The air blast creates a shock wave that causes the bag to flex as the air wave travels down (up) the length of the filter bag. Since the duration of the compressed-air burst is short (0.1 s), it acts as a rapidly moving air bubble, traveling through the entire length of the bag (see Fig. 18). As the bag flexes, the cake (inside) fractures and particulate is released into the hopper below.

In most baghouse designs, a venturi seated at the top (or the bottom) of each bag is used (as shown if Fig. 19) to increase air velocity in order to create a large enough pulse to travel down and back up the filter bag. These venturis are not systematically used, but they play the role of injectors and have a beneficial effect. The position and design of the venturi is critical.

In this way, it is not necessary to isolate an entire box (compartment), and during cake removal, neighboring bags can continue to operate. It should be noted that, during cleaning, a more or less important amount of liberated dust will return to stick on neighboring elements that are active, but this is of little consequence as long as the percentage of bags affected remains low (<20 %).

The advantages of this type of filter cleaning are its greatest efficiency, the fact that it allows higher filtration

rates, and the possibility of construction of non-compartmentalized filters. However, the bags are most stressed and their wear can be faster than reverse air. In addition, the energy consumption is high and can represent up to 40 % of the energy consumed by the main fan.

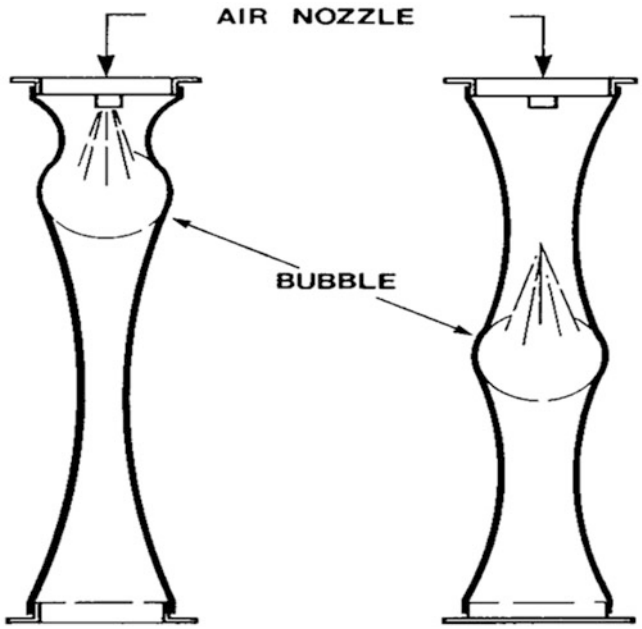

Fig. 18 Bubble movement in pulse jet cleaning

The instrumentation required to conduct bag filters consists primarily of a differential pressure sensor, a temperature sensor that can be used to trigger an emergency bypass and possibly a CO analyzer in the hopper to prevent the risk of fire. It should be noted also that during the shutdown and startup phases, it is often necessary to keep (or get) the filter temperature using heating batteries to avoid condensation problems.

3.3 Electrostatic Separators: Electrofilters

3.3.1 Definitions and Principles of Operation

The principle of operation of an electrostatic precipitator is based on the force applied by an electric field on a charged particle. A charged particle, often naturally, can adhere to a surface, but this natural charge is too low to give rise to a sufficient attractive force to be exploitable. It is thus necessary that the particle receives, by an external process, a sufficient charge to be used in a separation operation.

3.3.1.1 Charge of Particles or Droplets

The electric charge is supplied by ionization of the carrier gas, usually obtained by a wire to which a high potential current is applied which gives rise to the "corona" effect. In principle, a wire stretched between two plates or located in the middle of a cylinder is heated to a high negative voltage (positive voltage can also be used, but the process is less efficient). From a certain tension threshold, a bright purple

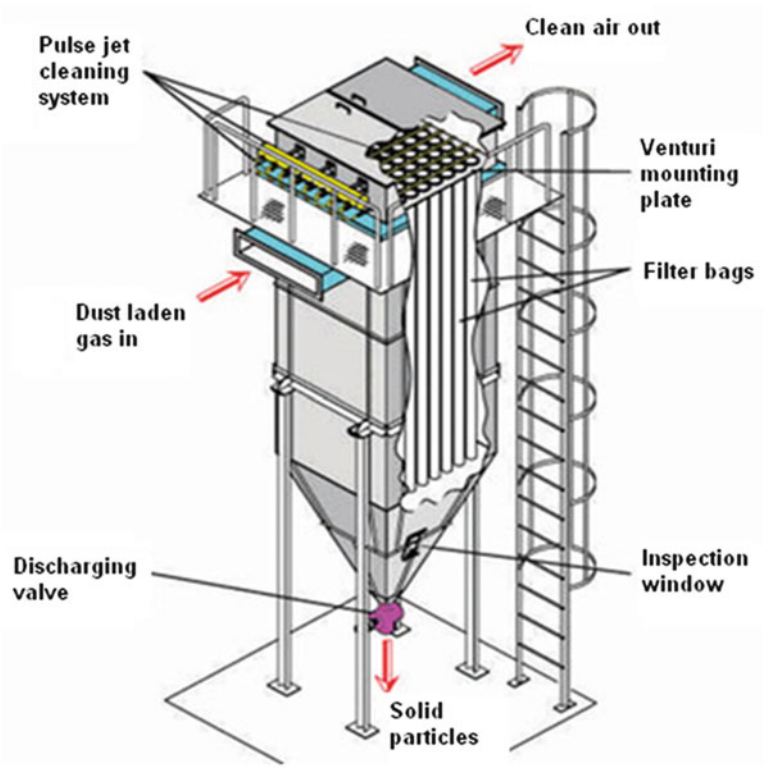

Fig. 19 A baghouse with pulse jet cleaning mechanism and venturi

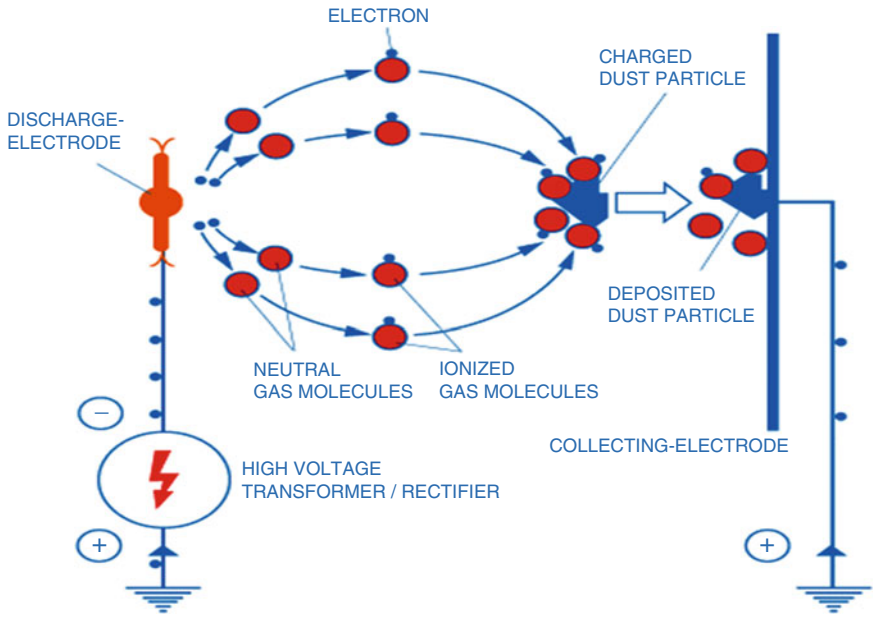

Fig. 20 Mechanism of the charge and movement of the particles in the electric field

halo appears around the wire. Within this halo appear many radical species and ozone. This phenomenon is stable in a range of high voltage, until, when increasing the voltage, arcs and sparks appear between the wire and the counter electrode. At this stage the breakdown voltage is reached. In the purple halo, the gas is in a state of intense excitement and that electrons are stripped by the collision cascade effect. This will provide an avalanche of ions and radicals and which will allow the particles to be charged as shown in Fig. 20 above.

The value of the threshold voltage at which the corona effect is obtained depends on the pressure and nature of the gases and of the geometry. Typically, for a gas such as air at atmospheric pressure, the threshold is about 20 kV. The current then follows a nonlinear law as a function of voltage.

As has been explained above, the particles are charged by shocks when they encounter electrons or other charged particles or by diffusion, due to the thermal motion of the ions. The diffusion mechanism is important only for very small submicron particles. In practice, the charge is reached within a few tenths of a second. It should be noted that for each particle with a given size, there is a maximum load (electric field) that will never be exceeded. E_{max} is about 10^9 V/m for electron emission and 2.10^{10} V/m in transmission of positive charges. For liquid particles, a different mechanism "Rayleigh" will limit the phenomenon beyond a certain load, the drop will explode. The corresponding charge value is given by

$$q_{max} = d^{1.5}\sqrt{2\pi\sigma} \tag{31}$$

where σ is the interfacial tension and d the diameter of the liquid droplet.

3.3.1.2 Movement of the Particles in the Electric Field and Collection Efficiency

A particle within an electric field is subjected to the force represented by

$$F = qE \tag{32}$$

where E is the electric field (V/m) and q the electric charge (in C) equal to the number of elementary charges multiplied by the charge of an electron.

The rate of migration will be, as in the case of gravitation, calculated by balancing the force resulting from the Stokes law to the electric force:

$$\frac{3\pi\mu d v_m}{C_D} = qE \tag{33}$$

in which C_D represents the drag coefficient, μ the gas viscosity, and d the particle diameter.

The collection efficiency of the global process is given by the Deutsch relationship (Deutsch 1922; Anderson 1924):

$$\eta = 1 - \exp(-v_m A/G) \tag{34}$$

where v_m is the migration velocity (see Table 6 for some example values), A the surface offered by the collecting electrodes, and G the gas flow rate.

A modified form of Eq. (34) was proposed by Matts and Ohnfeldt (1964) and takes into account the nature of the solid particles and the deviation from the average particle size (with an empirical parameter k):

$$\eta = 1 - \exp\left(-v_m (A/G)^k\right) \tag{35}$$

Table 5 Collection-efficiency estimations using the Deutsch-Anderson and Matts-Ohnfeldt equations (Gallaer 1983)

		Matts-Ohnfeldt		
Relative size of ESP (A/Q)	Deutsch $k = 1.0$	$k = 0.4$	$k = 0.5$	$k = 0.6$
1	90	90	90	90
2	99	95.1	96.2	97.2
3	99.9	97.2	98.1	98.8
4	99.99	98.1	99	99.5
5	99.999	98.7	99.6	99.76

Table 6 Typical effective particle-migration velocity rates for various applications (Gallaer 1983)

	Migration velocity	
Application	(ft/s)	(cm/s)
Utility fly ash	0.13–0.67	4.0–20.4
Pulverized coal fly ash	0.33–0.44	10.1–13.4
Pulp and paper mills	0.21–0.31	6.4–9.5
Sulfuric acid mist	0.19–0.25	5.8–7.62
Cement (wet process)	0.33–0.37	10.1–11.3
Cement (dry process)	0.19–0.23	6.4–7.0
Gypsum	0.52–0.64	15.8–19.5
Smelter	0.06	1.8
Open-hearth furnace	0.16–0.19	4.9–5.3
Blast furnace	0.20–0.46	6.1–14.0
Hot phosphorous	0.09	2.7
Flash roaster	0.25	7.6
Multiple-hearth roaster	0.25	7.9
Catalyst dust	0.25	7.6
Cupola	0.10–0.12	3.0–3.7

The constant k in this equation is generally between 0.4 and 0.6, depending on the standard deviation of the particle size distribution and other properties of the dust. However, most researchers have reported that a value of $k \sim 0.5$ gives satisfactory results (Gallaer 1983).

If $k = 1$, the equation of Matts-Ohnfeldt is identical to that of Deutsch-Anderson, i.e., Eq. (34). From Table 5, we can see that the estimate of the efficiency from the equation Matts-Ohnfeldt is moderate and probably more realistic than the estimation of the Deutsch-Anderson equation.

In general we can consider that:

- For $\eta < 95$ %, Deutsch-Anderson equation is used.
- For $\eta > 99$ %, Matts-Ohnfeldt equation is used.
- In between, an average value from the two equations could be used.

Table 6 gives some values of the rate of migration of solid particles in the dust encountered in some solid handling industries:

A typical efficiency-particle size curve is shown in Fig. 21; it exhibits a minimum which is a feature of many processes. At very low particle sizes, diffusion mechanisms show considerable importance and effectiveness increases

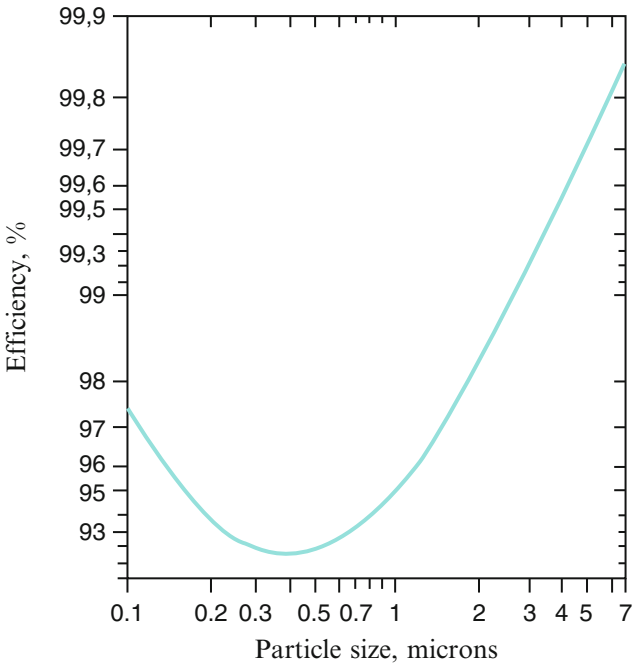

Fig. 21 Typical evolution of the efficiency of an electrostatic precipitator as a function of particle size

again. Once at the collector surface, the particles will be a more or less coherent deposit which must be eliminated. The most common method used for this is to hit the plates periodically with large hammers or rappers. Sound vibrations can also be used.

3.3.2 Main Types of Electrostatic Separators

There are basically dry electrostatic precipitators, wet electrostatic precipitators, and devices based on other processes using electrostatic forces.

3.3.2.1 Ordinary Dry Electrostatic Filters

In an electrostatic precipitator (ESP), the charged particles and which are subjected to an electrostatic force, will migrate to the counter electrode, planar or cylindrical, where they will be collected. The overall mechanism is presented in Fig. 20. Figure 22 shows a simplified form of this type of ESP. Dry ESPs, which have only small pressure losses, are particularly

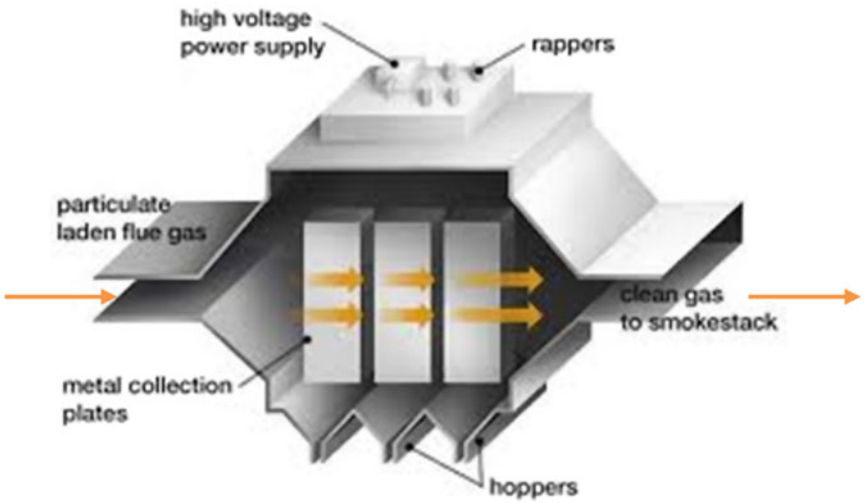

Fig. 22 Schematic representation of a dry electrostatic precipitator

suitable for very high flow rates (>100.000 Nm^3/h), such as found in the processes of energy generation.

In what follows, the main key parameters of a dry electrostatic separator will be discussed.

- The operating temperature is usually between room temperature and 400 °C. When condensable gases contain acidic pollutants such as HCl, SO_2, and SO_3, generally, the operation is carried out at temperatures above 180 °C, to avoid corrosion. Overall, the effect of an increase in temperature is negative, on the one hand, because the viscosity of the gas increases, reducing the mobility of the species, but on the other hand, as the gas volume increases, the time of passage between the collecting devices is reduced.
- An electrostatic precipitator normally operates in a voltage range between 40 and 100 kV (peak). Several types of control are available and are designed to raise the tension as much as possible to the breakdown threshold and stay there. Typical current intensity values are 0.1–0.5 mA/m^2 surface.
- The operating pressure is usually around atmospheric pressure. An electrostatic precipitator operating at a pressure substantially lower than the atmospheric pressure is very quickly penalized in terms of performance and efficiency.
- The operating velocity is typically 1–2.5 m/s, but in some cases, velocities of 7 m/s were achieved in pilot scale with success. Velocity, a contributing factor, to re-entrainment of the particles from the collecting electrode wall, each application is quite specific and sets a velocity that is good is not exceeded.
- The properties of the dust, and especially their resistivity, are essential. Indeed, the resistivity is an important factor that significantly affects the efficiency of collection. Although the resistivity is an important phenomenon in the space between the electrodes, where most of the particles are ionized, it has a particularly strong effect on the layer of dust collecting electrode. The particles which display a high resistivity (greater than about 1.10^{11} to 5.10^{11} $\Omega \cdot cm$) are difficult to be ionized. But once such a condition is reached, they do not easily unload when arriving at the collector electrode. On the other hand, particles of low resistivity (less than about 10^8 $\Omega \cdot cm$) are easily charged but also easily release their load to the collection plate. This is why we can say that a range of 10^8 to 10^{11} $\Omega \cdot cm$ is optimal.

It follows that for some applications such as collecting fly ash from power plants by coke burning, a conditioning is used to lower the resistivity. This conditioning consists mainly of injection of sulfur trioxide, ammonia, or water vapor. Figures 23 and 24 show the effect of temperature and composition of sulfur in coal ash and the percentage of moisture on the resistivity.

3.3.2.2 Humid Electrofilters

These devices are called WESP (wet electrostatic precipitator). Their mechanism is very similar to that of an ordinary electrostatic (dry), but the collector wall is flushed continuously or intermittently. The collector plates can be made of stainless alloy, or even lead, conductive plastic. Often the collecting electrodes are tubular. An example diagram of a wet electrostatic precipitator is given in Fig. 25 below.

The wet electrostatic precipitators are often designed for velocities of gas flow rather low (1–2 m/s) and their performance is excellent. It is not uncommon to see such units get output dust levels below 1 mg/Nm^3. Several concepts can be implemented for these ESPs. Cleaning the electrodes can be achieved by intermittent sprinkling or by the condensation of water. Although they are expensive, wet electrostatic precipitators, for their excellent performance, are developing rapidly, driven by more binding regulation for emissions of solid particles in the atmosphere.

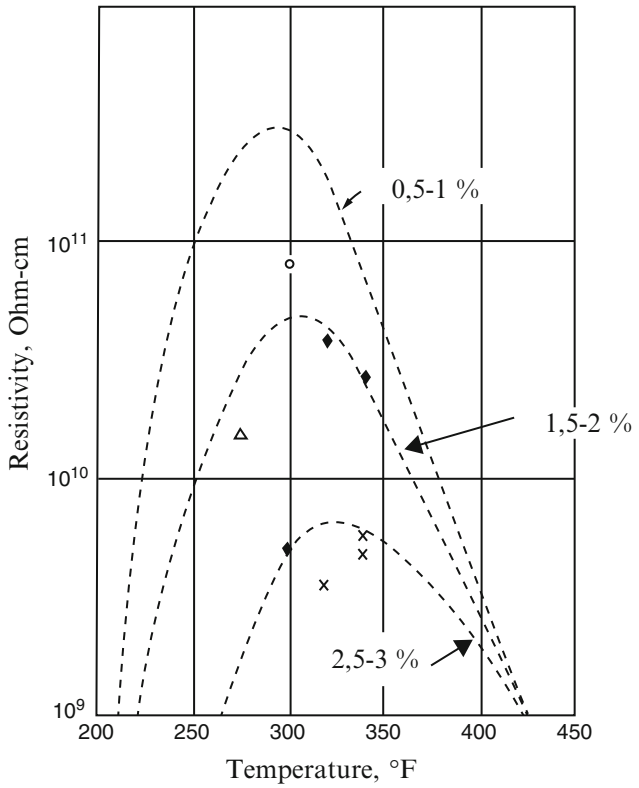

Fig. 23 Evolution of the ash resistivity as a function of flue gas temperature and composition of sulfur in coal (Oglesby and Nichols 1970)

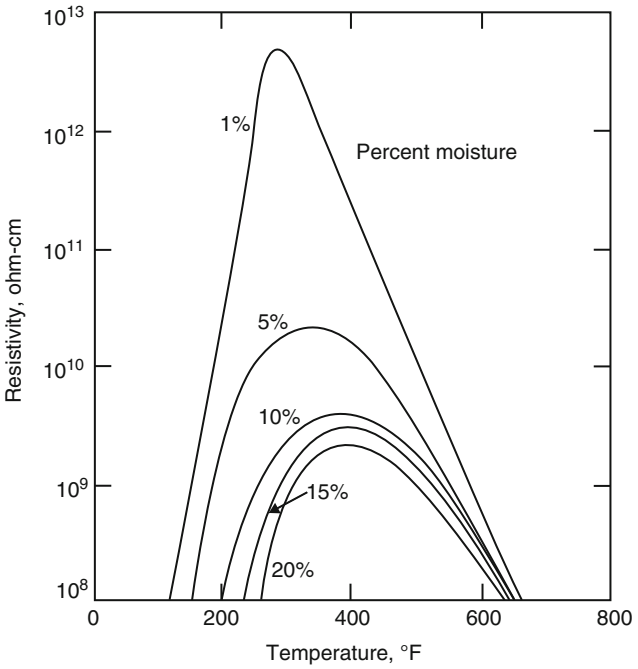

Fig. 24 Effect of temperature and humidity on the resistivity of cement dust (White 1977)

Fig. 25 A schematic diagram of a wet electrostatic precipitator

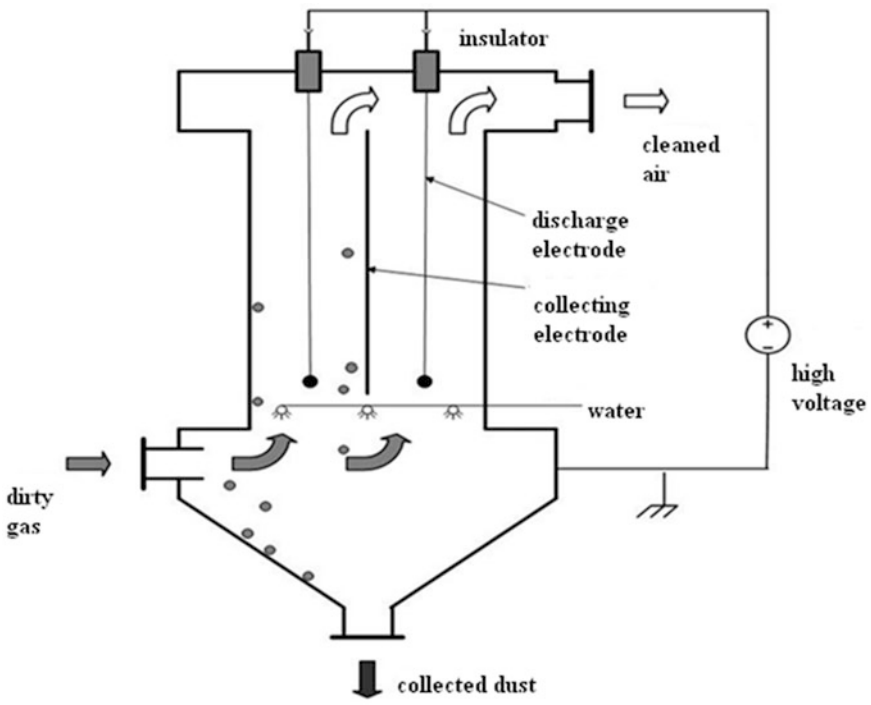

4 Conclusions

The choice of a cleaning technique, among all what was described in the two parts of this document, is based on the following parameters:

- Dust concentration and particle size
- Degree of dust collection required
- Purpose of dust collection
- Characteristics of airstream: temperature, humidity, nature of gas, volume to be treated, etc.
- Characteristics of dust: nature of particulate matter
- Methods of disposal: continuous or batch, dry or wet slurry

Generally, speaking, if there is a high concentration of wet and/or sticky particulate matter (PM), either a particulate wet scrubber or a wet electrostatic precipitator is used.

If the PM is primarily dry, mechanical collectors, wet scrubbers, conventional electrostatic precipitators, and fabric filters can be used. The selection depends on the particle size range and the efficiency requirements.

When selecting between mechanical collectors and wet scrubbers, mechanical collectors are the more economical choice. They have a lower purchase cost and a lower operating cost.

- If a significant portion of the PM in the gas stream is less than 0.5-mm size range, and high efficiency is needed, a fabric filter is the most common choice.
- If a significant portion of the PM is in the 0.5- to 5-mm size range, and high efficiency control is needed, fabric filters, electrostatic precipitators, or wet scrubbers could be used.
- If most of the particulate matter is larger than 5 mm, any of the four main types of particulate removing systems described here could be used.
- If gases and vapors in the gas stream are combustible or explosive, mechanical collectors or wet scrubbers can be used because both systems can be designed to minimize the risks of ignition. In some cases, a fabric filter can also be used if it includes the appropriate safety equipment. For these types of gases, electrostatic precipitator is not used due to the risk of ignition caused by electrical sparking in the precipitator fields.

References

Allen, H.S.: Motion of a Sphere in a viscous Fluid, Phys. Mag. **50**, 323 (1900)

Anderson, E.: Report, Western Precipitator Co, Los Angeles, CA. Trans. Am. Inst. Chem. Eng. **16**(69) (1924)

Billings, C.E., Wilder, J.: Handbook of Fabric Filter, vol. 1. N° APTD-0690, National Technical Information Service, NTIS: PB 200–648, US Environmental Protection Agency (1970)

Bouziani, A., Maâlmi, M., Tahiri, M.: Étude des Performances d'une Tour à Pulvérisation pour le Dépoussiérage de Gaz, Comptes Rendus Phys. **7**, 292 (2006)

Calvert, S., Goldshmid, J., Leith, D., Mehta, D.: Scrubber Handbook. NTIS, Springfield (1972). USI DE89 72 W271

Calvert, S., Goldshmid J., Leith D.: Scrubber performance for particle collection. AIChE Symp. Ser. **72**, 357 (1974)

Chen, C.Y.: Chem. Rev. **55**, 595 (1955)

Cooper, D., Alley, F.: Air Pollution Control: A Design Approach, 2nd edn. Waveland Press, Prospects Heights, IL (1994)

Deutsch, W.: Bewegung und Ledung der Elektricitatstrager in Zylinder Kondensator. Ann. Phys. (Leipzig) **68**, 335 (1922)

Dullien, F.A.L.: Introduction to Industrial Gas Cleaning. Academic Press, Inc., New York (1989)

Gallaer, C.A.: Electrostatic Precipitator Reference Manual. Electric Power. Research Institute. EPRI CS-2809, Project 1402–4 (1983)

Hesketh, H.E.: Atomization and Cloud Behavior in Wet Scrubbers, Symposium Control Fine Particulate Emissions, San Francisco, January (1974)

Koch, W.H., Licht, W.: New Design Approach Boosts Cyclone Efficiency, Chem. Eng. Int. Ed. **84**, 80 (1977)

Lamb, H.: Hydrodynamics. Dover, New York (1945)

Lapple, C.E.: In: Danielson, J. (ed.) Air Pollution Engineer Manual. US dept of Health, Education and Welfare, PHS No. 999-AP-40, p. 95 (1967)

Matts, S., Ohnfeldt, P.O.: Efficient Gas Cleaning with SF Electrostatic Precipitators. Flakten Rev, **6**, 105, Sweden (1964)

McCabe, W.L., Smith, J.C., Harriott, P.: Unit Operations of Chemical Engineering, 5th edn. McGraw-Hill, New York (1993)

Nukiyama, S., Tanasawa, Y.: Experimentation on atomization of liquid by means of air stream. Nippon Kikai Gakkai Ronbunshu B Hen. **4**, 86 (1938)

Nukiyama, S., Tanasawa, Y.: Experimentation on atomization of liquid by means of air stream. Trans. Soc. Mech. Eng. Jpn. **5**, 63 (1939)

Oglesby, S., Nichols, G.B.: A Manual of Electrostatic Precipitator Technology, Part II. Southern Research Institute, Birmingham (1970)

Pell, M., Dunson, J.B.: Gas-solid operations and equipment. In: Perry, R.H., Green, D. (eds.) Perry's Chemical Engineer's Handbook, 7th edn. McGraw-Hill Book Company, New York (1998)

Perry, R.H., And Green, D.: Perry's chemical engineer's handbook. In: Gas-Solid Operations and Equipment, 7th edn. McGraw-Hill Book Company, New York (1998)

Raguin, J.: "Techniques de Dépollution des rejets Atmosphériques Industriels", in "Techniques de l'Ingénieur, traité de Génie des Procédés", J-3920, ed. TI (1994)

Schiller, L., Naumann, A.: Ueber Die Grundlegenden Berechnungen bei der Schwerkraftaufbereitung. VDI Z. **77**, 318 (1933)

Siret, B.: Dépoussiérage et dévésiculage, in: "Tehniques de l'ingénieur, traité de Génie des Procédés", J-3580, ed. TI (1994)

Stairmand, C.J.: Pressure drop in cyclone separators. Engineering **168**, 409 (1949)

Stairmand, C.J.: Design and Performance of Cyclone Separators, Trans. Inst. Chem. Eng. **29**, 356 (1951)

Strauss, W.: Industrial gas cleaning, 2nd edn. Pergamon, Oxford (1975)

Swift, P.: Dust Control in Industry, Steam Heat Eng. **38**, 453 (1969)

White, H.J.: Electrostatic Precipitation of Fly Ash. Journal of Air Pollution Control Association, Pittsburgh (1977)

Williams, C.E., Hatch, T., Greenburg, L.: Determination of cloth area for industrial filters. Heat. Piping Air Cond. **12**, 259–263 (1940)

The Role of Catabolic Plasmids in Biodegradation of Petroleum Hydrocarbons

Alexander M. Boronin and Irina A. Kosheleva

Abstract

Genes encoding biodegradation of oil hydrocarbons are often localized on large conjugative plasmids. Transmissibility of catabolic plasmids ensures the dissemination of biodegradation features within indigenous microbial populations. Horizontal gene transfer mediated by plasmids plays an important role in the adaptation of bacteria to polluted environments and can be useful for genetic bioaugmentation.

Keywords

Biodegradation • Catabolic plasmids • Genetic bioaugmentation

1 Introduction

Environmental pollution by petroleum and the resulting ecological damage are a growing worldwide problem. A variety of environmental cleanup systems have been developed and utilized to try to provide environmental remediation and protection from recalcitrant organic pollutants. Bioremediation provides cost-effective and contaminant-specific treatments. Biodegradation is the main process that results in removing environmental pollutants and is carried out by microorganisms, predominantly bacteria. The capability of microorganisms to transform or degrade oil hydrocarbons is well documented and allows them to be used for the bioremediation of polluted environments. Great potential for developing new bioremediation technologies, and improving existing ones, lies in improving our understanding of the metabolism and genetic control of biodegradation processes, especially involvement of catabolic plasmids and ecology of microorganisms capable of degrading oil and oil products.

A.M. Boronin (✉)
Department of Microbiology & Biotechnology, Pushchino State Institute of Natural Sciences, Pushchino 142290, Russia
e-mail: boronin@ibpm.pushchino.ru

I.A. Kosheleva
Skryabin Institute of Biochemistry and Physiology of Microorganisms, Russian Academy of Sciences, Pushchino 142290, Russia

Mechanisms of bioremediation include biostimulation or bioaugmentation. Biostimulation is the addition of nutrient amendments to soil and/or groundwater to stimulate indigenous microorganisms capable of degrading environmental pollutants and consequently biodegradation. If biodegradative activity of indigenous microflora is not sufficient or absent, bacteria with degradation capacity can be introduced in situ in the soil of the site. It is particularly promising for heavy fractions of oil which are hard to degrade by microbes due to low bioavailability. Bioaugmentation is the addition of specifically selected pre-grown microorganisms to degrade contaminants. The enhancement of the microbial population present at a site subsequently improves contaminant cleanup through ensuring the presence of sufficient quantities of microorganisms in the soil to complete biodegradation and additionally reduces cleanup costs and time.

2 Degrader Microorganisms and Catabolic Plasmids

Crude oil is a complex mixture of hydrocarbons and other chemicals. The composition varies widely depending on where and how the oil was formed. The hydrocarbons in crude oil are mostly alkanes, cycloalkanes, and various aromatic hydrocarbons, while the other organic compounds

G. Cao and R. Orrù (eds.), *Current Environmental Issues and Challenges*,
DOI 10.1007/978-94-017-8777-2_9,

contain nitrogen, oxygen, and sulfur and trace amounts of metals such as iron, nickel, copper, and vanadium.

A large number of bacteria with oil hydrocarbon-degrading capabilities have been reported; among them are bacteria from different genera such as *Pseudomonas*, *Sphingomonas*, *Burkholderia*, *Mycobacterium*, *Corynebacterium*, *Aeromonas*, *Rhodococcus*, and *Bacillus*. Bacteria belonging to the genus *Pseudomonas* are noted possessing great metabolic potential and are able to acquire new capabilities during adaptation to specific conditions such as polluted environment.

Bacteria can degrade the following petroleum or hydrocarbon products with relative ease: gasoline, diesel, and fuel oil; hazardous crude oil compounds, such as benzene, toluene, and xylene; polycyclic aromatic hydrocarbons, such as naphthalene, phenanthrene, and pyrene; and alkanes.

Some chemicals are only partially degradable, or sometimes wastes are so mixed and variable that they degrade at different rates and may leave some toxic chemicals behind.

Degradation of different pollutants is often controlled by plasmids. Bacterial plasmids are mobile genetic elements able to replicate autonomously. Catabolic (degradative) plasmids confer their bacterial host's ability to degrade some unusual substrates such as oil hydrocarbons or synthetic compounds. The first reports of catabolic plasmids were made in the 1970s. To date a range of plasmids, catabolic transposons, and gene clusters have been identified which encode the degradation of naturally occurring and synthetic pollutants.

The generally accepted classification of plasmids is based on incompatibility groups. In 1971, Hedges and Datta proposed a plasmid classification scheme based on the instability of identical or related plasmids in one bacterial cell during growth, a phenomenon called incompatibility. Two plasmids are incompatible if they cannot coexist in the same bacterial cell simultaneously or if either is less stable in the presence of the other than it was by itself. Incompatibility group is determined by the genetic information specified by plasmid DNA, more specifically by their replication/partitioning functions. Generally, closely related plasmids are incompatible. Incompatibility grouping had been used to group plasmid of *Pseudomonas* species (Jacoby 1977) and the *Enterobacteriaceae* (Couturier et al. 1988). At present there are 14 listed plasmid incompatibility groups in *Pseudomonas* (Boronin 1992) and about 30 incompatibility groups in *Enterobacteriaceae*.

One of the fundamental properties of bacterial plasmids is their host range that is primarily determined by the plasmid replication system. A plasmid's host range is defined as the range of bacterial hosts in which the plasmid can replicate. Usually this range differs from the range of hosts into which plasmid can transfer by conjugation and the range of hosts in which plasmid is able to maintain stability without selective pressure. Most plasmids have a narrow host range (NHR) allowing only intraspecies transfer and replication. These plasmids are sometimes called "specialist." However, some plasmids have a broad host range (BHR) and can therefore maintain in many species of bacteria. BHR plasmids ("generalist") may be either self-transmissible (conjugative) or not self-transmissible but mobilizable (Sota and Top 2008). It seems that BHR plasmids are most important for horizontal gene transfer (HGT) between distantly related bacterial hosts. Plasmids can evolve to expand or at least shift their host range. High frequency of conjugal transfer of BHR plasmids belonging to IncP-1 group within an isogenic population accelerates the plasmids' adaptation and stability in new bacterial hosts which initially were unfavorable for these plasmids (Heuer et al. 2007).

Among the plasmids encoding degradation of naturally occurring organic molecules, IncP-9, IncP-7, and IncP-2 are dominant, whereas IncP-1 plasmids are prevalent among those determining degradation of man-made compounds (Top et al. 2000). There is at least one exception – CAP plasmids which determine degradation of ε-caprolactam and belong to P-2, P-7, and P-9 incompatibility groups. ε-Caprolactam, a man-made compound, is used as raw stuff to produce polymer materials (polycaproamide, nylon 6) for industry, agriculture, medicine, and household activities (Esikova et al. 1990). However, CAP plasmids are beyond the scope of this chapter.

Catabolic plasmids are large and often contain the full set of conjugal transfer genes as well as all genes organized in catabolic operons for biodegradation of various hydrocarbons. Transmissibility of such plasmids ensures the dissemination of biodegradation features within and between microbial populations and influences the process of bacterial microevolution. When hydrocarbon-degrading bacteria, containing appropriate plasmids, are introduced to polluted soils, these microorganisms not only degrade the contaminant but potentially also serve as plasmid donors for indigenous microorganisms. Degradative plasmids encode utilization of aliphatic compounds (octane, decane, hexadecane, etc.) and aromatic (phenol, toluene, xylene) and polycyclic aromatic hydrocarbons (naphthalene, phenanthrene, pyrene, etc.).

2.1 The OCT Plasmids

n-Octane is a common component of gasoline and other petroleum products. Many microorganisms, including genus *Pseudomonas*, are able to use linear alkanes as their sole source of carbon and energy (van Beilen et al. 1994).

The genetics and biochemical pathway of alkane metabolism have been well investigated for *Pseudomonas putida* (*oleovorans*), which is able to oxidize C_5–C_{12} n-alkanes.

Genes encoding biodegradation of octane are localized on the OCT plasmid and called *alk* genes. The naturally occurring OCT plasmid (IncP-2 group) consists of three distinct plasmids, namely, OCT plasmid responsible for octane utilization, MER plasmid encoding mercury resistance, and transfer plasmid (factor K). Initial OCT plasmid is conjugative; however, after dissociation into three distinct plasmids, OCT is non-conjugative but is mobilizable.

The OCT plasmid of *Pseudomonas oleovorans* contains two operons, *alkBFGHJKL* and *alkST*, which encode all proteins necessary for the degradation of n-octane and other 5- to 12-carbon linear alkanes to the corresponding acyl-CoA derivatives. Both clusters of the genes (*alkBFGHJKL* and *alkST*) encoding the *P. putida* GPo1 alkane degradation pathway are regulated by the AlkS protein. When no alkanes are present, *alkS* is expressed at low levels. The first catabolic operon of OCT plasmid encodes seven proteins, of which at least three are involved in alkane hydroxylation and alkanol dehydrogenation; the final product of this pathway, octanoyl-CoA, enters the beta-oxidation cycle and can be utilized as carbon and energy sources (van Beilen et al. 1994). Growth on alkanes requires a functional chromosomally encoded fatty acid degradation system in addition to the plasmid-borne *alk* system; such a system usually is active in *P. putida*. The nucleotide composition of the *alk* genes (47 % G + C) differs considerably from the G + C content of the *P. oleovorans* genome, suggesting that the alk regulon may originate from an unrelated organism. It has been shown that OCT plasmid encodes, among others, a methyl-accepting transducer protein (AlkN) that may be involved in chemotaxis to alkanes (van Beilen et al. 2001).

Two other plasmid-located genetic systems for alkane utilization have been partially characterized. *Pseudomonas maltophilia* N246-1 bears large IncP-2 plasmid allowing the host strain to grow on C_8–C14 of n-alkanes. The OCT plasmid can transfer to *Rhodopseudomonas sphaeroides* with a low frequency (Lee et al. 1993). The ability of *Pseudomonas* sp. strain C12B to utilize medium-chain-length n-alkanes (C_9–C_{12}) is encoded by plasmid pDEC. The enzyme system encoded by the putative *dec* genes present on plasmid pDEC differs from the system coded by the *alk* genes of plasmid OCT in the size range of hydrocarbons preferentially used (Kostal et al. 1998).

2.2 Plasmids Involved in Phenol Biodegradation (PHE Plasmids)

A common pathway for metabolizing an aromatic compound like phenol is to dihydroxylate the benzene ring to form a catechol. Catechol is oxidized via *ortho* pathway (intradiol cleavage) by catechol 1,2-dioxygenase or via *meta* pathway (extradiol cleavage) by catechol 2,3-dioxygenase. Further degradation is realized by distinct sets of enzymes. The final products of both the pathways are molecules that can enter the tricarboxylic acid cycle. Dihydroxylation is carried out by multi- or single-component phenol hydroxylases (Kivisaar et al. 1990).

The catabolic plasmid pVI150 of *Pseudomonas* sp. strain CF600 encodes all the genetic information required for the metabolism of phenol and some of its methyl-substituted derivatives as sole carbon and energy sources. The plasmid is very large and conjugative and belongs to the incompatibility group P-2. Biochemical pathway for the dissimilation of phenolic compounds involves a multicomponent phenol hydroxylase and subsequent *meta* cleavage pathway. These enzymes are encoded by 15 *dmp* structural genes in a single operon of pVI150. The operon is regulated by *dmp*R gene product belonging to the NtrC family of transcriptional activators that regulate transcription from -24/-12 promoters (Shingler et al. 1993).

The naturally occurring plasmid pPGH1 from *Pseudomonas putida* H also encodes inducible degradation of phenol and some of its methylated derivatives via the *meta* cleavage pathway (Herrmann et al. 1995). The plasmid DNA region about 16 kb contains all genetic information necessary for inducible degradation of phenolic compounds. Degradative genes are organized into a single operon encoding for a multicomponent phenol hydroxylase and *meta* cleavage pathway enzymes. Catabolic operon is subject to positive control by the product of regulatory gene.

Plasmids carrying genes for phenol degradation (*phe* genes) through catechol *ortho* cleavage pathway obtained as a result of long-term cultivation of the *Pseudomonas putida* multiplasmid strain EST1020 on phenol have been characterized (Kivisaar et al. 1990). PHE plasmids determine phenol monooxygenase (gene *pheA*) and catechol 1,2-dioxygenase (gene *pheB*), the key enzyme for *ortho* pathway. Sequencing of *pheB* has shown the relationship between the *pheB* gene and other C12O-encoding genes. The comparison of the *pheB* sequence with sequences of *catA* of *Alcaligenes calcoaceticus*, *tfdC* of *A. eutrophus*, and *clcA* of *P. putida* demonstrated that there are conserved residues in all the four protein products of these genes (Kivisaar et al. 1991).

Pseudomonas putida PaW85, carrying recombinant plasmid pAT1140 that contains the inducible pheBA operon, is able to degrade phenol using hybrid plasmid–chromosome-encoded pathway. The synthesis of the plasmid-encoded phenol monooxygenase and catechol 1,2-dioxygenase is induced by cis,cis-muconate. The pheBA operon is positively controlled by the regulatory protein CatR that is chromosomally encoded in *P. putida* (Kasak et al. 1993).

The bacterial strain *Pseudomonas putida* PhCN resistant to heavy metals has genetic systems for biodegradation of phenol. The strain contains two plasmids, a 120 kb catabolic plasmid that encodes the degradation of phenol (pPhCN1)

and pPhCN2 plasmid (100 kb) that codes for cadmium and copper resistance (El-Deeb 2009).

The analysis of nine oil-degrading strains isolated from contaminated soils in Western Siberia able to grow on phenol as sole carbon and energy sources reveled that at least for two strains, degradation of phenol is encoded by conjugative plasmids about 100 kb in size (Makarenko et al. 2002).

2.3 The TOL Plasmids

The ability to degrade toluene or BTEX compounds (benzene, toluene, ethylbenzene, xylene) is common among soil microorganisms such as *Pseudomonas*. Therefore, biochemical pathways and the genetic control of toluene degradation are well characterized. At least five different pathways are known for aerobic catabolism of toluene. The pathway for the catabolism of toluene and some substituted toluenes via *meta* cleavage of catechol utilization is very often encoded by plasmids collectively called TOL plasmids. The archetype TOL plasmid pWW0 was first described in 1974 (Williams and Murray 1974). Plasmid pWW0 was assigned to the P-9 incompatibility group. The *xyl* genes of *Pseudomonas putida* TOL plasmid encoding degradation of toluenes and xylenes are organized in four transcriptional units: the upper operon *xylUWCAMBN* for conversion of toluenes/xylenes into benzoates/alkylbenzoates; the *meta* operon *xylXYZLTEGFJQKIH*, which encodes the enzymes for further conversion of these compounds into Krebs cycle intermediates; and *xylS* and *xylR*, which are involved in transcriptional control. The XylS and XylR proteins are members of the XylS/AraC and NtrC families, respectively, of transcriptional regulators. The *xylS* gene is constitutively expressed at a low level from the Ps2 promoter. The XylS protein is activated by interaction with alkylbenzoates, and this active form stimulates transcription from Pm. The *xylR* gene is also expressed constitutively. The XylR protein, which in the absence of effectors binds in a non-active form to target DNA sequences, is activated by aromatic hydrocarbons and ATP; it subsequently undergoes multimerization and structural changes that result in stimulation of transcription from Pu of the upper operon. Once activated, the XylR protein also stimulates transcription from the Ps1 promoter of xylS without interfering with expression from Ps2 (Ramos et al. 1997). The pWW0 plasmid's degradative genes are located within class II (*Tn3*-like) catabolic transposons *Tn4651* (56 kb) and *Tn4653* (70 kb), and the latter transposon includes the former (Tsuda et al. 1989). The analysis of the complete pWW0 nucleotide sequence revealed 148 putative open reading frames. Of these, 77 showed similarity to predicting functions for plasmid replication, stable maintenance, conjugal transfer, catabolic determinants, and transposition (Greated et al. 2002). All identifiable transposition functions are located within the boundaries of transposon Tn*4653*, leaving a 46 kb region containing the IncP-9 plasmid's core functions. Thus, the sequence of pWW0 and its comparison to others suggest that the current structure can be derived from a single original insertion of the *Tn4563* transposon into IncP-9 ancestor plasmid. To the author's opinion, the complexity and size of pWW0 are largely the result of the mosaic organization of the transposable elements that it carries, rather than the backbone functions of IncP-9 plasmids.

Investigations of many environmental *Pseudomonas* isolates capable of growing on toluene, *m*-xylene, and *m*-toluate have shown that TOL-like plasmids are widely distributed in the environment. A number of TOL plasmids which carry *xyl* genes that are strongly homologous to those in pWW0 have been described. The plasmids differ in size, incompatibility, and ability to conjugal transfer. The plasmid pWW53 isolated from *Pseudomonas putida* MT53 is a 107 kb nontransmissible plasmid that does not belong to the P-9 incompatibility group. This plasmid carries a single upper pathway operon, two highly homologous but distinguishable *meta* operons, a single *xylR* gene, and three *xylS*-homologous genes (*xylS1*, *xylS2*, and *xylS3*) (Keil et al. 1985). Thus, the naturally occurring TOL plasmid may carry genes for two *meta* cleavage dioxygenases. The second homologous gene for catechol 2,3-dioxygenase also is present on naturally occurring TOL plasmids pWW5, pWW74, and pWW88. Other plasmids, pWW14 and pWW84, carried the second but nonhomologous C23O gene C23OII (Chatfield and Williams 1986).

The TOL plasmid pDK1 (129 kb in size) isolated from *Pseudomonas putida* HS1 and belonging to IncP-7 group carries two homologous but nonidentical copies of *xylS* regulatory genes. The comparison of the organization of the *xyl* catabolic operons on pDK1 and pWW53 indicates that the catabolic region on pDK1 was derived from a replicon on which the *xyl* genes are organized similarly to pWW53 and that a genetic rearrangement has taken place involving a reciprocal recombination internal to two of its *xylS* homologues (Assinder et al. 1993). Complete nucleotide sequence of pDK1 and comparative analysis revealed that toluene catabolic gene clusters of this plasmid were derived through homologous recombination, transposition, and site-specific recombination from the *xyl* gene clusters homologous to another TOL plasmid, pWW53. Moreover, recipient host range of conjugal transfer of pDK1is limited to only two *Pseudomonas* strains in spite of the fact that the mini-replicon of pDK1 is maintained in at least six *Pseudomonas* strains. These results indicate that IncP-7 plasmids have narrow host range and that IncP-7-specified conjugal transfer was narrower than that of its replication (Yano et al. 2010).

The majority of pSVS plasmids in *P. putida* strains isolated from different contaminated sites in Belarus carry *xyl* genes homologous to those of pWW53 and are organized in a similar manner (Sentchilo et al. 2000). These plasmids

contain two distinguishable *meta* operons, one upper pathway operon and three *xylS*-homologous regions. Two other pSVS plasmids carry one upper operon, one *meta* operon, and one copy of each regulatory gene.

Pseudomonas putida O_2C_2, isolated from oil-contaminated soil in the Netherlands, is able to grow on toluenes and methyl-substituted toluenes and contains the large plasmid pWW102 (the size is between 220 and 270 kb). The relative location of *xyl* operons differs from the organization of those in archetype plasmid pWW0: the upper pathway operon *xylUWCAMBN* being located downstream of the *meta* operon *xylXYZLTEGFJQKIH*, the two regulatory genes *xylS* and *xylR* are found immediately downstream of the *meta* pathway operon (Aemprapa and Williams 1998).

2.4 The NAH Plasmids

Naphthalene and its substituted derivatives are commonly found in crude oil and oil products. Naphthalene-degrading microorganisms are widely distributed in nature and are easy to isolate from different coal tar- and oil-contaminated soils. Among taxonomic groups of microorganisms able to degrade polycyclic aromatic hydrocarbons (PAH), a high proportion of the isolates belong to *Pseudomonas*, *Shingomonas*, and *Burkholderia* strains. The key intermediate of naphthalene biodegradation is salicylate, which is further catabolized via catechol or gentisate by catechol 2,3-dioxygenase (*meta* pathway) or catechol 1,2-dioxygenase (*ortho* pathway) and gentisate 1,2-dioxygenase, respectively.

Naphthalene biodegradation by *Pseudomonas* spp. is often determined by large conjugative plasmids. Plasmids carrying naphthalene catabolic genes represent a class of well-characterized degradation plasmids, known collectively as NAH plasmids. The plasmids NAH7 from *Pseudomonas putida* G7 and pDTG1 from *P. putida* NCIB 9816 are the best-studied naphthalene catabolic plasmids. The *nah* genes for naphthalene catabolism are organized in the upper pathway operon (*nahAaAbAcAdBFCQED*) which controls initial oxidation and subsequent degradation to salicylate (*nah* operon) and the lower operon (*nahGTHINLOMKJ*) for salicylate oxidation and further catechol *meta* cleavage pathway to tricarboxylic acid cycle intermediates (*sal* operon). Downstream of the *nahJ* gene of *P. putida* strain G7, two additional genes coding for an unknown function (*nahX*) and chemotaxis toward naphthalene transducer protein (*nahY*) were found (Habe and Omori 2003). A methyl-accepting chemotaxis protein, NahY, is cotranscribed with the degradation genes. In both strains a second operon encodes the enzymes for catabolism of salicylate to central metabolites via catechol and extradiol cleavage by catechol 2,3-dioxygenase. Both *nah* and *sal* operons are activated by a *trans*-acting positive regulator encoded by *nahR* gene and commonly are induced by a naphthalene intermediate – salicylate. The product of *nahR* gene, NahR is a member of the LysR family of transcriptional activators that are widely distributed in bacteria. Positive regulatory protein NahR binds to the promoters of *nah* and *sal* operons and activated their transcription after interaction with salicylate (Shell 1990). NahR proteins from different naphthalene-degrading *P. putida* strains exhibit a highly conserved helix–turn–helix motif and a putative enhancer-binding region in the N-terminal domain. Gene activation by NahR is consistent with the general transcriptional mechanism of class I transcription factors, by protein–protein interactions between alphaRNAP and NahR (Park et al. 2002).

Plasmids NAH7 and pDTG1 are conjugative and 83 kb in size and belong to incompatibility group P-9. Naphthalene catabolic genes on the NAH7 plasmid are located within a 37.5 kb region, which is the defective class II transposon, *Tn4655*.

The complete sequence of naphthalene-degrading 83 kb plasmid pDTG1 from *P. putida* strain NCIB 9816-4 has revealed that the upper and lower naphthalene-degrading operons occupy 9.5 kb and 13.4 kb, respectively (Dennis and Zylstra 2004).

The complete nucleotide sequence of 102 kb plasmid pND6-1 isolated from naphthalene-degrading *Pseudomonas* sp. strain ND6 was also determined. Among the 23 naphthalene catabolic genes in pND6-1, almost all have 99–100 % identity in amino acid sequences homologous to their nearest counterparts found in plasmids pDTG1 and NAH7 and in a chromosome region in *Pseudomonas stutzeri* AN10 except for two duplicated genes, ND013 and ND016 (Li et al. 2004). Interestingly, that plasmid pND6-1 contains two duplicate naphthalene catabolic genes. ND013 and ND016 were duplicate genes of ND058 (*nahF*) and ND091 (*nahG*), respectively. Later ND016 was identified as *nahU* (isofunctional gene of the classical salicylate hydroxylase gene), encoding a new salicylate hydroxylase, NahU, which possesses a higher binding ability to salicylate and cofactors and catalytic efficiency in comparison with NahG (Zhao et al. 2005).

In NAH7, the regulatory gene *nahR* is located between *nah* and *sal* operons and the direction of transcription of the two operons is identical. In pDTG1 and pND6-1, gene *nahR* is located upstream of *nah2* operon, and both operons are transcribed in opposite direction toward each other. The intervening region between the upper and lower *nah* operons of NAH7 does not show any homology with the corresponding regions of pDTG1 and pND6-1 plasmids. These data suggest that the *nah* operons on NAH7 have been acquired differently from those of pDTG1 and pND6-1 (Sota et al. 2006). The comparison of NAH7 with two other completely sequenced IncP-9 catabolic plasmids, pDTG1 and pWW0, revealed that the three plasmids share very high nucleotide similarities in a 39 kb region encoding the basic plasmid functions (the IncP-9 backbone). The backbone of NAH7 is phylogenetically more

related to that of pDTG1 than that of pWW0 (Sevastsyanovich et al. 2008). The IncP-9 naphthalene-degrading plasmid pNAH20 (83 kb in size) from multiplasmid *Pseudomonas fluorescens* strain PC20 exhibits a similarity to another naphthalene plasmid, pDTG1. However, the positions of insertion sequence (IS) elements significantly alter both catabolic and backbone functions provided by the two plasmids (Heinaru et al. 2009). The *P. fluorescens* strain PC20 harbors two large plasmids – self-transmissible pNAH20 and mobilizable pPHE20. These plasmids enable the host strain to degrade naphthalene and phenol simultaneously via catechol *meta* and *ortho* degradation pathways, respectively. The transfer frequency of pNAH20 is 100 times higher than that of pDTG1 probably due to the insertion of the pCAR1 IS*Pre2*-like element into the *mpfR* gene coding for a putative repressor of the *mpf* operon responsible for mating pilus formation. The plasmid pNAH20 can mobilize pPHE20, and the IncQ broad-host-range plasmid, the RSF1010-based PHE plasmid pEST1412 (Heinaru et al. 2009).

Naphthalene catabolic plasmids differ in size, restriction patterns, and incompatibility groups and revealed a high level of DNA homology among *nah* genes, and the gene order within either upper or *meta* pathway operons seems to be invariable. However, the relative position of both the operons and the regulatory genes varies. Naphthalene operons can be located in *trans* as it has been shown for *P. putida* strains bearing NPL-1, pBS1141, and pBS1191. In the first two cases, *nah* operon is located on the plasmids, and *sal* operon on the host bacterial chromosome; in the third case, the gene encoding key enzyme of *sal* operon (*salG*) is located on another plasmid – pBS1192. However, plasmids NPL-1, pBS1141, and pBS1191 contain nonfunctioning *salG* gene (Kosheleva et al. 2003). The plasmid NPL-1 contains at least two class II transposons of the Tn3 family; one of them is located between two catabolic operons near regulatory *nahR* gene. These transposons are involved in intraplasmid rearrangements, such as deletions and inversions, and can influence the expression of the catabolic and regulatory genes borne by biodegradation plasmids. The formation of a strong NahR-independent constitutive promoter by the inversion of a DNA fragment may be responsible for changing the character of naphthalene dioxygenase synthesis from inducible (in the case of plasmid NPL-1) to constitutive (in the case of plasmid NPL-41).

Most of the naphthalene biodegradation plasmids contain the genes for salicylate metabolism via *meta* pathway of catechol oxidation. However, genetic control of naphthalene biodegradation through salicylate and gentisate ("gentisate" pathway) also has been studied.

The *Pseudomonas putida* AK5 that was isolated from slime pit of Nizhnekamskneftekhim chemical factory can metabolize naphthalene via salicylate and gentisate. Naphthalene and salicylate catabolic genes are localized on non-conjugative IncP-7 plasmid pAK5, about 115 kb in size. The "classical" *nah* operon and the novel *sgp* operon (salicylate–gentisate pathway) are involved in naphthalene-degrading by *P. putida* AK5 (Izmalkova et al. 2013). The *sgp* operon contains six open reading frames (*sgpAIKGHB*). The four ORFs code for the entire salicylate 5-hydroxylase-oxidoreductase component (*sgpA*), large and small subunits of oxygenase component (*sgpG* and *sgpH*), and 2Fe–2S ferredoxin (*sgpB*). Genes for gentisate 1,2-dioxygenase (*sgpI*) and fumarylpyruvate hydrolase (*sgpK*) incorporate in salicylate 5-hydroxylase gene cluster between *sgpA* and *sgpG*. The putative positive regulator for *sgp* operon gene *sgpR* is located upstream from the *sgpA* gene and oriented in the opposite direction from *sgpA*. Putative maleylacetoacetate isomerase gene locates apart, directly downstream from the *sgp* operon. The *sgp* operon organization and phylogenetic analysis of deduced amino acid sequences indicate that this operon has a mosaic structure.

All NAH catabolic plasmids investigated to date encode a single upper pathway for the conversion of naphthalene to salicylate. High level of homology between NAH genes on different plasmids isolated from *Pseudomonas* sp. suggests that these catabolic plasmids are related.

Most of the naphthalene catabolic plasmids belong to incompatibility groups P-9 and P-7. Environmental studies have suggested a wide distribution of IncP-9-like replicons in nature and their involvement in natural horizontal gene transfer of the naphthalene-degrading trait. It should be noted that IncP-9 plasmids have a moderate range of host bacteria, whereas IncP-7 plasmids are those with a narrow host range. Naphthalene-degrading plasmids of IncP-7 group can be isolated more rarely than IncP-9.

A large collection of naphthalene-degrading fluorescent *Pseudomonas* strains isolated from sites contaminated with coal tar and crude oil were screened for the presence of degradative plasmids. About 50 % of strains were found to carry naphthalene catabolic plasmids of IncP-9 group ranging in size from 83 to 120 kb. The analysis of several strains bearing IncP-7 naphthalene catabolic plasmids revealed that the structure of IncP-7 plasmids is more various than the structure of IncP-9 plasmids. All IncP-7 plasmid-bearing strains were isolated from hardly contaminated soils, while IncP-9 plasmid-bearing strains were more widely spread and can be isolated from the relatively pristine environments too. Prevalence and diversity of IncP-7 and IncP-9 plasmids in polluted and pristine environments have been also determined by using primers specific for IncP-9 and IncP-7 backbone segments. While a pool of IncP-7 plasmids were detected in contaminated soil samples, IncP-9 plasmids seem to be ubiquitous. About 30 % of NAH plasmids have not been assigned to a particular group. It may be that these plasmids do belong to known groups, but at present they cannot be assigned to one. The absence of DNA probes or

DNA primers for PCR amplification for all the known groups makes it difficult to perform the classification easily. New incompatibility groups of catabolic plasmids could be established when the relation between unclassified plasmids and the defined groups will be studied in detail.

3 Genetic Bioaugmentation

3.1 Horizontal Transfer of Catabolic Plasmids

Horizontal gene transfer (HGT) is defined to be the movement of genetic material between bacteria other than by descent in which information travels through the generations as the cell divides. Plasmids as mobile genetic elements play an important role in HGT resulting in microbial adaptation to environmental changes and in the spread of existing catabolic pathways. Moreover horizontal exchange of degradative genes among bacteria in microbial communities plays a significant role in the evolution of catabolic pathways. It has been suggested that the complete catabolic pathways for degradation of at least aromatic hydrocarbons have evolved through modular fusion (Bosch et al. 1999). Catabolic operons are often located within transposons and bordered by insertion sequences. Transposons and IS elements play a significant role in recruitment of catabolic clusters by the replicon and also may increase further DNA rearrangements and exchange of the genes between different bacterial hosts and different replicons. The suggestion is made that the genes *nahAc* and *nahG* evolved independently and occur in *Pseudomonas* sp. strains in different combinations. Thus, *nah*-like genetic systems, despite conservative organization and high level of homology, demonstrate significant variability. Various configurations of the plasmids in different *Pseudomonas* sp. strains have arisen over time, and catabolic pathways are continuously subjected to selective pressure. Coexistence of duplicated genes or even operons within one plasmid as in the abovementioned TOL and NAH plasmids provides opportunities for recombination between them. Genetic plasticity of catabolic operons has appeared to play a significant role in adaptation of microorganisms to a wide variety of environmental conditions. In order to assess the prevalence of different hydrocarbon catabolic genotypes in nature and to monitor the evolution of modern catabolic pathways, there is a need for more complete nucleotide sequences for plasmids and degradative operons found in different hydrocarbon-degrading microorganisms. Bacterial plasmid genome sequence comparisons indicate that plasmids have complex genetic histories resulting from transposition, homologous recombination, and illegitimate recombinational events.

It is well documented that bacteria can readily exchange genetic information under artificial conditions typically used in most laboratory studies as well as to some extent in nature. The three mechanisms by which such genetic exchange can occur are transformation, transduction, and conjugation. Bacterial conjugation is the most widespread mechanism for horizontal DNA transfer in nature. As it has been mentioned above in addition to their degradative genes, most of the catabolic plasmids are transmissible via conjugation and contain clusters of transfer (*tra*) genes. Ecologically, plasmid-encoded pathways are advantageous because they provide genetically flexible systems and can be transferred between bacterial species.

When the in situ degradation potential is very low or absent, application of effective oil-degrading microorganisms is necessary. Introduced active microorganisms can themselves accelerate biodegradation of target pollutants; however, they have to compete with indigenous microbial flora which is usually more adapted to specific conditions of site. If the survival of used bacteria or bacterial consortium is poor, the introduction of degradative genes and operons, located on catabolic plasmids, into well-established, competitive indigenous microbial populations may play an important role in bioaugmentation. This approach is termed "plasmid-mediated" or "genetic" bioaugmentation. In genetic bioaugmentation, introduced microorganisms appear to be not only degrader strains but also donors of the catabolic genes for horizontal transfer to well-establish and competitive indigenous bacterial populations of a site. Spreading of catabolic genes increases the diversity of microorganisms capable of degrading target hydrocarbons and therefore accelerates the bioremediation process.

The occurrence of HGT in natural microbial communities has been well documented (Top and Springael 2003). These data were obtained by either retrospective analysis or by direct experimental studies. The retrospective approach is the investigation of distribution of very similar or highly homologous plasmids and genes among different microorganisms. For example, the presence of highly conserved *nahAc* allele among phylogenetically diverse bacteria bearing naphthalene catabolic plasmids (pDTG1-like) and isolated from geographically distant regions provides evidence for in situ horizontal transfer at coal tar-contaminated sites (Herrick et al. 1997). Data that horizontal transfer of naphthalene catabolic plasmids has indeed occurred between microorganisms in the soil bacterial community was also obtained in different experiments with soil microcosms using conjugative plasmids labeled by additional selectable marker. Conjugation transfer of catabolic plasmids was demonstrated in naphthalene-contaminated laboratory soil microcosms (Akhmetov, et al. 2008). The soil used in this work contained indigenous bacterial degraders of naphthalene which were isolated and identified as *Pseudomonas putida* and *Pseudomonas fluorescens*. In these

experiments, both indigenous microorganisms and the introduced laboratory strain *Pseudomonas putida* BS394 (pNF142::Tn*Mod*-OTc) served as donors of naphthalene biodegradation plasmids. As a recipient for indigenous catabolic plasmids, well-characterized *P. putida* strain KT2442 was used. Transconjugant strains harboring indigenous catabolic plasmids possessed high salicylate hydroxylase and low catechol 2,3-dioxygenase activities, in contrast to indigenous degraders, which had a high level of catechol 2,3-dioxygenase activity and a low level of salicylate hydroxylase. The transfer of the labeled plasmid pNF142::Tn*Mod*-OTc to the introduced plasmid-free recipient *P. putida* KT2442 and to indigenous soil microorganisms of the genus *Pseudomonas* was shown both under selective pressure (in the presence of naphthalene) and in its absence. The isolated transconjugant strains belonged to several species of the genus *Pseudomonas* (Filonov et al. 2010). This work has demonstrated that the plasmid-bearing *P. putida* strains KT2442 (pNF142::Tn*Mod*-OTc) and BS394 (pNF142::Tn*Mod*-OTc) could dominate over indigenous naphthalene destructors under selective pressure (soil contamination) and were quickly eliminated in the absence of the pollutant. The transfer of naphthalene biodegradation plasmids in soil microbial populations seems to enhance the efficiency of hydrocarbon biodegradation under field conditions due to the increase of microbial degradative potential. The occurrence of new bacterium-plasmid combinations resulting from horizontal transfer can lead to appearance of more efficient and competitive degrader strains that can be used for a successful bioremediation. However, authors could not present direct evidence for plasmid conjugal transfer-mediated biodegradation of naphthalene, since introduced strains themselves could survive, compete with indigenous microorganisms, and effectively degrade aromatic hydrocarbon.

Another example of HGT was demonstrated in a field bioaugmentation experiment with the abovementioned multiplasmid *P. fluorescens* strain PC20 (pNAH20, pPHE20) which is an effective degrader of pollutants (Heinaru et al. 2009). Occurrence of a natural transconjugant of pNAH20 was observed in birch rhizosphere. During in vitro transfer experiments, transconjugants of both plasmids pNAH20 and pPHE20 were obtained. It has been proposed that mobilization of the pPHE20 plasmid by the helper plasmid pNAH20 into the indigenous bacteria of the genus *Pseudomonas* might take place under natural conditions as well.

The best-studied catabolic plasmid pWW0 also has been used as a model for development of bioremediation strategies involving environmental release of plasmid-containing strains. Horizontal transfer of pWW0 in microbial biofilm communities has been investigated. The results demonstrated that plasmid transfer does occur when a donor interacts with a growing or established biofilm but that transfer to endogenous bacteria only occurs at the interface between the donor and recipient cultures and does not spread throughout the recipient population (Christensen et al. 1998). The mycorrhizosphere *Pseudomonas fluorescens* strain OS81 supplied with the TOL plasmid pWW0::Km was inoculated in microcosms with and without pine seedlings mycorrhized with *Suillus bovinus* (Sarand et al. 2000). After 3 months of regular treatment with *m*-toluate, the introduced catabolic plasmid was disseminated in the indigenous populations in both mycorrhizosphere and soil uncolonized by the fungus. Transconjugants were represented by the genera *Pseudomonas* and *Burkholderia*. It has been shown that inoculation of *P. fluorescens* OS81 (pWW0::Km) into microcosms influences the development of plants in contaminated soil protecting them from *m*-toluate. Since the inoculated strain was not detected after 3 months, protective effect was attributed to transconjugants receiving TOL plasmid and capable of degrading *m*-toluate.

3.2 Factors Affecting Horizontal Transfer and Expression of Catabolic Genes

Horizontal gene transfer is affected by many factors (environmental conditions) such as temperature, pH, soil textural type, moisture, and nutrient availability. A major factor was shown to be the level of nutrients as far as they stimulate plasmid transfer by enhancing the numbers and activities of donor and recipient bacteria (van Elsas et al. 2000). The presence of plant roots providing additional organic substrates allows higher frequency of catabolic gene transfer as well as higher metabolic activity compared to bulk soils. Exudates derived from the plant can help to stimulate the survival and action of bacteria, which subsequently results in a more efficient degradation of pollutants. Plant roots have nutrient-rich surfaces which provide conditions for microbial colonization and activities, e.g., plasmid conjugal transfer. The very important factor which dramatically affects the plasmid transfer rate in soil is selective pressure. Top et al. proposed that positive effect of the presence of the pollutant on the number of transconjugants is almost certainly due to the proliferation of the transconjugants, but not to a direct effect of the pollutant on the conjugation efficiency (Top et al. 2002). For successful bioaugmentation, it is desirable that effectively degrading pollutant transconjugants would be the numerically dominant population in the bacterial community. In order to grow to high density, the transconjugants need to have a selective advantage over the other indigenous bacteria which are usually more competitive without pollutants. Moisture, temperature, and soil pH influence on cell physiology in whole, and obviously these factors also effect on plasmid transfer. Indeed, plasmid transfer rates were highest at near-neutral pH values, whereas under acid conditions transfer was not detected and it was only detected at a favorable temperature for bacterial cells (van Elsas et al. 2000).

Even if transfer of degradative plasmid into some indigenous recipients was successful, expression of catabolic genes in new transconjugants can be limited. Alternative substrate availability may significantly change expression of catabolic genes transferred in a new recipient strain. The presence of glucose concurrently with toluene has been shown to trigger catabolite repression in *Pseudomonas putida* cells harboring the TOL plasmid (del Castillo and Ramos 2007). *E. coli* RP-1 cells containing the same TOL plasmid exhibited very low degradative functions when toluene is a sole carbon source. Large enhancement of toluene degradation rate and enzyme activities was observed when cells were exposed simultaneously on toluene and glucose or toluene and Luria-Bertani broth as easily degradable carbon source (Ikuma and Gunsch 2012). In spite of bacteria belonging to the *Enterobacteriaceae* family being very unlikely to use in bioremediation technology, these results indicated that additional carbon source may play a significant role in enhancement of catabolic abilities of degrader strains.

4 Conclusions

The role of plasmids and their horizontal transfer in evolution of bacterial genomes and adaptation of microbial populations to specific environmental changes is generally accepted nowadays. Despite that only a few reports have clearly demonstrated a direct effect of gene transfer on accelerated biodegradation, genetic bioaugmentation seems to be perspective for environmental cleanup biotechnology. For successful genetic bioaugmentation, knowledge about microbial communities of bioremediated sites is necessary to predict possible changes in their biodegradative potential. Changes in bacterial community structure in response to the contamination as well as the addition of nonindigenous microorganisms should be taken into account in the development of cleanup strategy. To access the fate and behavior of introduced plasmid in an open environment, preliminary studies are necessary concerning incompatibility group, host range, stability, and expression of catabolic genes in a new bacterial host's background. Catabolic plasmids are of great environmental significance. The type of catabolic plasmids and their horizontal transfer should be monitored for estimation of biodegradative potential of oil-contaminated soil.

References

Aemprapa, S., Williams, P.A.: Implication of the *xylQ* gene of TOL plasmid pWW102 for the evolution of aromatic catabolic pathways. SGM Microbiol. **144**, 1387–1396 (1998)

Akhmetov, L.I., Filonov, A.E., Puntus, I.F., Kosheleva, I.A., Nechaeva, I.A., Yonge, D.R., Petersen, J.N., Boronin, A.M.: Horizontal transfer of catabolic plasmids in the process of naphthalene biodegradation in model soil systems. Microbiology **77**, 29–39 (2008)

Assinder, S.J., De Marco, P., Osborne, D.J., Poh, C.L., Shaw, L.E., Winson, M.K., Williams, P.A.: A comparison of the multiple alleles of xylS carried by TOL plasmids pWW53 and pDK1 and its implications for their evolutionary relationship. J. Gen. Microbiol. **139**, 557–568 (1993)

Boronin, A.M.: Diversity of *Pseudomonas* plasmids: to what extent? FEMS Microbiol. Lett. **79**, 461–467 (1992)

Bosch, R., Garcia-Valdes, E., Moore, E.R.B.: Genetic characterization and evolutionary implications of a chromosomally encoded naphthalene-degradation upper pathway from *Pseudomonas stutzeri* AN10. Gene **236**, 149–157 (1999)

Chatfield, L.K., Williams, P.A.: Naturally occurring TOL plasmids in *Pseudomonas* strains carry either two homologous or two nonhomologous catechol 2,3-oxygenase genes. J. Bacteriol. **168**, 878–885 (1986)

Christensen, B.B., Sternberg, C., Andersen, J.B., Eberl, L., Moller, S., Givskov, M., Molin, S.: Establishment of new genetic traits in a microbial biofilm community. Appl. Environ. Microbiol. **64**, 2247–2255 (1998)

Couturier, M., Bex, F., Bergquist, P.L., Maas, W.K.: Identification and classification of bacterial plasmids. Microbiol. Rev. **52**, 375–395 (1988)

del Castillo, T., Ramos, J.L.: Simultaneous catabolite repression between glucose and toluene metabolism in *Pseudomonas putida* is channeled through different signaling pathways. J. Bacteriol. **189**, 6602–6610 (2007)

Dennis, J.J., Zylstra, G.J.: Complete sequence and genetic organization of pDTG1, the 83 kilobase naphthalene degradation plasmid from Pseudomonas putida strain NCIB 9816–4. J. Mol. Biol. **341**, 753–768 (2004)

El-Deeb, B.: Natural combination of genetic systems for degradation of phenol and resistance to heavy metals in phenol and cyanide assimilating bacteria. Malays. J. Microbiol. **5**(2), 94–103 (2009)

Esikova, T.Z., Grishchenkov, V.G., Kulakov, L.A., Morenkova, M.A., Boronin, A.M.: Incompatibility groups of caprolactam degradative plasmids of *Pseudomonas* sp. Mol. Genet. Microbiol. Virusol. **4**, 25–28 (1990)

Filonov, A.E., Akhmetov, L.I., Puntus, I.F., Esikova, T.Z., Gafarov, A. B., Kosheleva, I.A., Boronin, A.M.: Horizontal transfer of catabolic plasmids and naphthalene biodegradation in open soil. Microbiology **79**, 184–190 (2010)

Greated, A., Lambertsen, L., Williams, P.A., Thomas, C.M.: Complete sequence of the IncP-9 plasmid pWW0 from *Pseudomonas putida*. Environ. Microbiol. **4**, 856–871 (2002)

Habe, H., Omori, T.: Genetics of polycyclic aromatic hydrocarbon metabolism in diverse aerobic bacteria. Biosci. Biotechnol. Biochem. **67**, 225–243 (2003)

Heinaru, E., Vedler, E., Jutkina, J., Merit, A., Heinaru, A.: Conjugal transfer and mobilization capacity of the completely sequenced naphthalene plasmid pNAH20 from multiplasmid strain *Pseudomonas fluorescens* PC20. FEMS Microbiol. Ecol. **70**, 563–574 (2009)

Herrick, J.B., Stuart-Keil, K.G., Ghiorse, W.C., Madsen, E.L.: Natural horizontal transfer of a naphthalene dioxygenase gene between bacteria native to a coal tar-contaminated field site. Appl. Environ. Microbiol. **63**, 2330–2337 (1997)

Herrmann, H., Muller, C., Schmidt, I., Mahnke, J., Petruschka, L., Hahnke, K.: Localization and organization of phenol degradation genes of *Pseudomonas putida* strain H. Mol. Gen. Genet. **247**, 240–246 (1995)

Heuer, H., Fox, R.E., Top, E.M.: Frequent conjugal transfer accelerates adaptation of broad-host-range plasmid to an unfavorable *Pseudomonas putida* host. FEMS Microbiol. Ecol. **59**, 738–748 (2007)

Ikuma, K., Gunsch, C.K.: Genetic bioaugmentation as an effective method for in situ bioremediation. Bioengineered **3**(4), 236–241 (2012)

Izmalkova, T.Y., Sazonova, O.I., Nagornih, M.O., Sokolov, S.L., Kosheleva, I.A., Boronin, A.M.: The organization of naphthalene

degradation genes in *Pseudomonas putida* strain AK5. Res. Microbiol. **164**, 244–253 (2013)

Jacoby, G.A.: Classification of plasmid Pseudomonas aeruginosa. In: Schlessinger, D. (ed.) Microbiology-1977, pp. 119–126. American Society of Microbiology, Washington, DC (1977)

Kasak, L., Hôrak, R., Nurk, A., Talvik, K., Kivisaar, M.: Regulation of the catechol 1,2-dioxygenase- and phenol monooxygenase-encoding pheBA operon in Pseudomonas putida PaW85. J. Bacteriol. **175**, 8038–8042 (1993)

Keil, H., Keil, S., Pickup, R.W., Williams, P.A.: Evolutionary conservation of genes coding for *meta* pathway enzymes within TOL plasmids pWW0 and pWW53. J. Bacteriol. **164**, 887–895 (1985)

Kivisaar, M., Hõrak, R., Kasak, L., Heinaru, A., Habicht, J.: Selection of independent plasmids determining phenol degradation in Pseudomonas putida and the cloning and expression of genes encoding phenol monooxygenase and catechol 1,2-dioxygenase. Plasmid **24**(1), 25–36 (1990)

Kivisaar, M., Kasak, L., Nurk, A.: Sequence of the plasmid-encoded catechol 1,2-dioxygenase-expressing gene, *pheB*, of phenol-degrading *Pseudomonas* sp. strain EST1001. Gene **98**, 15–20 (1991)

Kosheleva, I.A., Izmalkova, T.Y., Sokolov, S.L., Sazonova, O.I., Boronin, A.M.: Structural and functional variability of genetic systems for catabolizing polycyclic aromatic hydrocarbons in *Pseudomonas putida* strains. Genetika **39**, 1185–1192 (2003)

Kostal, J., Suchanek, M., Klierova, H., Demnerova, K., Kralova, B., McBeth, D.L.: Pseudomonas C12B, an SDS degrading strain, harbors a plasmid coding for degradation of medium chain length n-alkanes. Int. Biodeter. Biodegr. **42**, 221–228 (1998)

Lee, M.-Y., Hwang, M.-O., Choi, S.-Y., Min, K.-H.: Min n-Alkane dissimilation by Rhodopseudomonas sphaeroides transferred OCT plasmid. Microb. Ecol. **26**, 219–226 (1993)

Li, W., Shi, J., Wang, X., Han, Y., Tong, W., Ma, L., Liu, B., Cai, B.: Complete nucleotide sequence and organization of the naphthalene catabolic plasmid pND6-1 from Pseudomonas sp. strain ND6. Gene **336**, 231–240 (2004)

Makarenko, A.A., Bezverbnaya, I.P., Kosheleva, I.A., Kuvichkina, T.N., Il'yasov, P.V., Reshetilov, A.N.: Development of biosensors for phenol determination from bacteria found in petroleum fields of West Siberia. Appl. Biochem. Microbiol. **38**, 29–34 (2002)

Park, W., Jeon, C.O., Madsen, E.L.: Interaction of NahR, a LysR-type transcriptional regulator, with the alpha subunit of RNA polymerase in the naphthalene degrading bacterium, Pseudomonas putida NCIB 9816-4. FEMS Microbiol. Lett. **213**, 159–165 (2002)

Ramos, J.L., Marqués, S., Timmis, K.N.: Transcriptional control of the Pseudomonas TOL plasmid catabolic operons is achieved through an interplay of host factors and plasmid-encoded regulators. Annu. Rev. Microbiol. **51**, 341–373 (1997)

Sarand, I., Haario, H., Jorgensen, K., Romantschuk, M.: Effect of inoculation of a TOL plasmid containing mycorrhizosphere bacterium on development of Scots pine seedlings, their mycorrhizosphere and the microbial flora in *m*-toluate-amended soil. FEMS Microbiol. Ecol. **31**, 127–141 (2000)

Sentchilo, V.S., Perebituk, A.N., Zehnder, A.J.B., van der Meer, J.R.: Molecular diversity of plasmid bearing genes that encode toluene and xylene metabolism in *Pseudomonas* strains isolated from different contaminated sites in Belarus. J. Bacteriol. **66**, 2842–2852 (2000)

Sevastsyanovich, Y.R., Krasowiak, R., Bingle, L.E.H., Haines, A.S., Sokolov, S.L., Kosheleva, I.A., Leuchuk, A.A., Titok, M.A., Smalla, K., Christopher, M., Thomas, C.M.: Diversity of IncP-9 plasmids of *Pseudomonas*. SGM Microbiol. **154**, 2929–2941 (2008)

Shell, M.A.: Regulation of the naphthalene degradation genes of plasmid NAH7: example of a generalized positive control system in Pseudomonas and related bacteria. In: Pseudomonas. Biotransformation, Pathogenesis, and Evolving Biotechnology, pp. 165–176. American Society for Microbiology, Washington, D.C (1990)

Shingler, V., Bartilson, M., Moore, T.: Cloning and nucleotide sequence of the gene encoding the positive regulator (DmpR) of the phenol catabolic pathway encoded by pVI150 and identification of DmpR as a member of the NtrC family of transcriptional activators. J. Bacteriol. **175**, 1596–1604 (1993)

Sota, M., Top, E.M.: Horizontal gene transfer mediated by plasmids. In: Lipps, G. (ed.) Plasmids: Current Research and Future Trends, p. 263. Horizon Scientific Press, Norfolk (2008)

Sota, M., Yano, H., Ono, A., Miyazaki, R., Ishii, H., Genka, H., Top, E., Tsuda, M.: Genomic and functional analysis of the IncP-9 naphthalene-catabolic plasmid NAH7 and its transposon Tn*4655* suggests catabolic gene spread by a tyrosine recombinase. J. Bacteriol. **188**, 4057–4067 (2006)

Top, E.M., Springael, D.: The role of mobile genetic elements in bacterial adaptation to xenobiotic organic compounds. Curr. Opin. Biotechnol. **14**, 262–269 (2003)

Top, E.M., Moenne-Loccoz, Y., Pembroke, T., Thomas, C.M.: Phenotypic traits conferred by plasmids. In: Thomas, C.M. (ed.) The Horizontal Gene Pool. Bacterial Plasmids and Gene Spread, p. 419. Harwood Academic Publishers, Amsterdam (2000)

Top, E.M., Springael, D., Boon, N.: Catabolic mobile elements and their potential use in bioaugmentation of polluted soils and waters. FEMS Microbiol. Ecol. **42**, 199–208 (2002)

Tsuda, M., Minegishi, K.-I., Iino, T.: Toluene transposons Tn*4651* and Tn*4653* are class II transposons. J. Bacteriol. **171**, 1386–1393 (1989)

van Beilen, J.B., Wubbolts, M.G., Witholt, B.: Genetics of alkane oxidation by Pseudomonas oleovorans. Biodegradation **5**(3–4), 161–174 (1994)

van Beilen, J.B., Panke, S., Lucchini, S., Franchini, A.G., Röthlisberger, M., Witholt, B.: Analysis of *Pseudomonas putida* alkane-degradation gene clusters and flanking insertion sequences: evolution and regulation of the *alk* genes. SGM Microbiol. **147**, 1621–1630 (2001)

Van Elsas, J.D., Fry, J., Hirsch, P., Molin, S.: Ecology of plasmid transfer and spread. In: Thomas, C.M. (ed.) The Horizontal Gene Pool. Bacterial Plasmids and Gene Spread, p. 419. Harwood Academic Publishers, Amsterdam (2000)

Williams, P.A., Murray, K.: Metabolism of benzoate and the methylbenzoates by *Pseudomonas putida* (*arvilla*) mt-2: evidence for the existence of a TOL plasmid. J. Bacteriol. **120**, 416–423 (1974)

Yano, H., Miyakoshi, M., Ohshima, K., Tabata, M., Nagata, Y., Hattori, M., Tsuda, M.: Complete nucleotide sequence of TOL plasmid pDK1 provides evidence for evolutionary history of IncP-7 catabolic plasmids. J. Bacteriol. **192**, 4337–4347 (2010)

Zhao, H., Chen, D., Li, Y., Cai, B.: Overexpression, purification and characterization of a new salicylate hydroxylase from naphthalene-degrading *Pseudomonas* sp. strain ND6. Microbiol. Res. **160**, 307–313 (2005)

On the Exploitation of Self-Propagating High-Temperature Reactions for Environmental Protection

Roberto Orrù and Giacomo Cao

Abstract

The major achievements obtained in the field of self-propagating reactions when exploited for environmental protection are reviewed in this chapter. In particular, the fixation and consolidation of high-level radioactive wastes; the treating and recycling of a highly toxic solid waste from electrolytic zinc plants; the recycling of silicon sludge and aluminum dross produced by semiconductor industries and aluminum foundries, respectively; the degradation of chlorinated aromatics; and the treatment of wastes containing asbestos are addressed. Future scientific and technological directions related to this promising field of reaction engineering are also foreseen.

Keywords

SHS exploitation for environmental protection • High-level radioactive wastes • Toxic solid waste from electrolytic zinc plants • Recycling • Degradation of chlorinated aromatics

1 Introduction

Integrated environmental protection can be implemented in the process industry as well as energy conversion plants by process redesign, reutilization of residues, and safer disposal of wastes with the aim of reducing and avoiding pollutants. Process innovation (i.e., production of the same or similar products using less raw material and energy and decreasing the pollutant output), material cycles (i.e., recycling of residues and produced wastes so that resources are reduced), and safe waste disposal (Manahan 1990) represent the characteristic elements of a sustainable development model. In this work, we address the use of self-propagating reactions for residue recycling and environmentally benign waste disposal.

It is well known that self-propagating reactions of either solid-solid or gas-solid type have been exploited in the establishment of the technique referred to in the literature with the acronym of SHS (Self-propagating High-temperature Synthesis) which represents an attractive alternative to conventional methods of materials synthesis (Merzhanov and Borovinskaya 1972; Munir and Anselmi-Tamburini 1989; Merzhanov 1994; Hlavacek and Puszynski 1996; Varma et al. 1998). As depicted in Fig. 1 for the case of the chemical reaction A + B → AB, this technique is characterized by the fact that once the starting mixture is ignited by means of external thermal sources for relatively short times, highly exothermic reactions are able to propagate through the mixture in the form of a self-sustained combustion wave leading to final products progressively without requiring additional energy. SHS is also characterized by process simplicity, short reaction time, easy-to-build equipments, low-energy requirements, and the possibility of obtaining complex or metastable phases.

Self-propagating reactions of thermite type where metallic or nonmetallic oxides, are exothermically reduced by certain metals to form more stable products (Wang et al. 1993) have been considered in the literature almost 50 years ago to address the important environmental problem related to the fixation of high-level radioactive wastes (Spector et al. 1968). The latter one can be considered as the pioneering work where the exploitation of combustion synthesis like

R. Orrù • G. Cao (✉)
Department of Mechanical, Chemical and Materials Engineering, University of Cagliari, Piazza d'Armi, 09123 Cagliari, Italy
e-mail: giacomo.cao@dimcm.unica.it

G. Cao and R. Orrù (eds.), *Current Environmental Issues and Challenges*,
DOI 10.1007/978-94-017-8777-2_10,

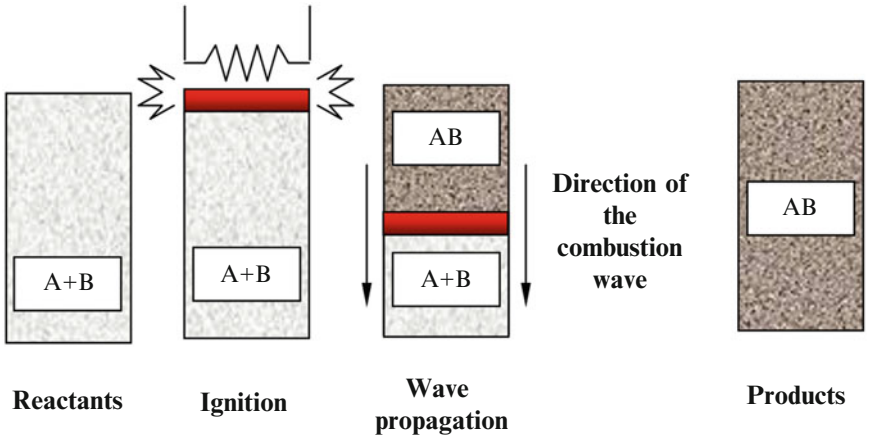

Fig. 1 Schematic representation of the SHS process

reaction for environmental protection is investigated. The proposed process consists of reducing the volume of radioactive liquid wastes and fixing products into a highly insoluble polysilicate structure by means of appropriate thermite reactions. Silicon, iron oxide, and silica are used to prepare the thermite mixture and to provide the desired reaction rate and final product composition. Leachability and final product tests were also performed, and although only the conceptual design of the process has been discussed, the investigation contributes toward the achievement of the permanent fixation of the fission products.

More recently (Cao and Orrù 2002; Orrù et al. 2003; Porcu et al. 2004, 2005; Vinokurov et al. 2007; Barinova et al. 2007, 2008a, b, 2011; Wang et al. 2009; Chen et al. 2009; Laverov et al. 2010; Qin et al. 2012; Zhang et al. 2011, 2012), the exploitation of self-propagating reactions for environmental protection has received renewed attention. In particular, interesting results have been obtained in the following areas: fixation and consolidation of high-level radioactive wastes, treating and recycling of a highly toxic solid waste from electrolytic zinc plants, degradation of chlorinated aromatics, treatment of wastes containing asbestos, recycling of silicon sludge and aluminum dross produced by semiconductor industries and aluminum foundries, etc.

The aim of this work is to provide an overview of the major achievements obtained in these areas. Future scientific and technological directions related to this promising field of reaction engineering are also discussed.

2 Major Achievements

2.1 Immobilization of Radioactive Wastes

As mentioned in the introduction, the first work available in the literature which takes advantage of self-propagating reactions for environmental applications deals with the fixation of radioactive waste (Spector et al. 1968). The process is based on the use of the following exothermic thermite reaction (Barin 1989):

$$4Fe_2O_3 + 3Si \rightarrow 3Fe_2SiO_4 + 2Fe \qquad \left(-\Delta H_r^0\right) = 1,142.714\ \text{kJ} \tag{1}$$

which gives rise to the formation of a polysilicate structure to incorporate the radioactive wastes. The thermite process was preceded by a pretreatment (evaporation, drying and denitration steps) of the radioactive waste which was originally in the form of an aqueous solution. Through this treatment all the salts present in the waste solution were converted to oxides. According to reaction (1), the thermite mixture consisted of Si and Fe_2O_3, where silica was sometimes used as an additive in order to control the reaction rate as well as the final product composition.

An alternative to the process described above was also proposed by Spector et al. (1968). It differs from the previous in that all salts are in this case converted to sulfates prior to the radioactive element fixation.

A different technology based on combustion reactions to prepare ceramic oxide materials like perovskite ($CaTiO_3$), zirconolite ($CaZrTi_2O_7$), hollandite ($Ba_{1.23}Al_{2.46}Ti_{5.54}O_{16}$), and sphene ($CaTiSiO_5$), which can be used for nuclear waste immobilization, has been also proposed in the literature (Muthuraman et al. 1994). In fact, these oxides are characterized by the presence of cavities and vacant interlayers in their structures capable of incorporating radioactive cations (Muthuraman et al. 1994). Basically, the method involves the wet combustion of metal nitrates, corresponding to the complex oxides to be prepared, together with some fuels, i.e., carbohydrazide (CH_6N_4O) and tetraformyl trisazine ($C_4H_{16}N_6O_2$), at 450 °C, according to the following reactions:

$$7Ca(NO_3)_2 + 7TiO(NO_3)_2 + 5C_4H_{16}N_6O_2 \rightarrow 7CaTiO_3 + 20CO_2 + 40H_2O + 29N_2 \tag{2}$$

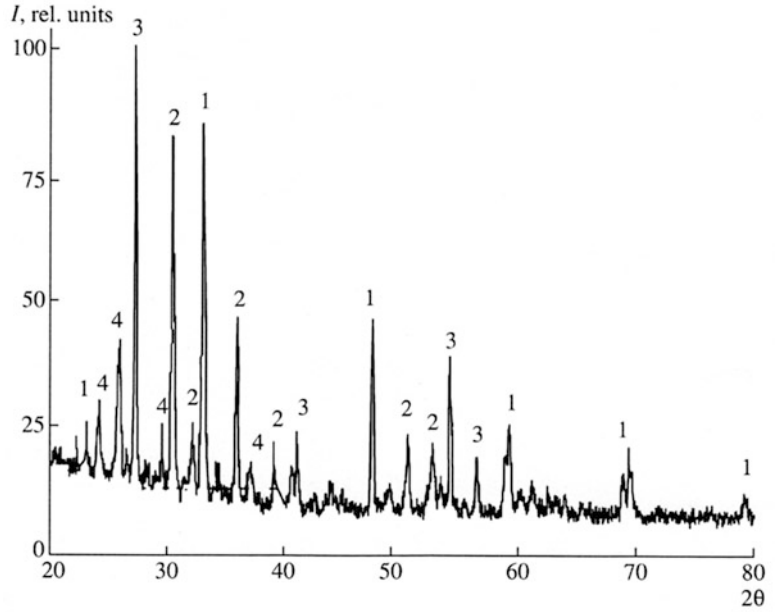

Fig. 2 XRD pattern of the product obtained from a green mixture containing 5 wt% of cesium: 1-perovskite, 2-zirconolite, 3-rutile, and 4-pollucite (Adapted from Barinova et al. 2007)

$$4Ca(NO_3)_2 + 4Zr(NO_3)_2 + 8TiO(NO_3)_2 + 25CH_6N_4O \rightarrow 4CaZrTi_2O_7 + 25CO_2 + 75H_2O + 70N_2 \quad (3)$$

$$2Ba(NO_3)_2 + 4Al(NO_3)_3 + 9TiO(NO_3)_2 + 21CH_6N_4O \rightarrow \text{Hollandite} + 21CO_2 + 63H_2O + 59N_2 \quad (4)$$

$$2Ca(NO_3)_2 + 2TiO(NO_3)_2 + 2SiO_2 + 5CH_6N_4O \rightarrow 2CaTiSiO_5 + 5CO_2 + 15H_2O + 14N_2. \quad (5)$$

More recently, the possibility of using SHS processes for the preparation of ceramics based on synthetic perovskite ($CaTiO_3$) and zirconolite ($CaZrTi_2O_7$) as matrix materials for immobilization of high-level waste (HLW) has been widely investigated (Borovinskaya 1998a, b; Barinova et al. 2007, 2008a, b). The perovskite and zirconolite lattices are able to incorporate almost all the elements available in HLW including Sr, Y, lanthanides, and actinides in oxidation states +3 and +4. Since Cs, owing to its larger atomic size, cannot be incorporated into crystal lattices of perovskite and zirconolite, oxides of Al and Si were added into the reacting mixture to form aluminosilicate glasses. The reactants typically used to perform the SHS reaction exploited to reach the objective of the proposed process are the following: reducing agent (Ti), oxidants ($Ca(NO_3)_2$, Fe_2O_3), additives (TiO_2, CaO, ZrO_2, Al_2O_3, SiO_2), and simulated high-level waste containing CsOH, SrO, FeO, NiO, Cr_2O_3, MnO, ZrO_2, MoO_3, MgO, La_2O_3, B_2O_3, Ce_2O_3, Pr_2O_3, Sm_2O_3, and Y_2O_3.

For instance, a mixture constituted by titanium oxide, calcium oxide, zirconium oxide, and titanium in powder form, where inactive isotopes like ^{90}Sr and ^{137}Cs are added, was considered to simulate a real composition of radioactive nuclear wastes. By adding calcium nitrate or iron oxides to the mixture above according to the following stoichiometries (Borovinskaya et al. 1998a, b)

$$2Ca(NO_3)_2 + 9Ti + 4CaO + TiO_2 \rightarrow 6CaTiO_3 + 4TiN \quad (6)$$

$$2Ca(NO_3)_2 + 9Ti + CaO + TiO_2 + 3ZrO_2 \rightarrow 3CaZrTi_2O_7 + 4TiN \quad (7)$$

$$2Fe_2O_3 + 3Ti + 4CaO + TiO_2 \rightarrow 4CaTiO_3 + 4Fe \quad (8)$$

as well as aluminum and silicon oxide, the resulting green mixture was ignited and simultaneously pressed into suitable molds. The total content of the simulated waste varied from 10 to 25 wt%. Along with perovskite and zirconolite phases, the resulting ceramics also contain rutile, as it may be seen from the diffraction pattern reported in Fig. 2. In addition, such ceramics exhibit low porosity, high mechanical strength, and strong fixation of Sr and lanthanides simulating actinides. On the other hand, significant losses of Cs (up to 20 %) are observed during the course of the proposed immobilization process. For this reason, the initial content of alumina and silica in the starting mixture was increased until the formation of pollucite ($CsAlSi_2O_6$) was guaranteed. However, it was found that the leaching rate of the obtained product increased probably due to an increase in the corresponding open porosity caused by lower temperature levels reached during the combustion process. The proposed process has been improved by promoting the formation of pyrochlore $Y_2Ti_2O_7$ to incorporate

actinides into the ceramic matrix as well as simultaneously compacting the reacting mixture and products (Barinova et al. 2011). High hydrolytic stability and mechanical strength of the latter ones have been found.

A similar approach has been adopted by Glagovskii et al. (1999). In particular, metallothermal processes performed under the SHS regime have been proposed to synthesize perovskite and zirconolite structures to immobilize radionuclides contained in calcinites into which liquid high-level wastes are transformed during the final stage of spent fuel processing. The same group has been investigating the immobilization by means of SHS processes of silica gel fixed cesium and strontium radionuclides into mineral-like matrices (Konovalov et al. 2002). It was found that virtually no cesium was lost by evaporation.

The immobilization of actinides in pyrochlore-type matrices produced by SHS has been also the subject of investigation of another Russian research group (Vinokurov et al. 2007). It should be noted that a mixture of actinide oxides, i.e., ^{237}Np, ^{237}Pu, ^{241}Am, and ^{238}U, has been used to test the validity of the proposed process. It was found that the obtained matrix has a high chemical stability. Russian and US scientists have been recently collaborating to develop a detailed analysis of the characteristics of actinide matrices based on oxides of the pyrochlore- and garnet-type structures (Laverov et al. 2010) in view of the immobilization of actinide-containing wastes. It was shown that the SHS technique is the optimal one to synthesize titanate and zirconate pyrochlore structures which can be used for ^{99}Tc incorporation.

More recently, several research groups from China have been addressing the use of SHS processing for immobilization of radioactive wastes. In particular, Qin et al. (2012) investigated the immobilization of simulated radioactive sandy soil waste. It was found that the considered tracer element, i.e., Ce, mainly forms $CeAl_{11}O_{18}$ and Ce_2SiO_5 as crystalline phases in the final product. In particular, the latter one displays a high chemical stability during a 28-day test, being the leaching rate of Ce much lower than that one of borosilicate glasses. Along these lines, the SHS was found to be a promising technique to immobilize Sr in high-level wastes (Zhang et al. 2012). In fact Sr directly took part in the synthesis process, thus forming strontium titanate synroc which represents a durable material with high-level waste loading. Such results were also ascribed to the use of chromium oxide as oxidant material which allows reaching high temperature levels during the combustion reaction that takes consequently place in the liquid state. Finally, it is worth mentioning that the leaching properties of strontium titanate ceramics have been also examined in detail in a separate publication (Zhang et al. 2011). In particular, it was found that the leaching rate of Sr resulted to be 2.29 10^{-3} $g^{-2}day^{-1}$.

2.2 Fixation of Toxic Species from Hydrometallurgical Wastes

Highly toxic solid wastes from electrolytic zinc plants, known as jarosite or goethite depending upon the treatment used for iron removal, are obtained as by-products (about 750,000 and 90,000 t/year in Europe and Sardinia, Italy, respectively). The large production, the high cost of disposal, and the increasing difficulty to find suitable disposal locations clearly provide a demonstration of their environmental impact (Pelino et al. 1994, 1996a, 1997).

Currently, a variety of processing options which give possible solutions to this acute environmental problem are proposed in the literature. These include hydrometallurgical and pyrometallurgical techniques (Pelino et al. 1996a), which are, to some extent, uneconomic or technically risky. On the other hand, glassification, i.e., vitrification of the waste so that hazard components are incorporated into an amorphous glassy structure, is not only an option for environmentally benign disposal but also a promising technique (Ionescu et al. 1997). For example, vitrification in borosilicate glass is currently used to solidify and stabilize certain forms of radioactive and hazardous wastes. In particular, it has been recently demonstrated that goethite and jarosite wastes can be mixed with raw materials and residues such as granite scraps and glass cullet, melted, and formed into glass or glass-ceramic matrix which incorporates a consistent amount of waste (Pelino et al. 1997). A preliminary flow sheet of the vitrification pilot plant has been also proposed (Pelino et al. 1996b).

Cao and coworkers (Orrù et al. 1999; Sannia et al. 2001) have developed a process for treating and recycling goethite wastes based upon self-propagating thermite reactions. In particular, taking advantage of the relatively high content of iron oxides in the waste, the following thermite reactions were exploited due to their high exothermic character (Barin 1989):

$$2Fe_2O_3 + 3Si \rightarrow 3SiO_2 + 4Fe \quad \left(-\Delta H_r^0\right) = 1,084.075\ \text{kJ} \tag{9}$$

$$Fe_2O_3 + 2Al \rightarrow Al_2O_3 + 2Fe \quad \left(-\Delta H_r^0\right) = 851.444\ \text{kJ} \tag{10}$$

$$Fe_2O_3 + 3Mg \rightarrow 3MgO + 2Fe \quad \left(-\Delta H_r^0\right) = 979.475\ \text{kJ} \tag{11}$$

$$Fe_2O_3 + 3Ca \rightarrow 3CaO + 2Fe \quad \left(-\Delta H_r^0\right) = 1,081.019\ \text{kJ}. \tag{12}$$

Indeed, it was found that by blending this waste with a suitable amount of reducing agents (aluminum, silicon,

magnesium, and calcium), to be used singularly or in combination, as well as ferric oxide, according to reactions (9), (10), (11), and (12), and igniting the resulting mixture, a combustion wave rapidly travels through the mixture without requiring additional energy, thus converting reactants into two different types of solid products, indicated as P_1 (the main one) and P_2, and a gas mainly containing SO_2. Specifically, the secondary product P_2 is distributed in powder form in the reaction chamber walls as a consequence of a probable expulsion occurring during the course of the reaction. On the other hand, the main product P_1 remains in the same position where the original sample was placed inside the reactor.

The occurrence of self-propagating reactions depends upon the combination of reducing agents and the waste content in the starting mixture. It was found that the combination of aluminum and silicon as reducing agents corresponds to the maximum value of the mass ratio of product P_1 with respect to starting mixture. In addition, on the basis of the leaching tests performed, the corresponding product P_1 was found to fulfill the very restrictive environmental regulations for heavy metals. This result was justified by the microstructural characterization of product P_1 obtained using the combination Al/Si as reducing agents. In fact, product P_1 is constituted by an amorphous glassy structure of iron aluminosilicates embodying heavy metals. A process for the treatment of zinc hydrometallurgical wastes has been proposed (Sannia et al. 2001). It was found that, due to its composition, the secondary solid product P_2 may be directly recycled in the roasting unit of the industrial zinc production plant. It should be noted that although commercial iron oxide, aluminum, and silicon have been used to demonstrate process feasibility, the possibility of taking advantage of the corresponding waste analogue is also addressed in what follows.

From the economical point of view, as it will be discussed in details subsequently, all the advantages of SHS processes are also valid when considering this method to be exploited for environmental applications. However, the utilization of commercial or generally relatively expensive reactants/additives makes the proposed processes often uneconomical. Along these lines, the self-propagating process of treatment of zinc hydrometallurgical wastes by totally or partially replacing the commercial additives previously employed (Orrù et al. 1999; Sannia et al. 2001) with industrial scraps has been investigated (Porcu et al. 2004). Specifically, the effect of substituting the added iron oxides with a steelmaking scrap and silicon with two different types of high Si content industrial wastes is systematically analyzed.

The obtained results demonstrated that, starting from a mixture containing 30 wt% of paragoethite wastes, the substitution of commercial silicon and ferric oxides with Si-rich wastes (Si content higher than 94 wt%) and Fe_2O_3-rich steelmaking (containing about 85 % of iron oxides) scraps provides reaction products analogous to those corresponding to commercial additives, where the toxic species are incorporated inside a silicate matrix. One example of the SEM investigation of product P_1 obtained by Porcu et al. (2004) is shown in Fig. 3 where a backscattered micrograph together with the corresponding Fe, Cu, and Pb maps is reported. The product is constituted by small globules dispersed into a dark matrix which consists of aluminosilicates, where crystals of hercinite are also present. This result is consistent with what has been observed by means of X-ray analysis. The map reveals that iron and, more importantly, lead are concentrated inside the lighter globules. This is an important aspect since it means that this hazardous heavy metal, initially present in the waste at relatively high content, is mainly confined in relatively small regions surrounded by a silicate glass matrix.

In addition, leaching test results confirm that the formation of the aluminosilicate phase which encapsulates the toxic species originally present in the waste leads to a highly water-resistant material. This represents an important result from the environmental point of view in the framework of preventing groundwater and surface water contamination. In particular, the starting mixture leading to the product which passes the leaching test consists of about 90 wt% of wastes. Further, additional cost reduction may be achieved through the replacement of commercial aluminum with analogous low-cost materials.

As the economic aspects of this process are more specifically taken into account, it is worth mentioning that SHS is an efficient process because of its relatively short synthesis time, the occurrence of self-heating up to high temperatures instead of external heating, the absence of external heating elements, and the simplicity of equipments required (Golubjatnikov et al. 1993; Merzhanov 1993, 1999). These intrinsic characteristics of SHS processes hold also true when dealing with self-propagating reactions for environmental protection. A detailed investigation of economic efficiency of SHS processes is typically performed by comparing physical parameters of SHS products with existing analogues. This procedure is in general extremely hard to carry out because of the lack of accessible "know-how" information (Miyamoto 1999). For the case of the recycling and treating of wastes by self-propagating reactions, such an investigation is even more difficult, due to the lack of existing industrial applications. However, the procedure for analyzing the treatment costs is constituted first by the description of the process steps followed by the definition of the unit costs for each category, i.e., raw materials, fixed costs, utilities, disposable materials, and labor, that form the basis of the cost analysis (Golubjatnikov et al. 1993). In particular, it was found that fixed costs are generally lower for SHS-based process as compared to conventional ones. On the other hand, while raw material costs are often higher when synthesizing materials by SHS, this

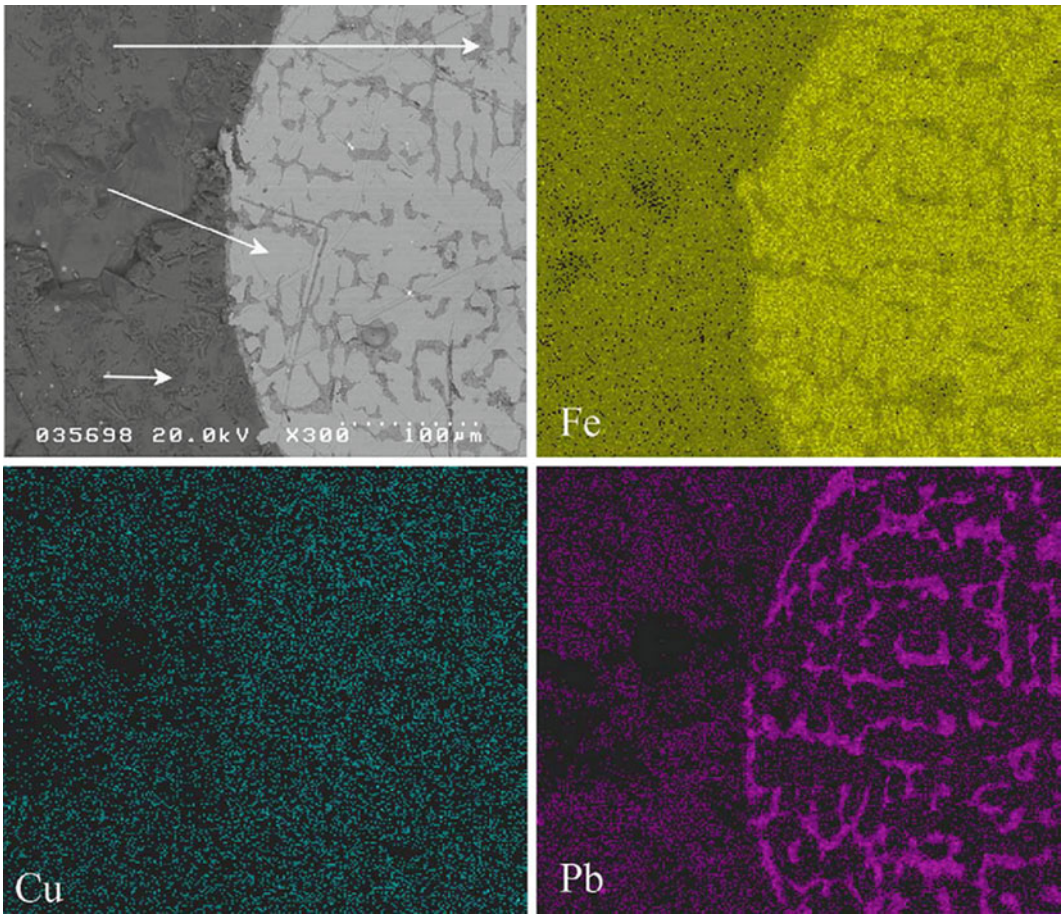

Fig. 3 SEM backscattered views of the microstructures of the product P_1, along with the corresponding Fe, Cu, and Pb maps, obtained when reacting mixtures containing steelmaking and silicon scraps, respectively (Adapted from Porcu et al. 2004)

cost category may be drastically reduced for the case of self-propagating reactions for environmental protection because recycled materials may be used as reactants.

2.3 Degradation of Chlorinated Aromatics

The destruction of health-threatening compounds has become one of the crucial problems in the area of hazardous waste management (Goldhaber and Chessin 1997). Organochlorine pesticides, polychloric biphenyls, dibenzofurans, dioxins, and other synthetically produced derivatives of chlorobenzene are some of the common and most politicized substances that must be dealt with. Indeed, aromatic rings with halogen substitution are highly resistant to oxidative degradation, and the possible emission of even worse by-products appears to be one of the main disadvantages of conventional incinerator technologies.

In this regard, the attention has been also directed to the exploitation of self-propagating reactions to degrade chlorinated aromatics (Cao et al. 1999; Cocco et al. 1999). Hexachlorobenzene (C_6Cl_6) and the racemate of 2-(2-4-dichlorophenoxy)propanoic acid ($C_9H_8Cl_2O_3$), a commercial herbicide known as dichlorprop, hereafter 2,4-DP, were used as chlorinated test species, while calcium hydride was proposed as reducing agent. Reactants were first mixed according to the following reactions:

$$3CaH_2 + C_6Cl_6 \rightarrow 3CaCl_2 + 6C + 3H_2 \quad (13)$$

$$6CaH_2 + C_6Cl_6 \rightarrow 6CaHCl + 6C + 3H_2 \quad (14)$$

$$4CaH_2 + C_9H_8Cl_2O_3 \rightarrow 3CaO + CaCl_2 + 9C + 8H_2 \quad (15)$$

$$5CaH_2 + C_9H_8Cl_{I2}O_3 \rightarrow 3CaO + 2CaHCl + 9C + 8H_2. \quad (16)$$

The resulting mixtures were then pressed into cylindrical pellets and fitted into the sample holder of the reaction chamber. The reaction was run under a slight overpressure of purified argon. Samples were fired by a power pulse (2 s) of about 2 kW by means of a tungsten coil. After the thermal spike, the reaction spreads spontaneously through the whole sample.

These features reflect the highly exothermic qualities of the reactions involved. From the reference data, a reaction

enthalpy of 1,709.6 kJ/mol is foreseen for the direct and complete reduction of hexachlorobenzene represented by reaction (13), which rises to 1,804.6 kJ/mol when an excess of CaH_2 is employed. In the case of 2,4-DP, reaction enthalpies of −1,295.4 kJ/mol and −1,321.7 kJ/mol for reactions (15) and (16), respectively, were calculated (Domalski and Hearing 1993).

The reaction heats above are large enough to maintain the self-sustaining character of the process within a wide range of compositions. Indeed the combustive regions are similar for the two test compounds and extend from a CaH_2/organohalide molar ratio of about 2–3 up to 15–18, i.e., up to a very large excess of calcium hydride. A combustion temperature above 2,650 K was registered using an infrared pyrometer for a CaH_2/C_6Cl_6 mixture with a molar ratio of 3. This value is similar to the calculated adiabatic temperature of 2,984 K. The reaction temperature progressively decreased with increasing the CaH_2 content in the mixture. This is due to the excess of CaH_2 which does not contribute to the reaction heat while increasing the total heat capacity of the system. It was found that the propagation rate of the reaction obtained from video records for the whole range of examined compositions was to be between 0.5 and 1.5 cm/s.

According to the straightforward pathways proposed in equations (13), (14), (15), and (16), relatively low CaH_2/organohalide benchmark ratios are demanded for the complete reduction of the chloroorganics. At least three moles of calcium hydride are required in the case of hexachlorobenzene and four or five in the case of 2,4-DP. Samples from the reactor's head space were analyzed by gas chromatography/mass spectroscopy (GC/MS). Hydrogen and methane (with CO and CO_2 in the case of 2,4-DP) were the main gaseous compounds (Cao et al. 1999). Traces of benzene; mono-, di-, and tri-chlorobenzene; dichloroethylene; dichloromethane; xylene; and trimethylbenzene were also found by utilizing the EPA (Environmental Protection Agency) Method TO15 (Cao et al. 1999). Organic solid end products in the reacted powders were also analyzed by high-resolution GC/MS. We found consistent concentrations of reaction products, the total organochlorine conversion resulting in each trial greater than 99.999 %.

The transformation of reactants into nontoxic end products was also confirmed by X-ray analysis. In the case of hexachlorobenzene, the burnt powders were found to consist of graphite, $CaCl_2$, and CaHCl, the hydride-chloride mixed salt becoming the predominant phase at the larger CaH_2 content. In the case of 2,4-DP, CaO was also found. These results suggest that self-activating processes can be an alternative to conventional thermal treatments of hazardous chlorinated aromatics. The advantages are obvious in that very high temperatures are locally reached with low pressure and under extent-controlled conditions. Solid and gaseous reaction products can be easily checked before their discharge. The simplicity and a very low-energy requirement are two other merits of the process (Cao and Orrù 2002; Orrù et al. 2003).

It should be noted that relatively simple facilities are required by large-scale SHS production up to 100t/year. However, the practical exploitation of the presented methodology for large-scale waste treatment requires further investigation. Along these lines it should be noted that the so-called self-propagating high-temperature dehalogenation (SPHTD) process has been included by the US Environmental Protection Agency as an ex situ technology to treat stockpiles containing hexachlorobenzene contamination in the reference guide to non-combustion processes for remediation of persistent organic pollutants in stockpile and soil (EPA 2005).

2.4 Treatment of Wastes Containing Asbestos

Asbestos materials had extensively been used in the past because of their useful properties for insulation and fireproofing. However, because of the health hazard caused by respiration of their fibers, the corresponding use has been dramatically reduced in recent years. While several methodologies, such as resin coating, encapsulation with concrete, chemical attack, thermal treatments, and mechanochemistry, have been proposed in several studies for the treatment of materials containing asbestos, the exploitation of self-propagating high-temperature thermite reactions to convert asbestos materials into harmless, nonfibrous species has been analyzed, to the best of our knowledge, in a unique investigation (Porcu et al. 2005). Specifically, it was found that by blending in appropriate proportions a waste containing about 85 wt% of chrysotile with ferric oxide and magnesium, the resulting mixture is able to generate, upon ignition, a combustion wave accompanied by a dramatic change in the starting material from both the chemical and microstructural points of view. Finally, the complete destruction of the fibrous structure of chrysotile is obtained by the proposed treatment. The effect of the SHS treatment on the microstructure of the final product as compared to that of the starting mixture can be seen in Fig. 4, where the corresponding SEM micrographs are reported for the case of a mixture constituted by 50 wt% of asbestos-containing material, 34.3 wt% of ferric oxide, and 15.7 % of magnesium. Forsterite, magnesium oxide, and iron are the only crystalline phases detected in the final product (Porcu et al. 2005).

Regarding the utilization of commercial Fe_2O_3 and Mg to be mixed with the asbestos-containing material to make the reaction mixture self-propagating, it is worth mentioning that they could be totally or partially substituted with analogous industrial scraps, similarly to the case described in Sect. 2.2.

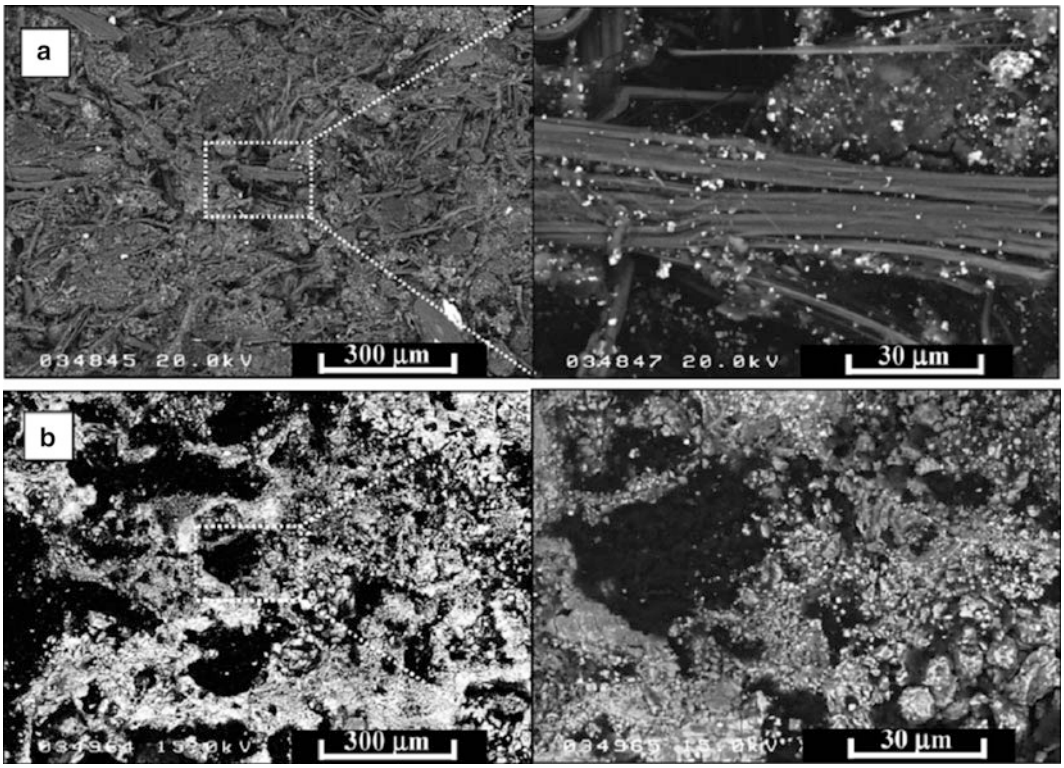

Fig. 4 General and detailed backscattered SEM micrographs of sample containing 60 wt% of asbestos-containing material, 27.4 wt% of ferric oxide, and 12.3 % of magnesium: (**a**) starting mixture and (**b**) product after treatment (Adapted from Porcu et al. 2005)

2.5 SHS Recycling

In addition to the application of self-propagating reactions described above and following previous studies related to the utilization of silicon wastes in zinc smelting (Miyamoto et al. 1995), a new recycling process based on the SHS nitriding combustion of silicon sludge from semiconductor industries and aluminum dross from aluminum foundries to obtain silicon-based ceramics has been proposed (Miyamoto et al. 1998, 2000).

The process treatment of silicon sludge is based on the combination of silicon with nitrogen to form Si_3N_4 according to the following exothermic reaction:

$$3Si + 2N_2 \rightarrow Si_3N_4 \quad (17)$$

which is characterized by a reaction enthalpy of −748 kJ/mol and an adiabatic temperature of 4,127 °C (Miyamoto et al. 1995). However, since the composition of the silicon sludge is Si (26 wt%), Al_2O_3 (14 wt%), $ZrSiO_4$ (31 wt%), Fe_2O_3 (27 wt%), and CaO (2 wt%), the silicon content is too low to make the nitridation of the sludge possible by SHS. To overcome this problem, reclaimed Si and Al powders produced by silicon and aluminum industries, respectively, were added to the waste.

The resulting mixture is then ignited by passing a current of 50 A for 5 s through a carbon ribbon heater in a pressurized nitrogen atmosphere until a self-propagating reaction takes place. The product consisted of three different sialon compositions (i.e., $Si_6Al_{10}O_{21}N_4$, $Si_{1.8}Al_{0.2}O_{1.2}N_{1.8}$, and $Si_3Al_3O_3N_5$), iron silicides ($FeSi_2$), and monoclinic zirconia (ZrO_2).

With the aim of improving the oxidation resistance, the iron oxide in the silicon sludge was eliminated by leaching it with hydrochloric acid. With this treatment, calcium oxide was also removed from the sludge, whose resulting composition became Si (31 wt%), Al_2O_3 (30 wt%), and $ZrSiO_4$ (35 wt%). In this case, the product consisted of sialon (80 wt %) and zirconia (20 wt%). It has been sintered at 1,600 °C for 2 h, and the resulting compact exhibits bending strength and thermal expansion coefficient of 270 MPa and $4.5{\cdot}10^{-6}$ K^{-1}, respectively. It is interesting to note that the product strength is lower than conventional sialon (about 360 MPa) but may be compared with silicon nitride obtained by reactive sintering (about 250 MPa).

The other SHS recycling process proposed in the literature which makes use of aluminum dross is based on the nitridation of aluminum according with the following reaction:

$$2Al + N_2 \rightarrow 2AlN \quad (18)$$

characterized by a combustion heat of 11,855 kJ/kg (Miyamoto et al. 2000). Aluminum dross, whose composition was 75 wt% AlN, 12.5 wt% Al_2O_3, and 12.5 wt% Al, was first pulverized and mixed with reclaimed silicon to make the self-propagation combustion possible, following

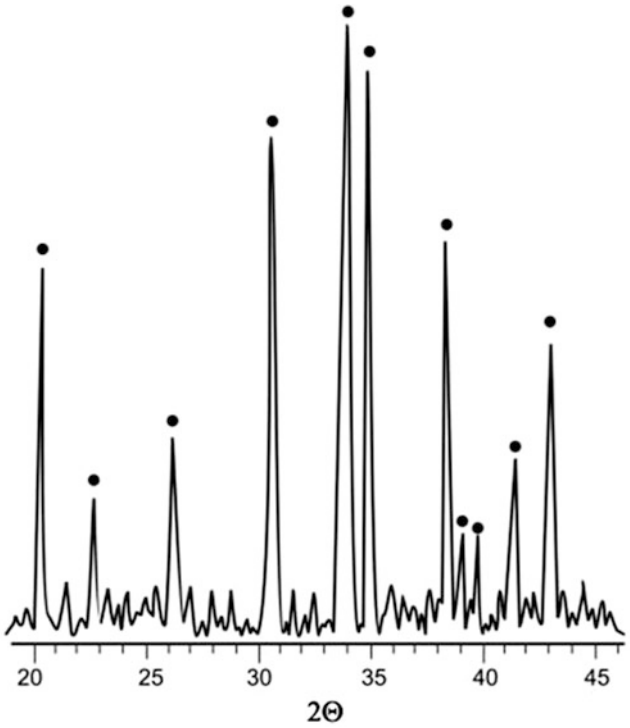

Fig. 5 XRD patterns of powders (●, α-sialon) synthesized by SHS (Adapted from Chen et al. 2002)

a procedure similar to the one described above. The resulting mixture was then combusted under nitrogen atmosphere and the resulting product consisted of $Si_{6-x}Al_xO_xN_{8-x}$ and other Si-Al-O-N phases.

Thus, by taking into account the large worldwide production of silicon wastes from semiconductor industries and aluminum dross, the proposed recycling process based on the exploitation of self-propagating reactions appears to be a promising alternative to the nonproductive disposal of these wastes.

The synthesis of (Ca, Mg)-α-sialon powders by SHS using slag from the Baoshan Steel Company (Shanghai, China) as a starting material has been also investigated (Chen et al. 2002). The slag from a blast furnace, whose composition is mainly constituted by CaO, SiO_2, Al_2O_3, and MgO, is mixed with aluminum and silicon in appropriate proportions, and the whole process was held in a sealed cabin with a high nitrogen pressure to obtain a nominal composition of the α-sialon of $Ca_{0.71}Mg_{0.23}Si_{9.18}Al_{2.82}O_{0.94}N_{15.06}$. α-Sialon is the only crystalline phase detected in the final product as it may be seen from the corresponding XRD pattern reported in Fig. 5. The SHS method has showed the inclusion of stabilizing cations into the α-sialon structure. The resulting powders have been attrition milled for 8 h and then hot pressed in flowing nitrogen at 1,750 °C for 1 h under a pressure of 20 MPa in a graphite furnace. The hardness and fracture toughness of the hot-pressed samples using SHS-synthesized powders reached 16 GPa and 5.1 $MPa \cdot m^{-1/2}$, respectively.

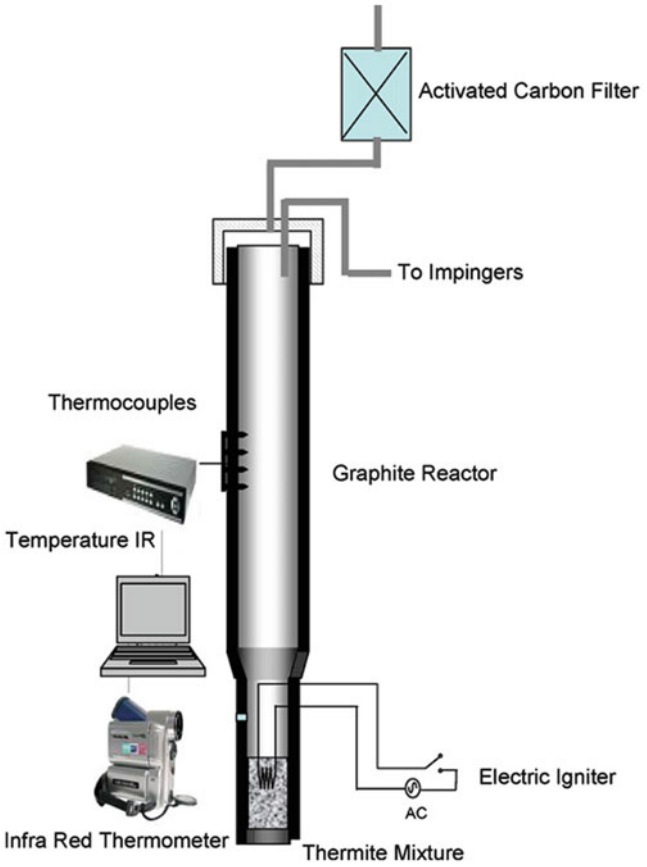

Fig. 6 Schematic representation of the experimental setup (Adapted from Wang et al. 2009)

2.6 Miscellanea

In addition to the specific cases described in detail in previous sections, it is interesting to note that SHS processes have been also recently proposed for unusual applications such as the melting of municipal solid waste incinerator fly ashes (Wang et al. 2009) as well as the detoxification of cathode ray tube glasses (Chen et al. 2009). In particular, the former approach (Wang et al. 2009) consisted first of mixing municipal solid waste incinerator fly ashes with aluminum and ferric oxide, the latter ones in stoichiometric proportions according to the corresponding well-known thermite reaction (10). Next, the reacting mixture was placed in a specifically designed reactor schematically reported in Fig. 6 which allows the monitoring of the temperature of the reaction and that one of the expulsed gases which can be also sampled. The results of such study demonstrated that a content of fly ashes up to 30 wt% was able to guarantee the self-propagating character of the reaction whose corresponding temperature was of about 1,350 °C. More than 91 wt% of iron was found to be present in the resulting alloy while the rest of nonreactive oxides remains in the slag where heavy metals have been partially incorporated. On the other hand, cadmium was mainly found in the flue gas generated during

the reaction occurrence, while lead and zinc were found not only in the slag but also in the secondary fly ashes generated from the melting process. On the other hand, the concentration of the various heavy metals determined by the performed toxic characteristic leaching procedure was within the regulatory thresholds which implied at least the environmental safety of the obtained slag.

A similar strategy has been proposed for the treatment of hazardous waste cathode ray tube glass which, together with computer monitors, accounts for about 70 wt% of the so-called e-wastes, i.e., electric and electronic equipment wastes (Chen et al. 2009). Since such wastes contain hazardous heavy metals like lead, barium, strontium, etc., they clearly represent a potential pollution danger to the environment. The proposed process consists first in blending various types of cathode ray tube glasses; once crushed, they are dry milled and sieved, with suitable amount of ferric oxide and magnesium. The molar ratio of the latter two reactants was chosen according to reaction (11). The mixture is then locally ignited by a thermal source to generate a self-propagating reaction which is capable of converting reactants into products constituted by forsterite (Mg_2SiO_4), magnesium oxide, and iron, where hazardous and toxic species were incorporated. It was found that self-propagating reactions are able to take place when the glass content in the initial mixture was less than 60 wt%. Leaching tests performed on the final products demonstrated the fulfillment of the corresponding environmental regulations concerning lead and barium. It is interesting to note that such behavior has been explained by considering Suitable X-ray photoelectron spectroscopy (XPS) experiments, where it was found that the bonding state of lead changed after the treatment from more ionic character to more covalent one.

3 Discussion and Future Scientific-Technological Directions

In the first part of this work, the major achievements in the field of self-propagating reactions exploited for environmental protection have been reviewed. It is shown that the applicability of this strategy of waste inertization, minimization, and reuse clearly depends upon the availability at relatively low cost of suitable reducing agents. This aspect may represent the main drawback of the proposed technologies based on self-propagating reactions. In fact, although reducing agents as scraps may be potentially available on the market, the use of the corresponding commercial products is often mandatory to overcome their unavailability. On the other hand, the exploitation of self-propagating reactions allows one to take advantage of the classical features of the technologies based on this type of reactions, i.e., short synthesis times, process simplicity, low-energy requirements, etc. (Yukhvid 1998), and to synthesize a wide variety of advanced materials (Varma et al. 1998).

It should be noted that the potential merit of SHS, i.e., the low process costs outlined above, tends to be canceled in many applications of materials synthesis by high cost of initial components such Ti, Mo, B, etc., to produce titanium carbide, molybdenum silicides, borides, etc. On the contrary, they may be fully utilized when ecological applications of self-propagating reactions are taken into account.

The practical exploitation of the SHS technology for environmental protection may be also improved through a deeper understanding of kinetics and mechanism of solid-solid and gas-solid self-propagating reactions. This represents a very complicated task, as recently pointed out in the literature (Varma et al. 1998), due to the unique aspects of complex physicochemical phenomena simultaneously taking place (melting and diffusion of reactants, chemical reactions with formation of intermediate phases, nucleation, grain growth, etc.). In fact, it should be noted that only few techniques are available to perform SHS kinetics and mechanistic studies, i.e., time-resolved XRD analysis, particle-foil experiments, and combustion front quenching, which allow identification of reactions and phase transformations taking place. Unfortunately, these investigation techniques are often characterized by difficulties in the experiments and their interpretation, even for systems constituted by two reactants. The complex nature of the systems investigated in the light of exploiting self-propagating reactions for environmental protection clearly prevents a comprehensive study of the corresponding kinetics and mechanisms of structure formation taking place. This difficulty is also enhanced by the limitation of experimental techniques discussed above. However, it should be noted that studies of this type, where the main goal is to establish direct and reciprocal relationships between the combustion conditions and structure formation, are known in the literature as structural macrokinetic investigations and represent one of the most promising research directions for the future exploitation of solid-solid and gas-solid self-propagating reactions.

Along these lines, the comparison between thermally and mechanically activated self-sustaining reactions may provide new insights and possible lines of inquiry may emerge. For the case of hexachlorobenzene degradation, according to reactions (13) and (14), these two processes which run under quite different regimes were compared (Cao et al. 1999). In particular, a well-defined activation barrier exists for the occurrence of a self-propagating thermal wave, while mechanochemical reactions are initiated under the conditions of continuous defect generation and progressive structural instabilities (Forrester and Schaffer 1995). Despite these features, it is shown that the same underlying mechanism seems operative in both processes as suggested by the close correspondence in the whole combustion range, between the temperature and the propagation wave velocity, and the values representing the instantaneous temperature reached in the milled powders at the spontaneous propagation stage. The same combustion products, found at the end of the

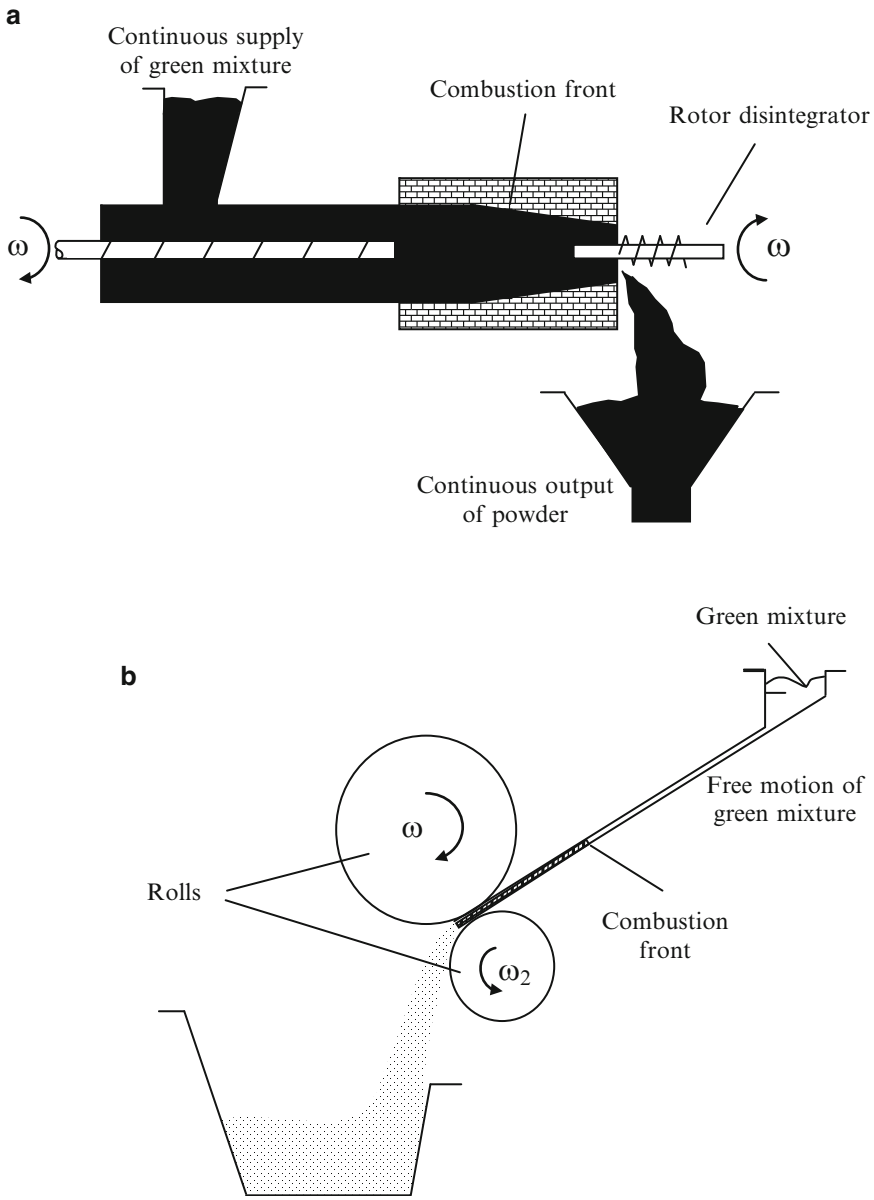

Fig. 7 Schematic representation of screw (**a**) and roll (**b**) reactors (Adapted from Cincotti et al. 2001)

reactions (Cao et al. 1999), confirm the similarity of the chemical transformations involved. A very promising research direction is to extend this strategy of investigation to other systems in order to highlight the mechanism involved during self-propagating reactions for environmental protection as well as other interesting application in the field of materials science and technology (Cao et al. 1997; Mulas et al. 2001).

In addition to the consideration above, the design of reactors for self-propagating reactions represents a very complex reactor problem, as pointed out by Hlavacek and coworkers (Hlavacek et al. 1990; Hlavacek and Puszynski 1996). This is mainly due to the rich spectrum of phenomena associated with solid-solid and gas-solid self-propagating reactions, such as the explosive expulsion of gases during reaction evolution, the melting of intermediate or final products, etc., which typically requires the design of a specific reactor. These aspects are of great importance when developing suitable technologies based on self-propagating reactions for residue recycling and environmental waste disposal. In addition, the availability of large-scale processes based on this technique should be taken into account due to the intensive production of wastes worldwide. While up to 1,000 t of material output may be handled by taking advantage of batteries of batch reactors, a very important technological challenge is represented by the development of continuous reactors where self-propagating reactions of solid-solid or gas-solid type take place (Merzhanov 1995). Along these lines, screw and roll reactors, whose sketches are reported in Fig. 7a, b, respectively, have been suggested for

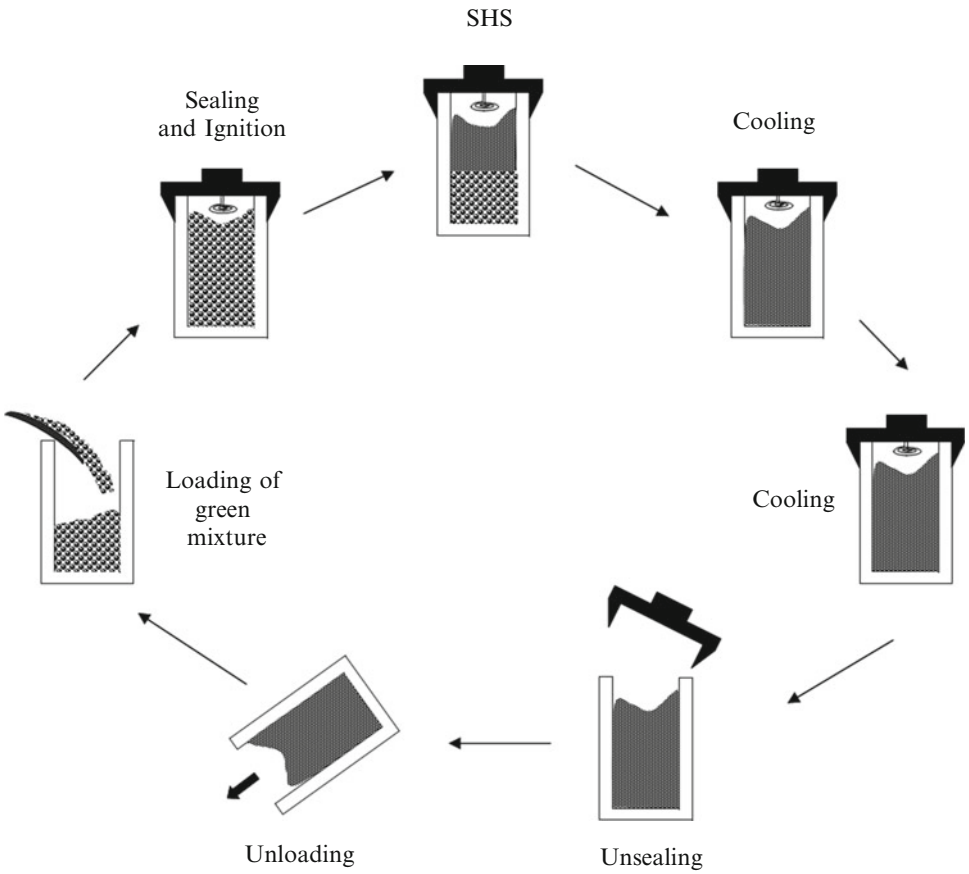

Fig. 8 Schematic representation of the various steps required by a batch SHS process (Adapted from Cincotti et al. 2001)

continuous powder production (Cincotti et al. 2001). In the first case (Fig. 7a), reactants are loaded into the reactor through a screw and subsequently reacted in a nozzle where the position of the combustion front is stabilized. Simultaneously, the products may be powdered in a rotor mill. The roll reactor (Fig. 7b) consists of two rotating rolls through which the obtained products are conveyed. However, practical exploitation of these continuous reactors seems to be very difficult for several reasons. Firstly, some operational problems may arise from the movement of the reacting mixture inside the reactor, since hard solid materials may cause strong erosion of the reactor tube. Moreover, reacting media can have the tendency to sinter which may stop the flow. The same problems may result if gas evolution occurs during the reacting process. All these inconveniences make the stabilization of the front difficult, which is, on the other hand, a necessary requirement for handling continuous reactors based on this technology.

On the other hand, it is worth noting that up to 1,000 t/year of material output can be handled for the large-scale production by SHS of titanium carbide in powder form (Merzhanov 1995; Miyamoto 1999) by taking advantage of batteries of batch reactors. This reactor technology, schematically shown in Fig. 8 (Cincotti et al. 2001), consists first of loading of the starting mixture prepared according to suitable ratios. After the reactor is sealed, the reaction is then initiated, thus generating a combustion front. Once the reaction is completed, a cooling step is required before the reactor is unsealed and unloaded to start a new cycle. The use of batteries of SHS batch reactors can satisfy the treatment of any amount of waste to be processed.

It should be noted that if reaction proceeds with gas evolution, an appropriate modification of the reaction configuration has to be adopted to facilitate gas escaping. This is not only due to safety concerns but also to prevent combustion front instabilities (and, consequently, the decreasing of degree of conversion) which may arise when gas evolution takes place. For example, this could be obtained by withdrawing it through a perforated tray at the end of the reactor.

Based on the considerations made previously, the batch technology is considered to be more easily applicable, due to its simplicity, with respect to the continuous reactor configurations reported in Fig. 7, for the exploitation of self-propagating reactions for environmental protection.

Apart from the technologies addressed in this paper, it is also worth mentioning that the comparison of different existing processes for residue recycling and waste disposal has to be performed to evaluate the most appropriate choice.

Acknowledgments The financial support of the Italian Ministry of Education, Universities and Research through the project "DINISAR" is gratefully acknowledged.

References

Barin, I.: Thermochemical Data of Pure Substances. VHC, Weinheim (1989)

Barinova, T.V., Borovinskaya, I.P., Ratnikov, V.I., Ignat'eva, T.I.: SHS immobilization of Cesium in mineral-like matrices. Int. J. SHS **16**, 133 (2007)

Barinova, T.V., Borovinskaya, I.P., Ratnikov, V.I., Ignat'eva, T.I.: SHS for immobilization of high-level waste in mineral-like ceramics: 1. Synthesis and study of titanate ceramics based on perovskite and zirconolite. Radiochemistry **50**(316) (2008a)

Barinova, T.V., Borovinskaya, I.P., Ratnikov, V.I., Ignat'eva, T.I.: SHS for immobilization of high-level waste in mineral-like ceramics: 2. Immobilization of cesium in ceramics based on perovskite and zirconolite. Radiochemistry **50**(321) (2008b)

Barinova, T.V., Borovinskaya, I.P., Ratnikov, V.I., Ignat'eva, T.I., Belikova, A.F., Skachkova, N.V., Khomenko, N.Y.: Mineral-like ceramics for immobilization of nuclear wastes by forced SHS compaction SHS. Int. J. SHS **20**, 67 (2011)

Borovinskaya, I.P.: Ecological aspects of SHS. In: Proceedings of 1st Russian-Japanese Workshop on SHS, Karlovy Vary, Czech Republic, 50 (1998a)

Borovinskaya, I.P., Barinova, T.V., Ratnikov, V.I., Zakorzhevsky, V. V., Ignat'eva, T.I.: Consolidation of radioactive wastes into mineral-like materials by the SHS method. Int. J. SHS **1**, 129 (1998b)

Cao, G., Orrù, R.: Self-propagating reactions for environmental protection: state of the art and future directions. Chem. Eng. J. **87**, 239–249 (2002)

Cao, G., Concas, G., Corrias, A., Orrù, R., Paschina, G., Simoncini, B., Spano, G.: Investigation of the reaction between Fe_2O_3 and Al accomplished by ball milling and self-propagating high-temperature techniques. Z. Naturforsch. **52a**, 539 (1997)

Cao, G., Doppiu, S., Monagheddu, M., Orrù, R., Sannia, M., Cocco, G.: The thermal and mechanochemical self-propagating degradation of chloro-organic compounds: the case of hexachlorobenzene over calcium hydride. Ind. Eng. Chem. Res. **38**, 3218 (1999)

Chen, W., Wang, P., Chen, D., Zhang, B., Jiang, J., Cheng, Y., Yan, D.: Synthesis of (Ca, Mg)-α-sialon from slug by self-propagating high-temperature synthesis. J. Mater. Chem. **12**, 1199 (2002)

Chen, M., Zhang, F.-S., Zhu, J.: Detoxification of cathode ray tube glass by self-propagating process. J. Hazard. Mater. **165**(1–3), 980–986 (2009)

Cincotti, A., Orrù, R., Pisu, M., Cao, G.: Self-propagating reactions for environmental protection: reactor engineering aspects. Ind. Eng. Chem. Res **40**, 5291–5299 (2001)

Cocco, G., Doppiu, S., Monagheddu, M., Cao, G., Orrù, R., Sannia, M.: Self-propagating high-temperature reduction of toxic chlorinated aromatics. Int. J. SHS **8**(4), 521 (1999)

Domalski, E.S., Hearing, E.D.: Estimation of the thermodynamic properties of C-H-N-O-S-halogen compounds. J. Phys. Chem. Ref. Data **22**(4), 805 (1993)

EPA-542-R-05-006: Reference Guide to Non-combustion Technologies for Remediation of Persistent Organic Pollutants in Stockpiles and Soil. http://www.cluin.org/download/remed/542r05006/final_pops_report_web.pdf (2005)

Forrester, J.S., Schaffer, G.B.: The chemical kinetics of mechanical alloying. Metall. Mater. Trans. A **26A**, 725 (1995)

Glagovskii, E.M., Kuprin, A.V., Pevelin, L.P., Konovalov, E.E., Starkov, O.V., Levakov, E.V., Postnikov, A.Y., Lisitsa, F.D.: Immobilization of high-level wastes in stable mineral-like materials in a self propagating high-temperature synthesis regime. Atom Energy **87**, 514 (1999)

Goldhaber, S.B., Chessin, R.L.: Comparison of hazardous air pollutant health risk benchmarks. Environ. Sci. Technol. **31**, 568 (1997)

Golubjatnikov, K.A., Stangle, G.C., Spriggs, R.M.: The economics of advanced self-propagating high-temperature synthesis materials fabrication. Am. Ceram. Soc. Bull. **72**(12), 96 (1993)

Hlavacek, V., Puszynski, J.A.: Chemical engineering aspects of advanced materials. Ind. Eng. Chem. Res. **35**, 349 (1996)

Hlavacek, V., Majorowski, S., Puszynski, J.: Engineering scale-up principles of SHS reactors. In: Kaieda, Y., Holt, J.B. (eds.) Proceedings of the First US-Japanese Workshop on Combustion Synthesis, p. 169. National Research Institute for Metals, Tokyo (1990)

Ionescu, D., Meadowcroft, T.R., Barr, P.V.: Glassification of EAF dust: the limit of Fe_2O_3 and ZnO content and an assessment of leach performances. Can. Metall. Quart. **36**, 269 (1997)

Konovalov, E.E., Starkov, O.V., Glagovskii, E.M., Myshkovskii, M.P., Kuprin, A.V., Pelevin, L.P., Gudkov, L.S., Nardova, A.K.: Immobilization of silica gel fixed cesium and strontium into mineral-like matrices in the SHS Mode. Radiochemistry **44**, 420 (2002)

Laverov, N.P., Yudintsev, S.V., Livshits, T.S., Stefanovsky, S.V., Lukinykh, A.N., Ewing, R.C.: Synthetic minerals with the pyrochlore and garnet structures for immobilization of actinide-containing wastes. Geochem. Int. **48**(1), 1–14 (2010)

Manahan, S.E.: Hazardous Waste Chemistry, Toxicology and Treatment. Lewis Publishers/CRC Press, Boca Raton (1990)

Merzhanov, A.G.: Theory and practice of SHS: world-wide state of the art and the newest results. Int. J. SHS **2**, 113 (1993)

Merzhanov, A.G.: Solid flames: discoveries, concepts, and horizon of cognition. Combust. Sci. Technol. **98**, 307 (1994)

Merzhanov, A.G.: Ten research directions in the future of SHS. Int. J. SHS **4**, 323 (1995)

Merzhanov, A.G., Borovinskaya, I.P.: Self-propagated high-temperature synthesis of refractory inorganic compounds. Dokl. Akad. Nauk SSSR **204**, 366 (1972)

Miyamoto, Y.: State of the art in R&D of SHS materials in the world. Int. J. SHS **8**, 375 (1999)

Miyamoto, Y., Li, Z., Tanihata, K.: Recycling processes of Si waste to advanced ceramics using SHS reaction. Ann. Chim. Fr. **20**, 197 (1995)

Miyamoto, Y., Arata, K., Yamaguchi, O.: Application of SHS to ecological problems – recycle of wastes in Si wafer production to sialon based ceramics. In: Proceedings of 1st Russian-Japanese Workshop on SHS, Karlovy Vary, Czech Republic, p. 46 (1998)

Miyamoto, Y., Kanehira, S., Yamagughi, O.: Development of recycling process for industrial wastes by SHS. Int. J. SHS **9**(357) (2000)

Mulas, G., Monagheddu, M., Doppiu, S., Cocco, G., Maglia, F., Anselmi Tamburini, U.: Metal-metal oxides prepared by MSR and SHS techniques. Solid State Ion. **141–142**(649) (2001)

Munir, Z.A., Anselmi-Tamburini, U.: Self-propagating exothermic reactions: the synthesis of high-temperature materials by combustion. Mater. Sci. Rep. **3**, 277 (1989)

Muthuraman, M., Arul Dhas, N., Patil, K.C.: Combustion synthesis of oxide materials for nuclear waste immobilization. Bull. Mater. Sci. **17**(977) (1994)

Orrù, R., Sannia, M., Cincotti, A., Cao, G.: Treatment and recycling of zinc hydrometallurgical wastes by self-propagating reactions. Chem. Eng. Sci. **54**, 3053 (1999)

Orrù, R., Cincotti, A., Concas, A., Cao, G.: Development of processes for environmental protection based on self-propagating reactions. Environ. Sci. Pollut. Res. **6**, 385–389 (2003)

Pelino, M., Cantalini, C., Vegliò, F., Plescia, P.: Crystallization of glasses obtained by recycling goethite industrial wastes to produce glass-ceramic materials. J. Mat. Sci. **29**, 2087 (1994)

Pelino, M., Cantalini, C., Abbruzzese, C., Plescia, P.: Treatment and recycling of goethite waste arising from the hydrometallurgy of zinc. Hydrometallurgy **40**, 25 (1996a)

Pelino, M., Cantalini, C., Ullu, F.: Re-utilization of Jarosite and goethite zinc hydrometallurgy wastes and granite mud in the glass-ceramic production. In: Ciccu, R. (ed.) Proceedings of SWEMP '96, p. 1011 (1996b)

Pelino, M., Cantalini, C., Ma Rincon, J.: Preparation and properties of glass-ceramic materials obtained by recycling goethite industrial wastes. J. Mat. Sci. **32**, 4655 (1997)

Porcu, M., Orrù, R., Cao, G.: On the use of industrial scraps for the treatment of zinc hydrometallurgical wastes by self-propagating reactions. Chem. Eng. J. **99**, 247–256 (2004)

Porcu, M., Orrù, R., Cincotti, A., Cao, G.: Self-propagating reactions for environmental protection: treatment of wastes containing asbestos. Ind. Eng. Chem. Res. **44**, 85–91 (2005)

Qin, Z., Mao, X., Chen, M., Yuan, X., Zhao, K., Liu, N.: Self-propagating high-temperature synthesis for immobilization of simulated radioactive sandy soil waste. Adv. Mater. Res. **518**, 2797 (2012)

Sannia, M., Orrù, R., Concas, A., Cao, G.: Self-propagating reactions for environmental protection: remarks on treatment and recycling of zinc hydrometallurgical wastes. Ind. Eng. Chem. Res. **40**, 801 (2001)

Spector, M.L., Suriani, E., Stukenbroker, G.L.: Thermite process for the fixation of high level radioactive wastes. I&EC Process Des. Dev. **7**, 117 (1968)

Varma, A., Rogachev, A.S., Mukasyan, A.S., Hwang, S.: Combustion synthesis of advanced materials: principles and applications. Adv. Chem. Eng. **24**, 79 (1998)

Vinokurov, S.E., Kulyako, Y.M., Perevalov, S.A., Myasoedov, B.F.: Immobilization of actinides in pyrochlore-type matrices produced by SHS. C. R. Chim. **10**, 1128 (2007)

Wang, L.L., Munir, Z.A., Maximov, Y.M.: Thermite reactions: their utilization in the synthesis and processing of materials. J. Mat. Sci. **28**, 3693 (1993)

Wang, K.-S., Lin, K.-L., Lee, C.-H.: Melting of municipal solid waste incinerator fly ash by waste-derived thermite reaction. J. Hazard. Mater. **162**(1), 338–343 (2009)

Yukhvid, V.I.: Solution of ecological problems by SHS – metallurgy method. In: Proceedings of 1st Russian-Japanese Workshop on SHS, Karlovy Vary, Czech Republic, p. 53 (1998)

Zhang, R., Gao, Y., Wang, J., Li, L., Su, W.: Leaching properties of immobilization of HLW into $SrTiO_3$ ceramics. Adv. Mater. Res. **332**, 1807 (2011)

Zhang, R., Shi, S., Zhang, T., Chen, G., Su, W.: Strontium titanate immobilization of simulated HLW by SHS. Adv. Sci. Lett. **12**, 381 (2012)

Glyphosate: Safety Risks, Biodegradation, and Bioremediation

A.V. Sviridov, T.V. Shushkova, I.T. Ermakova, E.V. Ivanova, and A.A. Leontievsky

Abstract

Problems and questions associated with worldwide success of glyphosate-based herbicide formulations are discussed. Controversy in glyphosate environmental safety assessments and the current state of research of the subject are reviewed. Glyphosate biodegradation is addressed, with particular emphasis on bacterial metabolism of the herbicide. Known degrader strains and corresponding enzyme systems are analyzed, and the prospects of their use in bioremediation of glyphosate contamination are discussed.

Keywords

Glyphosate • *N*-phosphonomethylglycine • Bioremediation • Glyphosate metabolism • Glyphosate safety • C–P lyase • Glyphosate oxidoreductase

1 Glyphosate: State of the Art

N-phosphonomethylglycine, known by its trivial name "glyphosate" (GP), is the widespread compound with direct carbon-to-phosphorus (C–P) covalent bond in its structure. Such unusual chemically inert bond is a typical feature of organophosphonates in contrast to more common organophosphates with phosphodiester bond. GP is a unique inhibitor of 5-enolpyruvyl 3-phosphate synthase (EPSPS) – the key enzyme of shikimate pathway of aromatic amino acid biosynthesis in plants, bacteria, and fungi, but absent in animals. The effects of EPSPS being "switched off" in plants include the impairment of protein, flavonoids, lignin, coumarins, and tannins biosynthesis, energy metabolism deregulation, and overaccumulation of shikimic acid, resulting in plant withering in 3–7 days after GP treatment (Jaworski 1972; Kishore and Shah 1988; Duke and Powles 2008; Dill et al. 2010).

GP was the first and only success among numerous attempts conducted in the late 1960s to produce an effective inhibitor of EPSPS which was considered to be a very promising and environmentally safe replacement for 2,4-D (2,4-dichlorophenoxyacetic acid). John E. Frantz, a chemist in Monsanto Company Inc., discovered GP after taking notice of EPSPS inhibition by phosphonic acid and conducting a search among its derivates. Soon after GP isopropylamine salt solution was patented as a herbicide and introduced on the market, thus bringing a spectacular commercial success to Monsanto (Lévesque and Rahe 1992; Herrmann and Weaver 1999; Duke and Powles 2008).

Today, GP is commonly used as acting compound in numerous commercial formulations of nonselective herbicides (glyphosate-based herbicides, GBH). GBH have quickly become an essential part of agriculture and forestry; their importance has been further amplified by the introduction of transgenic glyphosate-resistant crops in 1996. More than 80 % of the transgenic plants on the vast and ever-increasing farming area planted with these crops are GP resistant. Such cultures include soybean, maize, cotton, canola, sugar beet,

A.V. Sviridov (✉) • T.V. Shushkova • I.T. Ermakova
G. K. Skryabin Institute of Biochemistry and Physiology of Microorganisms RAS, Laboratory of Microbial Enzymology, Prospekt Nauki 5, Pushchino 142290, Russia
e-mail: alhummen@rambler.ru

E.V. Ivanova • A.A. Leontievsky
G. K. Skryabin Institute of Biochemistry and Physiology of Microorganisms RAS, Laboratory of Microbial Enzymology, Prospekt Nauki 5, Pushchino 142290, Russia

Pushchino State Institute of Life Science, Department of Microbiology and Biotechnology, Prospekt Nauki 3, Pushchino 142290, Russia

G. Cao and R. Orrù (eds.), *Current Environmental Issues and Challenges*,
DOI 10.1007/978-94-017-8777-2_11,

wheat, etc. Accordingly, the GP production has exceeded 500 thousand tons per annum and is estimated to reach one million ton in a few years. As a summary, the use of GP with resistant crops is the most important weed management technology in agronomic crops in the western hemisphere (Malik et al. 1989; Lévesque and Rahe 1992; James 2003; Duke and Powles 2008; Dill et al. 2010; Duke 2011).

2 Environmental Safety of Glyphosate

2.1 Controversy in GP Safety Considerations

GP environmental impact and its potential toxicity to animals and mammals in particular are highly disputed matter. The target enzyme of GP, and the shikimate pathway as a whole, is not present in animal cells; therefore the low toxicity of GP for animals was a natural assumption. This idea gained popular support after a number of studies which indicated a low-to-none effect of GP on test animals (e.g., rats, chicken), with LD_{50} comparable to this of sodium chloride (Williams et al. 2000; Taylor et al. 2004; Duke and Powles 2008; Dill et al. 2010).

Test made on several species of frogs (which are known to be highly susceptible to adverse effects of xenobiotics due to permeable skin) yielded comparable results. Commercial GBH were estimated as practically nontoxic (in terms of acute toxicity); the harmful impact of acidic form of GP was rather noticeable but was associated with general acid intolerance (Mann and Bidwell 1999).

Earlier studies on environmental fate of GP were quite promising as well: it became a common opinion that GP was susceptible to rapid and complete decomposition via photolysis and microbial degradation to aminomethylphosphonic acid (AMPA), which was regarded as physiologically neutral. GP accumulation and mobility in soils was considered insignificant, as its ability to be absorbed by plant roots and the impact on soil microbiota (Rueppel et al. 1977; Torstensson 1985; Lund-Høie and Friestad 1986; Williams et al. 2000; Duke and Powles 2008; Duke 2011).

Still it is important to note that the most cited part of the data published during the evaluation stages of GP/GBH safety were provided by the industry (i.e., Rueppel et al. 1977; Williams et al. 2000; Taylor et al. 2004), while academic studies on the matter are somewhat lacking. It is clear that a reasonable corpus of independent studies is necessary to fully evaluate the effects of GP on human health. This is particularly important when significant economic interests are concerned (Paganelli et al. 2010).

Indeed, the controversy in GP safety issues came forth with a number of papers which made evident the lack of deep studies of GP interaction with animal metabolism, specifically chronic and remote effects.

One of the most serious concerns expressed in recent studies of the matter was the possibility of embryonic development disruption caused by GP or GBH. It was based on the evidence of adverse effects of GBH on people living in areas where herbicides are intensively used. Agricultural workers using GBH were reported to have pregnancy problems; women exposed to GBH during pregnancy delivered the increased percentage of offspring with congenital malformations, including microcephaly, anencephaly, and cranial malformations (Savitz et al. 1997; Benitez-Leite et al. 2007).

It is argued that these phenomena are due to the fact that GP acts as a partial inactivator of microsomal aromatase by binding to its active center. This exerted cytotoxic and endocrine-disrupting effects on human placental and embryonic cells and on equine testicular cells in a time-dependent manner. Aromatase is a member of cytochrome P450 superfamily and plays a significant role in irreversible conversion of androgens to estrogens, thus affecting gametogenesis, placenta formation, and sex differentiation. Roundup formulation impact is even stronger due to synergic effects of glyphosate and surfactants it contains. These data suggest that glyphosate exposure may affect human reproduction and fetal development in case of contamination (Richard et al. 2005; Benachour et al. 2007).

Interestingly, the ability of GP to inhibit microsomal P450 cytochromes in plants was known heretofore (Lamb et al. 1998). The noncompetitive inhibition occurred as a result of GP nitrogen binding to heme of cytochrome P450 as a sixth ligand (Xiang et al. 2005).

Other potential cause of development abnormalities was the ability of GP to induce oxidative stress in liver cells and leukocytes. One percent GP oral exposure resulted in excessive lipid peroxidation in livers of pregnant rats and fetuses, which led to an overload of maternal and fetal antioxidant defense systems, primarily, glutathione peroxidase. Nevertheless, the exact mechanisms of reactive oxygen species formation resulting from GP exposure is still a matter of investigation (Beuret et al. 2005). Similar phenomena were observed in bovine lymphocytes, where the contact with GP affected cell proliferation and induced overexpression of glucose 6-phosphate dehydrogenase – a marker enzyme for changes in normal cell redox state, specifically, for reduced glutathione depletion. The increased rate of chromosome aberration occurrences was also observed (Lioi et al. 1998).

These data were confirmed in later studies, where hepatotoxic effect of GP formulations in sub-agricultural doses was investigated. Aromatase transcription and activity in human liver cells was disrupted within 24 h of incubation with 10 ppm of Roundup; acute cytotoxic and genotoxic effects were made evident as well. Although, it was noted that adverse effects were more dependent on specific herbicide formulation than on GP concentration. Thus, the real effect of GP on animal cells can be strongly mediated by

adjuvants present in specific formulation, yet these compounds alone do not exert the same effect as when they are coupled with GP (Gasnier et al. 2009).

GP concentrations used for agricultural purposes (about 10,000 ppm) was found to have acute cytotoxic effect on Sertoli cells from rat testicles, while its Roundup formulation affected Leydig cells as well, inducing necrosis and apoptosis. Minor concentrations of GP (about 1 ppm), comparable to these found in human urine after ingestion of GP-treated crops, had no cytotoxic potential, but disrupted endocrine function of testicular cells, resulting in testosterone production decrease by 35 %. This does not anticipate the chronic toxicity of GP which is generally not investigated (Clair et al. 2012).

Another line of evidence supporting adverse effects of GP was provided by data on GP and its principal metabolite, AMPA being able to alter cell cycle checkpoints by interfering with the physiological DNA repair machinery. Several GBH were assayed, and all of them induced cell cycle dysfunction from the first cell division in sea urchin embryos (Marc et al. 2002). GP interference with mRNA synthesis in pacific oyster gills was argued as well (Boutet et al. 2004).

Amphibians were found to be susceptible to develop abnormalities caused by GP exposure as well. Research conducted on embryos and tadpoles of sharp-snouted tree frog (*Scinax nasicus*) demonstrated high percentage of morphology alterations when incubated with sub-agricultural concentrations of GP (3.0–7.5 mg/L). The effect was dose and time dependent. External malformations observed in tadpoles included eye and cranial abnormalities and mouth deformities. In contradiction to previous data of Mann and Bidwell (1999), acute toxic effects were also evidential (Lajmanovich et al. 2003).

The same was demonstrated for embryos of clawed frogs (*Xenopus laevis*). Incubation with both pure GP and Roundup (0.02 % solution) resulted in high rate of abnormalities in cephalic and neural crest development. The same effects were observed for chicken embryos after similar treatment. Surfactants commonly used in GBH did not induce these effects per se. The mechanism of teratogenic effect was found to be a result of the increased production of endogenous retinoid acid which was a direct consequence of GP treatment. Retinoic acid plays an important role in early embryonic development as it helps to determine position along the embryonic anterior/posterior axis by serving as an intercellular signaling molecule (Paganelli et al. 2010).

Therefore the problem of GP safety requires very serious consideration, as there is notable amount of data suggesting that GP can accumulate in arable soil layer, through the roots it can get into leaves, berries, and fruit and finally to mammals via food chains (Gougler and Geiger 1981; Archer and Stokes 1984; Roy et al. 1989; Pline et al. 2002; Shushkova et al. 2010). The situation is further aggravated by the worldwide spread of transgenic GP-resistant crops and resulting application of GBH directly during the period of vegetation. In some cases, GBH are used to accelerate grain ripening of cereals and sugar cane. As a result, GP residues may be present in a variety of feed and food (Lévesque and Rahe 1992; Low et al. 2005; Gasnier et al. 2009).

2.2 GP-Resistant Weeds

Another aspect of worldwide GP usage is the inevitable emergence of resistant weeds. For any herbicide, the speed of this process depends upon several factors, including the mechanism of herbicide interaction with plants, its lethality, and its ability to persist in soil in sublethal doses. The development of the resistance can be sped up by using the same herbicide with the same application method for prolonged period of time, which is the case in GBH–GP-resistant crops agricultural system (Holt et al. 1993; Baerson et al. 2002). For GP, the onset of resistant weeds began only in 10 years after the introduction of GBH on the market (Nafziger et al. 1984). By the present moment, more than 20 species of weeds with spontaneous resistance to GBH are known, including particularly hazardous horseweed, ryegrass, and goosegrass (Pratley et al. 1996; Baerson et al. 2002; Duke and Powles 2008; Dill et al. 2010; Duke 2011; Gonzalez-Torralva et al. 2012a, b). More common mechanisms of GP resistance in weeds vary from simple overexpression of EPSPS (Nafziger et al. 1984) and reduced translocation of GP in leaves and stems (Dill et al. 2010; Gonzalez-Torralva et al. 2012b) to mutations in EPSPS genes making them similar to gene of GP-insensitive EPSPS of *Salmonella typhimurium*, used to produce GP-resistant transgenic crops (Baerson et al. 2002). A distinct and peculiar mechanism of GP resistance involves plant metabolism of this compound. This matter remains surprisingly unstudied despite 35-year history of GP usage, as if there was a common agreement that GP action in plants is strictly limited to inhibition of EPSPS (Duke 2011). Still, there is a growing bulk of evidence that several plant species (i.e., *Conyza canadensis*, *Agropyron repens*, *Ipomea purpurea*) are able to degrade GP with formation of AMPA (thus mimicking an alternative strategy of GP-resistant crops engineering) and sarcosine (such ability was considered an exclusive attribute of bacteria). Yet it is still unclear what enzymes participate in these processes; there is even no certainty if GP degradation is an innate trait of studied plants or some exo- or endosymbionts are involved (Lévesque and Rahe 1992; Reddy et al. 2008; Duke 2011; Gonzalez-Torralva et al. 2012a).

Another conundrum of plant-GP interactions is phytotoxicity of AMPA, which was reported repeatedly (Hoagland 1980; Cessna et al. 2002; Nandula et al. 2007),

without providing a satisfactory explanation (Duke 2011). Given the abundance of AMPA as a primary product of GP breakdown by chemical, physical, and biological factors (Rueppel et al. 1977; Talbot et al. 1984; Torstensson 1985; Lund-Høie and Friestad 1986; Kishore and Jacob 1987), this makes the research of AMPA degradation a highly topical matter.

2.3 GP Mobility in Environment

Soils are the common endpoint of GP translocation after its application in agriculture and forestry. The behavior of GP in soil likewise was proven to be much more complex than it was assumed earlier. The rate of GP degradation, its mobility, bioavailability, and environmental impact depend on numerous factors and may vary considerably in different conditions (Lévesque and Rahe 1992; Veiga et al. 2001; Shushkova et al. 2010).

GP migration may be quite limited in clayey soils or soils enriched with humus due to strong (but reversible in most cases) adsorption of GP on aluminum silicates or humic acids. Though in sandy soils GP demonstrates increased horizontal and vertical mobility and may reach aquifer or surface waters (Dousset et al. 2004; Shushkova et al. 2010). In some cases, GBH concentration in lentic water bodies adjacent to agricultural areas may come up to toxic levels (Mann and Bidwell 1999). It is estimated that the total of 3 % of applied GP may be found in aquatic environments (Lajmanovich et al. 2003).

Glyphosate mobility can be augmented by rainfalls after recent application. Tests made on soddy-podzol soils demonstrated the intense watering as the factor that drastically increased the vertical mobility of GP; up to 40 % of applied GP could percolate deeper than first 10 cm of soil. That resulted in the decrease of the bioavailability of GP to microbial degraders whose population is denser in surface layers of the soil; the leaked GP was not susceptible to photodegradation as well (Shushkova et al. 2010). Field experiments in temperate coastal rainforests of British Columbia demonstrated even higher percolation of GP resulting in 0.16 mg/L of GP in water with initial GP concentration in soil being approximately 2 mg/kg (Lajmanovich et al. 2003). GP dispersion and its leakage to water bodies were recognized as an environmental risk in France (Bazot and Lebeau 2008).

2.4 GP Impact on Microbiota

The initial opinion of negligible effect of GP on bacterial microbiota (Rueppel et al. 1977; Torstensson 1985) was found to be premature after a series of studies which demonstrated substantial heterogeneity in soil microflora response to GP treatment. The impact of exposure to 3 mM GP could vary from complete growth retardation to the decrease in growth rate by 40–50 % in bacterial isolates from different sites. Naturally, bacteria isolated from soils previously treated with GP showed greater resistance, while displaying very distinct species composition in comparison with nontreated sites (Quinn et al. 1988; Dick and Quinn 1995b). Laboratory strains tended to be more susceptible to GP than wild types and demonstrated two typical modes of response to GP treatment: (1) toxic effect could easily be reverted by introduction of aromatic amino acids in culture medium (*E. coli*, *Pseudomonas* spp.); (2) toxic effect included deregulation of catabolism and resulting depletion of energy substrates and could not be reverted (*B. subtilis*) (Fischer et al. 1986). The former one is the prevalent mode of response in bacterial communities found in GP-polluted environments (Quinn et al. 1988); the latter one is most evident in symbiotic and free-living nitrogen fixers, where GP-induced energy metabolism disruption resulted in complete inhibition of nitrogenase complex (Maria et al. 2006). This prevented the formation of nodules even if host plant was GP resistant (Zablotowicz and Reddy 2004).

GP tolerance in bacteria can be in most cases attributed to presence of GP-insensitive forms of EPSPS (class II EPSPS). Amino acid composition of this enzyme varies in bacteria to much greater extent than in plants, the sensitivity to GP varying accordingly. The most known GP-insensitive form of EPSPS was discovered in *Salmonella typhimurium* and used in earlier attempts of GP-resistant crops engineering. Its sensitivity to GP was 9 times lower in comparison with plant form of the enzyme. Later, class II EPSPSs were revealed in *E. coli* and *Aerobacter aerogenes* mutants with more than 3,000-fold increase in IC_{50} for GP. The latter was used for a successful production of transgenic cotton, soybean, and canola (Kishore and Shah 1988; Duke and Powles 2008; Shaner et al. 2011). Class II EPSPS, when coupled with efficient systems of GP degradation, in rare cases may provide bacteria with remarkable tolerance to GP concentrations exceeding those used in agriculture thousandfold. Strain *Alcaligenes* sp. GL could survive 100 mM (17 g/L) GP (Lerbs et al. 1990), while *Pseudomonas* sp. GLC 11 (Selvapandiyan and Bhatnagar 1994), *Ochrobactrum anthropi* GPK 3 (Sviridov et al. 2012b), and *Ochrobactrum* sp. GDOS (Hadi et al. 2012) were able to tolerate presence of 120 mM (20 g/L) GP without noticeable retardation of growth. All of the strains listed were also able to mineralize GP with formation of orthophosphate (P_i) but via different pathways and with different efficiency.

Fungal part of soil microbiota is also susceptible to toxic effects of GP, as it possesses the target enzyme EPSPS, though in fungi it is usually a part of five-functional enzyme complex *arom* and tends to be less sensitive to GP than

monomeric EPSPSs in plants and bacteria (Kishore and Shah 1988). High doses of GP could be lethal to wild types of fungi (Bujacz et al. 1995), but the impact of agricultural and residual doses of GP could be alleviated by external sources of aromatic amino acids, which give the fungi a major advantage over plants. This advantage is furthered by the fact that even the residual amounts of GP interfere with biosynthesis of natural phenolic fungicides in plants. In some cases, this aspect facilitates the formation of mycorrhizae, but more often GP treatment serves as an activator for fungal phytopathogens such as *Phytophthora* sp. and *Fusarium* sp. (Lévesque and Rahe 1992).

3 Bacterial Degradation of GP

At the present moment, biodegradation of GP has been sufficiently studied in bacteria only. In most GP-polluted environments, i.e., soils or industrial waste-separating tanks, GP was degraded to AMPA in roughly equimolar quantities by bacterial consortia. The cometabolism was an essential part of the process, as no isolate of consortia was able to degrade GP in pure culture (Rueppel et al. 1977; Balthazor and Hallas 1986; Hallas et al. 1992). Isolates, capable of utilizing GP as a source of P_i, are quite sparse, the first one discovered being *Pseudomonas* sp. PG2982 which, surprisingly, metabolized GP not into AMPA, but into sarcosine by disrupting the C–P bond (Moore et al. 1983; Shinabarger and Braymer; 1986). The same mechanism was later discovered in *Alcaligenes* sp. GL (Lerbs et al. 1990), *Arthrobacter* sp. GLP-1 (Pipke et al. 1987b), *Pseudomonas* sp. GLC11 (Selvapandiyan and Bhatnagar 1994), *Pseudomonas* sp. 4ASW (Dick and Quinn 1995a), and *Achromobacter* sp. MPS 12A (Sviridov et al. 2012a, b). A number of bacteria which degraded GP via AMPA and could utilize it as a source of P_i was identified as well: *Pseudomonas* sp. SG-1 (Talbot et al. 1984), *Flavobacterium* sp. GD1 (Balthazor and Hallas 1986), *Pseudomonas* sp. LBr (Jacob et al. 1988), *Achromobacter* sp. LW9 (McAuliffe et al. 1990), *O. anthropi* LBAA (Kishore and Barry 1992), *O. anthropi* GPK 3 (Sviridov et al. 2012a, b), and *Ochrobactrum* sp. GDOS (Hadi et al. 2012). Known microbial degraders of GP are reported in Table 1.

However, the ability to use GP as the source on nutrients other than P_i appeared to be extremely rare: *Arthrobacter* sp. GLP-1/Nit mutant was able to use GP as a source of nitrogen (Pipke and Amrhein 1988c); *Streptomyces* sp. StC (Obojska et al. 1999) and *Achromobacter* sp. LW9 (McAuliffe et al. 1990) utilized GP as a source of nitrogen and carbon. The possible cause of this may be the low speed of GP transformation after its transport to cytoplasm (Liu et al. 1991) or the suppression of GP-metabolizing enzymes by resulting P_i (Dick and Quinn 1995b; Bazot and Lebeau 2008).

The fundamental work of Dick and Quinn (1995b), where 163 wild-type bacterial isolates were tested for their ability to metabolize GP, along with other data, allowed us to make several generalizations on the matter:

1. The most widespread pathway of GP breakdown is its conversion to AMPA. This trait is common among a number of laboratory and wild-type strains, including those ones never exposed to GP before (Rueppel et al. 1977; Quinn et al. 1988; Dick and Quinn 1995b).
2. Bacteria metabolizing GP to AMPA are generally unable to mineralize the latter one, except for few exceptions. In most cases, almost total amount of AMPA is excreted (Balthazor and Hallas 1986; Jacob et al. 1988; Pipke and Amrhein 1988a; Lerbs et al. 1990).
3. The strains able to break down AMPA to P_i, but unable to transform GP to AMPA, are significantly more abundant than those ones that can perform both processes (Dick and Quinn 1995b). Thus, we can assume that the enzymes degrading GP to AMPA did not evolve as a dedicated part of phosphorus metabolism.
4. There sarcosine pathway of GP metabolism is more widespread among the strains able to mineralize GP (Shinabarger and Braymer 1986; Pipke et al. 1987a; Liu et al. 1991; Selvapandiyan and Bhatnagar 1994; Dick and Quinn 1995a, b). On the other hand, the sarcosine pathway is strongly regulated by external P_i, thus rather inefficient for GP biodegradation in most environments except synthetic media (Kertesz et al. 1991; Imazu et al. 1998; Bazot and Lebeau 2008).
5. As a rule, GP-utilizing bacteria use it as a source of P_i only, with singular exceptions (Pipke and Amrhein 1988b; McAuliffe et al. 1990; Obojska et al. 1999).

These facts indicate a considerable variety in bacterial enzymatic pathways of GP degradation and their regulatory mechanisms. It is safe to say that while GP-degrading microorganisms have been quite well characterized at a bench level, the underlying biochemistry is seldom sufficiently clarified.

4 GP Metabolism

There are two most abundant pathways of enzymatic GP breakdown: (1) more "direct" disruption of the C–P bond with formation of sarcosine and P_i and (2) cleavage of the C–N bond with formation of glyoxylate and environmentally stable AMPA, which could either be excreted or undergo further metabolism yielding P_i as well.

Table 1 GP-degrading microorganisms with established type of metabolism and taxonomy

Microorganism	Source	Primary GP metabolite	Gram status	Reference
Bacteria				
Achromobacter sp. LW9	Activated sludge of GP process waste stream	AMPA	–	McAuliffe et al. (1990)
Achromobacter sp. MPS 12A	Methylphosphonate-contaminated soil	Sarcosine	–	Sviridov et al. (2012a, b)
Agrobacterium radiobacter	Activated sludge from water treatment plant	Sarcosine (presumably)	–	Wackett et al. (1987)
Alcaligenes sp. GL[a]	Subculturing of non-axenic *Anacystis nidulans* on selective medium	Sarcosine (95 %), AMPA (5 %)	–	Lerbs et al. (1990)
Arthrobacter atrocyaneus ATCC 13752[a]	German Collection of Microorganisms and Cell Cultures	AMPA	+	Pipke and Amrhein (1988b)
Arthrobacter sp. GLP-1[a]	Accidental contaminant of *Klebsiella pneumoniae*	Sarcosine	+	Pipke et al. (1987b)
Flavobacterium sp. GD1	Activated sludge of GP process waste stream	AMPA	–	Balthazor and Hallas (1986)
Geobacillus caldoxylosilyticus T20[a]	Domestic central heating system	AMPA	+	Obojska et al. (2002)
Ochrobactrum anthropi GDOS	GP-contaminated soil	AMPA	–	Hadi et al. (2012)
O. anthropi GPK 3	GP-contaminated soil	AMPA	–	Sviridov et al. (2012a, b)
O. anthropi LBAA	Soil	AMPA	–	Kishore and Barry (1992), Gard et al. (1997)
O. anthropi S5	Soil	AMPA	–	Gard et al. (1997)
P. pseudomallei 22	GP-contaminated soil	AMPA (presumably)	–	Penaloza-Vasquez et al. (1995)
Pseudomonas sp. 4ASW	GP-contaminated soil	Sarcosine	–	Dick and Quinn (1995a)
Pseudomonas sp. GLC11[a]	Subculturing of *Pseudomonas aeruginosa* PAO1 on selective medium	Sarcosine	–	Selvapandiyan and Bhatnagar (1994)
Pseudomonas sp. LBr	Activated sludge of GP process waste stream	AMPA (95 %), Sarcosine (5 %)	–	Jacob et al. (1988)
Pseudomonas sp. PG2982[a]	Subculturing of *P. aeruginosa* ATCC 9027 on selective medium	Sarcosine	–	Moore et al. (1983)
Rhizobium meliloti 1021	Spontaneous streptomycin-resistant mutant of wild type	Sarcosine	–	Liu et al. (1991)
Streptomyces sp. StC	Activated sludge from water treatment plant	Sarcosine	+	Obojska et al. (1999)
Fungi				
Aspergillus niger	Soil	AMPA	n/a	Krzysko-Lupicka et al. (1997)
Penicillium chrysogenum	Soil	AMPA (presumed)	n/a	Klimek et al. (2001)
Penicillium notatum	Spontaneous growth on hydroxyfluorenyl-9-phosphonate	AMPA	n/a	Bujacz et al. (1995)
Scopulariopsis sp.	Soil	AMPA	n/a	Krzysko-Lupicka et al. (1997)
Trichoderma harzianum	Soil	AMPA	n/a	Krzysko-Lupicka et al. (1997)

n/a not applicable
[a]Strains never exposed to GP prior the research (spontaneous GP-degrading capabilities)

4.1 C–P Lyase and the Sarcosine Pathway of GP Degradation

Two main strategies of C–P bond cleavage are known, one involving highly substrate-specific hydrolases and the other one based on the action of a comparatively non-specific C–P lyase. All known organophosphonate-degrading hydrolases require the C–P bond to be "activated," i.e., destabilized by oxygen of carboxyl, carbonyl, or epoxy groups in close proximity, which is not the case in GP (Shames et al. 1987; White and Metcalf 2007).

Nonactivated C–P bond is resistant to chemical and enzymatic hydrolysis, and its splitting requires the action of a multienzyme complex known as "C–P lyase," which can convert a wide range of phosphonates into P_i and corresponding (amino) carbon residue. The action of the most studied *E. coli* C–P lyase is determined by the products of 14 genes of *phn* operon. Some C–P lyase constituents provide for organophosphonates transport, exert regulatory or auxiliary functions; others are enzymes that catalyze C–P bond cleavage per se. The *phn* genes, being a part of the Pho regulon, are only expressed under phosphorus starvation. The composition of C–P lyases in both gram-negative and

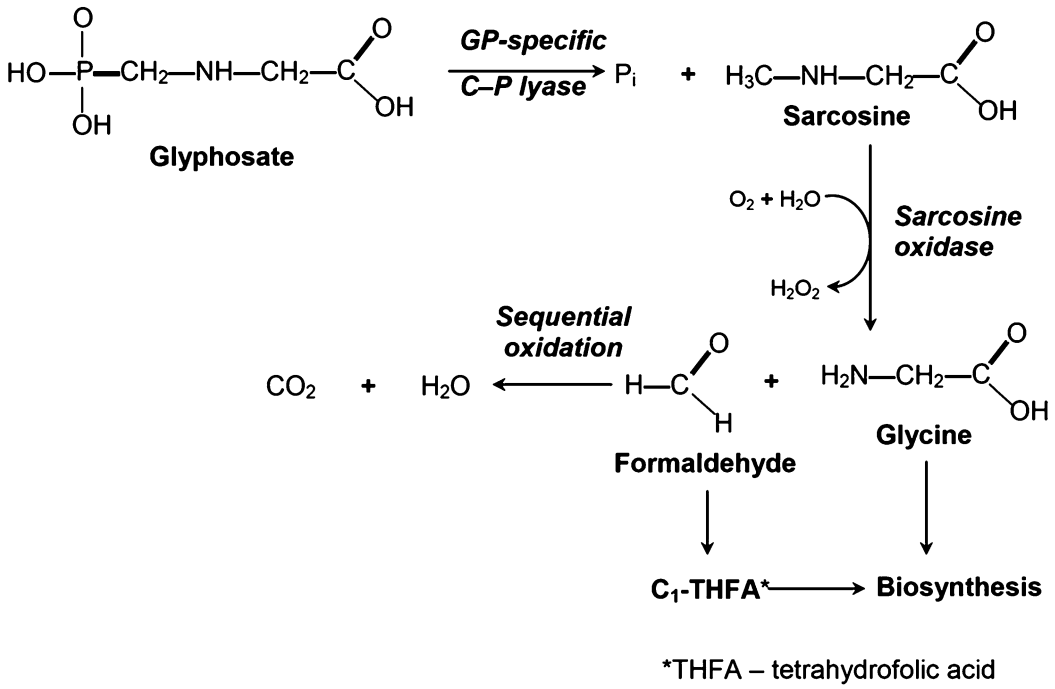

Fig. 1 GP metabolism via sarcosine (Shinabarger and Braymer 1986; Kishore and Jacob 1987)

gram-positive bacteria is presumed to be similar (White and Metcalf 2007). The catalytic core or C–P lyase constitutes a short metabolic pathway by itself; its complexity prevented the successful demonstration of C–P lyase activity in vitro for three decades until recently (Kamat et al. 2011; Zhang and van der Donk 2012).

Biochemical data on diverse patterns of different organophosphonate catabolism gave way to the assumption of two C–P lyase varieties in *Arthrobacter* sp. GLP-1 specific to (amino)alkylphosphonates (that were found earlier in *E. coli*) or GP. The same was discovered later in *Achromobacter* sp. MPS 12A. GP-specific C–P lyase was inhibited by the substrates of "*E. coli*-type" C–P lyase and its specificity seems to be limited to GP only (Kertesz et al. 1991; Sviridov et al. 2012b). The multiplicity of C–P lyases in single organism is not unique: two different C–P lyase operons that encoded enzymes with different substrate specificity were found in *Pseudomonas stutzeri*, though both lyases failed to degrade GP (White and Metcalf 2004).

Thereby the GP-specific C–P lyase still remains a conundrum, as it has never been characterized neither biochemically nor genetically and no natural substrates (if any) have been found. Surprisingly, the ability to degrade GP via sarcosine was found in strains that had never made contact with GP (see Table 1), and we may only speculate what were the causes for the evolution of such complex and highly specific enzyme system.

On the contrary, the metabolic fate of GP-derived sarcosine is ascertained quite well. This compound is rapidly metabolized by bacterial sarcosine oxidase into glycine and formaldehyde. The former is a common substrate for numerous anabolic processes; the latter could enter biosynthesis in a form or monocarbon residue coupled with tetrahydrofolic acid (Fig. 1) (Shinabarger and Braymer 1986; Kishore and Jacob 1987).

Bacterial strains with this type of GP metabolism may manifest excellent efficiency of GP degradation in laboratory conditions, where their P_i sources are limited to GP only, but in natural environments their capabilities could be reduced to nil. As a rule, the expression of C–P lyase is negatively regulated by the presence of extracellular P_i which is not uncommon in natural environments (Pipke and Amrhein 1988b; Dick and Quinn 1995a, b; Bazot and Lebeau 2008). A few exceptions are known, though, e.g., mutant *Arthrobacter* sp. GLP-1/Nit (Pipke and Amrhein 1988c) and *Alcaligenes* sp. GL (Lerbs et al. 1990) decomposed GP to sarcosine even in presence of P_i.

Sarcosine pathway of GP metabolism is depicted in Fig. 1.

4.2 AMPA Pathway of GP Metabolism

The second major pathway of GP degradation in bacteria starts with the enzyme known by its trivial name as "glyphosate oxidoreductase" (GOX) (Kishore and Barry 1992). It facilitates the breakdown of GP into stoichiometric amounts of AMPA and glyoxylate and is not subject to

regulation by P_i content. The recently purified GOX of *O. anthropi* GPK 3 was found to be a member of bacterial flavin monooxygenase superfamily. It contains one molecule of non-covalently bound FAD per subunit and exhibits maximum activity in alkalescent conditions with rather low affinity to GP (pH 8.0, $K_m = 0.2$ mM). The purified enzyme has somewhat low stability in normal conditions; its activity strongly depends on osmotic and oncotic pressure and is inhibited by ions of Cu^{2+}, Ag^{+}, and Mn^{2+} as well as by *p*-chloromercurybenzoic acid. GOX has rather wide substrate specificity, which includes iminodiacetic acid ($K_m = 0.1$ mM) and phosphonomethyliminodiacetic acid ($K_m = 2.4$ mM); the enzyme is also able to transform glycine, sarcosine, and D-alanine, albeit at a very slow rate (Sviridov et al. 2012a).

The thermostable form of GOX is presumed to exist in thermophilic *Geobacillus caldoxylosilyticus* T20 isolated from central heating system (Obojska et al. 2002).

The fate of products of GOX reaction may vary. Glyoxylate is a common energy substrate and can be utilized via glyoxylate shunt of Krebs cycle (Jacob et al. 1988), while the bulk of AMPA in most cases is excreted into extracellular environment (Balthazor and Hallas 1986; Jacob et al. 1988; Pipke and Amrhein 1988a; Lerbs et al. 1990). Alternatively, the C–P bond of AMPA can be disrupted by "*E. coli*-type" C–P lyase yielding P_i and methylamine or *N*-methylacetamide (in case AMPA is acetylated preliminary) (Avila et al. 1987; Pipke et al. 1987b; Kishore and Jacob 1987; Kishore and Barry 1992; Kertesz et al. 1994).

AMPA metabolism via C–P lyase was regarded as a sole way to decompose this compound until recently, when a novel phosphonatase pathway of glyphosate mineralization was discovered in *O. anthropi* GPK 3 (Sviridov et al. 2012a, b). Phosphonatase pathway is the most studied in phosphonates metabolism; it consists of two consequential reaction: (1) transamination of natural phosphonate ciliatine (2-aminoethylphosphonate, 2-AEP) by 2-AEP:pyruvate aminotransferase (EC 2.6.1.37), a 80 kDa homodimer with pH optimum of 8.5 (Kim et al. 2002) and (2) hydrolysis of C–P bond of resulting phosphonoacetaldehyde by phosphonatase (phosphonoacetaldehyde hydrolase, EC 3.11.1.1), a 62 kDa Mg^{2+}-dependent homodimer with optimal pH of 7.5 (Morais et al. 2004). These two enzymes are regarded as strongly substrate specific and were never directly reported to take part in GP metabolism (Quinn et al. 2007; White and Metcalf 2007; McGrath et al. 2013), though there were some indirect data on possibility of phosphonatase involvement in AMPA degradation (Talbot et al. 1984; Balthazor and Hallas 1986). In our recent study of GP metabolism in *O. anthropi* GPK 3, two distinct transaminase activities were detected: one corresponding with ordinary 2-AEP:pyruvate aminotransferase and the other specific to AMPA, with phosphonoformaldehyde as putative product (data not published). This product was subject to rapid hydrolysis by phosphonatase yielding P_i and formaldehyde both utilized intracellularly (Sviridov et al. 2012b).

AMPA pathway of GP metabolism in bacteria is depicted in Fig. 2.

4.3 Other Possible Ways of GP Biodegradation

Besides two major pathways of microbial GP degradation, some alternatives exist, though they still remain poorly studied in most cases.

GP could undergo modification and thus be detoxified by products of genes *igrA* (Fitzgibbon and Braymer 1990; Dalrymple et al. 1992), *glpA*, and *glpB* (Penaloza-Vasquez et al. 1995) found in *Pseudomonas* sp. PG2982 and *P. pseudomallei* 22, respectively. It was argued that the modification of the molecule of GP in these cases included decarboxylation, phosphorylation, and C–N bond cleavage, but no further studies were conducted.

Glyphosate *N*-acetyltransferase discovered in *Bacillus licheniformis* uses acetyl coenzyme A to transform GP into metabolically neutral *N*-acetyl glyphosate at very slow rate (Castle et al. 2004), which could be augmented by directed mutagenesis (Siehl et al. 2005, 2007). The enzyme with similar function was later discovered in *Salmonella typhimurium* LT 2, where it was encoded by *phnO* – a part of C–P lyase operon (Errey and Blanchard 2006). Physiological role of these proteins is under discussion.

Barett and McBride (2005) reported the phenomenon of abiotic GP and AMPA decomposition to P_i and primary amines in presence of manganese oxide, though it was noted that environmental quantities of manganese oxide are too low for noticeable contribution of this process in GP degradation.

Considerably higher rate of GP decomposition could be achieved in the presence of ligninolytic enzymes manganese peroxidase or laccase, Mn^{2+} ions, and surfactants, though in that case the final product was AMPA and no further decomposition was observed. Such mechanism could constitute a significant part of GP biodegradation in certain soils (Pizzul et al. 2009).

Recent studies of bacterial glycine oxidase showed its limited ability to break down GP into the same products as GOX but through different reaction mechanism (Pedotti et al. 2009). This data along with some controversy in reported GOX characteristics (Talbot et al. 1984; Kishore and Barry 1992; Obojska et al. 2002) gives ground to an assumption that there exist a number of bacterial oxidases with different structures, characteristics, and substrate specificity, which take part in metabolism of natural amino and imino acids, but are able to disrupt the C–N bond of GP as well due to broad substrate range.

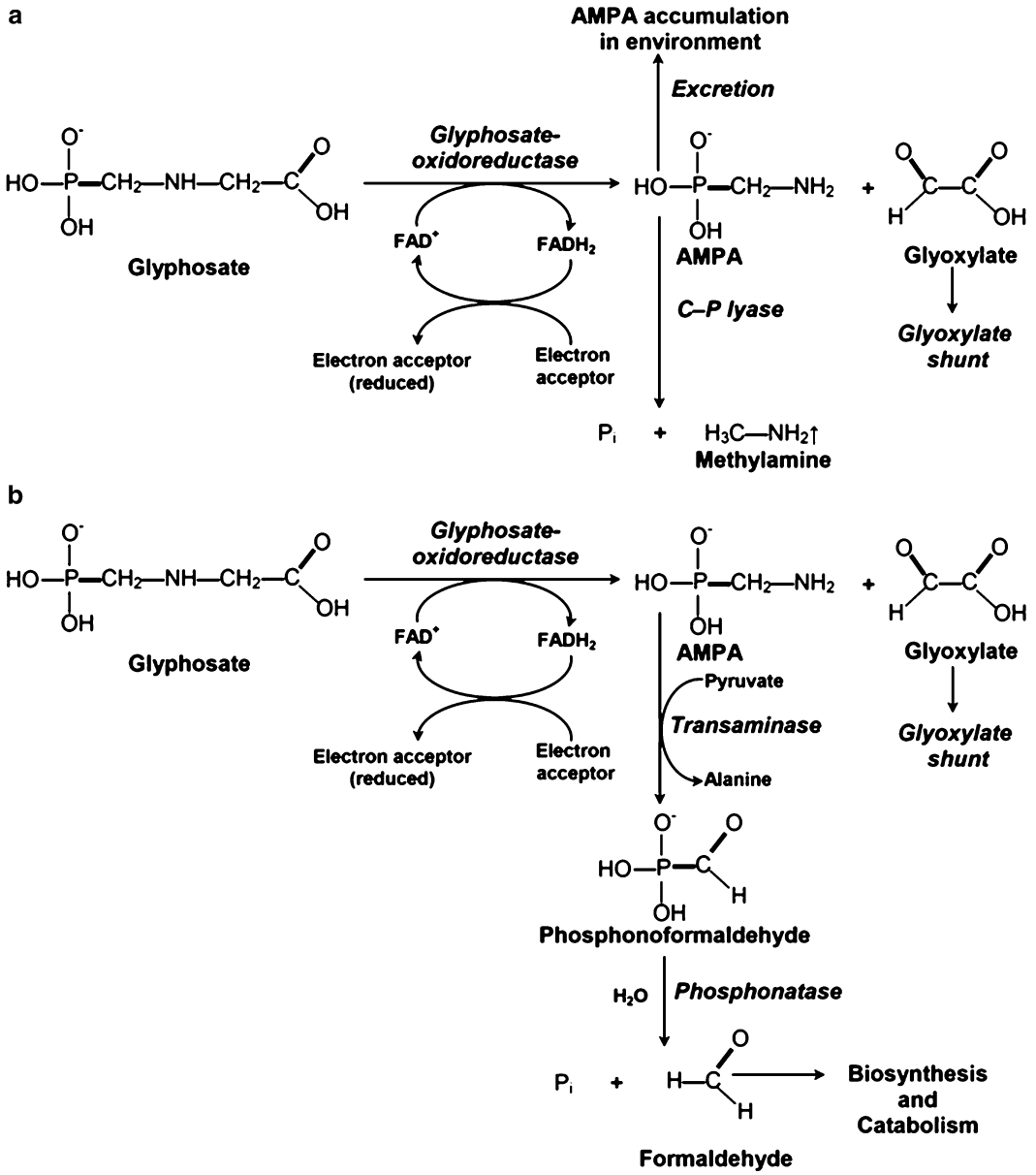

Fig. 2 GP metabolism via AMPA. (**a**) Pathway prevailing in most studied bacteria (Balthazor and Hallas 1986; Pipke et al. 1987b; Kishore and Jacob 1987; Kertesz et al. 1994); (**b**) Novel phosphonatase pathway in *O. anthropi* GPK 3 (Sviridov et al. 2012a, b)

In eukaryotes, GOX-like activity was found in some fungi (Bujacz et al. 1995; Krzysko-Lupicka et al. 1997), and one can speculate that fungal contribution into GP degradation in environment is comparable, if not greater, than bacterial (Kafarski et al. 2001), yet there are no biochemical data on the subject. Plant metabolism of GP remains vaguely studied as well, despite data suggesting its importance in evaluation of environmental fate of this herbicide (Reddy et al. 2008; Duke 2011; Gonzalez-Torralva et al. 2012a). GP transformation into AMPA and glyoxylate has even been detected in animals: a novel oxidase of pacific oyster *Crassostrea gigas* catalyzed the splitting of C–N bond of GP coupled with 4-electron reduction of oxygen. Unlike bacterial GOX, this enzyme required both flavin and nicotinamide cofactors and could play a major role in prevention of GP-induced protein biosynthesis impairment in mollusk gills (Boutet et al. 2004).

5 Bioremediation of GP-Contaminated Environments

Until recently, GP was not considered as a major environmental risk; therefore the research in the field of GP bioremediation was limited to microbial processing of industrial wastewater effluent of GP synthesis plants, which has been

used by Monsanto Company Inc. since the 1970s (Balthazor and Hallas 1986; Hallas et al. 1988). The introduction of columns with immobilized GP-degrading bacteria ensured 90 % extinction of GP in wastewater, provided the bacteria were sufficiently supplied with carbon and nitrogen sources (Hallas et al. 1992). A similar technology was found to be applicable for phosphonomethyliminodiacetate (PIA, GP precursor) waste treatment (Carson et al. 1997), although in both studies the percentage of mineralized GP was low and the bulk of GP and PIA was transformed into AMPA.

Treating GP contamination outside controlled environment of aerotanks is much more complex task, which requires microorganism cultures with very special set of physiological and biochemical traits: (1) low toxicity and pathogenicity; (2) high survival rate in short period but limited overall lifespan; (3) high GP biodegradation efficiency, not dependent on external conditions; and (4) ability to mineralize GP without accumulation of AMPA.

Literature contains some data on GP degradation by indigenous microbial communities (Rueppel et al. 1977; Veiga et al. 2001; Getenga and Kengara 2004; Sørensen et al. 2006); only a few studies of introduced GP degraders are known up to date. The attempt to use sarcosine-producing *Pseudomonas* sp. 4ASW – an effective laboratory GP degrader – was unsuccessful. Residual amounts of P_i present in freshwater was enough to abolish the expression of GP-specific C–P lyase, thus rendering the introduction of *Pseudomonas* sp. 4ASW futile (Bazot and Lebeau 2008).

Highly active form of GP acetyltransferase obtained through directed mutagenesis was proposed as a base of engineering GP-resistant transgenic plants suitable for phytoremediation of GP-contaminated soils (Siehl et al. 2007), though there is no data on practical application of this technology.

First successful remediation of GP-polluted soils in situ by introduced bacterial degraders *O. anthropi* GPK 3 and *Achromobacter* sp. Kg 16 was reported recently (Ermakova et al. 2010; Shushkova et al. 2010). Both strains exerted noticeable tolerance and biodestruction efficiency toward GP and were found to be safe for mammals. *O. anthropi* GPK 3 possessed a novel pathway of GP metabolism, where the complete herbicide mineralization is reached with no AMPA being excreted (Sviridov et al. 2012b) and GP is degraded more rapidly in liquid media. *Achromobacter* sp. Kg 16 displayed mediocre GP degradation rate in liquids, while the introduction of this strain in soil intensified GP decomposition threefold in comparison with native microflora (Ermakova et al. 2010). The use of consortium of *O. anthropi* GPK 3 and *Achromobacter* sp. Kg 16 as a universal microbial preparation for remediation of soils and water contaminated with GP, PIA, and AMPA is currently under research.

As a conclusion, it can be noted that the problem of glyphosate is very complex and versatile. On one hand, GP was named "once-in-a-century herbicide" for unprecedented weed control possibilities it has provided for agriculture and the impact it had on the rate of adoption of numerous transgenic crops (Duke and Powles 2008). On the other one, it is clear that there has always been a certain gap in GP-related research, i.e., environmental safety assessments of biochemistry studies. Only recently the deficiency of knowledge in this field was recognized, and a noticeable increase in a number of published GP-related works could be observed in the past 5 years. We can only look forward to obtain all the answers to the conundrums the GP could present us to facilitate a reasonable and controlled use of this unique yet ambiguous compound.

Acknowledgments The research of phosphonatase pathway of GP metabolism in *O. anthropi* GPK 3 was supported by the Ministry of Education and Science of the Russian Federation as a part of "A novel pathway for the catabolism of persistent organophosphonates in bacteria" project 2012–2014.

References

Archer, T.E., Stokes, J.D.: Residue analysis of glyphosate in blackberries by high-performance liquid chromatography and postcolumn reaction detection. J. Agric. Food Chem. **32**, 586–588 (1984)

Avila, L.Z., Loo, S.H., Frost, J.W.: Chemical and mutagenic analysis of aminomethylphosphonate biodegradation. J. Am. Chem. Soc. **109**, 6758–6764 (1987)

Baerson, S.R., Rodriguez, D.J., Minhtien, T., Feng, Y., Biest, N.A., Dill, G.M.: Glyphosate-resistant goosegrass. Identification of a mutation in the target enzyme 5-enolpyruvylshikimate-3-phosphate synthase. Plant Physiol. **129**, 1265–1275 (2002)

Balthazor, T.M., Hallas, L.E.: Glyphosate-degrading microorganisms from industrial activated sludge. Appl. Environ. Microbiol. **51**, 432–434 (1986)

Barrett, K.A., McBride, M.B.: Oxidative degradation of glyphosate and aminomethylphosphonate by manganese oxide. Environ. Sci. Technol. **39**, 9223–9228 (2005)

Bazot, S., Lebeau, T.: Simultaneous mineralization of glyphosate and diuron by a consortium of three bacteria as free-and/or immobilized-cells formulations. Appl. Microbiol. Biotechnol. **77**, 1351–1358 (2008)

Benachour, N., Sipahutar, H., Moslemi, S., Gasnier, C., Travert, C., Seralini, G.E.: Time- and dose-dependent effects of Roundup on human embryonic and placental cells. Arch. Environ. Contam. Toxicol. **53**, 126–133 (2007)

Benitez-Leite, S., Macchi, M.L., Acota, M.: Congenital malformation associated with toxic agricultural chemicals. Pediatr. (Asuncion) **34**, 111–121 (2007)

Beuret, C.J., Zirulnik, F., Gimenez, M.F.: Effect of the herbicide glyphosate on liver lipoperoxidation in pregnant rats and their fetuses. Reprod. Toxicol. **19**, 501–504 (2005)

Boutet, I., Tanguy, A., Moraga, D.: Molecular identification and expression of two non-P450 enzymes, monoamine oxidase A and flavin-containing monooxygenase 2, involved in phase I of xenobiotic biotransformation in the Pacific oyster. Biochim. Biophys. Acta **1679**, 29–36 (2004)

Bujacz, B., Wieczorek, P., Krzysko-Lupicka, T., Golab, Z., Lejczak, B., Kavfarski, P.: Organophosphonate utilization by the wild-type strain of *Penicillium notatum*. Appl. Environ. Microbiol. **61**, 2905–2910 (1995)

Carson, D.B., Heitkamp, M.A., Hallas, L.E.: Biodegradation of N-phosphonomethyliminodiacetic acid by microorganisms from industrial activated sludge. Can. J. Microbiol. **43**, 97–101 (1997)

Castle, L.A., Siehl, D.L., Gorton, R., Patten, P.A., Chen, Y.H., Bertain, S., Cho, H.-J., Duck, N., Wong, J., Liu, D., Lassner, M.W.: Discovery and directed evolution of a glyphosate tolerance gene. Science **304**, 1151–1154 (2004)

Cessna, A.J., Darwenet, A.L., Townley-Smith, L., Harker, K.N., Kirkland, K.J.: Residues of glyphosate and its metabolite AMPA in field pea, barley and flax seed following reharvest application. Can. J. Plant Sci. **82**, 485–489 (2002)

Clair, E., Mesnage, R., Travert, C., Seralini, G.-E.: A glyphosate-based herbicide induces necrosis and apoptosis in mature rat testicular cells in vitro, and testosterone decrease at lower levels. Toxicol. in Vitro **26**, 269–279 (2012)

Dalrymple, B.P., Peters, J.M., Vuocolo, T.: Characterisation of genes encoding two novel members of the aldo-keto reductase superfamily. Biochem. Int. **28**, 651–657 (1992)

de Maria, N., Becerril, J.M., Garcia-Plazaola, I., Hernandez, A., de Felipe, M.R., Fernandez-Pascual, M.: New insights on glyphosate mode of action in nodular metabolism: role of shikimate accumulation. J. Agric. Food Chem. **54**, 2621–2628 (2006)

Dick, R.E., Quinn, J.P.: Control of glyphosate uptake and metabolism in *Pseudomonas* sp. 4ASW. FEMS Lett. **134**, 177–182 (1995a)

Dick, R.E., Quinn, J.P.: Glyphosate-degrading isolates from environmental samples: occurrence and pathways of degradation. Appl. Microbiol. Biotechnol. **43**, 545–550 (1995b)

Dill, G.M., Sammons, R.D., Feng, P.C.C., Kohn, F., Kretzmer, K., Mehrsheikh, A., Bleeke, M., Honegger, J.L., Farmer, D., Wright, D., Haupfear, E.A.: Glyphosate: discovery, development, applications and properties. In: Nandula, V.K. (ed.) Glyphosate Resistance in Crops and Weeds: History, Development, and Management, pp. 1–33. Wiley, Hoboken (2010)

Dousset, S., Chauvin, C., Durlet, P., Thevenot, M.: Transfer of hexazinone and glyphosate through undisturbed soil columns in soils under Christmas tree cultivation. Chemosphere **57**, 265–272 (2004)

Duke, S.O.: Glyphosate degradation in glyphosate-resistant and -susceptible crops and weeds. J. Agric. Food Chem. **59**, 5835–5841 (2011)

Duke, S.O., Powles, S.B.: Glyphosate: a once-in-a-century herbicide. Pest Manag. Sci. **64**, 319–325 (2008)

Ermakova, I.T., Kiseleva, N.I., Shushkova, T., Zharikov, M., Zharikov, G.A., Leontievsky, A.A.: Bioremediation of glyphosate-contaminated soils. Appl. Microbiol. Biotechnol. **88**, 585–594 (2010)

Errey, J.C., Blanchard, J.S.: Functional annotation and kinetic characterization of PhnO from *Salmonella enterica*. Biochemistry **45**, 3033–3039 (2006)

Fischer, R.S., Berry, A., Gaines, C.G., Jensen, R.A.: Comparative action of glyphosate as a trigger of energy drain in eubacteria. J. Bacteriol. **168**, 1147–1154 (1986)

Fitzgibbon, J.E., Braymer, H.D.: Cloning of a gene from *Pseudomonas* sp. PG2982 conferring increased glyphosate resistance. Appl. Environ. Microbiol. **56**, 3382–3388 (1990)

Gard, J.K., Feng, P.C.C., Hutton, W.C.: Nuclear magnetic resonance timecourse studies of glyphosate metabolism by microbial isolates. Xenobiotica **27**, 633–644 (1997)

Gasnier, C., Dumont, C., Benachour, N., Clair, E., Chagnon, M.-C., Seralini, G.-E.: Glyphosate-based herbicides are toxic and endocrine disruptors in human cell lines. Toxicology **262**, 184–191 (2009)

Getenga, M., Kengara, F.O.: Mineralization of glyphosate in compost-amended soil under controlled condition. Bull. Environ. Contam. Toxicol. **72**, 266–275 (2004)

Gonzalez-Torralva, F., Rojano-Delgado, A.M., Luque de Castro, M.D., Mülleder, N., de Prado, R.: Two non-target mechanisms are involved in glyphosate-resistant horseweed (*Conyza canadensis* L. Cronq.) biotypes. J. Plant Physiol. **169**, 1673–1679 (2012a)

Gonzalez-Torralva, F., Gil-Humanes, J., Barro, F., Brants, I., de Prado, R.: Target site mutation and reduced translocation are present in a glyphosate-resistant *Lolium multiflorum* Lam. biotype from Spain. Plant Physiol. Biochem. **58**, 16–22 (2012b)

Gougler, J.A., Geiger, D.R.: Uptake and distribution of N-phosphonomethylglycine in sugar beet plants. Plant Physiol. **68**, 668–672 (1981)

Hadi, F., Mousavi, A., Akbari Noghabi, K., Ghaderi Tabar, H., Hatef Salmanian, A.: New bacterial strain of the genus Ochrobactrum with glyphosate-degrading activity. J. Environ. Sci. Health, Part B **48**, 208–213 (2012)

Hallas, L.E., Hahn, E.M., Korndorfer, C.: Characterization of microbial traits associated with glyphosate biodegradation in industrial activated sludge. J. Ind. Microbiol. **3**, 377–385 (1988)

Hallas, L.E., Adams, W.J., Heitkamp, M.A.: Glyphosate degradation by immobilized bacteria: field studies with industrial wastewater effluent. Appl. Environ. Microbiol. **58**, 1215–1219 (1992)

Herrmann, K.M., Weaver, L.M.: The shikimate pathway. Annu. Rev. Plant Physiol. Plant Mol. Biol. **50**, 473–503 (1999)

Hoagland, R.E.: Effects of glyphosate on metabolism of phenolic compounds: VI. Effect of glyphosine and glyphosate metabolites on phenylalanine ammonia-lyase activity, growth, and protein, chlorophyll, and anthocyanin levels in soybean (*Glycine max*) seedlings. Weed Sci. **28**, 393–400 (1980)

Holt, J.S., Powles, S.B., Holtum, J.A.M.: Mechanisms and agronomic aspects of herbicide resistance. Annu. Rev. Plant Physiol. Plant Mol. Biol. **44**, 203–229 (1993)

Imazu, K., Tanaka, S., Kuroda, A., Anbe, Y., Kato, J., Ohtake, H.: Enhanced utilization of phosphonate and phosphite by *Klebsiella aerogenes*. Appl. Environ. Microbiol. **64**, 3754–3758 (1998)

Jacob, G.S., Garbow, J.R., Hallas, L.E., Kimack, N.M., Kishore, G.M.: Metabolism of glyphosate in *Pseudomonas* sp. strain LBr. Appl. Environ. Microbiol. **54**, 2953–2958 (1988)

James, C.: Global review of commercialized transgenic crops: 2002 feature Bt maize. International service for the acquisition of agri-biotech applications. ISAAA Briefs 29. ISAAA, Ithaca (2003)

Jaworski, E.G.: Mode of action of *N*-phosphonomethylglycine: inhibition of aromatic amino acid biosynthesis. J. Agric. Food Chem. **20**, 1195–1198 (1972)

Kafarski, P., Lejczak, B., Forlani, G.: Biodegradation of pesticides containing carbon-to-phosphorus bond. ACS Sym. Ser. **777**, 145–163 (2001)

Kamat, S.S., Williams, H.J., Raushel, F.M.: Intermediates in the transformation of phosphonates to phosphate by bacteria. Nature **480**, 570–573 (2011)

Kertesz, M., Elgorriaga, A., Amrhein, N.: Evidence for two distinct phosphonate-degrading enzymes (C-P lyases) in *Arthrobacter* sp. GLP-1. Biodegradation **2**, 53–59 (1991)

Kertesz, M.A., Cook, A.M., Leisinger, T.: Microbial metabolism of sulfur- and phosphorus-containing xenobiotics. FEMS Microbiol. Rev. **15**, 195–215 (1994)

Kim, A.D., Baker, A.S., Dunaway-Mariano, D., Metcalf, W.W., Wanner, B.L., Martin, B.M.: The 2-aminoethylphosphonate-specific transaminase of the 2-aminoethylphosphonate degradation pathway. J. Bacteriol. **184**, 4134–4140 (2002)

Kishore, G.M., Barry, G.F.: Glyphosate tolerant plants. International patent WO92/00377 (1992)

Kishore, G.M., Jacob, G.S.: Degradation of glyphosate by *Pseudomonas* sp. PG2982 via a sarcosine intermediate. J. Biol. Chem. **262**, 12164–12168 (1987)

Kishore, G.M., Shah, D.M.: Amino acid biosynthesis inhibitors as herbicides. Ann. Rev. Biochem. **57**, 627–663 (1988)

Klimek, M., Lejczak, B., Kafarski, P., Forlani, G.: Metabolism of the phosphonate herbicide glyphosate by a non-nitrate-utilizing strain of Penicillium chrysogenum. Pest Manag. Sci. **57**, 815–812 (2001)

Krzysko-Lupicka, T., Strof, W., Kubs, K., Skorupa, M., Wieczorek, P., Lejczak, B., Kafarski, P.: The ability of soil-borne fungi to degrade

organophosphonate carbon-to-phosphorus bond. Appl. Microbiol. Biotechnol. **48**, 549–552 (1997)

Lajmanovich, R.C., Sandoval, M.T., Peltzer, P.M.: Induction of mortality and malformation in *Scinax nasicus* tadpoles exposed to glyphosate formulations. Bull. Environ. Contam. Toxicol. **70**, 612–618 (2003)

Lamb, D.C., Kelly, D.E., Hanley, S.Z., Mehmood, Z., Kelly, S.Z.: Glyphosate is an inhibitor of plant cytochrome P450: functional expression of *Thlaspi arvensae* cytochrome P45071B1/Reductase fusion protein in *Escherichia coli*. Biochem. Biophys. Res. Comm. **244**, 110–114 (1998)

Lerbs, W., Stock, M., Parthier, B.: Physiological aspects of glyphosate degradation in *Alcaligenes spec*. strain GL. Arch. Microbiol. **153**, 146–150 (1990)

Lévesque, C.A., Rahe, J.E.: Herbicide interactions with fungal root pathogens, with special reference to glyphosate. Annu. Rev. Phytopathol. **30**, 579–602 (1992)

Lioi, M.B., Scarfi, M.R., Santoro, A., Barbieri, R., Zeni, O., Berardino, D.D., Ursini, M.V.: Genotoxicity and oxidative stress induced by pesticide exposure in bovine lymphocyte cultures in vitro. Mutation Res. **403**, 13–20 (1998)

Liu, C.-M., McLean, P.A., Sookdeo, C.C., Cannon, F.C.: Degradation of the herbicide glyphosate by members of the family *Rhizobiaceae*. Appl. Environ. Microbiol. **57**, 1799–1804 (1991)

Low, F.L., Shaw, I.C., Gerrard, J.A.: The effect of *Saccharomyces cerevisiae* on the stability of the herbicide glyphosate during bread leavening. Lett. Appl. Microbiol. **40**, 133–137 (2005)

Lund-Høie, K., Friestad, H.O.: Photodegradation of the herbicide glyphosate in water. Bull. Environ. Contam. Toxicol. **36**, 723–729 (1986)

Malik, J., Barry, G., Kishore, G.: The herbicide glyphosate. Biofactors **2**, 17–25 (1989)

Mann, R.M., Bidwell, J.R.: The toxicity of glyphosate and several glyphosate formulations to four species of southwestern Australian frogs. Arch. Environ. Contam. Toxicol. **36**, 193–199 (1999)

Marc, J., Mulner-Lorillon, O., Boulben, S., Hureau, D., Durand, G., Belle, R.: Pesticide Roundup provokes cell division dysfunction at the level of CDK1/Cyclin B activation. Chem. Res. Toxicol. **15**, 326–331 (2002)

McAuliffe, K.S., Hallas, L.E., Kulpa, C.F.: Glyphosate degradation by *Agrobacterium radiobacter* isolated from activated sludge. J. Ind. Microbiol. **6**, 219–221 (1990)

McGrath, J.W., Chin, J.P., Quinn, J.P.: Organophosphonates revealed: new insights into the microbial metabolism of ancient molecules. Nat. Rev. Microbiol. **11**, 412–419 (2013)

Moore, J.K., Braymer, H.D., Larson, A.D.: Isolation of *Pseudomonas* sp. which utilizes the phosphonate herbicide glyphosate. Appl. Environ. Microbiol. **46**, 316–320 (1983)

Morais, M.C., Zhang, G., Zhang, W., Olsen, D.B., Dunaway-Mariano, D., Allen, K.N.: X-ray crystallographic and site-directed mutagenesis analysis of the mechanism of Schiff-base formation in phosphonoacetaldehyde hydrolase catalysis. J. Biol. Chem. **279**, 9353–9361 (2004)

Nafziger, E.D., Widholm, J.M., Steinrucken, H.C., Killmer, J.L.: Selection and characterization of a carrot cell line tolerant to glyphosate. Plant Physiol. **76**, 571–574 (1984)

Nandula, V.K., Reddy, K.N., Rimando, A.M., Duke, S.O., Poston, D. H.: Glyphosate-resistant and -susceptible soybean (*Glycine max*) and canola (*Brassica napus*) dose response and metabolism relationships with glyphosate. J. Agric. Food Chem. **55**, 3540–3545 (2007)

Obojska, A., Lejczak, B., Kubrak, M.: Degradation of phosphonates by *Streptomyces* isolates. Appl. Microbiol. Biotechnol. **51**, 872–876 (1999)

Obojska, A., Ternan, N.G., Lejczak, B., Kafarski, P., McMullan, G.: Organophosphonate utilization by the thermophile *Geobacillus caldoxylosilyticus* T20. Appl. Environ. Microbiol. **68**, 2081–2084 (2002)

Paganelli, A., Gnazzo, V., Acosta, H., Lopez, S.L., Carrasco, A.E.: Glyphosate-based herbicides produce teratogenic effects on vertebrates by impairing retinoic acid signaling. Chem. Res. Toxicol. **23**, 1586–1595 (2010)

Pedotti, M., Rosini, E., Molla, G., Moschetti, T., Savino, C., Vallone, B., Pollegioni, L.: Glyphosate resistance by engineering the flavoenzyme glycine oxidase. J. Biol. Chem. **284**, 36415–36423 (2009)

Penaloza-Vasquez, A., Mena, G.L., Herrera-Estrella, L., Bauley, A.M.: Cloning and sequencing of the genes involved in glyphosate utilization by *Pseudomonas pseudomallei*. Appl. Environ. Microbiol. **61**, 538–543 (1995)

Pipke, R., Amrhein, N.: Carbon-phosphorus lyase activity in permeabilized cells of *Arthrobacter* sp. GLP-1. FEBS Lett. **236**, 135–138 (1988a)

Pipke, R., Amrhein, N.: Degradation of the phosphonate herbicide glyphosate by *Arthrobacter atrocyaneus* ATCC 13752. Appl. Environ. Microbiol. **54**, 1293–1296 (1988b)

Pipke, R., Amrhein, N.: Isolation and characterization of a mutant of *Arthrobacter* sp. strain GLP-1 which utilizes the herbicide glyphosate as its sole source of phosphorus and nitrogen. Appl. Environ. Microbiol. **54**, 2868–2870 (1988c)

Pipke, R., Schulz, A., Amrhein, N.: Uptake of glyphosate by *Arthrobacter* sp. Appl. Environ. Microbiol. **53**, 974–978 (1987a)

Pipke, R., Amrhein, N., Jacob, G.S., Schaefer, J., Kishore, G.M.: Metabolism of glyphosate in an *Arthrobacter* sp. GLP-1. Eur. J. Biochem. **165**, 267–273 (1987b)

Pizzul, L., del P. Castillo, M., Stenström, J.: Degradation of glyphosate and other pesticides by ligninolytic enzymes. Biodegradation **20**, 751–759 (2009)

Pline, W.A., Wilcut, W., Duke, S.O., Edmisten, K.L., Wells, R.J.: Accumulation of shikimic acid in repose to glyphosate applications in glyphosate-resistant and conventional cotton (*Gossypium hirsutum* L.). J. Agric. Food Chem. **50**, 506–512 (2002)

Pratley, J., Baines, P., Eberbach, P., Incerti, M., Broster, J.: Glyphosate resistance in annual ryegrass. In: Proceedings of the 11th Annual Conference of the Grassland Society of NSW, p. 122. The Grassland Society of NSW Inc., Orange (1996)

Quinn, J.P., Peden, J.M.M., Dick, R.E.: Glyphosate tolerance and utilization by the microflora of soils treated with the herbicide. Appl. Microbiol. Biotechnol. **29**, 511–516 (1988)

Quinn, J.P., Kulakova, A.N., Cooley, N.A., McGrath, J.W.: New ways to break an old bond: the bacterial carbon-phosphorus hydrolases and their role in biogeochemical phosphorus cycling. Environ. Microbiol. **9**, 2392–2400 (2007)

Reddy, K.N., Rimando, A.M., Duke, S.O., Nandula, V.K.: Aminomethylphosphonic acid accumulation in plant species treated with glyphosate. J. Agric. Food Chem. **56**, 2125–2130 (2008)

Richard, S., Moslemi, S., Sipahutar, H., Benachour, N., Seralini, G.-E.: Differential effects of glyphosate and roundup on human placental cells and aromatase. Environ. Health Prospect **113**, 716–720 (2005)

Roy, D.N., Konar, S.K., Banerjee, S., Charles, D.A., Thompson, D.G., Prasad, R.P.: Uptake and persistence of the herbicide glyphosate (Vision®) in fruit of wild blue-berry and raspberry. Can. J. For. Res. **19**, 842–847 (1989)

Rueppel, M.L., Brightwell, B.B., Schaefer, J., Marvel, J.T.: Metabolism and degradation of glyphosate in soil and water. J. Agric. Food Chem. **25**, 517–528 (1977)

Savitz, D.A., Arbuckle, T., Kaczor, D., Curtis, K.M.: Male pesticide exposure and pregnancy outcome. Am. J. Epidemiol. **146**, 1025–1036 (1997)

Selvapandiyan, A., Bhatnagar, R.K.: Isolation of a glyphosate-metabolising *Pseudomonas*: detection, partial purification and

localization of carbon-phosphorus lyase. Appl. Microbiol. Biotechnol. **40**, 876–882 (1994)

Shames, S.L., Wackett, L.P., LaBarge, M.S., Kuczkowski, R.L., Walsh, C.T.: Fragmentative and stereochemical isomerization probes for hemolytic carbon to phosphorus bond scission catalyzed by bacterial carbon–phosphorus lyase. Bioorganic Chem. **15**, 366–373 (1987)

Shaner, D.L., Lindenmeyer, R.B., Ostlie, M.H.: What have the mechanisms of resistance to glyphosate taught us? Pest Manag. Sci. **68**, 3–9 (2011)

Shinabarger, D.L., Braymer, H.D.: Glyphosate catabolism by *Pseudomonas* sp. strain PG2982. J. Bacteriol. **168**, 702–707 (1986)

Shushkova, T., Ermakova, I., Leontievsky, A.: Glyphosate bioavailability in soil. Biodegradation **21**, 403–410 (2010)

Siehl, D.L., Castle, L.A., Gorton, R., Chen, Y.H., Bertain, S., Cho, H.-J., Keenan, R., Liu, D., Lassner, M.W.: Evolution of a microbial acetyltransferase for modification of glyphosate: a novel tolerance strategy. Pest Manag. Sci. **61**, 235–240 (2005)

Siehl, D.L., Castle, L.A., Gorton, R., Keenan, R.J.: The molecular basis of glyphosate resistance by an optimized microbial acetyltransferase. J. Biol. Chem. **282**, 11446–11455 (2007)

Sørensen, S.R., Schultz, A., Jacobsen, O.S., Aamand, J.: Sorption, desorption and mineralization of the herbicides glyphosate and MCPA in samples from two Danish soil and subsurface profiles. Environ. Pollut. **141**, 184–194 (2006)

Sviridov, A. V.: Enzyme systems of organophosphonate catabolism of soil bacteria *Achromobacter* sp. и *Ochrobactrum anthropi* GPK 3. PhD thesis (in Russian). Pushchinoa, 152 (2012a)

Sviridov, A.V., Shushkova, T.V., Zelenkova, N.F., Vinokurova, N.G., Morgunov, I.G., Ermakova, I.T., Leontievsky, A.A.: Distribution of glyphosate and methylphosphonate catabolism systems in soil bacteria *Ochrobactrum anthropi* and *Achromobacter* sp. Appl. Microbiol. Biotechnol. **97**, 787–796 (2012b)

Talbot, H.W., Johnson, L.M., Munnecke, D.M.: Glyphosate utilization by *Pseudomonas* sp. and *Alcaligenes* sp. isolated from environmental sources. Current Microbiol. **10**, 255–260 (1984)

Taylor, M.L., Stanisiewski, E.P., Riordan, S.G., Nemeth, M.A., George, B., Hartnell, G.F.: Comparison of broiler performance when fed diets containing Roundup ready (Event RT73), nontransgenic control, or commercial canola meal. Poult. Sci. **83**, 456–461 (2004)

Torstensson, L.: The Herbicide Glyphosate, pp. 137–149. Butterworths, London (1985)

Veiga, F., Zapata, J.M., Marcos, M.L.F., Alvarez, E.: Dynamics of glyphosate and aminomethylphosphonic acid in a forest soil in Galicia, north-west Spain. Sci. Total Environ. **271**, 135–144 (2001)

Wackett, L.P., Shames, S.L., Venditti, C.P., Walsh, C.T.: Bacterial carbon-phosphorus lyase: products, rates and regulation of phosphonic and phosphinic acid metabolism. J. Bacteriol. **169**, 710–717 (1987)

White, A.K., Metcalf, W.W.: Two C–P lyase operons in *Pseudomonas stutzeri* and their roles in the oxidation of phosphonates, phosphite and hypophosphite. J. Bacteriol. **186**, 4730–4739 (2004)

White, A.K., Metcalf, W.W.: Microbial metabolism of reduced phosphorus compounds. Ann. Rev. Microbiol. **61**, 379–400 (2007)

Williams, G.M., Kroes, R., Munro, I.C.: Safety evaluation and risk assessment of the herbicide Roundup and its active ingredient, glyphosate, for humans. Reg. Toxicol. Pharmacol. **31**, 117–165 (2000)

Xiang, W.-S., Wang, X.-J., Ren, T.-R., Ju, X.-L.: Expression of a wheat cytochrome P450 monooxygenase in yeast and its inhibition by glyphosate. Pest Manag. Sci. **61**, 402–406 (2005)

Zablotowicz, R.M., Reddy, K.N.: Impact of glyphosate of the *Bradyrhizobium japonicum* symbiosis with glyphosate-resistant transgenic soybean: a minireview. J. Environ. Qual. **33**, 825–831 (2004)

Zhang, Q., van der Donk, W.A.: Answers to the carbon-phosphorus lyase conundrum. ChemBioChem **13**, 627–629 (2012)

Bioleaching of Metals as Eco-friendly Technology

Mikhail Vainshtein

Abstract

Bioleaching occupies an important place among the available mining technologies. Its significance is based on the possibility to use an expanding source of low-grade mineral materials, while another profit of this bio-hydrometallurgical process is to reduce the relevant costs for pollution abatement. This chapter presents a review of data from different research articles, patents, and some proprietary experiments. Different directions and possible future trends of this technology are discussed.

Keywords

Metals • Hydrometallurgy • Leaching • Bioleaching • Bacteria • Environment

1 Introduction

Our civilization is based on the use and utilization of metals. Some stages of humane culture got appropriate names, for example, Bronze Age and Iron Age. A classic method of metal recovery, known since antique epochs, is based on melting of metals from ores or other mineral materials at high temperatures. In good accordance with the technology, the process was named as pyrometallurgy ("fire metallurgy"). The latter one is high effective when metals are presented in ores at high concentration levels. In contrast, a low concentration of metals excludes any possibility of their industrial recovery by melting: heating of dumps is too expensive and the minor production can be lost inside of the waste mineral material. As well, the overall cost price includes not only the corresponding ones of raw materials and energy but takes into account incineration of fuels with the following appropriate strategies against smokes, the atmosphere pollution, and following acid rains.

If metal content is low (<1 %), recovery is able only by means of hydrometallurgy ("water metallurgy"). Ores can be treated and partly dissolved with water solutions – in this case, metals are extracted and dissolved as cations usually. This method is known, at least, since the middle of the seventeenth century for copper recovery. In the eighteenth century, industrial recovery of copper was active by exploiting the contact of acid solutions through heaps of oxidized ore. This approach to metal recovery has been discovered by observing coloured water effluents from ore deposits. Till present, it is possible to see, for example, copper contamination from the abandoned mine near Mount Isa (Australia) where local waterways result to be bright blue. Acid mine drainage represents a long-term water pollution impact of mining so that in the coal fields of Appalachia (USA) or any other areas of coal and metal mining, polluted waters turn brown because of dissolved iron.

Nowadays, bioleaching is not a new developing method but a real industrial technology which represents an actual cost-effective alternative for the recovery of valuable metals (uranium, gold, copper, nickel, zinc, etc.) both from ores and solid wastes. A great number of large-scale bioleaching plants are located in developing countries that have significant reserves of minerals and a choice to select technology from the beginning.

M. Vainshtein (✉)
Pushchino State Institute of Natural Sciences, Prospect Nauki 3 and 5, Pushchino, Moscow Region 142290, Russia

Institute of Biochemistry and Physiology of Microorganisms, Russian Academy of Sciences, Prospect Nauki 3 and 5, Pushchino, Moscow Region 142290, Russia
e-mail: vain@ibpm.pushchino.ru

G. Cao and R. Orrù (eds.), *Current Environmental Issues and Challenges*,
DOI 10.1007/978-94-017-8777-2_12,

2 Major Achievements

2.1 Leaching and Bioleaching

There is an ancient international proverb "A drop hollows out a stone". Hydrometallurgy is a process where water and dissolved chemicals are used to extract the interesting element (metal) from the ore. The relevant examples of the reaction are the corrosion effects of acid rains on some historic monuments and constructions. In total, the mineral materials of ores and dumps are mostly insoluble in water. Thus, to recover the desired metals, destruction of the main structure of minerals and/or formation of metal chelates is required. The method of industrial recovery of metals from their solution has been named "leaching of metals".

There are two main groups of metal-bearing ores: sulphide and oxide ores. In the first group, some metals can be dissolved via oxidation of sulphide minerals. Low concentration of metal sulphides in ores does not create problems to bacteria which ignore surrounding mineral dumps. In the second group, metals from oxidized minerals can be brought into solution via chelation of metals or degrading of minerals. The most traditional leaching chemical agent is sulphuric acid.

The hydrometallurgical recovery of metals with water solutions normally includes three stages: (i) leaching with the metal transfer from solid mineral material into solution, (ii) solution treatment and metal concentrating, and (iii) recovery of the target product from the solutions. According to the disposition and localization of the process, leaching is described as (i) "heap leaching", i.e. a specific flow leaches through the heap of dumps; (ii) "tank leaching", mixing in a vat; or (iii) "in situ leaching" – for example, underground uranium leaching from ores of low grade. Leaching is especially applicable for rare and valuable metals.

The first patents on gold recovery with leaching method were claimed in 1887 in Britain and in 1889 in the USA (respectively, McArthur et al. 1887, 1889). Rate of leaching is determined by the composition of the raw mineral material, solution composition, temperature, pH, and redox potential (aeration).

It was found that the application of microbial strains can catalyse some chemical reactions during leaching. Specifically, the process of metal recovery can be hastened with bacteria which oxidize compounds of mineral material or degrade its structure. The first patent on *bioleaching*, i.e. leaching where solutions contained geochemically active bacteria, was claimed in the USA in 1958 (Zimmerley et al. 1958).

Different bacteria have different sources of energy and carbon. Historically, the bioleaching process was based on application of *thionic* (the Greek word "thio" means "sulphur") bacteria or thiobacilli for bioleaching of valuable metals from mineral sulphides because these microorganisms are chemolithotrophic: they receive energy from oxidation of inorganic sulphur compounds. As well, these bacteria can be of autotrophic character, i.e. they do not need organic substrates and build their cells with carbon available from carbon dioxide. The choice of chemolithoautotrophic bacteria permits to lower the operating cost and reach a high level of metal recovery.

Since ores are typically insoluble in water, the leaching processes are located mainly on the surface of sulphide minerals where bacterial cells have direct physical contact with the ore. Sulphides are then oxidized to receive energy – and some bacteria receive energy from iron oxidation too. The typical reactions of *Acidithiobacillus ferrooxidans* can be presented as the following:

$$4\,FeS_2 + 14\,O_2 + 4\,H_2O \rightarrow 4\,FeSO_4 + 4\,H_2SO_4,$$

$$4\,FeSO_4 + O_2 + 2\,H_2SO_4 \rightarrow 2\,Fe_2(SO_4)_3 + 2\,H_2O,$$

which can be combined in the next one:

$$4\,FeS_2 + 15\,O_2 + 2\,H_2O \rightarrow 2\,Fe_2(SO_4)_3 + 2\,H_2SO_4.$$

These and similar reactions of bioleaching of insoluble mineral sulphides result in production of sulphuric acid on spot. Some microbial species can produce also other sulphur compounds (polythionates, etc.) (Schippers et al. 1996):

$$FeS_2 + 6\,Fe(H_2O)_6^{3+} + 3\,H_2O \rightarrow 3\,Fe^{2+} + S_2O_3^{2-} + 6\,Fe(H_2O)_6^{2+} + 6\,H^+,$$

$$2\,Fe^{3+} + 2\,S_2O_3^{2-} \leftrightarrow 2\,FeS_2O_3^{+} \rightarrow 2\,Fe^{2+} + S_4O_6^{2-}.$$

Most of the modern bioleaching technologies are oriented to make use of super-acidophilic bacteria, such as *A. ferrooxidans* and *A. thiooxidans*, which produce sulphuric acid and can live at pH lower than 1.0.

2.2 Innovations in Bioleaching

It has been mentioned above that hydrometallurgy-leaching-bioleaching displays at least two advantages with respect to classic pyrometallurgy: (i) it permits to extract metals at low concentration from dumps, low-grade ores, etc., and (ii) it does not produce atmospheric pollutants.

As all existing industrial approaches, the applied methods can be developed and improved to increase production and to minimize acidification produced with sulphuric acid at the industrial mining sites. Acidification produced by biogenic sulphuric acid can be corrosive active (Fig. 1).

There are two main ways to develop the bioleaching biotechnologies: (i) improving of the process organization (optimizations of aeration, temperature, pretreatment of the raw material, etc.) and (ii) screening and selection of new strains which have more high oxidative activities or more expanded field of pH or which are more simple in culturing, etc.

The basic essence of the bioleaching in whole is described above: it is dissolution of metals from minerals; it is affiliated

Fig. 1 Acidification and destruction of concrete specimens by the strain *Acidithiobacillus* (*Thiobacillus*) *concretivorus* NCIMB 8345 in 6 months. (**a**) The blank specimen of concrete; (**b**) the inoculated specimen covered with biogenic crust of gypsum; (**c**) the inoculated specimen where part of the crust has been removed to show it thickness

with degrading and/or oxidation of the solid materials, despite the kind of metals. However, the applied technological conditions and techniques are changeable for each specific case and vary together with the types of the treated ores and with the used kinds of strains. For example, the usual one-step process of bioleaching suggests the temperature level that is not higher than 40–45 °C (Dew et al. 1999); otherwise, mesophilic bacteria will be inhibited and die. In contrast, thermophilic and super-thermophilic bacteria need higher temperature, for example, 70 °C for *Sulfolobus* spp. (Jordan et al. 2006; Mikkelsen et al. 2007). Application of super-acidophilic bacteria suggests that pH of the treated pulp is not higher than 2. From other hand, there are some bacteria which could oxidize the metal sulphides of the ores under more neural or alkaline conditions (Ostrowski and Sklodowska 1996; Xia et al. 2007). In whole, we can conclude that every new type of mineral material and, as well, every new technological version of treatment need in its turn application of some new strains selected for this specific case.

Innovations in the bioleaching can be determined as development of technologies in four fields, namely, (i) material pretreatment, (ii) optimization of the technological treatment conditions, (iii) addition of supplements to activate aborigenic and/or added industrial microorganisms, and iv) selection of new industrial strains. Some recent patents combined different applications together, for example. supplementation with salt for chemical treatment and with carbon substrate for microbial growth (Young et al. 2003). Some methodical applications are of great significance both for chemical and biological leaching. For example, increase of temperature affects rates of chemical and biochemical reactions; however, bioleaching at high temperature suggests application of other kinds of industrial strains, i.e. thermophilic bacteria which grow better at temperature above 45–50 °C or, at least, thermotolerant ones (resistant to high temperature). By this reason, some patents do not mention Latin names of the industrial leaching strains but identify the concrete temperature interval (Spencer et al. 1995; Kohr et al. 2002; Du Plessis and De Kock 2009).

Other physicochemical agents, which regulate both chemical and biochemical reactions of leaching, are pH and Eh (redox potential) of the industrial media. Usually the pH value is adjusted by addition of mineral acids, and the redox potential is regulated with aeration. Each type of raw mineral material and each kind of industrial microbial strains need its specific optimization of pH and Eh.

As distinct from physicochemical regulations, microbiological methods affect rates of biochemical reactions and permit also to expand field of application and to increase recovery of metals via formation of mutants with new properties. A good example of the mutation is a transformation of the leaching industrial thermophilic strain *Acidianus brierleyi* (formerly *Sulfolobus*) (Meng et al. 2007). In whole, we can conclude that bioleaching is a field of the hydrometallurgy with rapidly evolving technologies.

2.3 Search of New Industrial Leaching Strains

Development of leaching technologies based on new chemical supplements or increase in temperature and aeration suggests additional explicit costs. Thus, looking for new industrial strains could be cheaper. Search, screening, and selection of new leaching strains are the basement of the progressive biogeotechnology. There is a wide taxonomic diversity of potential industrial microbial strains which belong to the systematic *phyla* Bacteria and Archaea. For example, representatives of the following genera (i.e. formal groups identified by their genetic and metabolic features) are able

of oxidizing sulphides for the metal recovery: *Acidithiobacillus*, *Halothiobacillus*, *Thiobacillus*, *Leptospirillum*, *Acidiphilium*, *Sulfobacillus*, *Ferroplasma*, *Sulfolobus*, *Metallosphaera*, and *Acidianus*.

Search of new industrial leaching strains can be illustrated with an example of our proprietary research investigations oriented to the nickel bioleaching. We studied bacterial communities of the moderately acidic waste piles from the Canadian nickel ore dumps ("tails") (Vainshtein et al. 2011a). The structures of bacterial communities were determined by molecular biological techniques by the PCR profiles (eubacterial 16S rRNA gene). Sequencing of the DNA fragments was carried out, and the results were compared with the GenBank gene sequences. Analysis of the 16S rRNA gene sequences revealed predomination of some *Acidithiobacillus* species in the moderately acidic waste piles of sulphide nickel ore (Fig. 2). A number of these discovered bacteria belonged to species or subspecies which have never been obtained as pure culture by any microbiologists. These bacteria belong to the category of microorganisms described with a formal microbiological term "viable but not culturable" (VNC) (Barer 1997) or "unculturable". Meanwhile, molecular biological analyses showed and confirmed presence of the same bacteria in enrichment cultures obtained by inoculating the liquid medium with the waste pile samples (Fig. 3). Viability and activity of these bacteria were confirmed also by capacity to leach nickel from the added sulphide ore into liquid medium by the enriched "VNC" cultures. Thus, (i) it was obtained a new information concerning structure of the bacterial community of sulphide ore waste piles, (ii) the dominant forms were determined, (iii) their leaching activity was confirmed, and (iv) some new thiobacilli strains, which had not been isolated in pure cultures but were active in leaching, were received. Thus, the spectra of industrial bacterial cultures can be expanded with application of new strains, both maintained in the culture collections and, as well, the "VNC" ones. The last strains can be reinoculated with direct passage of the ore.

Historically, the first industrial bacterial strains for leaching belonged to the classic thionic group, namely, thiobacilli. All patents of 90-s include these species: *Thiobacillus* (in present *Acidithiobacillus*) *thiooxidans*, *T.* (*A.*) *ferrooxidans*, and *Leptospirillum ferrooxidans* (Hackl et al. 1991, 1992). However, since the beginning of the current century, the list of industrial species expanded and some patents included representatives of different genera together: *T. ferrooxidans*, *T. thiooxidans*, *L. ferrooxidans*, *T. caldus*, *Acidimicrobium* sp., and *Sulfolobus* sp. (Dew et al. 2001). Appearance of the last ones in the patent text is affiliated with ability of the mentioned strains to oxidize sulphur compounds at high temperature levels. Data on the bioleaching activity at different temperatures is a common object of discussion in research articles which are published during preparing patents (Dew et al. 1999). Recently a special attention was paid to the archaeal genus *Sulfolobus* including *S. metallicus* that was grown at 70 °C and was resistant against toxicity of dissolved heavy metals and floating agents (Jordan et al. 2006; Dopson et al. 2006). Toxicity of the leached heavy metals is not a limiting factor usually because bacteria can be adopted (Astudillo and Acevedoa 2008) or modified with specific plasmid of resistance (Filonov et al. 2009). Thus, formation of modified strains can be also a source of industrial microorganisms beside of direct expanding of the strain collections with new isolates.

2.4 Search of More Eco-friendly Technologies

In reality, industrial bioleaching is a combination of chemical and biological leaching. The most traditional approach suggested supplementing strong mineral acids, usually sulphuric acid. For example, in accordance with the US Patent 4,098,870 (Fekete et al. 1978), sulphuric acid has to be added to dry ore in proportion 4:5. The acid supplementation helps:

- To destroy/dissolve some minerals (e.g. carbonates)
- To stimulate oxidation of sulphide minerals
- To form favourable conditions for strict acidophilers

However, addition of the acid brings some economic negative effect and environmental damages too because:

- The acid is an expensive reagent.
- Its application leads to acidification of the industrial site and requires the following remediation of the environment that means increasing costs for pollution abatement.

Thus, it is possible to see fruitful ways and steps to create new biotechnology that shall be both profitable and more eco-friendly not only in comparison with pyrometallurgy but in competition with some modern biomining processes too. One of the most evident tasks for the green technology is to minimize input of sulphuric acid as an industrial supplement. The same effect of leaching can be reached with a minimum of the technical acid via application of (i) moderate acidophilic or neutrophilic leaching bacteria (Table 1) (Vainshtein et al. 2011b), (ii) leaching bacteria which produce sufficient amounts of sulphuric acid themselves, or, as well, (iii) these two groups combined together (Table 2) (Vainshtein et al. 2011b). Application of the moderate acidophilic bacteria decreased the local pH value in the treated pulp and changed it to threshold valuation that also permits the subsequent activity of the strong acidophilic bacteria without introducing chemical acidifying supplements.

The suggested replacement of strong acidophilic bacteria for moderate acidophilic ones shall decrease addition of sulphuric acid, shall decrease prime cost of nickel, and, as well, shall decrease expenses for the site remediation.

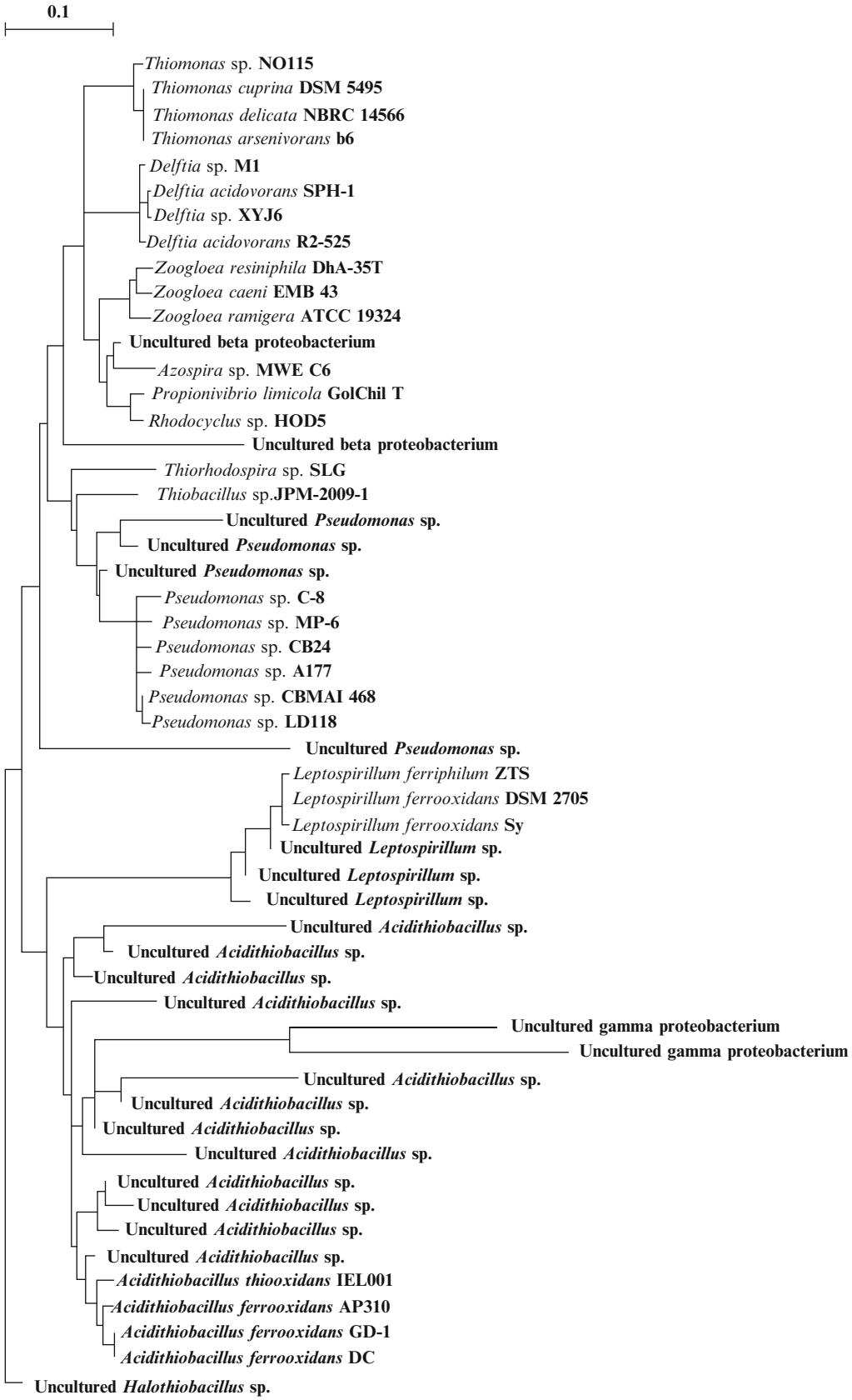

Fig. 2 Diversity of bacterial species in the tails of the Canadian sulphide nickel ores

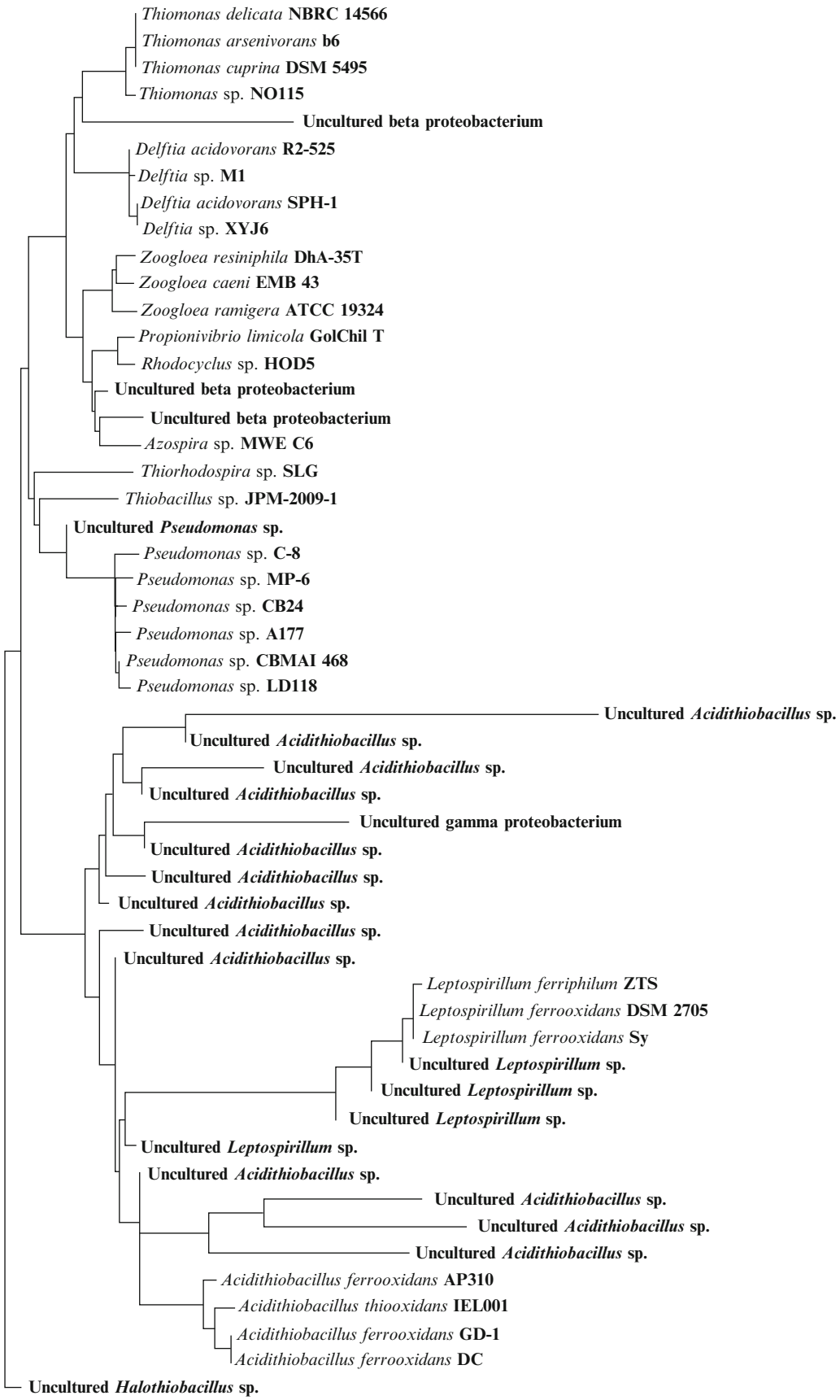

Fig. 3 Diversity of bacterial species in bench-scale leaching flasks inoculated with the Canadian ore tails

Table 1 Bioleaching of the Canadian nickel ores (B and C) by indigenous bacterial communities and by added moderate acidophilic strain *Halothiobacillus halophilus* DSM 6132 (Vainshtein et al. 2011b)

		Ni^{2+}, mg/l, recovered in solution	
Ore	Inoculation with	In 4 days	In 54 days
B	Ore	0.09 ± 0.01	2.07 ± 0.02
B	Tails	0.25 ± 0.03	11.4 ± 0.1
B	*H. halophilus*	0.19 ± 0.02	114 ± 1
C	Ore	1.68 ± 0.02	28.1 ± 0.2
C	Tails	1.43 ± 0.01	27.8 ± 0.2
C	*H. halophilus*	0.36 ± 0.04	131 ± 1

Table 2 Bioleaching of nickel from the Canadian ore C by moderate acidophilic bacteria *H. halophilus* DSM 6132 and by acidophilic *Acidithiobacillus* sp. KZ2 (Vainshtein et al. 2011b)

			Ni^{2+} extracted into solution		
Bacteria	Time, days	pH	mg/l	%	Biomass, mg protein/l
H. halophilus	2	7.5	<9	0.0	42.1 ± 0.1
	4	6	9.6 ± 0.0	0.6	–
	7	5	30.5 ± 0.3	2.0	–
	10	5	25.0 ± 0.2	1.6	59.8 ± 0.2
	15	5	36.2 ± 0.2	2.2	83.3 ± 0.6
Acidithiobacillus sp.	2	5	14.8 ± 0.0	0.9	107.8 ± 0.5
	4	4.5	61.7 ± 0.2	3.9	–
	7	4	146.0 ± 1.0	9.1	155.5 ± 0.5
	10	4	654 ± 5	40.9	146.7 ± 0.8
	15	3	619 ± 5	38.0	672.0 ± 3.0

Table 3 Changes in pH and Ni^{2+} and SO_4^{2-} during bioleaching of the Canadian ore C by population of the aborigenic bacteria combined with the added strain *H. halophilus* DSM 6132

	Methanol, 0.3 %			Format, 0.3 %			Blank		
Time, days	pH	Ni^{2+}, mg/l	SO_4^{2-}, mg/l	pH	Ni^{2+}, mg/l	SO_4^{2-}, mg/l	pH	Ni^{2+}, mg/l	SO_4^{2-}, mg/l
0	7.4	0.0	249 ± 2	7.4	0.0	156 ± 1	7.4	0.0	229 ± 2
8	6.0	0.7 ± 0.1	2,555 ± 18	6.0	1.6 ± 0.0	3,035 ± 20	6.0	0.1 ± 0.0	229 ± 2
14	5.8	1.1 ± 0.0	2,710 ± 18	5.8	3.1 ± 0.4	3,271 ± 25	6.2	0.9 ± 0.1	2,235 ± 14
20	5.8	6.2 ± 0.5	2,862 ± 24	5.4	572 ± 2	3,747 ± 26	6.0	1.8 ± 0.2	3,046 ± 23
34	5.8	12.1 ± 0.1	3,154 ± 24	5.4	1,008 ± 8	5,809 ± 39	5.8	13.8 ± 0.1	3,443 ± 27
43	5.8	31.2 ± 0.2	5,336 ± 31	5.4	1,116 ± 8	7,557 ± 52	5.6	35.4 ± 0.5	3,532 ± 22

Another attempt to increase productivity of bioleaching process with eco-friendly supplements could be reached with bacterial co-use of organic matter. It could be realized (i) by application of the pregrown biomass of heterotrophic bacteria or (ii) by stimulation of lithotrophic bacteria with especial organic supplements. A principal possibility of the last approach was shown two decades ago by J. G. Kuenen with coinvestigators (Pronk et al. 1991). These researchers showed that the chemolithoautotrophic strain *Acidithiobacillus* (former: *Thiobacillus*) *ferrooxidans* ATCC 21834 could be grown with format. The cell densities achieved with supplemented format were higher than cell densities reported for growth of *A. ferrooxidans* on ferrous iron or reduced sulphur compounds only. We found that format can stimulate growth/activity of some other thionic bacteria too (Vainshtein, M., Bykov, A., Repina, A., unpublished data) and used it in experiments on nickel extraction from the Canadian ore C (Table 3).

Stimulation of leaching heterotrophic under the neutral pH conditions seems especially interesting for recovery of metals from oxides, for example, from silicate laterite ores. In the absence of mineral sulphides, the thiobacilli are useless. Nevertheless, there are many other microorganisms which are able to destroy mineral structure, and this destruction is accompanied with some metal extraction (Vatsurina et al. 2008; Kim et al. 2008). The slime-producing

Table 4 Leaching of silicate ore and glassy slugs with slime of bacteria *Paenibacillus mucilaginosus* VKPM B-7519 and *P. edaphicus* VKM B-2665 at different pH (pH_0, initial pH value; pH_1, final one) (Yatskiv 2012)

		Final concentration of extracted metal in solution, mg/l				
	Mineral material	Ni^{2+}	Fe^{2+}	Co^{2+}	pH_0	pH_1
Blank	Glassy slags	0.08	6.82	0.21	9.0	9.0
P. mucilaginosus		0.86	143.45	1.55	9.0	9.5
P. edaphicus		0.78	134.82	0.65	9.0	9.0
Blank	Silicate ore	0.06	15.01	0.24	5.0	5.0
P. mucilaginosus		12.94	98.09	2.82	5.0	8.0
P. edaphicus		1,839	112.37	2.11	5.0	8.0

bacilli *Paenibacillus* could be used as an industrial perspective group of bacteria extracting valuable metals from silicates (Yatskiv 2012). At least, these bacteria can recover metals both from ores and from slugs without acidification of the media (Table 4).

3 Suggested Modern and Future Trends in Bioleaching

1. Classic pyrometallurgy provides civilization with metals in production quantities and on a global scale. However, this industrial approach is accompanied with the global warming, atmosphere pollution, and local environment contamination, and it is economically disadvantageous when the initial metal concentration in raw material is low. In contrast, bioleaching presents some more eco-friendly technology of metal recovery because the microbial leaching neither needs heating nor contaminates atmosphere, and it is effective when metal concentration in mineral raw material is 1 % or even less.
2. Industrial bioleaching needs improvements to increase metal production, to avoid acidification of the treated sites with chemical supplements, and to expand spectra of extracted raw mineral materials. These improvements can be reached with:
   (i) Expanding spectra of the leaching acidophilic chemolithoautotrophic strains; the chosen strains can include the "VNC" ones which are absent in the world culture collections.
   (ii) Application of the neutrophilic or moderate acidophilic strains; it can exclude or minimize volume of the supplemented sulphuric acid.
   (iii) Application of heterotrophic (chemoorganoheterotrophic) strains; these ones can be helpful especially to degrade non-sulphurous mineral materials.

Simplicity of equipment for bacterial leaching and the rapid multiplication of bacteria, especially when returning to the process from the used solutions containing living organisms, provide together an opportunity to reduce the prime cost of the metals production. This approach permits also to increase assortment and selection of sources of raw materials through the use of the poor and lost ores in tailings dumps, dust, slag, etc. At the same time, the use of bacterial leaching reduces contamination of the atmosphere and the environment, and thus it also reduces the relevant costs for pollution abatement. The main new trends of the biotechnology lie in the fact that, in addition to technical improvements in the basic method, developing new directions are based on the search of new organisms with new properties.

Acknowledgements The mentioned and presented own investigations were supported partially by the Russian Federal Special Purpose Programs, State Contracts 14.740.11.0414 (leaching of industrial wastes) and 14.512.11.0098 (microbial corrosion of constructional materials).

References

Astudillo, C., Acevedoa, F.: Adaptation of Sulfolobus metallicus to high pulp densities in the biooxidation of a flotation gold concentrate. Hydrometallurgy **92**(1–2), 11–15 (2008)

Barer, M.R.: Viable but not-culturable and dormant bacteria: time to resolve an oxymoron and a misnomer? J. Med. Microbiol. **46**, 629–631 (1997)

Dew, D.W., van Buuren, C., McEwan, K., Bowker, C.: Bioleaching of base metal sulphide concentrates: a comparison of mesophile and thermophile bacterial cultures. Process Metallurgy **9**(1), 229–238 (1999)

Dew, D.W., Miller, D.M.: Copper, nickel and cobalt recovery. US Patent 6,245,125 (2001)

Dopson, M., Sundkvist, J.-E., Lindström, E.B.: Toxicity of metal extraction and flotation chemicals to Sulfolobus metallicus and chalcopyrite bioleaching. Hydrometallurgy **81**(3–4), 205–213 (2006)

Du Plessis, C.A.R., De Kock, S.H.: Heap bioleaching process. US Patent 7,563,304 (2009)

Fekete, S.O., Wicker, G.R., Duyvesteyn, W.P.C., Shieh, D.F.: Acid leaching of nickeliferous oxide ores with minimized scaling. US Patent 4,098,870 (1978)

Filonov, A., Akhmetov, L., Vatsurina, A., Vainshtein, M.: Isolation of plasmids of nickel resistance from indigenous thiobacteria inhabiting nickel ores. The 3rd Congress of European Microbiologists, Gothenburg, 28 June–2 July 2009

Hackl, R.P., Wright, F.R., Bruynesteyn, A.: Bacteria for oxidizing multimetallic sulphide ores. US Patent 5,089,412 (1992)

Hackl, R.P., Wright, F.R., Bruynesteyn, A.: Chemical/biological process to oxidize multimetallic sulphide ores. US Patent 4,987,081 (1991)

Jordan, H., Sanhueza, A., Gautier, V., Escobar, B., Vargas, T.: Electrochemical study of the catalytic influence of Sulfolobus metallicus in the bioleaching of chalcopyrite at 70 °C. Hydrometallurgy **83**(1–2), 55–62 (2006)

Kim, E., Krylova, L., Adamov, E., Vatsurina, A., Vainshtein, M.: Nickel bio-opening under processing of silicate nickel ores. Abstr. IV Congr. Microbiol., Tashkent, Uzbekistan: 203 (2008)

Kohr, W.J., Shrader, V., Johansson, C.: High temperature heap bioleaching process. US Patent Application 20020194962 (2002)

McArthur, J.C., Forrest, R.W., Forrest, W.: Process obtaining gold and silver from ores. Brit. Patent 14174 (1887)

McArthur, J.C., Forrest, R.W., Forrest, W.: Process obtaining gold and silver from ores. US Patent 403,202 (1889)

Meng, C., Shia, X., Lina, H., Chena, J., Guoa, Y.: UV induced mutations in Acidianus brierleyi growing in a continuous stirred tank reactor generated a strain with improved bioleaching capabilities. Enzym. Microb. Technol. **40**(5), 1136–1140 (2007)

Mikkelsen, D., Kappler, U., Webb, R.I., Rasch, R., McEwan, A.G., Sly, L.I.: Visualization of pyrite leaching by selected thermophilic archaea: nature of microorganism–ore interactions during bioleaching. Hydrometallurgy **88**(1–4), 143–153 (2007)

Ostrowski, M., Sklodowska, A.: Acid leaching in alkaline environment. Bull. Polish Acad. Sci., Biol. Sci. **44**, 279–283 (1996)

Pronk, J.T., Meijer, W.M., Hazeu, W., Van Dijken, J.P., Bos, P., Kuenen, J.G.: Growth of Thiobacillus ferrooxidans on formic acid. Appl. Environ. Microbiol. **57**(7), 2057–2062 (1991)

Schippers, A., Jozsa, P.-G., Sand, W.: Sulphur chemistry in bacterial leaching of pyrite. Appl. Environ. Microbiol. **62**(9), 3424–3431 (1996)

Spencer, P.A., Budden, J.R., Barrett, J., Hughes, M.N., Poole, R.K.: Oxidation of metal sulphides using thermotolerant bacteria. US Patent 5,429,659 (1995)

Vainshtein, M.B., Vatsurina, A.V., Sokolov, S.L., Filonov, A.E., Adamov, E.V., Krylova, L.N.: Composition of microbial communities in sulphide nickel ore waste piles. Microbiology **80** (4), 566–572 (2011a)

Vainshtein, M.B., Abashina, T.N., Bykov, A.G., Ahmetov, L.I., Filonov, A.E., Smolyaninov, V.V.: Technologies of bacterial metal leaching. 3 (in Russian). Zoloto I Tehnologii (Gold and Technologies) **1**(11), 32–34 (2011b)

Vatsurina, A., Kim, E., Krylova, L., Adamov, E., Vainshtein, M.: Bioleaching activity of Tibi grains. Abstr. XII International Congr. Bacteriol. Appl. Microbiol., Istanbul: 88 (2008)

Xia, J., Penga, A., Hea, H., Yanga, Y., Liu, X., Qiu, G.: A new strain Acidithiobacillus albertensis BY-05 for bioleaching of metal sulphides ores. Trans. Nonferrous Metals Soc. China **17**(1), 168–175 (2007)

Yatskiv, A.: Leaching of silicate materials with bacteria of the genus Paenibacillus" (in Russian). M.S. Diss., Pushchino State Institute of Life Sciences (2012)

Young, T.L., Greene, M.G., Rice, D.R., Karlage, K.L., Premeau, S.P.: Methods for leaching of ores. US Patent Application 20030075021 (2003)

Zimmerley, S.R., Wilson, D.G., Prater, J.D.: Cyclic leaching process employing iron oxidizing bacteria. US Patent 2,829,964 (1958)

Biodiversity

Georgia Valaoras

Abstract

This chapter summarises the main issues facing biodiversity loss and focuses on three related topics: the threat of invasive alien species, the decline of agrobiodiversity and the valuation of biodiversity.

Keywords

Biodiversity • Genetic structures • World Conservation Union • Ecosystems • Alien species • Habitat

1 Introduction

Biodiversity, or biological diversity, is a term which encompasses many different aspects of the variety of life forms on the planet. It was coined in the mid-1980s by scientists and conservation biologists and became the conventional way of expressing the richness and variety of species, habitats and functions of the biological foundations which support life on Earth (Wilson 1988a).

There are several definitions of biodiversity, but most of them reflect the number of individual plant and animal species on the planet. Currently, around 2,000 separate species, excluding bacteria, are known and named by scientists, but these represent a small percentage of the total number of species estimated to inhabit Earth. Statements of the total number of species vary from 3 to 30 million, but we are not very certain of the actual range, which could rise as high as 50 or 100 million. The reason for this ignorance is that most of the species which have been identified are the most visible larger invertebrates and higher plants. There are, however, many thousands of species which belong to the lower taxonomic groups such as insects and microorganisms, which have not been studied sufficiently, partially due to the fact that the habitats in which they reside are inaccessible, such as the deep marine environment, or they are rapidly being destroyed before they can be adequately researched, such as the tropical rainforests (Wilson 1988b).

Biodiversity also refers to genetic biodiversity, the variety of genetic structures within populations of a species; functional biodiversity, meaning the full range of trophic levels within an ecosystem; as well as habitat or ecosystem diversity referring to the variety of microclimatic and geomorphological features which influence the conditions of living organisms. The full range of trophic levels should include primary producers; primary, secondary and tertiary consumers; and decomposers, in a well-functioning ecosystem. Ecological or ecosystem diversity refers to the complexity of a particular biological community including niches and trophic levels. Ecosystem characteristics are based on the type of soil or rock substrate, the microclimate, the altitude, the latitude and a host of other factors which combine to create a specific habitat in which plants and animals have evolved to coexist. All these levels of biodiversity are under threat today, by varying degrees of disruption or outright destruction, thus eroding the life-support system on which we all depend (Millenium Ecosystem Assessment 2005).

The Earth has finite resources in terms of air, land and water. This fact alone leads one to the understanding that the ‘natural capital’ which exists to support life is also limited.

G. Valaoras (✉)
General Education Department, Hellenic American University, Massalias 22, Athens 10680, Greece
e-mail: gvalaora@otenet.gr

G. Cao and R. Orrù (eds.), *Current Environmental Issues and Challenges*,
DOI 10.1007/978-94-017-8777-2_13,

Very few attempts have been made to actually estimate the abundance of life that can be supported. One early estimate of the amount of biomass that the Earth can support is that the total is equivalent to $1/10^9$ of the total mass of the planet (Valaoras 1977). This means that as human population expands and the rate of consumption of natural resources increases, many thousands of other life forms are inevitably pushed to extinction to make room for human activities. More recently, the Living Planet Index developed by the World Wide Fund for Nature estimated that our current consumption of natural wealth exceeds the Earth's carrying capacity by 50 % (World Wide Fund for Nature (WWF) 2012).

The term biodiversity was initially developed to highlight the extinction of many species caused directly by anthropogenic pressures. The most important of these is habitat loss, caused by converting natural landscapes into other uses such as agriculture, urbanisation, water management structures (such as dams) and other irreversible interventions which destroy the habitats of many species. Other threats to biodiversity include the increase in invasive alien species which tend to displace native, local and endemic species but also tend to homogenise the genetic make-up of species. Further threats include deforestation, the direct persecution of animals by poaching and poisoning, climate change and chemical contamination of the environment. Human population growth and associated consumption increase pressure on renewable resources such as freshwater systems and forests as well as nonrenewable resources such as fossil fuels and minerals which cause pollution to land and marine environments.

The World Conservation Union (IUCN) compiles data on the threatened and endangered species of the Earth. Using Red Data Book, IUCN publishes lists of these species and provides information gathered from world scientists on the number, location and threats that affect species at risk. From IUCN and other sources, the current state of the Earth's biodiversity can be reported. Extinction rates today are estimated to be up to 100 to 1,000 times the 'natural' rate. Twelve percent of bird species, 23 % of mammals and 25 % of conifers are currently threatened with extinction. Worldwide, 32 % of amphibians are threatened, although this is considered to be an underestimate. Some plants such as the cycads, a group of evergreen palm-like plants, have even higher rates: 52 % of these plants are estimated to be threatened with extinction (Millenium Ecosystem Assessment 2005). In the European Union, the rates are similar to global trends, and estimates report that 21 % of reptiles, 16 % of dragonflies and 7 % of butterflies are threatened with extinction in the 27 member states of the EU (European Commission 2011).

In terms of ecosystems, one-half of the world's wetlands have been lost in the past 100 years, and forests have been diminished by at least 50 %. Twenty percent of known coral reefs have been destroyed, and another 20 % degraded in the last decades (Millenium Ecosystem Assessment 2005). Forests have traditionally been cleared for timber uses such as shipping, metal ore extraction, building and fuelwood. Currently, forests are being logged to make room for expanding agriculture, especially in poorer societies found in the developing world. Developing countries and associated poverty are located in the areas of the globe that have the highest biodiversity. Successive clearing of forests followed by grazing and fires cause erosion and prevent re-growth, a phenomenon common in the Mediterranean area. Soil degradation affects two-thirds of the world's agricultural lands, and three quarters of the world's major marine fish stocks are overfished or are being harvested beyond their sustainable yield.

Most of the world's biodiversity concentrations are near the equator. As biodiversity is not evenly distributed around the globe, scientists and conservationists have made efforts to identify biodiversity 'hotspots' which urgently need to be protected as they contain the highest number of species and the most intact ecosystems which are currently under threat. To qualify as a biodiversity hotspot, a region must meet two strict criteria: it must contain at least 0.5 % of the world's total number or 1,500 species of vascular plants as endemics, and it has to have lost at least 70 % of its original habitat (Mittermeier et al. 2000). Endemic species are those which occur in only one area of the world. Their disappearance is an irreversible loss of biodiversity since they can no longer be reproduced, unless specimens have been saved in seed banks (plants) or in zoological parks (animals). Around the world, 34 areas currently qualify under the definition for a hotspot. These sites support nearly 60 % of the world's plant, bird, mammal, reptile and amphibian species, with a very high share of endemic species. They include the tropical rainforests of Central and South America, Africa and Asia. Coral reefs and coastal wetlands are the second most important habitats with high biodiversity and vulnerability to irreversible changes (Conservation International 2014) (Fig. 1).

Areas such as the Mediterranean have been identified as a biodiversity hotspot, mainly due to a combination of factors such as the confluence of three large land masses: Europe, Asia and Africa; the island and mountain geomorphology which enhances endemism; and the fact that most of the Mediterranean contains relict species dating before the last ice age (11,000 years ago), which wiped out most of the European species. The richness of ecosystems in the Mediterranean is based on the geological and topographical diversity due to the collision of African and Eurasian tectonic plates, which resulted in mountains with altitudes up to 4,500 m.a.s.l., peninsulas and several hundred islands. Diversity and endemism is mainly found on these islands,

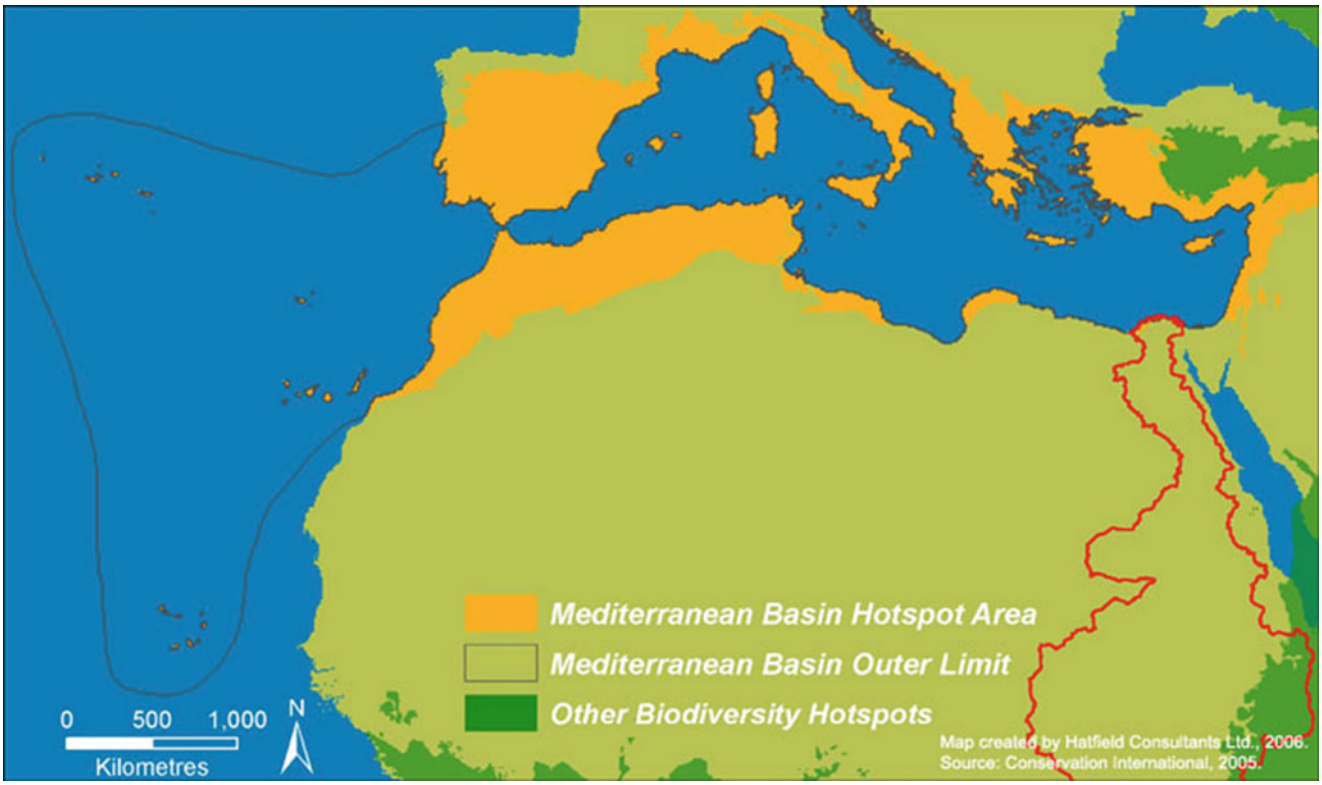

Fig. 1 The Mediterranean Basin hotspots (From Conservation International 2014)

peninsulas, rocky cliffs and mountain peaks It is also a region where migratory pathways of birds of the Western Palearctic cross twice a year, stopping, feeding and resting at Mediterranean coastal wetlands and lakes. Plant diversity is amongst the highest in the world, with 25,000 plant species of which 13,000 are endemic to the area. Of these, 290 are tree species, of which 201 are endemic (Cuttelod et al. 2008).

Yet the Mediterranean is also characterised by a long history of human habitation, dating at least 6,000–7,000 years, when the Neolithic period represented a shift from hunter-gatherers to subsistence agriculture and animal husbandry, as well as to the development of the first urban settlements (Diamond et al. 1997). This history of the Mediterranean ecoregion provides hope that biodiversity does not only flourish in untouched, primaeval forests or coastal wetlands but can also coexist with human habitation, provided that sustainable human practices allow natural cycles to continue. This, for example, is a principle which should govern harvesting of marine species. Allowing for the reproduction and repopulation of marine species by limiting the amount which is taken for human consumption can provide a continuous and sustainable yield which supports life.

Due to the lack of political will to protect biodiversity, and the fact that biodiversity is a complex and abstract topic which does not lend itself to widespread understanding, conservation biologists and scientists began to focus on the term ecosystem services as a means to provide direct evidence of the need to protect natural systems in order to support human life and prosperity. Ecosystem services support a whole range of human activities, such as water purification, soil formation, food and medicine supplies, climate regulation as well as non-material benefits such as recreation and spiritual inspiration.

This chapter will further highlight three aspects of biodiversity which are currently being studied and disseminated to the public and to policy makers, in an ongoing effort to stem the tide of species extinction and destruction of natural habitats which threaten to impoverish current and future generations on the planet. The three topics which will be briefly discussed here are the threat of invasive alien species, the preservation of agrobiodiversity and the valuation of biodiversity or ecosystem services.

2 Invasive Alien Species

Invasive alien species are a major and fast-growing threat to biodiversity. Alien species are also known as non-native, introduced or exotic species. They refer to plants, animals, fungi and microorganisms which have been transported accidentally or intentionally into areas outside their natural

range. Those that become invasive succeed in reproducing and establishing themselves in these new habitats, causing threats to native species. They do this by competing for food with local species, by spreading disease, by modifying habitats and also by direct predation. Another means by which biodiversity is diminished is hybridisation, or the homogenisation of the gene pool by breeding with local species. Native and endemic species are especially vulnerable to interbreeding with introduced species, which causes reduction of their unique genetic make-up and the characteristics which they have evolved to adapt to their habitats. Invasive alien species can also affect human health by the proliferation of infectious diseases spread by travellers or by contact with exotic species of birds, rodents and insects.

The EU 2020 Biodiversity Strategy estimates that costs associated with invasive alien species in Europe can reach up to € 12.5 billion per year, caused by human and animal health-care costs, crop yield losses, fish stock losses, damage to infrastructure, damage to navigation along water channels and damage to protected species. More than 11,000 alien species have already been documented in Europe (European Commission 2011).

According to the Millennium Ecosystem Assessment, invasive alien species are second only to habitat destruction as one of the main drivers for biodiversity loss (Millenium Ecosystem Assessment 2005). Islands and inland lakes are especially vulnerable to invasive species, due to the fact that in enclosed or isolated ecosystems, invasives have few, if any, natural enemies and can reproduce rapidly, adapting to a wide range of environmental conditions and food sources.

On isolated and uninhabited islets of the Mediterranean, the omnivorous ship rat or black rat (*Rattus rattus*) feeds on eggs and chicks, as well as nesting adults of endangered species such as Eleonora's Falcon or Audouin's Gull. First evidence of this species in the Near East is from 1000 B.C., while remains date back to 400 B.C. in the Western Mediterranean, having originated in SE Asia. Another species, the brown rat (*Rattus Norvegicus*), is equally widespread, but arrived later to Europe, most probably between the sixteenth and eighteenth century from NE China. An impressive 53 species of birds have been listed as its prey, of which 27 are seabirds. Rats were most likely transported by ships and easily colonised the lands which were visited. They are formidable swimmers and can reach isolated islets which are inhabited by seabirds, reptiles and other native species. Their prevalence can be attributed to their lack of specialisation, giving them the ability to adapt to any type of environment. Rapid reproduction allows them to make a quick recovery even when their survival is threatened by a temporary lack of food. A pair of rats can produce an amazing 15,000 individual new offspring in a single year (Fric, J., 2013, Knowing the opponent – basics of rat ecology, unpublished report, personal communication with the author).

Trade, tourism and transport of goods around the world accelerate the spread of alien species. Often invasive species are intentionally introduced by humans. Re-stocking of lakes with fish fry can introduce species which soon become invasive, destroying local fish fauna or causing ecological changes in lake water quality.

An example of this is the accidental introduction of the common sunfish (*Lepomis gibbosus*) of North American origin, to the Prespa lakes in Northwestern Greece in the 1990s. It was most likely mixed with other fish fry which are regularly added to the lakes to restock the commercial fisheries. The sunfish population is increasing; there is evidence that it competes with local fish for food resources and feeds on the eggs and fry of local species. There are also accounts of larger fish found starved due to the fact that the sunfish gets stuck in their throat. It is known to entangle the nets of local fishermen and causes a nuisance and unnecessary work (Koutseri et al. 2012).

Ornamental plants are often deliberately introduced by gardeners without realising the potential for taking over native flora and causing their extinction. On the island of Minorca, Spain, an ambitious elimination programme was conducted for the ornamental garden plant *Carpobrotus edulis*, a native of South Africa, which spread thickly throughout the entire island and endangered a number of endemic plants. It is commonly found on many other Mediterranean coasts and islands. On Minorca, eradication was conducted manually over a number of years, and the removal of plant remains off the island was especially difficult, sometimes using helicopters, since seed dispersal from plant remains is a constant threat for invasive regeneration (Jones et al. 2008).

The Mediterranean is unique amongst the world's seas and oceans for the high number of invasive species that have been documented during the last few decades. Starting in 1869 with the opening of the Suez Canal, a large number of species have entered from the Red Sea, and some have succeeded to reproduce and threaten local species; in other words, they have become invasive. Higher salinity and the higher water level of the Red Sea compared to the Mediterranean effectively cause seawater to be dumped into the Mediterranean due to gravity. Thus Red Sea species invaded the Mediterranean biota and not the other way around. Increasing global temperatures, which may be related to climate change, have warmed up the Mediterranean and favour the survival of species which come from warmer seas through the canal. The increase in temperature has been between 2.2 and 2.6 degrees centigrade between 1982 and 2003. The Aswan Dam built on the Nile in the 1960s reduced the freshwater inflow and the nutrient-rich silt to the Eastern Mediterranean, making conditions there even more favourable for invasive species.

It has been reported that up to 63 % of the exotic fishes of the Mediterranean are from Indo-Pacific origin, introduced

through the Suez Canal. Today even exotic, tropical Atlantic species have been entering through the Gibraltar Strait. Between 1996 and 2005 a total of 48 new alien species were recorded, representing 22 % of all registered aliens. Since December 2007, an average of one introduction every 3 weeks has been estimated since the year 2000 (Katsanevakis et al. 2010).

Another method of introduction of alien species is through shipping: ballast water emptied out during washing of ships at ports after travelling from faraway seas, often inadvertently dump marine species which are not native to local waters. However, the unlikely source of the highly toxic marine alga, *Caulerpa taxifolia*, nominated by IUCN as one of the worst 100 invaders of the world, was from dumping aquarium water into the Mediterranean from Jacques Cousteau's Oceanographic Museum of Monaco. This alga, which is native to the Indian Sea, has spread rapidly and has formed dense underwater meadows on the coasts of Croatia, France, Italy, Monaco, Spain and Tunisia. *Caulerpa taxifolia* has been associated with the reduction of commercial fish catches due to the elimination of fish habitats by entangling nets and boat propellers. The weed releases a potent repellent, *Caulerpenyne*, which is toxic to molluscs, sea urchins and herbivorous fish. It renders commercial fish such as the Mediterranean bream (*Sarpa salpa*) inedible because they accumulate toxins in their flesh (Vlachogianni et al. 2013).

These examples demonstrate how invasive alien species have become a growing threat to both water and land habitats of the world. The problem has only recently been studied in a systematic way, and reversing the trend is both costly and complex, as demonstrated by the case of Minorca. Prevention, early detection and stricter controls on trade are some of the actions which have been used to limit invasive species and contain the damage that they cause to local biodiversity. It remains to be seen whether the rate of colonisation of invasive species can be decreased effectively to reverse the loss of biodiversity on a global scale.

3 Agrobiodiversity

Agricultural biodiversity, or agrobiodiversity, is a term that refers to the wide variety of food, medicine, timber, animal breeds and wild plants which have been supporting human life on Earth since the introduction of agriculture 10,000 years ago. The great diversity of local varieties has been developed by farmers over thousands of years, based on local soil and climatic conditions and selection of traits such as size, shape, taste, resilience and breeding patterns. These varieties of plants and domesticated animals, in turn, have been the basis of a varied and locally developed cuisine and culinary methods which have evolved in all areas of the world. Their unique characteristics, such as the use of herbs and spices; methods of harvesting, preparing and cooking; and combinations of ingredients, become typical of local, ethnic and regionally distinct communities.

Another way of expressing agrobiodiversity is that it encompasses all crops, livestock and their wild relatives as well as all interacting species of pollinators, symbionts, pests, parasites, predators and competitors. These wild species are the source of *cultivars* or cultivated varieties which have been the basis of our food supply for centuries. It is estimated that only 3 % of our global food supply still come from the wild and consist mainly of fish species. The remaining 97 % are cultivated by farming or provided by domesticated animals. Plants account for over 80 % of the human diet. Around 30 crops account for 95 % of human food energy needs and just five of them – rice, wheat, maize, millet and sorghum – alone provide 60 %. Yet more than 7,000 plant species have been gathered and cultivated since people first learned to do so many thousands of years ago. And there are as many as 30,000 edible plant species in the world (SAVE eNews 2013).

As they have evolved over many centuries, local varieties are well adapted to local climate, soil and moisture conditions and are therefore an important source of food, medicine and biological products for human use. The importance of maintaining agrobiodiversity is directly related to saving such local varieties. Local varieties are more resistant to diseases, pests, climatic changes, water stress and other environmental pressures. The products are of high quality and nutritive value since they are based on limited chemical inputs such as artificial fertilizers or pesticides.

Local varieties cultivated over centuries are the basis of all commercially traded seeds and plants: the hybrids or patented seeds which are commercialised by agribusinesses and which form the basis for most of the world's food supply are based on locally developed varieties. In many cases of human history, pests or diseases have destroyed an entire crop, causing widespread famines and economic losses: agronomists have had to retrieve the original local varieties of a crop plant in order to propagate seeds and restore their cultivation. A variety of Turkish wheat, collected and stored in a seed gene bank in 1948, was rediscovered in the 1980s, when it was found to carry genes resistant to many types of disease-causing fungi. Plant breeders now use those genes to develop wheat varieties that are resistant to a range of diseases (SAVE eNews 2013).

Included in the broad term of agrobiodiversity are also the wild plants and seeds of regional origin. These have been harvested for thousands of years by local people and provide a wealth of practical uses for humans, including food, medicines, cosmetics and pharmaceuticals as well as fibres for ropes, baskets, clothing, fences and homes. In most of the world's forests, non-timber forest products have been

collected for years, contributing to the conservation of forests and sustainable coexistence with human settlements. These products include honey, cork, mushrooms, pine nuts, pine resin, oils, chestnuts and spices such as rosemary, thyme, oregano, lavender and myrtle (Moussouris and Regato 1999). Biomimicry, the field which derives modern technological inventions such as Velcro by imitating characteristics of wild species, relies entirely on a rich and diverse basis of plants, animals and the intact ecosystems which support them. In biologically diverse agroecosystems, wild plants and seeds of local origin coexist with local flora and fauna, preserving and conserving regional genotypes for future generations.

Maintaining and restoring agrobiodiversity is important to our livelihoods for the sustainable production of food and other useful products. Diverse agroecosystems maintain diversity of genetic resources and also provide support to ecosystem services such as soil microorganisms, pollinators, predators, soil fertility and protection of groundwater.

Crop breeding relies on a relatively narrow range of germplasm for the major crop species. But genetic resources have been lost through the loss of original crop species, chiefly due to the adoption of modern farming practices and through species extinctions. The Food and Agriculture Organization of the United Nations estimates that 75 % of varieties of agrarian crops have been lost and that only 12 plant species and five animal breeds provide three quarters of world food (Food and Agriculture Organisation 1999).

Despite the long history of agriculture on the planet, the last 50 years has seen rapid changes in the ways of growing food and fibre, resulting in an associated loss in agricultural biodiversity. Intensified agricultural systems are based on monocultural cultivation, mechanisation and the widespread use of artificial fertilizers and pesticides. Although industrialised agriculture has greatly increased production per capita and per land area, it has seriously depleted the Earth's agrobiodiversity.

Mechanised agriculture requires the clearing of shrubs and hedgerows, which removes habitats of important species such as birds and insects. This, in turn, eliminates natural pollinators. Pollination is essential for many plant-derived ecosystem services, but pollinators such as bees have been in decline for several years. Since many fruits and vegetables require pollinators, the provision of essential vitamins and minerals in the human diet is highly dependent on the bees, butterflies, hummingbirds, bats and other such species whose functions cannot be replaced by human intervention. About 87 of the 115 leading global food crops depend on pollination, including important cash crops such as cocoa and coffee (The Economics of Ecosystems and Biodiversity (TEEB) 2010). Habitat destruction and pesticide use associated with modern farming methods are the two most frequently cited reasons for their decline (Millenium Ecosystem Assessment 2005).

Local animal breeds include buffalos, cattle, goat, sheep, sheepdogs, pigs, horses and donkeys. They are best adapted to their local conditions and provide milk, meat, cheese, skins, transportation and other essential services to local communities. Unfortunately, many of these local breeds are becoming extinct, chiefly due to interbreeding or abandonment of traditional animal husbandry lifestyles. They are substituted with imported breeds which tend to be kept confined in stables, requiring expensive inputs such as feed, antibiotics and hormones. The trade-off between higher productivity and profit with adaptability, resilience and maintenance of genetic variability has often been lost in favour of the former, without a true assessment of the consequences for the future sustainability of our food supply.

Another threat to agrobiodiversity is the concentration in the trade of commercial seeds in very few large companies. There are only ten companies which own 73 % of the global market in seeds. In the 1930s, there were 150 companies which sell maize (corn) seeds, but today only four sell 68 % of them on the world market. The global commercial seed market in 2009 is estimated at 27,400 million USD. Just 3 companies control more than half (53 %) of the global commercial market for seed. Moreover, there is a convergence of ownership between the agrochemical (pesticide and fertilizer providers) and the seed owners, thus providing a whole 'package' to farmers, increasing their dependency on markets (Synthesis Report and Action Plan 2011).

The tendency is to 'patent' such seeds and to limit the ability of local seeds and varieties to be traded by local farmers and growers. In some cases, hybrid seeds which are patented and owned by companies cannot be re-planted each year, thereby forcing farmers to buy them annually. Increased reliance of farmers on expensive inputs for growing their crops and the reduction of agricultural prices on the world market is marginalising small- and medium-sized farms and forcing them to close. Rural abandonment and relative isolation as well as low expected income, long hours and hard work discourage young persons from following occupations in farming and animal husbandry. As traditional agricultural systems with high nature value and small farms tend to disappear, the decline of agrobiodiversity is very likely to continue.

New seed regulations are currently being drafted in the European Union. If realised, many of the old and rare varieties of fruits, vegetables and grains will disappear from the market. Under the proposed regulations, these diverse varieties and those grown by organic agriculture would be hampered by the bureaucracy of obligatory registrations. The proposed rules would effectively remove the possibility of local varieties to be traded commercially and transferred to places other than the sites where they are grown.

EU regulations also create difficulty in the marketing of local cheeses, meats, fruit preserves, teas and medicinal

products. The increasing burden of hygiene and health and safety rules in the European Union are obstacles to small producers. The small or medium farmer cannot invest in systems to comply with extensive regulations and therefore cannot bring products to the market.

The response of society to these threats to our food supply and to agricultural diversity on which it is based is significant. Several seed banks have been established, the most impressive being the one located inside permafrost 1,300 km from the North Pole, in Spitsbergen, Norway. Twenty million seeds have been stored here to date, equivalent to about two-thirds of the world's most important crop varieties. A wide range of plant seeds, duplicate samples and spare copies are similarly stored in other seed banks worldwide. Gene banks provide a measure of insurance against the loss of seeds and are a refuge in case of a large-scale regional or global crisis.

Another response to threats posed by declines in agrobiodiversity is a growing movement throughout the world by non-governmental organisations in support of food sovereignty: networks are being formed to support the maintenance of local varieties and to lobby to prevent regulations which discourage their free marketing. Many local movements are encouraging the exchange of local varieties and seeds, to save them from disappearance and to provide a reservoir for future cultivation in a sustainable manner (Synthesis Report and Action Plan 2011).

A special emphasis of these civil society movements is placed on local varieties because of their many advantages. As described above, they are well adapted to local conditions; they represent a rich genetic variability. They are based on small-scale extensive farming methods and tend to employ people locally. Organic farming or low impact methods of farming protect the environment, groundwater and soil. There are less waste of water and no use of artificial fertilizers, pesticides or genetically modified organisms. If marketed locally, they reduce the distance between producers and consumers and reduce the costs of consumer prices by limiting middlemen. Finally, reduction in agrochemical use and transport means less dependence on fossil fuels, higher nutritious value and better quality.

As threats to food security increase, as food-related diseases become more prevalent, and as the impacts from the loss of agrobiodiversity become more evident, the voice of civil society movements will become stronger and will provide a convincing counterbalance to the prevailing model of intensive, industrialised agriculture.

4 Valuation of Biodiversity

After 40 years of conservation action, the combined efforts of scientists, policy makers and NGOs have not been sufficient to reverse biodiversity loss. Ecological life-support systems are declining around the world, species continue to become extinct, and human pressures have reached a level that may cause abrupt global environmental disruption (Gomez-Baggethun and Ruiz-Perez 2011).

The focus of biodiversity from an economic perspective derives from four principles:

1. Biodiversity has strong public good characteristics.
2. Biodiversity is a basis for useful ecosystem services.
3. Biodiversity loss is due to anthropogenic influences.
4. Unregulated private markets cannot produce socially optimal biodiversity.

As a response to these circumstances, the concept of ecosystem services evolved as evidence that the basic conditions for human life and well-being are based on biodiversity, from which ecosystem services derive. Furthermore, one can value these ecosystem services in economic terms, in order to provide input into decisions regarding the allocation of funds for the use of land and natural resources.

The need to put a monetary value on biodiversity was explored to provide arguments to policy makers that biodiversity and ecosystem services are worth a significant amount of funds, and that saving this 'natural capital' can prevent spending much more money in the future for the restoration of habitats and species and/or the technological substitution of 'natural capital' (as far as this is possible) to provide equivalent benefits to humanity.

The economic valuation of ecosystem services cannot be used exclusively as a tool in decision-making. Other considerations must also be taken into account, which cannot be quantified or put into a cost-benefit analysis which would determine the outcomes of human intervention in the environment.

'Natural capital' is an economic term which refers to the limited amount of physical and biological resources of the Earth as well as the limited capacity of ecosystems to provide ecosystem services. 'Ecosystem services' are defined as the direct and indirect contributions to human well-being and are linked to biodiversity. They include provisioning services, regulating services, habitat or supporting services and cultural services.

A brief review of each of these follows:

Provisioning services are food; raw materials; freshwater, including surface and groundwater; and medicinal resources. Ecosystems provide conditions for growing food in wild habitats as well as in managed agroecosystems. Materials for construction and fuel are based on ecosystem services, and plants and animals are used as traditional medicines and pharmaceuticals.

Regulating services refer to the regulation of air quality and soil, the purification of water and the provision of flood and disease control. For example, trees provide shade and remove pollutants from the atmosphere. Trees and plants sequester carbon dioxide as they grow, and store it in their

tissues. Living organisms act as buffers for natural hazards such as floods, storms and landslides. Microorganisms in soil and in wetlands decompose human and animal wastes as well as pollutants. Soil erosion and land degradation from desertification are caused by soil degradation and the loss of soil quality. Pollination has already been mentioned as an essential service for major food crops, and the biological control of pests and vector-borne diseases is an example of the effective services of biological diversity.

Habitat or supporting services refer to the support of animal and plant life in well-functioning habitats as well as the provision of genetic diversity or biodiversity.

Cultural and spiritual services depend on a rich natural environment which provides rest and recreation, ecotourism, aesthetic and artistic inspiration and meditation (TEEB 2010). Since ancient times people have protected and revered sacred groves, sites which are often legally protected areas today because they have high biodiversity, having been saved from human interventions.

To varying degrees, the value of these ecosystem services can be quantified to provide input into policy making. The most effective of these attempts to put monetary value on ecosystem services have to do with watershed management, floodplain restoration and reforestation. The cost of creating water treatment systems can be demonstrated to be much higher than preventing contamination of soil and groundwater in the watershed which provides freshwater.

An example of this is the decision by New York City to pay landowners in the Catskill Mountains to improve farm management and reduce runoff of wastes and nutrients into the nearby waterways. This decision, estimated at $1 to $1.5 billion, was a substitute to building expensive water treatment plants, projected to cost $6 to $8 billion with an additional $300 to $500 million in annual operating costs (TEEB 2010).

Similarly, the costs of flood damage are much higher than the cost of rehabilitating littoral spaces and restoring floodplains next to major rivers. Other ecosystem services are more difficult to quantify and are often based on surrogate values such as 'willingness-to-pay', which are highly culturally dependent.

Removing subsidies and providing financial incentives are tools that are used by policy makers to encourage the protection of ecosystem services. Similarly, user charges for access to resources or the imposition of fines for overharvesting has been used to conserve wildlife sustainably in activities such as fishing and hunting.

The 'polluter pays' principle has been implemented for many years to assign liability for environmental damage.

A recent example of this principle is the compensation made by British Petroleum (BP) in response to the Deepwater Horizon accident in the Gulf of Mexico on 20 April 2010. Eleven people died as a result of the accident, and oil leaked into the Gulf of Mexico for weeks following the explosion. Two thousand three hundred and three birds, 18 sea turtles and 10 marine mammals were found dead and visibly oiled. As of 31 December 2012, BP spent more than $14 billion on response activities. $8.2 billion were paid to individuals and local businesses. Government entities received almost $1.4 billion in payments for claims, advances and settlements. A trust fund was set up for $20 billion to which BP contributed $4.9 billion for future litigation settlements, state and local response claims, natural resource damages and related costs (British Petroleum 2014).

On a larger scale, one innovative method applied to international biodiversity hotspots is the 'debt-for-nature' swaps which have successfully reduced foreign debt in developing countries such as Costa Rica, in exchange for setting aside substantial parts of their territory as strictly protected areas. Since 1987, when the first swap occurred between the non-governmental organisation Conservation International and Bolivia, another 36 swaps have been recorded, amounting to over $1 billion.

The Economics of Ecosystems and Biodiversity (TEEB) was an initiative of Germany and the EU in 2007. Its goals were to review the current state of sciences and economics of ecosystems and biodiversity and to recommend a valuation framework and methodology. In addition, it aimed to address the needs of end users: policy makers, local administrators, corporations and ordinary citizens. The goal was to mainstream the economics of ecosystems and biodiversity into policy decisions (TEEB 2010).

Valuation of ecosystems and their services could ensure that the true value of these services is taken into account. A total value framework includes both use and non-use values that individuals and society gain or lose from ecosystem services. The analysis of the TEEB group concluded that a change in the current economic mindset is needed to fully account for ecosystem-based activities. Amongst these are:

- Removing subsidies to intensive agriculture, large-scale commercial fisheries and fossil fuel-based energy
- Paying landowners in return for managing their lands to support ecosystem services
- Appropriate pricing for natural resources, e.g. freshwater
- Applying fees, taxes and fines to discourage activities that degrade biodiversity and ecosystem services
- Establishing market mechanisms to reduce pollution in the most cost-effective manner

Non-financial mechanisms to implement ecosystem-based activities include laws and regulations, individual and community property rights, access rights and restrictions, and the development of environmentally friendly technologies.

Returning to the basic assumptions, a question which arises is whether biodiversity conservation is too expensive for society. To assess the costs of protecting nature, an estimate was made of the costs of managing the Natura 2000 network of Europe, a system of over 11,000 sites with endangered habitats and species protected by the EU Birds Directive and the EU Habitats Directive. The estimates of the costs of the Natura network are € 5.8 billion euro per year for the EU-27 (Gantioler et al. 2000), or about € 11.6 per capita per annum. Global protected area costs are estimated at $45 billion per year, or less than $8 per capita per year. Biodiversity friendly agriculture is estimated to cost $240 billion per year or less than $40 per capita per year. These numbers stand in contrast to harmful environmental subsidies estimated for the OECD countries to be € 340 billion in 1999 alone for agriculture and € 19 billion for fisheries. The costs of not protecting nature have also been estimated. Over the period from 2000 to 2010, welfare losses from losses of ecosystem services are estimated to be around € 50 billion, amounting to a total of € 545 billion in 2010. The cumulative loss of ecosystem services in 2050 is projected to be € 14 trillion. This is equivalent to 7 % of the projected global GDP for 2050. As we lose more ecosystem services, the costs will rise – to ten times the costs of protecting nature in 2010 (TEEB 2010).

Assuming society wants to maintain ecosystem services and reverse the loss of biodiversity on the planet, how can this be financed? There are two basic categories: private and public finance. The public financing tools already mentioned are reducing subsidies, developing payments for ecosystem services, imposing fees and fines and internalising costs through taxes. Private financing can aid in debt-for-nature swaps and institutional investments in biodiversity and environmental protection. Green business initiatives are increasing worldwide and include a variety of market segments, sectors and approaches. These include ecotourism and ecolabelling, as well as developing strategies for 'Reduced Emissions from Deforestation and Forest Degradation (REDD)', which offer incentives for reduced impact logging with biodiversity benefits. (See also the chapter on Green Business in this volume.)

However, the UNEP finance initiative has stated that 'a key barrier to minimising private sector impacts on the environment is the failure of financial markets to adequately value the environmental and social impacts of goods and services. Despite rapid growth in socially responsible investment in financial markets, risk awareness within mainstream investment practices is lacking (UNEP Finance Initiative 2013)'.

Valuation of biodiversity through the quantification of ecosystem services is a step in the right direction to incorporate natural capital into resource and land use decisions on a large scale. However, the mechanisms of valuation are not yet thoroughly developed, sufficiently robust and widely accepted. The economic valuation of biodiversity is still a work in progress, and its impact on reversing the loss of biodiversity and ecosystem services to society has yet to be demonstrated.

References

British Petroleum: Deepwater horizon accident and response. http://www.bp.com/en/global/corporate/gulf-of-mexico-restoration/deepwater-horizon-accident-and-response.html (2014)

Conservation International: Mediterranean basin (Overview). http://www.conservation.org/where/priority_areas/hotspots/europe_central_asia/Mediterranean-Basin/Pages/default.aspx (2014)

Cuttelod, A., Garcia, N., Abdul Malak, D., Temple, H., Katariya, V.: The Mediterranean : A biodiversity hotspot under Threat. In: Hilton-Taylor, N., Stuart, S.N. (eds.) The 2008 Review of the IUCN Red List of Threatened Species. IUCN, Gland (2008)

Diamond, J.: Germs, Guns and Steel. W.W. Norton, New York (1997)

European Commission: The EU 2020 Biodiversity Strategy. ISBN 978-92-79-20762-4 (2011)

Food and Agriculture Organisation: Women: users, preservers, and managers of agrobiodiversity. www.fao.org/Focus/E/Women/Biodiversity.htm (1999)

Gantioler, S., Rayment, M., Bassi, S., Kettunen, M., McConville A., Landgrebe, R., Gerdes, H., ten Brink, P.: Costs and Socio-Economic Benefits associated with the Natura 2000 Network. Final report to the European Commission, DG Environment on Contract ENV. B.2/SER/2008/0038. Institute for European Environmental Policy/GHK/Ecologic, Brussels (2010)

Gomez-Baggethun, E., Ruiz-Perez, M.: Economic valuation and the commodification of ecosystem services. Prog. Phys. Geogr. **35**, 613 (2011)

Jones, W., Silva, J.P. (eds.): European Commission, DG ENV Nature Newsletter. In: Focus, Invasive Alien Species – a threat to Europe's Economy and Biodiversity, vol. 25. European Commission, Brussels (2008)

Katsanevakis, S., Zenetos, A., Belchior, C., Cardoso, A.C.: Invading European Seas: Assessing pathways of introduction of marine aliens. Ocean Coast. Manage. **76**, 64–74 (2013)

Koutseri, I.: Saving fish biodiversity in the Prespa basin. Society for the Protection of Prespa, LIFE09 INF GR 000319 project (2012)

Millenium Ecosystem Assessment: Ecosystems and Human Well-being: Biodiversity Synthesis. World Resources Institute, Washington, DC (2005)

Mittermeier, R.A., Myers, N., Mittermeier, C.G.: Hotspots: earth's biologically richest and most endangered terrestrial ecoregions. In: Conservation International. Conservation International, Arlington. www.conservation.org/. ISBN 978-968-6397-58-1 (2000)

Moussouris, Y., Regato, P.: Food and Agriculture Organisation of the United Nations. WWF Mediterranean Programme, Rome (1999)

Nyéléni Europe 2011: forum for food sovereignty 16th to 21st of August, 2011 in Krems/Austria Nyeleni. Synthesis Report and Action Plan. NYELENI Europe Coordination, Austria (2011)

SAVE eNews: Quarterly e-mail service of the European SAVE Foundation (Safeguard for Agricultural Varieties in Europe). www.safe-foundation.net; www.agrobiodiversity.net (2013)

The Economics of Ecosystems and Biodiversity (TEEB): Mainstreaming the Economics of Nature: A synthesis of the approach, conclusions and recommendations of TEEB. UNEP TEEB OFFICE, Geneva. http://www.teebweb.org/search/Synthesis+report (2010).

UNEP Finance Initiative: http://www.unepfi.org/ (2013)
Valaoras, V.G.: Perivallon kai Ygeia. Evgenidion Ydryma, Athens (1977)
Vlachogianni, T., Vogrin, M., Scoullos, M.: Aliens in the Mediterranean, report by the Mediterranean Information Office for Environment, Culture, and Sustainable Development–MIO-ECSDE (2013)
Wilson, E.O. (ed.): Biodiversity. National Academy Press, Washington, DC (1988a)
Wilson, E.O.: The current state of biological diversity. In: Biodiversity, pp. 3–18. National Academy Press, Washington, DC (1988b)
World Wide Fund for Nature WWF International (WWF): The Living Planet Report 2012. WWF International, Gland (2012)
Zenetos, A., et al.: Alien species in the mediterranean sea by 2010. A contribution to the application of European Union's Marine Strategy Framework Directive, Part I, Spatial Distribution. Mediterr. Marine Sci. **11,** 381–493 (2010)

Passive Sampling Technologies for the Monitoring of Organic and Inorganic Contaminants in Seawater

Marco Schintu, Alessandro Marrucci, and Barbara Marras

Abstract

Until now, water quality monitoring has relied on spot sampling followed by instrumental analytical measurements to determine pollutant concentrations. Despite a number of advantages, this procedure has considerable limitations in terms of temporal and spatial resolution. The passive sampling techniques, which basically consist of concentrating substances on a submerged device for a given period and analysing accumulated substances, should improve the monitoring practices by simplifying analytical issues (lower detection limits, analysis in a simpler matrix) and allowing time integration of the contamination. The performance and potential applications of passive sampling for water quality monitoring in coastal and marine environments are described.

Keywords

Passive sampling • Seawater • SPMDs • POCIS • DGT • Priority substances • Water Framework Directive

Abbreviations

AAS	atomic absorption spectrometry
AMAP	Arctic Monitoring and Assessment Programme
AP	alkylphenols
BFRs	brominated flame retardants
BSI	British Standards Institute
D4	octamethylcyclotetrasiloxane
D5	decamethylcyclopentasiloxane
DBT	dibutyltin
DDT	dichlorodiphenyltrichloroethane
DEHP	di(2-ethylhexyl)phthalate
DL-PCBs	dioxin-like PCBs
EPA	Environmental Protection Agency
EQSD	Environmental Quality Standards Directive
GC	gas chromatography
GMP	Global Monitoring Plan
GPC	gel-permeation chromatography
HBCD	hexabromocyclododecane
HCB	hexachlorobenzene
HCH	hexachlorocyclohexane
HELCOM	Baltic Marine Environment Protection Commission
ICES	International Council for the Exploration of the Sea
ICP-MS	inductively coupled plasma mass spectrometry
IMW	International Mussel Watch
JRC	Joint Research Centre European Commission
LDPE	low-density polyethylene
LOQ	limit of quantification
MBT	monobutyltin
MEDPOL	the Programme for the Assessment and Control of Marine Pollution in the Mediterranean region
MESCO	membrane-enclosed sorptive coating
MS	mass spectrometry
NOOA	National Oceanic Atmospheric Administration
NSTF	North Sea Task Force

M. Schintu (✉) • A. Marrucci • B. Marras
Department of Public Health, Clinical and Molecular Medicine, University of Cagliari, Via G.T. Porcell 4, 09124 Cagliari, Italy
e-mail: schintu@unica.it

G. Cao and R. Orrù (eds.), *Current Environmental Issues and Challenges*,
DOI 10.1007/978-94-017-8777-2_14,

OCPs	organochlorinated pesticides
OSPAR	Oslo and Paris Commission
PAHs	polycyclic aromatic hydrocarbons
PBDE	polybrominated diphenyl ether
PCBs	polychlorinated biphenyls
PCDD	polychlorinated dibenzo-p-dioxin
PCDE	polychlorinated diphenyl ether
PCDF	polychlorinated dibenzofuran
PES	polyethersulfone
PFCs	perfluorinated compounds
PFOA	perfluorooctanoic acid
PFOS	perfluorooctanesulfonic acid
POM	polyoxymethylene
POPs	persistent organic pollutants
PPCPs	pharmaceutical residues and personal care products
PS	passive sampler
QA/QC	quality assurance and quality control
REACH	Registration Evaluation Authorisation Chemicals
SC	Stockholm Convention
SCCPs	short-chain chlorinated paraffins
SPM	suspended particulate matter
SPMD	semipermeable membrane device
SPME	solid-phase microextraction
SR	silicone rubber
TBBPA	tetrabromobisphenol A
TCDD	2,3,7,8-tetrachlorodibenzo-p-dioxin
TWA	time-weighted average
UNEP	United Nation Environment Programme
USGS	United States Geological Survey
WFD	Water Framework Directive
WHO	World Health Organization

1 Introduction

A large number of international organisations and national, international, regional and sometimes global conventions study the monitoring of chemicals in the marine environment (e.g. AMAP, HELCOM, ICES, IMW, MEDPOL, NOOA, OSPAR, UNEP). The output of these programmes has been used to identify areas or regions of concern, estimate the hazards caused by chemicals to man and the marine environment and assess the effectiveness of the measures taken (Roose and Brinkman 2005). As instrumental analytical techniques have improved, greater numbers of substances have been detected in the aquatic environment and have subsequently become of interest to regulatory bodies. Some of this substances are hazardous because they are persistent, liable to accumulate and toxic. Personal care and household product components, pharmaceuticals and detergents are discharged to rivers via domestic waste treatment and industrial plants and then enter the marine environment with harmful effects on marine life and ultimately human health.

Until now, water quality monitoring has relied heavily on spot sampling followed by instrumental analytical measurements to determine pollutant concentrations. Despite a number of advantages, this procedure has considerable limitations in terms of (i) temporal and spatial resolution that may be achieved at reasonable cost and (ii) the information on bioavailability that may be obtained (Allan et al. 2006). Passive sampling represents an innovative monitoring tool for the measurement of bioavailable organic and inorganic contaminants in water and sediment. It is based on the deployment in situ of devices of simple construction capable of accumulating, via diffusion into a receiving phase, contaminants dissolved in water, mimicking an organism exposure. Contaminants are subsequently extracted and their concentration levels measured, allowing the quantification of time-weighted average (TWA) concentrations in water or equilibrium pore-water concentrations in sediment (e.g. Kot et al. 2000; Stuer-Lauridsen 2005; Vrana et al. 2005; Vrana et al. 2010).

This chapter aims to give an overview of the performance and potential applications of passive sampling for water quality monitoring in coastal and marine environments.

2 Passive Samplers

Trace elements and organic contaminants in the marine environment have traditionally been monitored in biota and sediments. Bivalve molluscs represent one of the most frequently used spatial and temporal trend indicators of contaminants in aquatic environments (Melwani et al. 2013). Sediments can act as a source or as sink of contaminants and are investigated almost always for local/regional reasons, due to contamination by industrial and urban waste sources. Moreover, data from sediments may not be representative of pollutant concentrations in the overlying water column and cannot give information on patterns of contamination at the higher levels of the food chain. Water concentrations often yield a clearer picture of the spatial distribution of pollutants than concentrations in biota or sediments, especially on regional and global scales. For instance, water concentrations of POPs in the oceans reflect a dynamic balance of inputs via rivers and atmospheric deposition, rerelease from sediments and removal pathways (Stemmler and Lammel 2013).

Seawater samples pose an analytical challenge because of the extremely low concentrations of dissolved contaminants and the salty aqueous matrix, which is not compatible with most sample introduction systems in the analytical instrumentation. Methods for monitoring concentrations of pollutants involve the use of spot (grab or bottle) sampling.

In some cases, large volumes of water (up to 100 L) have to be passed through an extraction device to concentrate the analytes of interest. Prevention of contamination of the samples during collection, handling and preparation is critical when dealing with samples that contain such low levels of contaminants. Analytical protocols and methodologies generally applied for routine environmental analyses cannot be used directly for seawater samples (Guitart et al. 2012).

The use of passive samplers (PSs) in monitoring the quality of ambient air is well recognised and accepted. There are established standards and official methods for the use of these devices, and these form part of legal frameworks. The application of passive sampling in monitoring water quality is some way behind the situation for air (Greenwood et al. 2007a). Over the past 20 years, several designs of PSs have been developed to monitor a range of pollutant types (nonpolar organic, polar organic, organometals and metals) present in the aquatic environment. PSs can be deployed directly in the environment and concentrate contaminants in situ, preserving chemicals sampled within the receiving phase. This enables improved sensitivity for a greater range of compounds, reducing the need to sample very large volumes of water or even eliminating the use of excessive volumes of toxic extraction solvents. Furthermore, PSs provide a TWA estimation of the dissolved-phase chemicals concentrations at the sampling stations. In contrast, conventional water samples provide a 'snap shot' of conditions at one moment in time that may not be representative of average or real concentrations to which receptors are exposed, especially where concentrations fluctuate (e.g. tidal waters). In these circumstances, costly monitoring campaigns employing either frequent and/or widespread spot sampling are needed.

For organic contaminants, the most commonly used PSs are (i) the nonpolar sampler semipermeable membrane device (SPMD) introduced by Huckins et al. (1990) and (ii) the polar organic chemical integrative sampler (POCIS) (Alvarez et al. 2004). Diffusive Gradients in Thin Films (DGT) (Davison and Zhang 1994) is most widely used passive sampling technique for metals. This section focuses on these three PSs but is applicable to most types of passive sampling devices. Further details on the different available designs of PSs for monitoring contaminants in water can be found elsewhere (e.g. Vrana et al. 2005; Greenwood et al. 2007a).

2.1 Passive Samplers Used for Monitor Organic Chemicals

Contaminants in seawater exhibit a partitioning preference between dissolved and particulate phase according to their physicochemical properties. For organics, several partition coefficients have been experimentally established under certain conditions and are commonly used, in particular the octanol–water coefficient (K_{OW}). The $\log K_{OW}$ defines nonpolar contaminants with values typically ranging from 3 to 8; polar contaminants have values <3. Nonpolar pollutants (e.g. PCBs, PCDDs and PCDFs) adsorb to suspended particulate matter (SPM) and thereby are removed by sedimentation faster from the water column. With increasing polarity of the pollutants, the portion which is freely dissolved in the water phase increases.

Nonpolar samplers consist of an amorphous polymer or resin for which nonpolar analytes have a high affinity. Nonpolar passive sampling devices can have high uptake rates (up to several litres per day) for compounds in the range of $\log K_{OW}$ 3.5–8. SPMDs have been widely used for screening and source identifications of a variety of nonpolar and moderately polar organic contaminants from aqueous and air environments (Esteve-Turrillas et al. 2008). A standard SPMD consists of 91.4 cm long, 2.5 cm wide layflat tube of low-density polyethylene (LDPE) membrane and 1 ml of pure triolein (>99 %). Dissolved, nonionic lipophilic contaminants from water column diffuse across various rate-limiting barriers which consist of the water boundary layer, the biofilm and the hydrophobic LDPE membrane prior to concentrating in the triolein. Theory and modelling of chemical partitioning and uptake from water phase to the SPMD has been described in detail by Huckins et al. (1990).

The SPMD and POCIS are integrative samplers which provide TWA concentrations of chemicals over deployment periods ranging from weeks to months. Field deployment of both samplers is usually accomplished on a stainless steel 'spider' in a canister (Fig. 1). Field blanks are simultaneously exposed to the ambient air (Fig. 2). Canisters are deployed rapidly to minimise exposure to atmospheric contaminants (Fig. 3).

The extracts from the devices need a clean-up step (e.g. using GPC or silica column chromatography) to remove residual triolein and LDPE oligomers prior to instrumental analysis. Contaminants sampled by SPMDs include PHAs, PCBs, PBDEs, OCPs and several 'new generation' pesticides, dioxins and furans. SPMDs have been used by a number of governmental agencies in the USA (USGS, EPA), the UK (Environment Agency for England and Wales) and the Czech Republic.

It was found (Rusina et al. 2007) that single-phase polymeric materials, such as LDPE, Tenax, SPME, POM and SR, show similar affinity for hydrophobic compounds, compared with SPMDs. These single-phase partition-type samplers have high uptake rates, similar to those of the SPMD, for many nonpolar priority pollutants. Other samplers for hydrophobic organic compounds ($\log K_{OW} > 3$) include the nonpolar version of the Chemcatcher (consisting of an n-octanol-soaked C18-3 M Empore™ disk overlaid by a

Fig. 1 SPMD (*left*) and POCIS assembled with proper supports to be inserted into the commercially available stainless steel canister (ExposMeter AB, Tavelsjö, Sweden)

Fig. 2 Field blanks of POCIS and SPMD simultaneously exposed during deployment (Marrucci et al. 2013). The PSs were transported in sealed clean metal cans and refrigerated at 4 °C. All of the canisters were subsequently sealed under an argon atmosphere for transport by boat

thin LDPE membrane) (Greenwood et al. 2007b) and various configurations of the MESCO sampler (Paschke et al. 2006).

Polar samplers consist of an adsorption phase overlaid by a thin polar diffusion-limiting membrane. They have been developed to monitor the more polar pollutants. POCIS (Alvarez et al. 2004) and the polar version of the Chemcatcher (Kingston et al. 2000) are the main samplers designs. POCIS are designed to sample the more water-soluble organic chemicals with $\log K_{OW} < 3$. This includes most pharmaceuticals, illicit drugs, polar pesticides, phosphate flame retardants, surfactants, metabolites and degradation products. However, compounds with $\log K_{OW} > 3$ such as steroidal hormones, fragrances, triclosan and other chemicals related to wastewater effluents are often preferentially sampled by the POCIS. In comparison with many of the samplers for nonpolar pollutants, polar samplers have relatively small sampling surface areas and associated lower sampling rates. The POCIS consists of a receiving phase (sorbent) sandwiched between two PES microporous (usually with 0.1 mm pore size) membranes. The membranes allow water and dissolved chemicals to pass

Fig. 3 Deployment in seawater of SMPDs for the work of Marrucci et al. (2013). The canisters were deployed 2 m below the water surface; they were hung from a buoy with a 1 cm polypropylene rope and were anchored to the bottom with a ballast, which weighed approximately 40 kg. All of the canisters were rolled up in a clean stainless steel wire net to prevent the photodegradation of the PAHs

through to the sorbent where the chemicals are trapped. Larger materials such as sediment and particulate matter are excluded. The sampler is generally compressed together using two stainless steel rings, which expose a surface area of 41–46 cm^2. Two configurations of the POCIS are commercially available. These are referred to as the *pharmaceutical* POCIS and the *pesticide* POCIS. The first contains the widely used Oasis hydrophilic–lipophilic balance (HLB) sorbent, while POCIS *pesticides* contain a triphasic sorbent admixture 80:20 (wt:wt) of hydroxylated polystyrene–divinylbenzene resin (Isolute ENV+) and a carbonaceous sorbent (Ambersorb 1500), dispersed on S-X3 biobeads. This second configuration provided superior uptake and recovery for certain classes of polar compounds including pesticides and hormones (Alvarez et al. 2004). Before chemical analysis or bioassay/toxicity testing, the general processing scheme of deployed POCIS samples includes exterior cleaning, solvent extraction and chemical recovery, enrichment and fractionation. A critical review on calibration and use of POCIS has been published by Harman et al. (2012).

Receiving phases that have been used for the polar Chemcatcher include C18, styrene–divinylbenzene or ion-exchange resins bound into 47 mm 3 M Empore™ disks. As for POCIS, a PES diffusion-limiting membrane is used to cover the receiving phase. The solid-phase absorption toxin tracker (SPATT), an integrative passive sampling for algal toxins, was first proposed by MacKenzie et al. (2004).

2.1.1 Estimating Water Concentrations from SPMD and POCIS Data

A comprehensive analysis of relevant uptake theory and modelling applicable to PSs in water monitoring is covered in detail elsewhere (e.g. Booij et al. 2007). The uptake of chemicals into PSs follows integrative (linear), curvilinear and equilibrium phases during the deployment/exposure period. In the initial stage of the exposure, the flux to the receiving phase is linearly proportional to the analyte's free concentration in the water column. Integrative (linear) uptake is the predominant phase for compounds with $\log K_{OW}$ values ≥ 5.0 and exposure periods of as much as 1 month in SPMDs. During the integrative uptake phase, the ambient chemical concentration (C_W) is determined by

$$C_W = \frac{N}{R_S t} \tag{1}$$

where N is the amount of the chemical accumulated by the sampler (typically ng), t is the exposure time (day) and R_S is the water sampling rate (L day^{-1}) that is measured in laboratory-based calibration studies. The product $R_S t$ can be interpreted as an extracted water volume and thereby forms a conceptual link between passive sampling and batch water sampling. R_S values need to be measured for each analyte of interest, and these values can vary according to water temperature, water turbulence and degree of biofouling on the diffusional surface of a sampler.

For long-exposure times, the flux to the sampler may decrease, because the analyte approaches its equilibrium concentration in the sampler. In the case of nonpolar samplers, the equilibrium conditions are well characterised by partition coefficients. This sampling stage is therefore known as equilibrium sampling. The time to reach equilibrium is a function of the compound's structure and can often be predicted based on K_{OW} values. The generalised equation

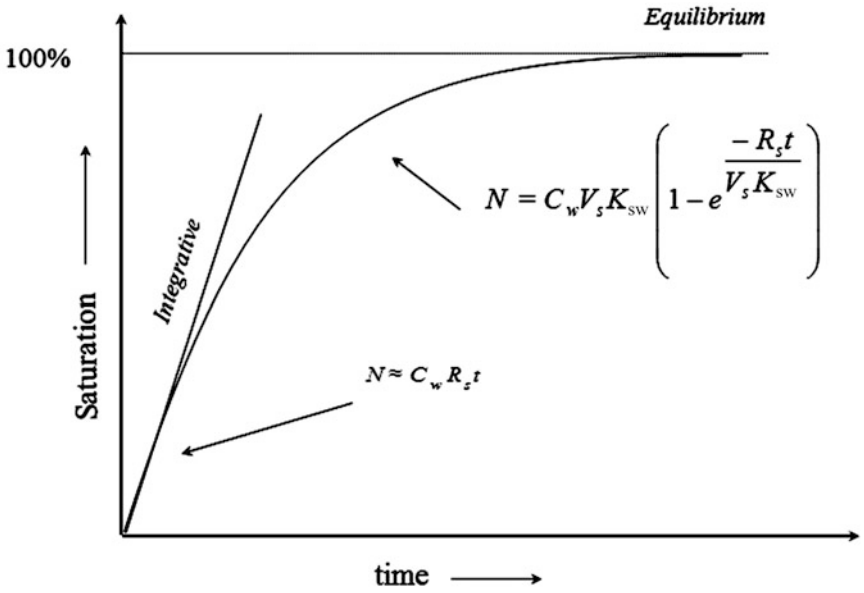

Fig. 4 The uptake kinetics in a partition passive sampler

governing the absorption of a nonpolar analyte with time is given by Huckins et al. (2006):

$$N = C_W V_S K_{SW}\left[1 - \exp\left(\frac{-R_S t}{V_S K_{SW}}\right)\right] \quad (2)$$

where N is the amount of analyte accumulated, C_W is the aqueous concentration V_S is the sampler volume, K_{SW} is the sampler–water partition coefficient (volume/volume units) and t is exposure time (Fig. 4). Accurate K_{SW} values should be available from calibration studies. In situ sampling rates should also be known; however, the R_S of many nonpolar compounds depends on the water flow and water temperature at the exposure site (Fig. 4).

2.1.2 Performance Reference Compounds (PRCs)

With SPMDs sampling rates can be estimated from the dissipation of PRCs. A PRC is an analytically noninterfering compound, such as certain perdeuterated PAHs, which has moderate-to-fairly high SPMD fugacity. The PRCs are introduced into a sampler prior to its deployment, and their loss rates during an exposure are influenced by the same environmental factors that affect the uptake rates of the compounds of interest (Huckins et al. 2002). Thus, PRC loss rate data can be used to adjust SPMD-derived estimates of ambient concentrations to reflect site-specific environmental conditions of an exposure. The PRC method for estimating uptake rates has been shown to account quantitatively for differences in water temperature, flow rates (degree of water turbulence) and biofouling (Booij et al. 2006b). A method for spiking performance PRCs into LDPE and silicone polymers was described by Booij et al. (2002a).

Samplers for polar analytes are almost exclusively used in the linear uptake stage, when the receiving phase can be regarded as an infinite sink. Estimating water concentrations from POCIS data is currently limited by the availability of experimentally derived R_S data. Based on results to date, POCIS remains in the integrative phase of sampling during exposure periods of at least 30 days (Alvarez et al. 2007); therefore, the use of the integrative uptake model (Eq. 1) for the calculation of ambient water concentrations is justified. However, it is critical to determine when a contaminant has achieved equilibrium between the dissolved phase and the sampler. One of the biggest challenges facing the quantitative use of POCIS is the lack of a method to correct for in situ exposure conditions (water flow rates, temperature, pH, etc.) which are known to affect uptake rates. PRCs cannot be used and so quantifying water concentrations with POCIS is very difficult.

2.2 Passive Samplers for Metals

Metallic species are present in a variety of chemical forms, such as free ions, inorganic complexes, organometallic species or large organic complexes. Transport of metals to the coastal systems from rivers and estuaries is dependent on the partitioning of metals between dissolved and particulate phases, which is modified by several factors including specific metal ion, metal concentration, nature of particles, particle concentration, pH, salinity and dissolved oxygen (Stumm and Morgan 1981). The fate between different compartments of the environment and their impact on biological organisms are regulated mainly by their chemical forms. It is well known that the toxicity of metals can be

related to their lability and mobility in the marine environment, which determines their availability to the biota. In this sense, several studies have demonstrated that the uptake is only related to the free-ion activity of the metal or to the labile metal forms rather than to the total concentration.

DGT was developed by Davison and Zhang (1994) at Lancaster University, UK. DGT is a monitoring tool of labile solute species in natural waters. DGT has been used for a wide range of inorganic analytes in natural waters, sediments and soils. Progress in understanding the use of DGT since the introduction of the technique has been reviewed by Davison and Zhang (2012).

The DGT technique is based on a simple device which accumulates solutes on a binding agent after passing through a well-defined diffusion layer of hydrogel. It relies on the establishment of a steady-state concentration gradient from solution to the binding agent (Zhang and Davison 1995).

In between the diffusive gel and the bulk solution, there is a diffusive boundary layer (DBL) of thickness δ in which transport of ions is solely by molecular diffusion.

Heavy metals have usually been measured using a binding layer of Chelex 100, known as the resin-gel layer. It is separated from the solution by an ion-permeable hydrogel of thickness Δg. According to the Fick's first law of diffusion, concentration in bulk solution (C_b) can be calculated from the mass of metal (M) accumulated in the resin layer after a known deployment time (t):

$$C_b = \frac{M\Delta g}{(D\,A\,t)}$$

where D is the diffusion coefficient of metal in the gel, t is deployment time and A is exposure surface area of the membrane ($A = 3.14\ \text{cm}^2$).

The mass of metal accumulated in the resin gel layer (M) can be calculated using equation

$$M = \frac{C_e\left(V_{\text{HNO}_3} + V_{\text{gel}}\right)}{f_e}$$

where C_e is the concentration of metals in the 1 M HNO_3 elution solution (in μg/L), V_{HNO_3} is the volume of HNO_3 added to the resin gel, V_{gel} is the volume of the resin gel, typically 0.15 mL and f_e is the elution factor; f_e has been reported to be between 0.7 and 0.98 for a suite of trace metals (Garmo et al. 2008). Concentration C_e in the acid extract can be measured using an appropriate analytical technique (AAS, ICP-MS). Ferrihydrite, an iron oxide mineral phase, has been used extensively as a DGT binding agent for the measurement of As, W, Se, V, Mo, Sb and dissolved reactive phosphorus. More recently, a DGT technique using a titanium dioxide-based adsorbent (Metsorb-DGT) has also been used to measure a variety of anionic species such as As, Se, P, Al and U (Panther et al. 2013). To measure mercury in river water using DGT, Docekalova and Divis (2005) used an agarose diffusive gel layer, since the normally used polyacrylamide gel type binds Hg covalently via the amide nitrogen groups. A Spheron-Thiol resin as well as Chelex 100 was used.

DGT adsorption does not depend on the concentration of other components in the solution; therefore, individual calibration in other media is unnecessary. However, it is crucial to have accurate estimates of D, and these are normally obtained from published diffusion coefficients or from laboratory experiments. A number of studies have been undertaken to determine diffusion coefficients for the DGT for a range of analytes from metals to radionuclides and in environments from freshwaters to marine systems (e.g. Scally et al. 2006). Garmo et al. (2003) assessed the diffusion coefficients of 55 different elements. The species diffusion rate depends on the pore size of the gel and the type of gel and resin selected. It is also possible to separate the labile organic species from the labile inorganic species when such diffusion parameters are optimised (Li et al. 2005).

The other main PS that has been used for metals is the Chemcatcher. Although this device has been used mainly for nonpolar and polar organics, a particular configuration has been developed for measuring the TWA concentration of metals. It consists of a Teflon watertight sampler body to hold in position a cellulose acetate diffusion-limiting membrane (0.45 μm pore size and thickness of 0.135 mm) that is placed over a 3 M Empore™ chelating disk (47 mm diameter) as the receiving phase (Greenwood et al. 2007b). Metal accumulation in the sampler is similar to that of the DGT and is based on the diffusion of metal species across the cellulose acetate membrane. The diffusion process is influenced by water temperature and by hydrodynamic conditions (water turbulence) at the surface of the sampler. Comparisons between the Chemcatcher and DGT were undertaken by Allan et al. (2008) in a 28-day trial during which fluctuating concentrations of metals (Cd, Cu, Ni, Pb, Zn) were observed in frequent spot samples. This study assessed the potential of these two devices for the regulatory monitoring of trace metals in surface water. It demonstrated that the two sampling devices provided similar information and were able to integrate concentrations reliably even where there were fluctuations in concentration during the deployment period.

2.3 Environmental Factors Affecting Passive Sampling

1. Dissolved organic carbon (DOC) can bind a large proportion of very hydrophobic compounds, significantly decreasing the freely dissolved concentration of many

contaminants (e.g. Dunnivant and Anders 2006). This can bias both calibration measurements and field evaluations.

2. Water turbulence affects the thickness of the unstirred layer of water that forms part of the diffusion-limiting barrier near the sampler surface and consequently also affects the mass transfer of the analytes. The rate-limiting step depends on the type and properties of the membrane, the environmental conditions prevailing during sampling and the properties of the compound being sampled (Alvarez et al. 2004).
3. The growth of bacterial mats, periphyton and even macrofauna can intuitively be expected to have a major impact on uptake rates (Flemming et al. 1997). The thickness and the composition of this biofilm (biofouling) vary significantly depending on the aquatic system. Biofouling can affect the overall resistance to mass transfer by increasing the thickness of the barrier and by blocking any water-filled pores in the diffusion-limiting membranes. Colonising organisms may damage the surface of membranes, if made of a degradable material. Uher et al. (2012) assessed the impact of biofouling on the DGT performance. Depending on the metals of interest, it is possible to limit bias due to biofilms by using an additional polycarbonate membrane.
4. Increasing temperature increases the water solubility of many organic compounds and decreases the partitioning to particles. Inversely, increasing salt concentration can decrease their water solubility. Since integrative PSs measure mainly the dissolved fraction of compounds, water temperature and salinity can have a large effect on the uptake of target analyte.
5. Many organic contaminants such as PAHs, some PBDEs, some pharmaceuticals and others are known to rapidly degrade upon exposure to sunlight. Chemicals sampled by SPMDs are susceptible to photodegradation as the polyethylene membrane of the SPMD is mostly transparent to UVA and UVB. The deployment canisters offer minimal protection from sunlight as the holes which allow water to pass through also allow substantial amounts of light to enter. Komarova et al. (2009) estimated the potential for photodegradation of PAHs accumulated in SPMDs deployed in different deployment devices. Options to help reduce the potential for photodegradation of sampled chemicals include placing the samplers out of direct sunlight or adding some type of sunshield (Fig. 3).

For nonpolar samplers, spiking devices prior to exposure with PRCs can compensate for the effect of environmental variables on the sampler performance (Booij et al. 2006b). Vandalism is the greatest risk to the use of PSs in the field. Careful consideration is necessary to avoid deploying the canisters in easily accessible areas.

2.4 Intercalibration Field Trials

Some of the prerequisites for the adoption of passive monitoring within legal frameworks are clear demonstrations of the performance and validity of the method and the development of recognised national and international standards for the technology (Greenwood et al. 2007a). Because of the difficulty of developing certified PSs and considering the large number of commercially available and homemade PSs, there is a need for new QA/QC approaches, which could involve the use of reference sites, or a need for interlaboratory exercises (Miège et al. 2012).

In 2006, the ICES working groups on Marine Sediments and Marine Chemistry organised a collaborative trial of the use of SR PSs in water and sediment. Passive sampling was carried out between October and December 2006 by 13 laboratories at up to 31 locations through the ICES PSTS project (Smedes et al. 2007). The European locations covered estuarine and coastal environments from Norway to Portugal and west to Ireland and the Faeroe Islands. Also, two locations in Brisbane, Australia, were sampled. The free dissolved or available concentrations of hydrophobic organic contaminants (the primary analytes were PAHs and chlorobiphenyls) in the aqueous phases were estimated from the uptake by SR PSs.

Very few in situ intercomparison exercises on passive sampling have been performed. Allan et al. (2009) tested in situ the performance of different PSs (i.e. nonpolar Chemcatcher, LDPE membranes, MESCO, SR and SPMD) for monitoring of PAHs, PCBs, HCB and p,p–DDE in the river Meuse (the Netherlands).

Another in situ intercomparison exercise on PSs was organised in summer 2010 within the framework of AQUAREF (http://www.aquaref.fr) to measure selected metals, PAHs and pesticides in surface waters (Miège et al. 2012). Various PSs were used and compared at two river sites and one marine lagoon. A total of 24 laboratories participated. The general objective of this study was to assess the potential function and the efficiency of PSs for monitoring priority pollutants in surface and coastal waters in the context of the WFD. The work clearly identified the need for reference or certified PSs to enable laboratories to demonstrate and to improve their mastery during the PSs analytical treatment in laboratory (conservation, extraction, purification steps and analysis). Furthermore, new QA/QC procedures need to be proposed to take into account field deployment. Finally, to extend their use to non-expert laboratories, there is a strong need of more detailed protocols with description of blanks (laboratory and field), PRCs, Rs and equations to use in calculating TWA concentration.

The organisation and initiation of interlaboratory studies is part of the regular activities of the Network of Reference Laboratories for Monitoring of Emerging Environmental Pollutants (NORMAN, http://www.norman-network.net).

An interlaboratory study on passive sampling of emerging pollutants was organised by NORMAN and JRC in 2011.

2.5 Guidance for Practical Use of Samplers

A Publicly Available Specification from BSI (*Determination of priority pollutants in surface water using passive sampling* PAS 61:2006) provides guidance for end users on the field deployment of PSs. This has led to the consideration of the development of an ISO/CEN standard to provide guidance of the field application of PSs, which was approved and published in 2011 (ISO 5667–23:2011. Water quality-Sampling Part 23: *Guidance on passive sampling in surface waters. It specifies procedures for the determination of TWA concentrations and equilibrium concentrations of the free dissolved fraction of organic and organometallic compounds and inorganic substances, including metals, in surface water by passive sampling, followed by analysis*).

USGS provided guidelines for the use of the SPMD and the POCIS in environmental monitoring studies (Alvarez 2010).

DGT Research (Lancaster University, UK) provides technical info for the use of DGTs in water, soils and sediments (http://www.dgtresearch.com).

2.6 Biological Assays of Extracts from Passive Samplers

In most cases, aquatic organisms are not exposed to a single substance but to a mixture of chemicals. It is now commonly acknowledged that data sets acquired in the framework of the environmental monitoring programmes of coastal ecosystems through conventional chemical analyses, while effective in describing types and levels of the most common potential pollutants, are not useful in inferring their biological effects on organisms living in the ambient environment, neither specific ones nor those interactive expected to arise from the actual mixture of contaminants (detected or even undetected). Coupling chemical analysis with biological assays of extracts from PSs can provide representative information on average exposures to sequestered biologically active pollutants. This approach can inform those involved in risk assessment of the toxicological significance of environmental pollutant loads. The extracts of SPMD and POCIS have been combined with an array of toxicity tests to determine the potential effect on biota from exposure to the complex mixtures of chemicals present at a site. Biological tests utilised have been including, but not limited to, Microtox, Mutatox, mixed-function oxygenase (MFO) induction-ethoxyresorufin-*O*-deethylase (EROD) activity, sister chromatid exchange, vitellogenin induction, enzyme-linked immunosorbent assay (ELISA), Daphtoxkit F, Ames mutagenicity tests and yeast oestrogen screen (YES) (e.g. Alvarez et al. 2008; Liscio et al. 2009; Shaw et al. 2010; Bargar et al. 2013). When receiving-phase extracts are to be used with bioassay procedures, samplers must be deployed without any PRCs added in order to avoid the toxic effects of these chemicals, since these would directly influence the results. Emelogu et al. (2013) demonstrate that extracts of SR PS devices deployed in surface water can be applied with minimal preparation to in vitro cell line bioassays. Toxic effects of extracts prepared from both spot water samples and PSs were determined in the pulse-amplitude-modulation (PAM) fluorometry bioassay by Booij et al. (2013).

2.7 Passive Sampling and Concentrations in Biota

Strategies to monitor levels and trends of trace metals and other pollutants, such as PAHs and PCBs, in coastal waters have been widely based on the use of mussels, since Mussel Watch concept was proposed by Goldberg (1975). Bioaccumulation by these test organisms provides biologically relevant data on available concentrations of pollutants in the water, since it may be several orders of magnitude greater than that found in seawater, reducing the frequency of sampling and costs of analysis. However, interpreting biomonitoring data reveals some difficulties related to numerous biotic and abiotic factors that can influence the results. Problems identified with the use of bivalves as bioindicators have included the effects on the uptake of toxicants of biotic factors such as age, size, sex, feeding activity and reproductive state and abiotic factors such as organic carbon levels, temperature, pH, dissolved oxygen levels and hydrology and dissolved metals interactions (Amiard-Triquet and Amiard 1998). Importantly, all biomonitor species have a restricted biogeographical distribution; thus different biomonitor species with different metal accumulation strategies have to be used in different geographical or hydrographical regimes, making comparison of metal levels among regions difficult, if not impossible. There is no single species that could be used across the entire world. Wu et al. (2007) developed a new chemical sampling device (the 'artificial mussel', AM) for monitoring metals in aquatic environments. AM consists of Chelex 100 suspended in artificial seawater within Perspex tubing and enclosed with semipermeable polyacrylamide gel at both ends. AM can overcome problems associated with variable biological attributes and pre-exposure history in the mussel and provides a standardised and representative time-integrated estimate of dissolved metal concentrations in different marine environments.

Similarly, to mussels, passive sampling devices are able to pre-concentrate dissolved trace metals and organic

Fig. 5 Parallel deployment of caged mussels and DGT devices in seawater in Mediterranean sampling sites for the work of Schintu et al. (2008)

compounds furnishing a time-integrated measure of their levels in water. Moreover, it is well accepted that mussels can accumulate contaminants from two ways: the uptake from the environment driven by the concentration of freely dissolved chemical in the water and by feeding on suspended particles to which pollutants are bound (Wang et al. 1996).

SPMDs were originally designed as monitoring tools to mimic the uptake on hydrophobic chemicals by a biological organism. The molecular size-exclusion limit of the LPDE membrane is similar to that of biological membranes while triolein, usually used in triolein-SPMD, constitutes a significant fraction of the lipid pool of most aquatic organisms (Huckins et al. 1990). A number of studies have compared the uptake of nonpolar compounds such as PAHs, PCBs, OCPs and PBDEs by SPMD with that of mussels (e.g. Richardson et al. 2001; Boehm et al. 2005; Booij et al. 2006a; Bourgeault and Gourlay-Francé 2013). Caution was suggested in directly interpreting the results from the two monitoring approaches, as SPMDs measure only the water-soluble fraction of pollutants, while mussels can sequester pollutants present in both the water-soluble and particle-bound fractions. However, both methods can give complementary information on bioavailability of POPs to higher marine organisms and transfer of these chemicals through the food chain. Uptakes of PAHs and PCBs by *Mytilus edulis* and by large SR sheet samplers were compared by Smedes (2007). Eight sampling stations in the Wadden Sea, Eastern Scheldt and Western Scheldt off the coast of the Netherlands were used. Overall, there was a close relationship between concentrations found in mussels and those derived from the PS exposures. Seasonal variations in pollutant profiles and concentrations were reflected in both monitoring methods.

DGTs have been postulated as a possible chemical alternative to bivalves for providing integrated records of trace metal pollution (Davison and Zhang 1994). Only labile species such as ionic forms and easily dissociable complexes are taken up by DGT, and these species are more likely to represent a bioavailable fraction than the total metal. Schintu et al. (2008) evaluated the usefulness of a combination of biomonitoring and DGT techniques for a better understanding of trace metal availability in coastal waters. Mussel (*Mytilus galloprovincialis*) and DGT devices were deployed together for three 1-month periods between 2004 and 2006 in sampling sites along the coast of Sardinia (Italy) (Fig. 5). The levels of Cd, Cu, Ni and Pb were then measured in both mussel tissues and seawater. They concluded that it is difficult to compare the results of the two methods since mussels respond to contaminants from water and food, while DGT only estimate concentrations of dissolved phase metals. However, the combination of biomonitors with DGTs allowed for the obtainment of different and complementary types of information about metal bioavailability in the study areas.

As far as regards comparison between DGTs and biomonitors other than mussels, Stark et al. (2006) monitored the water quality of a marine embayment during the remediation of an abandoned waste disposal site at Casey Station, East Antarctica. They used in parallel DGT devices and the amphipod *Paramoera walkeri* as a biomonitor. DGT samplers were less sensitive than amphipods in detecting differences in metal concentrations between sites, indicating that metals bound to suspended particulates were a potentially significant source of contamination. They pointed out that it is difficult to interpret the DGT results with respect to biota which may uptake contaminants from different routes of exposure. Schintu et al. (2010) determined the levels of Cd, Cu, Pb and Zn in the commonest species of green, red and brown algae collected from five coastal sites in SE Sardinia (Western Mediterranean, Italy), an area with a long history of mining and smelting. DGT devices were used to measure dissolved metals in seawater (Fig. 6).

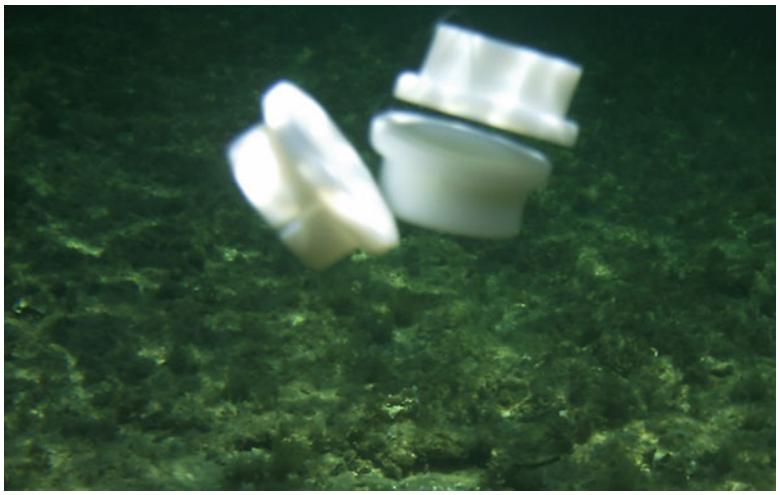

Fig. 6 DGT devices exposed in seawater for the work of Schintu et al. (2010)

A significant relationship was found between the content of Pb in *Padina pavonica* and DGT-labile Pb in seawater, suggesting that gross elemental concentrations of nonessential metals such as Pb in algal tissues are apparently controlled by the abundance of dissolved metal species in the ambient seawater. Clarisse et al. (2012) conducted a series of laboratory experiments to test the ability of the DGT technique to mimic monomethylmercury (MMHg) accumulation by a clam (*Macoma balthica*). The study demonstrates that DGT results reasonably predict MMHg uptake by clams from the aqueous phase and provide the basis for application of the DGT device as a surrogate for sentinel organism for monitoring bioavailable MMHg.

According to several authors (e.g. Smedes 2007; Vrana et al. 2010) monitoring by PSs has some advantages over the use of living organisms:

1. Initial concentration of contaminants is negligible. In contrast to PSs, biomonitors often contain background contamination levels.
2. The uptake process is simple compared with that found in organisms.
3. PSs can be applied in almost any environment with a broad range of water quality properties and even in sites where biomonitoring organisms may not survive (e.g. temperature, pH, pollution and salinity).

3 Field Applications of Passive Sampling in Seawater

3.1 Compounds Detectable by PSs in the Coastal and Marine Environment

POPs are a group of chemicals that have been intentionally or inadvertently (by-products) produced and introduced into the environment. The initial list of the Stockholm Convention (SC) on POPs included 12 substances (pesticides, industrial chemicals or by-products of industrial processes and combustion): aldrin, chlordane, DDT, dieldrin, endrin, heptachlor, HCB, mirex, toxaphene, PCBs, PCDDs and PCDFs. In 2011, endosulfan became the 22nd POP. With the addition of PFOS, chlordecone, HCH isomers and endosulfan to the SC, the chemicals addressed no longer comprise solely hydrophobic organics. Because of their high fat solubility, such chemicals tend to accumulate in animals, especially in species at the top of the food chain. Exposure to POPs can lead to serious health effects including certain cancers, birth defects and dysfunctional immune and reproductive systems (Xu et al. 2013). Due to their stability and long-range transport properties, POPs are now ubiquitous around the world. Although the production and use of many hazardous chemicals has been banned, ongoing commitments to exposure reductions are constrained by uncertainties in the extent and hence impact of both past and new control measures and concentration changes due to global climate change (Klanova et al. 2011). Almost all POPs targeted by the SC are nonpolar or weakly polar, hydrophobic substances, making them ideal targets (e.g. PCBs) for sampling in water using nonpolar PS devices (Muir and Lohmann 2013). Lohmann and Muir (2010) have proposed the establishment of a global passive sampling network (AQUA-GAPS) to monitor the concentrations of POPs. The same type of PSs can be used across all waters of the world, ensuring statistically comparable results. PSs are inexpensive, can be deployed by personnel with minimal training and are sufficiently well characterised to obtain meaningful results. This would be a natural extension of the successful global atmospheric monitoring scheme (GAPS) currently in operation for this class of pollutants. Low-cost polymeric samplers, such as polyethylene (PE) samplers, rather than SPMDs, have being targeted for this purpose.

SPMDs have been widely used for the monitoring of PAHs in seawater. Low levels of oil and hence PAHs are naturally present in the marine environment, although levels have increased significantly following human extraction and use of oil and gas. A distinction is generally made between petrogenic (oil-derived) and pyrogenic (combustion-derived) PAHs. Although petrogenic PAHs appear to be bioavailable to a large extent, pyrogenic PAHs are often associated with soot particles and less available for uptake into organisms. Most studies have focused on high-molecular-weight, carcinogenic PAHs such as benzo[a]pyrene. There is a need for increased research efforts to clarify biological effects of two- and three-ring PAHs, PAH mixtures and adaptation processes in marine ecosystem (Hylland 2006).

The ubiquitous worldwide occurrence of endocrine disrupting compounds (EDCs) and chemicals of emerging concern (CECs) and their effects on marine biota and public health have become a major concern. EDCs include pesticides; fungicides; insecticides; industrial chemicals like PCBs, PAHs, APs, phthalates and dioxins; chemicals in personal care products and synthetic oestrogens in pharmaceutical products such as oral contraceptives and hormone replacement therapy drugs (EEA 2011). A previous assessment on EDCs was primarily on POPs, but this has broadened more recently to include less persistent and less bioaccumulative organic chemicals (e.g. bisphenol A) and metals (WHO/UNEP 2013). EDCs in the aquatic environment have received significant attention because they can interfere with the normal function of exposed organisms, resulting in a variety of reproductive abnormalities, including feminisation and decreased fertility. In coastal areas, higher concentrations of the EDCs are usually found close to sewage-impacted areas, harbours and river estuaries (Arditsoglou and Voutsa 2008). Improvements in analytical methods, primarily the introduction of more sensitive and specific MS techniques, have increased awareness of the presence of CECs from many sources at trace levels (low ng L^{-1}) in the aquatic environment. CECs are chemicals which do not fall under standard monitoring and regulatory programmes but may be candidates for future regulation once more is known about their toxicity and health effects. The most discussed emerging CECs in the aquatic environment include complex mixtures of new generation pesticides, antifouling compounds, brominated flame retardants (BFRs), pharmaceutical and personal care products (PPCPs) and EDCs. Ibrahim et al. (2013) provided an in situ calibration of POCIS for the sampling of polar pesticides and metabolites in surface water. Perfluorinated compounds (PFCs) have been used in stain repellents and in polishes, paints and coatings. Some fluorosurfactants, such as PFOS and PFOA, have caught the most attention because of their persistence, toxicity and widespread occurrence in the blood of general populations and wildlife.

The use of POCIS for the detection of pharmaceuticals in the environment has been well documented (e.g. Alvarez et al. 2004). Togola and Budzinski (2007) determined the sampling rates (expressed as effective volumes of water extracted daily) of POCIS devices for 14 pharmaceuticals in several conditions of temperature, salinity and analyte concentration.

Applications of PSs for some important groups of emerging substances are discussed by Vrana et al. 2010. In comparison with devices designed for sampling hydrophobic organic compounds, sampling of most CECs is more complex. In addition to the common factors (temperature, water turbulence and biofouling), other factors (e.g. salinity, DOC level, pH and the presence of complex mixtures of contaminants) may significantly affect the performance of samplers of emerging substances and these need to be evaluated. Several of the polar organic compounds have a number of functional groups that can be ionised or neutral at various pH. If neutral and ionised forms of the target analytes are taken up differently, the pH could affect their R_s in the polar PS. A detailed overview of type of PS designs available for monitoring emerging polar organic compounds and their classes of target compounds and field of applications was given by Söderström et al. (2009). Developments in water analysis for emerging environmental contaminants have been reviewed by Richardson and Ternes (2011).

To date, at least 75 different brominated flame retardants (BFRs) have been commercially produced (Alaee et al. 2003). So far, studies have been primarily focused on three groups: PBDEs and PBBs, HBCDs and TBBP-A. These BFRs are persistent, bioaccumulative and toxic chemicals (Johnson-Restrepo and Kannan 2009). As PBDEs are extremely hydrophobic compounds (logK_{OW} values 4–10), they are dissolved in the aqueous phase at extremely low (sub-ppb) concentrations. PBDEs are being phased out; however, an increasing number of alternative flame retardant chemicals (e.g. phosphorus flame retardants) have been introduced to comply with consumer product fire safety standards. TBBP-A and HBCD are now the most commonly used BFRs (OSPAR 2010; Covaci et al. 2011).

Concern over pharmaceutical residues and personal care products (PPCPs) entering the aquatic environment has been growing since the mid-1990s. Effluent from wastewater treatment works is the most common source of pharmaceutical residues in streams and rivers. A complex mixture of chemicals is often present comprising the parent molecule, associated metabolites and environmental degradation products. Some of these substances may subsequently enter the food chain. The biological effects of pharmaceutical residues on aquatic organisms have been reviewed by Christen et al. (2010). An important class of emerging pollutants is the organosiloxanes. Over the last 30 years,

organosiloxanes (silicones) have been extensively used in a number of consumer products, such as antiperspirants, and hair and skin care items. The most commonly used organosiloxane is D5 although others such as D4 and their linear versions can be used in products (Horii and Kannan 2008). Several organosiloxanes are under assessment for classification as very persistent and very bioaccumulative in the environment.

Heavy metals are natural and, depending on the hydrogeological situation, their background concentration may vary from place to place. Since heavy metals are major contaminants of coastal and estuarine waters due to anthropogenic inputs, pollution may add to this background concentration, creating harmful concentrations in the environment. Heavy metals have become a global problem due to their toxicity, wide sources, non-biodegradable properties and accumulative behaviours. Cadmium, Pb, Ni and Hg are considered priority pollutants. Mercury, particularly its organic form (MeHg), is a global contaminant and toxicant of major concern for humans and wildlife (Chen 2012). Some trace metals (e.g. Cu, Zn) are considered to be essential; however, all of them can exert toxicity if present over a threshold concentration. Most organometallic compounds are more toxic than inorganic complexes or free forms of the parent metal. Due to their bioaccumulation potential and toxicity, organometallic substances are considered as CECs. Organotins are pollutants that are used as biocides in antifouling paints. In many countries the use of TBT for this application has been banned. At present, triorganotin compounds, such as TBT, have been demonstrated to produce imposex and mammalian reproductive and metabolic toxicity. For most mammals, triorganotin exposure predominantly occurs through the ingestion, and this compound can cross the placenta (Graceli et al. 2013).

3.2 SPMDs and POCIS

The offshore oil and gas industry contributes a significant input of organic pollutants to the marine environment through routine operational discharge. By far the most significant discharge is that of produced water which is largely a mixture of water injected to aid oil extraction and formation water which is naturally occurring within the reservoir (OSPAR 2010). The composition of produced water is both complex and highly variable. Of the organic constituents, PAHs and APs are often regarded to contribute significantly to the environmental risk. The oil companies operating in the Norwegian sector of the North Sea have conducted field studies since the mid-1990s in order to monitor produced water discharges to the ocean. SPMDs and blue mussels (*Mytilus edulis*) have been used to determine the bioavailable fraction of PAHs from oil field-produced water (Røe Utvik and Johnsen 1999). The profile was mainly dominated by alkylated naphthalenes, phenanthrenes and dibenzothiophenes. Harman et al. (2011) deployed SPMDs and POCIS in waters surrounding oil platforms. Passive sampling devices were coupled with in vitro bioassay techniques, testing the suitability of biological approaches and chemical-based PSs to determine exposure to PAHs and APs.

Roach et al. (2009) deployed SPMDs samplers along a 25 km transect around Sydney Harbour, Australia. The devices were able to measure sub-picograms per litre of a range of PCDDs, PCDFs and PCBs in the water column over a 28-day trial. Even at these trace levels, statistically significant spatial and temporal trends in concentration of the pollutants within the harbour system were identifiable. In the Mediterranean aqueous concentrations of individual PAHs and PCBs were first determined by Marrucci et al. (2013) in coastal waters of marine protected areas in Sardinia (Western Mediterranean Sea). The use of SPMDs enabled the detection of very low concentrations of dissolved PAHs and PCBs (pg L^{-1}) in seawater. The results reveal significant differences between the two sampling areas in terms of the concentration of individual PAHs, providing information on pollution sources in relatively pristine environments. The PCBs were generally at levels below the detection limits of the method utilised. Karacik et al. (2013) estimated water concentrations of PAHs, PCBs and OCPs from SPMDs and from sediment pollutant concentrations. SPMDs were deployed in the Istanbul Strait and Marmara Sea.

There is an increasing use of SPMDs, LPDE and PDMS tubing or SR strip samplers in large-scale monitoring programmes to map the distribution of hydrophobic pollutants. For over a year, beginning in May 2010, Allan et al. (2012) used LDPE passive sampling devices to assess bioavailable PAHs in the coastal waters of the Gulf of Mexico impacted by the Deepwater Horizon oil spill. Monteyne et al. (2013) used SR PSs in a 4-year monitoring performed to study the freely dissolved water concentrations of PAHs and PCBs in three coastal harbours and at an offshore station in the North Sea. Schintu et al. (Schintu M, Marrucci A, Marras B, 2014, unpublished raw data), since May 2012, have been using SPMDs, POCIS and DGT devices to monitor the bioavailable concentrations of PAHs, PCBs and EDCs and trace metals in the area of the sinking of the Costa Concordia cruise ship (Isola del Giglio, Italy) (Fig. 7).

Numerous studies have been dedicated to the passive sampling of hydrophobic OCPs and organophosphate pesticides, while the sampling of moderately hydrophobic to hydrophobic ($2 < \log K_{OW} > 5$) pesticides is poorly documented (Assoumani et al. 2013). Most of the studies have been carried out in streams or rivers located in

Fig. 7 Since May 2012, passive sampling monitoring of contaminants released by the wreck of the Costa Concordia cruise ship (Isola del Giglio, Italy) has been carried out by the authors of this chapter

agricultural watersheds. According to NORMAN, there is an increased demand for environmental monitoring of pesticides because some of them either already identified as priority substances under the WFD (e.g. atrazine, simazine, diuron, isoproturon) or may become priority substances in the future or are relevant as river basin-specific pollutants in selected European regions (Vrana et al. 2010). In seawater polar sampler devices have been used in ecologically sensitive environments, such as offshore reefs, to gain a better understanding of the effects of the run-off pollutants, such as polar herbicides, on delicate marine species. Solvent extracts of the receiving phase have been used in short-term bioassay tests to gain a further understanding of the toxicological relevance of individual fractions of the complex mixture of sequestered pollutants (Shaw et al. 2009). Different PSs (polar and nonpolar) proved to be sensitive tools capable of capturing a broad array of applied pesticides relevant to the Great Barrier Reef environment and provide the basis of a holistic approach to monitoring of land-sourced pesticides (Shaw et al. 2010). Booij et al. (2002b) used SPMDs for sampling and in situ pre-concentration of PBDEs from water at several sampling stations in the Scheldt estuary and North Sea along the Dutch coast. The application of integrative sampling enabled the back-calculation of extremely low concentrations (in range 0.1–5 pg L^{-1}) of PBDE congeners in water from SPMD-accumulated amounts.

Trends in monitoring PPCPs in the aquatic environment by use of passive sampling devices were discussed by Mills et al. (2007). Although passive sampling devices are showing promise in aquatic environmental monitoring of PPCPs, there is a need for demonstration of their robustness and reliability. This will necessitate a combination of laboratory calibration and field studies for this range of emerging pollutants. Interlaboratory method validations may be necessary for their acceptance as a regulatory tool. Arditsoglou and Voutsa (2008) examined the two types of POCIS (pharmaceutical and pesticide) for their sampling efficiency of selected EDCs (4-alkyl-phenols, their ethoxylate oligomers, bisphenol A, selected estrogens and synthetic steroids). The sampling efficiency of POCISs under various field conditions was assessed after their deployment in different aquatic environments, including coastal waters. Bueno et al. (2009) used POCIS to monitor a wide range of veterinary medicines (including antibiotics, pesticides and biocides) over a period of a year in a fish farm placed on the Mediterranean Sea. Munaron et al. (2012) investigated 21 pharmaceuticals, 6 APs and 27 hydrophilic pesticides and biocides using POCIS during a large-scale study of contamination of French Mediterranean coastal waters. The results showed that the French Mediterranean coastal waters were contaminated with a large range of emerging contaminants, detected at low concentrations during the summer season. Alvarez et al. (2013) used POCIS, PE and SPME samplers to sample a diverse set of chemicals in the coastal waters of San Francisco Bay and the Southern California Bight. Seventy-one chemicals (including fragrances, phosphate flame retardants, pharmaceuticals, PAHs, PCBs, PBDEs and pesticides) were measured in at least 50 % of the sites. The chemical profile from the San Francisco Bay sites was distinct from profiles from the sites in the Southern California Bight. This distinction was not due to a single compound or class, but by the relative abundances/concentrations of the chemicals. Comparing the PS devices to mussel (*Mytilus* spp.) tissues, a positive correlation exists for the 25 and 26 chemicals in common for the PE and SPME samplers, respectively.

Kaserzon et al. (2013) using a sampler based on a modified POCIS with a weak anion exchange sorbent as a

receiving phase in order to estimate trace level concentrations of PFCs in Sydney Harbour, Australia. The results were in good agreement with concentrations obtained from analysis of grab samples.

TBT has very low water solubility and, hence, is present at only very low concentrations in the water column. Passive sampling devices have been used to measure a number of organometallic species, including those of lead, mercury and tin. Følsvik et al. (2002) used SPMDs, caged mussels and water samples to monitor the levels of organotin compounds in the inner Oslofjord, Norway, over a period of 12 weeks. A good correlation was also found between the TBT concentration in SPMDs and mussels at the end of the experiment. Aguilar-Martínez et al. (2011) assessed the performance of Chemcatcher as aquatic monitoring technology for inorganic Hg and the organotin pollutants MBT, DBT and TBT in both fresh and marine waters.

3.3 DGT

Field trials in marine waters have been limited, with the emphasis being on research ad hoc deployments. DGT has been successfully applied to in situ metal speciation in seawater since its development in the mid-1990s. The first DGT deployments in a marine environment were carried out in the Menai Strait (UK) and the North Atlantic Ocean by Zhang and Davison (1995). They demonstrated the application of DGT to the in situ measurement of Cd, Fe, Mn and Cu in coastal and open seawater and discussed the more general applicability of DGT as a pollution monitoring tool and for measuring an in situ flux, as a surrogate for bioavailability. Twiss and Moffett (2002) compared Cu speciation in coastal marine waters measured using analytical voltammetry and DGT. Accumulation rates of Cu were substantially higher in contaminated waters than in pristine waters, suggesting that DGTs may be useful as tracking tools to detect episodic sources of contamination. Munksgaard and Parry (2003) investigated DGTs for in situ monitoring of labile metals in north Australian coastal seawater. DGT devices provided adequate detection limits, accuracy and precision for monitoring of near-pristine levels of labile Mn, Co, Cu, Cd and Pb when deployed for periods of 3 days. Larner et al. (2006) deployed DGT devices in the Antarctic environment to assess concentrations of trace metals in water and sediment porewater. DGT water sampling was restricted to quantification of Cd, Fe and Ni, while pre-concentration using Empore chelating disks provided results for additional elements. Forsberg et al. (2006) used DGTs and ultrafiltration to measure trace metal concentrations in the Baltic Sea. The results provide the first comparison of these two different speciation methods for trace metals. DGT appears to be a good alternative to 1 kDa ultrafiltration for measurement of truly dissolved Mn, Cd and Zn in seawater. Scoullos et al. (2006) investigated in shallow coastal areas of the Aegean Sea (Eastern Mediterranean) Cu and Cd partitioning and their interaction with organic matter. Dunn et al. (2007) monitored trace metal concentrations in dynamic estuarine waters in the Gold Coast Broadwater, Australia. They demonstrated that time-integrated, in situ DGT measurements could be used to monitor changes in various heavy metal (Ni, Cu, Zn and Pb) concentrations in response to different processes/conditions: tidal cycles, tidal flushing, urban storm water run-off and number of vessels with Cu-antifouled hulls. Sherwood et al. (2009) reported the deployment of DGT in relatively deep oceanic waters (50–150 m) and the first application of the technique to study plume dispersal from a deep sea tailings outfall. The authors measured total, filterable and DGT-labile concentrations of nine metals (Al, Cd, Cr, Cu, Fe, Pb, Mn, Ni and Zn) at five sites up to 4.2 km from a deep sea tailings outfall at Lihir Island, Papua New Guinea. In a large trial undertaken by IFREMER, Gonzalez et al. (2009) deployed DGTs (as well as POCIS and stir-bar sorptive extraction devices) in areas of the Indian Ocean (Reunion, Mayotte, French Guiana). Montero et al. (2012) in a study carried out in the Bay of Biscay (Spain) evaluated the potential use of DGTs for the chemical evaluation of transitional water bodies within the WFD.

Slaveykova et al. (2009) and Dakova et al. (2011) studied speciation of Cd, Cu, Ni and Pb in surface waters of Black Sea coast. The Black Sea is a unique marine ecosystem characterised by a large river inflow and very limited exchange of water with the Mediterranean Sea, which determines its low salinity and particular aquatic chemistry. In Brazil Costa and Wallner-Kersanach (2013) analysed the dissolved labile and labile particulate fractions of Cu and Zn during different seasons and salinity conditions in estuarine waters of marina, port and shipyard areas in the southern region of the Patos Lagoon. Some studies proved the ability of DGTs to measure radionuclides in seawater (French et al. 2005; Turner et al. 2012; Stockdale and Bryan 2013).

As far as regards Chemcatcher, the majority of work with trace metals has been undertaken in freshwater environments.

4 The Potential Use of Passive Sampling in WFD Monitoring

The Water Framework Directive of the European Union (WFD, EC 2000) establishes a framework for the protection and improvement of surface waters (inland, transitional and coastal waters) attempting to achieve ‘good status’ by 2015. The Marine Strategy Framework Directive (MSFD, EC

2008a), focusing on 'good environmental status' of marine waters, overlaps the WFD as far as regards the chemical quality of coastal water.

For the WFD, concentrations of contaminants in water are assessed against Environmental Quality Standards (EQS). EQS means the concentration of a particular pollutant or group of pollutants in water, sediment or biota which should not be exceeded in order to protect human health and the environment. The Environmental Quality Standards Directive (EQSD, EC 2008b) established limits on concentrations for 33 priority substances and eight other pollutants. The list includes trace metals (Cd, Hg, Ni, Pb and TBT), different pesticide groups, seven PAHs, chlorinated solvents and other compounds such as nonylphenol and PBDE. A number of substances or groups of substances that are toxic, persistent and liable to bioaccumulate, or assessed as giving rise to an equivalent level of concern, have been designated as priority hazardous substances (PHSs). For PHSs, discharges, emissions and losses must be stopped or phased out. The European Commission (EC) subsequently reviewed the list and in 2012 it put forward a proposal (EC 2012) for a directive amending the WFD and the EQSD as regards priority substances. Among the features of the proposal is the addition of 15 priority substances, 6 of them designated as PHSs.

A major contribute to the prioritisation of chemical compounds in the European Community comes from REACH (Registration, Evaluation, Authorisation and Restriction of Chemical Substances) (EC Regulation 1907/2006). REACH is a set of relatively new regulations put in place 'to ensure a high level of protection of human health and the environment' from chemicals used in industry. Authorisation is required for use of chemicals that cause cancer, mutations or problems with reproduction; that are persistent, bioaccumulative and toxic or very persistent and very bioaccumulative or that are identified from scientific evidence as causing probably serious effects on humans or the environment.

Several authors have reviewed the analytical challenges in monitoring water quality under the WFD. Current regulatory practice based on spot samples of water and comparisons of measured levels of priority pollutants with EQS will not provide data of the required reliability (Roig et al. 2007). Coquery et al. (2005) have highlighted (i) the need for defining new analytical methods for priority substances; (ii) the development of analytical methods capable of attaining detection limits consistent with the established quality objectives; (iii) the development of new certified reference materials, in order to ensure the accuracy and traceability of the results; and (iv) the organisation of interlaboratory trials, to improve the comparability of analytical results on water pollution, at an European level. These quality objectives should be, ideally, the concentration of a chemical, or the level of a physical factor, that would not produce any adverse effect on the environment. Both Coquery et al. (2005) and Lepom et al. (2009) pointed out that as WFD requires monitoring of unfiltered samples for organic contaminants, more attention needs to be paid to the distribution of chemical pollutants between SPM and the liquid phase. Methods allowing complete extraction of organic contaminants from whole-water samples are required. Furthermore, Lepom et al. (2009) found that monitoring in water encounters difficulties for some substances, e.g. SCCPs, PBDEs, TBT compounds, certain OCPs and six-ring PAHs, mainly due to a lack of validated, sufficiently sensitive methods that are applicable in routine laboratory conditions. Loos (2012) collected information on chemical analytical methods for the analysis of the new proposed priority substances of the WFD (EC 2012). He concluded that, in general, it is very difficult to reach with currently available analytical instruments LOQs in the low picogram per litre concentration range. Moreover, lower LOQs can be achieved by extracting higher volumes of water (10–1,000 L). These large-volume techniques, however, are very work and time intensive, and very costly, and are therefore not useful for routine WFD compliance monitoring (analysis of one sample per month).

According to Allan et al. (2006), successful implementation of the WFD will require the establishment and use of emerging and low-cost tools as part of monitoring programmes. These techniques may complement monitoring already in place by providing additional information with the aim to obtain a more representative picture of the quality of a water body. Emerging biological and chemical monitoring tools may become part of a 'toolbox' of techniques for use by those in charge of assessing water quality. Biological monitoring techniques include biomarkers, biosensors, biological early warning systems and whole-organism bioassays. Sampling and analytical tools developed for chemical assessment comprise biosensors, immunoassays, passive samplers and sensors.

It is now being recognised that PSs can play a valuable role in monitoring water quality within a legislative framework such as the WFD. The PSs, in particular the SPMD, can be used to monitor the 75 % of the organic micropollutants that are listed in the WFD (Table 1) (Stuer-Lauridsen 2005; Bergqvist and Zaliauskiene 2007). Passive samplers can provide information on environmental concentrations, fate and behaviour of substances of concern. They can potentially replace biota in the assessment of bioavailability, having advantages including lower cost and variability. The data from these devices can be used alongside the results obtained from conventional spot or bottle sampling to improve risk assessments and to inform decisions on undertaking potentially expensive remedial actions. Such monitoring techniques may have uses within the REACH

Table 1 Organic compounds identified in the WFD that can be monitored by SPMD or POCIS samplers

Compound	Sampler
Alachlor	POCIS
Anthracene	SPMD
Atrazine	POCIS
Benzene	SPMD
PBDE	SPMD
C10-13-chloroalkanes	SPMD
Chlorfenvinphos	SPMD
Chlorpyrifos	POCIS
1,2-Dichloroethane	–
Dichloromethane	–
DEHP	SPMD
Diuron	POCIS
Endosulfan	SPMD
Fluoranthene	SPMD
HCB	SPMD
Hexachlorobutadiene	SPMD
HCH	SPMD/POCIS
Isoproturon	POCIS
Naphthalene[a]	SPMD/POCIS
Nonylphenols[a]	SPMD/POCIS
Octylphenols[a]	SPMD/POCIS
Pentachlorobenzene[a]	SPMD/POCIS
Pentachlorophenol[a,b]	SPMD/POCIS
PAHs	SPMD
Simazine	POCIS
TBT compounds	SPMD
Trichlorobenzenes[a]	SPMD/POCIS
Trichloromethane (chloroform)	–
Trifluralin	SPMD

Adapted from Bergqvist and Zaliauskiene (2007)
[a]Compounds that can be sampled by both SPMDs and POCIS
[b]Ionised species

Directive (Greenwood et al. 2009; Söderström et al. 2009; Mills et al. 2011) and the MSFD. It is expected that the aquatic monitoring sector will follow a transition similar to that which occurred in air monitoring where data obtained from PSs can be used within a legal framework (Mills et al. 2011).

However, the fractions measured by these devices differ from those measured in spot samples. PSs accumulate the freely dissolved fractions, while spot samples allow to measure the total (without filtration) or a sub-fraction defined by the method of filtration used (e.g. ultrafiltration or filtration at 0.45 μm).

Pollutant concentration can be expressed as:

1. Freely dissolved
2. Dissolved (by filtration of water, thus removing the fraction associated with SPM and colloidal material)
3. In 'whole' water (dissolved + particulate)

As far as regards organic contaminants, EU Directive specifies that the EQSs 'are expressed as total concentrations in the whole water sample', meaning that the priority substance fraction bound to the SPM, especially relevant for hydrophobic compounds, also needs to be taken into account when reporting the measurement result. Since passive sampling is based on the measurement of freely dissolved phase pollutants, additional information on non-dissolved fractions of compounds can be obtained in parallel measurements of these compounds in SPM or bottom sediments. The sum of the contaminant concentration in the dissolved phase and that bound to colloids and particles will provide the measure of total concentration that can be applied in compliance checking with EQSs. Allan et al. (2009) showed that the measurements of hydrophobic organic pollutants in the freely dissolved phase in the marine environment carried out with passive sampling are less variable than those in the total water phase, which is strongly influenced by SPM content. This means that the frequency of sampling could be reduced by the use of PSs.

As far as regards metals, concentrations calculated from DGT deployment are generally lower than spot-sampling concentrations, since DGT measures only a part of total dissolved metal concentrations, represented by labile forms (inorganic complexes and small inorganic- or organic-complexed metals). Nevertheless, it has been suggested that water quality guidelines should be more appropriately expressed in terms of the bioavailable forms, as better proxy to toxicity, rather than in total or filterable concentrations (Montero et al. 2012). Eventually it might be important to rethink the definition of WFD EQSs to be compared with passive sampling data.

5 Conclusions

The numerous advantages that the use of PSs offers over conventional methods for the evaluation of the chemical quality of water bodies have been documented. Passive samplers provide a useful indication of the bioavailable fraction and a measure of the TWA concentration even where the environmental concentrations of a pollutant fluctuate in time. Under the WFD, they can be used for monitoring long-term trends and for screening a large range of contaminants at very low concentrations and reasonable costs. Future challenges for this technology include the improvement of calibration models, the availability of measurements of uptake rates for pollutants of current or emerging interest, the impacts of biofouling on performance and the development of quality assurance procedures.

References

Aguilar-Martínez, R., Gómez-Gómez, M.M., Palacios-Corvillo, M.A.: Mercury and organotin compounds monitoring in fresh and marine

waters across Europe by Chemcatcher passive sampler. Int. J. Environ. Anal. Chem. **91**(11), 1100–1116 (2011)

Alaee, M., Arias, P., Sjodin, A., Bergman, A.: An overview of commercially used brominated flame retardants, their applications, their use patterns in different countries/regions and possible modes of release. Environ. Int. **29**, 683–689 (2003)

Allan, I.J., Vrana, B., Greenwood, R., Mills, G.A., Roig, B., Gonzalez, C.: A 'toolbox' for biological and chemical monitoring requirements for the European Union's Water Framework Directive. Talanta **69**(2), 302–322 (2006)

Allan, I.J., Knutsson, J., Guigues, N., Mills, G.A., Fouillac, A.M., Greenwood, R.: Chemcatcher® and DGT passive sampling devices for regulatory monitoring of trace metals in surface water. J. Environ. Monit. **10**(7), 821–829 (2008)

Allan, I.J., Booij, K., Paschke, A., Vrana, B., Mills, G.A., Greenwood, R.: Field performance of seven passive sampling devices for monitoring of hydrophobic substances. Environ. Sci. Technol. **43**, 5383–5390 (2009)

Allan, S.E., Smith, B.W., Anderson, K.A.: Impact of the Deepwater Horizon oil spill on bioavailable polycyclic aromatic hydrocarbons in Gulf of Mexico coastal waters. Environ. Sci. Technol. **46**, 2033–2039 (2012)

Alvarez, D.A.: Guidelines for the use of the semipermeable membrane device (SPMD) and the polar organic chemical integrative sampler (POCIS) in environmental monitoring studies: U.S. Geological Survey, Techniques and Methods 1–D4, 28 p. (2010)

Alvarez, D.A., Petty, J.D., Huckins, J.N., Jones-Lepp, T.L., Getting, D. T., Goddard, J.P., Manahan, S.E.: Development of a passive, in situ, integrative sampler for hydrophilic organic contaminants in aquatic environments. Environ. Toxicol. Chem. **23**, 1640–1648 (2004)

Alvarez, D.A., Huckins, J.N., Petty, J.D., Jones-Lepp, T., Stuer-Lauridsen, F., Getting, D.T., Goddard, J.P., Gravell, A.: Chapter 8. Tool for monitoring hydrophilic contaminants in water: polar organic chemical integrative sampler (POCIS). Compr. Anal. Chem. 16 May 2013, **48**, 171–197 (2007)

Alvarez, D.A., Cranor, W.L., Perkins, S.D., Clark, R.C., Smith, S.B.: Chemical and toxicologic assessment of organic contaminants in surface water using passive samplers. J. Environ. Qual. **37**(3), 1024–1033 (2008)

Alvarez, D.A., Maruya, K.A., Dodder, N.G., Lao, W., Furlong, E.T., Smalling, K. L.: Occurrence of contaminants of emerging concern along the California coast (2009–10) using passive sampling devices. Mar. Pollut. Bull. http://dx.doi.org/10.1016/j.marpolbul.2013.04.022

Amiard-Triquet, C., Amiard, J.C.: Influence of ecological factors on accumulation of metal mixtures. In: Langston, W.J., Bebianno, M.J. (eds.) Metal Metabolism in Aquatic Environments, pp. 351–386. Chapman & Hall, London (1998)

Arditsoglou, A., Voutsa, D.: Passive sampling of selected endocrine disrupting compounds using polar organic chemical integrative samplers. Environ. Pollut. **146**, 316–324 (2008)

Assoumani, A., Lissalde, S., Margoum, C., Mazzella, N., Coquery, M.: In situ application of stir bar sorptive extraction as a passive sampling technique for the monitoring of agricultural pesticides in surface waters. Sci. Total Env. **463–464**, 829–835 (2013)

Bargar, T.A., Garrison, V.H., Alvarez, D.A., Echols, K.R.: Contaminants assessment in the coral reefs of Virgin Islands National Park and Virgin Islands Coral Reef National Monument. Mar. Pollut. Bull. **70**(1–2), 281–288 (2013)

Bergqvist, P.-A., Zaliauskiene, A.: Chapter 14. Field study considerations in the use of passive sampling devices in water monitoring. Compr. Anal. Chem. **48**, 311–328 (2007)

Boehm, P.D., Page, D.S., Brown, J.S., Neff, J.M., Bence, A.E.: Comparison of mussels and semi-permeable membrane devices as intertidal monitors of polycyclic aromatic hydrocarbons at oil spill sites. Mar. Pollut. Bull. **50**(7), 740–750 (2005)

Booij, P., Sjollema, S.B., Leonards, P.E.G., de Voogt, P., Stroomberg, G. J., Vethaak, A.D., Lamoree, M.H.: Extraction tools for identification of chemical contaminants in estuarine and coastal waters to determine toxic pressure on primary producers. Chemosphere **93**(1), 107–14 (2013). http://dx.doi.org/10.1016/j.chemosphere.2013.04.095

Booij, K., Smedes, F., Van Weerlee, E.M.: Spiking of performance reference compounds in low density polyethylene and silicone passive water samplers. Chemosphere **46**, 1157–1161 (2002a)

Booij, K., Zegers, B.N., Boon, J.P.: Levels of some polybrominated diphenyl ether (PBDE) flame retardants along the Dutch coast as derived from their accumulation in SPMDs and blue mussels (*Mytilus edulis*). Chemosphere **46**(5), 683–688 (2002b)

Booij, K., Smedes, F., Van Weerlee, E.M., Honkoop, P.J.C.: Environmental monitoring of hydrophobic organic contaminants: the case of mussels versus semipermeable membrane devices. Environ. Sci. Technol. **40**(12), 3893–3900 (2006a)

Booij, K., van Bommel, R., Mets, A., Dekker, R.: Little effect of excessive biofouling on the uptake of organic contaminants by semipermeable membrane devices. Chemosphere **65**(11), 2485–2492 (2006b)

Booij, K., Vrana, B., Huckins, J.N.: Chapter 7. Theory, modelling and calibration of passive samplers used in water monitoring. Compr. Anal. Chem. **48**, 141–169 (2007)

Bourgeault, A., Gourlay-Francé, C.: Monitoring PAH contamination in water: comparison of biological and physico-chemical tools. Sci. Total Environ. **454–455**, 328–336 (2013)

Bueno, M.J.M., Hernando, M.D., Agüera, A., Fernández-Alba, A.R.: Application of passive sampling devices for screening of micropollutants in marine aquaculture using LC–MS/MS. Talanta **77**, 1518–1527 (2009)

Chen, C.: Methylmercury effects and exposures: who is at risk? Environ. Health Perspect. **120**(6), 224–225 (2012)

Christen, V., Hickmann, S., Rechenberg, B., Fent, K.: Highly active human pharmaceuticals in aquatic systems: a concept for their identification based on their mode of action. Aquat. Toxicol. **96**, 167–181 (2010)

Clarisse, O., Lotufo, G.R., Hintelmann, H., Best, E.P.H.: Biomonitoring and assessment of monomethylmercury exposure in aqueous systems using the DGT technique. Sci. Total Environ. **416**, 449–454 (2012)

Coquery, M., Morin, A., Becue, A., Lepot, B.: Priority substances of the European Water Framework Directive: analytical challenges in monitoring water quality. Trend. Anal. Chem. **24**, 117–127 (2005)

Costa, L.D.F., Wallner-Kersanach, M.: Assessment of the labile fractions of copper and zinc in marinas and port areas in Southern Brazil. Environ. Monit. Assess. **185**(8), 6767–6781 (2013)

Covaci, A., Harrad, S., Abdallah, M.A.E., Ali, N., Law, R.J., Herzke, D., de Wit, C.A.: Novel brominated flame retardants: a review of their analysis, environmental fate and behaviour. Environ. Int. **37**, 532–556 (2011)

Dakova, I., Vasileva, P., Karadjova, I., Karadjov, M., Slaveykova, V.: Solid phase extraction and Diffusive Gradients in Thin Films techniques for determination of total and labile concentrations of Cd(II), Cu(II), Ni(II) and Pb(II) in Black Sea water. Int. J. Environ. Anal. Chem. **91**(1), 62–73 (2011)

Davison, W., Zhang, H.: In situ speciation measurements of trace components in natural waters using thin-film gels. Nature **367**, 546 (1994)

Davison, W., Zhang, H.: Progress in understanding the use of Diffusive Gradients in Thin Films (DGT) back to basics. Environ. Chem. **9**(1), 1–13 (2012)

Docekalova, H., Divis, P.: Application of diffusive gradient in thin films technique (DGT) to measurement of mercury in aquatic systems. Talanta **65**, 1174–1178 (2005)

Dunn, R.J.K., Teasdale, P.R., Warnken, J., Jordan, M.A., Arthur, J.M.: Evaluation of the in situ, time-integrated DGT technique by

monitoring changes in heavy metal concentrations in estuarine waters. Environ. Pollut. **148**(1), 213–220 (2007)
Dunnivant, F.M., Anders, E.: A Basic Introduction to Pollutant Fate and Transport. Wiley, New York (2006)
EC: Directive 2000/60/EC of the European Parliament and of the Council of 23 October 2000 establishing a framework for Community action in the field of water policy. Off. J. Eur. Union **L327**, 1–77 (2000)
EC: Directive 2008/56/EC establishing a framework for community action in the field of marine environmental policy (Marine Strategy Framework Directive). OJ L164, 25 Jun 2008, pp. 19–39 (2008a)
EC: Directive 2008/105/EC of the European Parliament and of the Council of 16 December 2008 on environmental quality standards in the field of water policy. Off. J. Eur. Union **L348**, 84–97 (2008b)
EC: Proposal for a Directive of the European Parliament and of the Council amending Directives 2000/60/EC and 2008/105/EC as regards priority substances in the field of water policy. COM (2011) 876 final (2012)
EEA: Hazardous substances in Europe's fresh and marine waters. A review. Technical Report No. 8, Copenhagen (2011)
Emelogu, E.S., Pollard, P., Robinson, C.D., Smedes, F., Webster, L., Oliver, I.W., et al.: Investigating the significance of dissolved organic contaminants in aquatic environments: coupling passive sampling with in vitro bioassays. Chemosphere **90**(2), 210–219 (2013)
Esteve-Turrillas, F.A., Yusà, V., Pastor, A., de la Guardia, M.: New perspectives in the use of semipermeable membrane devices as passive samplers. Talanta **74**, 443–457 (2008)
Flemming, H.-C., Schaule, G., Griebe, T., Schmitt, J., Tamachkiarowa, A.: Biofouling—the achilles heel of membrane processes. Desalination **113**(2–3), 215–225 (1997)
Følsvik, N., Brevik, E.M., Berge, J.A.: Organotin compounds in a Norwegian fjord. A comparison of concentration levels in semipermeable membrane devices (SPMDs), blue mussels (*Mytilus edulis*) and water samples. J. Environ. Monit. **4**(2), 280–283 (2002)
Forsberg, J., Dahlqvist, R., Gelting-Nyström, J., Ingri, J.: Trace metal speciation in brackish water using Diffusive Gradients in Thin Films and ultrafiltration: comparison of techniques. Environ. Sci. Technol. **40**(12), 3901–3905 (2006)
French, M.A., Zhang, H., Pates, J.M., Bryan, S.E., Wilson, R.C.: Development and performance of the Diffusive Gradients in Thin-Films technique for the measurement of technetium-99 in seawater. Anal. Chem. **77**(1), 135–139 (2005)
Garmo, Ø.A., Røyset, O., Steinnes, E., Flaten, T.P.: Performance study of Diffusive Gradients in Thin Films for 55 elements. Anal. Chem. **75**(14), 3573–3580 (2003)
Garmo, Ø.A., Davison, W., Zhang, H.: Interactions of trace metals with hydrogels and filter membranes used in DET and DGT techniques. Environ. Sci. Technol. **42**(15), 5682–5687 (2008)
Goldberg, E.D.: The mussel watch – a first step in global marine monitoring. Mar. Pollut. Bull. **6**, 111 (1975)
Gonzalez, J-L., Turquet, J., Cambert, H., Budzinski, H., Tapie, N., Guyomarch, J., Andral, B.: Projet PEPS La Réunion (Pré étude: Echantillonnage Passif pour la Surveillance de la contamination chimique). Mise en place d'échantillonneurs passifs pour la caractérisation de la contamination chimique des masses d'eau côtières réunionnaises. Rapport Convention Ifremer/DIREN Contract no. 07/1216859/F, p. 89 (2009).
Graceli, J.B., Sena, G.C., Lopes, P.F.I., Zamprogno, G.C., da Costa, M. B., Godoi, A.F.L., dos Santos Fernandez, M.A.: ,Organotins: a review of their reproductive toxicity, biochemistry, and environmental fate. Reprod. Toxicol. **36**, 40–52 (2013)
Greenwood, R., Mills, G., Vrana, B. (eds.): Passive Sampling Techniques in Environmental Monitoring. Comprehensive Analytical Chemistry, vol. 48. Elsevier, Amsterdam (2007a)
Greenwood, R., Mills, G.A., Vrana, B., Allan, I., Aguilar-Martínez, R., Morrison, G.: Chapter 9. Monitoring of priority pollutants in water using Chemcatcher passive sampling devices. Compr. Anal. Chem. **48**, 199–229 (2007b)
Greenwood, R., Mills, G.A., Vrana, B.: Potential applications of passive sampling for monitoring non-polar industrial pollutants in the aqueous environment in support of REACH. J. Chromatogr. A **1216**(3), 631–639 (2009)
Guitart, C., Readman, J.W., Bayona, J.M.: 1.16. Seawater organic contaminants. In: Pawliszyn, J. (ed.) Comprehensive Sampling and Sample Preparation, pp. 297–316. Academic, Oxford (2012)
Harman, C., Brooks, S., Sundt, R.C., Meier, S., Grung, M.: Field comparison of passive sampling and biological approaches for measuring exposure to PAH and alkylphenols from offshore produced water discharges. Mar. Pollut. Bull. **63**, 141–148 (2011)
Harman, C., Allan, I.J., Vermeirssen, E.L.M.: Calibration and use of the polar organic chemical integrative sampler-a critical review. Environ. Toxicol. Chem. **31**(12), 2724–2738 (2012)
Horii, Y., Kannan, K.: Survey of organosilicone compounds, including cyclic and linear siloxanes, in personal-care and household products. Arch. Environ. Contam. Toxicol. **5**, 701–710 (2008)
Huckins, J.N., Tubergen, M.W., Manuweera, G.K.: Semipermeable membrane devices containing model lipid: a new approach to monitoring the bioavailability of lipophilic contaminants and estimating their bioconcentration potential. Chemosphere **20**, 533–552 (1990)
Huckins, J.N., Petty, J.D., Lebo, J.A., Almeida, F.V., Booij, K., Alvarez, D.A., Cranor, W.L., Clark, R.C., Mogensen, B.B.: Development of the permeability/performance reference compound approach for in situ calibration of semipermeable membrane devices. Environ. Sci. Technol. **36**(1), 85–91 (2002)
Huckins, J.N., Petty, J.D., Booij, K.: Monitors of Organic Chemicals in the Environment Semipermeable Membrane Devices. Springer, New York (2006)
Hylland, K.: polycyclic aromatic hydrocarbon (PAH) ecotoxicology in marine ecosystems. J. Toxicol. Environ. Health Part A **69**(1–2), 109–123 (2006)
Ibrahim, I., Togola, A., Gonzalez, C.: In-situ calibration of POCIS for the sampling of polar pesticides and metabolites in surface water. Talanta **116**, 495–500 (2013)
Johnson-Restrepo, B., Kannan, K.: An assessment of sources and pathways of human exposure to polybrominated diphenyl ethers in the United States. Chemosphere **76**(4), 542–548 (2009)
Karacik, B., Okay, O.S., Henkelmann, B., Pfister, G., Schramm, K.W.: Water concentrations of PAH, PCB and OCP by using semipermeable membrane devices and sediments. Mar. Pollut. Bull. **70**, 258–265 (2013)
Kaserzon, S.L., Vermeirssen, E.L.M., Hawker, D.W., Kennedy, K., Bentley, C., Thompson, J., Mueller, J.F.: Passive sampling of perfluorinated chemicals in water: flow rate effects on chemical uptake. Environ. Pollut. **177**, 58–63 (2013)
Kingston, J.K., Greenwood, R., Mills, G.A., Morrison, G.M., Persson, L.B.: Development of a novel passive sampling system for the time-averaged measurement of a range of organic pollutants in aquatic environments. J. Environ. Monit. **2**, 487–495 (2000)
Klánova, J., Diamond, M., Jones, K., Lammel, G., Lohmann, R., Pirrone, N., Scheringer, M., et al.: Identifying the research and infrastructure needs for the global assessment of hazardous chemicals ten years after establishing the Stockholm Convention. Environ. Sci. Technol. **45**(18), 7617–7619 (2011)
Komarova, T.V., Bartkow, M.E., Rutishauser, S., Carter, S., Mueller, J. F.: Evaluation and in situ assessment of photodegradation of polyaromatic hydrocarbons in semipermeable membrane devices deployed in ocean water. Environ. Pollut. **157**(3), 731–736 (2009)
Kot, A., Zabiegała, B., Namieśnik, J.: Passive sampling for long-term monitoring of organic pollutants in water. Trend. Anal. Chem. **19** (7), 446–459 (2000)
Larner, B.L., Seen, A.J., Snape, I.: Evaluation of Diffusive Gradients in Thin Film (DGT) samplers for measuring contaminants in the

Antarctic marine environment. Chemosphere **65**(5), 811–820 (2006)
Lepom, P., Brown, B., Hanke, G., Loos, R., Quevauviller, P., Wollgast, J.: Needs for reliable analytical methods for monitoring chemical pollutants in surface water under the European Water Framework Directive. J. Chromatogr. A **1216**(3), 302–315 (2009)
Li, W., Zhao, H., Teasdale, P.R., John, R., Wang, F.: Metal speciation measurement by Diffusive Gradients in Thin Films technique with different binding phases. Anal. Chim. Acta. **533**(2), 193–202 (2005)
Liscio, C., Magi, E., Di Carro, M., Suter, M.J.-F., Vermeirssen, E.L.M.: Combining passive samplers and biomonitors to evaluate endocrine disrupting compounds in a wastewater treatment plant by LC/MS/MS and bioassay analyses. Environ. Pollut. **157**, 2716–2721 (2009)
Lohmann, R., Muir, D.: Global aquatic passive sampling (AQUA-GAPS): using passive samplers to monitor POPs in the waters of the world. Environ. Sci. Technol. **44**(3), 860–864 (2010)
Loos, R.: Analytical Methods Relevant to the European Commission's 2012 Proposal on Priority Substances Under the Water Framework Directive, JRC N° JRC73257, Publications Office of the European Union. http://publications.jrc.ec.europa.eu/repository/handle/111111111/26936 (2012)
MacKenzie, L., Beuzenberg, V., Holland, P., McNabb, P., Selwood, A.: Solid phase adsorption toxin tracking (SPATT): a new monitoring tool that simulates the biotoxin contamination of filter feeding bivalves. Toxicon **44**(8), 901–918 (2004)
Marrucci, A., Marras, B., Campisi, S.T., Schintu, M.: Using SPMDs to monitor the seawater concentrations of PAHs and PCBs in marine protected areas (Western Mediterranean). Mar. Pollut. Bull. **75**(1/2), 69–75 (2013). http://dx.doi.org/10.1016/j.marpolbul.2013.08.004
Melwani, A.R., Gregorio, D., Jin, Y., Stephenson, M., Ichikawa, G., Siegel, E., Crane, D., Lauenstein, G., Davis, J.A.: Mussel watch update: long-term trends in selected contaminants from coastal California 1977–2010. Mar. Pollut. Bull. 24 May 2013 http://dx.doi.org/10.1016/j.marpolbul.2013.04.025
Miège, C., Schiavone, S., Dabrin, A., Coquery, M., Mazzella, N., Berho, C., et al.: An in situ intercomparison exercise on passive samplers for monitoring metals, polycyclic aromatic hydrocarbons and pesticides in surface waters. Trend. Anal. Chem. **36**, 128–143 (2012)
Mills, G.A., Vrana, B., Allan, I., Alvarez, D.A., Huckins, J.N., Greenwood, R.: Trends in monitoring pharmaceuticals and personal-care products in the aquatic environment by use of passive sampling devices. Anal. Bioanal. Chem. **387**(4), 1153–1157 (2007)
Mills, G.A., Greenwood, R., Vrana, B., Allan, I.J., Ocelka, T.: Measurement of environmental pollutants using passive sampling devices – a commentary on the current state of the art. J. Environ. Monit. **13**(11), 2979–2982 (2011)
Montero, N., Belzunce-Segarra, M.J., Gonzalez, J.L., Larreta, J., Franco, J.: Evaluation of Diffusive Gradients in Thin-Films (DGTs) as a monitoring tool for the assessment of the chemical status of transitional waters within the Water Framework Directive. Mar. Pollut. Bull. **64**(1), 31–39 (2012)
Monteyne, E., Roose, P., Janssen, C.R.: Application of a silicone rubber passive sampling technique for monitoring PAHs and PCBs at three Belgian coastal harbours. Chemosphere **91**, 390–398 (2013)
Muir, D., Lohmann, R.: Water as a new matrix for global assessment of hydrophilic POPs. Trend. Anal. Chem. **46**, 162–172 (2013)
Munaron, D., Tapie, N., Budzinski, H., Andral, B., Gonzalez, J.L.: Pharmaceuticals, alkylphenols and pesticides in Mediterranean coastal waters: results from a pilot survey using passive samplers. Estuar. Coast. Shelf Sci. **114**, 82–92 (2012)
Munksgaard, N.C., Parry, D.L.: Monitoring of labile metals in turbid coastal seawater using Diffusive Gradients in Thin-Films. J. Environ. Monit. **5**(1), 145–149 (2003)
OSPAR Commission. Quality Status Report 2010. London (2010)
Panther, J.G., Stewart, R.R., Teasdale, P.R., Bennett, W.W., Welsh, D. T., Zhao, H.: Titanium dioxide-based DGT for measuring dissolved As(V), V(V), Sb(V), Mo(VI) and W(VI) in water. Talanta **105**, 80–86 (2013)
Paschke, A., Schwab, K., Brümmer, J., Schüürmann, G., Paschke, H., Popp, P.: Rapid semi-continuous calibration and field test of membrane-enclosed silicone collector as passive water sampler. J. Chromatogr. A **1124**(1–2), 187–195 (2006)
Richardson, S.D., Ternes, T.A.: Water analysis: emerging contaminants and current issues. Anal. Chem. **83**, 4614–4648 (2011)
Richardson, B.J., Zheng, G.J., Tse, E.S.C., Lam, P.K.S.: A comparison of mussels (*Perna viridis*) and semi-permeable membrane devices (SPMDs) for monitoring chlorinated trace organic contaminants in Hong Kong coastal waters. Chemosphere **45**(8), 1201–1208 (2001)
Roach, A.C., Muller, R., Komarova, T., Symons, R., Stevenson, G.J., Mueller, J.F.: Using SPMDs to monitor water column concentrations of PCDDs, PCDFs and dioxin-like PCBs in Port Jackson (Sydney Harbour), Australia. Chemosphere **75**(9), 1243–1251 (2009)
Røe Utvik, T.I., Johnsen, S.: Bioavailability of polycyclic aromatic hydrocarbons in the North Sea. Environ. Sci. Technol. **33**, 1963–1969 (1999)
Roig, B., Valat, C., Berho, C., Allan, I.J., Guigues, N., Mills, G.A., Ulitzur, N., Greenwood, R.: The use of field studies to establish the performance of a range of tools for monitoring water quality. Trend. Anal. Chem. **26**(4), 274–286 (2007)
Roose, P., Brinkman, U.A.T.: Monitoring organic microcontaminants in the marine environment: principles, programmes and progress. Trend. Anal. Chem. **24**(11), 897–926 (2005)
Rusina, T.P., Smedes, F., Klanova, J., Booij, K., Holoubek, I.: Polymer selection for passive sampling: a comparison of critical properties. Chemosphere **68**, 1344–1351 (2007)
Scally, S., Davison, W., Zhang, H.: Diffusion coefficients of metals and metal complexes in hydrogels used in diffusive gradients in thin films. Anal. Chim. Acta. **558**, 222–229 (2006)
Schintu, M., Durante, L., Maccioni, A., Meloni, P., Degetto, S., Contu, A.: Measurement of environmental trace-metal levels in Mediterranean coastal areas with transplanted mussels and DGT techniques. Mar. Pollut. Bull. **57**(6–12), 832–837 (2008)
Schintu, M., Marras, B., Durante, L., Meloni, P., Contu, A.: Macroalgae and DGT as indicators of available trace metals in marine coastal waters near a lead-zinc smelter. Environ. Monit. Assess. **167**(1–4), 653–661 (2010)
Scoullos, M., Plavšić, M., Karavoltsos, S., Sakellari, A.: Partitioning and distribution of dissolved copper, cadmium and organic matter in Mediterranean marine coastal areas: the case of a mucilage event. Estuar. Coast. Shelf Sci. **67**(3), 484–490 (2006)
Shaw, M., Negri, A., Fabricius, K., Mueller, J.F.: Predicting water toxicity: pairing passive sampling with bioassays on the Great Barrier Reef. Aquat. Toxicol. **95**, 108–116 (2009)
Shaw, M., Furnas, M.J., Fabricius, K., Haynes, D., Carter, S., Eaglesham, G., Mueller, J.F.: Monitoring pesticides in the Great Barrier Reef. Mar. Pollut. Bull. **60**, 113–122 (2010)
Sherwood, J.E., Barnett, D., Barnett, N.W., Dover, K., Howitt, J., Ii, H., Kew, P., Mondon, J.: Deployment of DGT units in marine waters to assess the environmental risk from a deep sea tailings outfall. Anal. Chim. Acta. **652**(1–2), 215–223 (2009)
Slaveykova, V.I., Karadjova, I.B., Karadjov, M., Tsalev, D.L.: Trace metal speciation and bioavailability in surface waters of the Black Sea coastal area evaluated by HF-PLM and DGT. Environ. Sci. Technol. **43**(6), 1798–1803 (2009)
Smedes, F.: Chapter 19. Monitoring of chlorinated biphenyls and polycyclic aromatic hydrocarbons by passive sampling in concert with deployed mussels. Compr. Anal. Chem. **48**, 407–448 (2007)
Smedes, F., van der Zande, T., Roose, P., Davies, I. M.: ICES passive sampling trial survey for water and sediment (PSTS) (2006–2007). ICES CM 2007/J:04 (2007)

Söderström, H., Lindberg, R.H., Fick, J.: Strategies for monitoring the emerging polar organic contaminants in water with emphasis on integrative passive sampling: tools for the REACH programme – analytical methods for the evaluation of industrial contaminants. J. Chromatogr. A **1216**, 623–630 (2009)

Stark, J.S., Johnstone, G.J., Palmer, A.S., Snape, I., Larner, B.L., Riddle, M.J.: Monitoring the remediation of a near shore waste disposal site in Antarctica using the amphipod *Paramoera walkeri* and diffusive gradients in thin films (DGTs). Mar. Pollut. Bull. **52** (12), 1595–1610 (2006)

Stemmler, I., Lammel, G.: Evidence of the return of past pollution in the ocean: a model study. Geophys. Res. Lett. **40**(7), 1373–1378 (2013)

Stockdale, A., Bryan, N.D.: Application of DGT to high pH environments: uptake efficiency of radionuclides of different oxidation states onto Chelex binding gel. Environ. Sci. Process. Impact. **15**(5), 1087–1091 (2013)

Stuer-Lauridsen, F.: Review of passive accumulation devices for monitoring organic micropollutants in the aquatic environment. Environ. Pollut. **136**, 503–524 (2005)

Stumm, W., Morgan, J.J.: Aquatic Chemistry, 2nd edn. Wiley Interscience, New York (1981)

Togola, A., Budzinski, H.: Development of polar organic integrative samplers for analysis of pharmaceuticals in aquatic systems. Anal. Chem. **79**(17), 6734–6741 (2007)

Turner, G.S.C., Mills, G.A., Teasdale, P.R., Burnett, J.L., Amos, S., Fones, G.R.: Evaluation of DGT techniques for measuring inorganic uranium species in natural waters: interferences, deployment time and speciation. Anal. Chim. Acta. **739**, 37–46 (2012)

Twiss, M.R., Moffett, J.W.: Comparison of copper speciation in coastal marine waters measured using analytical voltammetry and Diffusion Gradient in Thin-Film techniques. Environ. Sci. Technol. **36**(5), 1061–1068 (2002)

Uher, E., Zhang, H., Santos, S., Tusseau-Vuillemin, M.-H., Gourlay-Francé, C.: Impact of biofouling on diffusive gradient in thin film measurements in water. Anal. Chem. **84**, 3111–3118 (2012)

Vrana, B., Mills, G.A., Allan, I.J., Dominiak, E., Svensson, K., Knutsson, J., Morrison, G., Greenwood, R.: Passive sampling techniques for monitoring pollutants in water. Trend. Anal. Chem. **24**(10), 845–868 (2005)

Vrana, B., Vermeirssen, E.L.M., Allan, I.J., Kohoutek, J., Kennedy, K., Mills, G.A., Greenwood, R.: Passive sampling of environmental pollutants in the aquatic environment: state of the art and perspectives. Position paper. http://www.norman-network.net/public_docs/slides_prague/norman_position_paper_pas_sampling.pdf (2010)

Wang, W.X., Fisher, N.S., Luoma, S.N.: Kinetic determination of trace element bioaccumulation in the *Mytilus edulis*. Mar. Ecol. Prog. **140**, 91–113 (1996)

WHO: State of the science of endocrine disrupting chemicals-2012. In Bergman, Å., Heindel, J.J., Jobling, S., Kidd, K.A., Zoeller, R.T. United Nations Environment Programme and the World Health Organization (2013)

Wu, R.S.S., Lau, T.C., Fung, W.K.M., Ko, P.H., Leung, K.M.Y.: An 'artificial mussel' for monitoring heavy metals in marine environments. Environ. Pollut. **145**, 104–110 (2007)

Xu, W., Wang, X., Cai, Z.: Analytical chemistry of the persistent organic pollutants identified in the Stockholm Convention: a review. Anal. Chim. Acta. **790**, 1–13 (2013)

Zhang, H., Davison, W.: Performance characteristics of Diffusion Gradients in Thin Films for the in situ measurement of trace metals in aqueous solution. Anal. Chem. **67**(19), 3391–3400 (1995)

A Review of Green Business

Theoharis Tziovaras and Georgia Valaoras

Abstract

This chapter critically examines the role of business in fostering a more sustainable society. It offers a short historical review of the wider institutional role of business within the framework of global environmental governance and underlines the factors that have encouraged businesses in taking into account sustainability in their business model. It surveys some practices and tools that businesses utilise in this venture. It outlines the role of sustainable production by discussing tools such as eco-efficiency, biomimicry and life-cycle analysis. It also offers insights into the role of environmental management systems and environmental certification. A discussion on the significance of corporate social responsibility is included, along with an inspection of the emerging role of benefit corporations. Finally, some remarks are offered on the wider institutional changes needed for businesses to be aided in their drive to become more sustainable.

Keywords

Green business • Sustainable business • Triple bottom line • Sustainable production and consumption • Environmental management systems • Corporate social responsibility • Benefit corporations

1 Introduction

The term "green business" refers to the ongoing effort by a number of enterprises to minimise the negative impact of their operations to the environment, society and economy. It emerged as a direct response to the increasing appeals towards the corporate sector over the past 40 years to address the issues of pollution and general environmental degradation (Hoffman and Georg 2013). Corporations – particularly multinational ones – have contributed significantly to global resource depletion and pollution (Elliott 2004), particularly through negative externalities, i.e. impacts and costs that are not included in the final price of the product. Moreover, business-as-usual practices have a serious non-environmental impact, including the loss of livelihoods of many people, as local businesses slowly give way to huge corporate supply chains (Sukhdev 2012). On the other hand, businesses hold remarkable know-how, expertise, innovation and entrepreneurship, availability of funds and structural flexibility that can enable them to become leaders in fostering more sustainable practices. Therefore, the business community can be viewed both as part of the problem and as part of the solution of the severe sustainability challenges we currently face. Green business is a vast field which encompasses a great number of initiatives leading to the mitigation of those challenges. This chapter offers a short historical review on their emerging role and a look into a few practices (sustainable production, environmental management systems and corporate social responsibility) of a green business. It also provides some insights on the institutional framework and current trends which enable the transition towards sustainable business.

T. Tziovaras (✉) • G. Valaoras
Hellenic American University, Massalias 22, 10680 Athens, Greece
e-mail: Ttziovaras@hauniv.us

G. Cao and R. Orrù (eds.), *Current Environmental Issues and Challenges*,
DOI 10.1007/978-94-017-8777-2_15,

2 Short Historical Review

2.1 From Rio to Johannesburg

The emerging role of business in fostering sustainability was recognised during the Earth Summit at Rio in 1992, which provided a forum where the business community could voice its own relevant concerns and ideas. Within the next decade, considerable progress took place, with the launching of the first environmental management system standard in 1992 by the BSI Group, the formation of the influential World Business Council for Sustainable Development in 1995 and the emergence of relevant scientific publications such as *Business Strategy & the Environment* (1992) and the *Journal of Industrial Ecology* (1997). The conceptualisation of the triple bottom line by Elkington (1997) provided a framework of business practices that take care of "people, planet, profit". The triple bottom line measures organisational success on an expanded set of criteria, such as community relations, human rights and irresponsible marketing (social); use and protection of natural resources and life cycle impact of products and services (environmental); and cost competitiveness, profit margin and level of innovation (economic).

However, those initiatives did not suffice. The inability of global environmental governance to advance adequately the goals of Agenda 21 within the next decade led to the growing realisation that international treaties could only set the framework for such initiatives, which however needed the involvement of more stakeholders other than governments (Müller-Kraener 2003). Thus, the growing role of business was further solidified during the World Summit on Sustainable Development (WSSD) in Johannesburg in 2002, with the introduction of "Type-II partnerships". Those envisioned the cooperation of governments, businesses and civil society, offering corporations a new arena and motivation to operationalise sustainability and include it into their practices (Feldman 2009).

2.2 Three Crucial Factors

Yet, indicators of environmental degradation continued only to worsen; even this, more favourable institutional framework did not seem to be sufficient for the diffusion of sustainable practices at the level needed – and as Feldman (2009) noted, many feared that only a crisis would spur such action. Real change took place only after the influence of three crucial factors, which in a way convinced to a large extent the business community to jump on the sustainability bandwagon.

Firstly, Stern's (2006) review on the economics of climate change was a pivotal point in reframing the greatest environmental challenge of our times in economic terms. It clearly stipulated that it is more cost-effective to address climate change now than to pay for it in the future – either we pay 1 % of global GDP now to mitigate it or 5–20 % of global GDP in the future. Therefore, many companies, but also major industries, such as the insurance industry, understood that their long-term economic viability was compromised by this environmental challenge.

Secondly, awareness of approaching resource scarcity in the face of a growing population and the embracing of a Western standard of life in many parts of the developing world led many corporations and investors to realise that the core of their business is threatened by the degradation of such invaluable natural resources such as water and soil (Grantham 2011; Martenson 2011). Shortly afterwards, more robust sustainability initiatives were enacted, for instance, of cleaning agent companies initiating aggressive campaigns for water conservation at the industrial and the consumer level. Meanwhile, global investment companies warned that firms which do not take proactive measures to "insulate themselves against the threat of scarcity" (KPMG 2012: 2) would face severe problems in the future – or as Hawken (2012) put it, "when a limiting factor arises, the intelligent company works toward minimising the use of what is limited" (28).

Finally, companies understood that environmental challenges provide ample opportunity for creating business value. DeSimone and Popoff (1997) noted that companies adhering to the triple bottom line assume a competitive advantage by catering to the needs of ethical consumers while reducing costs and liabilities stemming from waste and pollution. Added business value also follows the rise of socially responsible investing, i.e. investing on companies fulfilling a set of ethical criteria, which has seen a boom during the past decade. According to the Social Investment Forum Foundation (2010), assets which have followed socially responsible investing strategies rose from US$639 billion in 1995 to US$3.07 trillion in 2010 in the USA, a rise of 380 %. At the same time, Henderson et al. (2013) noted a soaring in green investment funds, with over US$4 trillion having been invested in renewable energy, energy efficiency, green construction, clean tech and corporate R&D since 2007. Meanwhile, in 2011, investment on renewable sources of energy surpassed for the first time that of fossil fuels (Winston 2011). The increase of environmental challenges has also fostered entrepreneurship and innovation, through the development of companies such as Regenersis, which recycles mobile phones, and TerraCycle, which "recycles everything", from baby diapers to cigarette butts.

2.3 A Business Megatrend

This shift in thinking has been facilitated by the multi-stakeholder framework established during the World Summit on Sustainable Development and sustainability has progressively entered the agenda of both the international conferences and the boardroom. For instance, the European Commission (2008) has developed an action plan that aims to promote sustainable production and consumption, with policies such as promoting eco-design, eco-labelling, green procurement and cleaner production, leading to relevant business practices. This shift is so momentous and requires such a radical restructuring of corporate practices – even of what a corporation is! – that it has been fairly characterised as a "business megatrend", similar to electrification and the rise of mass production (Lubin and Esty 2012), that can change the face of business forever.

3 Sustainable Production

At the core of business practices lies the production of goods and services. Sustainable production refers to the creation of such goods and services in a way that minimises or even reverses negative environmental impact, is economically viable and is safe and healthy for all stakeholders involved. A number of innovations, practices and tools have emerged so as to constitute production sustainable. Although many times complementary, such tools can also be contradictory, particularly as far as the underlying principles guiding their usage are concerned.

3.1 Eco-efficiency

One of the main tools, developed by the World Business Council for Sustainable Development, is eco-efficiency, defined as the "delivery of competitively priced goods and services that satisfy human needs and bring quality of life, while progressively reducing ecological impacts and resource intensity throughout the life cycle, to a level at least in line with the earth's carrying capacity" (DeSimone and Popoff 1997, 47). Eco-efficiency is characterised by seven guidelines: (a) reduction of the material intensity of goods and services, (b) reduction of the energy intensity of goods and services, (c) reduction of toxic dispersion, (d) enhancing material recyclability, (e) maximising sustainable use of renewable resources, (f) extending product durability and (g) increasing the service intensity of products (DeSimone and Popoff 1997, 56–57).

The concept of eco-efficiency, although undoubtedly useful, has been criticised for putting the emphasis on efficient use of resources, rather than on the overall reduction of resource use, and for adhering to the tenet that growth can continue forever on a finite planet. For instance, McDonough and Braungart (2002) posited that eco-efficiency will never be enough to foster the desired transition to sustainability, since it would only reduce the rate of destruction rather than reverse it. Their aim is instead an "eco-effective" approach that promotes a fully closed-loop production system that mimics nature – i.e. a "cradle-to-cradle" design.

3.2 Biomimicry

Concepts such as the closed-loop production system draw from a larger body of thought known as biomimicry: imitating or being inspired from nature's models in order to solve human problems. Adherents of biomimicry point out that the planet is a vast resource of ideas, designs, models and applications that are the outcome of over 3.8 billion years of evolution – or "R&D". Thus, drawing from nature is wise, since natural systems often perform the same functions that human ingenuity does but using simpler processes that are extremely efficient, recycle everything, use only the energy they need (and mostly from sunlight) and have much less cost to the planet (Benyus 2009).

Biomimicry has inspired a remarkable array of industrial applications that alter mainly the design and manufacturing procedure of goods and services. From adhesives without glue to colouring without pigments, biomimicry is a field that promises significant innovation for the future, for instance, in solar collectors inspired by butterfly wings (see Fig. 1). But it has also encouraged ways of thinking. One of the greatest design inspirations coming from nature is the aforementioned closed-loop production, which aims to essentially eliminate the concept of waste. In nature, the waste of one organism is the food of another, in a cyclical system where no material is left unused. In contrast, the current material flow in human society is linear in nature, starting from the extraction of raw materials to their processing, the manufacture of products, their distribution, their use and their eventual disposal.

All this process is called the life cycle of a product and is one of the most important analysis tools utilised by businesses in their attempt to identify and address the stages of a product's life where environmental damage takes place. Although filled with high uncertainty due to its complexity, life cycle analysis is particularly useful when comparing two products or processes (Hendrickson et al. 2006). Such analysis can frequently uncover counter-intuitive results, since it addresses often unlooked factors of environmental impact. For instance, Jolliet et al. (1994) found through a life cycle analysis that biodegradable packing materials, such as popcorn, actually cause more environmental damage than

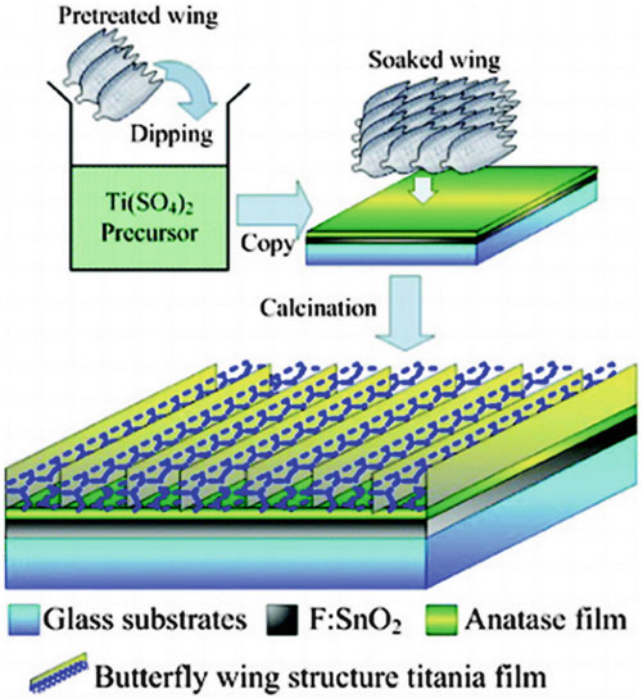

Fig. 1 An example of biomimicry: butterfly-wing solar collectors which absorb light more efficiently than dye-sensitised cells (Zhang et al. 2009)

polystyrene chips, due to the drainage of pesticides, phosphates and nitrates to groundwater caused by industrial agriculture. Companies such as Patagonia, with its Footprint Chronicles, have divulged the entire life cycle of their products, aiming for increased consumer awareness and transparency in its operations. One of the most important aspects of the life cycle analysis is that its results often influence a company to request better environmental performance up the supply chain.

3.3 From Goods to Services

An increasingly closed-loop production system reduces the requirement for new resources on the one end and waste/pollution on the other. This is extremely important, when one realises how wasteful the current production system is. According to Hawken (2012), only 0.28 % of the original mass of materials mined, grown or harvested in the USA is finally retained in durable products, while only 1/50th of this percentage produces more value later on through remanufacturing or recycling. Apart from the immense business opportunities that arise from the necessity to rectify this unsustainable situation, a closed-loop production can also provide significant benefits for companies utilising it, since they take advantage of materials which would otherwise end up in a landfill, using processes that often cost less than actually acquiring raw materials in the first place. An example of such an initiative is the ReEntry programme of Interface which reclaims old carpets and recycles/downcycles/repurposes them, having "reclaimed" 110 million kilos of carpets since 1994 (Interface Inc. 2013).

This trend signifies a gradual shift in companies from providers of goods to providers of services, retaining ownership of the materials used and recycling/reusing them when they have reached the end of their meaningful life for the consumer. It is then only natural that companies are looking for ways to design their products so that they are recyclable to begin with, or designed for remanufacturing – a practice that has reduced carbon emissions, 15 % less energy expenditure than manufacturing and double profit margins (Oakdene Hollins Ltd. 2004).

In this process, the chemical components of products have gone under the microscope, leading to the development of green chemistry, which is the promotion of "innovative chemical technologies that reduce or eliminate the use or generation of hazardous substances in the design, manufacture and use of chemical products" (Lancaster 2010: 4). Green chemistry is yet another tool that facilitates sustainable production and consumption, the result of lessons learned from the release of substances such as DDT in the environment. A few key principles of green chemistry are that it is better to prevent pollution than to clean it up afterwards, that chemical products should degrade in the environment and that safer chemicals should be designed; the application of those principles also leads to reduced expenditure, through the reduction of materials usage, lower costs of treating waste, etc. (Lancaster 2010).

4 Environmental Management Systems and Certification

The complicated nature of the production process and the inclusion of relevant tools leading to sustainable production necessitated a management approach regarding environmental impact. Environmental management systems were developed as a method used by an organisation to systematically manage the environmental aspects of its production processes. In practice, environmental management systems differ considerably, depending on the precise industry sector and the aims that top management wishes to achieve. Yet the underlying principles remain the same. Environmental management systems usually follow Deming's Plan-Do-Check-Act cycle: environmental targets, aims and objectives are planned; those are implemented by setting up relevant structures and training initiatives; the outcomes are checked using monitoring and audits; then the whole procedure passes through management review, aiming for continuous improvement, leading to the formation of new targets.

Environmental management systems are completely voluntary and have surfaced as an alternative to the command-and-control approach that characterised environmental regulation.

4.1 ISO-14001 and EMAS

A company's environmental management system can be certified using a number of certification schemes, the most prominent of which are ISO-14001 and the EU Eco-Management and Audit Scheme (EMAS). Certification of environmental management systems arose as a necessity to compare the environmental performance of different companies and for benchmarking. The ISO-14000 family was developed in 1996 and clearly indicated to the business community that a more strategic and systematic approach was needed in order to address environmental challenges (Horne et al. 2009). EMAS was developed in 1993 but was revised to incorporate the principles of ISO-14001 in 2001. EMAS has added further elements required for certification, such as an initial environmental review and an environmental statement. It also requires third-party auditing and has developed a set of key performance indicators to measure environmental performance, in materials, water, energy, waste, emissions and biodiversity. It should be noted that both ISO-14001 and EMAS do not have specific requirements for environmental performance; the environmental targets of a company are still set by management, guided by an environmental management system so as to comply with the minimum standards set by relevant legislation.

Significant advantages follow the adoption of an environmental management system. One of the key benefits is the minimisation of liability stemming from compliance with regulations. Moreover, the continuous improvement process facilitates cost-saving measures such as increased energy and materials efficiency and reduced operating costs. The adoption of an environmental management system in business practices also offers a competitive advantage, since it indicates to consumers that the company aims to improve its environmental performance. The inclusion of the ISO-14001 or EMAS logo in a company's appearance is thought to enhance its reputation and therefore its brand value.

4.2 Certification

EMAS and ISO-14001 certify environmental management systems; however, certification has expanded in the past two decades to include a wide variety of goods and services. Environmental certification is the process through which a company complies with a set of quality standards. Certification schemes have been developed for timber products (Forest Stewardship Council), marine products (Marine Stewardship Council), energy consumption (Leadership in Energy and Environmental Design), fair distribution of income and humane working conditions (FairTrade), organic agriculture (International Federation of Organic Agriculture Movements), sustainable tourism (EU Ecolabel for hotels) and others. The process is voluntary in most cases and is another example of a market-driven mechanism which can promote sustainability.

Even though this mechanism is non-state, Hackett (2011) noted that the success of certification and eco-label programmes relies on the inclusion of governments, along with environmental NGOs and companies, in developing and supporting the relevant standards. Other factors of success include the fact that consumers are informed about the impact of their product choices, that companies can make a profit by selling certified goods and that certification and auditing takes place by third-party agencies.

Most organisations offering certification are non-profit, multi-stakeholder ones. The requirements for a company to achieve certification vary considerably, depending on the sector. For instance, the Marine Stewardship Council has a set of 3 principles and 31 criteria which include setting catch levels that will maintain the target population, making use of fishing gear that avoids catching nontarget species and not using destructive fishing practices such as dynamite (Marine Stewardship Council 2010). The Forest Stewardship Council functions under a set of ten principles which include compliance with relevant laws and treaties, recognition and respect of indigenous people's rights and maintenance of high conservation value forests, i.e. forests that have significant biodiversity or endangered species, or provision of important ecosystem or cultural services to local communities (Forest Stewardship Council 1996).

There is significant controversy regarding the impact environmental certification on actually delivering more sustainable practices. On the one hand, there are important benefits stemming from environmental certification. The use of a recognisable eco-label offers a competitive advantage to companies and a benefit in its public relations practices. Thus, companies aiming for greater market share pursue better environmental and/or social performance and include those concerns in the management process, possibly through the simultaneous development of an environmental management system. Moreover, consumers have at their disposal more environmentally friendly products and can consume ethically. Finally, environmental certification adds a market mechanism which reduces the necessity for a state-driven "command-and-control" process.

On the other hand, there are several drawbacks with the recent rise of such certification. The fact that they are voluntary means exactly that many companies do not actually join

such a scheme – particularly companies without an environmental management system. Moreover, costs for acquiring an eco-label are usually fixed and high (for instance, certification from the Marine Stewardship Council can cost up to US$120,000) therefore large corporations have a distinct advantage over small and medium enterprises. Furthermore, a few big certification companies have assumed a much greater market share and have come to dominate the market. Finally, it can also be argued that a rebound effect can take place, in which "ethical consuming" actually leads to more consuming of a resource, which can be detrimental even if this is harvested or grown in a more environmentally friendly way. It should be noted that in some cases certification has been granted in practices that have been accused as being controversial, for instance, with fishing krill in the Antarctic sea (Pew Environment Group 2010).

In any case, environmental certification is a necessary tool that can help the consumer make more informed choices and which steers companies towards assuming better environmental performance. It is indicative of our times that environmental certification is actually needed; in a more sustainable society, products would be environmentally friendly by definition and thus the necessity for such schemes would eventually disappear.

5 Corporate Social Responsibility

Many companies have integrated sustainability practices within a larger framework of corporate social responsibility (CSR), a set of self-regulations that a company follows and which dictate its environmental and social performance. CSR looks at the impact of a company's activities on stakeholders other than the company's shareholders. It is quite a controversial concept, as it has been regarded both as a highly beneficial aspect of a company's overall returns to society and as a form of greenwashing by which companies choose to depict certain beneficial aspects of their workings in order to atone or draw attention away from unsustainable practices.

In any case, CSR has now been established as an integral part of a business model. Virtually all multinational corporations have established CSR principles in their operations, while in many cases they pursue philanthropy which is not directly related with the company's portfolio. Examples include women empowerment schemes pursued by Nestlé, public health initiatives by Coca-Cola or capacity building in Iraq from Royal Dutch Shell. Corporations have been extremely favourable towards this particular governance approach (Hoffman and Georg 2013), mostly since they have the opportunity to dictate themselves what their responsibilities are instead of having those imposed by governmental regulation. Moreover, businesses have realised that their environmental reputation is one of the important factors shaping their image. Environmental reputation has been an element in surveys conducted by newspapers such as the Financial Times when assessing corporate reputation (DeSimone and Popoff 1997).

5.1 Sustainability Reporting

An integral part of a company's CSR practice is the reporting of its practices and their impact on the environment, society and economy. Many companies issue annual reports, aiming for higher transparency, accountability and compliance. This trend has existed for the past two decades and has led to the formation of relevant standards, such as the Global Reporting Initiative, which provides a set of norms that companies can follow in their reports. More than 5,000 companies from all over the world have adopted the Global Reporting Initiative framework, in over 30 indicators, ranging from weight of materials used up to environmental investment (Global Reporting Initiative 2011).

Similar in thought, the Carbon Disclosure Project is an organisation working with major corporations to provide a framework for the reporting of greenhouse gas emissions. The Carbon Disclosure Project holds significant leverage, since it cooperates with over 700 institutional investors, with a combined US$87 trillion held in assets, and which require the disclosure of carbon emissions in order to expose the investment's inherent risks. Over 2,000 major companies disclosed their carbon footprint through the Carbon Disclosure Project in 2008; among them 77 % of the Global 500 companies (Carbon Disclosure Project 2009).

Criticism of sustainability reporting states that its goal is mainly to improve corporate reputation by managing the impressions of stakeholders, many times providing the public with a distorted picture of the company's practices through the use of specific language and narrative structures, and is essentially a sophisticated form of greenwashing (Hoffman and Georg 2013). Others underline that such reporting has not stopped corporations from irresponsible advertising; Shaw (2008) emphasised that the concept of full disclosure challenges most forms of current advertising, since advertisements rarely depict the negative characteristics of a product or its environmental impact.

In this respect, a new form marketing is warranted: one which identifies that relentless consumption is hardly sustainable, even if goods are produced in a more environmentally friendly way. Such an approach was exemplified by the advertising campaign of the company Patagonia, through its Common Threads Initiative and its "Don't buy this jacket" advertisement. Patagonia has gone further, asking its customers to pledge that they will purchase only the amount of jackets they need (ideally just one). Such an approach steers away from the usual path of a corporation's drive to maximise its profits through selling as many products as it can.

5.2 Benefit Corporations

One of the strongest criticisms against the practice of CSR has come from Friedman (1970), who posited that businesses should aim only to increase profit for their stakeholders and that this constitutes their only social responsibility. Indeed, for the greatest part of the twentieth century, in the Unites States the corporation was legally obliged to look after its own self-interest, after the landmark ruling of Dodge v. Ford in 1919 (Sukhdev 2012). CEOs could actually be held liable if pursuing measures which detracted from the profits of a company.

This has recently changed with the advent of benefit corporations (B Corps), a new corporate form which explicitly considers public benefit in its business model. This was enabled by changes in corporate law that took place in 2010 in the state of Maryland in the USA, allowing for corporations to pursue the general public benefit and the consideration of all stakeholders in decision-making. Up until now, relevant legislation has been enacted in 12 states of the USA, while over 600 certified companies with a cumulative revenue of US$3.4 billion have registered for B Corp status (Network for Business Innovation and Sustainability 2012). Although B Corps do not have to be certified, some acquire relevant certification by non-profit organisations, such as B Lab.

The major difference between traditional CSR and a B Corp's practices is that the stated purpose of the latter is not to increase the benefits only for shareholders but for all stakeholders and for social benefit. Hence, the CEO of a B Corp can be held liable for not pursuing the company's stated environmental and social benefit goals, providing shareholders with a private right of action in such as case. B Corps are also obliged to issue an annual benefit report to the public, outlining how the company pursues social benefit. Essentially, B Corps are a reply to the accusation of greenwashing through CSR and an important option offered to companies that are genuinely interested in sustainability and have faced difficulties in linking related initiatives to increased profits (Network for Business Innovation and Sustainability 2012).

Sukhdev (2012) noted how the drive of conventional corporations to maximise their profit for shareholders while excluding other stakeholders has often led their directors to pursue practices such as externalising costs or irresponsible advertising that can be justified by their legal obligation for high short-term returns. In this respect, the legal provisions of holding liability for environmental and social performance usher a new corporate era, where business can avoid the accusation of caring mostly for corporate reputation and may let its genuine interest in the benefit of global society to shine through increased accountability and transparency.

6 Concluding Remarks

Even though corporations are extremely influential today and are arguably the most important institution of today's society (Sukhdev 2012), they do not exist in a vacuum. The systemic nature of modern society clearly indicates that corporations are embedded in a wider institutional framework, affected by national and international legislation, societal values and norms, consumer preferences and business ethics. Society's inclination towards competition rather than cooperation means that costly sustainable practices may not be adopted by corporations fearing that others, who would not pay the same costs, might assume an advantage over them. Hence, as Hoffman and Georg (2013) noted, the idea of a single company becoming greener or more sustainable is an oxymoron; wider institutional changes are needed that would facilitate a broader transition towards sustainability of the business community. It could even be argued that sustainability actually requires such a shift, particularly in way of thinking, from competition to cooperation, from growth to development and from a short-term towards a long-term approach (Daly 2005; Krosinsky and Robins 2008). This necessity was outlined by Schmidheiny (1992), who acted as the chief advisor for business and industry to the UN Secretary General during the Rio Summit and who wrote in the World Business Council for Sustainable Development publication "Changing Course" that the main reason why sustainability is accepted in principle but it's not put into practice as much is that "many of those with the power to effect the necessary changes have the least motivation to alter the status quo that gave them that power" (11). After all those years since the Rio Summit, much has changed in thought, but not that much in practice, demanding greater institutional changes.

In principle, it cannot be doubted that most serious businesses of today's world have understood the value and importance of sustainability and are trying to promote it, as they understand it. The important question to ask is what sustainability means and what it actually is (e.g. weak vs. strong sustainability). Many people talk about "sustainable business" as the set of practices that constitute that business itself sustainable, i.e. surviving in the long term. However, the science of sustainability necessitates a different approach, one that posits first and foremost prevalence to the environment: the life-support system of this planet without which no life, let alone business, can exist. Therefore, it is suggested that a sustainable business is the one which constitutes primarily the planet sustainable. In order for this to happen, the current prevalent social, political, economic and corporate structures need to understand the limits placed by the globe and that infinite growth (and therefore infinite profit) is a biophysical impossibility (Daly 2005). Based on those limits,

a set of international practices based on disclosing externalities, resource taxation, accountable advertising and limiting leverage of corporate behemoths is required, as famed economist Nicholas Stern wrote in the foreword of the book "Corporation 2020" (Sukhdev 2012). Sustainability also requires a marked reduction of today's consumption levels, within the carrying capacity of the planet, and thus a whole redesign of the modern lifestyle, which would shift the pursuit of happiness from the acquisition of material objects to more immaterial values (Grantham 2011).

Adhering solely to the triple bottom line as the primary decision-making tool in this process can be misleading, since this would mean that changes required to make the planet sustainable will not be endorsed by business when such changes also necessitate loss in profit. It cannot be doubted that there are environmentally friendly innovations which provide profits for companies; and many of the tools presented in the chapter actually deliver that. However, many of the changes required in order to transition towards a more sustainable society (such as reduced consumption in the developed world and the decrease of their ecological footprint to one planet) can actually be detrimental for business. The answer to this problem has been eloquently provided by Daly (2005) who wrote: "Free trade would not be feasible in a world having both sustainable and unsustainable economies, because the former would necessarily count many costs to the environment and future that would be ignored in the growth economies. Unsustainable economies could then underprice their sustainable rivals, not by being more efficient but simply because they had not paid the cost of sustainability" (105). The same applies for businesses.

References

Benyus, J.: Biomimicry – Innovation Inspired by Nature. HarperCollins e-books (2009)

Carbon Disclosure Project: Carbon Disclosure Project – Information Pack (2009)

Daly, H.E.: Economics in a full world. Sci. Am. **293**(3), 100–107 (2005)

DeSimone, L.D., Popoff, F.: Eco-Efficiency – The Business Link to Sustainable Development. MIT Press, Cambridge, MA (1997)

Elkington, J.: Cannibals with Forks: The Triple Bottom Line of 21st Century Business. Capstone Publishing, Oxford (1997)

Elliott, L.: The Global Politics of the Environment, 2nd edn. Palgrave Macmillan, Hampshire/New York (2004)

European Commission: Communication from the Commission to the European Parliament, the Council, the European Economic and Social Committee and Social Committee and the Committee of the Regions on the sustainable consumption and production and sustainable industrial policy action plan. http://eur-lex.europa.eu/LexUriServ/LexUriServ.do?uri=COM:2008:0397:FIN:EN:PDF (2008)

Feldman, I.: Business & industry: transitioning to sustainability. In: Dernbach, J. (ed.) Agenda for a Sustainable America. Island Press/ELI, Washington, DC (2009)

Forest Stewardship Council: FSC International Standard – FSC Principles and Criteria for Forest Stewardship (1996)

Friedman, M.: The Social Responsibility of Business Is to Increase Its Profits. *The New York Times Magazine*, 13 Sept (1970)

Global Reporting Initiative: Sustainability reporting guidelines. https://www.globalreporting.org/resourcelibrary/G3.1-Sustainability-Reporting-Guidelines.pdf (2011)

Grantham, J.: Time to wake up: days of abundant resources and falling prices are over forever. *GMO Quarterly Letter* (2011)

Hackett, S.C.: Environmental and Natural Resource Economics – Theory, Policy, and the Sustainable Society, 4th edn. M.E. Sharpe, New York (2011)

Hawken, P.: A predictor of performance. In: Krosinsky, C. (ed.) Evolutions in Sustainable Investing – Strategies, Funds, and Thought Leadership. Wiley, New Jersey (2012)

Henderson, H., Nash, T.J., Sanquiche, R.: Green Transition Inflection Point – Green Transition Scoreboard 2013 Report. Ethical Markets (2013)

Hendrickson, C.T., Lave, L.B., Matthews, H.S.: Environmental Life Cycle Assessment of Goods and Services – An Input–Output Approach. RFF Press, Washington, DC (2006)

Hoffman, A.J., Georg, S.: A history of research on business and the natural environment: conversations from the field, Introduction. In: Georg, S., Hoffman, A. (eds.) Business and the Environment: Critical Perspectives in Business and Management, vol. 1. Routledge, Oxford (2013)

Horne, R., Grant, T., Verghese, K.: Life cycle assessment – principles, practice and prospects. Csiro Publishing, Collingwood (2009)

Interface, Inc.: ReEntry 2.0. https://www.interfaceflor.com/Default.aspx?Section=3&Sub=4&Ter=18 (2013)

Jolliet, O., Cotting, K., Drexler, C., Farago, S.: Life-cycle analysis of biodegradable packing materials compared with polystyrene chips: the case of popcorn. Agric. Ecosyst. Environ. **49**(3), 253–266 (1994)

KPMG: Raw material scarcity and its impact on business. http://www.kpmg.com/NL/nl/IssuesAndInsights/ArticlesPublications/Documents/PDF/Consumer-Markets/Raw-material-scarcity-def.pdf (2012)

Krosinsky, C., Robins, N.: Sustainable Investing: The Art of Long-Term Performance. Earthscan, London (2008)

Lancaster, M.: Green Chemistry – An Introductory Text. Royal Society of Chemistry, Cambridge (2010)

Lubin, A.D., Esty, D.C.: The sustainability imperative. In: Krosinsky, C. (ed.) Evolutions in Sustainable Investing – Strategies, Funds, and Thought Leadership. Wiley, New Jersey (2012)

Marine Stewardship Council: MSC Fishery Standard – Principles and Criteria for Sustainable Fishing (2010)

Martenson, C.: The Crash Course – The Unsustainable Future of Our Economy, Energy and Environment. Wiley, New Jersey (2011)

McDonough, W., Braungart, M.: Cradle to Cradle: Remaking the Way We Make Things. North Point Press, New York (2002)

Müller-Kraener, S.: Partnerships as an instrument to implement the Johannesburg policy targets. In: Streck, C., Witte, J.M., Benner, T. (eds.) Progress or Peril? Networks and Partnerships in Global Environmental Governance – The Post-Johannesburg Agenda. Global Public Policy Institute, Berlin/Washington, DC (2003)

Network for Business Innovation and Sustainability: B Corporations, Benefit Corporations and Social Purpose Corporations: Launching a New Era of Impact-Driven Companies (2012)

Oakdene Hollins Ltd.: Remanufacturing in the UK: A Significant Contributor to Sustainable Development? The Resource Recovery Forum, Skipton (2004)

Pew Environment Group: Pew faults Marine Stewardship Council's decision. Press Release, 25 May 2010. http://www.pewenvironment.org/news-room/press-releases/pew-faults-marine-stewardship-councils-decision-8589935217 (2010)

Schmidheiny, S.: Changing Course – A Global Business Perspective on Development and the Environment. The MIT Press, Cambridge (1992)
Shaw, W.H.: Business Ethics. Thomson Wadsworth, Belmont (2008)
Social Investment Forum Foundation: 2010 Report on Socially Responsible Investing Trends in the United States (2010)
Stern, N.: Stern Review on the Economics of Climate Change; UK Government Economics Service. HM Treasury, London (2006)
Sukhdev, P.: Corporation 2020 – Transforming Business for Tomorrow's World. Island Press, Washington, DC (2012)
Winston, A.: Top 10 green business stories of 2011. *Bloomberg*, 20 Dec (2011)
Zhang, W., Zhang, D., Fan, T., Gu, J., Ding, J., Wang, H., Guo, Q., Ogawa, H.: Novel Photoanode Structure Template from Butterfly Wing Scales. Chem. Mater. **21**(1), 33–40 (2009)

Grid/Cloud Computing as New Paradigm for Collaborative Problem Solving and Shared Resources Management in Environmental Sciences

Z. Heilmann, G.P. Deidda, G. Satta, A. Vargiu, L. Massidda, and M. Marrocu

Abstract

Cloud computing is establishing worldwide as a new high-performance computing paradigm that offers formidable possibilities to industry and science. In this chapter, we discuss the impact of this paradigm change to scientific research. After introducing the basic concepts of cloud computing and discussing briefly the recent technological developments that led to its emergence, two cloud computing portals are presented as examples for a trend that will drastically change the way in which scientific research will be done in the future. We will discuss and exemplify why a cloud computing science portal offers, besides the obvious advantages over locally installed software packages such as computing power and storage capacity, completely new possibilities for scientific research, collaboration, education, and presentation of reproducible results.

Keywords

Cloud computing • Real-time data analysis • Remote collaboration • Mesoscale weather forecasting • Fire forecasting • CFD models • OpenFOAM • Seismics • Multi-offset GPR • Near surface • CRS stack • Residual static corrections • Velocity model building • Time migration

1 Introduction

Environmental scientists are concerned with multidisciplinary problems that incorporate various scales in space and time. Doing, for instance, an extreme weather condition forecast on a local scale, meteorologists use data from regional studies to define a background from which the initial model and boundary conditions can be derived. Similarly, regional weather forecasts use global atmospheric models. In the same way short-time weather predictions with high temporal resolution use long-time forecasts as background. Analogous considerations hold also, e.g., for hydrogeological studies, seismological risk management and monitoring of pollution on land and in the seas. But it is not only the different scales that are interwoven; environmental problems are seldom described by a single scientific discipline. For instance, a hydrogeological study might also include meteorological models, geological and geophysical data, and geographic information. The Earth must be seen as holistic system, and therefore, the collaboration between scientists in different places and from different disciplines is useful and necessary. The grid/cloud computing paradigm was developed during the last two decades as an answer to these challenges, to facilitate collaboration and sharing of data, means, methods, and results.

A second important factor that triggered this development was the sheer amount of available data and its continuously improving quality. Today the size of datasets and the computational demand for creating and analyzing them increased

Z. Heilmann (✉) • G. Satta • A. Vargiu • L. Massidda • M. Marrocu
Energy and Environment Sector, CRS4, Center for Advanced Studies, Research, and Development in Sardinia, Cagliari, Italy
e-mail: zeno.heilmann@crs4.it

G.P. Deidda
Department of Civil and Environmental Engineering and Architecture, University of Cagliari, Cagliari, Italy

G. Cao and R. Orrù (eds.), *Current Environmental Issues and Challenges*,
DOI 10.1007/978-94-017-8777-2_16,

dramatically. While in the year 2000 datasets of some hundreds of megabytes were a typical size, we work with terabytes of data today. The current limit for datasets that still can be managed and processed in a reasonable time lies in the order of exabytes. Scientific fields where this limit was reached are, for instance, meteorology, genomics, connectomics, complex physics simulations, and biological and environmental research (Reichman et al. 2011). The main reasons why datasets and especially environmental data grew so much are the ubiquitous mobile information-sensing devices, aerial sensory technologies (remote sensing), software logs, cameras, microphones, radio-frequency identification readers, and wireless sensor networks (Hilbert and López 2011). According to IBM, every day, 2.5 quintillion bytes of data is created—so much that 90 % of the data in the world today has been created in the last 2 years alone. For this so-called big data, big data platforms are needed that are often shared by multiple private and/or governmental organizations.

Even though also the computing power of supercomputers has increased from teraflops as used at the end of the last century to petaflops today, this increase could not keep pace with the increase of data and storage. However, the even faster increase of network connectivity could compensate for this. Research centers and universities in all parts of the world are today interconnected with fast broadband Internet connections.

For environmental science, i.e., mainly public and governmentally funded research, sharing of computing resources, applications, and storage is the natural solution that reflects the scale and complexity of the posed problems and the need for holistic solutions. The huge advances in network and communication technology that have been achieved so far strongly support this kind of effort. Over the last decades network performance doubled every 9 months, resulting in an improvement of six orders of magnitude within the last 17 years (Foster 2002). Since the exponential increase of storage capacity (doubling time 12 months) and in particular of computing power (doubling time 18 months) was falling behind the development in communication bandwidth, spatially distributed computation and storage grids became more and more attractive. As a consequence, grid computing emerged in both early 1990s as the most efficient answer to the global challenges of the twenty-first century that are threatening both natural environment and human society (Cossu et al. 2010; Hoffa et al. 2008). The basic idea was to create a distributed computing infrastructure able to provide computation in a similar way as electrical power or water is provided today. Ten years later, cloud computing emerged, mainly driven by the rise of virtualization technology, utility computing, and the fast evolution of commercial web services, as the successor of the so far coexisting standards: concurrent, parallel, distributed, and grid computing (Udoh 2011). Hashemi and Bardsiri (2012) define cloud computing as a model for enabling ubiquitous and convenient on-demand network access to a shared pool of configurable computing resources that can be allocated and released with minimal management effort. Apart from the historical development, it is difficult today to draw a clear line between grid and cloud computing. According to Hoffa et al. (2008), they became today indistinguishable from each other.

The main fields of applications of grid/cloud infrastructures are as follows: science portals, distributed computing, large-scale data analysis, computer in a loop instrumentation, and collaborative work (Foster 2002). In the following, two examples will be presented, both developed under the GRIDA3 project (Murgia et al. 2009; Lecca et al. 2011) and follow-up initiatives. The first example describes an innovative approach to real-time seismic data processing for near-surface imaging, based on combining open-source state-of-the-art processing software and cloud computing technology that allows the effective use of distributed computation and data management with administratively distant resources. We will discuss how user-side demanding hardware and software requirements can be substituted by remote access to high-performance cloud computing facilities. As a result, data processing can be done quasi in real time, being ubiquitously controlled via the Internet by a user-friendly web-browser interface. To demonstrate the functionality of this portal, we will present processing results for two different types of data obtained from seismic reflection- and multi-offset ground-penetrating radar experiments.

The second cloud computing portal presented in this chapter consists in an integrated system for weather and wildfire propagation forecast. The service may be used by the authorized personnel of fire-fighting units as an aid to coordinate their actions during an emergency, as a tool for training of personnel, and to provide scenarios that can be used for prevention activities. As an example for the application of this portal, we show the simulation of a real wildfire that has caused severe damage and compare the results with the effects of the real event. Another promising example from geoscience was recently published by Versteeg and Johnson (2013). Finally, in the conclusion, we will evaluate the completed tasks and discuss future developments.

2 GRIDA3: A Shared Resources Manager for Environmental Data Analysis and Applications

The GRIDA3 (shared resources manager for environmental data analysis and applications) project was started in 2006 as a multidisciplinary research project funded by the Italian Research Ministry. The goal was to develop an integrated

grid computing environment able to deliver solutions to current environmental challenges that serves for a wide range of users, from decision makers without technological expertise to technical and scientific experts. The main idea was to manage the complexity and size of environmental systems by setting up a single web portal that allows integration and sharing of data, skills, and human know-how; high-performance computing (HPC) resources, sensors, and instrumentation; and scientific applications for simulation, inversion, and visualization over multiple sites across federated domains. The target applications are restoration of polluted sites, sustainable use of natural resources, real-time imaging of near-surface structures, high-precision forecast of extreme meteorological events, and real-time forest fire simulation. From the user point of view, the GRIDA3 portal (http://grida3.crs4.it) constitutes the entry point from where users can access different grid-empowered science sub-portals. Its web pages are built on Web 2.0 technology interacting with the grid computing framework EnginFrame that provides a simple to use, efficient, and stable infrastructure to access grid computing resources via the Internet. The EnginFrame environment acts as an agent between web server and middleware, here the load sharing facility (LSF), and fulfills tasks like user authentication/authorization, monitoring of hardware resources, control of actions like data up- and download, execution and monitoring of jobs, and gathering and transformation of results into formats required on the client side. Application interfaces can be tailored to the specific users' skills or access rights permitting access and control to computing and engineering resources. Intuitive, standard-compliant web-browser-based user interfaces are built from service definition files that follow customizable XML schemata. Thanks to the use of advanced web widgets specifically designed for computing- and data-intensive activities, applications can be controlled in a user-friendly and effective way, preserving user productivity even when handling complex tasks. Summing up, the technological objective of the GRIDA3 portal is—following the distributed information system paradigm—to provide authorized users that are part of a system of virtual organizations a transparent, easy, and safe access point to cloud/grid computing and storage facilities, sensors, databases, and scientific software.

The grid-enabled web applications span over five domains:

- AGISGRID, dealing with the development of a series of applications based on GIS (geographic information system) technologies
- AQUAGRID, focused on subsurface hydrology and water resources management
- BONGRID, related to remediation and monitoring of contaminated sites
- EIAGRID, enabling geophysicists to perform real-time subsurface characterization in the field by on-the-fly seismic data processing
- PREMIAGRID, centered on atmospheric modeling, offering a wide range of services for weather forecast and climate studies at regional scale

Each tool was implemented using previously developed stand-alone applications. Porting these applications to the cloud/grid environment shifted the user interaction from a single desktop to a collaboratively used web-based HPC system. This made it on the one hand necessary to adopt the core algorithm to the use of a massive parallel environment as far as this was not already done and on the other hand to dedicate attention to an appropriate design of the user interaction with the portal, particularly in view of multi-user collaboration and sharing and implementing a fine-grained access policy for different user groups and virtual organizations. The experience with different kinds of applications and their specific needs gave also impulses for new features and further development of EnginFrame, e.g., for interacting with environments and tools for building spatially enabled Internet applications (MapServer, msCross) and databases (PostgreSQL). Regarding the multi-user management, it was important to consider different user experience levels, such as guest, standard, and expert users, when designing user interfaces and possible workflows users might perform, depending on the type of input/output data and on the actions allowed for a user category. The graphical user interface (GUI) elements offered by EnginFrame can be customized and combined via XML scripts that describe, e.g., actions represented by calls to external scripts written in XML, Perl, shell, or Java through which input parameters are read and commands related to the requested service are executed. For more complex services, auxiliary Java files are called that define specific features like including descriptive figures into the input parameter fields, choosing dates from a pop-up calendar, or displaying a progress bar for file uploading. Parallel job execution on the cloud/grid environment is managed by the middleware LSF and implemented by including LSF commands for job management into the executable instructions that launch the applications. Using LSF under EnginFrame enables useful features such as displaying the job evolution or cluster load directly in the browser. As a result of the project, the ability of EnginFrame for use in science portals was demonstrated and improved by applying it to the field of earth sciences, and some of the features requested by application porting have been finally integrated in the stable release of EnginFrame. In the following section, we will briefly summarize the technologies that were necessary to build GRIDA3.

2.1 The GRIDA3 Hardware Infrastructure

The system architecture of the GRIDA3 hardware infrastructure comprises a complex set of technologies that can be structured in four layers:

1. *Computing, storage, net connections, and basic services systems*. The computing system consists of a low-latency grid of three tiny Linux PC clusters with 70 quad-core nodes in total, interconnected at 2 Gbit/s. A high-speed storage, based on a distributed file system, is directly connected to the grid, sharing the same network switch. Backup and snapshot management are connected to medium-speed storage. The basic services on this level consist of user authentication and authorization, web servers, and security.
2. *Grid management*. It is performed by the commercially supported grid portal EnginFrame. The main building blocks of EnginFrame are services, defined by an XML representation of computing-related facilities such as a seismic-imaging application or a query to the load sharing facility, e.g., to find pending jobs. The use of pluggable server-side XML services allows the decoupling of the current grid environment and the grid computing framework and enables easy integration of common workload schedulers.
3. *Applications level*. It contains the set of scripts and configuration files required to run the different applications hosted on the portal.
4. *Web user interaction*. Thanks to intuitive Web 2.0 interfaces, the end users manage their computing and engineering resources via a web browser. The technology complexity of the lower levels is completely hidden from the end user.

Accessing a service of the GRIDA3 web portal, a registered end user can log in on the web site generated by the EnginFrame server and browse service offerings and documentation as on a normal web site. He or she can monitor jobs and computing resources status, select services from the left-side frame, and interact with the selected service, e.g., upload data from remote, insert parameters, select input files, or submit jobs and view or download the job output. After the service is executed, the results are collected in a spooler zone, a system scratch area, private to the user which allows him to browse and download output files.

3 EIAGRID Portal for Real-Time Imaging of Seismic and GPR Data

The basic idea that led to the development of the EIAGRID cloud computing portal for real-time imaging of seismic and GPR data is depicted in Fig. 1. In-field processing, equipment is substituted by remote access to high-performance grid computing facilities which can be controlled by a user-friendly web-browser interface from the field using a wireless Internet connection. For the development, it was necessary to focus on two main aspects: the geophysical applications hosted on the portal and the computing framework in which these applications were embedded. Even though EIAGRID started as a grid computing portal, we will use in the following the terms grid and cloud synonymously. At the current state of development, the portal can be classified as a private cloud that provides software as a service (SaaS). With an increasing number of users and hosted applications, it could evolve to a community cloud providing a platform as a service (PaaS) for geophysical studies.

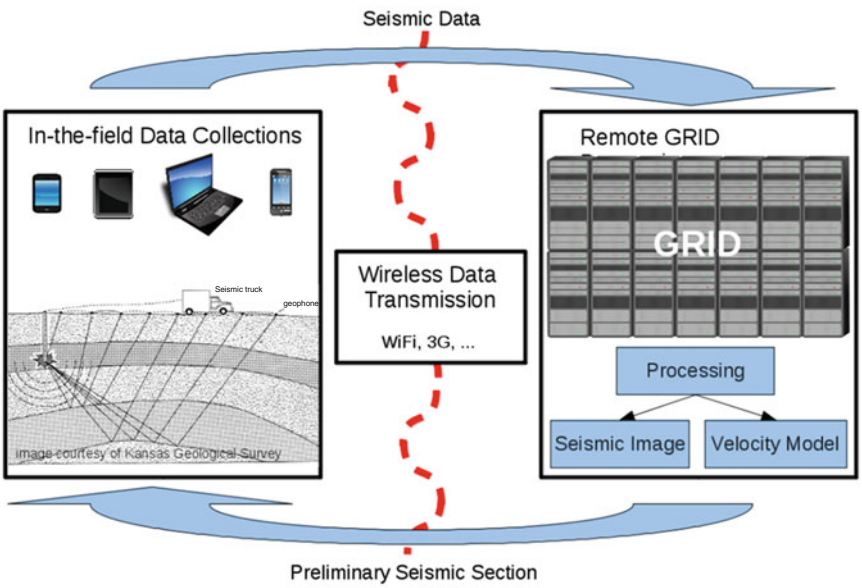

Fig. 1 Main scheme of the cloud computing service: in-field processing equipment is substituted by remote access to high-performance grid computing facilities which can be controlled by a user-friendly web-browser interface even from the field using a wireless Internet connection

3.1 Reflection Methods for Subsurface Imaging

In order to make aim, scope, and functionality of the EIAGRID portal more transparent to readers from other fields of environmental sciences, a brief introduction in the fundamentals of seismic reflection imaging will be given in the next three sections. There, we will discuss how the data is acquired, which preprocessing steps it has to undergo before entering the imaging phase, and what imaging methods are used to produce a structural image of the subsurface together with important subsurface properties as needed by many kinds of environmental, geotechnical, hydrogeological, and archaeological studies. We use the example of reflection seismics for this introduction but want to point out that EIAGRID and the presented methods are also valid for multi-offset ground-penetrating radar (GPR) data. The main difference between these methods is the type of waves that are used to probe the subsurface and thus also the source and receiver technology. GPR uses high-frequency (~1 to 1,000 MHz, usually polarized) radio waves generated by an emitting antenna and transmitted into the subsurface. There, waves are reflected or diffracted by buried objects or boundaries with different dielectric constants. That part of the wavefield that finally reemerges at the surface is recorded by receiving antennas. The principles involved are similar to reflection seismology, except that electromagnetic energy is used instead of elastodynamic energy and reflections appear at boundaries with different dielectric constants instead of acoustic impedances. Electromagnetic waves used for GPR have a much smaller wavelength and therefore a higher resolution power (~0.01 to 1 m) but also a smaller penetration depth (~0.1 to 25 m) than the different types of elastodynamic waves used for reflection seismic surveys (resolution power ~1 to 25 m and penetration depth ~10 to 10000 m).

3.1.1 Seismic Data Acquisition

The first seismic reflection survey in history was carried out near Oklahoma City, USA, on the 4th of June in the year 1921 (Brown 2002). Since that time, seismic exploration methods have been highly evolved, and seismic data acquisition is carried out all over the world—on land as well as at sea. For marine surveys, 3D acquisition has become standard, routinely applied by the oil industry. On the open sea, sources and receivers can be distributed without problems on the measurement surface, resulting in a 5D multi-coverage[1] dataset from which a 3D image of the subsurface structure can be produced. Just to give an idea on the dimensions, in the year 2013, the multiclient data library of PGS, a big geophysical service company, covered 425,000 km^2 of 3D and 294,000 km of 2D data. For land seismics, data acquisition is in general more demanding due to topography, housing, infrastructure, etc., and thus, 2D surveys, where sources and receivers follow a line and a 2D cross section of the subsurface is produced, are still frequently applied, particularly for environmental projects. The cloud computing portal presented in the following is limited to this 2D case. Therefore, also our introduction is confined to this case. A future update of the presented cloud portal services to 3D is straightforward, and 3D versions already exist for all the implemented 2D applications.

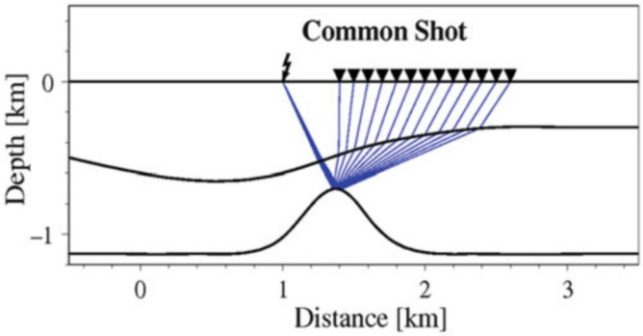

Fig. 2 Common shot experiment. A common shot (*CS*) gather contains all traces that have one and the same shot coordinate in common. The rays depicted in *blue* are transmitted by the first and reflected by the second interface (Figure according to Höcht 2002)

Moving-coil electromagnetic geophones that sense particle velocity or acceleration in vertical direction (P-waves) or horizontal direction (S-waves) are usually employed as receivers in land seismic acquisition. The seismic source on land is usually either a sledgehammer, an explosive planted in a borehole, a seismic shotgun, or Vibroseis, a vibrating mechanism mounted on a heavyweight.

Typically, for a reflection seismic survey, hundreds (2D) to tens of thousands (3D) of seismic source events, so-called shots, are generated. The typical geometry of a single shot experiment is depicted in Fig. 2. Each shot emits seismic energy into the subsurface that is partly transmitted and partly reflected at velocity/density discontinuities. The reflected energy which finally reaches the surface is then recorded at different distances from the source by receivers called geophones that transform ground movement or pressure into an electrical voltage. The amplitudes of this voltage, representing the subsurface response at a receiver location in a certain moment, are recorded in a time series called seismogram or trace. All traces of a certain shot use the time of the source event as reference time zero. For 2D acquisition the data can be represented by a 3D data cube, e.g., with the axes: shot coordinate, shot–receiver distance, and time. As we will see in the following, for processing, it is often preferable to use another coordinate system where the

[1] The subsurface is illuminated under a multitude of different angles.

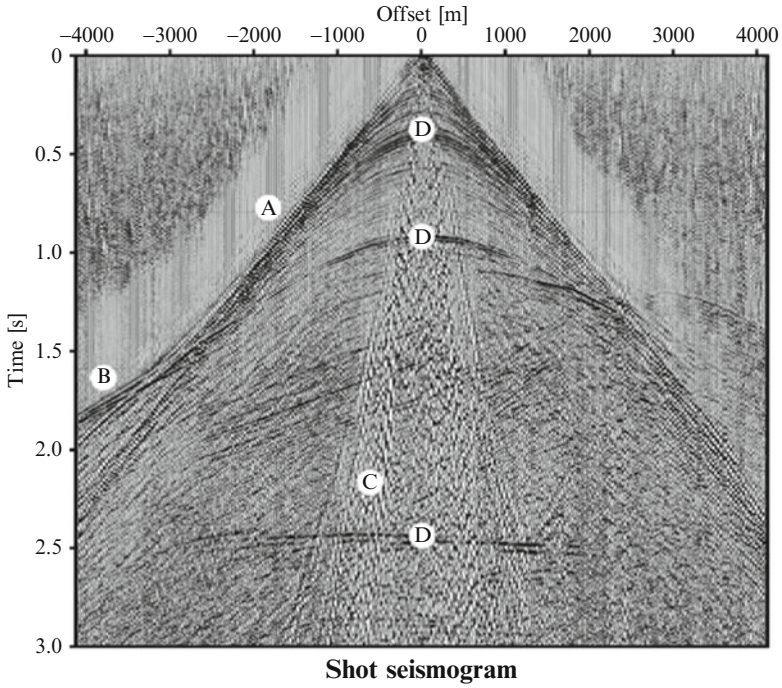

Fig. 3 Shot gather extracted from a land seismic dataset. In addition to the reflection events (some of them marked by the letter *D*), various other kinds of events can be observed, e.g., the direct wave (*A*), head wave (*B*), and ground roll (surface waves) (*C*) (Figure according to Mann et al. 2004)

traces are sorted with respect to the midpoint position x_m of shot and receiver and half-offset h, i.e., half of the distance between shot and receiver.

3.1.2 Preprocessing

Before an acquired dataset can enter the processing phase (imaging/inversion), it is subject to many preprocessing steps. Initially, it contains a multitude of different wave types. For seismic reflection imaging, only primary body waves of a specified wave mode, usually compressional waves (P-waves), but sometimes also shear waves (S-waves), are considered as signal.

All other wave types including multiply reflected waves (multiples), surface waves, refracted waves, converted waves, and often also primary reflections of other wave modes are treated as coherent noise. In addition, the data contains also incoherent noise, i.e., random noise, caused, for instance, by traffic, industry, or wind shaking of trees. Examples for some of the different kinds of coherent and incoherent noise can be seen in the shot seismogram depicted in Fig. 3.

Generally speaking, the main issue of every seismic-imaging workflow is, besides the imaging itself, the removal of all components of the data which are not intended to be imaged. The first step in this direction is the preprocessing phase during which:

- Geometry information is assigned to the traces, and bad traces, e.g., resulting from a corrupted receiver, are zeroed out.
- Small traveltime(s) are muted, which are not expected to be related to reflection events.
- Deconvolution[2] is applied to increase the temporal resolution. During a predictive deconvolution, reverberations or short-period multiple reflections are removed from seismic traces by applying a prediction-error filter.
- Band-pass filtering is used to suppress noise that lies outside the expected signal bandwidth.
- A dip filter serves to remove coherent noise in the f–k domain, since such events can often be distinguished by their much steeper traveltime-versus-offset dip.
- Trace balancing is applied to correct for amplitude variations along the line caused, e.g., by varying geophone ground coupling and changing near-surface conditions.
- Field static corrections compensate the influence of the topography and the weathering layer as far as possible.

For a more comprehensive list of preprocessing steps, we refer the reader to Yilmaz (1987). In practice seismic preprocessing is cumbersome and detail-laden. The applied corrections typically vary with respect to location within the survey area, source event, source–receiver offset, and time within the seismic trace. As a result, the seismic processor must usually perform a tedious analysis of the dataset to select appropriate parameter values for every processing operation.

[2] According to the *convolutional model* (Robinson and Treitel 1980), a recorded seismic trace can be seen as the convolution of the Earth's reflectivity function, a series of spikes representing reflectors, with a wavelet, i.e., the source signal (assumed to be stationary).

3.1.3 Seismic Imaging/Data Processing

Generally speaking, the final aim of seismic reflection imaging is to obtain a depth image of the subsurface from the time-domain multi-coverage prestack data. This process can be roughly divided into two principal tasks:

- *Stacking*, i.e., suitable summation of the recorded prestack data with the purpose to reduce its amount for further processing and to use its inherent redundancy to attenuate incoherent noise. Assuming a perfect summation of all seismic energy that stems from the same reflection point in depth, the signal-to-noise ratio can theoretically be improved by a factor of $\sqrt{N}$ (Yilmaz 1987), where N is the number of contributing traces. Aside from improving the signal-to-noise ratio, the illumination of one and the same subsurface point by many different experiments is necessary to obtain information about the wave propagation velocity that provides the link between traveltime and distance.
- *Migration*, i.e., a transformation of the time-domain records to a depth-domain image by placing reflections at the correct reflector positions and focusing diffractions at the associated diffraction points. An intermediate process is the so-called time migration where the reflected energy is represented in time but at a location where a diffracted (image) ray would emerge vertically at the surface. Besides a view exceptions (e.g., Mann 2002; Bonomi et al. 2012), virtually all time/depth migration procedures demand at least the knowledge of an initial macro-velocity model. In contrast to the short-wavelength velocity variation which gives rise to the recorded seismic reflection events, this model can be thought of as representing the long-wavelength component of the true subsurface velocity distribution. Information about the velocity model is obtained from the seismic data itself, together with existing geological information.

The order in which stacking and migration are applied is not fixed. On the one hand, it is possible to stack the data in the time domain and to apply the migration afterward (poststack migration). On the other hand, the migration can be applied first, before the migrated data is stacked (prestack migration). In practice, both approaches are closely interrelated since the information used to build an initial macro-velocity model for migration is usually obtained by stacking in the time domain. Since no depth axis has to be introduced, a time-domain velocity model which is far easier to obtain than its depth-domain counterpart suffices for the time-migration process.

Various migration methods exist, but most of them are based on the assumption that each reflection point in the subsurface can be treated as a diffraction point. Utilizing a known macro-velocity model, the associated diffraction operator is calculated analytically, by ray tracing or by finite-difference methods, and all seismic energy along this operator is summed up. In other words, a summation over all possible reflections at the common-reflection-point (CRP) is carried out, with the assumption that only the true reflection will constructively contribute to the summation result and that everything else will be subject to destructive interference. Under this assumption, prestack migration theoretically provides the best possible image of the subsurface. Practically, the required velocity model is not known a priori. It has to be derived from an initial model by means of iterative application of prestack migration itself and sophisticated methods to update the velocity model until the migration result is consistent with the data.

In order to separate the summation of amplitudes from the migration, which requires a velocity model, a macro-velocity model-independent stacking approach can be deployed. In the ideal case the stacking process would have to identify and sum up all amplitudes related to one and the same reflection point in depth. In other words, the stack would have to be applied along the so-called CRP trajectories. However, a strict identification of the CRP trajectories and their associated reflection points in depth is generally impossible as the exact velocity distribution of the subsurface would need to be known. A pragmatic solution to solve this problem is to employ an approximate description of the CRP trajectories by parameterizing them in such a way that the parameters can be directly determined from the prestack data. Doing this allows a summation of the amplitudes pertaining to a certain reflector point performed directly in the prestack data.

The depth location of the reflection points remains unknown and, thus, subject to a subsequent migration algorithm, whereas the offset dependency of the reflection traveltime(s) associated with a single CRP then provides the information needed for the construction of a velocity model, apart from borehole measurements and geological a priori knowledge. The parameterization of the CRP response should make as little assumptions as possible regarding the subsurface structure but involve only a reasonable number of free parameters. Furthermore, a sound physical interpretation of these parameters should exist. Such a space–time adaptive, data-driven approach for stacking and migration in the time domain is used by the EIAGRID portal that will later be presented in detail. Here we will have a brief look at the fundamentals on which the methods implemented in EIAGRID are built. The classical but still frequently used approach for stacking and velocity analysis is the common-midpoint (CMP) stack, an early predecessor of the common-reflection-surface (CRS) stack used in EIAGRID. The CMP stack method introduced by Mayne (1962) was a breakthrough in the early days of seismic data processing. In these times, the available computing power was still very limited. Therefore, the parameterization of reflection events used for stacking had to be as simple as possible. Mayne

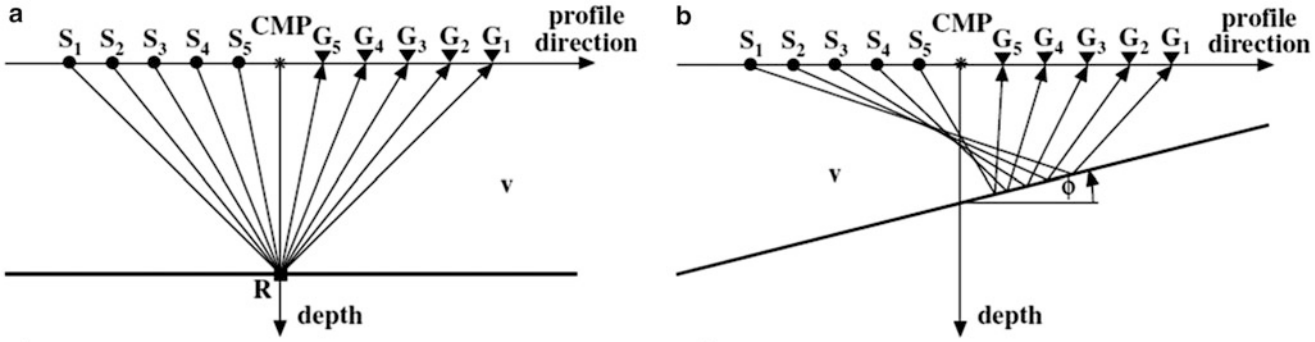

Fig. 4 Common-midpoint geometry. (**a**) CMP geometry for a horizontal reflector. (**b**) CMP geometry for a dipping reflector. In (**a**) the model consists of a single horizontal reflector embedded into two constant velocity layers. All rays associated with one CMP location illuminate the same subsurface point. In (**b**) a single dipping reflector separates two constant velocity layers. In this case, the CMP experiment illuminates more than one subsurface point (reflection point dispersal) (Figure was taken from Müller 1999)

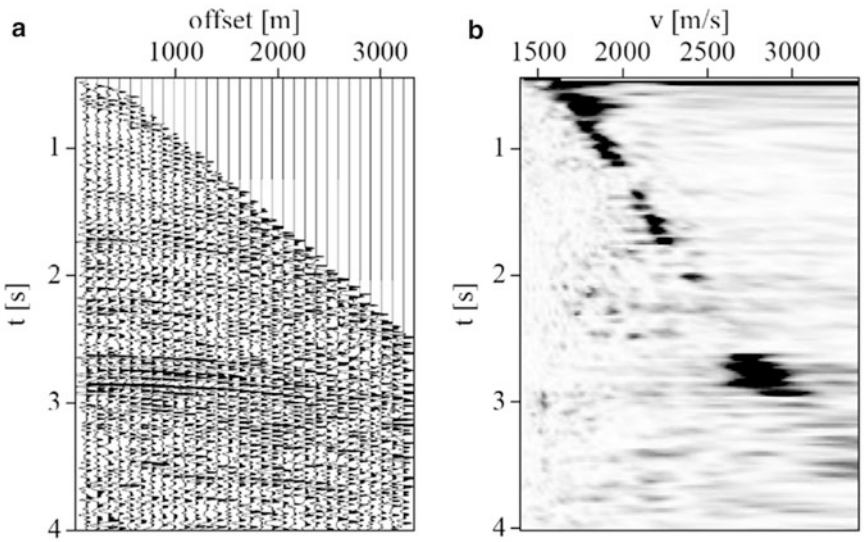

Fig. 5 Stacking velocity analysis. (**a**) Muted CMP gather. (**b**) Velocity spectrum. Semblance values are plotted as a function of ZO traveltime and NMO velocity. Maxima (*dark*) correspond to reflection events in (**a**) (Figure was taken from Duveneck 2004)

assumed a horizontally layered medium, where the reflection events measured on different traces in a CMP gather stem from a CRP in the subsurface located directly beneath the CMP location (see Fig. 4a).

For a horizontal reflector over a homogeneous layer, the reflection response of a CRP is exactly described by the equation

$$t^2(h) = t_0^2 + \frac{4h^2}{v_{\mathrm{NMO}}^2}. \qquad (1)$$

This hyperbolic equation is parameterized by a single parameter, the so-called normal moveout (NMO) velocity, which is for such a simple medium equal to the root-mean-square (RMS) velocity. Such a simple geometry is of course not always met. If the reflector dip is not zero, it comes to reflection point smearing as shown in Fig. 4b, degrading the lateral resolution of the stacking result.

For CMP processing, a time-dependent NMO velocity function is created for every CMP gather (or a representative subset) by interpolating the NMO velocities detected for the most prominent reflection events. The latter is done using the so-called semblance spectra that display for every time sample and for every velocity value within a certain range the coherence between moveout prediction and measured data (see Fig. 5). Normally, handpicked maxima of these spectra provide the searched-for NMO velocities.

If only a subset of CMPs was used, the CMP velocity functions need to be laterally interpolated to perform the NMO correction of the complete multi-coverage data. During this process, the offset-dependent reflection times are corrected to the corresponding ZO reflection time which is related to the configuration depicted in Fig. 6. After NMO correction, reflection events recorded on different traces of a single CMP gather should be flat and sum up constructively when stacked in offset direction. The result is a single trace

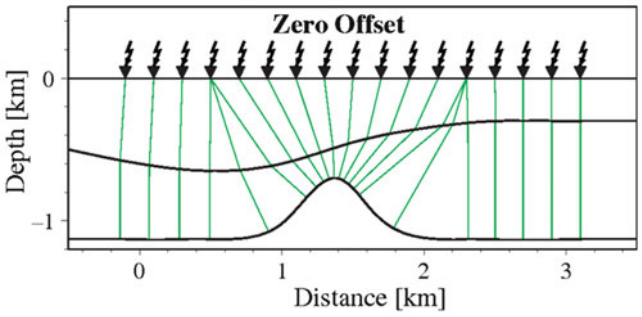

Fig. 6 In zero-offset configuration, the single experiments have coincident shot and receiver locations, a geometry that is very favorable for interpretation but not practical for seismic experiments. Standard GPR data acquisition uses this configuration (Figure according to Höcht 2002)

per CMP with a signal-to-noise ratio that is much higher than that of the initial prestack traces. In other words, the prestack dataset is replaced by a much smaller poststack dataset of much higher signal quality.

Later, Levin (1971) added a correction term to Eq. (1) to consider plane reflectors with dip Φ:

$$t^2(h) = t_0^2 + \frac{4h^2 \cos^2 \Phi}{v_{\mathrm{NMO}}^2}. \qquad (2)$$

However, this correction removes only the influence of the dip on the velocity but does not remove the reflection point dispersal itself.

Nowadays, the so-called dip moveout (DMO) correction (see, Deregowski 1986; Hale 1991) is applied to precondition the data for CMP processing. This process can be seen as a partial migration with the aim to remove the influence of the reflector dip from the prestack data in such a way that the reflection response of a CRP is again located within the CMP gather—as in case of a non-dipping reflector. This is done for a specific ZO traveltime by summing up for each offset the contributions of all possible dips along the DMO operator and putting the result into the CMP gather. This is justified by a similar assumption as used by prestack depth migration and many other migration methods: it is assumed that only the amplitudes along the true CRP trajectory will result in a constructive summation of signal, whereas the summation along the remaining trajectories will be subject to destructive interference of noise. A drawback of such a "blind" stack approach is that no explicit knowledge of reflector dips is obtained that could later complement the NMO velocity information. DMO processing has greatly extended the accuracy and usefulness of the CMP method. While oil exploration seismics is shifting more and more to imaging workflows based on prestack depth migration, the workflow NMO/DMO/stack plus poststack migration has remained the workhorse in environmental science for its robustness and low hardware requirements.

4 EIAGRID Project

During the last two decades, the successful employment of seismic reflection surveys using P- or S-wave data has been reported for many engineering, geotechnical, environmental, and hydrogeological studies (e.g., Goforth and Hayward 1992; Woorely et al. 1993; Ghose et al. 1998; Liberty 1998; Benjumea et al. 2003; Guy et al. 2003; Bradford et al. 2006; Pugin et al. 2009). In a quite similar way, multi-offset ground-penetrating radar (GPR) surveys have demonstrated their great potential for imaging archaeological targets, geological stratigraphy, and hydrogeological structure of shallow and ultra-shallow subsurface regions (e.g., Berard and Maillol 2006, 2008; Booth et al. 2008; Perroud and Tygel 2005; Goodman et al. 2011). These developments were going hand in hand with improvements in instrumentation and acquisition methods. As a result, the acquisition both of seismic data and of multi-offset GPR data got much more economic in view of instrumentation cost and required field work (see, e.g., Van der Veen et al. (2001), Sambuelli et al. 2001; Pugin et al. 2009). Nevertheless, reflection seismics and multi-offset GPR are still not considered as standard tools in the abovementioned fields even though these high-resolution imaging methods can provide very useful results. In our opinion there are two main reasons for this.

With respect to the stacking velocity analysis and the residual static corrections, the following considerations could be drawn. For shallow and ultra-shallow surveys, seismic velocities have large and often unpredictable variations (Miller and Xia 1998 and references given therein). Velocity changes of an order of magnitude can happen within only a few meters of vertical or horizontal displacement. Huge changes of velocity are typically encountered at the interface between bedrock and overlying sediments as well as at the separation between the unconsolidated part of the vadose zone and the underlying saturated zone (Birkelo et al. 1987; Miller and Xia 1997). The searched-for normal moveout (NMO) velocities are integral values that depend on all the layers above the reflector under consideration. Therefore, depth acts as a smoothing filter, and NMO velocities in several hundred or thousand meters of depth vary much smoother than for shallow and ultra-shallow surveys where target depth lies between a few meters and a few hundred meters. Residual static corrections are usually considered to be surface consistent and thus independent of target depth. Nevertheless, we find a higher static shift-to-dominant-period ratio in shallow and ultra-shallow surveys. Obtaining a good stack section, correctly interpretable from both structural and stratigraphic points of view, depends much on the detail with which velocity analysis and residual static corrections are carried out. Carefully analyzing velocity spectra for every

single CMP gather is a very time-consuming and usually the most expensive processing step for shallow seismic imaging. In addition, severe stretch muting, as required by conventional NMO correction techniques to avoid stretch-related artifacts, can harm seriously the signal-to-noise ratio, and more sophisticated methods require much time commitment (Miller and Xia 1998; Brouwer 2001; Masoomzadeh et al. 2010).

Acquisition parameters such as maximum offset, source spacing, receiver spacing, recording time, sampling interval, or source energy must be chosen with respect to the aim of the survey but also with respect to the a priori often unknown surface and subsurface conditions encountered at the site at the day of acquisition. Above all, temporal changes of the soil moisture can have a significant influence on near-surface data (Jefferson et al. 1998). Despite the large improvements in acquisition technology, finding the optimum acquisition parameters remained a difficult task that requires much experience and intuition. Till this day, in-field processing equipment able to do real-time data analysis and imaging directly in the field is mostly unavailable for near-surface studies. The reasons for this are, besides the economic constraints and the brief acquisition time frames, also the aforementioned near-surface specific difficulties for processing. Often, only the raw traces can be displayed by the recording device, and a trial-and-error adjustment of acquisition parameters in the field is not possible. If days later, when the data is finally processed, the results turn out to be disappointing because a crucial acquisition parameter was chosen wrong, the whole acquisition campaign has to be repeated or considered as a failure. For this reasons the development of real-time data processing tools for the field was anticipated by environmental geophysicists and engineers for a long time (see, e.g., Steeples et al. 1997).

In hydrocarbon exploration, where reflection seismic surveys always have been the standard high-resolution imaging tool, these problems are less severe due to the larger target depth, acquisition time frame, and budget that allow for the use of recording trucks equipped with powerful in-field processing hardware. The presented grid computing portal aims at reducing these problems also in near-surface applications and to support in this way a broader use of seismic reflection profiling and multi-offset GPR surveys.

4.1 Web Portal

The primary objective of the EIAGRID computing portal was to emulate, according to the scheme depicted in Fig. 1, heavy and expensive in-field processing equipment by a cloud computing solution that requires just a simple laptop or PC that is connected via the Internet to a cloud of high-performance computing resources. Besides this, the portal serves as a platform for sharing and remote collaboration that can be useful not only for data acquisition but also on a much broader scope. A user-friendly web-browser interface provides secure and transparent access for a group of authorized users, displays the status of the computing resources, allows the creation of projects, and—most important—controls a set of advanced visualization and processing tools. For mobile use a fast wireless Internet connection is required to upload the raw data and to ensure a smooth functioning web interface. The need for time-consuming human interaction is minimized by the implementation of computationally intensive but highly data-driven algorithms. For the parallelized applications, the huge available computing power allows to reduce processing times significantly. Furthermore, the grid deployment permits the parallel testing of alternative processing sequences and parameter settings, a feature which considerably shortens the time needed to obtain the final results.

The hosted applications were selected with the objective to construct typical 2D time-domain seismic-imaging workflows as used for shallow and ultra-shallow applications. For data visualization and preprocessing, we chose the free software package Seismic Un*x provided by the Colorado School of Mines (Cohen and Stockwell 2000). We ported tools for trace balancing, amplitude gaining, muting, frequency filtering, dip filtering, deconvolution, and image rendering as services on the cloud computing portal, each one with a customized choice of options. For structural imaging and velocity analysis, we developed a grid version of the common-reflection-surface (CRS) stack (see, e.g., Jäger et al. 2001; Mann 2002; Heilmann 2007). This data-driven imaging method can largely benefit from the hardware parallelism provided by the cloud deployment due to its high level of automation. CRS-based residual static corrections (Koglin et al. 2006) are calculated as a by-product of the stack and can be applied in an iterative way. Besides a simulated zero-offset section of high signal-to-noise ratio, also a coherence section and three stacking parameter sections are obtained. The latter provide the input for the estimation of a smooth time-migration velocity model. As a final imaging step, a parallelized prestack time-migration scheme reverses the effects of wave propagation in order to transform the preprocessed data into an image which resembles shape and location of the geological interfaces better than a simulated zero-offset section. We chose time migration because it is far less sensitive to velocity errors than depth migration. The resulting time-migrated image is still defined in the space–time domain, but diffraction events are collapsed to points and triplications are transformed to synclinal structures.

Processing can be done step-by-step or using a graphical workflow editor that can launch a series of pipelined tasks. The status of the cluster and of submitted jobs is monitored by dedicated services. An example for viewing the status of

ID	Project	Time	Status		Host	Name
161699	g3zeno	Aug 12 18:57		RUN	stria15	EIAGRID:MOptimization
161692	g3zeno	Aug 12 18:57		RUN	stria05	EIAGRID:MOptimization
161697	g3zeno	Aug 12 18:57		RUN	stria07	EIAGRID:MOptimization
161695	g3zeno	Aug 12 18:57		RUN	stria10	EIAGRID:MOptimization
161688	g3zeno	Aug 12 18:57		RUN	stria08	EIAGRID:MOptimization
161701	g3zeno	Aug 12 18:57		RUN	stria08	EIAGRID:MOptimization
161689	g3zeno	Aug 12 18:57		RUN	stria06	EIAGRID:MOptimization
161690	g3zeno	Aug 12 18:57		RUN	stria13	EIAGRID:MOptimization
161702	g3zeno	Aug 12 18:57		RUN	stria13	EIAGRID:MOptimization
161691	g3zeno	Aug 12 18:57		RUN	stria01	EIAGRID:MOptimization
161693	g3zeno	Aug 12 18:57		RUN	stria02	EIAGRID:MOptimization
161694	g3zeno	Aug 12 18:57		RUN	stria09	EIAGRID:MOptimization
161696	g3zeno	Aug 12 18:57		RUN	stria12	EIAGRID:MOptimization
161698	g3zeno	Aug 12 18:57		RUN	stria16	EIAGRID:MOptimization
161700	g3zeno	Aug 12 18:57		RUN	stria04	EIAGRID:MOptimization
161703	g3zeno	Aug 12 18:57		PEND		EIAGRID:catfiles_Opt
161704	g3zeno	Aug 12 18:57		PEND		EIAGRID:OptVelocities
161705	g3zeno	Aug 12 18:57		PEND		EIAGRID:optstack.pdf
161706	g3zeno	Aug 12 18:57		PEND		EIAGRID:optcoher.pdf
161707	g3zeno	Aug 12 18:57		PEND		EIAGRID:optangle.pdf
161708	g3zeno	Aug 12 18:57		PEND		EIAGRID:optVnmo.pdf
161709	g3zeno	Aug 12 18:57		PEND		EIAGRID:allcrsresults.pdf
161710	g3zeno	Aug 12 18:57		PEND		EIAGRID:MOptimization2
161711	g3zeno	Aug 12 18:57		PEND		EIAGRID:ResidualStaticCorrection
161528	g3zeno	Aug 12 18:22		DONE	stria15	EIAGRID:prepare
161534	g3zeno	Aug 12 18:22		DONE	stria12	EIAGRID:MCMPstack
161537	g3zeno	Aug 12 18:22		DONE	stria10	EIAGRID:MCMPstack
161532	g3zeno	Aug 12 18:22		DONE	stria09	EIAGRID:MCMPstack
161535	g3zeno	Aug 12 18:22		DONE	stria16	EIAGRID:MCMPstack
161533	g3zeno	Aug 12 18:22		DONE	stria13	EIAGRID:MCMPstack

Fig. 7 *My Jobs* view of the grid portal, showing 15 jobs that are currently running (*yellow*), 9 jobs that are pending (*gray*), and 6 jobs that are already done (*green*)

the submitted jobs is depicted in Fig. 7 that shows the *My Jobs* view after starting the CRS stacking service. Under *My Data*, all imaging results, stored in the project spooler as image files, can be downloaded or viewed directly in the browser. Processing results are stored in permanent storage folders as data files that can be chosen as input for successive processing steps.

4.2 Services

In the following, we will discuss the principal services provided by the portal: data upload and format conversion, data visualization, data preprocessing, stacking, residual static correction, velocity model estimation, and time migration.

4.2.1 Data Upload

A typical seismic 2D survey is carried through by applying a multitude of the so-called common shot experiments. The portal allows uploading the recorded data to the remote computing facilities immediately after each shot. Using the web-browser-based graphical user interface, a single shot gather or the complete range of shots can be uploaded, preprocessed, processed, and visualized while the acquisition still takes place (see Fig. 8). Particularly for the wireless data upload, high-speed 3G networks using UMTS (Universal Mobile Telecommunications System) or HSUPA/HSDPA (High-Speed Uplink/Downlink Packet Access) protocols are required. Supported data formats are SEGY and SEG2. At any stage of the data collection, newly uploaded shot gathers can be concatenated with those that were already on the server, creating a new dataset ready to be processed.

4.2.2 Visualization and Preprocessing

For GPR and seismic reflection imaging, accurate preprocessing has much influence on the reliability of the final subsurface image. During data acquisition a basic

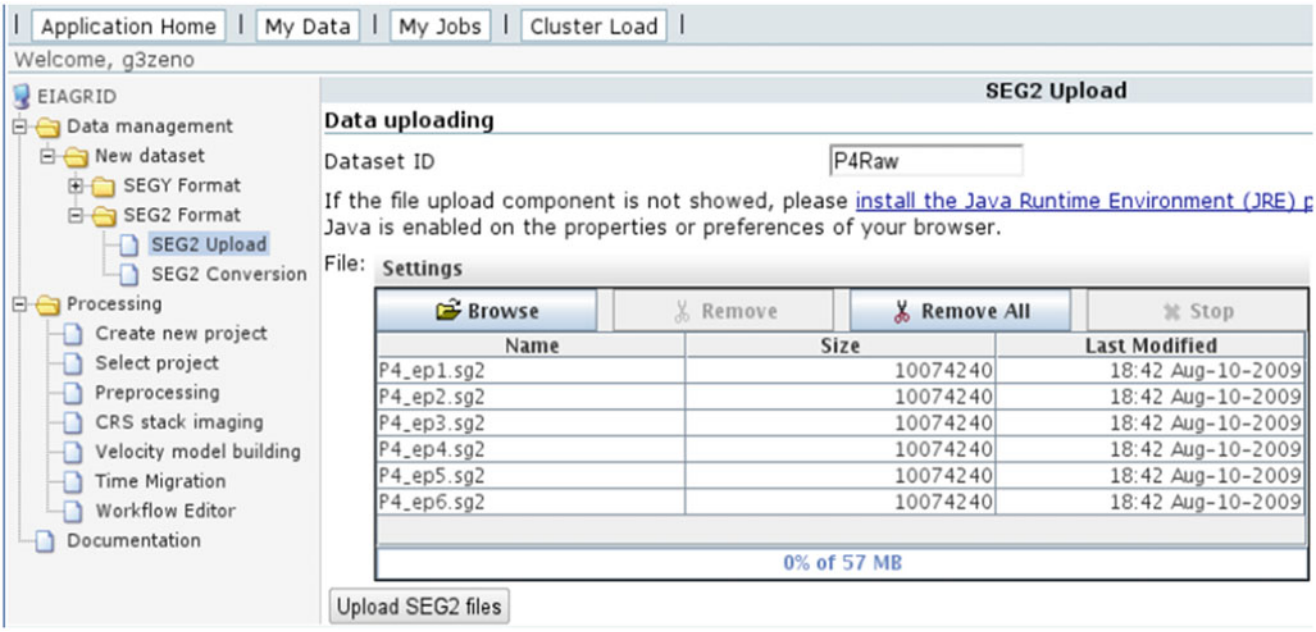

Fig. 8 Simultaneous upload of several shot gathers in the SEG2 format

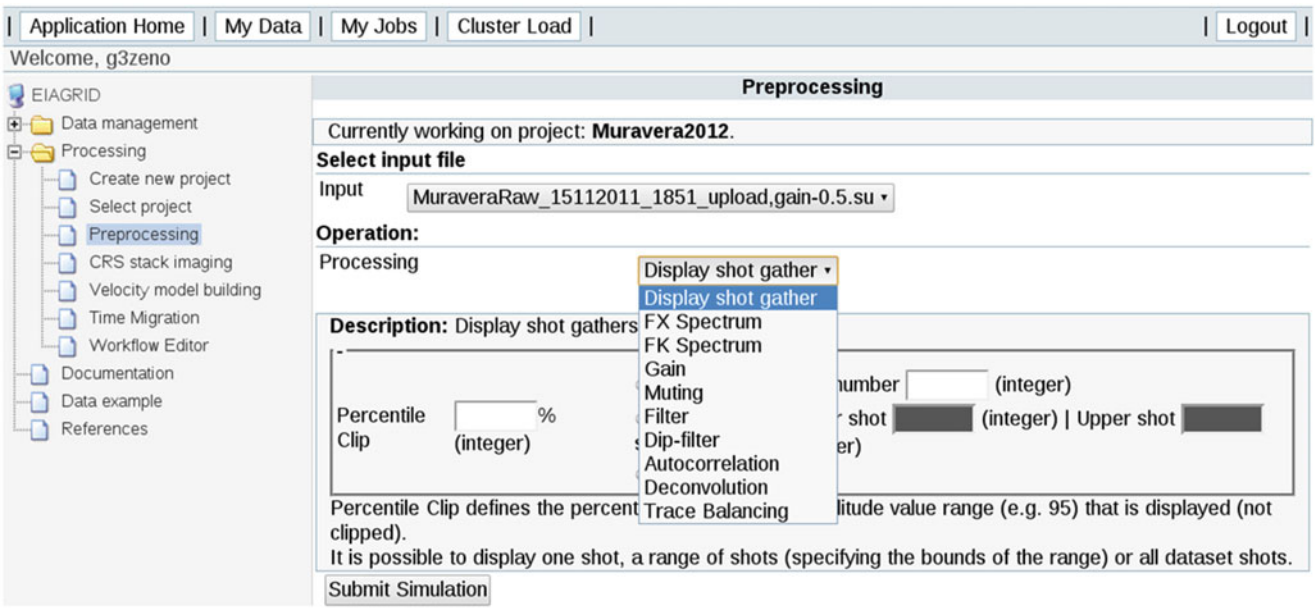

Fig. 9 Tools for data preprocessing and visualization. The output of the previous process (*Gain*) can be viewed (*Display shot gathers*) and used as input for the next process (e.g., *Filter*) to conduct a complete preprocessing workflow

collection of preprocessing tools with a limited choice of parameter settings is usually sufficient for a quality control (QC) of the acquired data. For the visualization and preprocessing services, we chose the applications of the free software package Seismic Un*x. This package features a multitude of data visualization, manipulation, and processing tools that are applied via command line in a Unix-like manner. We included a small subset of these tools with a customized choice of options into the EIAGRID GUI (see Fig. 9). In this way the following preprocessing tasks can be performed conveniently from any device that supports a web browser:

- Visualization of shot gathers, frequency–, frequency–wavenumber–, and autocorrelation spectra
- Muting, e.g., early arrivals not related to reflection events
- Application of a time-dependent gain function, e.g., to remove the effect of spherical divergence
- Trace amplitude balancing, e.g., to correct for variations along the line

- Band-pass filtering, e.g., to suppress the noise that lies outside the signal bandwidth
- Dip filtering in the f–k domain, e.g., to suppress ground roll or air blast
- Deconvolution to increase the temporal resolution and/or to remove reverberations and short-period multiple reflections

4.2.3 CRS Stack-Based Imaging

The graphical user interfaces for *CRS stack imaging* (including residual static corrections), as well as for *velocity model building* and *time migration*, are very similar to the one of *preprocessing*. The user has to choose one of the existing input data files and fill the field for the process parameters before he or she can press the Submit Simulation button. Shortly after, the *My Jobs* view will open and display the status of the submitted job and its subprocesses, as displayed in the example given in Fig. 7.

4.2.4 CRS Stack and Velocity Analysis

To date, many examples of 2D and 3D CRS stack applications in the field of oil and gas exploration have been reported from both academic and industrial research teams for many different areas of this world (e.g., Mann et al. 1999; Bergler et al. 2002; Heilmann et al. 2006; Prüssmann et al. 2008). Besides the generation of a simulated zero-offset section of high resolution and signal-to-noise ratio, also residual static corrections can be obtained from CRS results (Koglin et al. 2006; Heilmann et al. 2006), and valuable input for velocity model building is provided (Perroud and Tygel 2005; Heilmann 2007; Prüssmann et al. 2008). We believe that the CRS method offers a great potential also for shallow and ultra-shallow seismic reflection imaging. To justify this argument, we will briefly review the main concepts and principles behind CRS stacking and discuss basic processing parameters that are important for our field data examples. For a more extensive and profound description of the CRS stack method in general and its various target-specific extensions (e.g., rough topography, common offset, vertical seismic profiling, prestack data enhancement), other sources in literature are available (e.g., Müller 1998; Jäger et al. 2001; Höcht 2002; Mann 2002; Bergler et al. 2002; Hertweck et al. 2007; Heilmann 2007; von Steht 2008; Baykulov et al. 2011).

The CRS method is based on a generalized velocity analysis and stacking procedure. In case of 2D data, a three-parameter stacking surfaces is employed to obtain a simulated zero-offset section. The stacking process is not confined to single CMP gathers (stacking in offset direction), but it also includes neighboring CMPs (stacking in midpoint direction). The stacking aperture is the so-called CRS supergathers that covers all traces which contain energy reflected from a certain common reflector segment in depth centered at the theoretical reflection point of the zero-offset ray. Different to the normal moveout (NMO) or normal moveout/dip moveout (NMO/DMO) methods (Deregowski 1986; Yilmaz 1987), which assume to approximate reflection traveltime(s) a planar horizontal (NMO) or a planar dipping (NMO/DMO) reflector segment, the CRS method assumes a reflector segment of arbitrary dip and curvature including diffraction points and planar reflectors. For a more detailed comparison between these conventional methods and CRS, see Hertweck et al. (2007). The hyperbolic CRS traveltime operator is defined by the following approximation:

$$t^2(x_m,h) = \left[t_0 + \frac{2\sin(\alpha)(x_m - x_0)}{v_0}\right]^2 + \frac{2t_0\cos^2\alpha}{v_0}\left[\frac{(x_m - x_0)^2}{R_{\mathrm{N}}} + \frac{h^2}{R_{\mathrm{NIP}}}\right], \quad (3)$$

where x_m and h are the midpoint and half-offset coordinates, respectively. The summation result is placed in the zero-offset section at the point $(x_0,\ t_0)$, which represents traveltime and emergence point of the zero-offset (or central) ray, i.e., the ray reflected at the center of the common reflection segment. The three stacking parameters in Eq. (3), α, R_{NIP}, and R_{N}, are the emergence angle of the zero-offset ray and the two wavefront curvatures of the theoretical eigen-waves denoted as normal incident point wave and normal wave (Hubral 1983; Jäger et al. 2001). These kinematic wavefield attributes are determined automatically from the prestack data by means of coherence analysis. Finally, v_0 denotes the near-surface velocity in x_0. This a priori information does not influence the stack itself but provides the link between the searched-for reflection traveltime surface and the physical interpretation of the stacking parameters, α, R_{NIP}, and R_{N}.

The use of a spatial stacking operator increases the number of contributing traces which allows the use of sparser surveys without loss in imaging quality (Gierse et al. 2009) and/or a more stable velocity analysis and higher signal-to-noise ratio, particularly for very shallow, strongly curved, or steeply dipping reflectors. The data-driven implementation determines independently for every zero-offset sample $(x_0,\ t_0)$ those three stacking parameter values that maximize the coherence of the prestack data along the stacking operator given by Eq. (3). Semblance is used as coherence measure (Neidell and Taner 1971). As a result, time-consuming human interaction in prestack velocity analysis such as manual picking in velocity spectra can be avoided as well as the detrimental stretching effects that result on the traces from conventional NMO correction (Mann and Höcht 2003). The latter allows to use larger offset ranges for velocity analysis and stack, and thus, a better signal-to-noise ratio can be expected.

For CRS stacking, a spatial definition of the stacking aperture is required. In practice, the choice of the right stacking apertures is crucial as it substantially affects the lateral resolution and signal-to-noise ratio. The software used for our portal is based on the *CRS stack version 4.7* (see Mann 2002) but includes several additional features such as residual static corrections, redatuming, and the support of rough top-surface topography (see Heilmann 2007). It employs a tapered traveltime-dependent stacking aperture of elliptic shape in the midpoint/offset plane with user-defined half axes given by a midpoint aperture for $h = 0$ and an offset aperture for $x_m = x_0$. This choice accounts for the approximate nature of the CRS operator, which is a hyperbolic approximation of a second-order Taylor expansion of the reflection traveltime centered at $h = 0, x_m = x_0$. By default the software creates two stacked sections, one that corresponds to the user-defined aperture and one that corresponds to a midpoint aperture that is an approximation of the projected Fresnel zone W_F calculated from the stacking parameters and the estimated dominant period T of the source wavelet (for details see Mann 2002) according to the formula

$$\frac{W_F}{2} = |x_m - x_0| = \frac{1}{\cos\alpha}\sqrt{\frac{v_0 T}{2\left|\frac{1}{R_N} - \frac{1}{R_{NIP}}\right|}}. \qquad (4)$$

If velocity information is needed for other tasks such as poststack and/or prestack migration, time-to-depth conversion, and/or geotechnical site characterization, it can be obtained from the kinematic wavefield attributes that are determined for each stacking operation through coherence (semblance) analysis on the prestack data. As, e.g., shown by Perroud and Tygel (2005), this process fully replaces the traditional CMP velocity analysis and allows to substitute the 1D Dix velocity conversion (Dix 1955) with a 2D tomographic inversion approach (Duveneck 2004).

4.2.5 Residual Static Correction

The estimation of surface-consistent residual static corrections is part of the CRS stack implementation. Usually, several iterations of stacking and residual static corrections have to be applied to obtain optimum results. The algorithm to estimate the static time shifts is based on a maximization of the stack power, similar to the super-trace cross-correlation method of Ronen and Claerbout (1985). The cross-correlations between stacked pilot traces and measured prestack traces are performed within the moveout-corrected CRS supergathers. The moveout correction makes use of the previously obtained wavefield attributes. Due to the spatial extent of the stacking operator, such a supergather contains many neighboring CMP gathers. For each supergather, corresponding to a specific zero-offset location, the moveout correction will, in general, be different. Since each prestack trace is included in many different supergathers, it contributes to far more cross-correlations than in methods using individual common shot or common receiver gathers. The cross-correlations of the stacked pilot trace and the moveout-corrected prestack traces are summed for each shot and receiver location. This summation is performed for all supergathers contained in the specified target zone. The searched-for residual time shifts which are finally used to correct the prestack traces are associated with the maxima in the cross-correlation stacks and can be extracted in different ways (see Koglin et al. 2006). Here we take 30 % of the global or local maximum closest to a zero time shift as minimum threshold and take the center of the area that exceeds this threshold as the estimated time shift. Furthermore, more than 50 cross-correlations have to contribute to a cross-correlation stack for the time shift to be applied. For the next iteration of residual static correction, the entire attribute search and stacking process is repeated, now using the corrected prestack dataset.

4.2.6 Velocity Model Estimation

Time-migration velocity v_{tm} can be calculated from the CRS attributes, according to Mann (2002):

$$v_{tm}^2 = \frac{2v_0^2 R_{NIP}}{2R_{NIP}\sin^2\alpha + v_0 t_0 \cos^2\alpha}. \qquad (5)$$

Besides the stack, coherence, and NMO velocity section, a time-migration velocity panel is created by the portal as default output. The latter is used by the velocity model building service for creating a smooth time-migration velocity model by means of an iterative 2D smoothing and regularization algorithm which fills the gaps between reflections where no reliable wavefield attributes and thus no time-migration velocity can be obtained. The algorithm is fast and highly automated. Only a coherency threshold to discriminate unreliable attributes and an initial time-migration velocity range have to be specified. For the first iteration, all low-coherency gaps in the previously obtained time-migration velocity section are filled with a 1D gradient model based on the user-given velocity range. The resulting velocity model is smoothed using the Seismic Un*x command *smooth2* that smooths uniformly sampled 2D arrays in a user-defined window, via a damped least square technique. To make it more simple for the user, the window size is set by default to ten grid points in time and space direction. For the next iteration, the gaps between reliable velocity values on reflection events are filled by the result of the previous iteration. After a sufficiently large number of iterations ($n > 100$), the gaps are filled with a two-dimensional inhomogeneous

Table 1 CRS stack processing parameters used for the Muravera (Cagliari, Italy) and the Larreule (France) datasets

Processing parameter	Muravera (Cagliari, Italy)	Larreule (France)
CRS stacking	5 iterations	Single run
Near-surface velocity	1,700 m/s	6,500 cm/μs
Average wavelet frequency	100 Hz	120 MHz
Minimum NMO velocity	1,800 m/s	6,500 cm/μs
Maximum NMO velocity	2,800 m/s	8,500 cm/μs
Maximum allowed deviation from gradient velocity model	20 %	30 %
Minimum offset aperture	30 m	200 cm
Maximum offset aperture	245 m	650 cm
Minimum offset time	0.02 s	0.02 μs
Maximum offset time	0.25 s	0.08 μs
Minimum midpoint aperture	10 m	100 cm
Maximum midpoint aperture	50 m	400 cm
Minimum emergence angle	−70°	−80°
Maximum emergence angle	70°	80°
Residual static correction	5 iterations	Not applied
Minimum time for window	0.16 s	0.02 μs
Maximum time for window	0.7 s	0.10 μs
Maximum time shift per trace	5 ms	3 ns

The time variant search and stacking apertures in offset and midpoint direction (see Mann 2002) are defined by the time window between *minimum offset time* and *maximum offset time* during which the offset aperture increases linear from *minimum offset aperture* to *maximum offset aperture*. The midpoint aperture increases linearly between *minimum midpoint aperture* and *maximum midpoint aperture* for the entire recorded time range. Furthermore, for the residual static correction, a cross-correlation time window is specified by *minimum time for window* and maximum time for window together with the *maximum time shift per trace*

velocity distribution that fits well to the velocities picked at the events. For a more accurate velocity model building approach, it would have been necessary to move before the regularization the zero-offset time-migration velocity values to the apex location of the corresponding diffraction operator (see, Spinner and Mann 2005), i.e., the origin of a so-called image ray that emerges vertically at the surface (Hubral and Krey 1980). We omitted this step since time migration is anyway less sensible to velocity model errors than depth migration and results in well-focused images even for a roughly approximated velocity model.

4.2.7 Time Migration

For the prestack time-migration service, we chose a parallelized implementation, described in Spinner (2007), which employs the so-called straight-ray assumption to calculate analytically the approximate diffraction traveltime surface of a scattering point in the subsurface using a double-square-root equation. It assumes a medium that can be described by an effective velocity above each scatterer. This approach leads on the one hand to significant savings in computational time since no ray tracing is needed but is on the other hand less general than time-migration schemes that utilize complex non-hyperbolic operators in order to account for ray bending (see Robein 2003 and references given therein). Since our current velocity model building approach cannot resolve velocity distributions that are laterally strongly heterogeneous, the straight-ray assumption is sufficient for our purpose. Furthermore, this implementation calculates for each zero-offset location from the previously obtained CRS results an optimum migration aperture, which corresponds to the projected Fresnel zone, centered at the stationary point, where migration operator and reflection event are tangent.

4.3 Data Examples

In the following we will present two real-data examples for which a detailed description of survey, geological setting, processing results, and their interpretation was published in Perroud and Tygel (2005) and Deidda et al. (2006), respectively. The aim of these examples is to demonstrate the ability of the presented grid computing portal to obtain results close to the published ones, which were obtained with much more elaborate and time-consuming methods. We do not want to repeat the published results here; instead we would like to invite the reader to conduct his or her own comparison. The processing parameters that we used for stacking these two datasets are displayed in Table 1. Another test that we successfully concluded with an ultra-shallow S-wave dataset (see, Deidda et al. 2012) is omitted here for the sake of brevity. So far we used preexistent data, but we will soon have the occasion to use the portal also directly during data acquisition.

4.3.1 P-Wave Dataset from Muravera (Cagliari, Italy)

The seismic reflection survey used for the first test was conducted in the Flumendosa River Delta, close to the

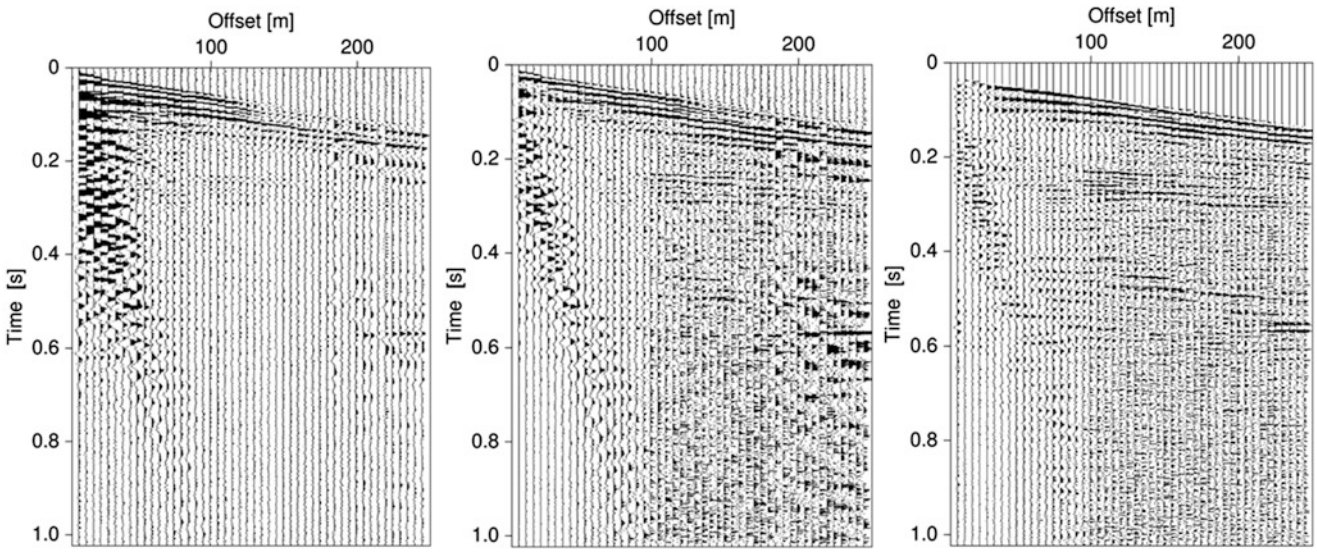

Fig. 10 Shot gather no. 77 of seismic data recorded in the Flumendosa delta close to Muravera (Cagliari, Italy). Before preprocessing (*left*), after application of gain and trace balancing (*middle*), and after dip filter, deconvolution, band-pass filter, muting, and residual static corrections (*right*)

South Sardinian town of Muravera (Cagliari, Italy). As described in Deidda et al. (2006), P-wave data was recorded using explosive sources along two seismic lines, both approximately 1.1 km long. The acquisition area lies only a few meters above the sea level, and the topography is flat with a maximum variation of ±0.5 m. The data was acquired using single 50 Hz geophones attached to a 48-channel seismograph system with 18 bit recording capability. The sample interval was 0.5 ms and the record length 1,024 ms. A 50 Hz low-cut filter with 24 dB/octave roll-off helped to attenuate the ground roll, while a standard common-midpoint (CMP) roll-along technique in an end-on configuration with 48 active geophones was employed for data recording. The 0.25 kg explosive sources were buried at approximately 2 m depth. With a few exceptions, all source locations lay below the groundwater table. Geophone spacing of 5 m and source spacing of 10 m provided twelvefold CMP coverage with a CMP spacing of 2.5 m. The maximum source–receiver offset of 245 m was chosen to allow the determination of stacking velocities for reflections from a depth of about 200–300 m, which was expected to be the depth of the bedrock surface. Because topography was flat, only residual static corrections were calculated and applied. We use here the data of line 1 that has a total size of 35 MB.

Starting from the raw seismograms, we applied trace balancing by dividing all amplitudes by the RMS amplitude value of the respective trace and spherical divergence correction by multiplying the amplitudes with the square root of the traveltime. To attenuate air wave and ground roll components, a dip filter rejecting phase velocities between 250 and 500 m/s and a trapezoidal band pass with the corner frequencies 30, 50, 270, and 300 Hz were applied. Finally, a deconvolution served to eliminate ringing and to reduce the temporal extent of the wavelet. To give an example of the data quality and the different preprocessing steps applied, a single shot gather is depicted in Fig. 10 in three states of preprocessing.

Similar to the conventional processing described in Deidda et al. (2006), five iterations of surface-consistent residual statics with a maximum allowable shift per iteration of ±5 ms were applied to improve the continuity of the events. The cross-correlation stacks for the source locations 100–150 and a time window of ±5 ms are displayed in Fig. 11 for the original data (a) and the data after five iterations of residual static corrections (b). In Fig. 12, the CRS stack section obtained for the Muravera (Cagliari, Italy) data is depicted. Figure 13 shows the migration velocity model created from the CRS stack results by extracting and regularizing attribute values on events with a coherence larger than 0.25. Even though this process runs sequentially on a single node, it took just half a minute. Figure 14 shows the prestack time-migration results for the Muravera (Cagliari, Italy) data. Using 20 cores it took less than 1 min to obtain this result.

Both the stacked and the migrated sections we obtained with EIAGRID agree quite well with the ones obtained in the original work (Deidda et al. 2006). However, there are some stratigraphic and structural features that appear less clearly imaged. For instance, the bowtie features (crossing reflections) are to some extent unresolved. In addition, in some parts of the sections, the shallowest reflection shows a very ringing character. To understand these differences, one has to note that great importance was given to processing rapidity; as a consequence, a rough and not shot record-oriented preprocessing was carried out, unable to address

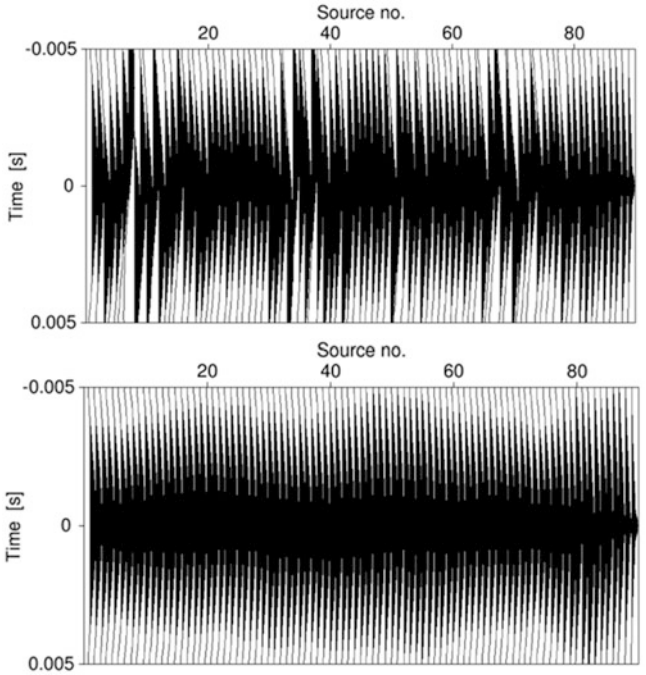

Fig. 11 Cross-correlation stack for the source locations for a P-wave dataset from Muravera (Cagliari, Italy). For the original data (*top*), the maxima are not centered at 0 ms but indicate residual static time shifts. The data after five iterations of residual static corrections (*bottom*) does hardly show any remaining residual statics. Similar pictures were obtained for the receiver positions

noise and signal variations along the line as well as to effectively improve S/N ratio. Thus, the quick-and-dirty preprocessing strongly impacts both CRS stack and time migration and constitutes the main reason for the differences. The minor processing-related reasons are a mixing of reflection events with small discontinuities caused in some locations by too large midpoint aperture and artifacts caused by poorly resolved conflicting dips (Deidda et al. 2012; Garabito et al. 2012). However, the main subsurface structures, and in particular the bedrock surface, appear so well imaged as to quickly detect the primary and somewhat surprising result highlighted in Deidda et al. (2006): a maximum bedrock depth twice as deep as expected. This demonstrates clearly the pressing need for in-field real-time data analysis and imaging. Concerning data acquisition, the wrong depth of the bedrock, assumed to set up the far offset, did not allow to estimate stacking velocities with the accuracy needed to do seismic data migration well or simply to do the time-to-depth conversion correctly. Besides, Deidda et al. (2006) also noticed the closeness of the bedrock dipping reflector to the section ends, which was a further problem for seismic imaging.

4.3.2 Ground-Penetrating Radar Dataset from Larreule (France)

As a second data example, we present results of the reprocessing of a multi-offset GPR dataset recorded close to Larreule (France) for which detailed results are presented in Perroud and Tygel (2005). The authors of this publication kindly provided to us the dataset as a test case for multi-offset

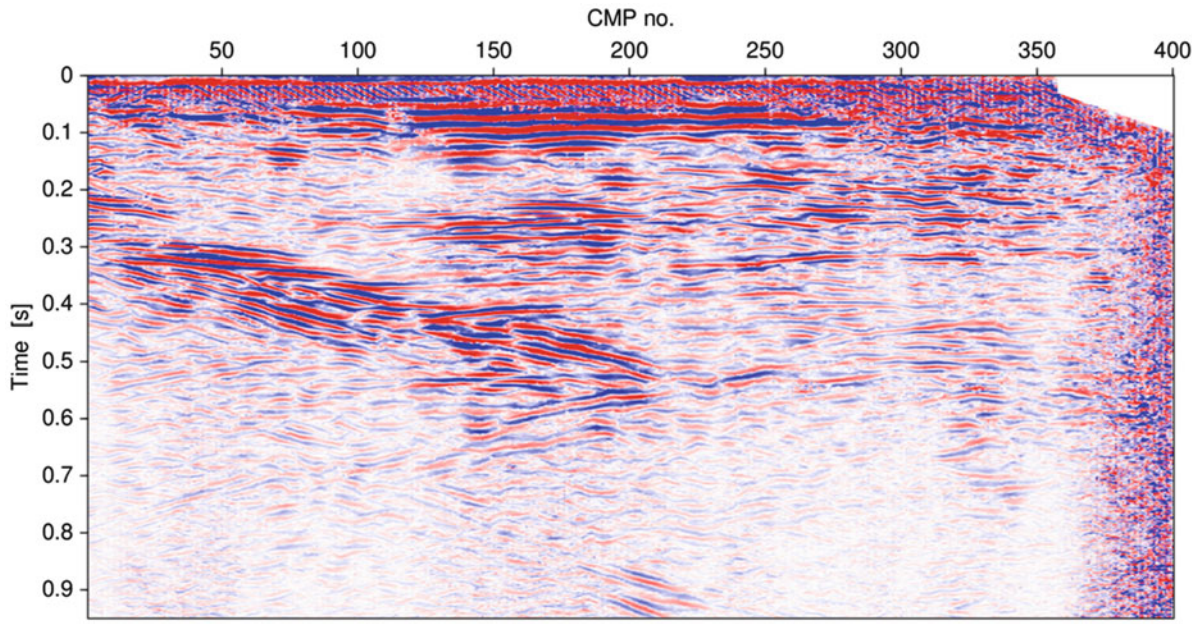

Fig. 12 Stack section obtained after five iterations of residual static corrections for a P-wave dataset from Muravera (Cagliari, Italy)

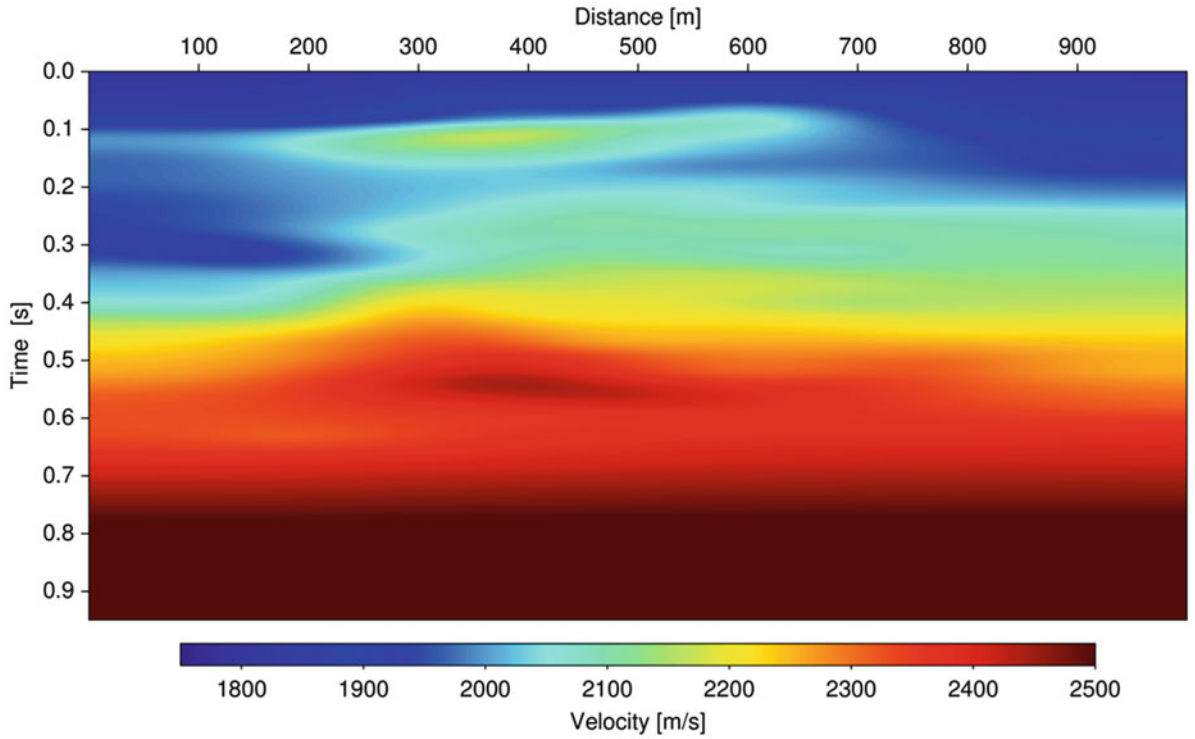

Fig. 13 Migration velocity model created for the Muravera (Cagliari, Italy) data from the coherence and stacking parameter sections by extracting and regularizing attribute values on events with a coherence larger than 0.25

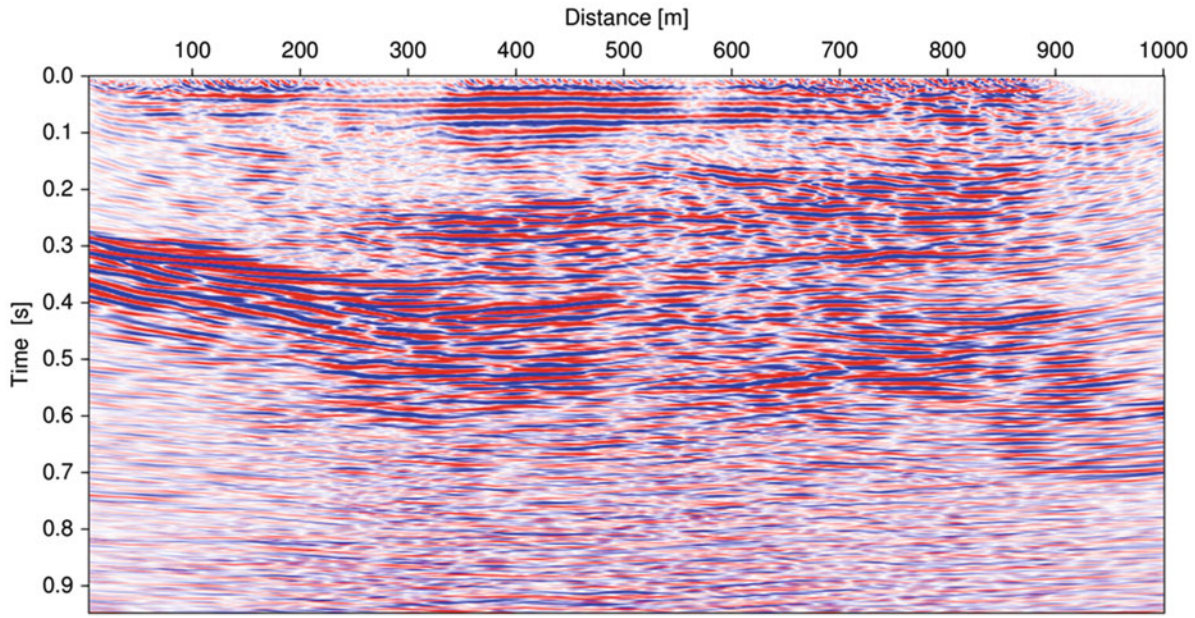

Fig. 14 Prestack time-migration results created for the Muravera (Cagliari, Italy) data obtained by using the velocity model depicted in Fig. 13

GPR processing. It was recorded using a Mala Geophysics RAMAC-2 four-channel control unit and two pairs of unshielded 200 MHz antennas. The aim was to obtain besides a structural image also velocity information that can be used to recover groundwater properties such as water content and water conductivity. As described in Perroud and Tygel (2005), repeated profiling was performed with four antennas mounted on a PVC cart with varying spacings. 56 CMPs were recorded, every 0.1 m on a 55 m-long profile, each one with 28 different offsets, ranging from 0.6 to 6 m. The maximum recording time was 150 ns, which corresponds roughly to a 6 m penetration depth for a mean velocity of 7.5 cm/ns. The data provided to us

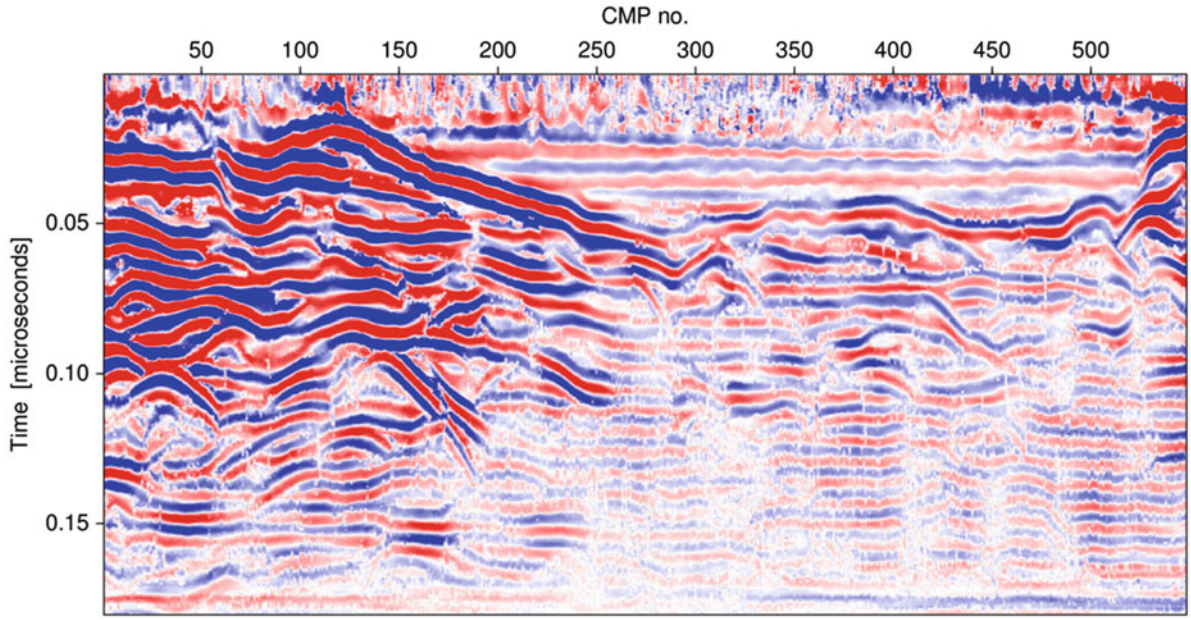

Fig. 15 Stack section obtained for the GPR dataset from Larreule (France)

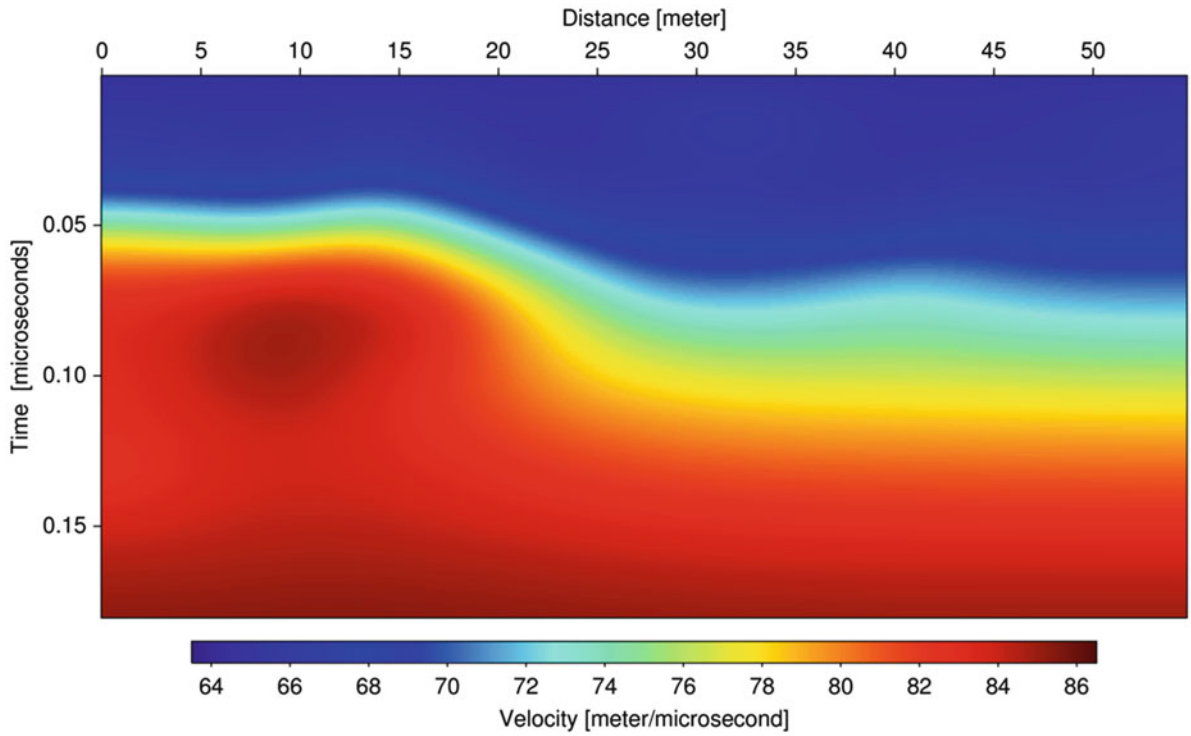

Fig. 16 Migration velocity model created for the Larreule (France) data from the coherence and stacking parameter sections by extracting and regularizing attribute values on events with a coherence larger than 0.25

was already preprocessed including, besides the geometry setup, also static shifts to zero time, mean amplitude removal, tapered band-pass filtering, muting of airwaves, and amplitude balancing. The stack result obtained by using our portal is depicted in Fig. 15. In Fig. 16, the smooth time-migration velocity model is shown that was generated by iteratively smoothing from coherency windowed CRS stacking parameters and a gradient model ranging between 6.5 and 9.0 cm/ns that served as an initial model for closing the gaps. The time-migration result is depicted in Fig. 17. The turnaround times for processing this dataset were very similar to those of the Muravera (Cagliari, Italy) example. The obtained results

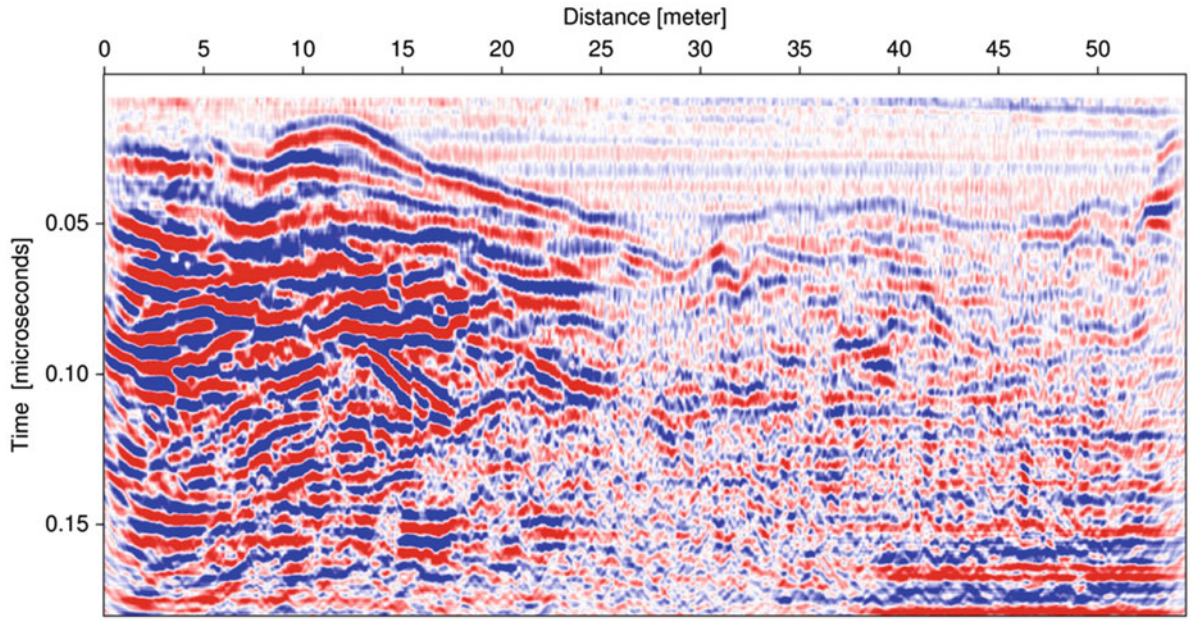

Fig. 17 Prestack time-migration results created for the Larreule (France) data obtained by using the velocity model depicted in Fig. 16

are very close to the original work. Different to the preceding data example, preprocessing was not an issue for this test since the same preprocessed data as used by Perroud and Tygel (2005) was taken as input for the EIAGRID imaging workflow.

4.4 Concluding Remarks

In-field real-time processing systems are a commonplace in electrical and electromagnetic surveys for several years now, as they allow efficient data acquisition and cost-effective results. Unfortunately, such systems are still a need both for shallow reflection seismics and for multichannel GPR surveys. For this reason, we have combined the powerful computational capabilities of a cloud computing architecture with a data-driven CRS stack-based imaging workflow, setting up an innovative, easy to use, and reliable imaging system. We simulated the in-field real-time processing for two different datasets, showing that our highly automated imaging workflow is able to produce stacked and migrated sections comparable to the ones obtainable with conventional CMP processing. The given examples highlight the practical applicability of the grid/cloud portal during acquisition as a tool supporting field geophysicists in improving acquisition geometry, gauging data quality, and estimating characteristic values of the subsurface, in a cost-effective way. Moreover, in case of low-quality records, it is possible to run an imaging workflow repeatedly along the line, until the operator reaches an optimum trade-off between different processing settings, obtaining the best possible image to optimize his or her acquisition setup.

In conclusion, we have devised a cutting-edge procedure that could become a commonplace for shallow seismic reflection and multi-offset GPR surveys in hydrogeological, environmental, agricultural, archaeological, and geotechnical studies, similar to what happened to electrical and electromagnetic methods in the past decades. We are aware that wireless Internet access and bandwidth are key requirements to employ our cloud computing imaging procedure. This may be a weak point, as today there still are locations with poor wireless coverage and poor capacity/speed connectivity or with no connectivity at all. However, we trust in the ongoing rapid improvement of mobile Internet connectivity and bandwidth, such as the upcoming G4 standard, which surely will push cloud computing and applications, such as the EIAGRID portal, on mobile devices. The latter will be particularly useful in the management of the huge data volume that the incoming new acquisition systems, equipped with wireless receivers and high-density shooting, will make available. Furthermore, we hope that our cloud computing proposal is a step ahead to stand up to in-field data interpretation, the next challenge for the near-surface community, as it fosters the integration of seismic data with other geophysical data, as well as gives rise to more collaboration and knowledge-sharing opportunities.

5 The Forest Fire Web Portal, PREMIAGRID Project

5.1 Introduction

In the following we briefly describe the forest fire service, an integrated system for weather and wildfire propagation forecast developed inside the PREMIAGRID portal.

The purpose of such service is to provide a tool that could be used to understand and predict the behavior of wildland fire, in order to increase the safety of the public and of the firefighters and to reduce the risk and possibly minimize the economic and environmental damage in case of an event.

The prediction of fire behavior is certainly not a new concept; several attempts to produce models have been done in the past with different levels of complexity, different purposes, and effective usage in fire suppression activities.

The simplest models are purely empirical and are based on observation and extrapolation of the fire spread velocity and fire intensity for a given type of vegetation under given conditions of wind and terrain slope.

The interpretation of these empirical data and the integration with data from controlled conditions experiment have led to the development of semiempirical models that, given some fundamental assumptions on the mechanism of fire spread, allow a good extrapolation of the fire behavior, based on measurable data on the vegetation characteristics and on the terrain and atmospheric conditions.

These models can only give point-wise estimation of the fire behavior but are extremely useful in the field, since these may give quick and efficient information to support firefighters.

Several models of this kind have been developed in the world, and of particular importance are those of the US, Canadian, and Australian forest services. The US Rothermel set of equation will be our reference model in the development of our fire propagation system (Rothermel 1972).

A second step in model complexity comes from proper consideration of the variation of the fire environment with position. The terrain slope, the characteristics of the vegetation, and the weather conditions too are clearly not constant with position and time; therefore, the fire behavior changes from place to place. It is thus possible to calculate in each geographic point the potential behavior of a fire and, by adding a fire spread model, to predict the fire propagation in a limited geographic area from a given ignition point.

These models do not require much computational power and can be used efficiently in the analysis of fire behavior with satisfactory results. They are difficult to use in real time, for instance, during an emergency, due to the long setup time required by the geographic information system that supports them for all the information on vegetation characteristics, terrain slope, and weather conditions; they furthermore suffer from the lack of fine-scale information on wind data to give maximum accuracy. An excellent example of such systems is the FARSITE model developed by the US forest service (Finney 2004).

Apart from the need of high-quality and high-resolution data, the principal limitation of such kind of approach is the lack of feedback between the fire and the weather and atmospheric conditions. A wildfire constitutes a power source for the atmospheric system; the energy release of the combustion process can affect the local winds. To include such effects in the modeling of the phenomena, a coupling between the fire spread model and the atmospheric model is required; the model is much more complex and requires significant computational costs. Several attempts are being made to obtain such coupling. The computational power required in any case does not allow to have a real-time prediction of the fire behavior and is therefore beyond the scope of our service.

It is worth reminding that there are several attempts for a full three-dimensional fluid dynamics modeling of wildfire behavior; in such models, the whole set of mass, momentum, and energy balance equations are solved for a system involving both air and fuel. Such models may allow a deeper understanding of some fire behavior but are clearly limited by the enormous computing power required for a relatively small model size.

The service we developed should be used by skilled and authorized personnel of the firefighting service to help the planning during an emergency, to help in the training of the personnel, and to provide scenarios that could be used for prevention activities. It is accessible through a web portal and is composed of a geographic information system for the management of soil and vegetation data, a limited area meteorological model chain that generates a high-resolution weather forecast, a very high-resolution fluid dynamic calculation of the wind in the fire area, and finally a fire spread model that allows to predict and visualize the evolution of the flame front position in time.

None of the skills required to manage such systems should be required to the final user, who can focus quickly on the interpretation of the results and make decisions more efficiently.

The behavior of wildfires is deeply affected by the weather, vegetation characteristics, and topography (Hanson et al. 2000).

The factors related to vegetation, the fuel of this combustion process, include the type of vegetation present in the area, its moisture, and its size and shape, density, and arrangement. The topography influences fire propagation through the terrain slope that partly determines the rate of spread of a fire front and through features such as narrow canyons which determine the direction of local winds or barriers such as creeks, roads, and areas without burnable vegetation.

These two factors are constant in time or have very limited variations; weather-related factors on the other side are difficult to predict and are subject to very high variations even during an event, not to mention the fact that the energy and gases released by the combustion can deeply influence the local characteristics of weather and winds (fire creates its own weather).

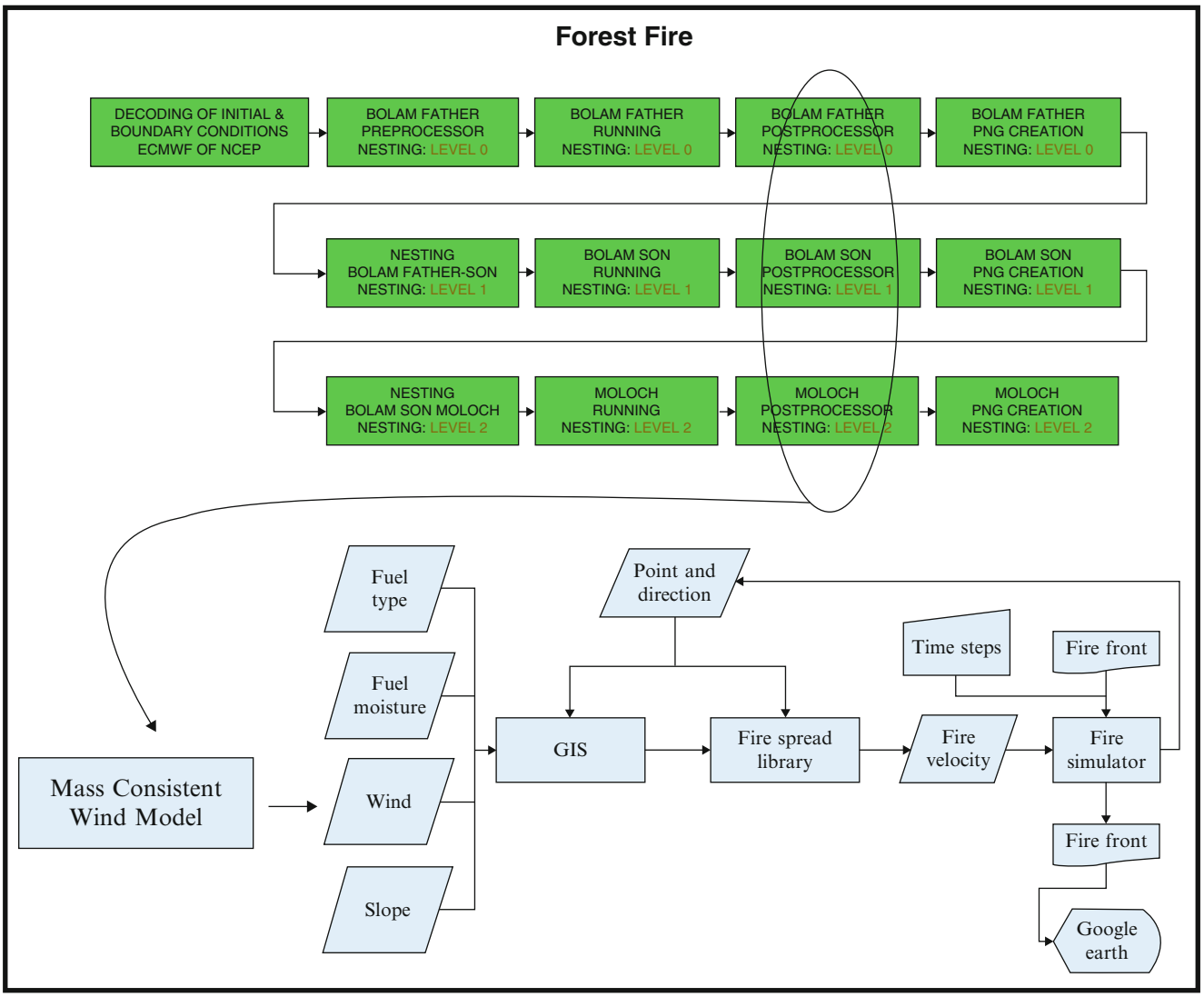

Fig. 18 Forest fire service algorithm scheme. The blocks in *green* are relative to the meteorological models representing the three levels of nested simulations. The results constitute the input of the wind modeling application. The high-resolution wind data and the GIS data on vegetation and terrain constitute the input for the fire spread algorithm, whose constitutive blocks are shown in *blue*

Weather influences fire propagation through winds, temperature, relative humidity, and precipitations, and even minimum variations on these quantities can have dramatic effects on the wildfire intensity and propagation direction. These factors are not constant in time as mentioned but also have strong variations in space. Winds in particular at the ground level may have strong variations in direction and intensity due to a complex topography or changes in the vegetation cover.

Wind deeply influences the rate and direction of spread of a fire front, and it is probably the most difficult and important factor to evaluate in order to obtain a reliable fire propagation forecast. It has to be determined with high precision at scales of the order of 20 m or less, comparable to the scale of flame length.

Our service is intended to give a real-time service to the user; the model complexity shall therefore be limited, and the user interaction for data input minimized.

Therefore, we set up within the GRIDA3 infrastructure the fire forest service, assembling and connecting the following modeling task (as it is shown in Fig. 18):

- A hydrostatic–nonhydrostatic limited area weather forecast chain based on the ISAC-CNR models BOLAM (Buzzi et al. 1994) and MOLOCH (Tettamanti et al. 2002), with up to four nesting levels and initial and boundary conditions from NCEP-GFS daily data (NCEP Office Note 442, 2003) or from ECMWF ERA Interim dataset (Dee et al. 2011).
- A preprocessing and GIS module used to prepare topography and fuel input data (elevation, slope, aspect, canopy cover and fuel model) to manage raster layers and interpolate the weather forecast results at the proper resolution required for the fluid dynamic and fire propagation analysis.

- A mass-consistent fluid dynamic analysis of the wind in the area of interest that allows to have the wind field with a spatial resolution of the order of 10 m, over a terrain of 10 km side, realized through a finite volume solver based on the public domain library OpenFOAM (http://www.openfoam.org).
- A fire spread analysis that gives the evolution in time of the fire line and the burned area. This module takes as input the geographic data on the terrain configuration, the land use and type of vegetation, the meteorological conditions, and the wind conditions near the ground and gives as output the time required for a fire starting from a given ignition point to reach any point in the map. The solver is developed on a well-established library for the calculation of the velocity of advancement of the fire front and on an in-house developed solver based on the level set method for the calculation of the front evolution on the ground surface.

As example of the fire forest portal, we show the simulation of the wildfire that occurred near the village of Budoni (Olbia, Italy) on August 26, 2004, where thousands of people (residents and tourists) were evacuated from their lodging due to the fire danger.

5.2 BOLAM–MOLOCH Chain

For the forest fire service, we arranged a complex BOLAM–MOLOCH chain consisting of four levels of nesting, starting from the BOLAM model used at 0.33 degrees of resolution and ending with the MOLOCH model (the last level of nesting) used at 0.01 degrees (about 1 km at our latitudes).

BOLAM and MOLOCH are two models closely related: BOLAM is a hydrostatic meteorological model, with prognostic equations for the horizontal wind components, the absolute temperature, the surface pressure, the specific humidity, and the turbulent kinetic energy (TKE). Deep moist convection is parameterized using the Kain–Fritsch (Kain 2004) convective scheme. BOLAM implements a split-explicit temporal integration scheme, forward–backward for the gravity modes. MOLOCH is a nonhydrostatic, fully compressible model developed at ISAC-CNR from the BOLAM experience. The MOLOCH time integration scheme is characterized by an implicit scheme for the vertical propagation of sound waves and explicit, time-split schemes, the remaining terms of the equations of motion. It shares with BOLAM many physics parameterization (such as atmospheric radiation, sub-grid turbulence, water cycle microphysics, and a soil model), but solving equations for vertical momentum, MOLOCH can compute directly convective phenomena.

The BOLAM–MOLOCH chain can be scheduled to execute daily one or two runs (forecast up to +72 h) with GFS analysis starting at 00 UTC or 12 UTC. Setting three levels of nesting (MOLOCH at 0.033 degrees of resolution), the forecast chain can last about 4 h, depending on the grid load. MOLOCH, even though fully parallelized, is the bottleneck of the chain, partly because of its equation complexity and partly because of its dense grid and small timestep. So, if users need a fast forecast (in less than 2 h), the chain can be stopped before the MOLOCH run.

The meteorological model chain must run continuously over a given region (the Region of Sardinia in our case) to have continuously improved weather forecast data, which constitutes the initial approximation on which a limited area fast computational fluid dynamic model is run to produce the high-resolution wind data required by the fire model.

5.3 Wind Modeling

The high-resolution wind field necessary to evaluate the fire spread is calculated through a dedicated finite volume solver based on the open-source library OpenFOAM. The meteorological model chain gives the value of the wind distribution up to a scale of 3 km that is clearly not sufficient. The target spatial scale is in fact of the order of 10 m, and the area on which the wind data is required has a side of 10 km.

It is beyond the limits of the current computational power the possibility to realize a complete CFD analysis of such a domain by solving the whole set of the Navier–Stokes equations and some closure model for turbulence, in a short time, comparable to the typical duration of the wildfires in the Mediterranean area. In order to have a real-time service, it is therefore necessary to have some simplification; we found that some good approximation may be obtained through a simple mass-consistent fluid dynamic model: of all Navier–Stokes balance equations, only the mass consistency is forced; some inconsistencies in the momentum and energy balance for the wind flow are thus allowed.

The procedure that we adopted may be figured out as a clever interpolation technique for the meteorological data that fulfills the mass balance requirements and includes high-resolution data on the orography and the vegetation.

The three-dimensional wind field is calculated with a two-step procedure consisting of an initial guess based on the meteorological results followed by a correction step to force mass consistency (Ratto et al. 2002).

The initial guess of the wind field is calculated as an interpolation of the meteorological results, taking proper consideration of the higher-resolution orography and of the form of the atmospheric boundary layer that is in turn influenced by the high-resolution data on the vegetation. While the meteorological wind field satisfies the Navier–Stokes balance equation, this high-resolution interpolation introduces some inconsistencies in the field, which are partly corrected in the second phase.

The correction step takes the initial guess and modifies it, forcing the wind field to verify the mass balance equation of the Navier–Stokes set.

Let $\boldsymbol{v}_0$ be the initial guess for the wind field, which already is a good approximation of the real conditions; the aim is to apply to it the minimum possible correction in order to make it satisfy the divergence free condition on all the computational domain Ω. We identify the corrected wind field with $\boldsymbol{v}$. The variational problem consists in minimizing the variance of the difference between the adjusted and the initial wind field, subject to the constraint that the divergence should vanish. It is necessary to minimize the integral norm of the difference between the two vectorial fields over the computational domain

$$E(\boldsymbol{v}) = \int_{\Omega} \|\boldsymbol{v} - \boldsymbol{v}_0\|^2 d\Omega, \tag{6}$$

under the strong constraint of mass conservation

$$\nabla \boldsymbol{v} = 0. \tag{7}$$

Here, for the sake of simplicity of the formulation, the air density is assumed constant.

Introducing the Lagrangian multipliers λ, the problem may be rewritten as the minimization of the functional

$$J(\boldsymbol{v}, \lambda) = \int_{\Omega} \left(\|\boldsymbol{v} - \boldsymbol{v}_0\|^2 + \lambda \nabla \boldsymbol{v} \right) d\Omega, \tag{8}$$

which leads to the solution of the following elliptic equation:

$$\nabla^2 \lambda = -2 \nabla \boldsymbol{v}_0. \tag{9}$$

Once solved, the corrected wind field is calculated as

$$v = v_0 + \frac{1}{2} \nabla \lambda. \tag{10}$$

For this problem, suitable boundary conditions able to ensure stability of the solution are: a zero normal gradient of the wind stream on the lateral boundaries, a fixed zero value for λ on the sky boundary and the no-slip condition on the ground.

Given a good estimation of the starting wind, obtained by meteorological model chain, this procedure allows to correct the wind for mass consistency only where needed and has an estimation that is at least in part responsive to the real detailed orography.

5.4 Fire Spread

The fire spread is based on a semiempirical method for the calculation of flame front velocity, through the well-known and tested Rothermel model, and on the level set method (Osher and Sethian 1988) as the numerical tool.

The Rothermel model is a semiempirical fire model consisting of a set of equations that allow the prediction of the rate of spread (ROS) of a fire front given the characteristics of the fuel in terms of humidity, latent heat, and heat released when burned, as well as the slope and wind intensity in the direction normal to the fire front.

Fire spread calculations are implemented using the GPLv2 library "Fire Behavior Software Developer Kit" (Bevins 2006).

The level set is a powerful method to track moving interfaces originally introduced by Osher and Sethian. It uses a rich computational space for the tracking of the interface and a two-dimensional Cartesian grid to describe the evolution of the linear boundary. The method can automatically deal with topological changes that may take place during fire spreading, such as the merging of separate flame fronts or the formation of unburned "islands," making it particularly appropriate to wildfire propagation problems.

We denote with $\Gamma(x, t)$ the fire line contour; in a two-dimensional domain this can be represented as an isoline of an auxiliary function $\varphi(x, t)$, i.e., $\Gamma(x, t) = \{x, t: \varphi(x, t) = \varphi_0 = \text{constant}\}$. Hence, the evolution in time of the isoline is given by

$$\frac{D\varphi}{Dt} = \frac{\partial \varphi}{\partial t} + \frac{\mathrm{d}\boldsymbol{x}}{\mathrm{d}t} \cdot \nabla \varphi = \frac{D\varphi}{Dt}. \tag{11}$$

If the motion of the surface points is directed toward the outward normal direction, then

$$\frac{D\varphi}{Dt} = \frac{\partial \varphi}{\partial t} + \frac{\mathrm{d}\boldsymbol{x}}{\mathrm{d}t} = \boldsymbol{V}(\boldsymbol{x}, t) = V(\boldsymbol{x}, t)\boldsymbol{n}, \tag{12}$$

$$\boldsymbol{n} = \frac{\nabla \psi_0}{\|\nabla \psi_0\|}, \tag{13}$$

and the evolution of φ is calculated as

$$\frac{\partial \varphi}{\partial t} = V(\boldsymbol{x}, t) \|\nabla \varphi\|, \tag{14}$$

which is here referred to as the ordinary level set equation.

For our purpose, we take $V(\boldsymbol{x}, t)$ as the ROS of the fire front, the velocity at which the fire contour propagates along its normal, and we let $\varphi(\boldsymbol{x}, t)$ be an indicator function which takes positive values for an unburned point and negative for the burned points, such as the signed distance of any point from the fire boundary. The area burned by the wildland fire may be defined as $\Omega(t) = \{\boldsymbol{x}, t: \varphi(\boldsymbol{x}, t) < 0\}$. The boundary of Ω is Γ that is the front line contour of the wildland fire.

When the ROS $V(\boldsymbol{x}, t)$ depending on the environmental conditions and of the local orientation of the fire front is known, the evolution of the fire front can be efficiently simulated by the numerical solution of Eq. (14).

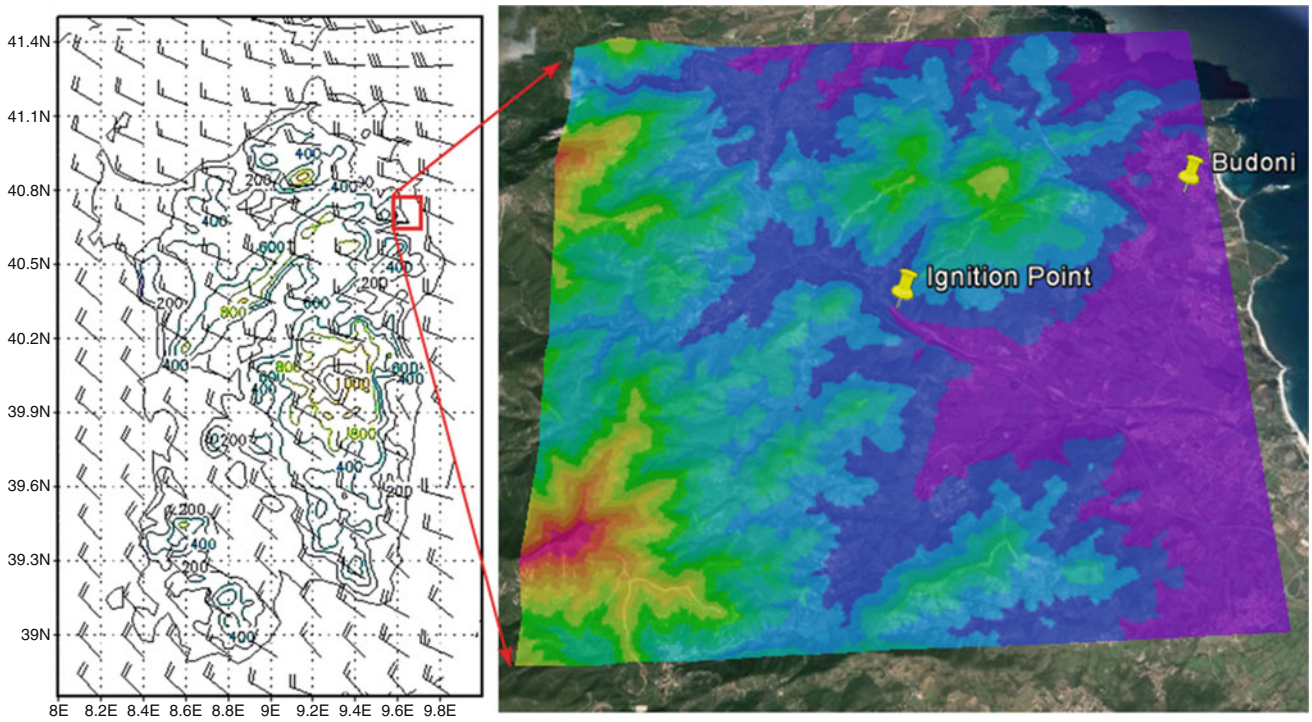

Fig. 19 The wind conditions and the ignition point for the Budoni (Olbia, Italy) wildfire on August 26, 2004. The picture on the *left* shows the wind condition on Sardinia 10 m above ground at 5 p.m. when the fire was started. The picture on the *right* shows the orography in color and the ignition point position

At any given time, the burned area is easily calculated from the value of the indicator function, and a map of the time of arrival of the fire may be easily deduced.

5.5 Budoni (Olbia, Italy) Wildfire Test Case

As an example the case of a wildfire in the hilly area close to the village of Budoni (Olbia, Italy) is examined where 145 ha were burnt on August 26, 2004. The burnt area was covered by the typical shrubland Mediterranean vegetation, and plant height in the range 1–4 m, with small surfaces covered by open wooded pastures and grasslands. The fire started at 5 p.m. in very windy weather conditions. The dominant wind came from north–west (as the MOLOCH forecast shows in Fig. 19) while locally near Budoni (Olbia, Italy) the wind came from west–southwest with an average speed of 35 km/h; the temperatures were moderate, ranging from a minimum of 20 °C to a maximum of 24 °C.

The fire spread quickly toward east, driven by the wind. In the south area, potentially interested by the fire, a fire suppression action was successfully conducted. On the opposite flank, the intervention was impossible, but the fire was naturally slowed down probably thanks to the terrain slope and wind intensity. The fire lasted 6 hours and a half; afterward it was definitively stopped by means of aerial interventions and thanks to the decrease of the wind speed.

5.5.1 Fire Model Setup and Test Procedure

The computational domain for the fire spread calculation has the same size and the same resolution of the wind grid on the ground (a side of 8 km and a grid spacing of 10 m). To forecast realistic rate of spread, suitable fuel models were chosen according to the land cover inferred from the CORINE map (Bossard et al. 2000). In particular the "chaparral" standard fuel model (Scott et al. 2005) for shrubland vegetation was replaced with a custom fuel model optimized for Mediterranean maquis (Bacciu et al. 2009). Figure 20 shows the CORINE land cover for the test area: every cover class represents a basic fuel model; we remapped these classes into standard fuel models plus a custom model for Mediterranean maquis.

Furthermore, to evaluate the sensitivity of the fire propagator to the wind conditions, we run several tests using different wind data: wind in output from the BOLAM–MOLOCH chain, wind downscaled with CFD models, and observed wind from the Regional Agency for Environmental Protection of Sardinia (SAR-ARPAS). All of these wind conditions were in agreement with the dominant mistral wind, but only the CFD downscaling was able to achieve a realistic interaction between mistral and the very fine orography used for the fire modeling. Figure 21 shows an example of high-resolution wind obtained with the mass-consistent model.

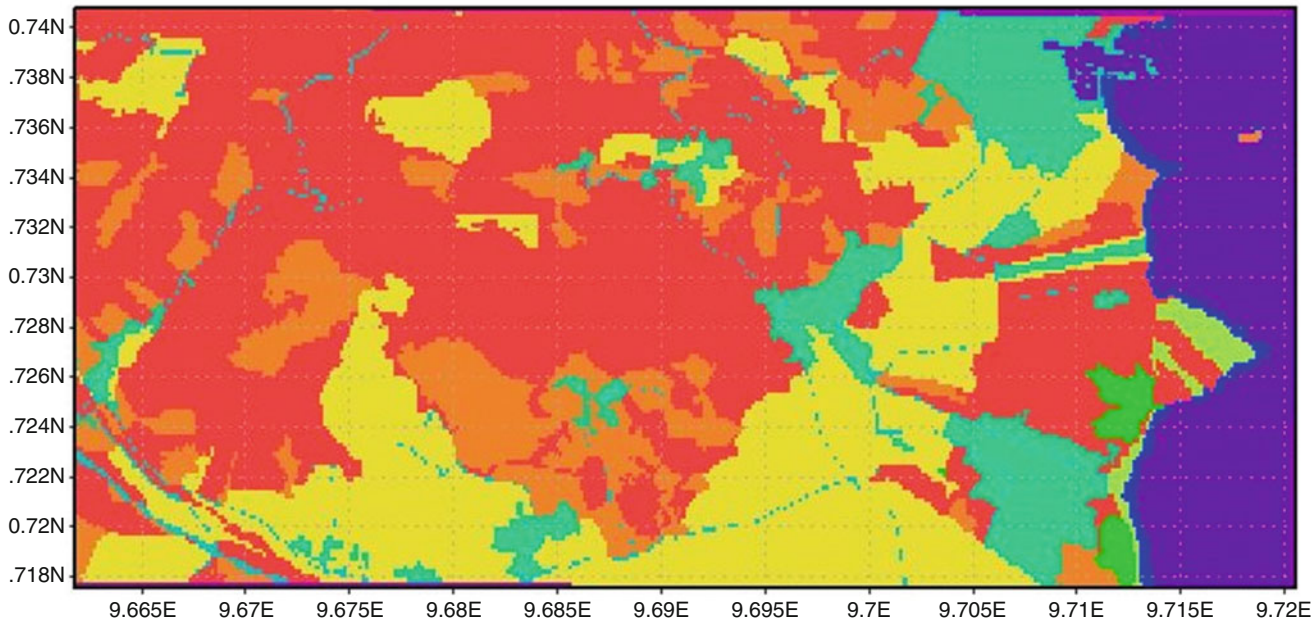

Fig. 20 GIS model of the land cover and terrain usage in the wildfire area. The different colors are representative of different terrain covers; *red* is for Mediterranean shrubland and *yellow* is for grasslands

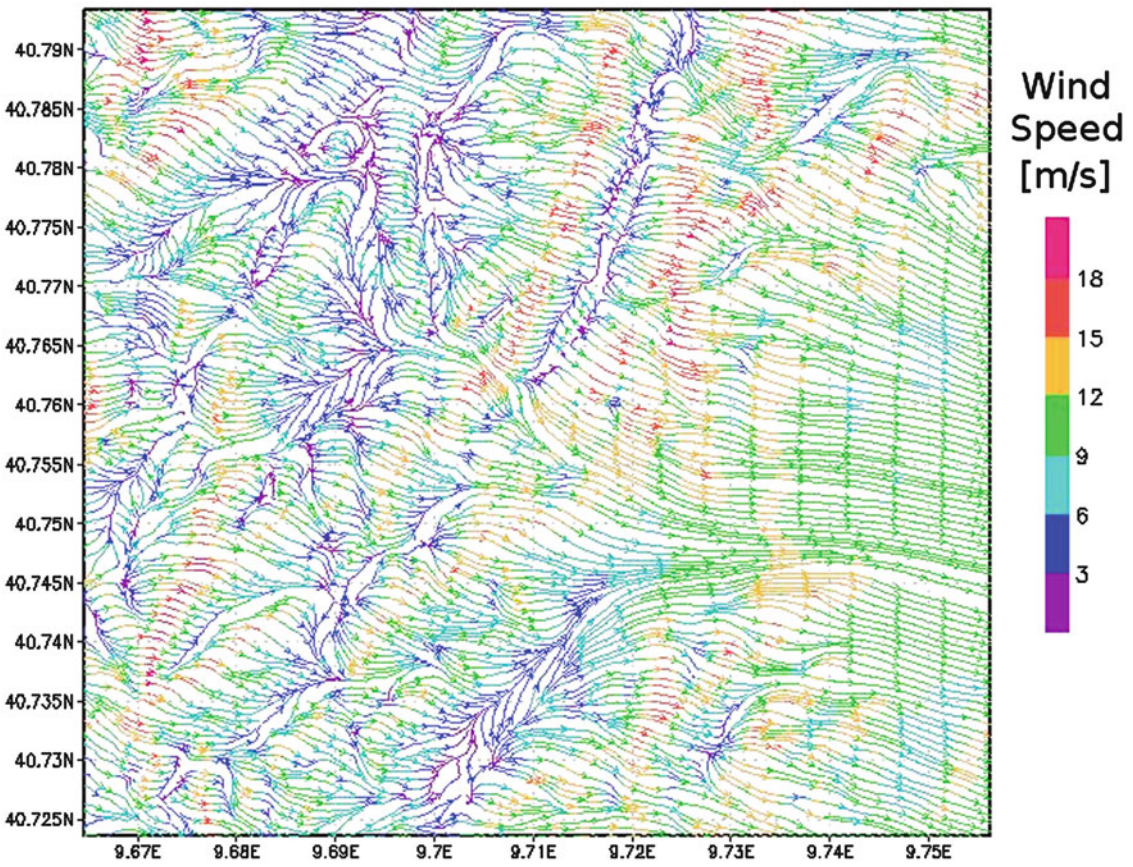

Fig. 21 High-resolution wind results on the area of the wildfire at the time the wildfire started. The domain spans an area of 8 km $\times$ 8 km on the ground centered at the point of ignition and 2 km above the ground. The grid resolution at which wind results are obtained is 10 m

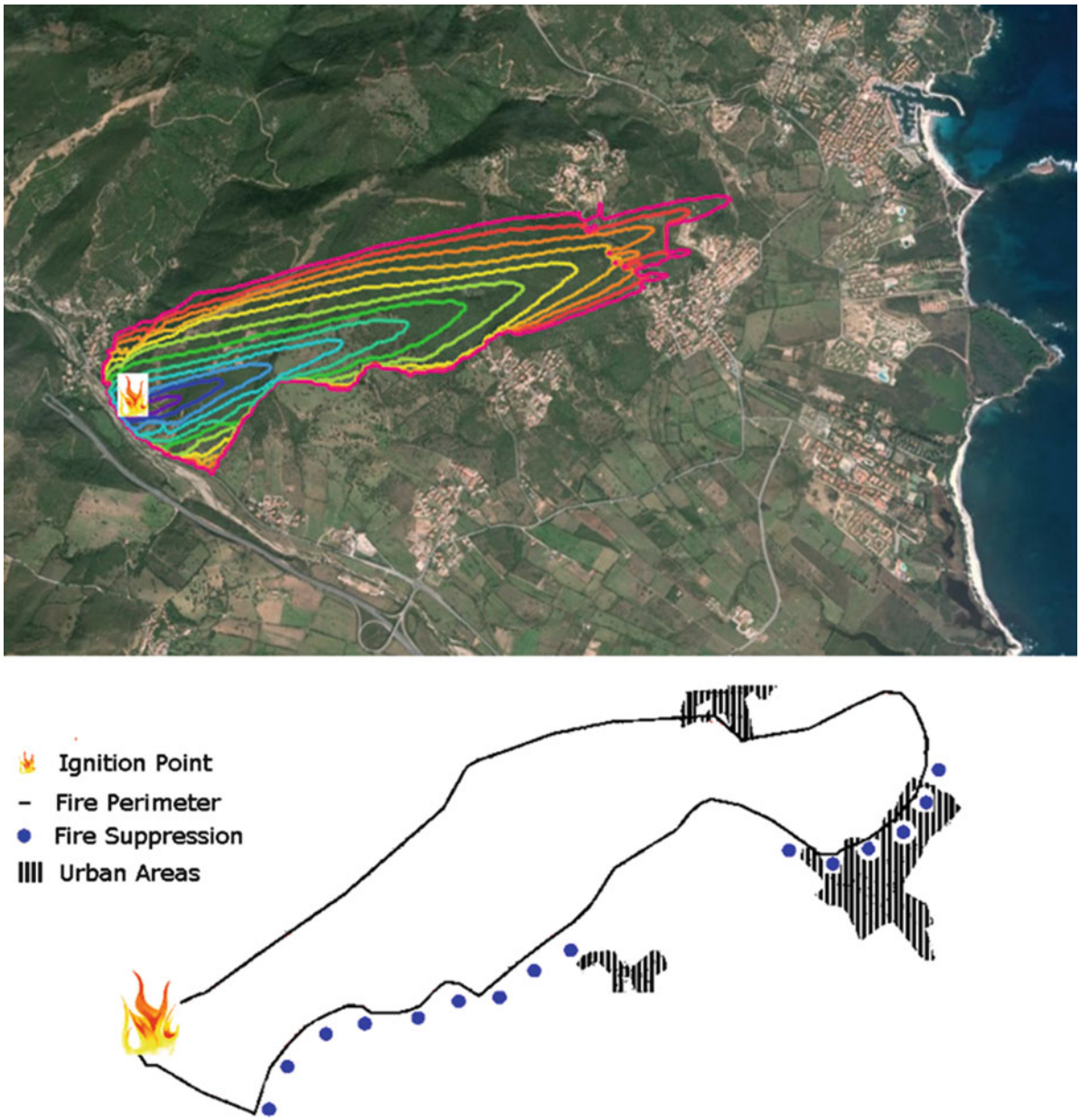

Fig. 22 Budoni (Olbia, Italy) wildfire, (at the *top* of the figure) time evolution of predicted front and (at the *bottom* of the figure) the observed fire perimeter after 6 h of burning

5.5.2 Test Results

A meaningful outcome for this test case is shown in Fig. 22: the forecast of fire front is tracked every 30 min (inert fuel has been set in areas where the wildfire was suppressed), and the total burned area is in good agreement with the perimeter tracked by the firefighters (as can be seen at the bottom of the figure). The pattern of the burned area is very similar, but there is a relevant overestimation in the upper area. These differences are due to uncertainties deriving mainly from:

- The simplified modeling of weather conditions at wildfire scale
- The nontrivial interaction among wildfire, local wind, and topography
- The simplified modeling of fuels and relative rate of spread
- The real position and time of the wildfire ignition
- Human action against the wildfire

We are confident that optimal results (for a real-time fire forecasting) can be achieved, improving some of these limits (as it is described in the following section).

5.6 Concluding Remarks

The service developed appears as a good example of the application of high-performance computing to the solution of complex environmental problems.

The results so far appear really promising, in terms of efficiency and quality of the results. Some important improvements are anyway possible and foreseen in all the steps of the computational chain.

The local meteorological models are quite stable and accurate. Nevertheless, more computing power would be necessary in order to have quicker forecast and more detailed output, possibly adding a further level of nesting to the described chain.

The wind analysis module may be greatly improved by adding a parameterization of the atmospheric instability calculated from the meteorological model and a feedback from fire related to the energy release. The model can be greatly improved by including the full set of balance equations and a closure model for turbulence. At the moment this upgrading is limited by the available computing power, since the run time of the simulation would be too long for an operational use.

The fire propagation model at the moment is limited to surface fires and cannot model the transition to crown fire and some phenomena that appear in extreme conditions; these models are available and their implementation is foreseen in the future.

6 Conclusions

A grid computing portal that can be accessed from all kind of devices via web browser provides the necessary computing power and gives much more freedom and flexibility to the user. Processing speed is increased (by a factor of 10 to 100 in out test cases) and even very large results can be stored safely on the cloud storage, from where they are directly accessible for colleagues and collaborators. Since data, application software, and results are on a central server that is location independent and accessible by multiple clients, a collaboration between researchers of spatially separated institutions is strongly facilitated. For example, meetings and seminars can be conducted via the Internet where participants can view examples or perform experiments with different workflows or parameter settings without having any software locally installed on their laptops. So far our work was focused on real-time data analysis and processing. To unfold the full potential of the remote collaboration capabilities, still a lot of work has to be done. We hope to find in the future the resources to make this portal accessible to a larger community of users in order to unfold the full potential of the cloud computing solution.

Acknowledgments The presented work was funded by the government of the Autonomous Region of Sardinia and by the Italian Ministry of Research and Education. We like to thank Hervé Perroud and Martin Tygel for providing us the GPR data and Miriam Spinner for allowing us to use her time-migration code. We are grateful to CNR IBIMET Sassari for providing material and hints for the forest fire portal.

References

Bacciu, V., Arca, B., Pellizzaro, G., Salis, M., Ventura, A., Spano, D., Duce, P.: Mediterranean Maquis Fuel Model Development and Mapping to Support Fire Modeling. In: Geophysical Research Abstracts, European Geosciences Union (EGU), General Assembly 2009, Vienna, Austria, p.13148 (2009)

Baykulov, M., Dümmong, S., Gajewski, D.: From time to depth with CRS attributes. Geophysics **76**(4), S151–S155 (2011)

Benjumea, B., Hunter, J.A., Aylsworth, J.M., Pullan, S.E.: Application of high-resolution seismic techniques in the evaluation of earthquake site response, Ottawa Valley, Canada. Tectonophysics **368**, 193–209 (2003)

Berard, B.A., Maillol, J.M.: Multi-offset ground penetrating radar data for improved imaging in areas of lateral complexity—application at a Native American site. J. Appl. Geophys. **62**(2), 167–177 (2006). doi:10.1016/j.jappgeo.2006.10.002

Berard, B.A., Maillol, J.M.: Common- and multi-offset ground-penetrating radar study of a Roman villa, Tourega, Portugal. Archaeol. Prospect. **15**(1), 32–46 (2008). doi:10.1002/arp.319

Bergler, S., Hubral, P., Marchetti, P., Cristini, A., Cardone, G.: 3D common- reflection-surface stack and kinematic wavefield attributes. Lead. Edge **21**, 1010–1015 (2002)

Bevins, C. D.: Fire behavior SDK documentation. Fire.org, http://www.fire.org/downloads/fbsdk/docs/html/main.html (2006)

Birkelo, B.A., Steeples, D.W., Miller, R.D., Sophocleous, M.A.: Seismic reflection study of a shallow aquifer during a pumping test. Ground Water **25**, 703–709 (1987)

Bonomi, E., Caddeo, G., Cristini, A., Marchetti, P.: Data-driven time imaging of 2D acoustic media without a velocity model. SEG Technical Program Expanded Abstracts 2012, pp. 1–5 (2012). doi:10.1190/segam2012-1095.1

Booth, A.D., Linford, N.T., Clark, R.A., Murray, T.: Three-dimensional, multi-offset ground-penetrating radar imaging of archaeological targets. Archaeol. Prospect. **15**(2), 93–112 (2008). doi:10.1002/arp.327

Bossard, M., Feranec, J., Otahel, J.: CORINE Land Cover Technical Guide – Addendum 2000. Technical report no 40. EEA, Copenhagen. http://terrestrial.eionet.eu.int (2000)

Bradford, J.H., Liberty, L.M., Lyle, M.W., Clement, W.P., Hess, S.: Imaging complex structure in shallow seismic-reflection data using prestack depth migration. Geophysics **71**(6), B175–B181 (2006)

Brouwer, J.H.: Improved NMO correction with a specific application to shallow-seismic data. Geophys. Prospect. **50**, 225–237 (2001)

Brown, R.: Historical Tidbit. Who was Irvine Perrine? Timelines, Jan. Issue, Geophysics Society, Tulsa (2002)

Buzzi, A., Fantini, M., Malguzzi, P., Nerozzi, F.: Validation of a limited area model in cases of Mediterranean cyclogenesis: surface fields and precipitation scores. Meteorol. Atmos. Phys. **53**, 137–153 (1994)

Cohen, J.K., Stockwell, J.J.W.: Seismic Un*x Release 34: a free package for seismic research and processing. Geophys. J. Int. **125**, 431–442 (2000)

Cossu, R., Petitdidier, M., Linford, J., Badoux, V., Fusco, L., Gotab, B., Hluchy, L., Lecca, G., Murgia, F., Plevier, C., Renard, P., Schwichtenberg, H., de Cerff, W.S., Tran, V., Vetois, G.: A

roadmap for a dedicated Earth Science Grid platform. Earth Sci. Inform. **3**(3), 135–148 (2010). doi:10.1007/s12145-010-0045-4

Dee, D.P., Uppala, S.M., Simmons, A.J., Berrisford, P., Poli, P., Kobayashi, S., Andrae, U., Balmaseda, M.A., Balsamo, G., Bauer, P., Bechtold, P., Beljaars, A.C.M., van de Berg, L., Bidlot, J., Bormann, N., Delsol, C., Dragani, R., Fuentes, M., Geer, A.J., Haimberger, L., Healy, S.B., Hersbach, H., Hólm, E.V., Isaksen, L., Kållberg, P., Köhler, M., Matricardi, M., McNally, A.P., Monge-Sanz, B.M., Morcrette, J.-J., Park, B.-K., Peubey, C., de Rosnay, P., Tavolato, C., Thépaut, J.-N., Vitart, F.: The ERA-Interim reanalysis: configuration and performance of the data assimilation system. Q. J. Roy. Meteorol. Soc. **137**, 553–597 (2011). doi:10.1002/qj.828

Deidda, G.P., Ranieri, G., Uras, G., Cosentino, V., Martorana, R.: Geophysical investigations in the Flumendosa River Delta, Sardinia, Italy—Seismic reflection imaging. Geophysics **71**(4), 121–128 (2006)

Deidda, G.P., Battaglia, E., Heilmann, Z.: Common-reflection-surface imaging of shallow and ultrashallow reflectors. Geophysics **77**(4), B177–B185 (2012). doi:10.1190/GEO2011-0401.1

Deregowski, S.M.: What is DMO? First Break **4**(7), 7–24 (1986)

Dix, C.H.: Seismic velocities from surface measurements. Geophysics **20**, 68–86 (1955)

Duveneck, E.: Velocity model estimation with data-derived wavefront attributes. Geophysics **69**, 265–274 (2004)

Finney, M.A.: FARSITE: Fire Area Simulator–Model Development and Evaluation. Research Paper RMRS-RP-4 Revised. U.S. Department of Agriculture, Forest Service, Rocky Mountain Research Station, Ogden, UT (2004)

Foster, I.: The grid: a new infrastructure for 21st century science. Phys. Today **55**(2), 42–47 (2002)

Garabito, G., Stoffa, P.L., Ferreira, C.A.S., Cruz, J.C.R.: Part II – CRS-beam PSDM: Kirchhoff-beam prestack depth migration using the 2D CRS stacking operator. J. Appl. Geophys. **85**, 102–110 (2012)

Ghose, R., Nijhof, V., Brouwer, J., Matsubara, Y., Kaida, Y., Takahashi, T.: Shallow to very shallow, high-resolution reflection seismic using a portable vibrator system. Geophysics **63**, 1295–1309 (1998)

Gierse, G., Trappe, H., Pruessmann, J., Eisenberg-Klein, G.: Enhanced velocity analysis, binning, gap infill, and imaging of sparse 2D/3D seismic data by CRS techniques. In: 79th Annual International Meeting, Society of Exploration Geophysicists, Extended Abstract, 3279–3283 (2009)

Goforth, T., Hayward, C.: Seismic reflection investigations of a bedrock surface buried under alluvium. Geophysics **57**, 1217–1227 (1992)

Goodman, D., Novo, A., Morelli, G., Piro, S., Kutrubes, D., Lorenzo, H.: Advances in GPR imaging with multi-channel radar systems from engineering to archaeology. Symp. Appl. Geophys. Eng. Environ. Probl. **24**(1) (2011). doi: 10.4133/1.3614128

Guy, E.D., Nolen-Hoeksema, R.C., Daniels, J.J., Lefchik, T.: High-resolution SH-wave seismic reflection investigations near a coal mine-related roadway collapse feature. J. Appl. Geophys. **54**, 51–70 (2003)

Hale, D.: Dip Moveout Processing. Course Notes Series, vol. 4. Society of Exploration Geophysicists, Tulsa (1991)

Hanson, H.P., Bradley, M.M., Bossert, J.E., Linn, R.R., Younker, L.W.: The potential and promise of physics-based wildfire simulation. Environ. Sci. Pol. **3**, 161–172 (2000)

Hashemi, S.M., Bardsiri, A.K.: Cloud computing Vs. grid computing. ARPN J. Syst. Softw. **2**(5), 188–194 (2012). ISSN 2222-9833

Heilmann, Z.: CRS-stack-based seismic reflection imaging for land data in time and depth domains. PhD thesis, University of Karlsruhe, Germany [online]. http://digbib.ubka.uni-karlsruhe.de/volltexte/1000005850 (2007)

Heilmann, Z., Mann, J., Koglin, I.: CRS-stack-based seismic imaging considering top-surface topography. Geophys. Prospect. **54**, 681–695 (2006)

Hertweck, T., Schleicher, J., Mann, J.: Data stacking beyond CMP. Lead. Edge **26**, 818–827 (2007)

Hilbert, M., López, P.: The world's technological capacity to store, communicate, and compute information. Science **332**(6025), 60–65 (2011). doi:10.1126/science.1200970. PMID 21310967

Höcht, G.: Traveltime approximations for 2D and 3D media and kinematic wavefield attributes. Ph.D. thesis, University of Karlsruhe (2002)

Hoffa, C., Mehta, G., Freeman, T., Deelman, E., Keahey, K., Berriman, B., Good, J.: On the use of cloud computing for scientific workflows. In: eScience'08, IEEE Fourth International Conference on eScience, Indianapolis, USA, Proceedings, pp. 640–645 (2008). doi:10.1109/eScience.2008.167

Hubral, P.: Computing true amplitude reflections in a laterally inhomogeneous earth. Geophysics **48**, 1051–1062 (1983)

Hubral, P., Krey, T.: Interval Velocities from Seismic Reflection Traveltime Measurements. Society of Exploration Geophysicists, Tulsa (1980)

Jäger, R., Mann, J., Höcht, G., Hubral, P.: Common-reflection-surface stack: images and attributes. Geophysics **66**, 97–109 (2001)

Jefferson, R.D., Steeples, D.W., Black, R.A., Carr, T.: Effects of soil-moisture content on shallow seismic data. Geophysics **63**(4), 1357–1362 (1998). doi:10.1190/1.1444437

Kain, J.S.: The Kain-Fritsch convective parameterization: an update. J. Appl. Meteorol. **43**, 170–181 (2004)

Koglin, I., Mann, J., Heilmann, Z.: CRS-stack-based residual static correction. Geophys. Prospect. **54**, 697–707 (2006)

Lecca, G., Petitdidier, M., Hluchy, L., Ivanovic, M., Kussul, N., Ray, N., Thieron, V.: Grid computing technology for hydrological applications. J. Hydrol. **403**, 186–199 (2011)

Levin, F.K.: Apparent velocity from dipping interface reflections. Geophysics **36**, 510–516 (1971)

Liberty, L.: Seismic reflection imaging of a geothermal aquifer in an urban setting. Geophysics **63**, 1285–1294, 8 (1998)

Mann, J.: Extensions and Applications of the Common-Reflection-Surface Stack Method. Logos Verlag, Berlin (2002)

Mann, J., Hoecht, G.: Pulse stretch effects in the context of data-driven imaging methods. In: 65th EAGE Conference, Stavanger, Norway, Extended Abstracts, P007 (2003)

Mann, J., Jäger, R., Müller, T., Höcht, G., Hubral, P.: Common-reflection-surface stack – a real data example. J. Appl. Geophys. **42**, 301–318 (1999)

Mann, J., Duveneck, E., Bergler, S., Hubral, P.: Chapter VIII.4: The Common-Reflection-Surface (CRS) stack – a data-driven space-time adaptive seismic reflection imaging procedure. In: Klemm, R. (ed.), Applications of Space-Time Adaptive Processing. The Institution of Electrical Engineers (IEE), London (2004)

Masoomzadeh, H., Barton, P.J., Singh, S.C.: Nonstretch moveout correction of long-offset multichannel seismic data for subbasalt imaging: example from the North Atlantic. Geophysics **75**(4), R83–R91 (2010)

Mayne, W.H.: Common reflection point horizontal data stacking techniques. Geophysics **27**(6), 927–938 (1962)

Miller, R.D., Xia, J.: High resolution seismic reflection survey to map bedrock and glacial/fluvial layers in Fridley, Minnesota. In: SAGEEP'97, 10th Annual Symposium on the Application of Geophysics to Engineering and Environmental Problems, Reno/Sparks, Nevada, USA, Proceedings, vol. 1, 281–290 (1997)

Miller, R.D., Xia, J.: Large near-surface velocity gradients on shallow seismic reflection data. Geophysics **63**(4), 1348–1356 (1998)

Müller, T.: Common Reflection Surface Stack versus NMO/STACK and NMO/DMO/STACK. In: 60th Annual International Meeting,

European Association Exploration Geophysicists, Extended Abstracts, Session. Bad Iburg, Germany 1–20 (1998)
Müller, T.: The Common Reflection Surface Stack Method – Seismic Imaging Without Explicit Knowledge of the Velocity Model. Der Andere Verlag, Bad Iburg (1999)
Murgia, F., Biddau, R., Concas, A., Demontis, R., Fanfani, L., Heilmann, B.Z., Lai, C., Lecca, G., Lorrai, E., Marrocu, M., Marrone, V., Vittorio, A., Muscas, L., Peneva, E., Piras, A., Pisu, M., Pusceddu, G., Satta, G., Theis, D., Vacca, A., Valera, P., Vallenilla, A.M., Bonomi, E.: GRIDA3—a shared resources manager for environmental data analysis and applications. Earth Sci. Inform. **2**, 5–21. NCEP Office Note 442, 2003, The GFS Atmospheric Model. http://www.emc.ncep.noaa.gov/officenotes/newernotes/on442.pdf (2009)
Neidell, N.S., Taner, M.T.: Semblance and other coherency measures for multichannel data. Geophysics **36**(3), 482–497 (1971)
Osher, S., Sethian, J.A.: Fronts propagating with curvature-dependent speed: algorithms based on Hamilton–Jacobi formulations. J. Comput. Phys. **79**, 12–49 (1988)
Perroud, H., Tygel, M.: Velocity estimation by the common-reflection-surface (CRS) method: using ground-penetrating radar data. Geophysics **70**(6), B43–B52 (2005). doi:10.1190/1.2106047
Prüssmann, J., Frehers, S., Ballesteros, R., Caballero, A., Clemente, G.: CRS-based depth model building and imaging of 3D seismic data from the Gulf of Mexico Coast. Geophysics **73**(5), VE303–VE311 (2008)
Pugin, A.J.-M., Pullan, S.E., Hunter, J.A., Oldenborger, G.A.: Hydrogeological prospecting using P- and S-wave landstreamer seismic reflection methods. Near Surf. Geophys. **7**, 315–327 (2009)
Ratto, C.F., Georgieva, E., Canepa, E., Mazzino, A.: WINDS Release 4.2 User's Guide. Scientific coordinator: Department of Physics – University of Genova (2002)
Reichman, O.J., Jones, M.B., Schildhauer, M.P.: Challenges and opportunities of open data in ecology. Science **331**(6018), 703–705 (2011). doi:10.1126/science.1197962
Robein, E.: Velocities, Time-Imaging and Depth-Imaging in Reflection Seismics: Principles and Methods. EAGE Publications, Houten (2003)
Robinson, E.A., Treitel, S.: Geophysical Signal Analysis. Prentice-Hall Inc., Upper Saddle River (1980)
Ronen, J., Claerbout, J.F.: Surface-consistent residual statics estimation by stack-power maximization. Geophysics **50**, 2759–2767 (1985)
Rothermel, R.C.: A Mathematical Model for Predicting Fire Spread in Wildland Fuels. Research Paper INT-115. U.S. Department of Agriculture, Forest Service, Intermountain Forest and Range Experiment Station, Ogden, UT (1972)
Sambuelli, L., Deidda, G.P., Albis, G., Giorcelli, E., Tristano, G.: Comparison of standard horizontal geophones and newly designed horizontal detectors. Geophysics **66**, 1827–1837 (2001)
Scott, J.H., Burgan, R.E.: Standard Fire Behavior Fuel Models: A Comprehensive Set for Use with Rothermel's Surface Fire Spread Model. General Technical Report RMRS-GTR-153. U.S. Department of Agriculture, Forest Service, Rocky Mountain Research Station, Fort Collins, CO (2005)
Spinner, M.: CRS-based minimum-aperture Kirchhoff migration in the time domain. [online] http://digbib.ubka.uni-karlsruhe.de/volltexte/1000007099 (2007)
Spinner, M., Mann, J.: True-amplitude CRS-based Kirchhoff time migration for AVO analysis. SEG Technical Program Expanded Abstracts 2005, 246–249 (2005). doi:10.1190/1.2144311
Steeples, D.W., Green, A.G., McEvilly, T.V., Miller, R.D., Doll, W.E., Rector, J.W.: A workshop examination of shallow seismic reflection surveying. Lead. Edge **16**, 1641–1647 (1997)
Tettamanti, R., Malguzzi, P., Zardi, D.: Numerical simulation of katabatic winds with a non-hydrostatic meteorological model. Polar Atmos. **1**, 1–95 (2002). ISSN 1591-3902
Udoh, E.: Cloud, Grid and High Performance Computing: Emerging applications. Premier Reference Source. IGI Global, Hershey (2011). ISBN 978-1-60960-603-9
van der Veen, M., Spitzer, R., Green, A.G., Wild, P.: Design and application of a towed landstreamer for cost-effective 2D and pseudo-3D shallow seismic data acquisition. Geophysics **66**, 482–500 (2001)
Versteeg, R., Johnson, D.: Efficient electrical hydrogeophysical monitoring through cloud-based processing, analysis, and result access. Lead. Edge **32**(7), 776–783 (2013). doi:10.1190/tle32070776.1
von Steht, M.: Imaging of vertical seismic profiling data using the common-reflection-surface stack. PhD thesis, University of Karlsruhe, Germany [online] http://digbib.ubka.uni-karlsruhe.de/volltexte/1000007747 (2008)
Woorely, E.W., Street, R.L., Wang, Z., Harris, J.B.: Near-surface deformation in the New Madrid seismic zone as imaged by high resolution SH-wave seismic methods. Geophys. Res. Lett. **20**, 1615–1618 (1993)
Yilmaz, O.: Seismic data processing: In Doherty, S.M., Neitzel, E.B. (eds.) Investigations in Geophysics, 2. Society of Exploration Geophysicists, Tulsa (1987)